DE GRUYTER
REFERENCE

Vasily E. Tarasov (Ed.)

HANDBOOK OF FRACTIONAL CALCULUS WITH APPLICATIONS

VOLUME 4: APPLICATIONS IN PHYSICS, PART A

Series edited by J. A. Tenreiro Machado

DE G

Vasily E. Tarasov (Ed.)

Handbook of Fractional Calculus with Applications

Handbook of Fractional Calculus with Applications

Edited by *J. A. Tenreiro Machado*

Volume 1: Theory
Anatoly Kochubei, Yuri Luchko (Eds.), 2019
ISBN 978-3-11-057081-6, e-ISBN (PDF) 978-3-11-057162-2,
e-ISBN (EPUB) 978-3-11-057063-2

Volume 2: Fractional Differential Equations
Anatoly Kochubei, Yuri Luchko (Eds.), 2019
ISBN 978-3-11-057082-3, e-ISBN (PDF) 978-3-11-057166-0,
e-ISBN (EPUB) 978-3-11-057105-9

Volume 3: Numerical Methods
George Em Karniadakis (Ed.), 2019
ISBN 978-3-11-057083-0, e-ISBN (PDF) 978-3-11-057168-4,
e-ISBN (EPUB) 978-3-11-057106-6

Volume 4: Applications in Physics, Part A
Vasily E. Tarasov (Ed.), 2019
ISBN 978-3-11-057088-5, e-ISBN (PDF) 978-3-11-057170-7,
e-ISBN (EPUB) 978-3-11-057100-4

Volume 6: Applications in Control
Ivo Petráš (Ed.), 2019
ISBN 978-3-11-057090-8, e-ISBN (PDF) 978-3-11-057174-5,
e-ISBN (EPUB) 978-3-11-057093-9

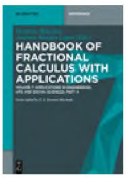

Volume 7: Applications in Engineering, Life and Social Sciences, Part A
Dumitru Băleanu, António Mendes Lopes (Eds.), 2019
ISBN 978-3-11-057091-5, e-ISBN (PDF) 978-3-11-057190-5,
e-ISBN (EPUB) 978-3-11-057096-0

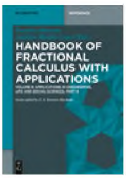

Volume 8: Applications in Engineering, Life and Social Sciences, Part B
Dumitru Băleanu, António Mendes Lopes (Eds.), 2019
ISBN 978-3-11-057092-2, e-ISBN (PDF) 978-3-11-057192-9,
e-ISBN (EPUB) 978-3-11-057107-3

Vasily E. Tarasov (Ed.)

Handbook of Fractional Calculus with Applications

Volume 5: Applications in Physics, Part B

Series edited by Jose Antonio Tenreiro Machado

DE GRUYTER

Editor
Prof. Dr. Vasily E. Tarasov
Lomonosov Moscow State University
Skobeltsyn Inst. of Nuclear Physics
Leninskie Gory
Moscow 119991
Russian Federation
tarasov@theory.sinp.msu.ru

Series Editor
Prof. Dr. Jose Antonio Tenreiro Machado
Department of Electrical Engineering
Instituto Superior de Engenharia do Porto
Instituto Politécnico do Porto
4200-072 Porto
Portugal
jtm@isep.ipp.pt

ISBN 978-3-11-057089-2
e-ISBN (PDF) 978-3-11-057172-1
e-ISBN (EPUB) 978-3-11-057099-1

Library of Congress Control Number: 2018967592

Bibliographic information published by the Deutsche Nationalbibliothek
The Deutsche Nationalbibliothek lists this publication in the Deutsche Nationalbibliografie; detailed bibliographic data are available on the Internet at http://dnb.dnb.de.

Cover image: djmilic / iStock / Getty Images Plus
Typesetting: VTeX UAB, Lithuania
Printing and binding: CPI books GmbH, Leck

www.degruyter.com

Preface

Fractional Calculus (FC) originated in 1695, nearly at the same time as conventional calculus. However, FC attracted a limited attention and remained a pure mathematical exercise in spite of the contributions of important mathematicians, physicists, and engineers. FC had a rapid development during the last few decades, both in mathematics and applied sciences, being nowadays recognized as an excellent tool for describing complex systems, phenomena involving long range memory effects and nonlocality. A huge number of research papers and books devoted to this subject have been published, and presently several specialized conferences and workshops are organized each year. The FC popularity in all fields of science is due to its successful application in mathematical models, namely in the form of FC operators and fractional integral and differential equations. Presently, we are witnessing considerable progress both on theoretical aspects and applications of FC in areas such as physics, engineering, biology, medicine, economy, or finance.

The popularity of FC has attracted many researchers from all over the world and there is a demand for works covering all areas of science in a systematic and rigorous form. In fact, the literature devoted to FC and its applications is huge, but readers are confronted with a high heterogeneity and, in some cases, with misleading and inaccurate information. The Handbook of Fractional Calculus with Applications (HFCA) intends to fill that gap and provides the readers with a solid and systematic treatment of the main aspects and applications of FC. Motivated by these ideas, the editors of the volumes involved a team of internationally recognized experts for a joint publishing project offering a survey of their own and other important results in their fields of research. As a result of these joint efforts, a modern encyclopedia of FC and its applications, reflecting present day scientific knowledge, is now available with the HFCA. This work is distributed by several distinct volumes, each one developed under the supervision of its editors.

The fourth and fifth volumes of HFCA are devoted to the application of fractional calculus (FC) and fractional differential equations in different areas of physics. These volumes describe the fundamental physical effects and, first of all, those that belong to fractional relaxation-oscillation or diffusion-wave phenomena. The FC allows describe spatial nonlocality and fading memory of power-law type, the openness of physical systems and dissipation, long-range interactions, and other physical phenomena. The most well-known physical phenomena and processes, which are described by fractional differential equations, include fractional viscoelasticity, spatial and frequency dispersion of power type, nonexponential relaxation, anomalous diffusion, and many others.

The fifth volume of HFCA focuses on the application of FC in various sections of electrodynamics, statistical physics and physical kinetics, quantum mechanics, and quantum field theory. In the 12 chapters, the most important models with nonlocality, memory of the power type, and openness and dissipation are described in such phenomena as the diffusion-wave, fractional and anomalous diffusion, advection-dispersion, nonexponential relaxation, the spatial and frequency dispersion of power-law type in electrodynamics and quantum mechanics, the openness of quantum systems and dissipation.

My special thanks go to the authors of individual chapters that are excellent surveys of selected classical and new results in several important fields of FC. The editors believe that the HFCA will represent a valuable and reliable reference work for all scholars and professionals willing to develop research in the challenging and timely scientific area.

Vasily E. Tarasov

Contents

J. A. Tenreiro Machado and António M. Lopes

Fractional electromagnetics

Abstract: This chapter addresses the application of fractional calculus (FC) in the area of electromagnetics, and studies four cases, namely the modeling of the electric potential generated by arbitrary charges, electric transmission lines, the skin effect in an electric conductor, and the behavior of a nonlinear electric inductor. The first generalizes the concept of integer to fractional electrostatic multipoles. The second interprets the telegraph equation in the light of FC. The third generalizes the skin effect to inductive effects of any fractional order. The fourth, focuses the modeling of inductors, including phenomena usually overlooked with classical approaches.

Keywords: Fractional calculus, electromagnetics, electric potential, transmission line, skin effect, electric inductor

PACS: 02.30.Jr, 02.60.Cb, 02.70.Bf

1 Introduction

Fractional calculus (FC) generalizes the concepts of classic differential calculus to noninteger orders [36]. During the last decades, FC was adopted for modeling natural and artificial signals and systems characterized by power-law behavior, long range memory effects, nonlocality, and fractal properties [49, 29]. In fact, FC opened new perspectives toward the generalization of classic laws and systems models [34, 41, 28, 7, 25, 6]. In the field of electromagnetics, the tools of FC were applied successfully to describe the behavior of electric machines, transformers, inductors, capacitors, and electronic devices [45, 8, 22, 38, 34, 47, 48].

This chapter addresses the application of FC for modeling several electromagnetic phenomena.

Having these ideas in mind, this chapter is organized as follows. Section 2 models the potential generated by electric charges. Section 3 studies the electric transmission lines. Section 4 addresses the skin effect (SE) in an electric conductor. Section 5 models a nonlinear electric inductor. Finally, Section 6 draws the main conclusions.

J. A. Tenreiro Machado, Institute of Engineering, Polytechnic of Porto, Dept. of Electrical Engineering, Rua Dr. António Bernardino de Almeida, 431, 4249-015 Porto, Portugal, e-mail: jtm@isep.ipp.pt
António M. Lopes, UISPA–LAETA/INEGI, Faculty of Engineering, University of Porto, Rua Dr. Roberto Frias, 4200-465 Porto, Portugal, e-mail: aml@fe.up.pt

2 Fractional order potential

Several well-known expressions for the electric potential are related through integer-order integrals and derivatives. Some researchers proposed their generalization based on the concept of fractional-order (FO) poles [23, 15, 42]. This section focuses on the analysis and synthesis of FO multipoles.

For homogeneous, linear, and isotropic media, the electric potential φ at a point P generated by different punctual charge configurations, namely a single charge, a dipole, and a quadrupole, is given by [3]:

$$\varphi = \frac{q}{4\pi\varepsilon_0}\frac{1}{r} + \varphi_0, \tag{1a}$$

$$\varphi = \frac{ql\cos\theta}{4\pi\varepsilon_0}\frac{1}{r^2} + \varphi_0, \quad r \gg l, \tag{1b}$$

$$\varphi = \frac{ql^2(3\cos^2\theta - 1)}{4\pi\varepsilon_0}\frac{1}{r^3} + \varphi_0, \quad r \gg l, \tag{1c}$$

where $\varphi_0 \in \mathbb{R}$ is a constant, ε_0 represents the permittivity, q is the electric charge, r and θ denote the radial distance and the corresponding angle with the axis, and l is the distance between the charges. Therefore, the relationship $\varphi \sim \{r^{-1}, r^{-2}, r^{-3}\}$ results.

For one long straight filament, two filaments with opposite charges and three filaments, carrying the charge λ per unit length, the potential is given by

$$\varphi = -\frac{\lambda}{2\pi\varepsilon_0}\ln r + \varphi_0, \tag{2a}$$

$$\varphi = \frac{\lambda l\cos\theta}{2\pi\varepsilon_0}\frac{1}{r} + \varphi_0, \quad r \gg l, \tag{2b}$$

$$\varphi = \frac{\lambda l^2(\cos^2\theta - 1)}{2\pi\varepsilon_0}\frac{1}{r^2} + \varphi_0, \quad r \gg l, \tag{2c}$$

and the relationship $\varphi \sim \{\ln r, r^{-1}, r^{-2}\}$ applies.

From (1)–(2), we conclude that the expressions for φ are related by integer-order derivatives and integrals.

A FO multipole produces at point P a fractional potential $\varphi \sim r^{\alpha}$, $\alpha \in \mathbb{R}$, meaning that the relationship between φ and r is not restricted to the integer-order integro-differential operator.

Let us consider the potential produced at a point $P = (x, y)$ by a straight filament with finite length l and charge q:

$$\varphi = \frac{1}{4\pi\varepsilon_0}\frac{q}{l}\ln\left[\frac{y + \frac{1}{2}l + \sqrt{x^2 + (y + \frac{1}{2}l)^2}}{y - \frac{1}{2}l + \sqrt{x^2 + (y - \frac{1}{2}l)^2}}\right] + \varphi_0. \tag{3}$$

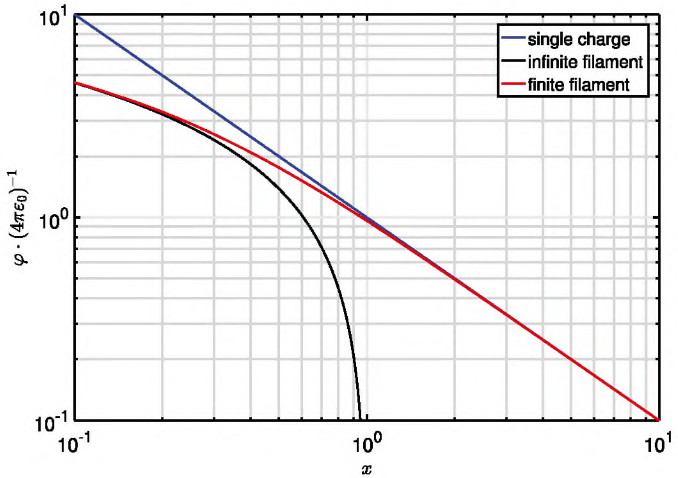

Figure 1: The potential φ of formula (3) versus x, for $y = 0$, and the two limits given by (1a) and (2a), for $q = 1$, $l = 1$, and $\varphi_0 = 0$.

For $y = 0$ and $x \to \infty$, the asymptotic expansion of the potential is $\varphi \to \frac{q}{4\pi\varepsilon_0}\frac{1}{x} + \varphi_0$, while for $y = 0$ and $x \to 0$ yields $\varphi \to \frac{1}{2\pi\varepsilon_0}\frac{q}{l}\ln(\frac{1}{x}) + \varphi_0$. These limits correspond to (1a) and (2a), that is, to the electric potentials produced by a single charge and by an infinite filament, respectively. Figure 1 depicts the potential (3) versus x and, for comparison, the two limits given by (1a) and (2a), for $q = 1$, $l = 1$ and $\varphi_0 = 0$.

We verify that expression (3) represents a potential changing smoothly between the two limit cases, leading to the conclusion that an intermediate FO relationship is possible, at least within a limited working range. Figure 2 shows the approximations $\varphi_A \approx 1.385x^{-0.532}$, within the interval $x \in [0.1, 0.3]$, and $\varphi_A \approx 1.031x^{-0.747}$, within $x \in [0.3, 0.8]$, for $y = 0$, $q = 1$, $l = 1$, and $\varphi_0 = 0$. We conclude that the standard integer-order potential relationships have a "global" nature, while FO potentials have a "local" nature, possible to capture only in a restricted interval of space.

In the follow-up, a numerical algorithm for generating a given FO potential is presented [38, 23].

The method fits the nth order approximation, $\varphi_A^n(x)$, based on single charges, to a reference model, $\varphi_R(x)$, while minimizing the optimization index, J [9]:

$$\varphi_A^n(x) = \sum_{i=1}^{n} \frac{1}{4\pi\varepsilon_0} \frac{q_i}{|x - x_i|}, \quad q_i, x_i \in \mathbb{R}, \tag{4}$$

$$\varphi_R(x) = mr^{\alpha}, \quad m, \alpha \in \mathbb{R}, \tag{5}$$

$$J = \frac{1}{K} \sum_{k=1}^{K} \frac{|\varphi_A^n(x_k) - \varphi_R(x_k)|}{|\varphi_A^n(x_k)| + |\varphi_R(x_k)|}, \quad x_k \in [x_a, x_b], \tag{6}$$

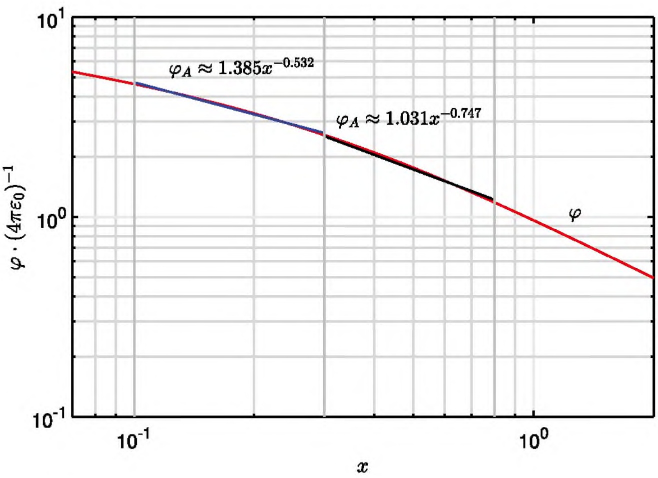

Figure 2: Approximations of the potential φ of formula (3), for $y = 0$, $q = 1$, $l = 1$, and $\varphi_0 = 0$, with $\varphi_A \approx 1.385x^{-0.532}$ and $\varphi_A \approx 1.031x^{-0.747}$, within the intervals $x \in [0.1, 0.3]$ and $x \in [0.3, 0.8]$, respectively.

where K represents the number of points in $x_k \in [x_a, x_b]$, q_i denotes electrical charges, x_i represents the ith charge position, m is a constant, and α is the FO. This means that the algorithm places n charges q_i, $i = 1, 2, \ldots, n$, at the positions x_i, so that $\varphi_A^n \approx mr^\alpha$, within the interval $x \in [x_a, x_b]$.

For example, Figure 3 shows the $n = 4$ charge approximations to the reference potentials of $\varphi_R = 1.5x^{-0.6}$ and $\varphi_R = 1.5x^{-1.3}$ for $K = 400$ points linearly spaced within the interval $x \in [1, 3]$. The charges and positions are $q_i = \{3.09 \times 10^{-5}, -6.59, 8.22, -0.99\}$ and $x_i = \{3.39, 0.21, 0.19, -1.79\}$, and $q_i = \{6.05, 0.01, 1.22, 0.94\}$ and $x_i = \{-23.75, 0.50, -1.95, -0.13\}$, respectively.

The results show a good fit between φ_A^n ($n = 4$) and φ_R. Nevertheless, for a given application, a superior precision may be required and, in that case, a larger number of charges must be used. Table 1 shows the values of J obtained for the n-charge approximations, $n = 1, \ldots, 10$, of $\varphi_R = 1.5x^{-1.6}$, $\varphi_R = 1.5x^{-1.4}$, $\varphi_R = 1.5x^{-0.6}$, and $\varphi_R = 1.5x^{-0.4}$, with $K = 400$ points linearly spaced within the interval $x \in [1, 3]$. Figure 4 depicts the $\{n, J\}$ locus. We verify that J diminishes as n increases, yielding a better approximation of φ_A^n to φ_R.

3 Fractional-order modeling of transmission lines

During the twentieth century, electric power transmission, telecommunications, and microwave engineering made popular the theory of transmission lines [10, 2]. In this section, the transmission lines are reviewed at light of FC [35].

Table 1: Values of J for the n-charge approximations, $n = 1, \ldots, 10$, of $\varphi_R = 1.5x^{-1.6}$, $\varphi_R = 1.5x^{-1.4}$, $\varphi_R = 1.5x^{-0.6}$, and $\varphi_R = 1.5x^{-0.4}$, within the interval $x \in [1, 3]$.

n	1	2	3	4	5	6	7	8	9	10
$\varphi_R = 1.5x^{-1.6}$										
J ($\times 10^{-7}$)	224934.4	500.5	343.7	297.1	272.9	268.5	234.7	127.0	83.9	54.3
$\varphi_R = 1.5x^{-1.4}$										
J ($\times 10^{-7}$)	127162.8	703.7	550.3	387.4	269.1	262.1	150.0	136.1	54.1	36.6
$\varphi_R = 1.5x^{-0.6}$										
J ($\times 10^{-7}$)	47473.3	225.4	21.5	5.8	4.5	3.7	2.1	1.2	1.1	0.6
$\varphi_R = 1.5x^{-0.4}$										
J ($\times 10^{-7}$)	46010.6	219.9	26.7	13.3	4.1	1.6	1.0	0.8	0.2	0.2

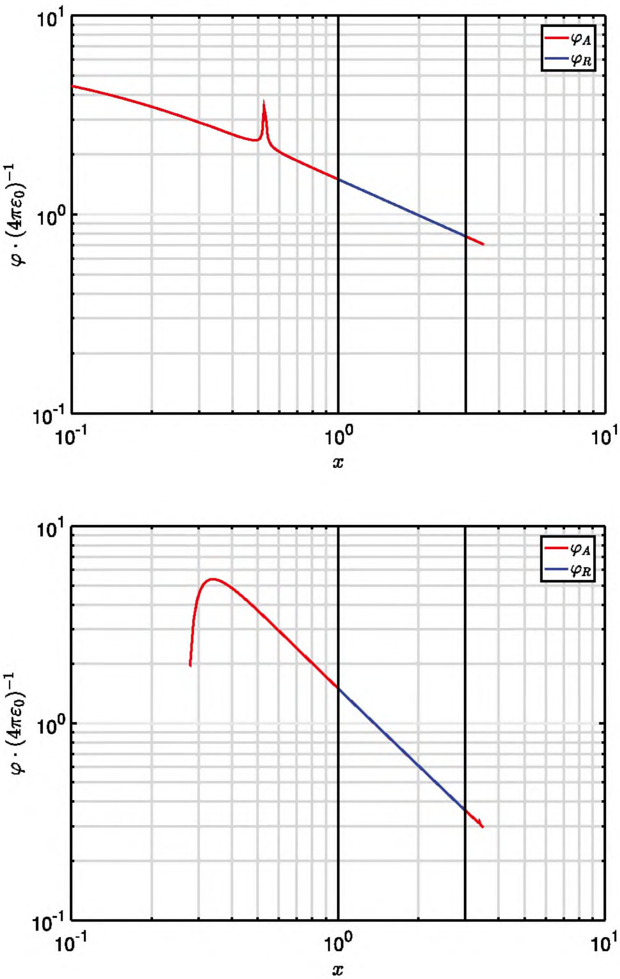

Figure 3: The $n = 4$ charge approximations of $\varphi_R = 1.5x^{-0.6}$ and $\varphi_R = 1.5x^{-1.3}$ for $K = 400$ points linearly spaced within the interval $x \in [1, 3]$.

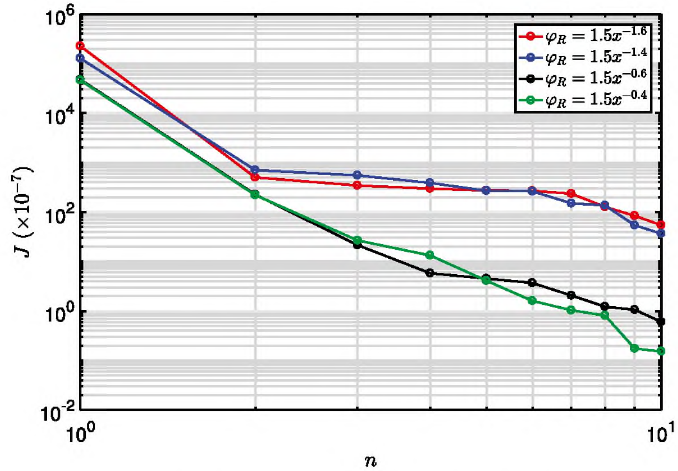

Figure 4: The relationship between J and n for $\varphi_R = 1.5x^{-1.6}$, $\varphi_R = 1.5x^{-1.4}$, $\varphi_R = 1.5x^{-0.6}$, and $\varphi_R = 1.5x^{-0.4}$, within the interval $x \in [1, 3]$.

The model of a uniform transmission line is derived by considering an infinitesimal length dx located at coordinate x. The model is also called telegrapher's equations and the values of the components are specified per unit length. Therefore, we have four parameters:

- distributed resistance R of the conductors, represented in series (with units Ohm per unit length).
- distributed self-inductance L, represented in series (expressed in Henry per unit length).
- distributed capacitance C between the two conductors, modeled by a shunt capacitor (in Farad per unit length).
- distributed conductance G of the dielectric material separating the two conductors, described by a shunt resistor (in Siemens per unit length).

The line segment has series resistance and inductance Rdx and Ldx, and shunt conductance and capacitance Gdx and Cdx, respectively (see the diagram of Figure 5, where t represents time, and v and i denote the electrical voltage and current).

The application of the Kirchoff's laws to the circuit leads to the set of partial differential equations:

$$\frac{\partial v(x,t)}{\partial x} = -L\frac{\partial i(x,t)}{\partial t} - Ri(x,t), \tag{7a}$$

$$\frac{\partial i(x,t)}{\partial x} = -C\frac{\partial v(x,t)}{\partial t} - Gv(x,t). \tag{7b}$$

Some additional calculations allow the elimination of one variable and to write the differential equation either with respect to v or to i, yielding

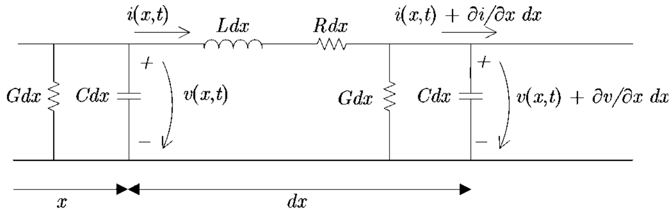

Figure 5: Electrical circuit of an infinitesimal portion of a uniform transmission line.

$$\frac{\partial^2 v(x,t)}{\partial x^2} = LC\frac{\partial^2 v(x,t)}{\partial t^2} + (LG + RC)\frac{\partial v(x,t)}{\partial t} + RGv(x,t), \tag{8}$$

or

$$\frac{\partial^2 i(x,t)}{\partial x^2} = LC\frac{\partial^2 i(x,t)}{\partial t^2} + (LG + RC)\frac{\partial i(x,t)}{\partial t} + RGi(x,t). \tag{9}$$

When $L = 0$ and $G = 0$, equations (8)–(9) reduce to the equivalent of the heat diffusion equation, where v and i are the analogs of the temperature and the heat flux, respectively.

To analyze the transmission line in the frequency domain, the Fourier transform operator $\mathcal{F}$ is applied to equation (7), yielding

$$\frac{dV(x,j\omega)}{dx} = -Z(j\omega)I(x,j\omega), \tag{10a}$$
$$\frac{dI(x,j\omega)}{dx} = -Y(j\omega)V(x,j\omega), \tag{10b}$$

where ω is the angular frequency, $j = \sqrt{-1}$, $I(x,j\omega) = \mathcal{F}\{i(x,t)\}$, $V(x,j\omega) = \mathcal{F}\{v(x,t)\}$, $Z(j\omega) = R + j\omega L$, and $Y(j\omega) = G + j\omega C$. In the same line of thought, equation (8) is transformed to

$$\frac{d^2 V(x,j\omega)}{dx^2} = -Z(j\omega)Y(j\omega)V(x,j\omega). \tag{11}$$

Equation (11) has solution in the frequency domain given by

$$V(x,j\omega) = A_1 e^{\gamma x} + A_2 e^{-\gamma x}, \tag{12a}$$
$$I(x,j\omega) = Z_c^{-1}(A_2 e^{-\gamma x} - A_1 e^{\gamma x}), \tag{12b}$$

where

$$Z_c(j\omega) = \sqrt{Z(j\omega)Y^{-1}(j\omega)} = \sqrt{(R + j\omega L)/(G + j\omega C)}, \tag{13}$$

is called characteristic impedance, and

$$\gamma(j\omega) = \sqrt{Z(j\omega)Y(j\omega)} = \alpha(\omega) + j\beta(\omega). \tag{14}$$

These expressions have two terms corresponding to waves traveling in opposite directions: the term proportional to $e^{-\gamma x}$ is due to the signal applied at the line input, while the term $e^{\gamma x}$ represents the reflected wave.

For a transmission line of length l, it is usual to adopt for variable the distance up to the end given by

$$x' = l - x. \tag{15}$$

If V_2 and I_2 represent the voltage and current at the end of the transmission line, then the Fourier transforms of equation (7) at coordinate x' are given by

$$V(x, j\omega) = V_2 \cosh(\gamma x') + I_2 Z_c \sinh(\gamma x'), \tag{16a}$$

$$I(x, j\omega) = V_2 Z_c^{-1} \sinh(\gamma x') + I_2 \cosh(\gamma x'). \tag{16b}$$

For a loading impedance $Z_2(j\omega)$, it results in $V_2(j\omega) = Z_2(j\omega) I_2(j\omega)$ and the input impedance $Z_i(j\omega)$ of the transmission line is given by

$$Z_i(x, j\omega) = [Z_2 \cosh(\gamma x') + Z_c \sinh(\gamma x')] \cdot [Z_2 Z_c^{-1} \sinh(\gamma x') + \cosh(\gamma x')]^{-1}. \tag{17}$$

Typically, at the end of the line three cases are considered: namely, short circuit, open circuit, and adapted line. These conditions simplify equation (17), yielding

$$\text{short circuit:} \quad V_2 = 0, Z_2(j\omega) = 0 \Rightarrow Z_i(j\omega) = Z_c(j\omega) \tanh(\gamma l), \tag{18a}$$

$$\text{open circuit:} \quad I_2 = 0, Z_2(j\omega) = \infty \Rightarrow Z_i(j\omega) = Z_c(j\omega) \coth(\gamma l), \tag{18b}$$

$$\text{adapted line:} \quad Z_2(j\omega) = Z_c(j\omega) \Rightarrow Z_i(j\omega) = Z_c(j\omega). \tag{18c}$$

The classic perspective is to study lossless lines (i. e., $R = 0$ and $G = 0$). This approach is reasonable in real-world power systems, and models in the frequency domain lead to two-port networks usually analyzed under the light of integer order elements. Nevertheless, the transcendental equations (17) and (18) yield both to integer and FO expressions. For example, in the case of an adapted line (with $R, C, L, G \in \mathbb{R}^+$), we can have half-order FO capacitances and half-order FO inductances, accordingly with the expressions:

$$L = 0, G = 0 \Rightarrow Z_c(j\omega) = \sqrt{(j\omega)^{-1} R C^{-1}}, \tag{19a}$$

$$R = kL, G = kC \Rightarrow Z_c(j\omega) = \sqrt{R L^{-1}}, \tag{19b}$$

$$R = 0, C = 0 \Rightarrow Z_c(j\omega) = \sqrt{j\omega L G^{-1}}, \tag{19c}$$

where $k \in \mathbb{R}^+$.

Since conditions (18a) and (18b) are easier to implement in practice than (18c), we follow the asymptotic expansions of $\tanh(\gamma l)$ and $\coth(\gamma l)$. Knowing that for low frequencies we have $\omega \to 0$, $\tanh(\gamma l) \to \gamma l$, $\coth(\gamma l) \to (\gamma l)^{-1}$, and that for high frequencies $\omega \to \infty$, $\tanh(\gamma l) \to 1$, $\coth(\gamma l) \to 1$, we obtain approximations for the short and open circuit cases, given by

$$Z_i(j\omega) = \begin{cases} Z(j\omega)l, & \omega \to 0, \\ Z_c(j\omega), & \omega \to \infty, \end{cases} \tag{20a}$$

$$Z_i(j\omega) = \begin{cases} [Y(j\omega)l]^{-1}, & \omega \to 0, \\ Z_c(j\omega), & \omega \to \infty. \end{cases} \tag{20b}$$

We conclude that both cases approximate the condition (18c) when $\omega \to \infty$.

These results are overlooked in the textbooks and suggest possible strategies for implementing FO impedances. Hardware strategies for implementing FO derivatives have been pointed out in order to avoid computational approximation schemes [51]. Therefore, it is relevant to explore fractal geometries and dielectric properties [46, 5] to achieve FO capacitors and inductors.

4 Fractional-order skin effect

The effect of a high-frequency electric current to distribute itself in a conductor so that the current density near the surface is higher than that at its core is called SE. This phenomenon reveals characteristics well modeled by the FC tools, exhibiting a dynamics of half-order. Moreover, the model development based on the Maxwell's equations suggests the implementation of inductive devices of FO [39, 4, 8, 44, 37].

Let us denote by ∇ the nabla operator. In the differential form, the Maxwell equations are given by [27]:

$$\nabla \times \mathbf{E} = -\frac{\partial \mathbf{B}}{\partial t}, \tag{21}$$

$$\nabla \times \mathbf{H} = \mathbf{J} + \frac{\partial \mathbf{D}}{\partial t}, \tag{22}$$

$$\nabla \cdot \mathbf{D} = \rho, \tag{23}$$

$$\nabla \cdot \mathbf{B} = 0, \tag{24}$$

where **E**, **D**, **H**, **B**, **J** represent the vectors of electric field intensity, electric flux density (or electric displacement), magnetic field intensity, magnetic flux density and the current density, respectively, and ρ is the charge density.

For homogeneous, linear, and isotropic media, we write

$$\mathbf{D} = \varepsilon \mathbf{E}, \tag{25}$$

$$\mathbf{B} = \mu \mathbf{H}, \tag{26}$$

$$\mathbf{J} = \gamma \mathbf{E}, \tag{27}$$

where ε, μ, and γ are the electrical permittivity, the magnetic permeability, and the conductivity, respectively.

We consider a cylindrical conductor with radius r_0 conducting a current I along its longitudinal axis. In a conductor, even for high frequencies, the term $\frac{\partial \mathbf{D}}{\partial t}$ is negligible in comparison with the conduction term $\mathbf{J}$, that is, the displacement current is much lower than the conduction current, and equation (22) simplifies to $\nabla \times \mathbf{H} = \mathbf{J}$. Therefore, for a radial distance $r < r_0$ the application of the Maxwell's equations with the simplification of (22) leads to the expression [26, 3]:

$$\nabla \times (\nabla \times \mathbf{J}) = -\gamma\mu \frac{\partial \mathbf{J}}{\partial t}. \tag{28}$$

Knowing that $\nabla\times(\nabla\times\mathbf{J}) = \nabla(\nabla\cdot\mathbf{J}) - \nabla^2\mathbf{J}$, where ∇^2 is the Laplacian, and that $\nabla\cdot\mathbf{J} = 0$, it results in

$$\nabla^2 \mathbf{J} = \gamma\mu \frac{\partial \mathbf{J}}{\partial t}. \tag{29}$$

For cylindrical coordinates and for $\mathbf{J}$ pointing in the direction of the z axis, the Laplacian can be expressed as $\nabla^2\mathbf{J} = \frac{1}{r}\frac{\partial}{\partial r}(r\frac{\partial \mathbf{J}}{\partial t})$. Therefore, rewriting (29) in terms of the electric field intensity E, it comes as

$$\frac{\partial^2 E}{\partial r^2} + \frac{1}{r}\frac{\partial E}{\partial r} = \gamma\mu \frac{\partial E}{\partial t}. \tag{30}$$

For a sinusoidal field $E \sin(\omega t)$, we adopt the complex notation $Ee^{j\omega t}$, yielding

$$\frac{d^2 E}{dr^2} + \frac{1}{r}\frac{dE}{dr} + q^2 E = 0, \tag{31}$$

with $v^2 = -j\omega\gamma\mu$.

Equation (31) is a particular case of the Bessel equation that has a solution:

$$E(r) = \frac{v}{2\pi r_0 \gamma} \frac{J_0(vr)}{J_1(vr_0)} I, \quad 0 \le r \le r_0, \tag{32}$$

where $J_0(\cdot)$ and $J_1(\cdot)$ are complex valued Bessel functions of the first kind of orders 0 and 1, respectively.

Equation (32) characterizes the SE phenomenon consisting of a nonuniform current density, namely a low density near the conductor axis and a high density on surface, the higher the frequency ω. Therefore, for a conductor of length l_0 the total voltage drop is $ZI = E(r = r_0)l_0$ and the equivalent electrical complex impedance Z is given by

$$Z = \frac{ql_0}{2\pi r_0 \gamma} \frac{J_0(vr)}{J_1(vr_0)}. \tag{33}$$

For small values of x, the Taylor series [43] leads to

$$J_0(x) = 1 - \frac{x^2}{2^2} + \cdots, \tag{34}$$

$$J_1(x) = \frac{x}{2} - \frac{x^3}{2^2 4} + \cdots, \tag{35}$$

while for large values of x the asymptotic expansion yields

$$J_n(x) = \sqrt{\frac{2}{\pi x}} \cos\left(x - n\frac{\pi}{2} - \frac{\pi}{4}\right), \quad n = 0, 1, \ldots. \tag{36}$$

Knowing the expansions (34), (35), and (36), the low and high frequency approximations of Z can be written as

$$\omega \to 0 \Rightarrow Z \to \frac{l_0}{\pi r_0^2 \gamma}, \tag{37}$$

$$\omega \to \infty \Rightarrow Z \to \frac{l_0}{2\pi r_0}\sqrt{\frac{\omega\mu}{2\gamma}}(1 + j). \tag{38}$$

The standard approach to avoid handling the transcendental equation (33) is to approximate Z by means of a resistance R_a and an inductance L_a given by $Z = R_a + j\omega L_a$. Nevertheless, this method is inadequate because the model parameters $\{R_a, L_a\}$ must vary with the frequency (see Figure 6).

Expression (38) reveals the half-order nature of the dynamic phenomenon, at high frequencies (i. e., $Z \sim \omega^{\frac{1}{2}}$) which is not captured by the classic integer-order modeling.

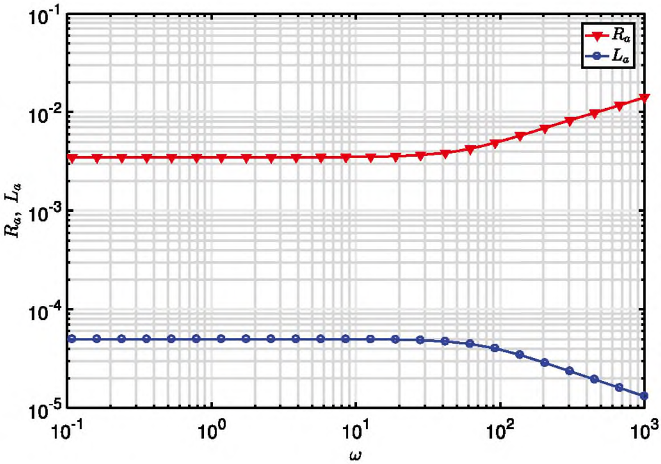

Figure 6: Variation of R_a and L_a for the integer order model $Z = R_a + j\omega L_a$ with $\gamma = 10^7\ \Omega^{-1}$m, $l_0 = 1$ m, $r_0 = 3.02 \cdot 10^{-3}$ m, $\mu_0 = 1.257 \cdot 10^{-6}$ Hm^{-1}, and $\mu_r = 10^3$.

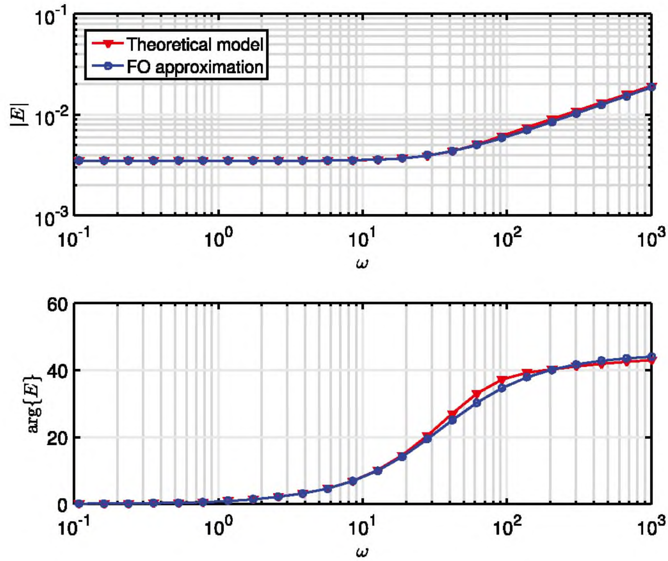

Figure 7: Amplitude and phase Bode diagrams of the electrical field at $r = r_0$, $E(r_0)$, for the theoretical and the approximate expression (39) with $\gamma = 10^7\ \Omega^{-1}\text{m}$, $l_0 = 1\,\text{m}$, $r_0 = 3.02 \cdot 10^{-3}\ \text{m}$, $\mu_0 = 1.257 \cdot 10^{-6}\ \text{Hm}^{-1}$, and $\mu_r = 10^3$.

The FC eliminates that limitation [35, 39]. A simple method is to join the two asymptotic expressions (37)–(38) by means of the FO reference (approximation) model:

$$Z_R = Z_0\left(1 + \frac{j\omega}{z}\right)^{\alpha}, \tag{39}$$

where $Z_0 = \frac{l_0}{\pi r_0^2 \gamma}$, $z = \frac{4}{r_0^2 \gamma \mu}$, and $\alpha = \frac{1}{2}$.

Figure 7 compares the Bode diagrams of amplitude and phase of $E(r_0)$ based on expressions (33) and (39) in the case of a conductor with $\gamma = 10^7\ \Omega^{-1}\text{m}$, $l_0 = 1\,\text{m}$, $r_0 = 3.02 \cdot 10^{-3}\ \text{m}$, $\mu_0 = 1.257 \cdot 10^{-6}\ \text{Hm}^{-1}$, and $\mu_r = 10^3$. We verify that (39) leads to a very good curve fitting.

Other values of α can be designed, either by varying the geometry of the conductor, or by modifying its electromagnetic properties.

Equation (31) is now integrated numerically adopting the Euler forward approximation for the first- and second-order derivatives of the sinusoidal electric field, E. We get the approximate

$$E(k+2) + \left(-2 + \frac{\Delta r}{r}\right)E(k+1) + \left(1 - \frac{\Delta r}{r}\right)E(k) - j\omega\mu\Delta r^2\gamma(r)E(k) = 0, \tag{40}$$

where k and $k+1$ represent two consecutive sampling points in space and Δr is the integration step along the conductor radius.

The numerical initialization must be obtained from the boundary conditions:

$$H = \frac{1}{j\omega\mu}\frac{dE}{dr}, \tag{41}$$

$$H_0 = H(r = r_0) = \frac{I}{2\pi r_0}. \tag{42}$$

The calculation of (40) requires initial conditions compatible with (41)–(42). The initial conditions are estimated by means of a Genetic Algorithm (GA) [40], with population $\{\mathbb{R}\{E(1)\}, \mathbb{R}\{E(0)\}, \mathbb{J}\{E(1)\}, \mathbb{J}\{E(0)\}\}$, and fitness function

$$J_{\text{init}} = \left[\frac{1}{\omega\mu}\frac{\mathbb{J}\{E(k+1)\} - \mathbb{J}\{E(k)\}}{\Delta r}\right]^2 + \left[\mathbb{R}\{E(k+1)\} - \mathbb{R}\{E(k)\}\right]^2, \tag{43}$$

$$H_0 = \frac{1}{\omega\mu}\frac{\mathbb{J}\{E(k_0)\} - \mathbb{J}\{E(k_0 - 1)\}}{\Delta r}, \tag{44}$$

where $k_0\Delta r = r_0$. It adopted a GA population of 2000 elements, crossover and mutation probabilities of $p_c = 0.5$ and $p_m = 0.1$, respectively, and elitism. Furthermore, the GA was executed during $n_{\text{GA}} = 2000$ iterations for a total of K testing frequencies, logarithmically spaced in the interval $\omega_{\min} < \omega < \omega_{\max}$, of the sinusoidal electric field E. In the numerical experiments a set of frequencies Ω was considered such that $\omega_{\min} = 10^{-2}$, $\omega_{\max} = 10^3$ and $K = 30$.

Expressions (43)–(44) pose a considerable computational load, for the initialization GA. In order to reduce the burden the integration step Δr was adjusted, from gross to fine, during three phases in the GA evolution, namely

$$\Delta r(n) = \begin{cases} \frac{r_0}{66} & n \le \frac{1}{3}n_{\text{GA}}, \\ \frac{r_0}{133} & \frac{1}{3}n_{\text{GA}} < n \le \frac{2}{3}n_{\text{GA}}, \\ \frac{r_0}{200} & \frac{2}{3}n_{\text{GA}} < n \le n_{\text{GA}}, \end{cases} \tag{45}$$

where the index n represents the GA iterations.

This algorithm guarantees the convergence of the numerical integration of (40) and leads to a reduction of 50 % in the computational burden of the fitness evaluation. In fact, several experiments, comparing the results of the variable and the fixed step sizes, demonstrated the feasibility of the proposed scheme.

The first approach for modifying the properties of the SE consists of adopting a conductor with a different geometry. One simple possibility is, for example, to have a annular conductor with inner and outer radius r_1 and r_0, respectively. Figure 8 shows the amplitude and phase Bode diagrams of the electrical field at $r = r_0$, $E(k_0)$, for $r_1 = \{0, 0.3, 0.5, 0.7\} \cdot r_0$. We verify that by eliminating the flow of current in the inner part of the conductor we can shift the frequency response.

The second approach for a different SE consists of varying the electrical conductivity with the conductor radial distance, that is, to have $\gamma = \gamma(r)$, $r_1 \le r \le r_0$. For the

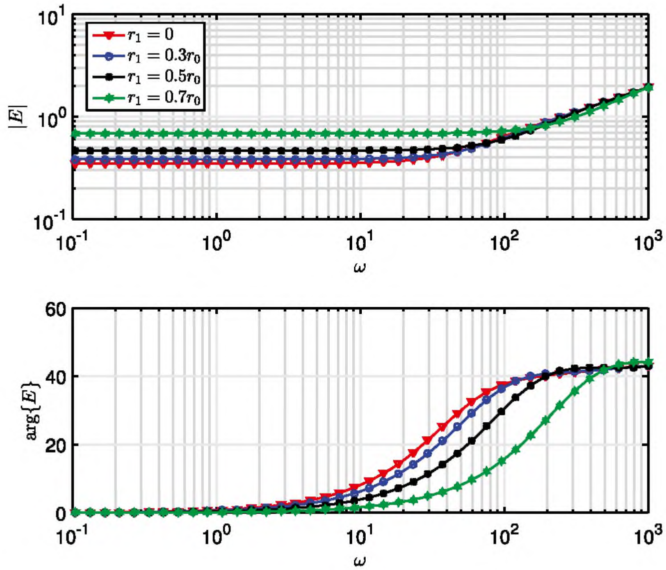

Figure 8: Amplitude and phase Bode diagrams of the electrical field at $r = r_0$, $E(r_0)$, for a annular conductor with inner and outer radius r_1 and r_0, such that $r_1 = \{0, 0.3, 0.5, 0.7\} \cdot r_0$, with $\gamma = 10^7\,\Omega^{-1}$m, $l_0 = 1$ m, $r_0 = 3.02 \cdot 10^{-3}$ m, $\mu_0 = 1.257 \cdot 10^{-6}$ Hm^{-1}, and $\mu_r = 10^3$.

electrical conductivity, the following expression was considered:

$$\gamma(r) = \gamma_0\left(1 - \frac{r - r_1}{r_0}\right)^{\beta}, \quad -\infty < \beta < +\infty, \tag{46}$$

Obviously, $\beta = 0$ yields the case of constant electrical conductivity that was analyzed above.

During the experiments the numerical values $\gamma = 10^7\,\Omega^{-1}$m, $r_0 = 3.02 \cdot 10^{-3}$ m, $\mu_0 = 1.257 \cdot 10^{-6}$ Hm^{-1}, $\mu_r = 10^3$, $\omega_{\text{min}} = 10^{-2}$ s^{-1}, and $\omega_{\text{max}} = 10^3$ s^{-1} were adopted.

Figure 9 depicts the Bode diagrams of amplitude and phase of $E(k_0)$ for $\beta = \{-1, -\frac{1}{2}, 0, \frac{1}{2}, 1\}$.

It was observed that when moving far away from the central case of $\beta = 0$ the results became more and more "unstable," that is, with considerable variations in the plots. Therefore, in the study were considered only those cases that depicted a sound numerical response.

The Bode plots reveal that at low frequencies we get the usual resistive behavior, but at high frequencies we have inductive effects of different FO. Therefore, it was decided to approximate the numerical results by a reference expression:

$$E_R = E_0\left(1 + \frac{j\omega}{z}\right)^{\alpha}, \quad E_0 > 0,\ z > 0,\ \alpha > 0, \tag{47}$$

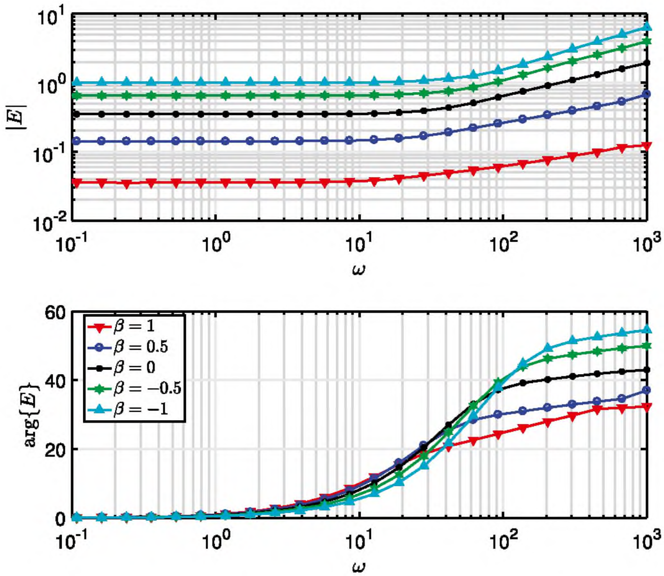

Figure 9: Amplitude and phase Bode diagrams of the electrical field at $r = r_0$, $E(r_0)$, for $\gamma = 10^7\ \Omega^{-1}\text{m}$, $r_0 = 3.02 \cdot 10^{-3}$ m, $\mu_0 = 1.257 \cdot 10^{-6}\ \text{Hm}^{-1}$, $\mu_r = 10^3$, and $\beta = \{-1, -\frac{1}{2}, 0, \frac{1}{2}, 1\}$.

For the estimation of the three parameters $\{E_0, z, \alpha\}$, an identification GA with fitness function:

$$J_{\text{ident}} = \sum \left[\Re(E_R) - \Re\{E(k_0)\}\right]^2 + \left[\Im(E_R) - \Im\{E(k_0)\}\right]^2, \tag{48}$$

was implemented, where Ω represents the set of K sampling frequencies such that $\omega_{\min} < \omega < \omega_{\max}$. The parameters of the identification GA are: population of $n_{\text{GA}} = 5000$ elements, crossover and mutation probabilities of $p_c = 0.5$ and $p_m = 0.1$, respectively, and elitism. The GA was executed during 1000 iterations, for $\omega_{\min} = 10^{-2}$, $\omega_{\max} = 10^3$ and $K = 30$.

Figure 10 depicts the parameters $\{E_0, z, \alpha\}$ of expression (47) versus β. We verify clearly that by varying the electrical conductivity in (46) we can design different values of α.

5 Fractional-model of an inductor

An ideal inductor is characterized by the impedance $Z(j\omega) = j\omega L$, where the parameter L denotes the inductance. However, such device has no physical correspondence, since the model ignores the ohmic resistance of the winding, the parasitic capacitance between neighbor turns, the hysteresis and eddy-current losses in the magnetic core,

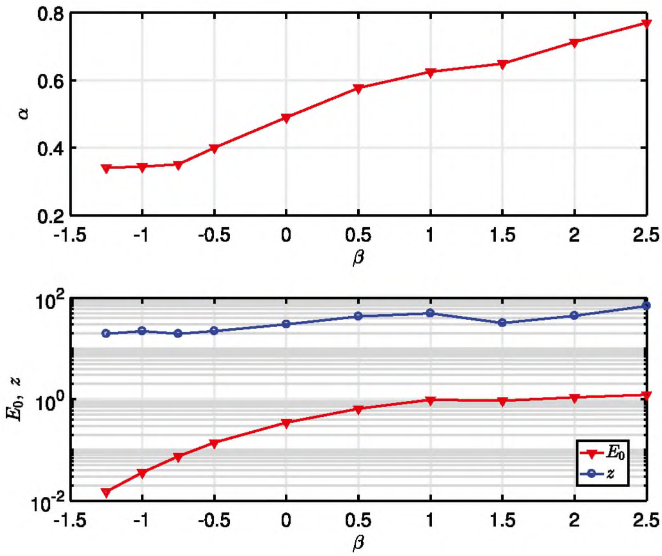

Figure 10: Variation of the parameters $\{E_0, z, \alpha\}$ versus β.

and the SE in the wire. Additionally, the nonlinearities are dependent on the amplitude and frequency, ω, being more critical when ω is high [47].

Classic models represent a real inductor by means of equivalent electric circuits, where the inductor is associated in series/parallel with resistances and capacitors. Nevertheless, these models reveal difficulties in describing the nonlinear and the SE that characterize many inductors, and their accurate modeling is a challenging exercise [48]. In this section, the FC perspective is adopted for describing an inductor [31]. The electrical impedance spectroscopy (EIS) technique is used for measuring the equivalent impedance of the device, and the experimental data is approximated by means of FO empirical transfer functions [11, 12, 20, 21].

The EIS technique measures the electrical impedance of a specimen object [29, 30]. The EIS is straightforward to implement, avoiding complicated procedures and time consuming measurements. The EIS has been used in the description of vegetable [14, 24] and animal [18] tissues, food liquids [32, 33], materials [50, 16], and electrical devices [17, 1].

The EIS starts by applying to the sample electric sinusoidal input signals, and registering the amplitude and phase shift of the output steady-state sinusoidal voltage, $v(t)$, and current, $i(t)$:

$$v(t) = V\cos(\omega t + \theta_V), \tag{49a}$$

$$i(t) = I\cos(\omega t + \theta_I), \tag{49b}$$

where $\{V, I\}$ and $\{\theta_V, \theta_I\}$ are the amplitudes and phase shifts of the voltage and current, respectively.

The signals $v(t)$ and $i(t)$ can be represented in the Fourier domain:

$$V(j\omega) = V \cdot e^{j\theta_V}, \tag{50a}$$

$$I(j\omega) = I \cdot e^{j\theta_I}, \tag{50b}$$

where the impedance $Z(j\omega)$ is given by

$$Z(j\omega) = \frac{V(j\omega)}{I(j\omega)} = \frac{V}{I} \cdot e^{j(\theta_V - \theta_I)} = |Z(j\omega)| \cdot e^{j \arg [Z(j\omega)]}. \tag{51}$$

The diagram of Figure 11 shows the experimental set-up [29, 30] using general purpose equipment. The inductor is connected in series with an adaptation metal film resistance, $R_s = 27\,\Omega$, for achieving good signal/noise ratio, while avoiding interference at high frequencies [19]. A Hewlett Packard/Agilent 33220A function generator applies a sinusoidal AC voltage with amplitude V_{ab} to the circuit (i. e., the voltage divider) and a Tektronix TDS 2002C two channel oscilloscope measures the voltages V_{ab} and V_{cb}. The oscilloscope bandwidth is 70 MHz, with DC vertical accuracy of $\pm(3\,\% \times \text{reading} + 0.1\,\text{div} + 1\,\text{mV})$, and delta time accuracy equal to $\pm(1\,\text{sample interval} + 100\,\text{ppm} \times \text{reading} + 0.6\,\text{ns})$.

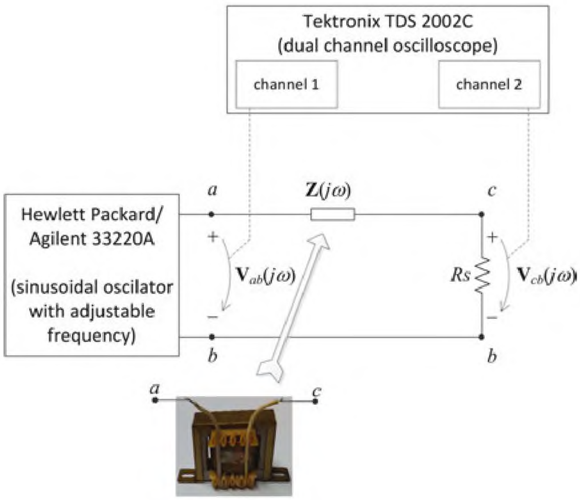

Figure 11: Experimental set-up EIS for measuring $Z(j\omega)$.

The tested inductor has a closed iron core, a resistance $R = 0.6\,\Omega$, measured by a Keithley 2000 digital multimeter by means of the 4-wire method, and an inductance $L = 11.5\,\text{mH}$, measured with a Escort ELC-131D LCR bridge at the frequency of 120 Hz. The experiments consist of measurements with linearly spaced exciting voltages $V_{ab} = \{1, \ldots, 10\}$ V. For each fixed-amplitude V_{ab}, the impedance $Z(j\omega)$ is obtained for the frequency range $2\pi \cdot 10 \leq \omega \leq 2\pi \cdot 10^4$ rad/s, at $K = 27$ logarithmically spaced points using the expression:

$$Z(j\omega) = R_s \cdot \left(\frac{V_{ab}(j\omega)}{V_{cb}(j\omega)} - 1 \right), \tag{52}$$

where the signals $v_{ab}(t) = V_{ab}\cos(\omega t)$ and $v_{cb}(t) = V_{cb}\cos(\omega t + \theta)$ are measured directly by the oscilloscope, and θ denotes the phase shift between $v_{cb}(t)$ and $v_{ab}(t)$.

In the follow-up we shall denote by Z_A and Z_R the impedances corresponding to the measured values and the reference (approximation) model, respectively.

The FO description is fitted into the data by minimizing the Canberra distance, J, between Z_A and Z_R, according with the expression:

$$J = \frac{1}{K} \sum_{k=1}^{K} \left(\frac{|\Re[Z_A(j\omega_k)] - \Re[Z_R(j\omega_k)]|}{|\Re[Z_A(j\omega_k)]| + |\Re[Z_R(j\omega_k)]|} + \frac{|\Im[Z_A(j\omega_k)] - \Im[Z_R(j\omega_k)]|}{|\Im[Z_A(j\omega_k)]| + |\Im[Z_R(j\omega_k)]|} \right), \tag{53}$$

where K is the total number of measuring points, as defined previously.

Expression (53) captures the relative error of the curve fitting. This avoids saturation effects that occur when using the standard Euclidean norm due to the simultaneous presence of large and small values.

A good fit occurs for the 5-parameter reference model:

$$Z_R(j\omega) = Z_0 \cdot \frac{(1 + \frac{j\omega}{z})^{\beta}}{(1 + \frac{j\omega}{p})^{\alpha}}, \tag{54}$$

where $Z_0 = 0.6$ is the inductor resistance measured in DC. Expression (54) represents a compromise between model complexity and quality of fitting between experimental and analytical results.

The polar, Nichols and Bode diagrams of $Z_A(j\omega)$ and $Z_R(j\omega)$ are depicted in Figure 12 for the excitation voltage $V_{ab} = 5$ V. The charts reveal the adequacy of expression (54) when modeling the inductor. For the other values of V_{ab}, the results are identical.

Table 2 summarizes the values of the parameters and the fitness function obtained for the 10 excitation voltages $V_{ab} = \{1, \ldots, 10\}$ V. We observe that the parameters z and p diminish for increasing values of the excitation voltage. On the other hand, α and β have a very small variation, revealing average and standard deviation values of $\{\mu_\alpha, \sigma_\alpha\} = \{0.536, 0.028\}$ and $\{\mu_\beta, \sigma_\beta\} = \{0.905, 0.025\}$, respectively. The fitness function, J, is minimal for intermediate values of V_{ab}, corresponding to a closer fit between $Z_A(j\omega)$ and $Z_R(j\omega)$.

Figure 13 depicts the Nichols diagrams of the inductor obtained with the experimental impedances, for $V_{ab} = \{1, \ldots, 10\}$ V. The points corresponding to the same frequency are also connected [13], so that we have the locus of constant frequency/amplitude versus variable amplitude/frequency. We observe that the impedance Z_A depends on V_{ab}, reflecting the nonlinear nature of the device. At low frequencies, Z_A is more

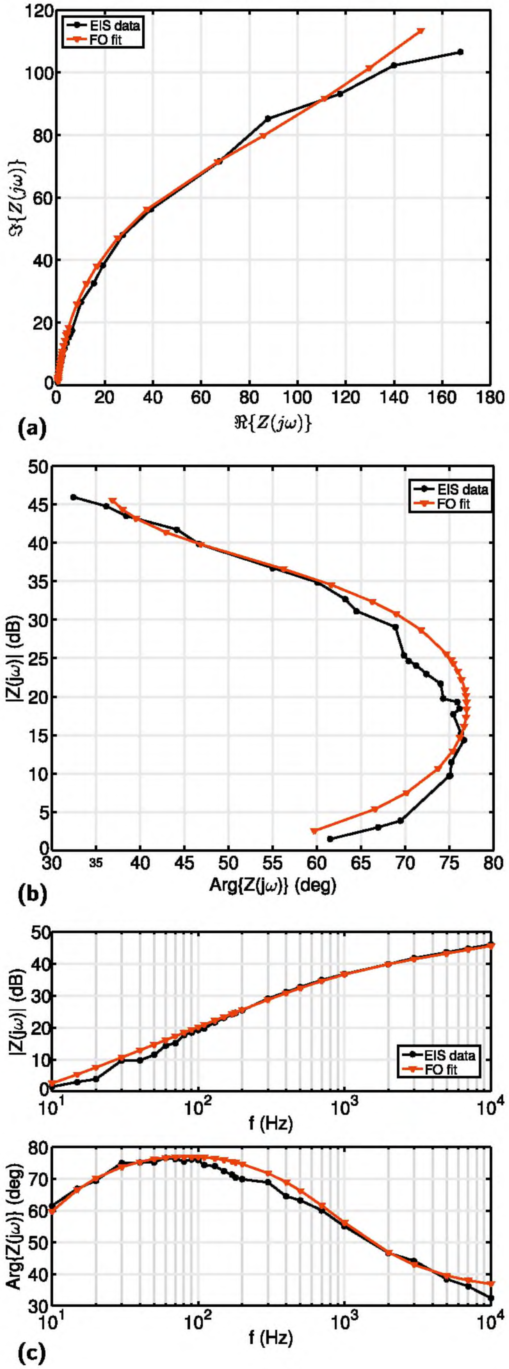

Figure 12: Diagrams of the experimental and model impedances, $Z_A(j\omega)$ and $Z_R(j\omega)$, of the inductor for $V_{ab} = 5$ V: (a) Polar; (b) Nichols; (c) Bode.

Table 2: Values of the parameters of the model and the fitness function for $V_{ab} = \{1, \dots, 10\}$ V.

V_{ab}	z	β	p	α	J
1	38.96	0.92	8400	0.60	0.22
2	33.93	0.93	6200	0.55	0.16
3	32.67	0.92	6600	0.54	0.13
4	28.90	0.92	5100	0.54	0.11
5	28.90	0.92	5500	0.54	0.13
6	26.39	0.92	4800	0.54	0.10
7	22.62	0.90	4000	0.52	0.10
8	21.36	0.90	4000	0.52	0.14
9	16.34	0.86	4200	0.51	0.15
10	15.71	0.86	3900	0.50	0.20

sensitive to the excitation voltage, meaning that the nonlinear component represents a larger part of the total value.

The results demonstrate that model (54) yields a quantitative description and reliable characterization of the inductor. Nevertheless, the number of model parameters necessary is high and the adherence between the heuristic model and the experimental data in Figure 12 is limited.

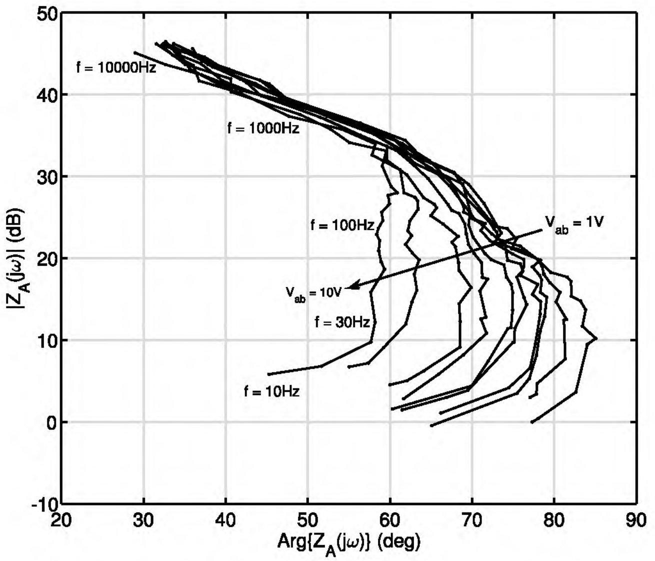

Figure 13: The Nichols diagrams of the inductor obtained with the experimental impedances, for $V_{ab} = \{1, \dots, 10\}$ V.

6 Conclusion

This chapter presented four applications of FC in the area of electromagnetics, namely for modeling the electric potential generated by arbitrary charges, the electric transmission lines, the SE in an electric conductor, and the behavior of a nonlinear electric inductor. The phenomena and devices are well known and described by classic models. However, a closer look reveals that the FC formalism leads to a news perspective for evaluating more deeply all details. It was verified that the FO models characterize more accurately effects overlooked by standard approaches.

Bibliography

[1] M. Adachi, M. Sakamoto, J. Jiu, Y. Ogata, and S. Isoda, Determination of parameters of electron transport in dye-sensitized solar cells using electrochemical impedance spectroscopy, *J. Phys. Chem. B*, **110**(28) (2006), 13872–13880.

[2] R. B. Adler, L. J. Chu, and R. M. Fano, *Electromagnetic energy transmission and radiation*, Wiley, 1960.

[3] L. Bessonov, *Applied Electricity for Engineers*, MIR Publishers, Moscow, 1968.

[4] P. Bidan, Commande diffusive d'une machine electrique: une introduction, in *ESAIM Proceedings, France*, vol. 5, 1998.

[5] K. Biswas, G. Bohannan, R. Caponetto, A. Lopes, and J. A. T. Machado, *Fractional Order Devices*, Springer, 2017.

[6] A. Buscarino, R. Caponetto, G. Di Pasquale, L. Fortuna, S. Graziani, and A. Pollicino, Carbon black based capacitive fractional order element towards a new electronic device, *AEÜ, Int. J. Electron. Commun.*, **84** (2018), 307–312.

[7] M. Busłowicz, Stability analysis of continuous-time linear systems consisting of *n* subsystems with different fractional orders, *Bull. Pol. Acad. Sci., Tech. Sci.*, **60**(2) (2012), 279–284.

[8] S. Canat and J. Faucher, Fractional order: frequential parametric identification of the skin effect in the rotor bar of squirrel cage induction machine, in *ASME Design Engineering Technical Conferences 2003VIB-48393*, vol. 48393, 2003.

[9] S. H. Cha, Comprehensive survey on distance/similarity measures between probability density functions, *Int. J. Math. Models Methods Appl. Sci.*, **4** (2007), 300–307.

[10] R. A. Chipman, *Transmission Lines*, McGraw-Hill, 1968.

[11] K. S. Cole and R. H. Cole, Dispersion and absorption in dielectrics I. Alternating current characteristics, *J. Chem. Phys.*, **9**(4) (1941), 341–351.

[12] D. W. Davidson and R. H. Cole, Dielectric relaxation in glycerol, propylene glycol, and *n*-propanol, *J. Chem. Phys.*, **19**(12) (1951), 1484–1490.

[13] F. Duarte and J. A T. Machado, Describing function of two masses with backlash, *Nonlinear Dyn.*, **56**(4) (2009), 409–413.

[14] D. El Khaled, N. N. Castellano, J. A. Gazquez, R. M. García Salvador, and F. Manzano-Agugliaro, Cleaner quality control system using bioimpedance methods: A review for fruits and vegetables, *J. Clean. Prod.*, **140** (2017), 1749–1762.

[15] N. Engheta, On fractional calculus and fractional multipoles in electromagnetism, *IEEE Trans. Antennas Propag.*, **44**(4) (1996), 554–566.

[16] S. Ghasemi, M. T. Darestani, Z. Abdollahi, and V. G. Gomes, Online monitoring of emulsion polymerization using electrical impedance spectroscopy, *Polym. Int.*, **64**(1) (2015), 66–75.

[17] M. Glatthaar, M. Riede, N. Keegan, K. Sylvester-Hvid, B. Zimmermann, M. Niggemann, A. Hinsch, and A. Gombert, Efficiency limiting factors of organic bulk heterojunction solar cells identified by electrical impedance spectroscopy, *Sol. Energy Mater. Sol. Cells*, **91**(5) (2007), 390–393.
[18] F. Groeber, L. Engelhardt, S. Egger, H. Werthmann, M. Monaghan, H. Walles, and J. Hansmann, Impedance spectroscopy for the non-destructive evaluation of in vitro epidermal models, *Pharm. Res.*, **32**(5) (2015), 1845–1854.
[19] S. Guinta, Ask the applications engineer–resistors, *Analog Dialogue: A Forum for the Exchange of Circuits, Systems and Software for Real-World Signal Processing*, **31**(1) (1997), 1–24.
[20] S. Havriliak and S. Negami, A complex plane analysis of α-dispersions in some polymer systems, *J. Polym. Sci., C Polym. Symp.*, **14** (1966), 99–117.
[21] C. Ionescu, A. M. Lopes, D. Copot, J. A. T. Machado, and J. H. T. Bates, The role of fractional calculus in modeling biological phenomena: A review, *Commun. Nonlinear Sci. Numer. Simul.*, **51** (2017), 141–159.
[22] A. Jalloul, J.-C. Trigeassou, K. Jelassi, and P. Melchior, Fractional order modeling of rotor skin effect in induction machines, *Nonlinear Dyn.*, **73**(1–2) (2013), 801–813.
[23] I. S. Jesus and J. A. T. Machado, Implementation of fractional-order electromagnetic potential through a genetic algorithm, *Commun. Nonlinear Sci. Numer. Simul.*, **14**(5) (2009), 1838–1843.
[24] Á. Kertész, Z. Hlaváčová, E. Vozáry, and L. Staroňová, Relationship between moisture content and electrical impedance of carrot slices during drying, *Int. Agrophys.*, **29**(1) (2015), 61–66.
[25] M. S. Krishna, S. Das, K. Biswas, and B. Goswami, Fabrication of a fractional order capacitor with desired specifications: a study on process identification and characterization, *IEEE Trans. Electron Devices*, **58**(11) (2011), 4067–4073.
[26] K. Küpfmüller, *Einführung in die Theoretische Elektrotechnik*, Springer-Verlag, Berlin, 1939.
[27] R. B. Leighton, R. P. Feynman, and M. Sands, *The Feynman Lectures on Physics: Mainly Electromagnetism and Matter*, Addison-Wesley Pub. Company, Reading, Massachusetts, 1964.
[28] M. Lewandowski and M. Orzyłowski, Fractional-order models: The case study of the supercapacitor capacitance measurement, *Bull. Pol. Acad. Sci., Tech. Sci.*, **65**(4) (2017), 449–457.
[29] A. Lopes and J. A. T. Machado, Fractional order models of leaves, *J. Vib. Control*, **20**(7) (2014), 998–1008.
[30] A. Lopes and J. A. T. Machado, Modeling vegetable fractals by means of fractional-order equations, *J. Vib. Control*, **22**(8) (2016), 2100–2108.
[31] A. Lopes and J. A. T. Machado, Fractional-order model of a non-linear inductor, 2018, in press.
[32] A. Lopes, J. A. T. Machado, and E. Ramalho, On the fractional-order modeling of wine, *Eur. Food Res. Technol.*, **243**(6) (2017), 921–929.
[33] A. Lopes, J. A. T. Machado, E. Ramalho, and V. Silva, Milk characterization using electrical impedance spectroscopy and fractional models, in *Food Analytical Methods*, pp. 1–12, 2017.
[34] J. A. T. Machado and A. Galhano, Generalized two-port elements, *Commun. Nonlinear Sci. Numer. Simul.*, **42** (2017), 451–455.
[35] J. A. T. Machado and I. S. Jesus, A suggestion from the past? *Fract. Calc. Appl. Anal.*, **7**(4) (2004), 403–407.
[36] J. A. T. Machado and A. Lopes, The persistence of memory, *Nonlinear Dyn.*, **79**(1) (2015), 63–82.
[37] J. A. T. Machado M. W. Albert, J. Fernando Silva, and M. T. Correia de Barros, Fractional order calculus on the estimation of short-circuit impedance of power transformers, in *Proc. 1st IFAC Workshop on Fractional Differentiation and Its Applications, Bordeaux, France*, 2004.
[38] J. A. T. Machado, I. S. Jesus, A. Galhano, and J. B. Cunha, Fractional order electromagnetics, *Signal Process.*, **86**(10) (2006), 2637–2644.

[39] J. A. T. Machado, I. S. Jesus, A. Galhano, J. B. Cunha, and J. K. Tar, Fractional calculus analysis of the electrical skin phenomena, in O. P. Agrawal, J. Sabatier, and J. A. T. Machado (eds.), *Advances in Fractional Calculus: Theoretical Developments and Applications in Physics and Engineering*, pp. 323–332, Springer, Dordrecht, The Netherlands, 2007.
[40] J. A. T. Machado, A. Galhano, A. Oliveira, and J. K. Tar, Optimal approximation of fractional derivatives through discrete-time fractions using genetic algorithms, *Commun. Nonlinear Sci. Numer. Simul.*, **15**(3) (2010), 482–490.
[41] J. A. T. Machado, A. Lopes, F. Duarte, M. Ortigueira, and R. Rato, Rhapsody in fractional, *Fract. Calc. Appl. Anal.*, **17**(4) (2014), 1188–1214.
[42] P. Melchior, B. Orsoni, O. Lavialle, A. Poty, and A. Oustaloup, Consideration of obstacle danger level in path planning using A* and Fast-Marching optimisation: comparative study, *Signal Process.*, **83**(11) (2003), 2387–2396.
[43] A. Milton and I. A. Stegun, *Handbook of Mathematical Functions with Formulas, Graphs, and Mathematical Tables*, Dover Pub. Inc., New York, 1965.
[44] T. Poinot, A. Benchellal, S. Bachir, and J.-C. Trigeassou, Identification of a non-integer model of induction machines, in *Proc.1st IFAC Workshop on Fractional Differentiation and Its Applications, Bordeaux, France*, 2004.
[45] S. Racewicz, Identification and non-integer order modelling of synchronous machines operating as generator, *Acta Energ.*, 2012.
[46] H. Samavati, A. Hajimiri, A. R. Shahani, G. N. Nasserbakht, and T. H. Lee, Fractal capacitors, *IEEE J. Solid-State Circuits*, **33**(12) (1998), 2035–2041.
[47] I. Schäfer and K. Krüger, Modelling of coils using fractional derivatives, *J. Magn. Magn. Mater.*, **307**(1) (2006), 91–98.
[48] I. Schäfer and K. Krüger, Modelling of lossy coils using fractional derivatives, *J. Phys. D, Appl. Phys.*, **41**(4) (2008), 045001.
[49] V. E. Tarasov, Review of some promising fractional physical models, *Int. J. Mod. Phys. B*, **27**(09) (2013), 1330005.
[50] A. R. West, D. C. Sinclair, and N. Hirose, Characterization of electrical materials, especially ferroelectrics, by impedance spectroscopy, *J. Electroceram.*, **1**(1) (1997), 65–71.
[51] S. Westerlund, Dead matter has memory! *Phys. Scr.*, **43**(2) (1991), 174.

Vasily E. Tarasov

Fractional electrodynamics with spatial dispersion

Abstract: Nonlocal electrodynamics of media with power-law spatial dispersion (PLSD) are described. Spatial dispersion is a phenomenon in which the absolute permittivity of the media depends on the wave vector. Power-law spatial dispersion is described by derivatives and integrals of noninteger orders. Fractional differential equations for the electric fields in these media are suggested. The generalizations of Coulomb's law and Debye's screening for power-law nonlocal media are proposed. Simple models of anomalous behavior of media with PLSD are described as nonlocal properties of power-law type. As examples, we consider electric fields of point charge and dipole in media with PLSD, infinite charged wire, uniformly charged disk, capacitance of spherical capacitor, and multipole expansion for media with PLSD. A microscopic model, which is based on fractional kinetics, is proposed to describe spatial dispersion of power-law type. The fractional Liouville equation is used to obtain the power-law dependence of the absolute permittivity on the wave vector. The proposed fractional nonlocal electrodynamics is characterized by universal spatial behavior of electromagnetic fields in media with PLSD by analogy with the universal temporal behavior of low-loss dielectrics.

Keywords: Spatial dispersion, electrodynamics, fractional calculus, fractional Laplacian, Riesz potential

PACS: 03.50.De, 45.10.Hj, 41.20.-q, 05.20.-y, 51.10.+y

1 Introduction

Spatial dispersion is a phenomenon of the dependence of the absolute permittivity tensor of the medium on the wave vector [28, 7, 5]. This dependence leads to different effects, including the rotation of the plane of polarization, anisotropy of cubic crystals and others [4, 3, 2, 6, 17, 18, 12, 26, 10, 11, 8, 1]. The spatial dispersion is caused by nonlocal connection between the electric induction **D** and the electric field **E**. Vector **D** at any point **r** of the medium is not uniquely defined by the values of **E** at this point. It also depends on the values of **E** at neighboring points $\mathbf{r}'$.

Media with high spatial dispersion are called plasma-like media. The term "plasma-like media" was proposed by Viktor P. Silin and Henri A. Rukhadze in 1961 in book [28]. Plasma-like medium is medium, in which the motion of free charge carriers cre-

Vasily E. Tarasov, Skobeltsyn Institute of Nuclear Physics, Lomonosov Moscow State University, Moscow 119991, Russia, e-mail: tarasov@theory.sinp.msu.ru

ates electric and magnetic fields that significantly distorts the external field and the effect on the motion of the charges themselves [28, 7, 5]. Examples of these media are ionized gas, metals and semiconductors, molecular crystals, and colloidal electrolytes.

The fractional calculus [27, 16, 38–40] is a powerful tool to describe the behavior of media and fields that are characterized by power-law nonlocality. Power-law spatial dispersion of the media have been described by using derivatives and integrals of noninteger order in [54, 48, 41–43]. The fractional differential equations for electric fields in media with power-law spatial dispersion are derived in [54]. The particular solutions of these equations for the electric field of point charge are also considered in [54, 48, 41]. The difference between the point charge potential in the media with PLSD and the Couloumb's and Debye's potentials are described in [54].

As it was shown in [30, 31, 38], the equations with fractional derivatives of noninteger orders are directly connected with microstructural models with long-range interactions. A connection between the dynamics of system with long-range interactions and the fractional differential equations of continuum is proved by using the transform operation [30, 31, 55, 56, 19, 57, 13, 44, 45]. This allows us to formulate the lattice fractional calculus [44, 45, 49] and the exact fractional differences [50, 46, 53, 51, 52].

A microscopic model based on the fractional kinetics has been suggested in [41] to describe spatial dispersion of power-law type. Using fractional calculus, we proposed generalizations of the Liouville equation [29, 32, 33, 47, 38] that can be used in the fractional kinetics [58, 38]. In paper [41], the Liouville equation with the spatial fractional derivatives of noninteger order is used to get the power-law dependence of the absolute permittivity on the wave vector for PLSD-media.

In this chapter, models of anomalous behavior of media with power-law spatial dispersion are described as nonlocal properties of power-law type by using the methods of the fractional calculus. We demonstrate that media with PLSD are characterized by universal spatial behavior of electromagnetic fields by analogy with the universal temporal behavior of low-loss dielectrics [14, 15, 34, 37, 35].

2 Linear nonlocal electrodynamics

Let us give some basic concepts and equations of electrodynamics of continuous media to fix the notation (see also [28, 7, 5]).

The state of the electric field is described by the vectors $(\mathbf{E}(t,\mathbf{r}), \mathbf{D}(t,\mathbf{r}))$, where $\mathbf{E}(t,\mathbf{r})$ is the electric field strength and $\mathbf{D}(t,\mathbf{r})$ is the electric displacement field. The state of magnetic field is described by the vectors $(\mathbf{B}(t,\mathbf{r}), \mathbf{H}(t,\mathbf{r}))$, where the field $\mathbf{B}(t,\mathbf{r})$ is the magnetic induction and the vector $\mathbf{H}(t,\mathbf{r})$ is the magnetic field strength.

Dynamics of electric and magnetic fields in continuous media can be described by the differential Maxwell's equations

$$\operatorname{div} \mathbf{D}(t,\mathbf{r}) = \rho(t,\mathbf{r}), \quad \operatorname{curl} \mathbf{E}(t,\mathbf{r}) = -\frac{\partial \mathbf{B}(t,\mathbf{r})}{\partial t}, \tag{1}$$

$$\operatorname{div} \mathbf{B}(t,\mathbf{r}) = 0, \quad \operatorname{curl} \mathbf{H}(t,\mathbf{r}) = \mathbf{j}(t,\mathbf{r}) + \frac{\partial \mathbf{D}(t,\mathbf{r})}{\partial t}, \tag{2}$$

where the charge density $\rho(t,\mathbf{r})$ and the current density $\mathbf{j}(t,\mathbf{r})$ describe external sources of fields.

In order to apply the Maxwell's equations, it is necessary to specify the constitutive relations (material equations). In the linear electrodynamics, the constitutive relations for electromagnetic fields, which are changed slowly in the space-time, have the form $D_i(t,\mathbf{r}) = \varepsilon_{ij}E_j(t,\mathbf{r})$, $B_i(t,\mathbf{r}) = \mu_{ij}H_j(t,\mathbf{r})$, where ε_{ij} and μ_{ij} are second-rank tensors.

For fields, which are changed in space rapidly, we should take into account an influence of the field at remote points $\mathbf{r}'$ on the electromagnetic properties of the medium at a given point $\mathbf{r}$. The field at a given point $\mathbf{r}$ of the medium will be determined not only the value of the field at this point, but the field in the areas of environment, where the influence of the field is transferred. For example, it can be caused by the transport processes in the medium. In this case, we should use nonlocal relations instead of relations $D_i(t,\mathbf{r}) = \varepsilon_{ij}E_j(t,\mathbf{r})$, $B_i(t,\mathbf{r}) = \mu_{ij}H_j(t,\mathbf{r})$. For linear electrodynamics, the nonlocal constitutive relation between electric fields $\mathbf{E}$ and $\mathbf{D}$ is given by

$$D_i(t,\mathbf{r}) = \int_{\mathbb{R}^3} \hat{\varepsilon}_{ij}(\mathbf{r},\mathbf{r}')E_j(t,\mathbf{r}')\, d\mathbf{r}'. \tag{3}$$

For simplification, we will assume that the constitutive relation for the magnetic fields $\mathbf{H}$ and $\mathbf{B}$ is local, $B_i(t,\mathbf{r}) = \mu_{ij}H_j(t,\mathbf{r})$.

We also will assume that the medium is not limited in space and homogeneous. Then the kernel of the integral operator (3) is a function of the position difference, $\varepsilon_{ij}(\mathbf{r},\mathbf{r}') = \varepsilon_{ij}(\mathbf{r}-\mathbf{r}')$. In this case, equation (3) has the form

$$D_i(t,\mathbf{r}) = \int_{\mathbb{R}^3} \hat{\varepsilon}_{ij}(\mathbf{r}-\mathbf{r}')E_j(t,\mathbf{r}')\, d\mathbf{r}'. \tag{4}$$

Using the Fourier transforms $\mathcal{F}$, the electric field can be represented as a set of plane monochromatic waves, such that relation (4) takes the form

$$D_i(\omega,\mathbf{k}) = \varepsilon_{ij}(\mathbf{k})E_j(\omega,\mathbf{k}), \tag{5}$$

where the direct Fourier transform $\mathcal{F}$ is given by

$$(\mathcal{F}f)(\mathbf{k}) = \mathcal{F}[f(\mathbf{r})](\mathbf{k}) = \int_{\mathbb{R}^3} e^{-i(\mathbf{kr})} f(\mathbf{r})\, d^3\mathbf{r}. \tag{6}$$

The inverse Fourier transform $\mathcal{F}^{-1}$ is defined as

$$\hat{g}(\mathbf{r}) = (\mathcal{F}^{-1}g)(\mathbf{r}) = \mathcal{F}^{-1}[g(\mathbf{k})](\mathbf{r}) = \frac{1}{(2\pi)^3}\int_{\mathbb{R}^3} e^{+i(\mathbf{kr})} g(\mathbf{k})\, d^3\mathbf{k}. \tag{7}$$

We do not use the hat for $\mathbf{D}(t,\mathbf{r})$ and $\mathbf{E}(t,\mathbf{r})$ to have usual notation. From the context, it will be easy to understand if the field is considered in the space-time of its the Fourier transforms.

The function $\varepsilon_{ij}(\mathbf{k})$ is called the tensor of the absolute permittivity of the material

$$\varepsilon_{ij}(\mathbf{k}) = \int\limits_{\mathbb{R}^3} e^{-i\mathbf{kr}} \hat{\varepsilon}_{ij}(\mathbf{r})\, d\mathbf{r}. \tag{8}$$

The dependence of the tensor $\varepsilon_{ij}(\mathbf{k})$ of the wave vector $\mathbf{k}$ preserves [28, 7, 5] the tensor form

$$\varepsilon_{ij}(\mathbf{k}) = \left(\delta_{ij} - \frac{k_i k_j}{|\mathbf{k}|^2}\right)\varepsilon_{\perp}(|\mathbf{k}|) + \frac{k_i k_j}{|\mathbf{k}|^2}\varepsilon_{\parallel}(|\mathbf{k}|), \tag{9}$$

where $\varepsilon_{\perp}(|\mathbf{k}|)$ is the transverse permittivity, and $\varepsilon_{\parallel}(|\mathbf{k}|)$ is the longitudinal permittivity. The representation (9) should be used even for an isotropic linear medium.

The differential Maxwell's equations for the electromagnetic fields can be represented [28, 7, 5] in the form

$$i(\mathbf{k}, \mathbf{E}(\omega,\mathbf{k}))\varepsilon(\mathbf{k}) = \rho(\omega,\mathbf{k}), \tag{10}$$

$$[\mathbf{k}, \mathbf{E}(\omega,\mathbf{k})] = \omega\mathbf{B}(\omega,\mathbf{k}), \tag{11}$$

$$(\mathbf{k}, \mathbf{B}(\omega,\mathbf{k})) = 0, \tag{12}$$

$$\frac{i}{\mu(\mathbf{k})}[\mathbf{k}, \mathbf{B}(\omega,\mathbf{k})] = -i\omega\varepsilon(\mathbf{k})\mathbf{E}(\omega,\mathbf{k}) + \mathbf{j}(\omega,\mathbf{k}). \tag{13}$$

For simplification, we will neglect the frequency dispersion. This can be done when the inhomogeneous field can be approximately considered as static. For the static case, we have inhomogeneous electric field $\mathbf{E}(t,\mathbf{r}) = \mathbf{E}(\mathbf{r})$. In this case, the electric field can be represented through the scalar potential $\Phi(\mathbf{r})$ by the equation

$$\mathbf{E}(\mathbf{r}) = -\operatorname{grad}\Phi(\mathbf{r}). \tag{14}$$

The Fourier transform of (14) is written as

$$\mathbf{E}(\mathbf{k}) = -i\mathbf{k}\Phi_{\mathbf{k}}. \tag{15}$$

Substitution of (15) into (10) gives

$$|\mathbf{k}|^2\varepsilon_{\parallel}(|\mathbf{k}|)\Phi_{\mathbf{k}} = \rho_{\mathbf{k}}, \tag{16}$$

where $\rho_{\mathbf{k}} = \rho(0,\mathbf{k})$. Note that equation (16) does not depend of the transverse permittivity $\varepsilon_{\perp}(|\mathbf{k}|)$.

For the case, when the resting point charge is a source of fiedls, the charge density is described by the delta-function

$$\rho(\mathbf{r}) = Q\delta^{(3)}(\mathbf{r}). \tag{17}$$

Therefore, the electrostatic potential of the point charge in the isotropic medium, according to the equation (16), has the form

$$\Phi(\mathbf{r}) = \frac{Q}{(2\pi)^3} \int_{\mathbb{R}^3} e^{+i\mathbf{k}(\mathbf{r})} \frac{1}{|\mathbf{k}|^2 \varepsilon_{\|}(|\mathbf{k}|)} d^3\mathbf{k}, \tag{18}$$

where $\Phi(\mathbf{r})$ is the electric potential created by a point charge Q at a distance $|\mathbf{r}|$ from the charge.

Let us note the two following well-known cases [28, 7, 5].

The first case [28, 7, 5] is described by $\varepsilon_{\|}(|\mathbf{k}|) = \varepsilon_0$, where the constant ε_0 is the vacuum permittivity ($\varepsilon_0 \approx 8.854\,10^{-12}\,\mathrm{F{\cdot}m^{-1}}$). Substituting $\varepsilon_{\|}(|\mathbf{k}|) = \varepsilon_0$ into (16), we obtain

$$|\mathbf{k}|^2 \Phi_{\mathbf{k}} = \frac{1}{\varepsilon_0} \rho_{\mathbf{k}}. \tag{19}$$

The inverse Fourier transform of (19) gives

$$\Delta\Phi(\mathbf{r}) = -\frac{1}{\varepsilon_0} \rho(\mathbf{r}), \tag{20}$$

where Δ is the Laplace operator (the Laplacian), and $\mathcal{F}[\Delta f(\mathbf{r})](\mathbf{k}) = -|\mathbf{k}|^2 \mathcal{F}[f(\mathbf{r})](\mathbf{k})$. In this case, the electrostatic potential of the point charge (17) has the Coulomb's form

$$\Phi(\mathbf{r}) = \frac{1}{4\pi\varepsilon_0} \frac{Q}{|\mathbf{r}|}. \tag{21}$$

The second case [28, 7, 5] is described by the expression

$$\varepsilon_{\|}(|\mathbf{k}|) = \varepsilon_0 \left(1 + \frac{1}{r_D^2 |\mathbf{k}|^2}\right). \tag{22}$$

Substitution of (22) into (16) gives

$$\left(|\mathbf{k}|^2 + \frac{1}{r_D^2}\right) \Phi_{\mathbf{k}} = \frac{1}{\varepsilon_0} \rho_{\mathbf{k}}. \tag{23}$$

The inverse Fourier transform of (23) has the form

$$\Delta\Phi(\mathbf{r}) - \frac{1}{r_D^2} \Phi(\mathbf{r}) = -\frac{1}{\varepsilon_0} \rho(\mathbf{r}). \tag{24}$$

As a result, we get the screened potential of the point charge (17) in the Debye's form

$$\Phi(\mathbf{r}) = \frac{1}{4\pi\varepsilon_0} \frac{Q}{|\mathbf{r}|} \exp\left(-\frac{|\mathbf{r}|}{r_D}\right), \tag{25}$$

where r_D is the Debye's radius of screening. The Debye's potential differs from the Coulomb's potential by factor $C_D(|\mathbf{r}|) = \exp(-|\mathbf{r}|/r_D)$. Such factor is a decay factor for the Coulomb's law, where the parameter r_D defines the distance over which significant charge separation can occur. The Debye's sphere is a region with Debye's radius r_D, in which there is an influence of charges, and outside of which charges are screened.

3 Power-law of nonlocality and generalized screening

3.1 General power-law spatial dispersion

Let us consider the power-law form of the absolute permittivity

$$\varepsilon_{\|}(|\mathbf{k}|) = \varepsilon_0 \left(\sum_{j=1}^{m} a_j |\mathbf{k}|^{\alpha_j - 2} + \frac{a_0}{|\mathbf{k}|^2} \right). \tag{26}$$

Substitution of (26) into (16), and using the inverse Fourier transform gives the fractional partial differential equation

$$\sum_{j=1}^{m} a_j ((-\Delta)^{\alpha_j/2} \Phi)(\mathbf{r}) + a_0 \Phi(\mathbf{r}) = \frac{1}{\varepsilon_0} \rho(\mathbf{r}), \tag{27}$$

where $\alpha_m > \cdots > \alpha_1 > 0$, and $a_j \in \mathbb{R}$ $(1 \leq j \leq m)$ are constants, $(-\Delta)^{\alpha_j/2}$ are fractional Laplacians in the Riesz form [24, 25, 27, 16, 22]. Note that the Fourier transform of the fractional Laplace operator has the form $\mathcal{F}[(-\Delta)^{\alpha/2} f(\mathbf{r})](\mathbf{k}) = |\mathbf{k}|^{\alpha} \hat{f}(\mathbf{k})$. Here, we consider $\mathbf{r}$ and r_D as dimensionless variables.

Using the Fourier transform $\mathcal{F}$ to both sides of (27), the fractional analog of the Green function (see Section 5.5.1 in [16]) and Lemma 25.1 of [27] (see also Theorem 5.22 in [16]), we can obtain the solution. If $\alpha_m > 1$ and $A_m \neq 0$, $A_0 \neq 0$, then equation (27) (see, e. g., Section 5.5.1, pp. 341–344 in [16]) has a particular solution is given by

$$\Phi(\mathbf{r}) = \frac{1}{\varepsilon_0} \int_{\mathbb{R}^3} G_{\alpha}(\mathbf{r} - \mathbf{r}') \rho(\mathbf{r}')\, d^3\mathbf{r}', \tag{28}$$

where the Green function $G_{\alpha}(z)$ can be given [54] in the form of the one-dimensional integral

$$G_{\alpha}(\mathbf{r}) = \frac{|\mathbf{r}|^{-1/2}}{(2\pi)^{3/2}} \int_0^{\infty} \left(\sum_{j=1}^{m} a_j |\lambda|^{\alpha_j} + a_0 \right)^{-1} \lambda^{3/2} J_{1/2}(\lambda |\mathbf{r}|)\, d\lambda, \tag{29}$$

where $\alpha = (\alpha_1, \ldots, \alpha_m)$ and J_{ν} is the Bessel function of the first kind such that

$$J_{1/2}(z) = \sqrt{\frac{2}{\pi z}} \sin(z). \tag{30}$$

Solution (28) is represented in the form of the convolution of the functions $G(\mathbf{r})$ and $\rho(\mathbf{r})$.

The fractional partial differential equation (27) with $a_0 = 0$, $a_1 \neq 0$, when $m \in \mathbb{N}$, $m \geq 1$ has the particular solution that is described by (28) with (29) with $a_0 = 0$ (see Theorem 5.23 in [16]).

These particular solutions allows us to describe electrostatic field in the plasma-like media with the spatial dispersion of power-law type.

3.2 Generalizations of Coulomb's law and Debye's screening for media with PLSD

Let us describe power-law type generalizations of the Coulomb's law and the Debye's permittivity by consideration of the simplest power-law forms of the longitudinal permittivity $\varepsilon_{\parallel}(|\mathbf{k}|)$ and equations for the electrostatic potential. The suggested simple models allow us to consider new possible types of an anomalous behavior of media with nonlocality.

We can generalize the Coulomb's law and the Debye's screening by the deformation of two terms in equation (22) in the form

$$\varepsilon_{\parallel}(|\mathbf{k}|) = \varepsilon_0\left(|\mathbf{k}|^{\alpha-2} + \frac{1}{r_D^2|\mathbf{k}|^{2-\beta}}\right). \tag{31}$$

The parameter α characterizes the deviation from Coulomb's law due to non-local properties of the medium. The parameter β characterizes the deviation from Debye's screening due to noninteger power-law type of nonlocality in the medium. For $\alpha = 2$ and $\beta = 0$, equation (31) gives (22).

Substituting (31) into (16), we obtain

$$\left(|\mathbf{k}|^{\alpha} + \frac{1}{r_D^2}|\mathbf{k}|^{\beta}\right)\Phi_{\mathbf{k}} = \frac{1}{\varepsilon_0}\rho_{\mathbf{k}}. \tag{32}$$

Using the inverse Fourier transform of (32), we get

$$((-\Delta)^{\alpha/2}\Phi)(\mathbf{r}) + \frac{1}{r_D^2}((-\Delta)^{\beta/2}\Phi)(\mathbf{r}) = \frac{1}{\varepsilon_0}\rho(\mathbf{r}), \tag{33}$$

where $(-\Delta)^{\alpha/2}$ and $(-\Delta)^{\beta/2}$ are the fractional Laplacian in the Riesz form [24, 25, 27, 16, 22]. Note that $\mathbf{r}$ and r_D are dimensionless variables.

Let us consider properties of electrostatic potentials for fractional differential model of media with PLSD that is described by the fractional partial differential equation

$$((-\Delta)^{\alpha/2}\Phi)(\mathbf{r}) + a_{\beta}((-\Delta)^{\beta/2}\Phi)(\mathbf{r}) = \frac{1}{\varepsilon_0}\rho(\mathbf{r}), \tag{34}$$

where $1 < \alpha$, $0 < \beta < \alpha$, $\beta < 3$, and $a_{\beta} = r_D^{-2}$. Note that $\mathbf{r}$ and r_D are dimensionless. Equation (34) has the particular solution

$$\Phi(\mathbf{r}) = \frac{1}{\varepsilon_0}\int_{\mathbb{R}^3} G_{\alpha,\beta}(\mathbf{r}-\mathbf{r}')\rho(\mathbf{r}')\,d^3\mathbf{r}', \tag{35}$$

where the Green-type function is given by

$$G_{\alpha,\beta}(\mathbf{r}) = \frac{|\mathbf{r}|^{-1/2}}{(2\pi)^{3/2}}\int_0^{\infty}\left(|\lambda|^{\alpha} + a_{\beta}|\lambda|^{\beta}\right)^{-1}\lambda^{3/2}J_{1/2}(\lambda|\mathbf{r}|)\,d\lambda. \tag{36}$$

Therefore, the electrostatic potential of the point charge (17) has form

$$\Phi(\mathbf{r}) = \frac{1}{4\pi\varepsilon_0}\frac{Q}{|\mathbf{r}|} \cdot C_{\alpha,\beta}(|\mathbf{r}|), \tag{37}$$

with

$$C_{\alpha,\beta}(|\mathbf{r}|) = \frac{2}{\pi}\int\limits_0^\infty \frac{\lambda \sin(\lambda|\mathbf{r}|)}{|\lambda|^\alpha + a_\beta|\lambda|^\beta}\, d\lambda, \tag{38}$$

where $C_{\alpha,\beta}(|\mathbf{r}|)$ describes the difference of Coulomb's potential.

Electric field $\mathbf{E}$ is defined as a gradient of the potential $\mathbf{E} = -\nabla\Phi$. Using

$$\frac{\partial}{\partial r}\left(\frac{\sin(\lambda r)}{r}\right) = \frac{(\lambda r)\cos(\lambda r) - \sin(\lambda r)}{r^2}, \tag{39}$$

where $r = |\mathbf{r}|$, we obtain the electric field

$$\mathbf{E}(\mathbf{r}) = \frac{Q}{4\pi\varepsilon_0}\frac{\mathbf{r}}{r^3} \cdot B_{\alpha,\beta}(r), \tag{40}$$

where

$$B_{\alpha,\beta}(r) = \frac{2}{\pi}\int\limits_0^\infty \frac{\lambda(\sin(\lambda r) - (\lambda r)\cos(\lambda r))}{\lambda^\alpha + a_\beta\lambda^\beta}\, d\lambda. \tag{41}$$

The function $B_{\alpha,\beta}(r)$ describes the nonlocal properties of media with PLSD. For $\alpha = 2$ and $a_\beta = 0$, we get the well-known equation with $B_{\alpha,\beta}(r) = 1$.

In order to describe the properties of on-local deformation of the Coulomb's law and the Debye's screening separately, we will consider the following special cases:

(1) Non-local deformation of Coulomb's law in the media with PLSD is defined by equation (31) with $\beta = 0$,

$$\varepsilon_\parallel(|\mathbf{k}|) = \varepsilon_0\left(|\mathbf{k}|^{\alpha-2} + \frac{1}{r_D^2|\mathbf{k}|^2}\right), \tag{42}$$

where $\alpha > 1$, $\alpha \neq 1$. Then equation (16) has the form

$$\left(|\mathbf{k}|^\alpha + \frac{1}{r_D^2}\right)\Phi_\mathbf{k} = \frac{1}{\varepsilon_0}\rho_\mathbf{k}, \tag{43}$$

and the equation for electrostatic potential is

$$((-\Delta)^{\alpha/2}\Phi)(\mathbf{r}) + \frac{1}{r_D^2}\Phi(\mathbf{r}) = \frac{1}{\varepsilon_0}\rho(\mathbf{r}). \tag{44}$$

This model allows us to describe a deviation from Coulomb's law in the media with nonlocal properties defined by the power-law spatial dispersion.

(2) Nonlocal deformation of Debye's screening in the media with PLSD is defined by equation (31) with $\alpha = 2$, is given by

$$\varepsilon_{\|}(|\mathbf{k}|) = \varepsilon_0\left(1 + \frac{1}{r_D^2|\mathbf{k}|^{2-\beta}}\right). \tag{45}$$

Equation (16) with (45) is

$$\left(|\mathbf{k}|^2 + \frac{1}{r_D^2}|\mathbf{k}|^{\beta}\right)\Phi_{\mathbf{k}} = \frac{1}{\varepsilon_0}\rho_{\mathbf{k}}, \tag{46}$$

where $0 < \beta < 2$. Then the equation for generalized potential has the form

$$-\Delta\Phi(\mathbf{r}) + \frac{1}{r_D^2}((-\Delta)^{\beta/2}\Phi)(\mathbf{r}) = \frac{1}{\varepsilon_0}\rho(\mathbf{r}), \tag{47}$$

which involve two different differential operators. Such model allows us to describe a possible deviation from Debye's screening by nonlocal properties of the media with PLSD.

(3) We also consider the case $\alpha \neq 2$ and $\beta > 0$ that deformation of the Coulomb's law and Debye's screening.

Let us describe a behavior of electrostatic potentials for the suggested fractional differential models described by equations (44) and (47). We will give explicit solutions of these fractional differential equations.

3.3 Nonlocal deformation of Coulomb's law

The nonlocal deformation of Coulomb's law in the media with PLSD is defined by the equation

$$((-\Delta)^{\alpha/2}\Phi)(\mathbf{r}) + \frac{1}{r_D^2}\Phi(\mathbf{r}) = \frac{1}{\varepsilon_0}\rho(\mathbf{r}), \tag{48}$$

where $\alpha > 1$, and $a_0 = r_D^{-2} > 0$. The electrostatic potential $\Phi(\mathbf{r})$ is described by equation (37) with

$$C_{\alpha,0}(|\mathbf{r}|) = \frac{2}{\pi}\int_0^{\infty} \frac{\lambda \sin(\lambda|\mathbf{r}|)}{|\lambda|^{\alpha} + a_0}\, d\lambda. \tag{49}$$

The asymptotic at $|\mathbf{r}| \to 0$ is described [54] by the expression

$$C_{\alpha,0}(|\mathbf{r}|) \approx \frac{2^{2-\alpha}\Gamma((3-\alpha)/2)}{\sqrt{\pi}\Gamma(\alpha/2)}\frac{1}{|\mathbf{r}|^{2-\alpha}}, \quad (1 < \alpha < 2), \tag{50}$$

$$C_{\alpha,0}(|\mathbf{r}|) \approx \frac{2^{2-\alpha}\Gamma((3-\alpha)/2)}{\sqrt{\pi}\Gamma(\alpha/2)}|\mathbf{r}|^{\alpha-2}, \quad (2 < \alpha < 3), \tag{51}$$

$$C_{\alpha,0}(|\mathbf{r}|) \approx \frac{2\Gamma(3/\alpha)\Gamma(1-3/\alpha)}{\pi\alpha a_0^{1-3/\alpha}}|\mathbf{r}|, \quad (\alpha > 3). \tag{52}$$

Note that asymptotic (50)–(51) for $1 < \alpha < 2$ and $2 < \alpha < 3$ does not depend on the parameter a_0. Note that for $\alpha = 2$ we get the Debye's exponents $C_{2,0}(|\mathbf{r}|) = C_D(|\mathbf{r}|) = \exp(-|\mathbf{r}|/r_D)$.

As a result, the electrostatic potential of the point charge on small distances $|\mathbf{r}| \ll 1$ has the power-law form

$$\Phi(\mathbf{r}) \approx \frac{Q}{4\pi\varepsilon_0}\frac{2^{2-\alpha}\Gamma((3-\alpha)/2)}{\sqrt{\pi}\Gamma(\alpha/2)}\frac{1}{|\mathbf{r}|^{3-\alpha}} \quad (1 < \alpha < 2,\ 2 < \alpha < 3) \tag{53}$$

For $\alpha > 3$, we have the constant value

$$\Phi(\mathbf{r}) \approx \frac{1}{4\pi\varepsilon_0}\frac{Q}{R_{\text{eff}}}, \quad (\alpha > 3), \tag{54}$$

where R_{eff} is an effective sphere radius that is equal to

$$R_{\text{eff}} = \frac{\pi\alpha a_0^{1-3/\alpha}}{2\Gamma(3/\alpha)\Gamma(1-3/\alpha)}. \tag{55}$$

We can state that for $\alpha > 3$ the electric field of a point charge in the media with PLSD is analogous to the field inside a conducting charged sphere of the radius R_{eff}, for small distances $|\mathbf{r}| \ll 1$.

3.4 Nonlocal deformation of Debye's screening

Let us consider nonlocal deformation of Debye's screening in the media with spatial dispersion is described by equation (34) with $\alpha = 2$, given by

$$-\Delta\Phi(\mathbf{r}) + a_\beta((-\Delta)^{\beta/2}\Phi)(\mathbf{r}) = \frac{1}{\varepsilon_0}\rho(\mathbf{r}), \tag{56}$$

where $0 < \beta < 2$. The electrostatic potential of the point charge (17) has the following form:

$$\Phi(\mathbf{r}) = \frac{1}{4\pi\varepsilon_0}\frac{Q}{|\mathbf{r}|} \cdot C_{2,\beta}(|\mathbf{r}|), \tag{57}$$

where

$$C_{2,\beta}(|\mathbf{r}|) = \frac{2}{\pi}\int_0^\infty \frac{\lambda\sin(\lambda|\mathbf{r}|)}{|\lambda|^2 + a_\beta|\lambda|^\beta}\,d\lambda. \tag{58}$$

In paper [54], we present some plots of the Debye exponential factor $C_D(|\mathbf{r}|) = \exp(-|\mathbf{r}|/r_D)$ and factor $C_{2,\beta}(|\mathbf{r}|)$ for different orders of $1.5 < \beta < 2$ and $a_\beta = 1$.

The asymptotic behavior for $C_{2,\beta}(|\mathbf{r}|)$ with $\beta < 2$, when $|\mathbf{r}| \to \infty$ has [54] the form

$$C_{2,\beta}(|\mathbf{r}|) \approx A_0(\beta)\frac{1}{|\mathbf{r}|^{2-\beta}} + \sum_{k=1}^{\infty} A_k(\beta)\frac{1}{|\mathbf{r}|^{(2-\beta)(k+1)}}, \tag{59}$$

where

$$A_0(\beta) = \frac{2}{\pi a_\beta}\Gamma(2-\beta)\sin\left(\frac{\pi}{2}\beta\right), \tag{60}$$

$$A_k(\beta) = -\frac{2}{\pi a_\beta^{k+1}}\int_0^\infty z^{(2-\beta)(k+1)-1}\sin(z)\,dz. \tag{61}$$

As a result, nonlocal media with PLSD deform the Debye's screening such that the exponential decay is replaced by the generalized power-law

$$C_{2,\beta}(|\mathbf{r}|) \approx \frac{A_0}{|\mathbf{r}|^{2-\beta}} \quad (0 < \beta < 2,\ |\mathbf{r}| \to \infty). \tag{62}$$

The electrostatic potential of the point charge in the media with this type of spatial dispersion is given by

$$\Phi(\mathbf{r}) \approx \frac{A_0}{4\pi\varepsilon_0}\cdot\frac{Q}{|\mathbf{r}|^{3-\beta}} \quad (0 < \beta < 2,\ |\mathbf{r}| \to \infty) \tag{63}$$

on the long distance $|\mathbf{r}| \gg 1$.

3.5 Nonlocal deformation of Coulomb's law and Debye's screening

The electrostatic potential of nonlocal media that is described by equation (34) includes two parameters (α,β), where $\alpha > \beta > 0$. In this case, nonlocal properties deform Coulomb's law and Debye's screening, which are described by the asymptotic behavior with the fractional power-law decay

$$C_{\alpha,\beta}(|\mathbf{r}|) \approx \frac{2\Gamma(2-\beta)\sin(\pi\beta/2)}{\pi a_\beta}\cdot\frac{1}{|\mathbf{r}|^{2-\beta}} \quad (|\mathbf{r}| \to \infty), \tag{64}$$

for $0 < \beta < 3$ and $\alpha > \beta$. Note that this asymptotic behavior $|\mathbf{r}| \to \infty$ does not depend on the parameter α. The field on the long distances is determined only by term with $(-\Delta)^{\beta/2}$ $(\alpha > \beta)$ that can be interpreted as a nonlocal deformation of Debye's (second) term in equation (24).

The new type of behavior of the media with PLSD is presented by power-law decreasing of the field at long distances instead of exponential decay [54].

The asymptotic behavior $C_{\alpha,\beta}(|\mathbf{r}|)$ for $|\mathbf{r}| \to 0$ is given by

$$C_{\alpha,\beta}(|\mathbf{r}|) \approx \frac{2^{2-\alpha}\Gamma((3-\alpha)/2)}{\sqrt{\pi}\Gamma(\alpha/2)}\cdot\frac{1}{|\mathbf{r}|^{2-\alpha}}, \quad (1 < \alpha < 2,\ |\mathbf{r}| \to 0), \tag{65}$$

$$C_{\alpha,\beta}(|\mathbf{r}|) \approx \frac{2^{2-\alpha}\Gamma((3-\alpha)/2)}{\sqrt{\pi}\Gamma(\alpha/2)} \cdot |\mathbf{r}|^{\alpha-2}, \quad (2 < \alpha < 3, |\mathbf{r}| \to 0), \tag{66}$$

$$C_{\alpha,\beta}(|\mathbf{r}|) \approx \frac{2}{\alpha a_\beta^{1-3/\alpha} \sin(3\pi/\alpha)} \cdot |\mathbf{r}|, \quad (\alpha > 3, |\mathbf{r}| \to 0). \tag{67}$$

Note that the above asymptotic behavior does not depend on the parameter β, and relations (65–66) does not depend on a_β. The field on the short distances (64) is determined only by term with $(-\Delta)^{\alpha/2}$ $(\alpha > \beta)$ that can be considered as a nonlocal deformation of Coulomb's (first) term in equation (24). It should be noted the remarkable that exist a maximum for the factor $C_{\alpha,\beta}(|\mathbf{r}|)$ in the case $0 < \beta < 2 < \alpha$ [54].

4 Weak power-law spatial dispersion

To describe the weak spatial dispersion [28, 7, 4, 1], it is enough to know the dependence of the tensor $\varepsilon_{ij}(\mathbf{k})$ only for small values $\mathbf{k}$. This allows us to replace the function by the Taylor polynomial. The weak spatial dispersion in the media with PLSD cannot be correctly described by the standard Taylor approximation. The fractional Taylor series is very useful for approximating noninteger power-law functions [54]. It is based on fact that the fractional Taylor series of power-law function can give an exact expression instead of approximation of the standard Taylor series [54].

Let us consider properties of the media with weak PLSD that is described by the functions $\varepsilon_\parallel(|\mathbf{k}|)$ of noninteger power-law type. These media can demonstrate new type of behavior of complex media with nonlocality.

The weak spatial dispersion (and the permittivity) will be called α-type, if the function $\varepsilon_\parallel(|\mathbf{k}|)$ satisfies the condition

$$\lim_{|\mathbf{k}|\to 0} \frac{\varepsilon_\parallel(|\mathbf{k}|) - \varepsilon_\parallel(0)}{\varepsilon_0 |\mathbf{k}|^\alpha} = a_\alpha, \tag{68}$$

where $\alpha > 0$ and $0 < |a_\alpha| < \infty$. Here, the constant ε_0 is the vacuum permittivity ($\varepsilon_0 \approx 8.854\, 10^{-12}$ F·m^{-1}).

The weak spatial dispersion (the permittivity) will be called (α, β)-type, if the function $\varepsilon_\parallel(|\mathbf{k}|)$ satisfies the conditions (68) and

$$\lim_{|\mathbf{k}|\to 0} \frac{\varepsilon_\parallel(|\mathbf{k}|) - \varepsilon_\parallel(0) - a_\alpha \varepsilon_0 |\mathbf{k}|^\alpha}{\varepsilon_0 |\mathbf{k}|^\beta} = a_\beta, \tag{69}$$

where $\beta > \alpha > 0$ and $0 < |a_\beta| < \infty$.

Note that these definitions are similar to definitions of nonlocal alpha-interactions between lattice particles (see Section 8.6 in [38] and [30, 31]) that give continuous medium equations with spatial fractional derivatives.

For the weak spatial dispersion of the (α,β)-type, the permittivity can be represented in the form

$$\varepsilon_{\|}(|\mathbf{k}|) = \varepsilon_0(\varepsilon + a_\alpha|\mathbf{k}|^\alpha + a_\beta|\mathbf{k}|^\beta) + R_{\alpha,\beta}(|\mathbf{k}|), \tag{70}$$

where $\varepsilon = \varepsilon_{\|}(0)/\varepsilon_0$ can be considered as the relative permittivity of material, and

$$\lim_{|\mathbf{k}|\to 0} \frac{R_{\alpha,\beta}(|\mathbf{k}|)}{|\mathbf{k}|^\beta} = 0. \tag{71}$$

As a result, we can use the following approximation for weak spatial dispersion:

$$\varepsilon_{\|}(|\mathbf{k}|)/\varepsilon_0 \approx \varepsilon + a_\alpha|\mathbf{k}|^\alpha + a_\beta|\mathbf{k}|^\beta. \tag{72}$$

If $\alpha = 1$ and $\beta = 2$, equation (72) has the standard form

$$\varepsilon_{\|}(|\mathbf{k}|)/\varepsilon_0 \approx \varepsilon + a_\alpha|\mathbf{k}|^1 + a_2|\mathbf{k}|^2. \tag{73}$$

Equation (73) is used for an isotropic linear medium, such as crystals with high symmetry [4]. In this case, we have the well-known case of the weak spatial dispersion [4, 3, 2, 6, 17, 18, 12, 26, 10, 11, 8, 1]. Note that to explain the natural optical activity (e. g., optical rotation, gyrotropy) is sufficient to consider the linear dependence on $\mathbf{k}$ in (73). For nongyrotropic crystals, it is necessary to take into account the terms quadratic in $\mathbf{k}$.

In general, we should use a fractional generalization of the Taylor series [54]. If the orders of the fractional Taylor series is correlated with the type of weak spatial dispersion, then the fractional Taylor series approximation of $\varepsilon_{\|}(|\mathbf{k}|)$ will be exact ($R_{\alpha,\beta}(|\mathbf{k}|) = 0$).

Let us consider a weak PLSD of (α,β)-type. Then substituting (72) into (16), we obtain

$$(\varepsilon|\mathbf{k}|^2 + a_\alpha|\mathbf{k}|^{\alpha+2} + a_\beta|\mathbf{k}|^{\beta+2})\Phi_{\mathbf{k}} = \frac{1}{\varepsilon_0}\rho_{\mathbf{k}}, \tag{74}$$

where $\varepsilon = \varepsilon_{\|}(0)\varepsilon_0$ and $\beta > \alpha > 0$. The inverse Fourier transform of (74) gives

$$a_\beta((-\Delta)^{(\beta+2)/2}\Phi)(\mathbf{r}) + a_\alpha((-\Delta)^{(\alpha+2)/2}\Phi)(\mathbf{r}) - \varepsilon\Delta\Phi(\mathbf{r}) = \frac{1}{\varepsilon_0}\rho(\mathbf{r}). \tag{75}$$

This fractional differential equation describes a weak spatial dispersion of the (α,β)-type. Equation (75) has the particular solution

$$\Phi(\mathbf{r}) = \frac{1}{\varepsilon_0}\int_{\mathbb{R}^3} G_{2,\alpha,\beta}(\mathbf{r}-\mathbf{r}')\rho(\mathbf{r}')\, d^3\mathbf{r}', \tag{76}$$

where

$$G_{2,\alpha,\beta}(\mathbf{r}) = \frac{|\mathbf{r}|^{-1/2}}{(2\pi)^{3/2}} \int_0^\infty \frac{\lambda^{3/2} J_{1/2}(\lambda|\mathbf{r}|)}{a_\alpha|\lambda|^{\alpha+2} + a_\beta|\lambda|^{\beta+2} + \varepsilon|\lambda|^2} \, d\lambda. \tag{77}$$

For the point charge (17) in media with weak PLSD, the electrostatic potential has the form

$$\Phi(\mathbf{r}) = \frac{1}{4\pi\varepsilon_0} \frac{Q}{|\mathbf{r}|} \cdot C_{2,\alpha,\beta}(|\mathbf{r}|), \tag{78}$$

where $0 < \alpha < \beta$, and

$$C_{2,\alpha,\beta}(|\mathbf{r}|) = \frac{2}{\pi} \int_0^\infty \frac{\lambda \sin(\lambda|\mathbf{r}|)}{a_\alpha|\lambda|^{\alpha+2} + a_\beta|\lambda|^{\beta+2} + \varepsilon|\lambda|^2} \, d\lambda. \tag{79}$$

The weak spatial dispersion of α-type is described by equations (75), (78), and (79) with $a_\beta = 0$.

To describe properties of electric field of the point charge in the media with the weak PLSD, we consider properties of function (79) with $\beta > \alpha$.

Using the values for the sine integral $\mathrm{Si}(x)$ for the infinite limit and the equation for the integral transform (equation (1) in Section 2.3 of [9]), we obtain [54] the asymptotic expression:

$$C_{2,\alpha,\beta}(|\mathbf{r}|) \approx \frac{2}{\pi\varepsilon}\left(\frac{\pi}{2} - \frac{1}{|\mathbf{r}|^\alpha}\frac{a_\alpha}{\varepsilon}\Gamma(\alpha)\sin\left(\frac{\pi\alpha}{2}\right) - \frac{1}{|\mathbf{r}|^\beta}\frac{a_\beta}{\varepsilon}\Gamma(\beta)\sin\left(\frac{\pi\beta}{2}\right)\right). \tag{80}$$

As a result, we get the asymptotic behavior of the electrostatic potential

$$\begin{aligned}\Phi(\mathbf{r}) \approx \; & \frac{Q}{4\pi\varepsilon\varepsilon_0}\frac{1}{|\mathbf{r}|} - \frac{a_\alpha Q}{4\pi\varepsilon^2\varepsilon_0}\frac{2\Gamma(\alpha)\sin(\pi\alpha/2)}{\pi}\frac{1}{|\mathbf{r}|^{\alpha+1}} \\ & - \frac{a_\beta Q}{4\pi\varepsilon^2\varepsilon_0}\frac{2\Gamma(\beta)\sin(\pi\beta/2)}{\pi}\frac{1}{|\mathbf{r}|^{\beta+1}},\end{aligned} \tag{81}$$

where $0 < \alpha < \beta < 1$. The first term in (81) describes the well-known Coulomb's field. The second and third terms in equation (81) can be interpreted [54] as generalized dipole fields, which are represented as

$$\Phi_{\mathrm{eff}}(\mathbf{r}) = -\frac{d_{\mathrm{eff}}(\alpha)\cos\theta_{\mathrm{eff}}(\alpha)}{4\pi\varepsilon_0|\mathbf{r}|^{\alpha+1}} - \frac{d_{\mathrm{eff}}(\beta)\cos\theta_{\mathrm{eff}}(\beta)}{4\pi\varepsilon_0|\mathbf{r}|^{\beta+1}}, \tag{82}$$

where $0 < \alpha < \beta < 1$, and we used the effective values $d_{\mathrm{eff}}(\alpha) = 2\Gamma(\alpha)a_\alpha Q/\pi\varepsilon^2$, $\theta_{\mathrm{eff}} = \frac{\pi}{2}(1-\alpha)$.

5 Special cases of electric field in media with PLSD

5.1 Electric dipole in media with PLSD

For the point charge (17) in the PLSD-media, the electrostatic potential (35) has the form (37). The electric dipole is a combination of the two equal in magnitude of opposite point charges, located at some distance from each other.

The electrostatic potential of dipole in the PLSD-media is

$$\Phi(\mathbf{r}) = \frac{Q}{4\pi\varepsilon_0}\left(\frac{C_{\alpha,\beta}(r_+)}{r_+} - \frac{C_{\alpha,\beta}(r_-)}{r_-}\right), \tag{83}$$

where $\mathbf{r}_\pm$ are vectors from point charges of signs ± to a given observation point.

The vectors $\mathbf{r}_\pm$ are connected by the equation $\mathbf{r}_- = \mathbf{r}_+ + \mathbf{l}$, where $\mathbf{l}$ is the vector from the point with a negative charge to a point with a positive charge.

Substitution of expression (38) of $C_{\alpha,\beta}(r)$ into (83) gives

$$\Phi(\mathbf{r}) = \frac{Q}{4\pi\varepsilon_0}\frac{2}{\pi}\int_0^\infty d\lambda \frac{\lambda}{\lambda^\alpha + a_\beta \lambda^\beta}\left(\frac{\sin(\lambda r_+)}{r_+} - \frac{\sin(\lambda r_-)}{r_-}\right). \tag{84}$$

In work [48], the electrostatic potential of an electric dipole in the media with PLSD is derived in the form

$$\Phi(\mathbf{r}) = \frac{Q}{4\pi\varepsilon_0}\frac{(\mathbf{l},\mathbf{r})}{r^3}A_{\alpha,\beta}(r), \tag{85}$$

where

$$A_{\alpha,\beta}(r) = \frac{1}{\pi}\int_0^\infty d\lambda \frac{\lambda}{\lambda^\alpha + a_\beta \lambda^\beta}(\sin(\lambda r) - (\lambda r)\cos(\lambda r)). \tag{86}$$

The function $A_{\alpha,\beta}(r)$ describes the nonlocal properties of a dipole field in PLSD media. Product of the vector $\mathbf{l}$, which is drawn from the negative charge to positive, and the absolute value of the charge Q is the dipole moment $\mathbf{d} = Q\mathbf{l}$. For $\alpha = 2$ and $a_\beta = 0$, equation (85) gives $A_{\alpha,\beta}(r) = 1$ and the standard equation for the potential $\Phi(\mathbf{r})$ of the electric dipole.

5.2 Infinite charged wire in media with PLSD

Let us consider the electric potential of a uniformly charged wire with a linear density τ. Let the wire be located along the z-axis. If we have an "infinitely long" and uniformly linearly distributed charge, we can determine the potential by integration.

At a given point at distance R from the wire, we can obtain [48]; the potential from an infinitesimal part of wire of length dz' by the integration over z from $-\infty$ to $+\infty$

gives the potential of the infinite wire

$$\Phi(R) = \frac{1}{4\pi\varepsilon_0} \int_{-\infty}^{+\infty} \frac{\tau}{\sqrt{R^2 + (z - z')^2}} \cdot C_{\alpha,\beta}\left(\sqrt{R^2 + (z - z')^2}\right) dz', \tag{87}$$

where $\tau dz'$ is the charge on that section of wire.

Using the integral 2.5.6.2 of [23], we can get [48] the electric field of infinite wire in the media with PLSD in the form

$$\Phi(R) = \frac{\tau}{2\pi\varepsilon_0} \int_0^{\infty} \frac{\lambda J_0(\lambda R)}{\lambda^\alpha + a_\beta \lambda^\beta} d\lambda, \tag{88}$$

where J_0 is the Bessel function of the first kind

$$J_0(z) = \sum_{k=0}^{\infty} \frac{(-1)^k (z/2)^{2k}}{(k!)^2}. \tag{89}$$

The electric field $\mathbf{E} = -\nabla\Phi$ at the points perpendicularly away from the wire, and is inversely proportional to the first power of the separation distance.

5.3 Uniformly charged disk in media with PLSD

Let us consider a uniformly charged disk of radius a with the total charge Q. The potential at a distance h at the perpendicular to the disk plane passing through its center is

$$\Phi(h) = \frac{1}{4\pi\varepsilon_0} \int_S dx\, dy \frac{\sigma}{\sqrt{x^2 + y^2 + h^2}} C_{\alpha,\beta}\left(\sqrt{x^2 + y^2 + h^2}\right), \tag{90}$$

where $\sigma = Q/(\pi a^2)$ is the charge density per unit area of the disk plane.

Using cylindrical coordinates (R, α, h) instead of the Cartesian (x, y, z), we get [48] the expression

$$\Phi(h) = \frac{Q}{\pi^2 a^2 \varepsilon_0} \int_0^{\infty} \frac{\sin^2(\lambda\sqrt{a^2 + h^2}/2)}{\lambda^\alpha + a_\beta \lambda^\beta} d\lambda. \tag{91}$$

Equation (91) described the electric field of uniformly charged disk in the PLSD-media [48].

5.4 Capacitance of spherical capacitor with PLSD media

The capacitance for spherical conductors can be obtained by evaluating the voltage difference between the conductors for a given charge on each.

The voltage between the spheres is given [48] by the equation

$$\Phi_2 - \Phi_1 = \Phi(\mathbf{r}_2) - \Phi(\mathbf{r}_1) = \frac{Q}{4\pi\varepsilon_0}\left(\frac{C_{\alpha,\beta}(r_1)}{r_1} - \frac{C_{\alpha,\beta}(r_2)}{r_2}\right). \quad (92)$$

Using (38), we get

$$\Phi_2 - \Phi_1 = \frac{Q}{4\pi\varepsilon_0}\int_0^\infty d\lambda \frac{\lambda}{\lambda^\alpha + a_\beta\lambda^\beta}\left(\frac{\sin(\lambda r_1)}{r_1} - \frac{\sin(\lambda r_2)}{r_2}\right). \quad (93)$$

From the definition, the capacitance of spherical capacitor is

$$C = \frac{Q}{\Phi_2 - \Phi_1} = \frac{4\pi\varepsilon_0 r_1 r_2}{r_2 C_{\alpha,\beta}(r_1) - r_1 C_{\alpha,\beta}(r_2)}, \quad (94)$$

where $C_{\alpha,\beta}(r)$ is defined by equation (38).

5.5 Multipole expansion for media with PLSD

In work [48], we consider an electric multipole expansion for a distribution of charged particles in the PLSD media. Let $\mathbf{R}$ be a vector from a fixed reference point to the observation point, and $\mathbf{r} = x_k\mathbf{e}_k$ be a vector from the reference point to a point in the distribution of charges. The potential $\Phi(\mathbf{R})$ of the electric field of this distribution is defined by the equation

$$\Phi(\mathbf{R}) = \frac{1}{4\pi\varepsilon_0}\int_W \frac{\rho(\mathbf{r})}{|\mathbf{R} - \mathbf{r}|} C_{\alpha,\beta}(|\mathbf{R} - \mathbf{r}|)\, d^3r, \quad (95)$$

where $(\mathbf{R} - \mathbf{r})$ is a vector from a point in the distribution to the observation point. The multipole expansion for media with PLSD is given [48].

6 Fractional Liouville equation

It is known that the Liouville equations [20, 21] are used to describe kinetics for plasma-like media with spatial dispersion [28, 7, 5]. The fractional Liouville equations can also be applied to describe fractional kinetics for media with the spatial dispersion of power-law type [41]. In the work [41], the Liouville equation with the fractional derivatives is used to obtain the power-law dependence of the absolute permittivity on the wave vector. This approach, which is proposed in [41], gives a microscopic model for the media with PLSD that is described in [54].

The Liouville equation is a mathematical expression of the conservation of probability in the phase-space [20, 21]. Let us consider dynamics of system in the phase space with dimensionless coordinates $(\mathbf{x}, \mathbf{p}) = (x_1, \ldots, x_n, p_1, \ldots, p_n)$. The function $\rho(t, \mathbf{x}, \mathbf{p})$ describes probability density to find a system in the phase volume $d^n\mathbf{x}d^n\mathbf{p}$. The evolution of $\rho = \rho(t, \mathbf{x}, \mathbf{p})$ is described by the Liouville equation

$$\frac{\partial \rho}{\partial t} + \frac{p_i}{m} D^1_{x_i}\rho + F_i D^1_{p_i}\rho = 0, \tag{96}$$

where $F_i = F_i(\mathbf{x}, \mathbf{p})$ is the force field (here and later, we mean the sum on the repeated index i from 1 to n). Equation (96) describes the probability conservation for the volume element of the phase space. If ρ is the one-particle reduced distribution function, then the Liouville equation describes a collisionless system.

Using fractional calculus, we can consider a different generalization of the Liouville equation [29, 32, 33, 47, 38] that includes derivatives of noninteger orders. The fractional Liouville equation has been proposed [29, 32, 33, 47, 38] in the form

$$\frac{\partial \rho}{\partial t} + \frac{p_i}{m} {}_0^C D^{\alpha_i}_{x_i}\rho + F_i \, {}_0^C D^{\beta_i}_{p_i}\rho = 0, \tag{97}$$

where we use dimensionless variables x_i, p_i, $(i = 1, \ldots, n)$, and ${}_0^C D^\alpha_x$ and ${}_0^C D^\beta_x$ are the Caputo fractional derivatives of order α and β. The Caputo fractional derivatives are used since a consistent formulation of fractional vector calculus, which contains fractional differential and integral vector operations, can be realized for the Caputo differentiation and Riemann–Liouville integration only [36]. It allows to prove the correspondent fractional generalizations of the Green's, Stokes', and Gauss' theorems [36]. The main distinguishing feature of the Caputo fractional derivative is the form of the fractional generalization of the Newton–Leibniz formula (see Lemma 2.22 of [16]). The other feature of the Caputo fractional derivative is that the Caputo fractional derivative of a constant is equal to zero.

For simplification, we will consider the case $\alpha_i = \alpha$, and $\beta_i = 1$ for all $i = 1, \ldots, n$. Then the fractional Liouville equation is

$$\frac{\partial \rho}{\partial t} + \frac{p_i}{m} {}_0^C D^{\alpha}_{x_i}\rho + F_i D^{1}_{p_i}\rho = 0. \tag{98}$$

The fractional Liouville equation (98) will be used to describe properties of nonlocal media with PLSD.

7 Permittivity of plasma-like media with PLSD

For the case $F_i = 0$, the Liouville equation (98) is

$$\frac{\partial \rho}{\partial t} + \frac{p_i}{m} {}_0^C D^{\alpha}_{x_i}\rho = 0. \tag{99}$$

The solution of (98) is the distribution function $\rho_0 = \rho(t, \mathbf{x}, \mathbf{p})$ that is unperturbed by the fields.

For a weak force field $\mathbf{F} = \mathbf{e}_i F_i$, we use the charge distribution function in the form

$$\rho = \rho_0 + \delta\rho, \tag{100}$$

where ρ_0 is the stationary isotropic homogeneous distribution function unperturbed by the fields, and $\delta\rho$ is the change of ρ_0 by the fields. Using the linear approximation with respect to perturbations (the function $\delta\rho$ and the field $\mathbf{F}$), the Liouville equation has the form

$$\frac{\partial \delta\rho}{\partial t} + \frac{p_i}{m}({}_0^C D^{\alpha}_{x_i} \delta\rho) + F_i D^1_{p_i} \rho_0 = 0. \tag{101}$$

For the plasma-like media, the force is the Lorentz force $\mathbf{F} = q\mathbf{E}(t, \mathbf{x}) + q[\mathbf{v}, \mathbf{B}]$, where q is charge of particle moves with velocity $\mathbf{v} = \mathbf{p}/m$ in the presence of an electric field $\mathbf{E} = \mathbf{e}_i E_i(t, \mathbf{x})$ and a magnetic field $\mathbf{B}$. Here and later, we use the International System of Units (SI).

Foe isotropic media, the distribution function depends only on the momentum, $\rho_0 = \rho_0(|\mathbf{p}|)$. Then the direction of the vector $\mathbf{e}_i D^1_{p_i} \rho_0$ is the same as $\mathbf{p} = m\mathbf{v}$, and its scalar product with $[\mathbf{v}, \mathbf{B}]$ is equal to zero. Therefore, the magnetic field does not affect the distribution function in the linear approximation. As a result, we have

$$\frac{\partial \delta\rho}{\partial t} + \frac{p_i}{m}({}_0^C D^{\alpha}_{x_i} \delta\rho) + qE_i D^1_{p_i} \rho_0 = 0. \tag{102}$$

We assume that the perturbations (the function $\delta\rho$ and the field $\mathbf{E}$) are proportional to

$$\delta\rho, \mathbf{E} \sim E_{\alpha}[i(\mathbf{k}, \mathbf{x})^{\alpha}] \cdot \exp\{-i\omega t\}, \tag{103}$$

where $E_{\alpha}[z]$ is the Mittag-Leffler function [16]. Note that the exponent for $\alpha = 1$, $E_1[z] = \exp\{z\}$.

Choosing the x-axis along $\mathbf{k}$, we get $k_x = |\mathbf{k}|$, $(\mathbf{k}, \mathbf{v}) = |\mathbf{k}| v_x$. Then equation (102) gives

$$i(|\mathbf{k}|^{\alpha} v_x - \omega)\delta\rho + q(E_i D^1_{p_i} \rho_0) = 0, \tag{104}$$

where we use ${}_0^C D^{\alpha}_x E_{\alpha}[\lambda x^{\alpha}] = \lambda E_{\alpha}[\lambda x^{\alpha}]$, $\alpha > 0$, $\lambda \in \mathbb{C}$, (see Lemma 2.23 of [16]).

As a result, we get

$$\delta\rho = -\frac{q(E_i D^1_{p_i} \rho_0)}{i(|\mathbf{k}|^{\alpha} v_x - \omega)}. \tag{105}$$

In an unperturbed plasma-like media, the charge density ρ_{charge} is equal zero, since the media are isotropic. The charge density perturbed by the field is

$$\rho_{\text{charge}} = q \int \delta\rho \, d^3\mathbf{p} = iq^2 \int \frac{(E_i D^1_{p_i} \rho_0)}{|\mathbf{k}|^{\alpha} v_x - \omega} \, d^3\mathbf{p}, \tag{106}$$

where ρ_{charge} is the bound charge density. The electric polarization vector $\mathbf{P}$ is defined by the relations $\operatorname{div}\mathbf{P} = -\rho_{\text{charge}}$, and we get

$$i(\mathbf{k},\mathbf{P}) = -\rho_{\text{charge}}. \tag{107}$$

The polarization $\mathbf{P}$ defines $\mathbf{D} = \varepsilon_0\mathbf{E} + \mathbf{P}$, where ε_0 is the electric permittivity. If the field $\mathbf{E}$ be parallel to $\mathbf{k}$, then $\mathbf{P}$ be parallel to $\mathbf{k}$, and

$$\mathbf{P} = (\varepsilon_{\parallel}(|\mathbf{k}|) - \varepsilon_0)\mathbf{E}, \tag{108}$$

where $\varepsilon_{\parallel}(|\mathbf{k}|)$ is the longitudinal permittivity.

Substitution of (106) and (108) into (107) gives

$$(\varepsilon_{\parallel}(|\mathbf{k}|) - \varepsilon_0)(\mathbf{k}|,\mathbf{E}) = -q^2 \int \frac{E_i D^1_{p_i}\rho_0}{|\mathbf{k}|^{\alpha}v_x - \omega - i0}\, d^3\mathbf{p}. \tag{109}$$

Since we take the x-axis along the vector $\mathbf{k}$, then $\mathbf{E} = (E,0,0)$, and $(\mathbf{k},\mathbf{E}) = |\mathbf{k}|E_x$, $E_i D^1_{p_i}\rho_0 = E_x D^1_{p_x}\rho_0$.

As a result, the longitudinal permittivity can be derived [41] from the equation

$$\varepsilon_{\parallel}(|\mathbf{k}|) = \varepsilon_0 - \frac{q^2}{|\mathbf{k}|} \int \frac{D^1_{p_x}\rho_0(p_x)}{|\mathbf{k}|^{\alpha}p_x/m - \omega - i0}\, dp_x, \tag{110}$$

where we use the function

$$\rho_0(p_x) = \int \rho_0(|\mathbf{p}|)dp_y dp_z. \tag{111}$$

For the isotropic homogeneous case, we can use an equilibrium distribution $\rho_0(p_x)$.

Let us consider the case of the equilibrium Maxwell's distribution

$$\rho_0(p_x) = \frac{N_q}{\sqrt{2\pi m k_B T}} \exp\left(-\frac{p_x^2}{2mk_B T}\right), \tag{112}$$

where $k_B = 1.38065 \cdot 10^{-23}\ \text{m}^2{\cdot}\text{kg}/(\text{s}^2{\cdot}\text{K})$ is the Boltzmann constant, and N_q is the particles number density. In this case, equation (110) is written in the form

$$\varepsilon_{\parallel}(|\mathbf{k}|) = \varepsilon_0 + \frac{q^2 N_q}{|\mathbf{k}|^{1+\alpha}} \frac{2m}{\sqrt{\pi}(2mk_B T)^{3/2}} \int_{-\infty}^{+\infty} \frac{p_x \exp(-\frac{p_x^2}{2mk_B T})}{p_x - m\omega/|\mathbf{k}|^{\alpha} - i0}\, dp_x. \tag{113}$$

Let us define the variables:

$$z = \frac{p_x}{\sqrt{2mk_B T}}, \quad x = \sqrt{\frac{m}{2k_B T}} \cdot \frac{\omega}{|\mathbf{k}|^{\alpha}}. \tag{114}$$

Using these variables, equation (113) takes the form

$$\varepsilon_{\parallel}(|\mathbf{k}|) = \varepsilon_0 + \frac{q^2}{|\mathbf{k}|^{1+\alpha}} \frac{1}{\sqrt{\pi} k_B T} \int_{-\infty}^{+\infty} \frac{z e^{-z^2}}{z - x - i0} dz, \tag{115}$$

where the integral can be represented as

$$\int_{-\infty}^{+\infty} \frac{z e^{-z^2}}{z - x - i0} dz = \sqrt{\pi} + V.P. \int_{-\infty}^{+\infty} \frac{x e^{-z^2}}{z - x} dz + i\pi x e^{-x^2}. \tag{116}$$

Using equation (115), the special cases with for large and small x have been considered in the work [41].

For $x \ll 1$, the expression for the function $\varepsilon_{\parallel}(|\mathbf{k}|)$ was obtained [41] in the form

$$\varepsilon_{\parallel}(|\mathbf{k}|) = \varepsilon_0 + \frac{q^2 N_q}{k_B T |\mathbf{k}|^{1+\alpha}} - \frac{q^2 N_q m \omega^2}{k_B^2 T^2 |\mathbf{k}|^{3\alpha+1}} + \frac{q^2 N_q m^2 \omega^4}{4 k_B^3 T^3 |\mathbf{k}|^{5\alpha+1}} + \cdots. \tag{117}$$

The imaginary part of the permittivity is relatively small (not exponentially small), and in this case the condition $|\mathbf{k}|^{\alpha} p_x / m - \omega = 0$ is satisfied because of the smallness of the phase volume. We can use the standard notation of the Debye radius of screening

$$r_D = \sqrt{\frac{\varepsilon_0 k_B T}{N_q q^2}}, \tag{118}$$

and the Langmuir frequency for charged particle

$$\Omega_L = \sqrt{\frac{N_q q^2}{m \varepsilon_0}}. \tag{119}$$

Then equation (117) takes the form

$$\varepsilon_{\parallel}(|\mathbf{k}|) \approx \varepsilon_0 + \varepsilon_0 \frac{1}{r_D^2 |\mathbf{k}|^{1+\alpha}} - \varepsilon_0 \frac{\omega^2}{r_D^4 \Omega_L^2 |\mathbf{k}|^{3\alpha+1}} + \varepsilon_0 \frac{\omega^4}{4 r_D^6 \Omega_L^4 |\mathbf{k}|^{5\alpha+1}}. \tag{120}$$

Note that $\mathbf{k}$, $\mathbf{r}$, and x_i are dimensionless variable. Using (120), we can derive an equation for the scalar potentials of the electric field.

For $x \gg 1$, the expression for the function $\varepsilon_{\parallel}(|\mathbf{k}|)$ was obtained [41] in the form

$$\varepsilon_{\parallel}(|\mathbf{k}|) = \varepsilon_0 - \frac{q^2 N_q}{|\mathbf{k}|^{1+\alpha}} \frac{1}{k_B T} \left(\frac{k_B T}{m \omega^2} |\mathbf{k}|^{2\alpha} + \frac{3 k_B^2 T^2}{m^2 \omega^4} |\mathbf{k}|^{4\alpha} + \cdots \right). \tag{121}$$

The imaginary part of $\varepsilon_{\parallel}(|\mathbf{k}|)$ is exponentially small, since in a Maxwell's distribution only an exponentially small part of the charged particles have the velocity v_x =

$\omega/|\mathbf{k}| \gg v_T = \sqrt{k_B T/m}$, where v_T is the average velocity of charged particles. Then equation (121) takes the form

$$\varepsilon_{\|}(|\mathbf{k}|) \approx \varepsilon_0 - \varepsilon_0 \frac{\Omega_L^2}{\omega^2} |\mathbf{k}|^{\alpha-1} - \varepsilon_0 \frac{3r_D^2 \Omega_L^4}{\omega^4} |\mathbf{k}|^{3\alpha-1}, \tag{122}$$

where we used the Debye radius (118) and the Langmuir frequency (119).

Using equation (122), we can obtain the scalar potentials of the electric field in power-law nonlocal media, and then describe the difference of these potentials from the well-known Couloumb's and Debye's potentials.

8 Electric field in plasma-like media with PLSD

The case of the Coulomb potential corresponds to the first term in equation (120), that is, $\varepsilon_{\|}(|\mathbf{k}|) = \varepsilon_0$. The electrostatic potential of the point charge (17) is described by equation (21), which is the Coulomb's form of the potential.

If we consider only the first two terms in equation (120) with $\alpha = 1$, then we get that the standard expression of the differential equation for potential is (24) and the screened potential of the point charge (17).

If we consider the first two terms in equation (120) with $\alpha \neq 1$, then the longitudinal permittivity $\varepsilon_{\|}(|\mathbf{k}|)$ is

$$\varepsilon_{\|}(|\mathbf{k}|) = \varepsilon_0 \left(1 + \frac{1}{r_D^2 |\mathbf{k}|^{\alpha+1}} \right). \tag{123}$$

The equation of electrostatic potential has the form

$$-\Delta\Phi(\mathbf{r}) + \frac{1}{r_D^2} (-\Delta)^{(1-\alpha)/2} \Phi(\mathbf{r}) = \frac{1}{\varepsilon_0} \rho(\mathbf{r}), \tag{124}$$

where $(-\Delta)^{\alpha/2}$ is the fractional Laplacian in the Riesz form [24, 25, 27, 16, 22]. The particular solution (124) has the form

$$\Phi(\mathbf{r}) = \frac{1}{\varepsilon_0} \int_{\mathbb{R}^3} G_{1-\alpha,2}(\mathbf{r} - \mathbf{r}') \rho(\mathbf{r}')\, d^3\mathbf{r}', \tag{125}$$

where

$$G_{1-\alpha,2}(\mathbf{r}) = \frac{|\mathbf{r}|^{-1/2}}{(2\pi)^{3/2}} \int_0^\infty \left(r_D^{-2} \lambda^{1-\alpha} + \lambda^2 \right)^{-1} \lambda^{3/2} J_{1/2}(\lambda |\mathbf{r}|)\, d\lambda. \tag{126}$$

The electrostatic potential of the point charge (17) is

$$\Phi(\mathbf{r}) = \frac{1}{4\pi\varepsilon_0} \frac{Q}{|\mathbf{r}|} \cdot C_{1-\alpha,2}(|\mathbf{r}|), \quad (0 < \alpha < 1), \tag{127}$$

where the function

$$C_{1-\alpha,2}(|\mathbf{r}|) = \frac{2}{\pi}\int_0^{\infty} \frac{\lambda \sin(\lambda|\mathbf{r}|)}{r_D^{-2}\lambda^{1-\alpha} + \lambda^2}\, d\lambda, \tag{128}$$

describes the difference between this potential and the Coulomb's potential (21). The asymptotic behavior of $C_{\alpha,\beta}(|\mathbf{r}|)$ for $|\mathbf{r}| \to \infty$ and for $|\mathbf{r}| \to 0$ is described in [54] (see Sections 3.3.2 and 3.3.3 of [41]).

Let us consider the case of the first three terms in equation (120) with $\alpha \neq 1$. Then

$$\varepsilon_{\parallel}(|\mathbf{k}|) = \varepsilon_0\left(1 + \frac{1}{r_D^2|\mathbf{k}|^{1+\alpha}} - \frac{\omega^2}{r_D^4\Omega_L^2|\mathbf{k}|^{3\alpha+1}}\right). \tag{129}$$

For this case, the equation for potential has the form

$$-\Delta\Phi(\mathbf{r}) + \frac{1}{r_D^2}(-\Delta)^{(1-\alpha)/2}\Phi(\mathbf{r}) - \frac{\omega^2}{r_D^4\Omega_L^2}(-\Delta)^{(1-3\alpha)/2}\Phi(\mathbf{r}) = \frac{1}{\varepsilon_0}\rho(\mathbf{r}). \tag{130}$$

The particular solution of (130) is given [41] by the equation

$$\Phi(\mathbf{r}) = \frac{1}{\varepsilon_0}\int_{\mathbb{R}^3} G_{1-\alpha,1-3\alpha,2}(\mathbf{r}-\mathbf{r}')\rho(\mathbf{r}')\, d^3\mathbf{r}'. \tag{131}$$

The function $G_{1-\alpha,1-3\alpha,2}(\mathbf{r})$ is defined by

$$G_{1-\alpha,1-3\alpha,2}(\mathbf{r}) = \frac{|\mathbf{r}|^{-1/2}}{(2\pi)^{3/2}}\int_0^{\infty} \frac{\lambda^{3/2}J_{1/2}(\lambda|\mathbf{r}|)}{a_1\lambda^{1-\alpha} - a_2\lambda^{1-3\alpha} + \lambda^2}\, d\lambda, \tag{132}$$

where

$$a_1 = \frac{1}{r_D^2}, \quad a_2 = \frac{\omega^2}{r_D^4\Omega_L^2}. \tag{133}$$

For the of the point charge (17) we have

$$\Phi(\mathbf{r}) = \frac{1}{4\pi\varepsilon_0}\frac{Q}{|\mathbf{r}|}C_{1-\alpha,1-3\alpha,2}(|\mathbf{r}|), \tag{134}$$

where $0 < \alpha < 1/3$, and the function

$$C_{1-\alpha,1-3\alpha,2}(|\mathbf{r}|) = \frac{2}{\pi}\int_0^{\infty} \frac{\lambda \sin(\lambda|\mathbf{r}|)}{a_1\lambda^{1-\alpha} - a_2\lambda^{1-3\alpha} + \lambda^2}\, d\lambda, \quad (0 < \alpha < 1/3) \tag{135}$$

describes the difference between this potential and the Coulomb's potential.

Let us consider the case of the first three terms in the equation (122) with $\alpha \neq 1$. Then

$$\varepsilon_{\parallel}(|\mathbf{k}|) = \varepsilon_0\left(1 - \frac{\Omega_L^2}{\omega^2}|\mathbf{k}|^{\alpha-1} - \frac{3r_D^2\Omega_L^4}{\omega^4}|\mathbf{k}|^{3\alpha-1}\right). \tag{136}$$

The differential equation of the potential is

$$-\Delta\Phi(\mathbf{r}) - \frac{\Omega_L^2}{\omega^2}(-\Delta)^{(\alpha+1)/2}\Phi(\mathbf{r}) - \frac{3r_D^2\Omega_L^4}{\omega^4}(-\Delta)^{(3\alpha+1)/2}\Phi(\mathbf{r}) = \frac{1}{\varepsilon_0}\rho(\mathbf{r}). \tag{137}$$

If we consider only the first two terms in equation (137), then we have the equation

$$-\Delta\Phi(\mathbf{r}) - \frac{\Omega_L^2}{\omega^2}(-\Delta)^{(\alpha+1)/2}\Phi(\mathbf{r}) = \frac{1}{\varepsilon_0}\rho(\mathbf{r}). \tag{138}$$

For this case of the point charge (17), the electrostatic potential has the form

$$\Phi(\mathbf{r}) = \frac{1}{4\pi\varepsilon_0}\frac{Q}{|\mathbf{r}|}\cdot C_{\alpha+1,2}(|\mathbf{r}|). \tag{139}$$

The function

$$C_{\alpha+1,2}(|\mathbf{r}|) = \frac{2}{\pi}\int_0^\infty \frac{\lambda\sin(\lambda|\mathbf{r}|)}{\lambda^2 - (\Omega_L^2/\omega^2)\lambda^{\alpha+1}}\,d\lambda \tag{140}$$

describes the difference between this potential and the Coulomb's potential. The asymptotic behavior of $C_{\alpha,\beta}(|\mathbf{r}|)$ for $|\mathbf{r}| \to \infty$ and for $|\mathbf{r}| \to 0$ is described in [54] (see Sections 3.3.2 and 3.3.3).

9 Conclusion

In this chapter, we consider an application of fractional calculus to the nonlocal electrodynamics of media with power-law spatial dispersion (PLSD) that is proposed in [54, 48, 41]. We describe a new area of fractional nonlocal electrodynamics that deals with electric and magnetic fields in complex media with power-law spatial dispersion. The proposed fractional nonlocal electrodynamics is characterized by universal spatial behavior of electromagnetic fields in such media by analogy with the universal temporal behavior of low-loss dielectrics [14, 15, 34, 37, 35].

The media with PLSD are described by the noninteger power-law type of functions $\varepsilon_{\parallel}(|\mathbf{k}|)$. Equations for electrostatic potential $\Phi(\mathbf{r})$ in media with PLSD involve the fractional generalization of the Laplacian [24, 25, 27, 16, 22]. The simplest power-law forms of the longitudinal permittivity $\varepsilon_{\parallel}(|\mathbf{k}|) = \varepsilon_0(|\mathbf{k}|^{\alpha-2} + r_D^{-2}|\mathbf{k}|^{\beta-2})$ where $\alpha \geq 2$,

$0 < \beta \leq 2$ are considered. The parameter α characterizes the deviation from Coulomb's law due to nonlocal properties of the medium. The parameter β characterizes the deviation from Debye's screening due to noninteger power-law type of nonlocality in the medium. The fractional differential equations for electrostatic potential $\Phi(\mathbf{r})$ has the form $((-\Delta)^{\alpha/2}\Phi)(\mathbf{r}) + r_D^{-2}((-\Delta)^{\beta/2}\Phi)(\mathbf{r}) = \varepsilon_0^{-1}\rho(\mathbf{r})$, where $(-\Delta)^{\alpha/2}$ and $(-\Delta)^{\beta/2}$ are the Riesz fractional Laplacian [24, 25, 27, 16, 22], and $\mathbf{r}$, r_D are dimensionless variables. Analytic solutions of the fractional differential equations, which describe the electrostatic potentials in media with PLSD are suggested. For the point charge, the electrostatic potential has form $\Phi(\mathbf{r}) = Q/(4\pi\varepsilon_0|\mathbf{r}|)\cdot C_{\alpha,\beta}(|\mathbf{r}|)$, where $C_{\alpha,\beta}(|\mathbf{r}|)$ describes the differences of Coulomb's potential and Debye's screening. Using the analytic solutions of the fractional differential equations for electrostatic potentials, we describe the asymptotic behaviors of the electrostatic potential. The universal behavior of the media with PLSD at short and long distances is described. We also consider the electric field in the media with weak PLSD. The fractional Taylor series is very useful for approximating noninteger power-law functions. Using fractional generalization of the Taylor series, we get approximations for such type of media. If the orders of the fractional Taylor series approximation will be correlated with the type of weak spatial dispersion, then the fractional Taylor series for $\varepsilon_{\parallel}(|\mathbf{k}|)$ will be exact.

We describe the fractional kinetics of plasma-like media, which is proposed in [41], as a microscopic model for the electrodynamics of continuous media with PLSD. This fractional kinetics is based on the fractional Liouville equations, which are proposed in [47] and [29, 32, 33, 38]. Using the fractional Liouville equation, we obtain the power-law dependence of the absolute permittivity on the wave vector. This dependence leads to fractional differential equations for electrostatic potential that includes Riesz fractional derivatives. Particular solutions of these equations, which describe the electric potential of the point charge in the media with PLSD are suggested.

Bibliography

[1] V. M. Agranovich and Yu. N. Gartstein, Spatial dispersion and negative refraction of light, *Phys. Usp. (Adv. Phys. Sci.)*, **49**(10) (2006), 1029–1044.

[2] V. M. Agranovich and V. L. Ginzburg, *Crystal Optics with Spatial Dispersion and Theory of Exciton*, 1st ed., Moscow, Nauka, 1965; 2nd ed., Nauka, Moscow, 1979 (Russian).

[3] V. M. Agranovich and V. L. Ginzburg, *Spatial Dispersion in Crystal Optics and the Theory of Excitons*, Interscience Publishers, John Wiley and Sons, 1966, 316 pp.

[4] V. M. Agranovich and V. L. Ginzburg, *Crystal Optics with Spatial Dispersion and Excitons: An Account of Spatial Dispersion*, 2nd ed., Springer-Verlag, Berlin, 1984, 441 pp.

[5] A. F. Alexandrov and A. A. Rukhadze, *Lectures on the Electrodynamics of Plasma-Like Media*, Moscow State University Press, 1999, 336 pp. (Russian).

[6] A. F. Alexandrov and A. A. Rukhadze, *Lectures on the Electrodynamics of Plasma-Like Media, vol. 2. Nonequilibrium Environment*, Moscow State University Press, 2002, 233 pp. (Russian).

[7] A. F. Alexandrov, L. S. Bogdankevich, and A. A. Rukhadze, *Principles of Plasma Electrodynamics*, Vysshaya Shkola, Moscow, 1978 (Russian), and Springer-Verlag, Berlin, 1984.
[8] N. B. Baranova and B. Ya. Zeldovich, Two approaches to spatial dispersion in molecular scattering of light, *Sov. Phys. Usp.*, **22**(3) (1979), 143–159.
[9] H. Bateman and A. Erdelyi, *Tables of Integral Transforms, vol. 1*, McGraw-Hill, New York, 1954; or Moscow, Nauka, 1969 (Russian).
[10] V. L. Ginzburg and V. M. Agranovich, Crystal optics with allowance for spatial dispersion; exciton theory. I, *Sov. Phys. Usp.*, **5**(2) (1962), 323–346.
[11] V. L. Ginzburg and V. M. Agranovich, Crystal optics with allowance for spatial dispersion; exciton theory. II, *Sov. Phys. Usp.*, **5**(4) (1963), 675–710.
[12] P. Halevi, *Spatial Dispersion in Solids and Plasmas*, North-Holland, Amsterdam, New York, 1992, 681 pp., ISBN: 9780444874054.
[13] R. Ishiwata and Y. Sugiyama, Relationships between power-law long-range interactions and fractional mechanics, *Physica A*, **391** (2012), 5827–5838.
[14] A. K. Jonscher, The universal dielectric response, *Nature*, **267** (1977), 673–679.
[15] A. K. Jonscher, *Universal Relaxation Law*, Chelsea Dielectrics, London, 1996.
[16] A. A. Kilbas, H. M. Srivastava, and J. J. Trujillo, *Theory and Applications of Fractional Differential Equations*, Elsevier, Amsterdam, 2006.
[17] M. V. Kuzelev and A. A. Rukhadze, *Methods of Waves Theory in Dispersive Media*, World Scientific, Zurich, 2009; Fizmatlit, Moscow, 2007 (Russian).
[18] L. D. Landau and E. M. Lifshitz, *Course of Theoretical Physics, vol. 8. Electrodynamics of Continuous*, 2nd ed., pp. 358–371, Pergamon, Oxford, 1984, Chapter XII.
[19] N. Laskin and G. M. Zaslavsky, Nonlinear fractional dynamics on a lattice with long-range interactions, *Physica A*, **368** (2006), 38–54.
[20] R. L. Liboff, *Kinetic Theory: Classical, Quantum and Relativistic Description*, 2nd ed., Wiley, New York, 1998.
[21] G. A. Martynov, *Classical Statistical Mechanics*, Kluwer, Dordrecht, 1997.
[22] C. Pozrikidis, *The Fractional Laplacian*, CRC Press, Taylor and Francis Group, Boca Raton, 2016, 274 pp.
[23] A. P. Prudnikov, Yu. A. Brychkov, and O. I. Marichev, *Integrals and Series, vol. 2. Special Functions*, Gordon Breach Science Publishers/CRC Press, 1988–1992; Nauka, Moscow, 1983.
[24] M. Riesz, L'integrale de Riemann–Liouville et le probleme de Cauchy pour l'equation des ondes, *Bull. Soc. Math. Fr.*, **67** (1939), 153–170, in French.
[25] M. Riesz, L'integrale de Riemann–Liouville et le Probleme de Cauchy, *Acta Math.*, **81**(1) (1949), 1–222, in French.
[26] A. A. Rukhadze and V. P. Silin, Electrodynamics of media with spatial dispersion, *Sov. Phys. Usp.*, **4**(3) (1961), 459–484.
[27] S. G. Samko, A. A. Kilbas, and O. I. Marichev, *Integrals and Derivatives of Fractional Order and Applications*, Nauka i Tehnika, Minsk, 1987; *Fractional Integrals and Derivatives Theory and Applications*, Gordon and Breach, New York, 1993.
[28] V. P. Silin and A. A. Ruhadze, *Electromagnetic Properties of Plasmas and Plasma-like Media*, Gosatomizdat, Moscow, 1961; 2nd ed., USSR, Librikom, Moscow, 2012 (Russian).
[29] V. E. Tarasov, Fractional systems and fractional Bogoliubov hierarchy equations, *Phys. Rev. E*, **71**(1) (2005), 011102.
[30] V. E. Tarasov, Continuous limit of discrete systems with long-range interaction, *J. Phys. A*, **39**(48) (2006), 14895–14910, arXiv:0711.0826.
[31] V. E. Tarasov, Map of discrete system into continuous, *J. Math. Phys.*, **47**(9) (2006), 092901, 24 pp., arXiv:0711.2612.

[32] V. E. Tarasov, Fractional statistical mechanics, *Chaos*, **16**(3) (2006), 033108.
[33] V. E. Tarasov, Liouville and Bogoliubov equations with fractional derivatives, *Mod. Phys. Lett. B*, **21**(5) (2007), 237–248.
[34] V. E. Tarasov, Universal electromagnetic waves in dielectrics, *J. Phys. Condens. Matter*, **20**(17) (2008), 175223, arXiv:0907.2163.
[35] V. E. Tarasov, Fractional equations of Curie–von Schweidler and Gauss laws, *J. Phys. Condens. Matter*, **20**(14) (2008), 145212, 5 pp.
[36] V. E. Tarasov, Fractional vector calculus and fractional Maxwell's equations, *Ann. Phys.*, **323**(11) (2008), 2756–2778.
[37] V. E. Tarasov, Fractional integro-differential equations for electromagnetic waves in dielectric media, *Theor. Math. Phys.*, **158**(3) (2009), 355–359.
[38] V. E. Tarasov, *Fractional Dynamics: Applications of Fractional Calculus to Dynamics of Particles, Fields and Media*, Springer, New York, 2010.
[39] V. E. Tarasov, *Theoretical Physics Models with Integro-Differentiation of Fractional Order*, IKI, RCD, Moscow, Izhevsk, 2011 (Russian).
[40] V. E. Tarasov, Review of some promising fractional physical models, *Int. J. Mod. Phys. B*, **27**(9) (2013), 1330005, arXiv:1502.07681.
[41] V. E. Tarasov, Power-law spatial dispersion from fractional Liouville equation, *Phys. Plasmas*, **20**(10) (2013), 102110, arXiv:1307.4930.
[42] V. E. Tarasov, Lattice model with power-law spatial dispersion for fractional elasticity, *Cent. Eur. J. Phys.*, **11**(11) (2013), 1580–1588, arXiv:1501.01201.
[43] V. E. Tarasov, Fractional gradient elasticity from spatial dispersion law, *ISRN Condens. Matter Phys.*, **2014** (2014), 794097, arXiv:1306.2572.
[44] V. E. Tarasov, Toward lattice fractional vector calculus, *J. Phys. A*, **47**(35) (2014), 355204, 51 pp., DOI: 10.1088/1751-8113/47/35/355204.
[45] V. E. Tarasov, Lattice fractional calculus, *Appl. Math. Comput.*, **257** (2015), 12–33, DOI: 10.1016/j.amc.2014.11.033.
[46] V. E. Tarasov, Exact discrete analogs of derivatives of integer orders: Differences as infinite series, *J. Math.*, **2015** (2015), 134842, DOI: 10.1155/2015/134842.
[47] V. E. Tarasov, Fractional Liouville equation on lattice phase-space, *Phys. A, Stat. Mech. Appl.*, **421** (2015), 330–342, arXiv:1503.04351.
[48] V. E. Tarasov, Electric field in media with power-law spatial dispersion, *Mod. Phys. Lett. B*, **30**(10) (2016), 1650132, 11 pp., DOI: 10.1142/S0217984916501323.
[49] V. E. Tarasov, United lattice fractional integro-differentiation, *Fract. Calc. Appl. Anal.*, **19**(3) (2016), 625–664, DOI: 10.1515/fca-2016-0034.
[50] V. E. Tarasov, Exact discretization by Fourier transforms, *Commun. Nonlinear Sci. Numer. Simul.*, **37** (2016), 31–61, DOI: 10.1016/j.cnsns.2016.01.006.
[51] V. E. Tarasov, Exact discretization of Schrodinger equation, *Phys. Lett. A*, **380**(1–2) (2016), 68–75, DOI: 10.1016/j.physleta.2015.10.039.
[52] V. E. Tarasov, Exact discrete analogs of canonical commutation and uncertainty relations, *Mathematics*, **4**(3) (2016), DOI: 10.3390/math4030044.
[53] V. E. Tarasov, Exact discretization of fractional Laplacian, *Comput. Math. Appl.*, **73**(5) (2017), 855–863, DOI: 10.1016/j.camwa.2017.01.012.
[54] V. E. Tarasov and J. J. Trujillo, Fractional power-law spatial dispersion in electrodynamics, *Ann. Phys.*, **334** (2013), 1–23, arXiv:1503.04349.
[55] V. E. Tarasov and G. M. Zaslavsky, Fractional dynamics of coupled oscillators with long-range interaction, *Chaos*, **16**(2) (2006), 023110.
[56] V. E. Tarasov and G. M. Zaslavsky, Fractional dynamics of systems with long-range interaction, *Commun. Nonlinear Sci. Numer. Simul.*, **11**(8) (2006), 885–898.

[57] T. L. Van Den Berg, D. Fanelli, and X. Leoncini, Stationary states and fractional dynamics in systems with long-range interactions, *Europhys. Lett.*, **89**(5) (2010), 50010, DOI: 10.1209/0295-5075/89/50010.
[58] G. M. Zaslavsky, Chaos, fractional kinetics, and anomalous transport, *Phys. Rep.*, **371**(6) (2002), 461–580.

Aleksander Stanislavsky and Karina Weron

Fractional-calculus tools applied to study the nonexponential relaxation in dielectrics

Abstract: Motion of charges, their accumulation, and discharge arise in many physical, chemical, and biological processes in nature. The simplest theoretical description of the relaxation phenomenon as a function of time is the exponential law. However, the relaxation properties of various physical systems (dielectrics, amorphous semiconductors and insulators, ferroelectrics, polymers, and others) strongly deviate from the classical exponential decay. They relax in a nonexponential fashion and have attracted an immediate interest of scientists and technologists for a long time. A theoretical description of the nonexponential relaxation is one of the most important problems of modern physics. In this chapter, we show the role played by the fractional calculus tools in a realistic physical treatment of dielectric relaxation.

Keywords: Power-law memory, fractional derivative, relaxation

MSC 2010: 35R11, 26A33

1 Introduction

It is generally accepted to distinguish materials by their electrical behavior as conductors, semiconductors, and insulators (or dielectric materials). Applied to dielectrics, the main property, namely complex susceptibility, is typically measured as a function of frequency in dielectric/impedance spectroscopy. The characteristics represent interaction of an external field with the electric dipole moment of a dielectric sample. Now dielectric materials play an extremely important role in science and technology. It is enough to recall that every electronic circuit needs a dielectric medium to build an appropriate system. Hence, the relaxation behavior of different dielectric materials attracts much interest of the dielectric society.

Any relaxation process is experimentally observed as a physical macroscopic magnitude (concentration, current, etc.) monotonically decays or grows in time. In case

Acknowledgement: A. S. is grateful to the Faculty of Pure and Applied Mathematics and the Hugo Steinhaus Center for pleasant hospitality during his visit in Wrocław University of Science and Technology. He is also grateful for a partial support from the NCN Maestro grant No. 2012/06/A/ST1/00258.

Aleksander Stanislavsky, Institute of Radio Astronomy, National Academy of Sciences of Ukraine, Mystetstv St., 4, 61002 Kharkiv, Ukraine; and V. N. Karazin Kharkiv National University, Svobody Sq., 4, 61022 Kharkiv, Ukraine, e-mail: a.a.stanislavsky@rian.kharkov.ua
Karina Weron, Faculty of Fundamental Problems of Technology, Wrocław University of Science and Technology, Wybrzeże Wyspiańskiego 27, 50-370 Wrocław, Poland, e-mail: karina.weron@pwr.edu.pl

of the dielectric relaxation, this process is defined as an approach to equilibrium of a dipolar system driven out of equilibrium by a step or alternating external electric field. The relaxation function $\phi(t)$ (satisfying $\phi(0) = 1$ and $\phi(\infty) = 0$) could be considered as a solution of the kinetic (master) equation

$$\frac{d\phi(t)}{dt} = -r(t)\phi(t), \quad \phi(0) = 1. \tag{1}$$

The nonnegative quantity $r(t)$ is the transition rate of the system. The time-domain function $\phi(t)$, describing damping of the electric dipole moment after the interaction of a dielectric material with an external field, relates to the complex susceptibility $\chi(\omega)$ as $\chi(\omega) = \phi^*(\omega)(\chi_0 - \chi_\infty) + \chi_\infty$, where the frequency domain relaxation function (or shape function) $\phi^*(\omega)$ is the inverse Stieltjes–Fourier transform of $\phi(t)$, namely

$$\phi^*(\omega) = \int_0^\infty e^{-it\omega}\, d(1 - \phi(t)). \tag{2}$$

The constant χ_∞ represents the asymptotic value of $\chi(\omega)$ at high frequencies, and χ_0 is the complex susceptibility for small ω. Sometimes, it is also useful to know the derivative $f(t) = -d\phi(t)/dt$, called the response function and connected with the shape function $\phi^*(\omega)$ by the one-side Fourier transform. The relaxation function describes the decay of polarization, and the response function is its decay rate. Thus, experimental characterization of dielectric properties in a wide range of materials is just contained in the specified parameters such as relaxation or response functions and complex dielectric susceptibility.

Over the past 100 years, a huge number of dielectric experimental data, covering 17 decades (10^{-5}–10^{12} Hz in frequency or 10^{-12}–10^5 s in time), manifests strong deviation from the exponential decay. For this reason, many empirical relaxation laws have been proposed. They may be regarded as generalizations of the exponential (or Debye, D) relaxation law. The most known of them, established empirically for a very wide range of materials, are the Cole-Cole (CC) law [3, 4], the Cole–Davidson (CD) law [5, 6], and the Havriliak–Negami (HN) law [18, 19]. Their form, utilized in the frequency domain, is convenient to write as

$$\phi^*_{\mathrm{HN}}(\omega) = \frac{1}{[1 + (i\omega/\omega_p)^\alpha]^\gamma}, \quad 0 < \alpha, \gamma \le 1. \tag{3}$$

The D case has $\alpha = \gamma = 1$, and the CD law originates from $\alpha = 1$, $0 < \gamma < 1$, whereas $0 < \alpha < 1$, $\gamma = 1$ is CC. The stretched exponential relaxation, known also as the Kohlrausch–Williams–Watts (KWW) law, has a simpler form in time [58], where it reads

$$\phi_{\mathrm{KWW}}(t) = e^{-(t/\tau_p)^\alpha} \tag{4}$$

with $0 < \alpha < 1$. The value $\tau_p = \omega_p^{-1}$ is the time constant characteristic for a given material. If $\alpha = 1$, the KWW function gives the simple exponential form.

Following Jonscher [22, 23], the commonly observed nonexponential relaxation behavior is characterized by the high- and low-frequency fractional-power dependence in the complex dielectric susceptibility $\chi(\omega) = \chi'(\omega) - i\chi''(\omega)$:

$$\chi(\omega) \propto \left(\frac{i\omega}{\omega_p}\right)^{n-1} \quad \text{for } \omega \gg \omega_p \tag{5}$$

and

$$\Delta\chi(\omega) \propto \left(\frac{i\omega}{\omega_p}\right)^{m} \quad \text{for } \omega \ll \omega_p, \tag{6}$$

where positive constant ω_p is the loss peak frequency characteristic for the dielectric material under consideration, and $\Delta\chi(\omega) = \chi_0 - \chi(\omega)$. Eventually, a great majority of dielectric materials is characterized only by two parameters (power-law exponents) m and $1 - n$, both falling strictly within the range (0,1], and this feature is independent on particular details of examined dielectric materials.

From the physical point of view, nonexponential relaxation in dielectrics is characterized by the fact that relaxing entities (dipoles) interact not only among themselves, but also with the surrounding medium to modify disorder of this medium and to affect other entities. Consequently, the motion of dipoles (change of their direction) can be very similar to a random walk, drawing parallels between relaxation and diffusion in literature (see, e. g., [40, 28, 16, 10]). Then any excited dielectric material tending to equilibrium passes from less disordered states to more disordered ones. Its macroscopic evolution is a result of averaging over local random properties of dipoles, and features of microscopic stochastic dynamics (of dipoles) is manifested in the macroscopic behavior of the dielectric systems as a whole. One of such manifestations is the need to describe the dielectric evolution in fractional calculus. The aim of this chapter is to present the elementary exposition to the theory of nonexponential relaxation in dielectrics, which is manifested in the need to involve fractional calculus. In Section 2, we discuss the fractional description of macroscopic dielectric properties, arising from the susceptibility. Microscopic evolution of dipoles (many-body problem) in dielectrics preferably describe probabilistic methods. Subsequent sections are just devoted to the concepts. Although dynamical processes in such systems have a stochastic background, their characterization wholly is deterministic (universal relaxation laws). The summary is contained in the Conclusions section.

2 Relaxation paradigms

The theoretical description of nonexponential relaxation can be conditionally divided into two directions: deterministic and probabilistic. The former approach, based on the time-independent transition rate of the relaxing system, suggests a macroscopic description of the dielectric properties with equations of a new fractional-equation type. Using the common universal pattern, equations (5) and (6), in the papers [49–51] from the definition of polarization density $\mathbf{P}(t,r)$ and the fractional power law $\tilde{\chi}(\omega) = \chi_\alpha(i\omega)^{-\alpha}$ with a positive constant χ_α and $0 < \alpha < 1$, one can obtain the polarization density $\mathbf{P}(t,r)$ in the high-frequency domain proportional to the fractional Riemann–Liouville (RL) integral I_t^α of the electric field $\mathbf{E}(t,r)$ [39], namely

$$\mathbf{P}(t,r) = \varepsilon_0\chi_\alpha(I_t^\alpha\mathbf{E})(t,r).$$

Similarly, for the low-frequency domain from the fractional power law $\tilde{\chi}(\omega) = \tilde{\chi}(0) - \chi_\beta(i\omega)^\beta$ with positive constants χ_β, $\tilde{\chi}(0)$ and $0 < \beta < 1$, the polarization density yields

$$\mathbf{P}(t,r) = \varepsilon_0\tilde{\chi}(0)\mathbf{E}(t,r) - \varepsilon_0\chi_\beta(D_t^\beta\mathbf{E})(t,r).$$

Note that this equation is expressed in terms of the fractional RL derivative D_t^β [39] of the electric field. Next, using the Maxwell equations, expressing in terms of $\mathbf{P}(t,r)$ and $\mathbf{E}(t,r)$ (or the magnetic field $\mathbf{B}(t,r)$), one obtains the fractional differential equation for the electric (or magnetic, respectively) field with $\omega \ll \omega_p$ or $\omega \gg \omega_p$. An important property of the fractional differential equations is that their solutions have fractional power-law tails.

The concept of time-dependent transition rate $r(t)$ in the study of nonexponential relaxation is not always convenient because of its overloaded form. Really, it becomes very cumbersome in the HN case. Even in the case of the CC relaxation function the transition rate $r(t)$ is expressed in terms of a ratio of functions. In [54], it was shown that the CC relaxation function is described by the one-parameter Mittag-Leffler (ML) function [8]. If we want to save $r(t) = \text{const}$ as in the D law, the differentiation operator in equation (1) must be replaced by the so-called Caputo fractional derivative [2]. For $0 < \alpha < 1$, the relationship between RL and Caputo fractional derivatives is

$${}^{\mathrm{C}}D_t^\alpha f(t) = D_t^\alpha f(t) - \frac{t^{-\alpha}}{\Gamma(1-\alpha)}f(0),$$

where $\Gamma(z)$ is the Euler's gamma function. Then the CC relaxation equation takes the following fractional form [31, 20]:

$$({}^{\mathrm{C}}D_t^\alpha + \tau_p^{-\alpha})\phi_{\mathrm{CC}}(t) = 0 \tag{7}$$

with the initial condition $\phi_{\mathrm{CC}}(0) = 1$. Introducing the fractional pseudo-differential operator $(D_t^\alpha + \tau^{-\alpha})^\gamma$ from the Fourier inversion of equation (3), some attempts have been made to find robust and practical characterizations of the HN model [36, 1, 11, 15, 12–14]. Using the function,

$$e_{\alpha,\beta}^\gamma(t;\lambda) = t^{\beta-1}E_{\alpha,\beta}^\gamma(t^\alpha\lambda),$$

where $E^{\gamma}_{\alpha,\beta}(z)$ is the Prabhakar (or three-parameter ML) function [37], according to [11], the above mentioned fractional pseudo-differential operator can be written as a convolution

$$(D_t^{\alpha} + \tau^{-\alpha})^{\gamma} f(t) = \frac{d}{dt} \int_0^t e^{-\gamma}_{\alpha,1-\alpha\gamma}(t-u; -\tau^{-\alpha}) f(u)\, du. \tag{8}$$

Moreover, the operator is regularized in the Caputo sense. They are clearly generalizations of the classical fractional derivatives of the RL and Caputo type. In the limiting case $\gamma = 1$, it is immediate to obtain that $e^{-1}_{\alpha,1-\alpha}(t; -\tau^{-\alpha}) = t^{-\alpha}/\Gamma(1-\alpha)$, that is, there is the limit passage to conventional fractional operators.

3 Stochastic nature of relaxation

In comparison with the deterministic methodology, the probabilistic formalism approaches to description of the nonexponential relaxation differently. It helps to build bridges between the local random characteristics of dielectric materials and the universal deterministic relaxation laws. Stochastic tools hidden behind the empirical dielectric relaxation laws (5) and (6) were detailed in the recent review [46]. Therefore, we briefly describe the achievements of this approach with an emphasis on fractional calculus. In the framework of the paradigm, there are several successful concepts. To derive the nonexponential decay, one of them is based on a picture of parallel relaxations, in which each degree of freedom (each relaxation channel) relaxes independently with random relaxation time (see, e. g., [29, 34, 7]). From the probabilistic point of view, the idea reveals the weighted average $\langle\cdots\rangle$ of an exponential decay

$$\phi(t) = \langle e^{-t\tilde{\beta}} \rangle = \int_0^{\infty} \exp(-tb) w(b)\, db, \tag{9}$$

with respect to the distribution $w(b)db$ of the random effective relaxation rate $\tilde{\beta}$ being a normalized sum of individual relaxation rates $\{\beta_i\}$ with support of $b \in [0, \infty)$. It is assumed that the random variable β_i is the relaxation rate of the ith dipole, $\{\beta_i\}$ where $i = 1, \dots, N$ form a sequence of nonnegative independent identically distributed random variables, and any dielectric system consists of a large number N of relaxing dipoles. This approach allows studying different dielectric systems that follow not only the stretched exponential relaxation (KWW) law but also the case of HN and other patterns (see [46] and the references therein). In deriving the probability density function (pdf) $w(b)$, the interaction of dipoles and their environment is described by a mixture of random variables, which can follow Lévy α-stable distributions, the gamma distribution, etc. As an example, we illustrate the concept using the recent results from [45].

In each dielectric system, capable of responding to an external electric field and demonstrating nonexponential relaxation, only a part (in general, random) of the total number N of dipoles in the system is able to follow the changes of the external field [22, 23]. A core of the cluster model [55], leading to the Jonscher's two-power-law relaxation behavior [18] and [19], includes random cluster sizes N_i, random supercluster sizes M_j, and random individual relaxation rates β_{iN}. On the basis of limit theorems of the probability theory, it is possible to find the distribution of the limit $\overline{\beta}$ representing a large relaxing system, even with rather limited knowledge about the distributions of micro/mesoscopic quantities [24]. Assume that $M = \{M_j,\ j = 1, 2, \ldots\}$, $N = \{N_i,\ i = 1, 2, \ldots\}$ and $\beta = \{\beta_i,\ i = 1, 2, \ldots\}$ are independent sequences, each of which consists of independent and identically distributed positive random variables, M_j and N_i being integer-valued. Let both N_j and β_j have heavy-tailed distributions. Underestimating the number of clusters and superclusters [45], the relaxation rate of the clustered system considered above is

$$\overline{\beta}_{\mathrm{JWS}} \overset{d}{=} \frac{1}{\tau_p} \frac{Z_\alpha}{S_\alpha} (\mathcal{B}_\gamma)^{1/\alpha}, \tag{10}$$

where $\overset{d}{=}$ means the equality in distribution, random variables S_α and Z_α are distributed with one-sided (Lévy) α-stable distributions, and $\mathcal{B}_\gamma$ behaves as a random variable under the generalized arcsine distribution. The abbreviation JWS happened historically [15, 52]. Notice that for $0 < \alpha, \gamma < 1$ the relaxation function $\phi_{\mathrm{JWS}}(t)$ can be represented by a weighted average of an exponential decay $\langle e^{-t\overline{\beta}_{\mathrm{JWS}}} \rangle$ with respect to the distribution of the above effective relaxation rate. In this case, the pdf of the effective relaxation rate $\overline{\beta}_{\mathrm{JWS}}$ reads

$$w_{\mathrm{JWS}}(b) = \begin{cases} \frac{\sin(\gamma\psi(b))(\pi b)^{-1}}{[(\tau_p b)^{-2\alpha} + 2(\tau_p b)^{-\alpha}\cos(\pi\alpha) + 1]^{\gamma/2}} & \text{for } b > 0, \\ 0 & \text{for } b \le 0, \end{cases}$$

where $\psi(b) = \frac{\pi}{2} - \arctan(\frac{(b\tau_p)^\alpha + \cos(\pi\alpha)}{\sin(\pi\alpha)})$ [25]. Consequently, the JWS relaxation function is of the following form:

$$\phi_{\mathrm{JWS}}(t) = \frac{1}{\Gamma(\gamma)\Gamma(1-\gamma)} \int_0^1 E_\alpha(-zt^\alpha/\tau_p^\alpha) z^{\gamma-1}(1-z)^{-\gamma}\, dz, \tag{11}$$

including the one-parameter ML function $E_\alpha(x) = \sum_{k=0}^{\infty} x^k/\Gamma(\alpha k+1)$ in convolution. The above result can be expressed in terms of the three-parameter ML function, namely

$$\phi_{\mathrm{JWS}}(t) = E^{\gamma}_{\alpha,1}[-(t/\tau_p)^\alpha].$$

Finally, it is useful to write the kinetic equation for the JWS relaxation function. If one applies the Laplace table formula (see, e. g., [32]),

$$\int_0^\infty e^{-st} t^{\beta-1} E^{\gamma}_{\alpha,\beta}(\pm\lambda t^{\alpha})\, dt = \frac{s^{\alpha\gamma-\beta}}{(s^{\alpha} \mp \lambda)^{\gamma}},$$

then $\phi_{\mathrm{JWS}}(t)$ is the solution of the fractional pseudodifferential equation

$$(D^{\alpha}_t + \tau_p^{-\alpha})^{\gamma} \phi_{\mathrm{JWS}}(t) = \frac{t^{-\alpha\gamma}}{\Gamma(1-\alpha\gamma)} \tag{12}$$

with the initial condition $\phi_{\mathrm{JWS}}(0) = 1$. For $\gamma \to 1$, the kinetic equation (12) transforms into the kinetic equation for the CC relaxation; see equation (7). Note that appearance of the fractional derivative in (12) originates from the one-sided α-stable law, and the exponent γ is an "echo" of the generalized arcsine distribution. Together they describe the major features of stochastic processes in the dielectric systems. Generally, this extends the probabilistic interpretation of the fractional calculus suggested in [43]. According to [22], the above mentioned type of relaxation responses takes about 20 % from the general number of the fractional two-power relaxation dependencies, whereas each of the CC and CD patterns occurs in ~10 % and together with the HN law give (~80 %). Therefore, the JWS relaxation law may be termed as atypical. It should be pointed out that the procedure of overestimating the number of clusters and superclusters leads to the HN relaxation law (see more details in [55]).

The JWS law has the frequency-domain shape function itself [46, 45], namely

$$\phi^*_{\mathrm{JWS}}(\omega) = \int_0^\infty e^{-(i\omega/\omega_p)^{\alpha} t} \varrho_{\gamma}(t)\, dt,$$

where

$$\varrho_{\gamma}(x) = \frac{1}{\Gamma(\gamma)\Gamma(1-\gamma)} \int_0^1 e^{-xz} z^{\gamma}(1-z)^{-\gamma}\, dz$$

for $x > 0$. Consequently, we get the simple expression

$$\phi^*_{\mathrm{JWS}}(\omega) = 1 - \frac{(i\omega/\omega_p)^{\alpha\gamma}}{[1 + (i\omega/\omega_p)^{\alpha}]^{\gamma}}. \tag{13}$$

This result points to the following relationship with the HN relaxation function

$$\phi^*_{\mathrm{JWS}}(\omega) = 1 - (i\omega/\omega_p)^{\alpha\gamma} \phi^*_{\mathrm{HN}}(\omega).$$

It is interesting to compare the power-law characteristics of the relaxation response for both laws (Figure 1). For them, the exponents n and m fall in the range $(0, 1)$, and are defined by the parameters $0 < \alpha < 1$ and $0 < \gamma < 1$. The HN relaxation is characterized by the exponents $m = \alpha$ and $m > 1 - n = \alpha\gamma$, and it fits the so-called typical dielectric spectroscopy data, while the JWS case demonstrates up-down with $m = \alpha\gamma$ and $m < 1 - n = \alpha$ and it fits the atypical two-power-law relaxation pattern which, as shown by the experimental evidence (see, e. g., [22, 23] and references therein), cannot be neglected.

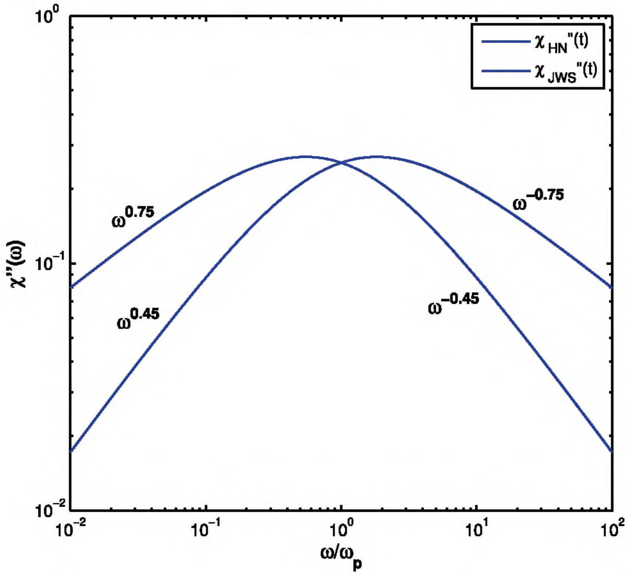

Figure 1: Log-log plots of the frequency-domain relaxations functions, corresponding to the HW and JWS laws, with $\alpha = 0.75$ and $\gamma = 0.6$.

4 Two-state systems

Relaxation, following the D law, may be simply explained by means of a two-state system [38]. Let N be the common number of entities in a dielectric system. If $N_\uparrow$ is the number of dipoles in the state $\uparrow$, $N_\downarrow$ is the number of dipoles in the state $\downarrow$ so that $N = N_\uparrow + N_\downarrow$. Assume that for $t = 0$ the system is stated in such an order so that the states $\uparrow$ dominate, namely

$$\frac{N_\uparrow(t=0)}{N} = n_\uparrow(0) = 1, \qquad \frac{N_\downarrow(t=0)}{N} = n_\downarrow(0) = 0,$$

where $n_\uparrow$ is the part of dipoles in the state $\uparrow$, $n_\downarrow$ the part in the state $\downarrow$. Denote the transition rates by B defined from microscopic properties of the system (for instance, according to the given Hamiltonian of interaction and the Fermi's golden rule). In this case, the kinetic equation describing the ordinary relaxation (D relaxation) takes the form

$$\begin{cases} \dot{n}_\uparrow(t) - B\{n_\downarrow(t) - n_\uparrow(t)\} = 0, \\ \dot{n}_\downarrow(t) - B\{n_\uparrow(t) - n_\downarrow(t)\} = 0, \end{cases} \tag{14}$$

where, as usual, the dotted symbol means the first-order time derivative. The relaxation function for the simple two-state system is

$$\phi_D(t) = 1 - 2n_\downarrow(t) = 2n_\uparrow(t) - 1 = \exp(-2Bt), \tag{15}$$

where $2B = \tau_p^{-1}$ is the characteristic material constant. It is easy to see that the steady state of the system corresponds to equilibrium with $n_\uparrow(\infty) = n_\downarrow(\infty) = 1/2$. Clearly, its response has an exponential character. However, this happens to be the case when entities relax irrespectively of each other and of their environment. If the entities interact with their environment, and the interaction is complex (or random), their contribution in relaxation already will not result in any exponential decay. This idea gives a new breath to the study of dielectric relaxation.

4.1 Time arrow with irregular steps

The system of equations (14) is a particular case of the general kinetic equation used for the description of evolution of Markov random processes [53]. It is governed by the deterministic array of time. As it was shown in [43, 41, 42], if one accounts for the subordination of $n_\uparrow(\tau)$ and $n_\downarrow(\tau)$ by an appropriate random process, the kinetic equation (14) changes its form in dependence of chosen subordinators. Recall [9], a subordinator itself is a stochastic process (with independent, stationary, nonnegative increments) describing the evolution of time within another stochastic process. Such a subordinator introduces a new time clock (stochastic time arrow). In fact, the notion of a subordinator allows determining the random number of "time steps." This concept is very helpful to account for appearance of traps in the evolution of relaxing entities.

Let us consider time evolution of the number of dipoles in the states $\downarrow$ and $\uparrow$ as parent random processes in the sense of subordination, assuming that they may be subordinated by another random process with a pdf, say $p(t,\tau)$. Then the entity ratio $m_\uparrow(t)$ in the state $\uparrow$ and the entity ratio $m_\downarrow(t)$ in the state $\downarrow$ under the temporal subordination are determined by the following integral relations:

$$m_\uparrow(t) = \int_0^\infty n_\uparrow(\tau)p(t,\tau)\,d\tau, \quad m_\downarrow(t) = \int_0^\infty n_\downarrow(\tau)p(t,\tau)\,d\tau. \tag{16}$$

To derive the equations describing the evolution $m_\downarrow(t)$ and $m_\uparrow(t)$, it is necessary to know a subordinator in the clear form.

If a new time clock is the inverse Lévy α-stable subordinator, then the equation of the two-state system (16) takes the following form:

$$\begin{cases} {}^{C}D_t^\alpha m_\uparrow(t) - B\{m_\downarrow(t) - m_\uparrow(t)\} = 0, \\ {}^{C}D_t^\alpha m_\downarrow(t) - B\{m_\uparrow(t) - m_\downarrow(t)\} = 0, \end{cases} \tag{17}$$

expressed in terms of the Caputo derivative with $0 < \alpha \le 1$. In this case, the relaxation function reads

$$\phi_{CC}(t) = 1 - 2m_\downarrow(t) = 2m_\uparrow(t) - 1 = E_\alpha(-2Bt^\alpha).$$

Evolution of the states $\downarrow$ and $\uparrow$ is shown in Figure 2. Following equation (2), the frequency-domain CC function is

$$\phi^*_{CC}(\omega) = \frac{1}{1 + (i\omega/\omega_p)^\alpha}, \quad 0 < \alpha \le 1. \tag{18}$$

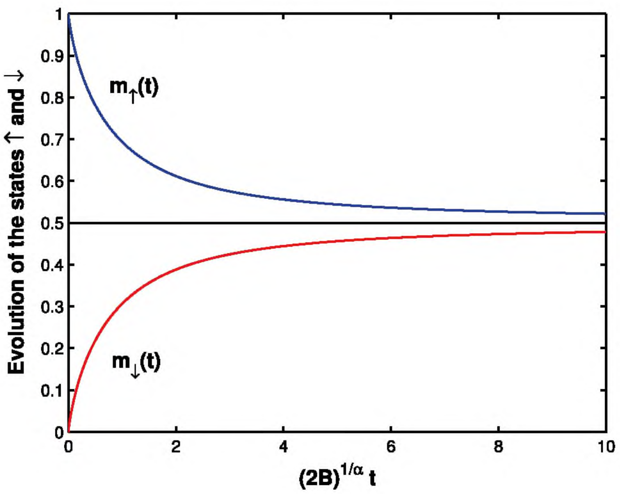

Figure 2: Relaxation of the part $m_\uparrow$ of dipoles in the state $\uparrow$ and the part $m_\downarrow$ of dipoles in the state $\downarrow$ (for $\alpha = 0.8$).

With reference to the theory of subordination [30], the CC law shows that the dipoles tend to equilibrium via motion alternating with stops so that the temporal intervals between them are random.

Notice, by a slight change in the method we can easily obtain not only the CC law of relaxation. The approach has a wide potential that will be presented in the next subsection.

4.2 Memory function

If the distribution of a nonnegative stochastic process $U(\tau)$ is infinitely divisible, then its Laplace transform takes the form

$$\langle e^{-sU(\tau)} \rangle = e^{-\tau\Psi(s)}, \tag{19}$$

where $\Psi(s)$ is the Laplace exponent according to the Lévy–Khintchine formula [9] (called also as the Lévy exponent). Many examples of such distributions are well known [21]. Among them are such as Gaussian, inverse Gaussian, α-stable, tempered α-stable, exponential, gamma, compound Poisson, Pareto, Linnik, Mittag-Leffler, and others, including completely asymmetric α-stable distributions. Let $f(\tau, t)$ be the pdf of $U(\tau)$. Then the mean $\langle e^{-sU(\tau)} \rangle$ is the Laplace transform of $f(\tau, t)$ equal to

$$\langle e^{-sU(\tau)} \rangle = \int_0^\infty e^{-st} f(\tau, t)\, dt.$$

Knowing $f(\tau, t)$, it is not difficult to find the pdf $g(t, \tau)$ of its inverse process. Based on the Laplace transform of $g(t, \tau)$ with respect to t, we come to

$$\tilde{g}(s, \tau) = \frac{\Psi(s)}{s} e^{-\tau\Psi(s)}. \tag{20}$$

It should be pointed out that the exponential term in the Laplace image $\tilde{g}(s,\tau)$ allows one to simplify further calculations by reducing them to algebraic transformations.

Let us now come back to the two-state system where interactions of dipoles with their environment are taken into account with help of the temporal subordination under an infinitely divisible processes mentioned above. We will analyze the time evolution of the number of dipoles in the states $\downarrow$ and $\uparrow$. They are parent random processes in the same manner as in the case of the previous subsection. To account for interaction of dipoles with the environment, we subordinate the latter processes by another random process with a probability density $g(t,\tau)$ according to the relations (16). In the steady state, the system supports the relation $m_\uparrow(\infty) = m_\downarrow(\infty) = 1/2$ conventionally. Then the relaxation function can be written as

$$\phi(t) = \int_0^\infty \phi_D(\tau) g(t,\tau)\,d\tau = \int_0^\infty \exp(-2B\tau) g(t,\tau)\,d\tau. \tag{21}$$

Using the Laplace image $\tilde{g}(s,\tau)$ as applied to infinitely divisible random processes (20), we find the frequency-domain response in a simple form

$$\phi^*(\omega) = \frac{1}{1+\Psi(i\omega)/(2B)}, \tag{22}$$

where B is a constant transition rate. The latter equation clearly shows that the relaxation behavior will be determined by the Laplace exponent $\Psi(s)$.

In the subordination framework, relaxation of the two-state system is described by the following equations:

$$\begin{cases} m_\uparrow(t) = m_\uparrow(0) + B\int_0^t M(t-\tau)\{m_\downarrow(\tau) - m_\uparrow(\tau)\}\,d\tau, \\ m_\downarrow(t) = m_\downarrow(0) + B\int_0^t M(t-\tau)\{m_\uparrow(\tau) - m_\downarrow(\tau)\}\,d\tau, \end{cases}$$

where the kernel $M(t)$ plays the role of a memory function. Note that memory is a key feature of fractional systems. The time-dependent function $M(t)$ can be written as an inverse Laplace transform $\mathcal{L}_t^{-1}$, that is,

$$M(t) = \frac{1}{2\pi i}\int_{c-i\infty}^{c+i\infty} \frac{e^{st}}{\Psi(s)}\,ds = \mathcal{L}_t^{-1}\frac{1}{\Psi(s)}, \tag{23}$$

where c is large enough that $1/\Psi(s)$ is defined for $\operatorname{Re} s \geq c$, and $i^2 = -1$. Then the relaxation function satisfies the following equation:

$$\phi(t) = 1 - 2B\int_0^t M(t-\tau)\phi(\tau)\,d\tau. \tag{24}$$

Using equation (23), we get

$$\phi(t) = 1 - 2B \int_0^t \mathcal{L}_\tau^{-1} \frac{1}{2B + \Psi(s)} \, d\tau .$$

The relaxation response $f(t) = -\frac{d\phi(t)}{dt}$ obeys another integral equation

$$f(t) = 2BM(t) - 2B \int_0^t M(t-\tau) f(\tau) \, d\tau . \tag{25}$$

From the above formula, it follows immediately an interesting relationship between $f(t)$ and $M(t)$:

$$\lim_{B\to 0} \frac{f(t)}{2B} = M(t).$$

Note that every infinitely divisible stochastic process is defined by its Laplace (or Lévy) exponent $\Psi(s)$. There exists one-to-one connection between the exponent and the corresponding memory function. Thus, the memory function $M(t)$ has the same important characteristics for relaxing systems as their time-domain relaxation responses. However, it is not easy to detect $M(t)$ in experiments. The physical significance of the memory function lies in its asymptotic properties. Power-law tails of memory functions in short or/and long times reflect directly similar properties in the asymptotic behavior of the corresponding relaxation responses.

4.3 Memory function formalism for empirical laws of relaxation

A significant amount of experimental data on relaxation of the disordered systems supports some types of empirical laws (it is about D, CD, CC, and HN) [22, 23]. According to [48], their memory functions take the following forms:

$$M_{\mathrm{D}}(t) = \tau_p^{-1} \theta(t),$$
$$M_{\mathrm{CC}}(t) = \tau_p^{-\alpha} t^{\alpha-1} \theta(t)/\Gamma(\alpha),$$
$$M_{\mathrm{CD}}(t) = e^{-\tau_p^{-1} t} \tau_p^{-\gamma} t^{\gamma-1} E_{\gamma,\gamma}(\tau_p^{-\gamma} t^\gamma) \theta(t),$$

where $0 < \alpha, \gamma \le 1$, $\theta(t)$ denotes the Heaviside step function, and $E_{\alpha,\beta}(x) = \sum_{j=0}^\infty x^j/\Gamma(\alpha j + \beta)$, with $\alpha, \beta > 0$, defines the well-known two-parameter ML function [8, 17].

The memory function connected with the HN law takes the cumbersome form

$$M_{\mathrm{HN}}(t) = \theta(t) \sum_{j=0}^\infty \tau_p^{-\alpha\gamma(j+1)} t^{\alpha\gamma(j+1)-1} E_{\alpha,\alpha\gamma(j+1)}^{\gamma(j+1)}(-\tau_p^{-\alpha} t^\alpha),$$

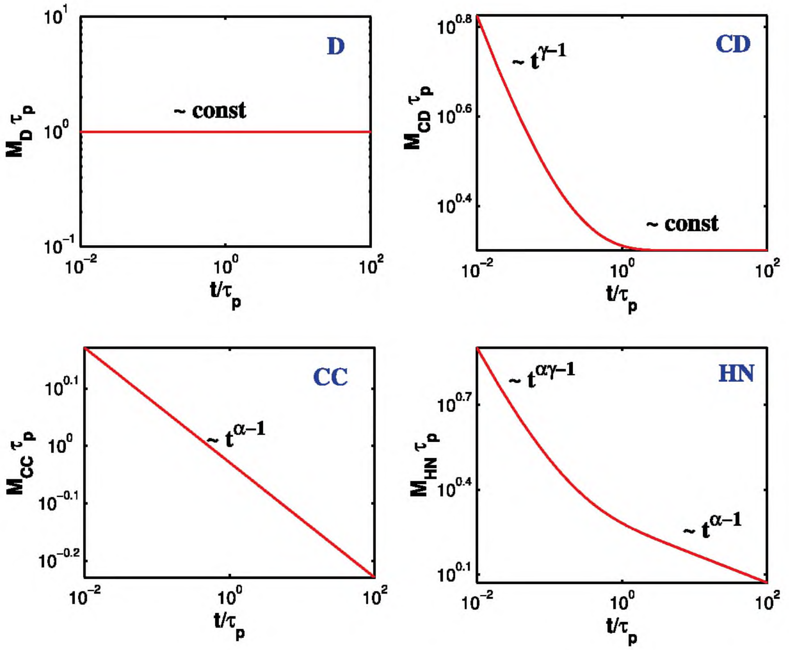

Figure 3: Memory functions corresponding to the empirical laws of relaxation ($\alpha = 0.9$, $\gamma = 0.5$).

expressed in terms of the three-parameter Mittag-Leffler function [37, 32, 33]. The shapes of all these (D, CC, CD, and HN) memory functions are shown in Figure 3. They clearly indicate that the memory function $M_{\mathrm{HN}}(t)$ is the most general case leading to particular cases $M_{\mathrm{D}}(t)$, $M_{\mathrm{CC}}(t)$, and $M_{\mathrm{CD}}(t)$ in limit values of parameters ($\alpha \to 1$ and/or $\gamma \to 1$). Really, based on relation $E^{\mu}_{1,\mu}(y) = e^y/\Gamma(\mu)$, the HN memory function easily transforms into the CD ($\alpha = 1$) and D ($\alpha = \gamma = 1$) memory ones. When $\gamma = 1$, we obtain the CC memory function using the sum $\sum_{j=0}^{\infty} \tau_p^{-\alpha j} t^{\alpha j} E^{j+1}_{\alpha,\alpha(j+1)}(-\tau_p^{-\alpha} t^{\alpha}) = 1/\Gamma(\alpha)$. Returning to [11, 15, 12–14], equation (24) may be considered as a generalization to fractional calculus.

5 Evolution of diffusive fronts

Each relaxation process as a change in time (growth or decay) of a macroscopic physical magnitude characteristic for the observed system (e. g., polarization-depolarization of a dielectric material) is accompanied with diffusion of a corresponding physical variable (in particular, dipole orientations). In this context, the nonexponential relaxation of dielectric systems can be modeled as an excitation undergoing diffusion [16, 10]. The relaxation function $\phi(t)$ is found from the temporal decay of a given mode k, and in the framework of the one-dimensional continuous time random walks

(CTRWs), it is given by the following Fourier transform (supported on whole the real axis):

$$\phi(t) = \langle e^{ik\tilde{R}(t)} \rangle, \tag{26}$$

where $k > 0$ has the physical sense of a wave number, and $\tilde{R}(t)$ denotes the diffusion front (scaling limit of the CTRW) under consideration. In the classical waiting-jump CTRW idea [35], in which the jump R_i occurs after the waiting-time T_i, the random number of the particle jumps performed by time $t > 0$ is given by the renewal counting process N_t. In the alternative jump-waiting CTRW scenario, the particle jump R_i precedes the waiting time T_i. Then the counting process $N_t + 1$ gives the number of jumps by time t, and the particle location at time t is defined by the following sum:

$$R^+(t) = R(N_t + 1) = \sum_{i=1}^{N_t+1} R_i. \tag{27}$$

This model is called the overshooting CTRW, or briefly OCTRW; see [27]. In this connection, it should be noticed that the anomalous diffusion fronts $\tilde{R}^+(t)$ have the frequency-domain shape function identified as the HN function [56, 47]. The OCTRW is an important and useful example of the coupled CTRW. In this case, the waiting time and the subsequent jump are both random sums with the same random number of summands, and as a consequence, this type of the CTRW is coupled, even if the original CTRW before clustering had no dependence between the corresponding waiting times and jumps.

The diffusion front $\tilde{R}^+(t) = X_\eta(Y_\gamma[S_\alpha(t)])$ is determined by the compound subordination [56, 44], where the process $S_\alpha(t)$ subordinates the process $Y_\gamma(y)$ independent on $S_\alpha(t)$, and the process $Y_\gamma(y) = U_\gamma[S_\gamma(y)]$ itself is expressed in terms of $U_\gamma(s)$, being a strictly Lévy γ-stable motion. Hence, we have

$$S_\gamma(s) = \inf\{s : U_\gamma(s) > y\},$$

being inverse to $U_\gamma(s)$. As the process $U_\gamma(y)$ is one-self-similar, we get

$$Y^O_\gamma(y) \stackrel{d}{=} y Y^O_\gamma(1).$$

Fixing of the space structure (clusters and super-clusters) in the system at one instance is equivalent to

$$X_\eta(Y^O_\gamma[S_\alpha(t)]) \stackrel{d}{=} (Y^O_\gamma[S_\alpha(t)])^{1/\eta} X_\eta(1) \stackrel{d}{=} t^{\alpha/\eta}[U_\alpha(1)]^{-\alpha/\eta}[Y^O_\gamma(1)]^{1/\eta} X_\eta(1).$$

The random variable $Y^O_\gamma(1) \stackrel{d}{=} 1/\mathcal{B}_\gamma$ is reciprocal to the beta-distributed variable $\mathcal{B}_\gamma$. The beta distribution with parameters γ and $1-\gamma$ is known also as the generalized arcsine distribution [9]. In this scenario, the HN relaxation function is written as

$$\phi_{\mathrm{HN}}(t) = \int_0^\infty E_\alpha(-C_\alpha C_\eta k^\eta t^\alpha x) h_\gamma(x)\, dx, \tag{28}$$

where $h_\gamma(x) = [\Gamma(\gamma)\Gamma(1-\gamma)]^{-1}x^{-1}(x-1)^{-\gamma}$ is supported for $x > 1$ and 0 otherwise. Here, C_α and C_η the constants dependent on the tail exponents, and the integrand function $E_\alpha[-(t/\tau_p)^\alpha x]$ describes an evolution in the distributions of microscopic quantities (like relaxation rates of clusters) whereas the distribution $h_\gamma(x)$ relates to the mesoscopic level of relaxation rates in super-clusters.

If $p^+(x,t)$ are the pdf of the anomalous diffusion process $\tilde{R}^+(t)$, then

$$\langle e^{ik\tilde{R}^+(t)}\rangle = \int_{-\infty}^{\infty} e^{ikx}p^+(x,t)dx. \tag{29}$$

Hence, the Fourier–Laplace (FL) images $\mathcal{J}_{\mathrm{FL}}(p^+)(k,s)$ of the functions $p^+(x,t)$ are just the Laplace images of the corresponding time-domain HN relaxation function. It is interesting [44, 26, 57] that the pdf $p^+(x,t)$ is a mild solution of equation

$$\begin{aligned}
&(C^\eta D_x^\eta + \tau_0^\alpha D_t^\alpha)^\gamma p^+(x,t)\\
&= \frac{\gamma}{C\Gamma(1-\gamma)}\int_0^\infty u^{-\gamma-1}p^X(x/C,u)\int_0^{\tau_0^\alpha u} p^S(t,\tau)\,d\tau\,du,
\end{aligned}$$

where $p^X(x,t)$ and $p^S(t,\tau)$ are the pdfs of $X_\eta(t)$ and $S_\alpha(t)$, respectively. Here, C is a positive constant dependent on the tail exponents α and η. Equivalently,

$$\mathcal{L}(\phi_{\mathrm{HN}})(s) = \mathcal{J}_{\mathrm{FL}}(p^-)(k,s) = \frac{1}{s}\left\{1-\left(\frac{|Ck|^\eta/\tau_0^\alpha}{s^\alpha + |Ck|^\eta/\tau_0^\alpha}\right)^\gamma\right\} \tag{30}$$

with $|Ck|^\eta/\tau_0^\alpha = \omega_p^\alpha$. Taking $\gamma = 1$, the diffusion front $\tilde{R}^+(t)$ is simplified to $X_\eta(S_\alpha(t))$, and the relaxation function is the CC law. If $\alpha = 1$, we come to the CD relaxation pattern. The interested reader can find many other examples in [46] and can become more familiar with this approach.

6 Conclusions

In this chapter, we have shown that fractional calculus plays an important role in the study of dielectric relaxation. The tools allow one to describe the macroscopic (deterministic) behavior of dielectric materials. From the physical point of view, the appearance of fractional operators is explained by coupled interaction of dipoles each other. This leads to the emergence of memory effects in such physical systems, and for their description we need operators such as ones in fractional calculus. Note that the fractional models of dielectric systems are fundamental and universal, independent of the physical and chemical structures of their interacting entities (dipoles, clusters, etc). However, the macroscopic evolution of dielectric systems is not attributed to any particular entity taken from those forming the system. The relationship between the local random characteristics of dielectric systems and the universal deterministic empirical laws of relaxation is performed by the limit theorems of probability theory ("averaging principles" like the law of large numbers). It should be stressed that the deterministic and probabilistic methods for the theoretical description of nonexponential relaxation do not compete with each other. On the contrary, they help each other to provide a more comprehensive description and effective understanding of dielectric phenomena from their analysis with help of experimental data.

Bibliography

[1] E. Capelas de Oliveira, F. Mainardi, and J. Vaz Jr., Models based on Mittag-Leffler functions for anomalous relaxation in dielectrics, *Eur. Phys. J. Spec. Top.*, **193** (2011), 161–171.

[2] M. Caputo, A model for the fatigue in elastic materials with frequency independent Q, *J. Acoust. Soc. Am.*, **66** (1979), 176–179.

[3] K. S. Cole and R. H. Cole, Dispersion and absorption in dielectrics I. Alternating current characteristics, *J. Chem. Phys.*, **9** (1941), 341–351.

[4] K. S. Cole and R. H. Cole, Dispersion and absorption in dielectrics II. Direct current characteristics, *J. Chem. Phys.*, **10** (1942), 98–105.

[5] D. W. Davidson and R. H. Cole, Dielectric relaxation in glycerine, *J. Chem. Phys.*, **18** (1950), 1417.

[6] D. W. Davidson and R. H. Cole, Dielectric relaxation in glycerol, propylene glycol, and n-propanol, *J. Chem. Phys.*, **19** (1951), 1484–1490.

[7] M. R. de la Fuente, M. A. Perez Jubindo, and M. J. Tello, Two-level model for the nonexponential Williams–Watts dielectric relaxation, *Phys. Rev. B*, **37** (1988), 2094–2101.

[8] A. Erdélyi, Higher Transcendental Functions, vol. 3, McGraw-Hill, New York, 1955.

[9] W. Feller, *An Introduction to Probability Theory and Its Applications*, vol. 2, John Wiley, New York, 1966.

[10] S. Fujiwara and F. Yonezawa, Anomalous relaxation in fractal structures, *Phys. Rev. E*, **51** (1995), 2277–2285.

[11] R. Garra, R. Gorenflo, F. Polito, and Z. Tomovski, Hilfer–Prabhakar derivatives and some applications, *Appl. Math. Comput.*, **242** (2014), 576–589.

[12] R. Garrappa, Grunwald–Letnikov operators for fractional relaxation in Havriliak–Negami models, *Commun. Nonlinear Sci. Numer. Simul.*, **38** (2016), 178–191.

[13] R. Garrappa and G. Maione, Fractional Prabhakar derivative and applications in anomalous dielectrics: A numerical approach, in A. Babiarz, A. Czornik, J. Klamka, and M. Niezabitowski (eds.) *Theory and Applications of Non-integer Order Systems*, Lecture Notes in Electrical Engineering, vol. 407, pp. 429–439, Springer, Cham, 2017.

[14] R. Garrappa and G. Maione, The Prabhakar or three parameter Mittag-Leffler function: theory and application, *Commun. Nonlinear Sci. Numer. Simul.*, **56** (2018), 314–329.

[15] R. Garrappa, F. Mainardi, and G. Maione, Models of dielectric relaxation based on completely monotone functions, *Fract. Calc. Appl. Anal.*, **19** (2016), 1105–1160.

[16] S. Gomi and F. Yonezawa, Anomalous relaxation in the fractal time random walk model, *Phys. Rev. Lett.*, **74** (1995), 4125–4128.

[17] R. Gorenflo, J. Loutchko, and Yu. Luchko, Computation of the Mittag-Leffler function and its derivative, *Fract. Calc. Appl. Anal.*, **5** (2002), 491–518.

[18] S. Havriliak and S. Negami, A complex plane analysis of α-dispersion in some polymer systems, *J. Polym. Sci.*, **14** (1966), 99–117.
[19] S. Havriliak and S. Negami, A complex plane representation of dielectric and mechanical relaxation processes in some polymers, *Polymer*, **8** (1967), 161–210.
[20] R. Hilfer (ed.), *Applications of Fractional Calculus in Physics*, pp. 87–130, World Scientific, Singapore, 2000.
[21] N. L. Johnson and S. Kotz, *Distributions in Statistics: Continuous Univariate Distributions*, vol. 2, Wiley, New York, 1970.
[22] A. K. Jonscher, *Dielectric Relaxation in Solids*, Chelsea Dielectrics Press, London, 1983.
[23] A. K. Jonscher, *Universal Relaxation Law*, Chelsea Dielectrics Press, London, 1996.
[24] A. Jurlewicz and K. Weron, A general probabilistic approach to the universal relaxation response of complex systems, *Cell. Mol. Biol. Lett.*, **4** (1999), 55–86.
[25] A. Jurlewicz, K. Weron, and M. Teuerle, Generalized Mittag-Leffler relaxation: Clustering-jump continuous-time random walk approach, *Phys. Rev. E*, **78** (2008), 011103.
[26] A. Jurlewicz, M. M. Meerschaert, and H. P. Scheffler, Cluster continuous time random walks, *Stud. Math.*, **205** (2011), 13–30.
[27] A. Jurlewicz, P. Kern, M. M. Meerschaert, and H. P. Scheffler, Fractional governing equations for coupled random walks, *Comput. Math. Appl.*, **64** (2012), 3021–3036.
[28] J. Klafter and M. F. Shlesinger, On the relationship among three theories of relaxation in disordered systems, *Proc. Natl. Acad. Sci. USA*, **83** (1986), 848–851.
[29] C. P. Lindsey and G. D. Patterson, Detailed comparison of the Williams–Watts and Cole–Davidson functions, *J. Chem. Phys.*, **73** (1980), 3348–3357.
[30] M. Magdziarz and K. Weron, Anomalous diffusion schemes underlying the Cole–Cole relaxation: The role of the inverse-time α-stable subordinator, *Physica A*, **367** (2006), 1–6.
[31] F. Mainardi, Fractional relaxation-oscillation and fractional diffusion-wave phenomena, *Chaos Solitons Fractals*, **7** (1996), 1461–1477.
[32] A. M. Mathai and H. J. Haubold, *Special Functions for Applied Scientists*, Springer, New York, 2008.
[33] A. M. Mathai, R. K. Saxena, and H. J. Haubold, *The H-Function. Theory and Applications*, Springer, Amsterdam, 2009.
[34] E. W. Montroll and J. T. Bendler, On Lévy (or stable) distributions and the Williams–Watts model of dielectric relaxation, *J. Stat. Phys.*, **34** (1984), 129–162.
[35] E. W. Montroll and G. H. Weiss, Random walks on lattices. II, *J. Math. Phys.*, **6** (1965), 167–181.
[36] R. R. Nigmatullin and Ya. E. Ryabov, Cole–Davidson dielectric relaxation as a self-similar relaxation process, *Phys. Solid State*, **39** (1997), 87–90.
[37] T. R. Prabhakar, A singular integral equation with a generalized Mittag-Leffler function in the kernel, *Yokohama Math. J.*, **19** (1971), 7–15.
[38] G. Röpke, *Statistische Mechanik für das Nichtgleichgewicht*, VEB Deutscher Verlag der Wissenschaften, Berlin, 1987.
[39] S. G. Samko, A. A. Kilbas, and O. I. Marichev, *Fractional Integrals and Derivatives Theory and Applications*, Gordon and Breach, New York, 1993.
[40] M. F. Shlesinger, Williams–Watts dielectric relaxation: A fractal time stochastic process, *J. Stat. Phys.*, **36** (1984), 639–648.
[41] A. A. Stanislavsky, Fractional dynamics from the ordinary Langevin equation, *Phys. Rev. E*, **67** (2003), 021111.
[42] A. A. Stanislavsky, Subordinated random walk approach to anomalous relaxation in disordered systems, *Acta Phys. Pol. B*, **34** (2003), 3649–3660.
[43] A. A. Stanislavsky, Probabilistic interpretation of the integral of fractional order, *Theor. Math. Phys.*, **138** (2004), 418–431.

[44] A. Stanislavsky and K. Weron, Anomalous diffusion with under- and over-shooting subordination: A competition between the very large jumps in physical and operational times, *Phys. Rev. E*, **82** (2010), 051120.
[45] A. Stanislavsky and K. Weron, Atypical case of the dielectric relaxation responses and its fractional kinetic equation, *Fract. Calc. Appl. Anal.*, **19** (2016), 212–228.
[46] A. Stanislavsky and K. Weron, Stochastic tools hidden behind the empirical dielectric relaxation laws, *Rep. Prog. Phys.*, **80** (2017), 036001.
[47] A. Stanislavsky, K. Weron, and J. Trzmiel, Subordination model of anomalous diffusion leading to the two-power-law relaxation responses, *Europhys. Lett.*, **91** (2010), 40003.
[48] A. Stanislavsky, K. Weron, and A. Weron, Anomalous diffusion approach to non-exponential relaxation in complex physical systems, *Commun. Nonlinear Sci. Numer. Simul.*, **24** (2015), 117–126.
[49] V. E. Tarasov, Universal electromagnetic waves in dielectrics, *J. Phys. Condens. Matter*, **20** (2008), 175223.
[50] V. E. Tarasov, Fractional equations of Curie–-von Schweidler and Gauss laws, *J. Phys. Condens. Matter*, **20** (2008), 145212.
[51] V. E. Tarasov, Fractional integro-differential equations for electromagnetic waves in dielectric media, *Theor. Math. Phys.*, **158** (2009), 355–359.
[52] J. Trzmiel, T. Marciniszyn, and J. Komar, Generalized Mittag-Leffler relaxation of $NH_4H_2PO_4$: Porous glass composite, *J. Non-Cryst. Solids*, **357** (2011), 1791–1796.
[53] N. G. van Kampen, *Stochastic Processes in Physics and Chemistry*, North-Holland Physics Publishing, Amsterdam, 1984.
[54] K. Weron and M. Kotulski, On the Cole–Cole relaxation function and related Mittag-Leffler distribution, *Physica A*, **232** (1996), 180–188.
[55] K. Weron, A. Jurlewicz, and A. K. Jonscher, Energy criterion in interacting cluster systems, *IEEE Trans. Dielectr. Electr. Insul.*., **8** (2001), 352–358.
[56] K. Weron, A. Jurlewicz, M. Magdziarz, A. Weron, and J. Trzmiel, Overshooting and undershooting subordination scenario for fractional two-power-law relaxation responses, *Phys. Rev. E*, **81** (2010), 041123.
[57] K. Weron, A. A. Stanislavsky, A. Jurlewicz, M. M. Meerschaert, and H. P. Scheffler, Clustered continuous time random walks: Diffusion and relaxation consequences, *Proc. R. Soc. Lond., Ser. A, Math. Phys. Eng. Sci.*, **468** (2012), 1615–1628.
[58] G. Williams and D. C. Watts, Non-symmetrical dielectric relaxation behaviour arising from a simple empirical decay function, *Trans. Faraday Soc.*, **66** (1970), 80–85.

Yuri Luchko and Francesco Mainardi

Fractional diffusion-wave phenomena

Abstract: In this chapter, basic properties of the fundamental solutions to the initial-value problems for the fractional diffusion-wave equations with the time-fractional Caputo derivative and the Riesz–Feller space-fractional derivative or the Riesz derivative (fractional Laplacian) are discussed. We start with the Mellin–Barnes representations of the fundamental solution to the one-dimensional diffusion-wave equation with the Riesz–Feller space-fractional derivative and continue with a discussion of its properties. In the multidimensional case, we restrict ourselves to analysis of the diffusion-wave equation with the fractional Laplacian. For its fundamental solution, we provide both its Mellin–Barnes representation and several important results that follow from this representation including some closed-form formulas for its particular cases and connection between solutions in different dimensions. The main focus of presentation is on both probabilistic and physical interpretations of solutions to the initial-value problems for the fractional diffusion-wave equations. In particular, their interpretations as anomalous diffusion processes or diffusive waves, respectively, are discussed.

Keywords: Fractional diffusion-wave equation, fundamental solution, Mellin–Barnes integral, Mittag-Leffler function, Wright function, probability density functions, entropy, entropy production rate, propagation speed

MSC 2010: 26A33, 35C05, 35E05, 35L05, 45K05, 60E99

1 Introduction

Time evolution of many complex systems can be interpreted as a kind of anomalous transport or wave propagation that is characterized by a large diversity of elementary particles that participate in the processes, by a strong interactions between them, and by an anomalous dynamics of the system in time. Attempts of mathematical description of anomalous transport and wave propagation processes with fractional partial differential equations become a fashion within the last few decades; see, e. g., [11, 40, 48], and numerous references therein. It is worth mentioning that anomalous transport models are usually first formulated in stochastic form in terms of the continuous time random walk processes. The time- and/or space-fractional differential equations are then derived from the stochastic models for a special choice of the jump

Yuri Luchko, Beuth University of Applied Sciences Berlin, Department of Mathematics, Physics, and Chemistry, Luxemburger Str. 10, 13353 Berlin, Germany, e-mail: luchko@beuth-hochschule.de
Francesco Mainardi, University of Bologna, Department of Physics and Astronomy, Via Irnerio 46, 40126 Bologna, Italy, e-mail: francesco.mainardi@bo.infn.it

probability density functions with infinite first or/and second moments (see, e. g., [13, 18, 38]). The fractional wave equation can also be obtained from the appropriate continuous time random walk models in the case of the waiting time and the jump length probability density functions with the same power law asymptotic behavior (see [17] for details).

The probably first model introduced in this field was formulated in terms of a single-term time-fractional diffusion equation with the Caputo fractional derivative of order $\alpha \in (0,1)$ and the spatial Laplace operator. In [46], the fundamental solution for this equation was shown to be a probability density function (pdf) evolving in time with the mean squared displacement of the diffusing particles of the form $C_\alpha t^\alpha$, $0 < \alpha < 1$. We refer also to [14] for an in-depth mathematical treatment of this and more general equations and to [10] for physical and probabilistic interpretations of its solutions.

Later on, one started investigation of the models in form of the space-time-fractional diffusion-wave equations. In [35], a model one-dimensional space-time fractional diffusion equation with the spatial Riesz–Feller derivative of order $\alpha \in (0,2]$ and skewness θ ($|\theta| \le \min\{\alpha, 2-\alpha\}$) and time-fractional Caputo derivative of order $\beta \in (0,2]$ was investigated in detail. In particular, a Mellin–Barnes representation of the first fundamental solution to the Cauchy problem for this equation was obtained and employed for derivation of its properties including series representations and asymptotic expansions. Moreover, several subordination formulas for fundamental solutions of this equation with different values of α and β and an extension of their probabilistic interpretation to the ranges $\{0 < \alpha \le 2\} \cap \{0 < \beta \le 1\}$ and $\{1 < \beta \le \alpha \le 2\}$ were presented in [35], too. It is worth mentioning that the solutions to the time-fractional diffusion-wave equations with the time-fractional Caputo derivative of order $\beta \in (1,2]$ inherit some characteristics of solutions to the wave equation, also. In particular, the propagation velocities of the maximum points, centers of gravity, and medians of the fundamental solutions to both the Cauchy and the signaling problems for the one-dimensional time-fractional diffusion-wave equations were shown to be finite and depending on the order β of the fractional derivative [28–30]. In the one-dimensional case and under some restrictions on the orders α and β of the fractional derivatives, the fundamental solution to the Cauchy problems for the space-time-fractional diffusion-wave equation can be interpreted both as a diffusive wave with the constant propagation velocity and as a spatial probability density function evolving in time. Thus one can speak about a wave-diffusion dualism of the processes described by this equation [21].

Multidimensional space-time-fractional diffusion-wave equations were considered, for example, in [1, 9, 24, 25], and [47]. In [9], fundamental solutions and propagators for these equations were obtained in integral form and then analyzed from the viewpoint of their unimodality and transition from diffusion to wave propagation. In [1, 24], and [25], the Mellin–Barnes integral representations of the fundamental solutions to the multidimensional space-time-fractional diffusion-wave equations were derived and employed to deduce some new closed-form formulas for their particular cases, integral representations of the Mellin convolution type with the special functions of the Wright type, and subordination formulas for the fundamental solutions with different orders α and β of the fractional derivatives.

It turned out that some particular cases of the multidimensional space-time-fractional diffusion-wave equation possess especially interesting and useful properties and were worth to be considered in deep. The first case is the so-called neutral-fractional equation or α-fractional wave equation that contains fractional derivatives of the same order α, $1 \le \alpha \le 2$ both in space and in time. From the mathematical viewpoint, the neutral-fractional equation was considered for the first time in [6], where an explicit formula for the fundamental solution of the one-dimensional neutral-fractional equation was derived. In [35], this equation was treated as a particular case of a more general space-time fractional diffusion-wave equation. In [39], a fundamental solution to the one-dimensional neutral-fractional equation was deduced and analyzed in terms of the Fox H-function. In [19], the one-dimensional neutral-fractional equation was investigated from the viewpoint of an interpretation of its solutions as some diffusive waves. The multidimensional neutral-fractional equation with a special focus given to the three-dimensional case was analyzed in [20]. In contrast to the one-dimensional case, the fundamental solution cannot be interpreted as a probability density function in the two- and three-dimensional cases, and thus these equations cannot be employed for modeling of any diffusion processes.

Another important particular case of the multidimensional space-time-fractional diffusion-wave equation is the so-called α-fractional diffusion-wave equation that contains the Caputo time-fractional derivative of the order $\alpha/2$ and the Riesz space-fractional derivative of the order α so that the ratio of the derivatives' orders is equal to one-half as in the case of the conventional diffusion equation. It turned out that the α-fractional diffusion-wave equation inherits some properties of both the conventional diffusion equation and of the wave equation. In particular, in the one- and two-dimensional cases, the fundamental solution to the α-fractional diffusion-wave equation can be interpreted as a probability density function and the entropy production rate of the stochastic process governed by this equation is exactly the same as in the case of the conventional diffusion equation [2, 22, 23]. The entropy of the processes governed by the time- and space-fractional diffusion equations was considered in [12, 16] and [42, 43], respectively. In the three-dimensional case, the fundamental solution is not nonnegative anymore, but can be interpreted as a kind of diffusive waves [2, 10].

The rest of the chapter is organized as follows. In the second section, basic definitions and some analytical results for the one-dimensional space-time-fractional equation as well as probabilistic and physical interpretation of the fundamental solutions to this equation are presented. The third section is devoted to the multidimensional space-time-fractional diffusion-wave equation including a treatment of the neutral-fractional (or α-fractional diffusion) equation and the α-fractional diffusion-wave equation. To illustrate analytical findings, some results of numerical calculations, plots, their physical interpretations, and discussions are presented.

2 One-dimensional space-time-fractional diffusion equation

2.1 Problem formulation and fundamental solution

In this section, we closely follow the presentation in [35] and discuss properties of the fundamental solution to the one-dimensional space-time-fractional diffusion equation

$$ {}_xD_\theta^\alpha u(x,t) = {}_tD_*^\beta u(x,t), \quad x \in \mathbb{R},\ t \in \mathbb{R}^+, \tag{1}$$

where the α, θ, β are real parameters restricted as follows:

$$0 < \alpha \le 2, \quad |\theta| \le \min\{\alpha, 2-\alpha\}, \quad 0 < \beta \le 2. \tag{2}$$

In the equation (1), ${}_xD_\theta^\alpha$ stays for the Riesz–Feller space-fractional derivative of order α and skewness θ, defined as a pseudo-differential operator in terms of its Fourier transform,

$$\mathcal{F}\{{}_xD_\theta^\alpha f(x);\kappa\} = -\psi_\alpha^\theta(\kappa)\hat{f}(\kappa), \tag{3}$$

with the symbol

$$\psi_\alpha^\theta(\kappa) = |\kappa|^\alpha e^{i(\operatorname{sign}\kappa)\theta\pi/2}, \quad 0 < \alpha \le 2, \quad |\theta| \le \min\{\alpha, 2-\alpha\} \tag{4}$$

and by ${}_tD_*^\beta$ the Caputo time-fractional derivative of order β ($m-1 < \beta \le m$, $m \in \mathbb{N}$) is denoted:

$$ {}_tD_*^\beta f(t) = \begin{cases} \frac{1}{\Gamma(m-\beta)} \int_0^t \frac{f^{(m)}(\tau)\,d\tau}{(t-\tau)^{\beta+1-m}}, & m-1 < \beta < m, \\ \frac{d^m}{dt^m} f(t), & \beta = m. \end{cases} \tag{5}$$

In this section, the first fundamental solution to the equation (1), that is, its solution that satisfies an initial condition with the Dirac δ-function, will be mainly discussed. Let us denote it by $G = G(x,t)$. Using the scaling properties of the equation (1), the fundamental solution can be represented in the form

$$G_{\alpha,\beta}^\theta(x,t) = t^{-\gamma} K_{\alpha,\beta}^\theta(x/t^\gamma), \quad \gamma = \beta/\alpha, \tag{6}$$

where the function $K_{\alpha,\beta}^\theta$ depends just on one (similarity) variable x/t^γ.

Application of the Fourier and Laplace transforms to the equation (1) and to the corresponding initial conditions leads to an initial-value problem for a simple ordinary fractional differential equation with a known solution (see [35] for details). Thus we arrive at the following integral representation of the function $K^{\theta}_{\alpha,\beta}$ from (6) for $x > 0$ (because of the symmetry relation $K^{\theta}_{\alpha,\beta}(-x) = K^{-\theta}_{\alpha,\beta}(x)$ we can restrict ourselves to this case w. l. o. g.):

$$K^{\theta}_{\alpha,\beta}(x) = \frac{1}{2\pi}\int_{-\infty}^{+\infty} e^{-i\kappa x} E_{\beta}[-\psi^{\theta}_{\alpha}(\kappa)]\, d\kappa = {}_{c}K^{\theta}_{\alpha,\beta}(x) + {}_{s}K^{\theta}_{\alpha,\beta}(x), \tag{7}$$

$${}_{c}K^{\theta}_{\alpha,\beta}(x) = \frac{1}{\pi}\int_{0}^{\infty} \cos(\kappa x)\Re[E_{\beta}(-\kappa^{\alpha} e^{i\theta\pi/2})]\, d\kappa, \tag{8}$$

$${}_{s}K^{\theta}_{\alpha,\beta}(x) = \frac{1}{\pi}\int_{0}^{\infty} \sin(\kappa x)\Im[E_{\beta}(-\kappa^{\alpha} e^{i\theta\pi/2})]\, d\kappa. \tag{9}$$

The next step is employing the Mellin integral transform technique to derive a Mellin–Barnes representation of $K^{\theta}_{\alpha,\beta}$ for $x > 0$ based on the formula (7) (for basic theory of the Mellin transform see, for example, [27] or [37]):

$$K^{\theta}_{\alpha,\beta}(x) = \frac{1}{\alpha x}\frac{1}{2\pi i}\int_{\gamma-i\infty}^{\gamma+i\infty} \frac{\Gamma(\frac{s}{\alpha})\Gamma(1-\frac{s}{\alpha})\Gamma(1-s)}{\Gamma(1-\frac{\beta}{\alpha}s)\Gamma(\rho s)\Gamma(1-\rho s)} x^{s}\, ds, \tag{10}$$

where $\rho = \frac{\alpha-\theta}{2\alpha}$, $0 < \gamma < \min\{\alpha, 1\}$, $|\theta| \le 2-\beta$. The case $x = 0$ can be also handled by employing the technique of the Mellin integral transform:

$$K^{\theta}_{\alpha,\beta}(0) = \begin{cases} \frac{1}{\pi\alpha}\frac{\Gamma(1/\alpha)\Gamma(1-1/\alpha)}{\Gamma(1-\beta/\alpha)}\cos(\frac{\theta\pi}{2\alpha}) & \text{if } 1 < \alpha \le 2,\ \beta \ne 1, \\ \frac{1}{\pi\alpha}\Gamma(1/\alpha)\cos(\frac{\theta\pi}{2\alpha}) & \text{if } 0 < \alpha \le 2,\ \beta = 1. \end{cases} \tag{11}$$

We note that $K^{\theta}_{\alpha,\beta}(0)$ is nonnegative except for $1 < \alpha < \beta \le 2$.

The Mellin–Barnes representation (10) can be interpreted as a formula for the inverse Mellin integral transform of the quotient of products of the Gamma functions and then used among other things to get closed-form formulas for the moments of the function $K^{\theta}_{\alpha,\beta}(x)$ that are written in form of its Mellin integral transform:

$$\int_{0}^{+\infty} K^{\theta}_{\alpha,\beta}(x) x^{s}\, dx = \frac{1}{\alpha}\frac{\Gamma(-s/\alpha)\Gamma(1+s/\alpha)\Gamma(1+s)}{\Gamma(1+\beta s/\alpha)\Gamma(-\rho s)\Gamma(1+\rho s)}, \quad -\min\{\alpha, 1\} < \Re(s) < 0.$$

In order to include the value $s = 0$ in the convergence strip of the integral at the left-hand side of the last formula (so, in particular, the integral of $K^{\theta}_{\alpha,\beta}(x)$ in $\mathbb{R}^{+}_{0}$ can be evaluated), the known property $\Gamma(1+z) = z\Gamma(z)$ of the Gamma-function is applied to the right-hand side of this formula and we obtain the relation

$$\int_0^{+\infty} K_{\alpha,\beta}^{\theta}(x)x^s\,dx = \frac{\rho\Gamma(1-s/\alpha)\Gamma(1+s/\alpha)\Gamma(1+s)}{\Gamma(1-\rho s)\Gamma(1+\rho s)\Gamma(1+\beta s/\alpha)}, \quad -\min\{\alpha,1\} < \Re(s) < \alpha.$$

The last equation allows us to evaluate the (absolute) moments of the fundamental solution $G_{\alpha,\beta}^{\theta}$ of order δ under the restriction $-\min\{\alpha,1\} < \delta < \alpha$.

The Mellin–Barnes integral (10) can be also used to get a series representation of $K_{\alpha,\beta}^{\theta}$, and thus of the fundamental solution $G_{\alpha,\beta}^{\theta}$. To do this, we distinguish three cases depending on the relationship between α and β:

$$\text{(i)}\ \alpha = \beta, \qquad \text{(ii)}\ \alpha < \beta, \qquad \text{(iii)}\ \alpha > \beta. \tag{12}$$

The idea behind our procedure for getting the series representations is to apply the Cauchy theorem for transforming the integration contour in the integral at the right-hand side of (10) either to the loop $L_{-\infty}$ starting and ending at infinity and encircling all poles of the function $\Gamma(s/\alpha)$ or to the loop $L_{+\infty}$ starting and ending at infinity and encircling all poles of the function $\Gamma(1-\frac{s}{\alpha})\Gamma(1-s)$. Then the Jordan lemma, well-known formula for the residuals of the gamma function, and the Cauchy residual theorem are applied to produce the final result.

If $\alpha = \beta$, we again have to distinguish two cases:

$$K_{\alpha,\alpha}^{\theta}(x) = \frac{1}{\pi x}\sum_{n=0}^{\infty} \sin\left[\frac{n\pi}{2}(\theta-\alpha)\right](-x^{\alpha})^n, \quad 0 < x < 1; \tag{13}$$

$$K_{\alpha,\alpha}^{\theta}(x) = \frac{1}{\pi x}\sum_{n=0}^{\infty} \sin\left[\frac{n\pi}{2}(\theta-\alpha)\right](-x^{-\alpha})^n, \quad 1 < x < \infty. \tag{14}$$

Remarkably, in this case we can obtain a closed-form formula for the fundamental solution (see [6, 35])

$$K_{\alpha,\alpha}^{\theta}(x) = \frac{1}{\pi}\frac{x^{\alpha-1}\sin[\frac{\pi}{2}(\alpha-\theta)]}{1+2x^{\alpha}\cos[\frac{\pi}{2}(\alpha-\theta)]+x^{2\alpha}}, \quad 0 < x < \infty \tag{15}$$

by using the known formula ($a \in \mathbb{R}$, $|r| < 1$)

$$\sum_{n=1}^{\infty} r^n \sin(na) = \Im\left(\sum_{n=1}^{\infty} r^n e^{ina}\right) = \Im\left(\frac{re^{ia}}{1-re^{ia}}\right) = \frac{r\sin a}{1-2r\cos a + r^2}. \tag{16}$$

If $\alpha < \beta$ (case (ii)), we get the series representation

$$K_{\alpha,\beta}^{\theta}(x) = \frac{1}{\pi x}\sum_{n=1}^{\infty}\frac{\Gamma(1+\alpha n)}{\Gamma(1+\beta n)} \sin\left[\frac{n\pi}{2}(\theta-\alpha)\right](-x^{-\alpha})^n, \quad 0 < x < \infty. \tag{17}$$

Finally, in the case (iii) ($\alpha > \beta$) the situation is more complicated because we have to transform the contour of integration in the Mellin–Barnes integral (10) to the loop $L_{+\infty}$ encircling all poles of the functions $\Gamma(1-\frac{s}{\alpha})$ and $\Gamma(1-s)$ and we have to consider the possibility of double poles occurring when $\alpha = (m+1)/(k+1)$, $m, k \in \mathbb{N}_0$.

When all poles are simple, we get the following representation by two convergent series:

$$K_{\alpha,\beta}^{\theta}(x) = \frac{1}{\pi x}\sum_{k=0}^{\infty}\frac{\Gamma(1-\alpha k)}{\Gamma(1-\beta k)}\sin\left[\frac{k\pi}{2}(\theta-\alpha)\right](-x^{\alpha})^{k}$$
$$+\frac{1}{\pi x}\sum_{k=0}^{\infty}\frac{\Gamma(1-\frac{k}{\alpha})\Gamma(1+\frac{k}{\alpha})}{k!\Gamma(1-\frac{\beta}{\alpha}k)}\sin\left[\frac{k\pi}{2\alpha}(\theta-\alpha)\right](-x)^{k}. \quad (18)$$

When some poles are not simple, the situation is more complicated and we refer the interested reader to [35] for details.

2.2 Important particular cases of the fundamental solution

Now let us shortly discuss the most important particular cases of the space-time-fractional diffusion-equation (1):
$\alpha = 2, \beta = 1$ (standard diffusion),
$0 < \alpha \le 2, \beta = 1$ (space-fractional diffusion),
$\alpha = 2, 0 < \beta \le 2, \beta \ne 1$ (time-fractional diffusion),
$0 < \alpha = \beta \le 2$ (neutral-fractional diffusion).

The fundamental solution of the standard diffusion equation ($\alpha = 2, \beta = 1$ in (1)) is known to be the Gaussian pdf,

$$G_{2,1}^{0}(x,t) = t^{-1/2}\frac{1}{2\sqrt{\pi}}\exp[-x^2/(4t)], \quad -\infty < x < +\infty,\ t \ge 0 \quad (19)$$

that evolves in time with the variance $\sigma^2 = 2t$ proportional to the first power of time according to the Einstein diffusion law. This representation easily follows from the Mellin–Barnes integral (10) or its series representation.

Equation (1) with $0 < \alpha \le 2, \beta = 1$ is called space-fractional diffusion equation. In this case, the fundamental function can be interpreted as a Lévy strictly stable pdf evolving in time:

$$G_{\alpha,1}^{\theta}(x,t) = t^{-1/\alpha}L_{\alpha}^{\theta}(x/t^{1/\alpha}), \quad -\infty < x < +\infty, \quad t \ge 0. \quad (20)$$

Let us note that the Lévy strictly stable pdf L_{α}^{θ} can be defined via its characteristic function according to the Feller parameterization introduced in [3] and revisited and modified in [5] in the form

$$\widehat{L_{\alpha}^{\theta}}(\kappa) = \mathrm{e}^{-\psi_{\alpha}^{\theta}(\kappa)}$$

with ψ_α^θ defined by (4). In the case $\alpha = 1$, $0 < |\theta| < 1$, we have the representation

$$L_1^\theta(x) = \frac{1}{\pi} \frac{\cos(\theta\pi/2)}{[x + \sin(\theta\pi/2)]^2 + [\cos(\theta\pi/2)]^2}, \quad -\infty < x < +\infty, \tag{21}$$

whereas for $\alpha = 1$, $\theta = \pm 1$ we get

$$L_1^{\pm 1}(x) = \delta(x \pm 1), \quad -\infty < x < +\infty. \tag{22}$$

For $0 < \alpha < 2$, the stable pdfs exhibit "fat tails" and their absolute moments of order ν are finite only if $-1 < \nu < \alpha$. For $0 < \alpha < 1$, the extremal pdfs (those that correspond to the extremal values of θ) are one-sided: for $\theta = -\alpha$, the support of pdf is $\mathbb{R}^+$ and it tends exponentially to zero as $x \to 0^+$ whereas for $\theta = +\alpha$ the support of pdf is $\mathbb{R}^-$ and it tends exponentially to zero as $x \to 0^-$. For $1 < \alpha < 2$, the extremal pdfs are two-sided and exhibit an exponential left tail (as $x \to -\infty$) if $\theta = +(2-\alpha)$ or an exponential right tail (as $x \to +\infty$) if $\theta = -(2-\alpha)$.

It is worth mentioning that for any α the corresponding stable pdf is unimodal and indeed bell-shaped, that is, its nth derivative has exactly n zeros.

Let us now consider the case of the time-fractional diffusion ($\alpha = 2$, $0 < \beta < 2$ in the equation (1)). Then the series representation (18) takes the form

$$G_{2,\beta}^0(x,t) = \frac{1}{2} t^{-\beta/2} M_{\beta/2}\big(|x|/t^{\beta/2}\big), \quad -\infty < x < +\infty,\ t \geq 0, \tag{23}$$

where $M_{\beta/2}$ denotes the so-called M-function of the Wright type that is defined for $\nu \in (0,1)$ and $\forall z \in \mathbb{C}$ by the convergent series

$$M_\nu(z) = \sum_{n=0}^{\infty} \frac{(-z)^n}{n!\Gamma[-\nu n + (1-\nu)]} = \frac{1}{\pi} \sum_{n=1}^{\infty} \frac{(-z)^{n-1}}{(n-1)!} \Gamma(\nu n) \sin(\pi \nu n). \tag{24}$$

The M-function is a special case of the Wright function that plays an important role in different areas of FC. For a detailed investigation of the M-function, we refer the readers to, say, [35].

In particular, it is known that the fundamental solution $G_{2,\beta}^0(x,t)$ with $0 < \beta < 2$ can be interpreted as a symmetric spatial pdf evolving in time with a stretched exponential decay. More precisely, we have

$$G_{2,\beta}^0(x,1) = \frac{1}{2} M_{\beta/2}(|x|) \sim A x^a \mathrm{e}^{-bx^c}, \quad x \to +\infty, \tag{25}$$

where

$$A = \left\{2\pi(2-\beta) 2^{\beta/(2-\beta)} \beta^{(2-2\beta)/(2-\beta)}\right\}^{-1/2}$$

with

$$a = \frac{2\beta - 2}{2(2-\beta)}, \quad b = (2-\beta) 2^{-2/(2-\beta)} \beta^{\beta/(2-\beta)}, \quad c = \frac{2}{2-\beta}.$$

The variance (second moment) of this pdf is $\sigma^2 = 2t^\beta/\Gamma(\beta+1)$. Comparing this expression with the variance of the Gaussian pdf, the time-fractional diffusion equation with $0 < \beta < 1$ can be connected with the anomalous slow diffusion whereas the case of anomalous fast diffusion is described by the same equation with $1 < \beta < 2$.

It is worth mentioning that in the slow diffusion case ($0 < \beta < 1$) the fundamental solution $G^0_{2,\beta}(x,t)$ attains its maximum value at $x = 0$ (where the first spatial derivative is discontinuous) and exhibits exponential tails fatter than the Gaussian. In the fast diffusion case ($1 < \beta < 2$), the $G^0_{2,\beta}(x,t)$ attains two symmetric maxima that move apart from the origin with time and it exhibits exponential tails thinner than the Gaussian.

We mention also an important relation of the M-function to the extremal stable distributions, namely,

$$\frac{1}{c^{1/\nu}} L_\nu^{-\nu}\left(\frac{r}{c^{1/\nu}}\right) = \frac{c\nu}{r^{\nu+1}} M_\nu\left(\frac{c}{r^\nu}\right), \quad 0 < \nu < 1,\ c > 0,\ r > 0. \tag{26}$$

Among other things, this relation can be used to show the nonnegativity of the M-function with the positive argument. Another noteworthy result is a very unexpected relation [34, 35]

$$G^0_{2,\beta}(x,t) = \frac{1}{\beta} G^{2/\beta-2}_{2/\beta,1}(x,t), \quad 1 < \beta < 2,\ x > 0,\ t > 0 \tag{27}$$

between the fundamental solutions to the time-fractional and the space-fractional diffusion equations.

In the case $\alpha = \beta$ (neutral-fractional diffusion equation) and for $x > 0$, the fundamental solution takes the form (see (15))

$$K^\theta_{\alpha,\alpha}(x) = N^\theta_\alpha(x) = \frac{1}{\pi} \frac{x^{\alpha-1} \sin[\frac{\pi}{2}(\alpha-\theta)]}{1 + 2x^\alpha \cos[\frac{\pi}{2}(\alpha-\theta)] + x^{2\alpha}}, \quad 0 < \alpha < 2.$$

This solution can be extended to negative values of x by setting $N^\theta_\alpha(-x) = N^{-\theta}_\alpha(x)$. It is evidently not negative and can be interpreted as a fractional generalization with skewness of the well-known Cauchy pdf.

2.3 Subordination formulas and probabilistic interpretation of the fundamental solution

Another important topic in connection with the one-dimensional space-time-fractional diffusion-wave equation (1) are subordination formulas that connect the fundamental solutions of this equation with different values of the derivatives' orders α and β (see [35, 36]). We start with the noteworthy formula

$$G^\theta_{\alpha,\beta}(x,t) = 2\int_0^\infty G^\theta_{\alpha,1}(x,u) G^0_{2,2\beta}(u,t)\, du \tag{28}$$

that express the fundamental solution to the general equations via the fundamental solutions to the space-fractional and the time-fractional equations. This formula can be also interpreted as a kind of variables separation. An equivalent form of the subordination formula (28) involves the functions L and M that were introduced above:

$$G^{\theta}_{\alpha,\beta}(x,t) = t^{-\beta}\int_0^{\infty} u^{-1/\alpha} L^{\theta}_{\alpha}\left(\frac{x}{u^{1/\alpha}}\right) M_{\beta}\left(\frac{u}{t^{\beta}}\right) du. \tag{29}$$

Specifying the formula (29) for the particular cases of the space-fractional and time-fractional diffusion equations, we get

$$G^{\theta}_{\alpha,1}(x,t) = t^{-1}\int_0^{\infty} u^{-1/\alpha} L^{\theta}_{\alpha}\left(\frac{x}{u^{1/\alpha}}\right) \delta\left(\frac{u}{t}-1\right) du = t^{-1/\alpha} L^{\theta}_{\alpha}\left(\frac{x}{t^{1/\alpha}}\right)$$

and

$$G^{0}_{2,\beta}(x,t) = \frac{t^{-\beta}}{2\sqrt{\pi}}\int_0^{\infty} \mathrm{e}^{-x^2/(4u)} M_{\beta}\left(\frac{u}{t^{\beta}}\right)\frac{du}{u^{1/2}} = \frac{t^{-\beta/2}}{2} M_{\beta/2}\left(\frac{|x|}{t^{\beta/2}}\right).$$

The last formula can be interpreted as a kind of (integral) duplication formula for the M-function with respect to the order. The subordination formula (29) can be also rewritten in terms of the L-function:

$$G^{\theta}_{\alpha,\beta}(x,t) = \int_0^{\infty}\left[u^{-1/\alpha} L^{\theta}_{\alpha}\left(\frac{x}{u^{1/\alpha}}\right)\right]\left[\frac{t}{u\beta} u^{-1/\beta} L^{-\beta}_{\beta}\left(\frac{t}{u^{1/\beta}}\right)\right] du.$$

By the variables substitution $y = u^{-1/\beta}$, the last formula at the point $t = 1$ takes the form

$$G^{\theta}_{\alpha,\beta}(x,1) = K^{\theta}_{\alpha,\beta}(x) = \int_0^{\infty} y^{\beta/\alpha} L^{\theta}_{\alpha}(xy^{\beta/\alpha}) L^{-\beta}_{\beta}(y)\, dy.$$

The subordination formulas presented above can be used among other things to show that the fundamental solution to the space-time-fractional diffusion equation (1) is nonnegative for any $x \in \mathbb{R}$ and $t \in \mathbb{R}^{+}_{0}$, when $0 < \alpha < 2$ and $0 < \beta \le 1$. We also know that the fundamental solutions to the time-fractional diffusion equation ($\alpha = 2$, $0 < \beta \le 2$) and to the neutral-fractional diffusion equation ($0 < \alpha = \beta \le 2$) are nonnegative.

Returning back to the Mellin–Barnes integral representation (10) of the function $K^{\theta}_{\alpha,\beta}$, we get for $x > 0$ and $0 < \alpha < 2$:

$$K^{\theta}_{\alpha,\beta}(x) = \begin{cases} \alpha\int_0^{\infty}[\xi^{\alpha-1}M_{\beta}(\xi^{\alpha})] L^{\theta}_{\alpha}(x/\xi)\frac{d\xi}{\xi}, & 0 < \beta < 1, \\ \int_0^{\infty} M_{\beta/\alpha}(\xi) N^{\theta}_{\alpha}(x/\xi)\frac{d\xi}{\xi}, & 0 < \beta/\alpha < 1. \end{cases} \tag{30}$$

The limiting cases $\beta = 1$, $\alpha = \beta$ and $\alpha = 2$ can be also included into the representation (30) by taking into account the properties of the Dirac δ-function.

Because the integrand of the integrals at the right-hand side of the formula (30) is a product of two non negative functions (related to the pdfs $L_\alpha^\theta(x)$, $M_{\beta/2}(x)$, and $N_\alpha^\theta(x)$), the fundamental solution $G_{\alpha,\beta}^\theta$ can be interpreted as a pdf in the ranges $\{0 < \alpha \le 2\} \cap \{0 < \beta \le 1\}$ and $\{0 < \alpha \le 2\} \cap \{0 < \beta/\alpha \le 1\}$ of the fractional derivatives' orders. Summarizing, the probability interpretation holds true for any $\alpha \in (0, 2]$ if $0 < \beta \le 1$, whereas, if $1 < \beta \le 2$, it is the case only for $1 < \beta \le \alpha \le 2$. The cases excluded from the probability interpretation turn out to be $\{0 < \alpha < \beta\} \cap \{1 < \beta < 2\}$. For other interesting subordination formulas for the one-dimensional space-time fractional diffusion-wave equation, we refer the reader to [36].

2.4 Interpretation of the fundamental solutions as diffusive waves

In this subsection, we deal with a particular case of the equation (1), namely, with the following one-dimensional time-fractional diffusion-wave equation:

$$\frac{\partial^2 u(x,t)}{\partial x^2} = {}_tD_*^\beta u(x,t), \quad x \in \mathbb{R},\ t \in \mathbb{R}^+,\ 0 < \beta \le 2. \tag{31}$$

In [32], this equation was shown to govern a propagation of the mechanical diffusive waves in viscoelastic media that exhibit a simple power-law creep. This problem of dynamic viscoelasticity was formerly treated in [15] and [41], however, without an interpretation by means of the fractional calculus operators.

Here, we follow the presentation in [28, 29], and [30] and consider the two basic boundary-value problems for the equation (31) in the form

$$\begin{cases} \text{(a) Cauchy problem:} & u(x,0^+) = f(x), \quad x \in \mathbb{R}; \quad u(\mp\infty, t) = 0 \quad t > 0; \\ \text{(b) Signaling problem:} & u(x,0^+) = 0, \quad x > 0; \quad u(0^+, t) = h(t), \quad t > 0. \end{cases} \tag{32}$$

For $1 < \beta \le 2$, the initial value of the first-order time derivative of the field variable $\frac{\partial}{\partial t} u(x, 0^+) = g(x)$ is required in the above problems. In what follows, we mainly limit ourselves to the case $g(x) \equiv 0$.

In view of our analysis, we find it convenient to put

$$\nu = \frac{\beta}{2}, \quad 0 < \nu < 1.$$

For the *Cauchy* and *signaling* problems, we introduce the fundamental solutions $\mathcal{G}_c(x,t;\nu)$ and $\mathcal{G}_s(x,t;\nu)$ that correspond to the initial conditions $f(x) = \delta(x)$ and $h(t) = \delta(t)$, respectively, where δ denotes the Dirac δ-function. It should be noted that the fundamental solution for the Cauchy problem turns out to be an even function of x, so $\mathcal{G}_c(x,t;\nu) = \mathcal{G}_c(|x|,t;\nu)$.

For $0 < \nu \leq 1$, the two fundamental solutions are connected by the following *reciprocity relation* (see, e. g., [33] and references therein):

$$2\nu x \mathcal{G}_c(x,t;\nu) = t\mathcal{G}_s(x,t;\nu) = F_\nu(r) = \nu r M_\nu(r), \quad x > 0,\ t > 0,\ r > 0, \tag{33}$$

with the *similarity variable*

$$r = x/t^\nu > 0 \tag{34}$$

and the *auxiliary functions* $F_\nu(r)$ and $M_\nu(r)$ of the Wright type that are defined as follows:

$$F_\nu(z) = \frac{1}{2\pi i}\int_{Ha} e^{\sigma - z\sigma^\nu}\,d\sigma = \sum_{n=1}^{\infty}\frac{(-z)^n}{n!\Gamma(-\nu n)}, \quad z \in \mathbb{C},\ 0 < \nu < 1, \tag{35}$$

$$M_\nu(z) = \frac{1}{2\pi i}\int_{Ha} e^{\sigma - z\sigma^\nu}\frac{d\sigma}{\sigma^{1-\nu}} = \sum_{n=0}^{\infty}\frac{(-z)^n}{n!\Gamma[-\nu n + (1-\nu)]}, \quad z \in \mathbb{C},\ 0 < \nu < 1, \tag{36}$$

where *Ha* denotes the Hankel path properly defined for the representation of the reciprocal of the Gamma function.

In [4], the fundamental solution $\mathcal{G}_c(x,t;\nu)$ of the Cauchy problem was shown to attain its maximum at the points

$$x_*(t) = \pm c_\nu t^\nu, \quad \nu = \beta/2 \tag{37}$$

for each $t > 0$, where $c_\nu > 0$ is a constant determined by ν, $1/2 < \nu < 1$. In [4], the formula (37) was derived from some probabilistic arguments and in [30] an analytical proof of this relation was given.

It follows from (37) that the maximum point of the fundamental solution $\mathcal{G}_c(x,t;\nu)$ propagates with a finite velocity

$$\mathbf{V}_c(t,\nu) = x_*'(t) = \nu c_\nu t^{\nu-1}. \tag{38}$$

For $\nu = 1/2$ (conventional diffusion equation), the propagation velocity is equal to zero because of $c_{1/2} = 0$ whereas for $\nu = 1$ (conventional wave equation) it remains constant and is equal to $c_1 = 1$. In Figure 1, some plots of the propagation velocity of the maximum point of the fundamental solution $\mathcal{G}_c$ are given for different values of ν.

The maximum value $\mathcal{G}_c^*(t;\nu)$ of $\mathcal{G}_c(x,t;\nu)$ is given by the formula

$$\mathcal{G}_c^*(t;\nu) = m_\nu t^{-\nu}, \quad m_\nu = \frac{1}{2}M_\nu(c_\nu) = \frac{1}{\pi}\int_0^\infty E_{2\nu}(-\tau^2)\cos(c_\nu\tau)\,d\tau, \tag{39}$$

where E_α is the Mittag-Leffler function defined by a convergent series as follows:

$$E_\alpha(z) = \sum_{n=0}^{\infty}\frac{z^n}{\Gamma(1+\alpha n)}, \quad \alpha > 0,\ z \in \mathbb{C}. \tag{40}$$

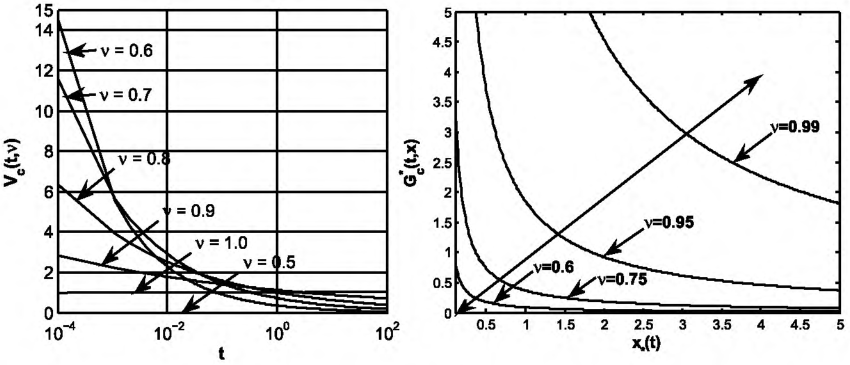

Figure 1: Propagation velocity $\mathbf{V}_c(t,\nu)$ of the maximum point of $\mathcal{G}_c$ in the log-lin scale (left) and the maximum locations and maximum values of $\mathcal{G}_c(x,t;\nu)$ (right).

The relations (37) and (39) implicate that the product

$$\mathcal{G}_c^*(t;\nu)\cdot x_*(t) = c_\nu m_\nu, \quad 0 < t < \infty \tag{41}$$

is a constant that depends only on ν, that is, that the maximum locations and the corresponding maximum values specify a certain hyperbola for a fixed value of ν and for $0 < t < \infty$.

In Figure 1, some plots of the parametric curve $(x_*(t),\ \mathcal{G}_c^*(t;\nu))$, $0 < t < \infty$ are presented. The vertex of the curve (in fact, a hyperbola) tends to the point $(0,0)$ as ν tends to $1/2$ (diffusion equation) and to infinity as $\nu \to 1$ (wave equation).

Finally, in Figure 2, the maximum locations c_ν and the maximum values m_ν as well as their product are plotted for $1/2 < \nu < 1$. As expected, the product $c_\nu m_\nu$ is a

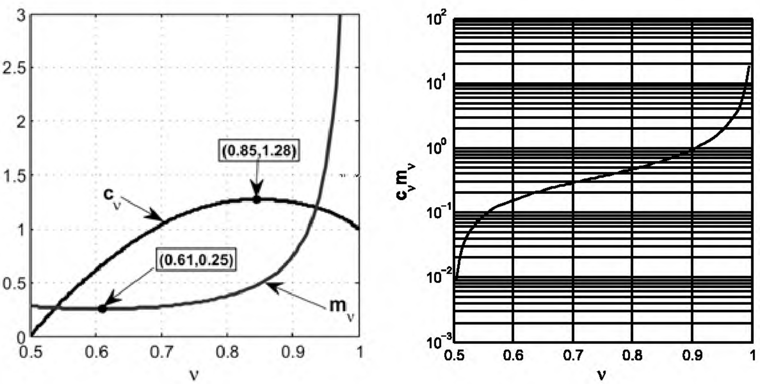

Figure 2: Maximum locations and maximum values of the fundamental solution $\mathcal{G}_c(x,1;\nu)$ (left) and their product (right).

monotonically increasing function that takes values between 0 (diffusion equation) and $+\infty$ (wave equation).

As to the fundamental solution $\mathcal{G}_s$ for the signaling problem, it was analyzed in [28] and [29].

This time, the maximum location $x_* = x_*(t, \nu)$ of the fundamental function $\mathcal{G}_s(x, t; \nu)$ is given by the formula

$$x_*(t, \nu) = Dt^\nu \quad \text{with} \quad D = x_*(1, \nu) = d_\nu. \tag{42}$$

The propagation velocity $\mathbf{V}_s(t, \nu)$ of the maximum point has then the form

$$\mathbf{V}_s(t, \nu) = \frac{dx_*}{dt} = \nu d_\nu t^{\nu-1}. \tag{43}$$

As we see, the propagation velocity $\mathbf{V}_s(t, \nu)$ of the maximum point of $\mathcal{G}_s$ is described by a formula of the same type as the one for the $\mathcal{G}_c$ (see the formula (38)). Its qualitative behavior is very similar to one presented on the plots of Figure 1. The only essential difference is in the curve for $\nu = 1/2$ (diffusion equation). Whereas the maximum location of the fundamental solution for the Cauchy problem for the diffusion equation does not move with the time ($c_{1/2} = 0$), its velocity for the signaling problem is equal to $\frac{\sqrt{2}}{2}\frac{1}{\sqrt{t}}$ (see the formula (43)).

The maximum value $\mathcal{G}_s^*(t; \nu)$ of $\mathcal{G}_s(x, t; \nu)$ in dependence of t and ν is given by the formula

$$\mathcal{G}_s^*(t; \nu) = \frac{n_\nu}{t} \quad \text{with} \quad n_\nu = F_\nu(d_\nu) = \frac{2}{\pi}\int_0^\infty \tau E_{2\nu,2\nu}(-\tau^2)\sin(d_\nu \tau)\, d\tau, \tag{44}$$

where $E_{\alpha,\beta}$ is the generalized Mittag-Leffler function defined by a convergent series as follows:

$$E_{\alpha,\beta}(z) = \sum_{n=0}^{\infty} \frac{z^n}{\Gamma(\beta + \alpha n)}, \quad \alpha > 0,\ \beta \in \mathbb{C},\ z \in \mathbb{C}. \tag{45}$$

The formulas (42) and (44) implicate that the product p_ν of the maximum location and the maximum value of the fundamental solution $\mathcal{G}_s(x, t; \nu)$ is given by the relation

$$p_\nu = p_n u(t) = \mathcal{G}_s^*(t; \nu) \cdot x_*(t) = d_\nu t^\nu n_\nu t^{-1} = d_\nu n_\nu t^{\nu-1}. \tag{46}$$

For further results regarding interpretation of the fundamental solutions to the one-dimensional diffusion-wave equation as diffusive waves, we refer the interested reader to [29]. In particular, in [29], the centers of gravity and the medians of the fundamental solution to the Cauchy and signaling problems and their propagation velocities were determined analytically and calculated numerically.

3 Multidimensional space-time-fractional diffusion equation

3.1 Problem formulation and fundamental solution

Fundamental solution to the multidimensional time-fractional diffusion-wave equation of type (1) with the Laplace operator was derived for the fist time by Kochubei in [14] and Schneider and Wyss in [46] independently from each other in terms of the Fox H-function. Moreover, in [14], the Cauchy problem for the general fractional diffusion equation with the regularized fractional derivative (the Caputo fractional derivative in the modern terminology) and the general second-order spatial differential operator was investigated, also. In the series of publications [9, 10, 8], Hanyga considered mathematical, physical, and probabilistic properties of the fundamental solutions to the multidimensional time-, space- and space-time-fractional diffusion-wave equations, respectively. Recently, Luchko and his co-authors started to employ the method of the Mellin–Barnes integral representation for in-depth investigation of the multidimensional space-time-fractional diffusion-wave equation (see, e. g., [1, 2, 19–25]). In this section, we shortly present some of the results obtained in the papers mentioned above.

We start with the multidimensional space- and time-fractional diffusion-wave equation in the following form:

$$-(-\Delta)^{\frac{\alpha}{2}}u(\mathbf{x},t) = {}_tD_*^{\beta}u(\mathbf{x},t), \quad \mathbf{x}\in\mathbb{R}^n,\ t>0,\ 1<\alpha\le 2,\ 0<\beta\le 2, \tag{47}$$

where $(-\Delta)^{\frac{\alpha}{2}}$ is the fractional Laplacian and ${}_tD_*^{\beta}$ stays for the Caputo time-fractional derivative of order β.

The fractional Laplacian $(-\Delta)^{\frac{\alpha}{2}}$ is defined as a pseudo-differential operator with the symbol $|\kappa|^{\alpha}$ [44, 45]:

$$(\mathcal{F}(-\Delta)^{\frac{\alpha}{2}}f)(\kappa) = |\kappa|^{\alpha}(\mathcal{F}f)(\kappa), \tag{48}$$

where $(\mathcal{F}f)(\kappa)$ is the Fourier transform of a function f at the point $\kappa\in\mathbb{R}^n$ defined by

$$(\mathcal{F}f)(\kappa) = \hat{f}(\kappa) = \int_{\mathbb{R}^n} e^{i\kappa\cdot\mathbf{x}}f(\mathbf{x})\,d\mathbf{x}. \tag{49}$$

For further properties and representations of the fractional Laplacian, we refer the reader to, for example, [45].

In this section, we deal with the Cauchy problem for the equation (47) with the Dirichlet initial conditions. If the order β of the time-derivative satisfies the condition $0<\beta\le 1$, we pose an initial condition in the form

$$u(\mathbf{x},0) = \varphi(\mathbf{x}), \quad \mathbf{x}\in\mathbb{R}^n. \tag{50}$$

For the orders β satisfying the condition $1 < \beta \le 2$, the second initial condition in the form

$$\frac{\partial u}{\partial t}(\mathbf{x}, 0) = 0, \quad \mathbf{x} \in \mathbb{R}^n \tag{51}$$

is added to the Cauchy problem.

Because the initial-value problem (47), (50) (or (47), (50)–(51), respectively) is a linear one, its solution can be represented in the form

$$u(\mathbf{x}, t) = \int_{\mathbb{R}^n} G_{\alpha,\beta,n}(\mathbf{x} - \zeta, t)\varphi(\zeta)\, d\zeta,$$

where $G_{\alpha,\beta,n}$ is the first fundamental solution to the fractional diffusion-wave equation (47), that is, the solution to the problem (47), (50) with the initial condition

$$u(\mathbf{x}, 0) = \prod_{i=1}^{n} \delta(x_i), \quad \mathbf{x} = (x_1, x_2, \dots, x_n) \in \mathbb{R}^n$$

or to the problem (47), (50)–(51) with the initial conditions

$$u(\mathbf{x}, 0) = \prod_{i=1}^{n} \delta(x_i), \quad \mathbf{x} = (x_1, x_2, \dots, x_n) \in \mathbb{R}^n$$

and

$$\frac{\partial u}{\partial t}(\mathbf{x}, 0) = 0, \quad \mathbf{x} \in \mathbb{R}^n,$$

for $0 < \beta \le 1$ or $1 < \beta \le 2$, respectively, with δ being the Dirac delta function.

Thus the behavior of the solutions to the problem (47), (50) (or (47), (50)–(51), respectively) is determined by the fundamental solution $G_{\alpha,\beta,n}(\mathbf{x}, t)$ and here we focus on the properties of the fundamental solution.

Applying the Fourier transform to (47) and to the initial conditions, solving the resulting initial-value problem for an ordinary fractional differential equations, returning back to the space domain by applying the inverse Fourier transform and representing it as a single integral, we arrive at the following integral representation ([1] and [24]):

$$G_{\alpha,\beta,n}(\mathbf{x}, t) = \frac{|\mathbf{x}|^{1-\frac{n}{2}}}{(2\pi)^{\frac{n}{2}}} \int_0^\infty E_\beta(-\tau^\alpha t^\beta)\tau^{\frac{n}{2}} J_{\frac{n}{2}-1}(\tau|\mathbf{x}|)\, d\tau, \tag{52}$$

whenever the integral in (52) converges absolutely or at least conditionally. In the formula (52), J_ν denotes the Bessel function with the index ν and E_β stays for the Mittag-Leffler function defined as in (40). Using the Mellin integral transform technique, the formula (52) can be transformed to the following important Mellin–Barnes representation of the fundamental $G_{\alpha,\beta,n}$ (see [1] and [24]):

$$G_{\alpha,\beta,n}(\mathbf{x},t) = \frac{1}{\alpha}\frac{t^{-\frac{\beta n}{\alpha}}}{(4\pi)^{\frac{n}{2}}}\frac{1}{2\pi i}\int_{\gamma-i\infty}^{\gamma+i\infty}\frac{\Gamma(\frac{s}{2})\Gamma(\frac{n}{\alpha}-\frac{s}{\alpha})\Gamma(1-\frac{n}{\alpha}+\frac{s}{\alpha})}{\Gamma(1-\frac{\beta}{\alpha}n+\frac{\beta}{\alpha}s)\Gamma(\frac{n}{2}-\frac{s}{2})}\left(\frac{|\mathbf{x}|}{2t^{\frac{\beta}{\alpha}}}\right)^{-s} ds \tag{53}$$

that is valid for $|\mathbf{x}| \neq 0$ under the conditions $\max(n-\alpha,0) < \gamma < n$. This formula can be used among other things for derivation of the series representations and asymptotics of $G_{\alpha,\beta,n}$, its nice particular cases, and connections between the fundamental solutions for different values of n, α, and β.

In the case $|\mathbf{x}| = 0$ ($\mathbf{x} = (0,\dots,0)$), we have the representation

$$G_{\alpha,\beta,n}(0,t) = \frac{1}{(2\pi)^n}\frac{2\pi^{\frac{n}{2}}}{\Gamma(\frac{n}{2})}\int_0^\infty E_\beta(-\tau^\alpha t^\beta)\tau^{n-1}\,d\tau, \tag{54}$$

where E_β is the Mittag-Leffler function (40). Its asymptotics ensures convergence of the integral of the right-hand side of (54) under the condition $0 < n < \alpha$ and thus for $1 < \alpha \leq 2$ the fundamental solution $G_{\alpha,\beta,n}$ is finite at $|x| = 0$ only in the one-dimensional case and we get the formula (see [1] and [24]):

$$G_{\alpha,\beta,1}(0,t) = \frac{t^{-\frac{\beta}{\alpha}}}{\alpha\pi}\frac{\Gamma(\frac{1}{\alpha})\Gamma(1-\frac{1}{\alpha})}{\Gamma(1-\frac{\beta}{\alpha})}$$

that is valid for $\alpha > 1$ if $0 < \beta < 2$ and for $\alpha > 2$ if $\beta = 2$.

3.2 Properties and particular cases of the fundamental solution

The representation (53) can be easily employed, say, for determination of the particular cases of the fundamental solution that have a simpler form compared to the general cases. The idea is very simple, namely to look for the cases when some of the Gamma-functions from the Mellin–Barnes representation (53) are canceled, that is, when the quotient

$$K_{\alpha,\beta,n}(s) = \frac{\Gamma(\frac{s}{2})\Gamma(\frac{n}{\alpha}-\frac{s}{\alpha})\Gamma(1-\frac{n}{\alpha}+\frac{s}{\alpha})}{\Gamma(1-\frac{\beta}{\alpha}n+\frac{\beta}{\alpha}s)\Gamma(\frac{n}{2}-\frac{s}{2})} \tag{55}$$

takes a simpler form. In [1], several of such cases were listed and here we present just some of them:

Case I: $\beta = 1$, $\alpha = 2$ (diffusion equation).
This case is especially simple because two pairs of the Gamma-functions are canceled in the quotient (55) that defines the function $K_{\alpha,\beta,n}$ from the Mellin–Barnes integral

representation (53) of the fundamental solution, namely, $\Gamma(\frac{n}{\alpha} - \frac{s}{\alpha})$ is canceled with $\Gamma(\frac{n}{2} - \frac{s}{2})$ and $\Gamma(1 - \frac{n}{\alpha} + \frac{s}{\alpha})$ is canceled with $\Gamma(1 - \frac{\beta}{\alpha}n + \frac{\beta}{\alpha}s)$. What is remaining, is the most simple Mellin–Barnes representation

$$G_{2,1,n}(\mathbf{x}, t) = \frac{t^{-\frac{n}{2}}}{2(4\pi)^{\frac{n}{2}}} \frac{1}{2\pi i} \int_{\gamma - i\infty}^{\gamma + i\infty} \Gamma\left(\frac{s}{2}\right) \left(\frac{|x|}{2\sqrt{t}}\right)^{-s} ds.$$

To put it into conventional form, the integration contour in the last integral is transformed to the loop $L_{-\infty}$ starting and ending in $-\infty$ and encircling all poles of $\Gamma(\frac{s}{2})$ and then application of the Jordan lemma and the Cauchy residue theorem leads to the well-known formula:

$$G_{2,1,n}(\mathbf{x}, t) = \frac{1}{(\sqrt{4\pi t})^n} \exp\left(-\frac{|\mathbf{x}|^2}{4t}\right).$$

The same procedure leads to the following particular cases:

Case II: $\beta = 1, 1 < \alpha \leqslant 2$ (space-fractional diffusion equation).

$$G_{\alpha,1,n}(\mathbf{x}, t) = \frac{2t^{-\frac{n}{\alpha}}}{(4\pi)^{\frac{n}{2}}} \, {}_1\Psi_1 \left[\begin{matrix} (\frac{n}{\alpha}, \frac{2}{\alpha}) \\ (\frac{n}{2}, 1) \end{matrix} ; -\frac{|x|^2}{4t^{\frac{2}{\alpha}}} \right], \tag{56}$$

where the generalized Wright function is defined by the following series (in the case it is a convergent one):

$${}_p\Psi_q \left[\begin{matrix} (a_1, A_1), \dots, (a_p, A_p) \\ (b_1, B_1) \dots (b_q, B_q) \end{matrix} ; z \right] = \sum_{k=0}^{\infty} \frac{\prod_{i=1}^{p} \Gamma(a_i + A_i k)}{\prod_{i=1}^{q} \Gamma(b_i + B_i k)} \frac{z^k}{k!}. \tag{57}$$

For details regarding the generalized Wright function, we refer the readers to the recent book [7].

Case III: $\beta = \frac{\alpha}{2}$, $n = 2$ (two-dimensional α-fractional diffusion equation).

$$G_{\alpha,\frac{\alpha}{2},2}(\mathbf{x}, t) = \frac{1}{4\pi t} \left(\frac{|x|}{2\sqrt{t}}\right)^{\alpha-2} E_{\frac{\alpha}{2},\frac{\alpha}{2}}\left(-\left(\frac{|x|}{2\sqrt{t}}\right)^{\alpha}\right), \tag{58}$$

where the generalized Mittag-Leffler function $E_{\beta,\gamma}$ is defined as in (45). Let us note that the formula (58) was deduced for the first time in [23], where it was also shown that the fundamental solution $G_{\alpha,\frac{\alpha}{2},2}$ can be interpreted as a spatial probability density function evolving in time and that the entropy production rate associated with the anomalous diffusion process described by the two-dimensional equation (47) with $\beta = \alpha/2$ is exactly the same as in the case of the classical diffusion equation.

Case IV: $\alpha = \beta$ and $n = 1$ (one-dimensional α-fractional wave equation).

$$G_{\alpha,\alpha,1}(\mathbf{x}, t) = \frac{1}{\pi} \frac{|x|^{\alpha-1} t^{\alpha} \sin(\pi\alpha/2)}{t^{2\alpha} + 2|x|^{\alpha} t^{\alpha} \cos(\pi\alpha/2) + |x|^{2\alpha}}. \tag{59}$$

For details of derivation of the formula (59), we refer the reader to [6, 19], or [21]. Let us note that the equation (47) with $\alpha = \beta$ is usually referred to as a neutral-fractional diffusion-wave equation (see [6] of [35] for discussion of the mathematical properties of its fundamental solution and its plots) or as α-fractional wave equation (see [19] or [21] for discussion of the physical properties of its fundamental solution).

For other interesting particular cases of the fundamental solution $G_{\alpha,\beta,n}$, we refer the interested reader to [1] and [24]. In the rest of this subsection, we present some important formulas hat connect the fundamental solutions with different values of n, α, and β.

We start with the formulas that connect the fundamental solutions for equations with different dimensions (see [1]):

$$G_{\alpha,\beta,n+2}(\mathbf{x},t) = -\frac{1}{2\pi|\mathbf{x}|}\frac{d}{d|\mathbf{x}|}G_{\alpha,\beta,n}(\mathbf{x},t), \tag{60}$$

$$G_{\alpha,\beta,n+2}(\mathbf{x},t) = \frac{1}{2\pi|\mathbf{x}|^2}\left(n + \frac{\alpha}{\beta}t\frac{d}{dt}\right)G_{\alpha,\beta,n}(\mathbf{x},t). \tag{61}$$

A particular case of (61) for the equation (47) with $\alpha = \beta$ has been deduced in [20].

Both formulas (60) and (61) connect the fundamental solutions $G_{\alpha,\beta,n+2}$ and $G_{\alpha,\beta,n}$, that is, the solutions in either odd or even dimensional spaces, respectively. Say, if a simple closed-form formula exists for $G_{\alpha,\beta,1}$ (one-dimensional case) or $G_{\alpha,\beta,2}$ (two-dimensional case), the relations (60) and (61) can be used for deriving the closed-form formulas for all odd or even dimensional fundamental solutions, respectively.

Another kind of connections between the fundamental solutions are the so-called subordination formulas that connect the fundamental solutions for different values of the fractional derivatives α and β. In the one-dimensional case, several of such formulas were derived in [35] and [36]. For subordination formulas in the multidimensional cases, we refer the readers to the recent paper [25]. In the rest of this subsection, we present the main result derived in [25].

For the fundamental solution $G_{\alpha,\beta,n}(\mathbf{x},t)$ to the multidimensional space-time-fractional diffusion-wave equation (47) with $0 < \beta \le 1$, $0 < \alpha \le 2$, and $2\beta + \alpha < 4$ the following subordination formula is valid:

$$G_{\alpha,\beta,n}(\mathbf{x},t) = \int_0^\infty t^{-\frac{2\beta}{\alpha}}\Phi_{\alpha,\beta}(st^{-\frac{2\beta}{\alpha}})G_{2,1,n}(\mathbf{x},s)\,ds, \tag{62}$$

where the fundamental solution to the conventional diffusion equation is given by

$$G_{2,1,n}(\mathbf{x},t) = \frac{1}{(\sqrt{4\pi t})^n}\exp\left(-\frac{|\mathbf{x}|^2}{4t}\right)$$

and the kernel function $\Phi_{\alpha,\beta}(\tau)$ is a probability density function that is defined as follows:

$$\Phi_{\alpha,\beta}(\tau) = \begin{cases} \tau^{\frac{\alpha}{2}-1} W_{(1-\beta,-\beta),(\frac{\alpha}{2},\frac{\alpha}{2})}(-\tau^{\frac{\alpha}{2}}) & \text{if } \frac{\beta}{\alpha} < \frac{1}{2}, \\ \tau^{-1} W_{(1,\beta),(0,-\frac{\alpha}{2})}(-\tau^{-\frac{\alpha}{2}}) & \text{if } \frac{\beta}{\alpha} > \frac{1}{2}, \\ \begin{cases} \frac{\tau^{\frac{\alpha}{2}-1}}{\pi} \sum_{k=0}^{\infty} \sin(\frac{\pi\alpha}{2}(k+1))(-\tau^{\frac{\alpha}{2}})^k & \text{if } 0 < \tau < 1 \\ -\frac{\tau^{-1}}{\pi} \sum_{k=0}^{\infty} \sin(\frac{\pi\alpha}{2}k)(-\tau^{-\frac{\alpha}{2}})^k & \text{if } \tau > 1 \end{cases} & \text{if } \frac{\beta}{\alpha} = \frac{1}{2}. \end{cases} \tag{63}$$

In the formula (63), $W_{(a,\mu),(b,\nu)}$ stays for the four parameters Wright function that is defined by the series

$$W_{(a,\mu),(b,\nu)}(z) = \sum_{k=0}^{\infty} \frac{z^k}{\Gamma(a+\mu k)\Gamma(b+\nu k)}, \quad \mu,\nu \in \mathbb{R},\ a,b,z \in \mathbb{C}. \tag{64}$$

This function was introduced in [51] for the positive values of the parameters μ and $\nu > 0$. When $a = \mu = 1$ or $b = \nu = 1$, respectively, the four parameters Wright function is reduced to the conventional Wright function. In [26], the four parameters Wright function was investigated in the case when one of the parameters μ or ν is negative.

Let us also mention that kernel function $\Phi_{\alpha,\beta}(\tau)$ from the formula (63) can be also represented in form of a Mellin–Barnes integral [25]

$$\Phi_{\alpha,\beta}(\tau) = \frac{2}{\alpha}\frac{1}{2\pi i}\int_{\gamma-i\infty}^{\gamma+i\infty} \frac{\Gamma(\frac{2}{\alpha}-\frac{2}{\alpha}s)\Gamma(1-\frac{2}{\alpha}+\frac{2}{\alpha}s)}{\Gamma(1-\frac{2\beta}{\alpha}+\frac{2\beta}{\alpha}s)\Gamma(1-s)}\tau^{-s}\,ds$$

and as the inverse Laplace transform of the Mittag-Leffler function $E_\beta(-\lambda^{\frac{\alpha}{2}})$:

$$E_\beta(-\lambda^{\frac{\alpha}{2}}) = \int_0^{\infty} \Phi_{\alpha,\beta}(\tau)e^{-\lambda\tau}\,d\tau. \tag{65}$$

3.3 Entropy of the fractional diffusion processes

One of the most important characteristics of the diffusion processes is their entropy and the entropy production rate. The entropy of the processes governed by some one-dimensional time- or space-fractional diffusion equations has been discussed in [12, 16] and [42, 43], respectively. According to [12, 42], the entropy production rates of the stochastic processes governed by these equations depend on the derivative order α of the time- or space-fractional derivative, respectively, and increase with α from 1 (diffusion) to 2 (wave propagation) that results in the so-called entropy production paradox.

The one-dimensional time- and space-fractional diffusion equation with the ratio of the orders of the time- and space-fractional derivatives equal to one-half (called the α-fractional diffusion equation) was studied in [21, 22], and the two-dimensional case was considered in [23]. It turned out that in the one- and two-dimensional cases the fundamental solution to the α-fractional diffusion equation can be interpreted as a spatial probability density function evolving in time. Moreover, the entropy production rate of the fundamental solution to the α-fractional diffusion equation does not depend on the equation order α and is exactly the same as in the case of the conventional diffusion equation. Thus in the one- and two-dimensional cases the α-fractional diffusion equation combines the properties of the anomalous diffusion (the mean squared displacement of the diffusing particles does not exist) and of the conventional diffusion (the same entropy production rate). However, in the three-dimensional case (and also in higher dimensions) the fundamental solution changes its sign, and thus describes rather an anomalous wave propagation and not anomalous diffusion anymore (see [9] for a mathematical characterization of the wave propagation processes).

Following [1, 21–23], we consider here the following initial-value problem for the n-dimensional α-fractional diffusion equation:

$$-(-\Delta)^{\frac{\alpha}{2}} u(\mathbf{x},t) = {}_tD_*^{\frac{\alpha}{2}} u(\mathbf{x},t), \quad \mathbf{x} \in \mathbb{R}^n,\ t > 0,\ 0 < \alpha \leqslant 2, \tag{66}$$

$$u(\mathbf{x},0) = \varphi(\mathbf{x}), \quad \mathbf{x} \in \mathbb{R}^n, \tag{67}$$

where $-(-\Delta)^{\frac{\alpha}{2}}$ is the fractional Laplacian and ${}_tD_*^{\frac{\alpha}{2}}$ stays for the Caputo time-fractional derivative of the order $\frac{\alpha}{2}$.

Again, we mainly focus on the fundamental solution to the problem (66), (67) that we denote by $G_{\alpha,n}$. Because the equation (66) is a particular case of the equation (47) we dealt with at the beginning of this section, we can employ all formulas derived there. In particular, by a linear variables substitution the representation (52) can be put into the form

$$G_{\alpha,n}(\mathbf{x},t) = t^{-\frac{n}{2}} L_{\alpha,n}(z), \quad z = \frac{|\mathbf{x}|}{2\sqrt{t}}, \tag{68}$$

with the auxiliary function

$$L_{\alpha,n}(z) = \frac{z^{1-\frac{n}{2}}}{2^{n-1}\pi^{\frac{n}{2}}} \int_0^\infty \tau^{\frac{n}{2}} E_{\frac{\alpha}{2}}(-\tau^\alpha) J_{\frac{n}{2}-1}(2z\tau)\, d\tau$$

that also can be represented as a Mellin–Barnes integral:

$$L_{\alpha,n}(z) = \frac{1}{\alpha 2^n \pi^{\frac{n}{2}}} \frac{1}{2\pi i} \int_{\gamma-i\infty}^{\gamma+i\infty} \Gamma\left(\frac{s}{2}\right) \frac{\sin(\frac{\pi s}{2} - \frac{n\pi}{2})}{\sin(\frac{\pi s}{\alpha} - \frac{n\pi}{\alpha})} (z)^{-s}\, ds, \tag{69}$$

where $n - \min(\alpha, n) < \gamma < n$. This representation will be used in the further discussions. As already mentioned in the previous subsection, in the one- and two-dimensional cases, the fundamental solution $G_{\alpha,n}$ can be interpreted as a probability density function evolving in time. In this subsection, we discuss the entropy and the entropy production rate of the underlying stochastic processes.

For an n-dimensional continuous random variable evolving in time with the probability density function $p(\mathbf{x},t)$, $\mathbf{x} \in \mathbb{R}^n$, $t > 0$, the Shannon entropy is defined by the formula

$$S(p,t) = -\int_{\mathbb{R}^n} p(\mathbf{x},t)\ln(p(\mathbf{x},t))\,d\mathbf{x} \tag{70}$$

with the entropy production rate given as

$$R(p,t) = \frac{d}{dt}S(p,t).$$

It is well known that the entropy production rate of an n-dimensional Gaussian random variable is given by the expression

$$R(G_{2,n},t) = \frac{n}{2t}$$

that is strictly positive and decreases with the time.

To calculate the entropy of the stochastic process governed by the multi-dimensional α-fractional diffusion equation (66), we employ the representation (68) of its fundamental solution in terms of the auxiliary function $L_{\alpha,n}$. Substituting (68) into (70) and using the formula (see, e. g., [45])

$$\int_{\mathbb{R}^n} f(|\mathbf{x}|)\,d\mathbf{x} = \frac{2\pi^{\frac{n}{2}}}{\Gamma(\frac{n}{2})}\int_0^\infty \tau^{n-1}f(\tau)\,d\tau, \tag{71}$$

we obtain the following chain of equalities:

$$\begin{aligned} S(\alpha,t) &= -\int_{\mathbb{R}^n} t^{-\frac{n}{2}}L_{\alpha,n}\left(\frac{|\mathbf{x}|}{2\sqrt{t}}\right)\ln\left(t^{-\frac{n}{2}}L_{\alpha,n}\left(\frac{|\mathbf{x}|}{2\sqrt{t}}\right)\right)d\mathbf{x} \\ &= -\frac{2\pi^{\frac{n}{2}}}{\Gamma(\frac{n}{2})}\int_0^\infty t^{-\frac{n}{2}}L_{\alpha,n}\left(\frac{\tau}{2\sqrt{t}}\right)\ln\left(t^{-\frac{n}{2}}L_{\alpha,n}\left(\frac{\tau}{2\sqrt{t}}\right)\right)\tau^{n-1}\,d\tau \\ &= -\frac{2^{n+1}\pi^{\frac{n}{2}}}{\Gamma(\frac{n}{2})}\int_0^\infty u^{n-1}L_{\alpha,n}(u)\left(-\frac{n}{2}\ln t + \ln(L_{\alpha,n}(u))\right)du \end{aligned}$$

or, equivalently,

$$S(\alpha,t) = A_{\alpha,n}\ln t + B_{\alpha,n}, \tag{72}$$

where

$$A_{\alpha,n} = \frac{n2^n\pi^{\frac{n}{2}}}{\Gamma(\frac{n}{2})}\int_0^\infty u^{n-1}L_{\alpha,n}(u)\,du,$$

$$B_{\alpha,n} = -\frac{2^{n+1}\pi^{\frac{n}{2}}}{\Gamma(\frac{n}{2})}\int_0^\infty u^{n-1}L_{\alpha,n}(u)\ln(L_{\alpha,n}(u))\,du.$$

The integral that defines $A_{\alpha,n}$ can be interpreted as the Mellin transform of the auxiliary function $L_{\alpha,n}$ at the point $s = n$. From (69), it is clear that

$$L^*_{\alpha,n}(s) = \int_0^\infty L_{\alpha,n}(\tau)\tau^{s-1}\,d\tau = \frac{1}{\alpha 2^n\pi^{\frac{n}{2}}}\Gamma\left(\frac{s}{2}\right)\frac{\sin(\frac{s\pi}{2}-\frac{n\pi}{2})}{\sin(\frac{s\pi}{\alpha}-\frac{n\pi}{\alpha})}, \tag{73}$$

assuming that $n - \min(\alpha, n) < \operatorname{Re} s < n$. To obtain the Mellin transform of $L_{\alpha,n}$ at $s = n$, we take the limit of the right-hand side of (73) as $s \to n$. Thus we get

$$A_{\alpha,n} = \frac{n2^n\pi^{\frac{n}{2}}}{\Gamma(\frac{n}{2})}\lim_{s\to n}L^*_{\alpha,n}(s) = \frac{n}{\alpha}\lim_{s\to n}\frac{\sin(\frac{s\pi}{2}-\frac{n\pi}{2})}{\sin(\frac{s\pi}{\alpha}-\frac{n\pi}{\alpha})} = \frac{n}{2}.$$

This representation along the formula (72) leads to the following expression for the entropy production rate:

$$R(t) = \frac{d}{dt}S(\alpha, t) = \frac{n}{2t}. \tag{74}$$

The formula (74) shows that the entropy production rate of the stochastic process governed by the α-fractional diffusion equation (47) with $n = 1, 2$ does not depend on the equation order α and agrees with the entropy production rates of the one- and two-dimensional diffusion equations.

3.4 Velocities of the fractional diffusive waves

In this subsection, a multidimensional α-fractional wave equation that describes propagation of diffusive waves is considered. In contrast to the fractional diffusion-wave equation, the α-fractional wave equation contains fractional derivatives of the same order α, $1 \le \alpha \le 2$ both in space and in time. This feature is a decisive factor for inheriting some crucial characteristics of the wave equation, such as, a constant phase velocity of the diffusive waves described by the fractional wave equation.

Following [19] and [20], we consider the following initial-value problem for the multi-dimensional α-fractional wave equation:

$$u(x,0) = \varphi(x), \quad \frac{\partial u}{\partial t}(x,0) = 0, \quad x \in \mathbb{R}^n, \tag{75}$$

$$-(-\Delta)^{\frac{\alpha}{2}}u(x,t) = {}_tD^\alpha_* u(x,t) =, \quad x \in \mathbb{R}^n,\ t \in \mathbb{R}_+,\ 1 \le \alpha \le 2. \tag{76}$$

In (76), $-(-\Delta)^{\frac{\alpha}{2}}$ stays for the fractional Laplacian and ${}_tD_*^\alpha$ for the Caputo time-fractional derivative of order α.

The one-dimensional case of the equation (76) was analyzed in detail in [19]. In this case, the fundamental solution can be expressed in terms of elementary functions [6, 19, 35]:

$$G_{\alpha,1}(x,t) = \frac{1}{\pi}\frac{|x|^{\alpha-1}t^\alpha \sin(\pi\alpha/2)}{t^{2\alpha} + 2|x|^\alpha t^\alpha \cos(\pi\alpha/2) + |x|^{2\alpha}}, \quad t > 0,\ x \in \mathbb{R},\ 1 \le \alpha < 2. \tag{77}$$

In [19], several kinds of velocities were determined for the diffusive waves that are described by the α-fractional wave equation (76).

The phase velocity $v_p(\alpha)$ is interpreted as velocity of propagation of the maximum location of the fundamental solution $G_{\alpha,1}$ (that we denote just by G_α). It is given by the expression

$$v_p(\alpha) = \left(\frac{-\cos(\pi\alpha/2) + \sqrt{\alpha^2 - \sin^2(\pi\alpha/2)}}{\alpha+1}\right)^{\frac{1}{\alpha}}. \tag{78}$$

For $\alpha = 1$ (modified advection equation), the propagation velocity of the maximum of G_α is equal to zero (the maximum point stays at $x = 0$) whereas for $\alpha = 2$ (wave equation) the maximum point propagates with the constant velocity 1.

The propagation velocity $v_g(\alpha)$ of the gravity center of G_α is given by the formula

$$v_g(\alpha) = \frac{2}{\alpha \sin(\pi/\alpha)}. \tag{79}$$

$v_g(\alpha)$ is thus time-independent and determined by the order α of the fractional wave equation. Evidently, $v_g(2) = 1$ and $v_g(\alpha) \to +\infty$ as $\alpha \to 1 + 0$.

The velocity $v_m(\alpha)$ of the “mass”-center of G_α or its pulse velocity is equal to

$$v_m(\alpha) = \frac{\int_0^\infty \tau^{-1} L_\alpha^2(\tau)\, d\tau}{\int_0^\infty L_\alpha^2(\tau)\, d\tau}, \tag{80}$$

where the function L_α is defined by

$$L_\alpha(\tau) = \frac{1}{\pi}\frac{\tau^\alpha \sin(\pi\alpha/2)}{\tau^{2\alpha} + 2\tau^\alpha \cos(\pi\alpha/2) + 1}, \quad \tau > 0,\ 1 < \alpha < 2. \tag{81}$$

Let us note here that the function $\frac{1}{|\tau|}L_\alpha(|\tau|)$ can be interpreted as a fractional Cauchy pdf of order α.

The second centrovelocity $v_2(\alpha)$ is defined as the mean pulse velocity computed from 0 to time t. For the diffusive wave that is described by the fundamental solution of the fractional wave equation, the second centrovelocity is equal to its pulse velocity $v_m(\alpha)$:

$$v_2(\alpha) = v_m(\alpha) = \frac{\int_0^\infty \tau^{-1} L_\alpha^2(\tau)\, d\tau}{\int_0^\infty L_\alpha^2(\tau)\, d\tau}. \tag{82}$$

The Smith centrovelocity $v_c(\alpha)$ of the waves describes the motion of the first moment of their energy distribution. For a diffusive wave that is described by the fundamental solution of the fractional wave equation, $v_c(\alpha)$ can be evaluated in explicit form:

$$v_c(\alpha) = \frac{\int_0^\infty L_\alpha^2(\tau)d\tau}{\int_0^\infty \tau L_\alpha^2(\tau)\,d\tau}, \tag{83}$$

where the function L_α is defined by (81). Because the integral $\int_0^\infty \tau L_\alpha^2(\tau)\,d\tau$ diverges for $\alpha = 1$, the Smith centrovelocity tends to 0 as $\alpha \to 1$.

Finally, the first centrovelocity $v_1(\alpha)$ that is defined as the mean centrovelocity from 0 to x is equal to the Smith centrovelocity $v_c(\alpha)$:

$$v_1(\alpha) = v_c(\alpha) = \frac{\int_0^\infty L_\alpha^2(\tau)\,d\tau}{\int_0^\infty \tau L_\alpha^2(\tau)\,d\tau}. \tag{84}$$

As we see, all velocities introduced above are constant in time and depend just on the order α of the fractional wave equation. The phase velocity, the velocity of the gravity center of G_α, the pulse velocity, and the Smith centrovelocity are different each to other whereas the first centrovelocity coincides with the Smith centrovelocity and the second centrovelocity is the same as the pulse velocity. For the physical interpretation and meaning of the velocities that were determined above, we refer to, for example, [31, 49, 50].

The plots of the propagation velocity v_p of the maximum of the fundamental solution G_α (phase velocity), the velocity v_g of its gravity center, its pulse velocity v_m and its centrovelocity v_c are presented in Figure 3. As expected, $v_p = v_c = 0$ for $\alpha = 1$ (modified advection equation) and all velocities smoothly approach the value 1 as $\alpha \to 2$ (wave equation). For $1 < \alpha < 2$, v_p, v_m, and v_c monotonously increase whereas v_g monotonously decreases. It is interesting to note that for all velocities $v = v(\alpha)$, the property $\frac{dv(\alpha)}{d\alpha}(2-0) = 0$ holds true, that is, in a small neighborhood of the point $\alpha = 2$ the velocities of G_α are nearly the same as in the case of the fundamental solution of the wave equation. The velocity v_g of the gravity center of G_α tends to $+\infty$ for $\alpha \to 1+0$

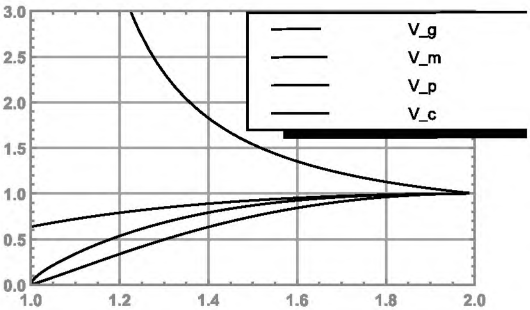

Figure 3: Plots of the gravity center velocity $v_g(\alpha)$, the pulse velocity $v_m(\alpha)$, the phase velocity $v_p(\alpha)$, and the centrovelocity $v_c(\alpha)$ for $1 \le \alpha \le 2$.

and $t > 0$ (modified advection equation) because the first moment of the Cauchy kernel does not exist. It is interesting to note that for all α, $1 < \alpha < 2$ the velocities v_p, v_g, v_m, v_c are different each to other and fulfill the inequalities $v_c(\alpha) < v_p(\alpha) < v_m(\alpha) < v_g(\alpha)$. For $\alpha = 2$, all velocities are equal to 1.

For a detailed discussion of the n-dimensional α-fractional wave equation with a special focus given to the three-dimensional case, we refer the interested reader to [20].

Bibliography

[1] L. Boyadjiev and Yu. Luchko, Mellin integral transform approach to analyze the multidimensional diffusion-wave equations, *Chaos Solitons Fractals*, **102** (2017), 127–134.

[2] L. Boyadjiev and Yu. Luchko, Multi-dimensional α-fractional diffusion-wave equation and some properties of its fundamental solution, *Comput. Math. Appl.*, **73** (2017), 2561–2572.

[3] W. Feller, On a generalization of Marcel Riesz' potentials and the semi-groups generated by them, in *Meddelanden Lunds Universitets Matematiska Seminarium*, Comm. Sém. Mathém. Université de Lund, Tome suppl. dédié à M. Riesz, Lund, pp. 73–81, 1952.

[4] Y. Fujita, Integrodifferential equation which interpolates the heat equation and the wave equation, I, II, *Osaka J. Math.*, **27** (1990), 309–321, 797–804.

[5] R. Gorenflo and F. Mainardi, Random Walk Models for Space-Fractional Diffusion Processes, *Fract. Calc. Appl. Anal.*, **1** (1998), 167–191.

[6] R. Gorenflo, A. Iskenderov, and Yu. Luchko, Mapping between solutions of fractional diffusion-wave equations, *Fract. Calc. Appl. Anal.*, **3** (2000), 75–86.

[7] R. Gorenflo, A. A. Kilbas, F. Mainardi, and S. V. Rogosin, *Mittag-Leffler Functions, Related Topics and Applications*, Springer, Berlin, 2014, second edition in preparation.

[8] A. Hanyga, Multidimensional solutions of space-fractional diffusion equations, *Proc. R. Soc. Lond. A*, **457** (2001), 2993–3005.

[9] A. Hanyga, Multi-dimensional solutions of space-time-fractional diffusion equations, *Proc. R. Soc. Lond. A*, **458** (2002), 429–450.

[10] A. Hanyga, Multidimensional solutions of time-fractional diffusion-wave equations, *Proc. R. Soc. Lond. A*, **458** (2002), 933–957.

[11] R. Hilfer, *Applications of Fractional Calculus in Physics*, World Scientific Publishing, Singapore, 2000.

[12] K. H. Hoffmann, C. Essex, and C. Schulzky, Fractional diffusion and entropy production, *J. Non-Equilib. Thermodyn.*, **23** (1998), 166–175.

[13] R. Klages, G. Radons, and I. M. Sokolov, *Anomalous Transport: Foundations and Applications*, Wiley–VCH, Hoboken, 2008.

[14] A. N. Kochubei, Fractional-order diffusion, *Differ. Equ.*, **26** (1990), 485–492.

[15] A. Kreis and A. C. Pipkin, Viscoelastic pulse propagation and stable probability distributions, *Q. Appl. Math.*, **44** (1986), 353–360.

[16] X. Li, C. Essex, M. Davison, K. H. Hoffmann, and C. Schulzky, Fractional diffusion, irreversibility and entropy, *J. Non-Equilib. Thermodyn.*, **28** (2003), 279–291.

[17] Yu. Luchko, Models of the neutral-fractional anomalous diffusion and their analysis, *AIP Conf. Proc.*, **1493** (2012), 626–632.

[18] Yu. Luchko, Anomalous diffusion: Models, their analysis, and interpretation, in *Advances in Applied Analysis*, pp. 115–146, Birkhäuser, Basel, 2012.

[19] Yu. Luchko, Fractional wave equation and damped waves, *J. Math. Phys.*, **54** (2013), 031505.

[20] Yu. Luchko, Multi-dimensional fractional wave equation and some properties of its fundamental solution, *Commun. Appl. Ind. Math.* **6** (2014), e-485.

[21] Yu. Luchko, Wave-diffusion dualism of the neutral-fractional processes, *J. Comput. Phys.*, **293** (2015), 40–52.

[22] Yu. Luchko, Entropy production rate of a one-dimensional alpha-fractional diffusion process, *Axioms*, **5** (2016), doi:10.3390/axioms5010006.

[23] Yu. Luchko, A new fractional calculus model for the two-dimensional anomalous diffusion and its analysis, *Math. Model. Nat. Phenom.*, **11** (2016), 1–17.

[24] Yu. Luchko, On some new properties of the fundamental solution to the multi-dimensional space- and time-fractional diffusion-wave equation, *Mathematics*, **5** (2017), 1–16.

[25] Yu. Luchko, Subordination principles for the multi-dimensional space-time-fractional diffusion-wave equation, arXiv:1802.04752 [math.AP].

[26] Yu. Luchko and R. Gorenflo, Scale-invariant solutions of a partial differential equation of fractional order, *Fract. Calc. Appl. Anal.*, **1** (1998), 63–78.

[27] Yu. Luchko and V. Kiryakova, The Mellin integral transform in fractional calculus, *Fract. Calc. Appl. Anal.*, **16** (2013), 405–430.

[28] Yu. Luchko and F. Mainardi, Some properties of the fundamental solution to the signalling problem for the fractional diffusion-wave equation, *Cent. Eur. J. Phys.*, **11** (2013), 666–675.

[29] Yu. Luchko and F. Mainardi, Cauchy and signaling problems for the time-fractional diffusion-wave equation, *ASME J. Vib. Acoust.*, **136**(5) (2014), 050904/1-7, 10.1115/1.4026892. [E-print arXiv:1609.05443].

[30] Yu. Luchko, F. Mainardi, and Yu. Povstenko, Propagation speed of the maximum of the fundamental solution to the fractional diffusion-wave equation, *Comput. Math. Appl.*, **66** (2013), 774–784.

[31] F. Mainardi, Energy propagation for dispersive waves in dissipative media, *Radiofisika [Radiophys. Quantum Electron.]*, **36** (1993), 650–664.

[32] F. Mainardi, Fractional diffusive waves in viscoelastic solids, in J. L. Wegner and F. R. Norwood (eds.), *IUTAM Symposium – Nonlinear Waves in Solids*, pp. 93–97, ASME/AMR, Fairfield, NJ, 1995.

[33] F. Mainardi, *Fractional Calculus and Waves in Linear Viscoelasticity*, Imperial College Press, London, 2010, second edition in preparation.

[34] F. Mainardi and M. Tomirotti, Seismic pulse propagation with constant Q and stable probability distributions, *Ann. Geofis.*, **40** (1997), 1311–1328.

[35] F. Mainardi, Yu. Luchko, and G. Pagnini, The fundamental solution of the space-time fractional diffusion equation, *Fract. Calc. Appl. Anal.*, **4** (2001), 153–192.

[36] F. Mainardi, G. Pagnini, and R. Gorenflo, Mellin transform and subordination laws in fractional diffusion processes, *Fract. Calc. Appl. Anal.*, **6** (2003), 441–459.

[37] O. I. Marichev, *Handbook of Integral Transforms of Higher Transcendental Functions. Theory and Algorithmic Tables*, Ellis Horwood, Chichester, 1983.

[38] R. Metzler and J. Klafter, The restaurant at the end of the random walk: Recent developments in the description of anomalous transport by fractional dynamics, *Phys. A., Math. Gen.*, **37** (2004), R161–R208.

[39] R. Metzler and T. F. Nonnenmacher, Space- and time-fractional diffusion and wave equations, fractional Fokker-Planck equations, and physical motivation, *Chem. Phys.*, **284** (2002), 67–90.

[40] R. Metzler, J.-H. Jeon, A. G. Cherstvy, and E. Barkai, Anomalous diffusion models and their properties: non-stationarity, non-ergodicity, and ageing at the centenary of single particle tracking, *Phys. Chem. Chem. Phys.*, **16** (2014), 24128.

[41] A. C. Pipkin, *Lectures on Viscoelastic Theory*, Springer Verlag, New York, 1986.

[42] J. Prehl, C. Essex, and K. H. Hoffmann, The superdiffusion entropy production paradox in the space-fractional case for extended entropies, *Physica A*, **389** (2010), 214–224.

[43] J. Prehl, C. Essex, and K. H. Hoffmann, Tsallis relative entropy and anomalous diffusion, *Entropy*, **14** (2012), 701–716.

[44] A. Saichev and G. Zaslavsky, Fractional kinetic equations: Solutions and applications, *Chaos*, **7** (1997), 753–764.

[45] S. G. Samko, A. A. Kilbas, and O. I. Marichev, *Fractional Integrals and Derivatives: Theory and Applications*, Gordon and Breach, New York, 1993.

[46] W. R. Schneider and W. Wyss, Fractional diffusion and wave equations, *J. Math. Phys.*, **30** (1989), 134–144.

[47] V. V. Uchaikin, Montroll–Weiss' problem, fractional equations and stable distributions, *Int. J. Theor. Phys.*, **39** (2000), 2087–2105.

[48] V. V. Uchaikin, *Fractional Derivatives for Physicists and Engineers. Vol. II: Applications*, Springer, Berlin, 2013.

[49] E. van Groesen and F. Mainardi, Energy propagation in dissipative systems, Part I: Centrovelocity for linear systems, *Wave Motion*, **11** (1989), 201–209.

[50] E. van Groesen and F. Mainardi, Balance laws and centrovelocity in dissipative systems, *J. Math. Phys.*, **30** (1990), 2136–2140.

[51] E. M. Wright, The asymptotic expansion of the generalized hypergeometric function, *J. Lond. Math. Soc.*, **10** (1935), 287–293.

Rudolf Gorenflo and Francesco Mainardi

Fractional diffusion and parametric subordination

Abstract: In this chapter, we consider simulation of spatially one-dimensional space-time fractional diffusion. After a survey on the operators entering the basic fractional equation via Fourier–Laplace manipulations, we obtain the subordination integral formula that teaches us how a particle path can be constructed by first generating the operational time from the physical time and then generating in operational time the spatial path. By inverting the generation of operational time from physical time, we arrive at the method of parametric subordination.

Keywords: Fractional derivatives and integrals, fractional diffusion, Mittag-Leffler function, Wright function, random walks, subordination, self-similar stochastic processes, stable distributions, infinite divisibility

MSC 2010: 26A33, 33E12, 33C60, 44A10, 45K05, 60G18, 60G50, 60G52, 60K05, 76R50

1 Introduction

The purpose of this chapter is to describe our method of parametric subordination to produce particle trajectories for the so-called fractional diffusion processes.

By replacing in the common diffusion equation the first-order time derivative and the second-order space derivative by appropriate fractional derivatives, we obtain a fractional diffusion equation whose solution describes the temporal evolution of the density of an extensive quantity, for example, of the sojourn probability of a diffusing particle.

After giving a survey on analytic methods for determination of the solution (this is the macroscopic aspect), we turn our attention to the problem of simulation of particle trajectories (the microscopic aspect). By some authors, such simulation is called “particle tracking”; see, for example, [63].

Note: Rudolf Gorenflo (31.07.1930–20.10.2017).

Acknowledgement: We acknowledge the valuable assistance of the former PhD students of FM: A. Mura and A. Vivoli in producing the figures. The research activity of FM has been carried out in the framework of the National Group of Mathematical Physics (GNFM-INdAM).

Rudolf Gorenflo, Department of Mathematics, Free University Berlin, Berlin, Germany
Francesco Mainardi, Department of Physics and Astronomy, University of Bologna, Via Irnerio 46, 40126 Bologna, Italy, e-mail: francesco.mainardi@bo.infn.it

As an approximate method among physicists, the so-called Continuous Time Random Walk (*CTRW*) is very popular. On the other hand, it is possible to produce a sequence of precise snapshots of a true trajectory. This is achieved by a change from the "physical time" to an "operational time" in which the simulation is carried out. By two Markov processes happening in operational time, the running of physical time and the motion in space are produced. Then elimination of the operational time yields a picture of the desired trajectory. It is remarkable that so by combination of two Markov processes, a non-Markovian process is generated.

The two Markov processes can be obtained and analyzed in two ways:

(a) from the *CTRW* model by a well-scaled passage to the "diffusion limit",

(b) directly from an integral representation of the fundamental solution of the fractional diffusion equation.

We have developed a way (a) in our 2007 paper [19] via passage to the diffusion limit in the Cox–Weiss solution formula for *CTRW*, and by the technique of splitting the *CTRW* into three separate walks and passing in each of these to the diffusion limit in our 2011 paper [17]. For another access (more oriented toward measure-theoretic theory of stochastic processes), see the papers [20, 21]. In [21], the authors also treat the problem of subordination for diffusion with distributed orders of time-fractional differentiation.

The plan of our chapter is as follows. In Section 2, we provide for the reader's convenience some preliminary notions and notation as a mathematical background for our further analysis. In Section 3, we introduce the *space-time fractional diffusion equation*, based on the *Riesz–Feller* and *Caputo* fractional derivatives, and we present the fundamental solution. In Section 4, we provide the stochastic interpretation of the space-time fractional diffusion equation discussing the concepts of subordination, the main goal of this chapter. Finally, in Section 5 we show some graphical representations along with conclusions.

2 Notions and notation

In this section, we survey some preliminary notions including Fourier and Laplace transforms, special functions of Mittag-Leffler and Wright type, and Lévy stable probability distributions.

Since in what follows we shall meet only real or complex-valued functions of a real variable that are defined and continuous in a given open interval $I = (a, b)$, $-\infty \le a < b \le +\infty$, except, possibly, at isolated points where these functions can be infinite, we restrict our presentation of the integral transforms to the class of functions for which the Riemann improper integral on I absolutely converges. In so doing, we follow Marichev [34] and we denote this class by $L^c(I)$ or $L^c(a, b)$.

2.1 The Fourier transform

Let

$$\widehat{f}(\kappa) = \mathcal{F}\{f(x); \kappa\} = \int_{-\infty}^{+\infty} e^{+i\kappa x} f(x)\, dx, \quad \kappa \in \mathbb{R}, \tag{2.1a}$$

be the Fourier transform of a function $f(x) \in L^c(\mathbb{R})$, and let

$$f(x) = \mathcal{F}^{-1}\{\widehat{f}(\kappa); x\} = \frac{1}{2\pi} \int_{-\infty}^{+\infty} e^{-i\kappa x} \widehat{f}(\kappa)\, d\kappa, \quad x \in \mathbb{R}, \tag{2.1b}$$

be the inverse Fourier transform.[1]

Related to the Fourier transform is the notion of the pseudo-differential operator. Let us recall that a generic pseudo-differential operator A, acting with respect to the variable $x \in \mathbb{R}$, is defined through its Fourier representation, namely

$$\int_{-\infty}^{+\infty} e^{i\kappa x} A[f(x)]\, dx = \widehat{A}(\kappa)\widehat{f}(\kappa), \tag{2.2}$$

where $\widehat{A}(\kappa)$ is referred to as symbol of A, formally given as $\widehat{A}(\kappa) = (Ae^{-i\kappa x})e^{+i\kappa x}$.

2.2 The Laplace transform

Let

$$\widetilde{f}(s) = \mathcal{L}\{f(t); s\} = \int_{0}^{\infty} e^{-st} f(t)\, dt, \quad \Re(s) > a_f, \tag{2.3a}$$

be the Laplace transform of a function $f(t) \in \mathcal{L}^c(0, T), \forall T > 0$ and let

$$f(t) = \mathcal{L}^{-1}\{\widetilde{f}(s); t\} = \frac{1}{2\pi i} \int_{\gamma-i\infty}^{\gamma+i\infty} e^{st} \widetilde{f}(s)\, ds, \quad \Re(s) = \gamma > a_f, \tag{2.3b}$$

with $t > 0$, be the inverse Laplace transform[2]

---

1 If $f(x)$ is piecewise differentiable, then the formula (2.1b) holds true at all points where $f(x)$ is continuous and the integral in it must be understood in the sense of the Cauchy principal value.

2 A sufficient condition of the existence of the Laplace transform is that the original function is of exponential order as $t \to \infty$. This means that some constant a_f exists such that the product $e^{-a_f t}|f(t)|$ is bounded for all t greater than some T. Then $\widetilde{f}(s)$ exists and is analytic in the half-plane $\Re(s) > a_f$. If $f(t)$ is piecewise differentiable, then the formula (2.3b) holds true at all points where $f(t)$ is continuous and the (complex) integral in it must be understood in the sense of the Cauchy principal value.

2.3 The auxiliary functions of Mittag-Leffler type

The Mittag-Leffler functions that we denote by $E_\alpha(z)$, $E_{\alpha,\beta}(z)$ are so named in honor of Gösta Mittag-Leffler, the eminent Swedish mathematician, who introduced and investigated these functions in a series of notes starting from 1903 in the framework of the theory of entire functions [45–47]. The functions are defined by the series representations, convergent in the whole complex plane $\mathbb{C}$

$$E_\alpha(z) := \sum_{n=0}^{\infty} \frac{z^n}{\Gamma(\alpha n + 1)}, \quad \mathrm{Re}(\alpha) > 0; \tag{2.4}$$

$$E_{\alpha,\beta}(z) := \sum_{n=0}^{\infty} \frac{z^n}{\Gamma(\alpha n + \beta)}, \quad \mathrm{Re}(\alpha) > 0,\ \beta \in \mathbb{C}. \tag{2.5}$$

Originally Mittag-Leffler assumed only the parameter α and assumed it as positive, but soon later the generalization with two complex parameters was considered by Wiman [58]. In both cases, the Mittag-Leffler functions are entirely of order $1/\,\mathrm{Re}(\alpha)$. Generally, $E_{\alpha,1}(z) = E_\alpha(z)$.

Using their series representations, it is easy to recognize

$$\begin{cases} E_{1,1}(z) = E_1(z) = \mathrm{e}^z, & E_{1,2}(z) = \dfrac{\mathrm{e}^z - 1}{z}, \\ E_{2,1}(z^2) = \cosh(z), & E_{2,1}(-z^2) = \cos(z), \\ E_{2,2}(z^2) = \dfrac{\sinh(z)}{z}, & E_{2,2}(-z^2) = \dfrac{\sin(z)}{z}, \end{cases} \tag{2.6}$$

and more generally

$$\begin{cases} E_{\alpha,\beta}(z) + E_{\alpha,\beta}(-z) = 2E_{2\alpha,\beta}(z^2), \\ E_{\alpha,\beta}(z) - E_{\alpha,\beta}(-z) = 2zE_{2\alpha,\alpha+\beta}(z^2). \end{cases} \tag{2.7}$$

We note that in Chapter 18 of Volume 3 of the handbook of the 1955 Bateman Project [4] devoted to Miscellaneous Functions, we find a valuable survey of these functions, which later were recognized as belonging to the more general class of Fox H-functions introduced after 1960. A more recent and complete survey on functions of the Mittag-Leffler type we refer the reader to the 2014 treatise by Gorenflo et al. [12].

For our purposes, relevant roles are played by the following auxiliary functions of the Mittag-Leffler type on support $\mathbb{R}^+$ defined as follows, where $\lambda > 0$, along with their Laplace transforms

$$e_\alpha(t;\lambda) := E_\alpha(-\lambda t^\alpha) \div \frac{s^{\alpha-1}}{s^\alpha + \lambda}, \tag{2.8}$$

$$e_{\alpha,\beta}(t;\lambda) := t^{\beta-1} E_{\alpha,\beta}(-\lambda t^\alpha) \div \frac{s^{\alpha-\beta}}{s^\alpha + \lambda}, \tag{2.9}$$

$$e_{\alpha,\alpha}(t;\lambda) := t^{\alpha-1} E_{\alpha,\alpha}(-\lambda t^\alpha) = \frac{d}{dt} e_\alpha(-\lambda t^\alpha) = \div - \frac{\lambda}{s^\alpha + \lambda}. \tag{2.10}$$

Here, we have used the sign ÷ for the juxtaposition of a function depending on t with its Laplace transform depending on s. Later we use this sign also for juxtaposition of a function depending on x with its Fourier transform depending on κ.

Remark. We outline that the above auxiliary functions (for restricted values of the parameters) turn out to be *completely monotone* (CM) functions so that they enter in some types of relaxation phenomena of physical relevance.

We recall that a function $f(t)$ is CM in $\mathbb{R}^+$ if $(-1)^n f^n(t) \geq 0$. The function e^{-t} is the prototype of a CM function. For a Bernstein theorem, more generally they are expressed in terms of a (generalized) real Laplace transform of a positive measure

$$f(t) = \int_0^\infty e^{-rt} K(r)\,dr, \quad K(r) \geq 0. \tag{2.11}$$

Restricting attention to the auxiliary function in two parameters, we can prove for $\lambda > 0$ that

$$e_{\alpha,\beta}(t;\lambda) := t^{\beta-1} E_{\alpha,\beta}(-\lambda t^\alpha) \quad \text{CM} \quad \text{iff} \quad 0 < \alpha \leq \beta \leq 1. \tag{2.12}$$

Using the Laplace transform, we can prove, following Gorenflo and Mainardi [13], that for $0 < \alpha < 1$ and $\lambda = 1$,

$$E_\alpha(-t^\alpha) \simeq \begin{cases} 1 - \frac{t^\alpha}{\Gamma(\alpha+1)} + \frac{t^{2\alpha}}{\Gamma(2\alpha+1)} \cdots & t \to 0^+, \\ \frac{t^{-\alpha}}{\Gamma(1-\alpha)} - \frac{t^{-2\alpha}}{\Gamma(1-2\alpha)} \cdots & t \to +\infty, \end{cases} \tag{2.13}$$

and

$$E_\alpha(-t^\alpha) = \int_0^\infty e^{-rt} K_\alpha(r)\,dr \tag{2.14}$$

with

$$K_\alpha(r) = \frac{1}{\pi} \frac{r^{\alpha-1} \sin(\alpha\pi)}{r^{2\alpha} + 2r^\alpha \cos(\alpha\pi) + 1} = \frac{1}{\pi r} \frac{\sin(\alpha\pi)}{r^\alpha + 2\cos(\alpha\pi) + r^{-\alpha}} > 0. \tag{2.15}$$

2.4 The auxiliary functions of the Wright type

The Wright function, that we denote by $W_{\lambda,\mu,}(z)$, is so named in honor of E. Maitland Wright, the eminent British mathematician, who introduced and investigated this function in a series of notes starting from 1933 in the framework of the asymptotic theory of partitions; see [59–61]. The function is defined by the series representation, convergent in the whole z-complex plane $\mathbb{C}$,

$$W_{\lambda,\mu}(z) := \sum_{n=0}^\infty \frac{z^n}{n!\,\Gamma(\lambda n + \mu)}, \quad \lambda > -1,\ \mu \in \mathbb{C}. \tag{2.16}$$

Originally, Wright assumed $\lambda \geq 0$, and, only in 1940 [62], he considered $-1 < \lambda < 0$. We note that in Chapter 18 of Volume 3 of the handbook of the 1955 Bateman Project [4] devoted to Miscellaneous Functions, we find an earlier analysis of these functions, which, similarly with the Mittag-Leffler functions, were later recognized as belonging to the more general class of Fox H-functions introduced after 1960. However, in that chapter, presumably for a misprint, the parameter λ of the Wright function is restricted to be nonnegative. It is possible to prove that the Wright function is entirely of order $1/(1+\lambda)$, hence it is of exponential type only if $\lambda \geq 0$. For this reason, we propose to distinguish the Wright functions in two kinds according to $\lambda \geq 0$ (*first kind*) and $-1 < \lambda < 0$ (*second kind*). Both kinds of functions are related to the Mittag-Leffler function via Laplace transform pairs: in fact, we have (see, for details, Appendix F of the recent book by Mainardi [29]), for the case $\lambda > 0$ (Wright functions of the first kind),

$$W_{\lambda,\mu}(\pm r) \div \frac{1}{s} E_{\lambda,\mu}\left(\pm\frac{1}{s}\right), \quad \lambda > 0, \tag{2.17}$$

and for the case $\lambda = -\nu \in (-1, 0)$ (Wright functions of the second kind),

$$W_{-\nu,\mu}(-r) \div E_{\nu,\mu+\nu}(-s), \quad 0 < \nu < 1. \tag{2.18}$$

For our purposes, relevant roles are played by the following auxiliary functions of the Wright type (of the second kind):

$$F_\nu(z) := W_{-\nu,0}(-z) = \sum_{n=1}^{\infty} \frac{(-z)^n}{n!\,\Gamma(-\nu n)}, \quad 0 < \nu < 1, \tag{2.19}$$

and

$$M_\nu(z) := W_{-\nu,1-\nu}(-z) = \sum_{n=0}^{\infty} \frac{(-z)^n}{n!\,\Gamma[-\nu n + (1-\nu)]}, \quad 0 < \nu < 1, \tag{2.20}$$

interrelated through $F_\nu(z) = \nu z M_\nu(z)$. The relevance of these functions was pointed out by Mainardi in his former analysis of the time fractional diffusion equation via Laplace transform. Restricting our attention to the M-Wright functions on support $\mathbb{R}^+$, we point out the Laplace transforms pairs

$$M_\nu(r) \div E_\nu(-s), \quad 0 < \nu < 1. \tag{2.21}$$

$$\frac{\nu}{r^{\nu+1}} M_\nu(1/r^\nu) \div \mathrm{e}^{-s^\nu}, \quad 0 < \nu < 1. \tag{2.22}$$

$$\frac{1}{r^\nu} M_\nu(1/r^\nu) \div \frac{\mathrm{e}^{-s^\nu}}{s^{1-\nu}}, \quad 0 < \nu < 1. \tag{2.23}$$

It was also proved in [29] that the M-Wright function on support $\mathbb{R}^+$ is a probability density function (pdf) that in the literature is sometimes known as the density related to Mittag-Leffler probability distribution. Its absolute moments of order $\delta > -1$ in $\mathbb{R}^+$ are finite and turn out to be

$$\int_0^\infty r^\delta M_\nu(r)\,dx = \frac{\Gamma(\delta+1)}{\Gamma(\nu\delta+1)}, \quad \delta > -1,\ 0 \le \nu < 1. \tag{2.24}$$

We point out that in the limit $\nu \to 1^-$ the function $M_\nu(r)$, for $r \in \mathbb{R}^+$, tends to the Dirac generalized function $\delta(r-1)$.

For our next purposes, it is worthwhile to introduce the *function in two variables*

$$M_\nu(x,t) := t^{-\nu} M_\nu(xt^{-\nu}), \quad 0 < \nu < 1,\ x,t \in \mathbb{R}^+, \tag{2.25}$$

which defines a spatial probability density in x evolving in time t with self-similarity exponent $H = \nu$. Of course, for $x \in \mathbb{R}$, we can consider the symmetric version obtained from (2.25) multiplying by 1/2 and replacing x by $|x|$. Hereafter, we provide a list of the main properties of this density, which can be derived from the Laplace and Fourier transforms for the corresponding Wright M-function in one variable.

From equation (2.23), we derive the Laplace transform of $M_\nu(x,t)$ with respect to $t \in \mathbb{R}^+$,

$$\mathcal{L}\{M_\nu(x,t); t \to s\} = s^{\nu-1} \mathrm{e}^{-xs^\nu}. \tag{2.26}$$

From equation (2.21), we derive the Laplace transform of $M_\nu(x,t)$ with respect to $x \in \mathbb{R}^+$,

$$\mathcal{L}\{M_\nu(x,t); x \to s\} = E_\nu(-st^\nu). \tag{2.27}$$

From the book by Mainardi [29], we recall the Fourier transform of $M_\nu(|x|,t)$ with respect to $x \in \mathbb{R}$,

$$\mathcal{F}\{M_\nu(|x|,t); x \to \kappa\} = 2E_{2\nu}(-\kappa^2 t^{2\nu}), \tag{2.28}$$

and, in particular,

$$\begin{cases} \displaystyle\int_0^\infty \cos(\kappa x) M_\nu(x,t)\,dx = E_{2\nu,1}(-\kappa^2 t^{2\nu}), \\ \displaystyle\int_0^\infty \sin(\kappa x) M_\nu(x,t)\,dx = \kappa t^\nu E_{2\nu,1+\nu}(-\kappa^2 t^{2\nu}). \end{cases} \tag{2.29}$$

It is worthwhile to note that for $\nu = 1/2$ we recover the Gaussian density evolving with time with variance $\sigma^2 = 2t$,

$$\frac{1}{2} M_{1/2}(x,t) = \frac{1}{2\sqrt{\pi} t^{1/2}} \mathrm{e}^{-x^2/(4t)}. \tag{2.30}$$

2.5 The Lévy stable distributions

The term stable has been assigned by the French mathematician Paul Lévy, who, in the twenties of the last century, started a systematic research in order to generalize the celebrated *central limit theorem* to probability distributions with infinite variance. For stable distributions, we can assume the following definition: *If two independent real random variables with the same shape or type of distribution are combined linearly with positive coefficients and the distribution of the resulting random variable has the same shape, the common distribution (or its type, more precisely) is said to be stable.*

The restrictive condition of stability enabled Lévy (and then other authors) to derive the *canonic form* for the characteristic function of the densities of these distributions. Here, we follow the parameterization by Feller [5] and revisited in [14] and in [31]. Denoting by $L_\alpha^\theta(x)$ a generic stable density in $\mathbb{R}$, where α is the *index of stability* and θ the asymmetry parameter, improperly called *skewness*; its characteristic function reads

$$\begin{cases} L_\alpha^\theta(x) \div \widehat{L}_\alpha^\theta(\kappa) = \exp[-\psi_\alpha^\theta(\kappa)], \quad \psi_\alpha^\theta(\kappa) = |\kappa|^\alpha e^{i(\operatorname{sign}\kappa)\theta\pi/2}, \\ 0 < \alpha \le 2, \quad |\theta| \le \min\{\alpha, 2-\alpha\}. \end{cases} \tag{2.31}$$

We note that the allowed region for the real parameters α and θ turns out to be a diamond in the plane $\{\alpha, \theta\}$ with vertices in the points $(0,0)$, $(1,1)$, $(1,-1)$, $(2,0)$, that we call the *Feller–Takayasu diamond*; see Figure 1. For values of θ on the border of the diamond (i. e., $\theta = \pm\alpha$ if $0 < \alpha < 1$, and $\theta = \pm(2-\alpha)$ if $1 < \alpha < 2$) we obtain the so-called *extremal stable densities*.

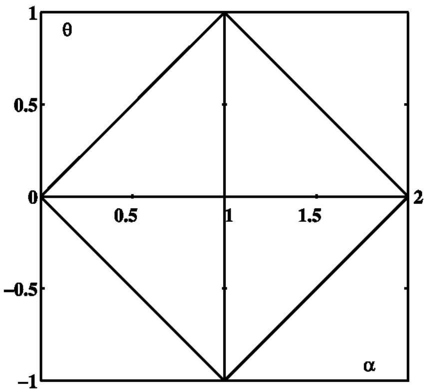

Figure 1: The Feller–Takayasu diamond.

We note the *symmetry relation* $L_\alpha^\theta(-x) = L_\alpha^{-\theta}(x)$, so that a stable density with $\theta = 0$ is symmetric.

Stable distributions have noteworthy properties on which the interested reader can be informed from the relevant existing literature. Hereafter, we recall some peculiar properties:

- *Each stable density L_α^θ possesses a domain of attraction*; see, for example, [5].
- *Any stable density is unimodal and indeed bell-shaped*, that is, its nth derivative has exactly n zeros in $\mathbb{R}$; see [8].
- *The stable distributions are self-similar and infinitely divisible.*

These properties derive from the canonic form (2.31) through the scaling property of the Fourier transform.

Self-similarity means

$$L_\alpha^\theta(x,t) \div \exp[-t\psi_\alpha^\theta(\kappa)] \Longleftrightarrow L_\alpha^\theta(x,t) = t^{-1/\alpha}[L_\alpha^\theta(x/t^{1/\alpha})], \tag{2.32}$$

where t is a positive parameter. If t is time, then $L_\alpha^\theta(x,t)$ is a spatial density evolving in time with self-similarity.

Infinite divisibility means that for every positive integer n, the characteristic function can be expressed as the nth power of some characteristic function, so that any stable distribution can be expressed as the n-fold convolution of a stable distribution of the same type. Indeed, taking in (2.31) $\theta = 0$, without loss of generality, we have

$$\mathrm{e}^{-t|\kappa|^\alpha} = \left[\mathrm{e}^{-(t/n)|\kappa|^\alpha}\right]^n \Longleftrightarrow L_\alpha^0(x,t) = \left[L_\alpha^0(x,t/n)\right]^{*n}, \tag{2.33}$$

where

$$\left[L_\alpha^0(x,t/n)\right]^{*n} := L_\alpha^0(x,t/n) * L_\alpha^0(x,t/n) * \cdots * L_\alpha^0(x,t/n) \tag{2.34}$$

is the multiple Fourier convolution in $\mathbb{R}$ with n identical terms.

Only in special cases the inversion of the Fourier transform in (2.31) can be carried out using standard tables, and provides well-known probability distributions.

For $\alpha = 2$ (so $\theta = 0$), we recover the *Gaussian pdf* that turns out to be the only stable density with finite variance, and more generally with finite moments of any order $\delta \geq 0$. In fact,

$$L_2^0(x) = \frac{1}{2\sqrt{\pi}}\mathrm{e}^{-x^2/4}. \tag{2.35}$$

All the other stable densities have finite absolute moments of order $\delta \in [-1,\alpha)$ as we will later show.

For $\alpha = 1$ and $|\theta| < 1$, we get

$$L_1^\theta(x) = \frac{1}{\pi}\frac{\cos(\theta\pi/2)}{[x+\sin(\theta\pi/2)]^2 + [\cos(\theta\pi/2)]^2}, \tag{2.36}$$

which for $\theta = 0$ includes the *Cauchy–Lorentz pdf*,

$$L_1^0(x) = \frac{1}{\pi}\frac{1}{1+x^2}. \tag{2.37}$$

In the limiting cases $\theta = \pm 1$ for $\alpha = 1$, we obtain the *singular Dirac pdfs,*

$$L_1^{\pm 1}(x) = \delta(x \pm 1). \tag{2.38}$$

In general, we must recall the power series expansions provided in [5]. We restrict our attention to $x > 0$ since the evaluations for $x < 0$ can be obtained using the symmetry relation. The convergent expansions of $L_\alpha^\theta(x)$ $(x > 0)$ turn out to be,

– for $0 < \alpha < 1$, $|\theta| \le \alpha$:

$$L_\alpha^\theta(x) = \frac{1}{\pi x}\sum_{n=1}^{\infty}(-x^{-\alpha})^n \frac{\Gamma(1+n\alpha)}{n!}\sin\left[\frac{n\pi}{2}(\theta-\alpha)\right]; \tag{2.39}$$

– for $1 < \alpha \le 2$, $|\theta| \le 2-\alpha$:

$$L_\alpha^\theta(x) = \frac{1}{\pi x}\sum_{n=1}^{\infty}(-x)^n \frac{\Gamma(1+n/\alpha)}{n!}\sin\left[\frac{n\pi}{2\alpha}(\theta-\alpha)\right]. \tag{2.40}$$

From the series in (2.39) and the symmetry relation, we note that *the extremal stable densities for* $0 < \alpha < 1$ *are unilateral*, precisely vanishing for $x > 0$ if $\theta = \alpha$, vanishing for $x < 0$ if $\theta = -\alpha$. In particular, the unilateral extremal densities $L_\alpha^{-\alpha}(x)$ with $0 < \alpha < 1$ have support $\mathbb{R}^+$ and Laplace transform $\exp(-s^\alpha)$. For $\alpha = 1/2$, we obtain the so-called *Lévy–Smirnov pdf*:

$$L_{1/2}^{-1/2}(x) = \frac{x^{-3/2}}{2\sqrt{\pi}}\mathrm{e}^{-1/(4x)}, \quad x \ge 0. \tag{2.41}$$

It is worth to note that the Gaussian *pdf* (2.35) and the Lévy–Smirnov *pdf* (2.41) are well known in the treatment of the Brownian motion: the former as the spatial density on an infinite real line, the latter as the first passage time density on a semi-infinite line; see, for example, [5].

As a consequence of the convergence of the series in (2.39)–(2.40) and of the symmetry relation, we recognize that the stable *pdf*s with $1 < \alpha \le 2$ are entire functions, whereas with $0 < \alpha < 1$ have the form

$$L_\alpha^\theta(x) = \begin{cases} (1/x)\Phi_1(x^{-\alpha}) & \text{for } x > 0, \\ (1/|x|)\Phi_2(|x|^{-\alpha}) & \text{for } x < 0, \end{cases} \tag{2.42}$$

where $\Phi_1(z)$ and $\Phi_2(z)$ are distinct entire functions. The case $\alpha = 1$ with $|\theta| < 1$ must be considered in the limit for $\alpha \to 1$ of (2.39)–(2.40), because the corresponding series reduce to power series akin with geometric series in $1/x$ and x, respectively, with a finite radius of convergence. The corresponding stable densities are no longer represented by entire functions, as can be noted directly from their explicit expressions (2.36)–(2.37).

From a comparison between the series expansions in (2.39)–(2.40) and in (2.19)–(2.20), we recognize that for $x > 0$ our *auxiliary functions of the Wright type are related to the extremal stable densities as follows* (see [30]):

$$L_\alpha^{-\alpha}(x) = \frac{1}{x} F_\alpha(x^{-\alpha}) = \frac{\alpha}{x^{\alpha+1}} M_\alpha(x^{-\alpha}), \quad 0 < \alpha < 1, \tag{2.43}$$

$$L_\alpha^{\alpha-2}(x) = \frac{1}{x} F_{1/\alpha}(x) = \frac{1}{\alpha} M_{1/\alpha}(x), \quad 1 < \alpha \le 2. \tag{2.44}$$

In the above equations, for $\alpha = 1$, the skewness parameter turns out to be $\theta = -1$, so we get the singular limit

$$L_1^{-1}(x) = M_1(x) = \delta(x-1). \tag{2.45}$$

We do not provide the asymptotic representations of the stable densities here, referring the interested reader to [31]. However, based on asymptotic representations, we can state the following: For $0 < \alpha < 2$, the stable densities exhibit *fat tails* in such a way that their absolute moment of order δ is finite only if $-1 < \delta < \alpha$. More precisely, one can show that for non-Gaussian, not extremal, stable densities the asymptotic decay of the tails is

$$L_\alpha^\theta(x) = O(|x|^{-(\alpha+1)}), \quad x \to \pm\infty. \tag{2.46}$$

For the extremal densities with $\alpha \ne 1$, this is valid only for one tail (as $|x| \to \infty$), the other (as $|x| \to \infty$) being of exponential order. For $1 < \alpha < 2$, the extremal *pdf*s are two-sided and exhibit an exponential left tail (as $x \to -\infty$) if $\theta = +(2-\alpha)$, or an exponential right tail (as $x \to +\infty$) if $\theta = -(2-\alpha)$. Consequently, the Gaussian *pdf* is the unique stable density with finite variance. Furthermore, when $0 < \alpha \le 1$, the first absolute moment is infinite so we should use the median instead of the nonexistent expected value in order to characterize the corresponding *pdf*.

Let us also recall a relevant identity between stable densities with index α and $1/\alpha$ (a sort of reciprocity relation) pointed out in [5], that is, assuming $x > 0$,

$$\frac{1}{x^{\alpha+1}} L_{1/\alpha}^\theta(x^{-\alpha}) = L_\alpha^{\theta^*}(x), \quad 1/2 \le \alpha \le 1, \quad \theta^* = \alpha(\theta+1) - 1. \tag{2.47}$$

The condition $1/2 \le \alpha \le 1$ implies $1 \le 1/\alpha \le 2$. A check shows that θ^* falls within the prescribed range $|\theta^*| \le \alpha$ if $|\theta| \le 2-1/\alpha$. We leave as an exercise for the interested reader the verification of this reciprocity relation in the limiting cases $\alpha = 1/2$ and $\alpha = 1$. For more details on Lévy stable densities, we refer the reader to specialized treatises, as [5, 26, 52, 53, 57, 64], where different notation are adopted. We like to refer also to the 1986 paper by Schneider [55], where he first provided the Fox H-function representation of the stable distributions (with $\alpha \ne 1$) and to the 1990 book by Takayasu [56], where he first gave the diamond representation in the plane $\{\alpha, \theta\}$.

3 The space-time fractional diffusion

We now consider the Cauchy problem for the (spatially one-dimensional) *space-time fractional diffusion* (STFD) equation,

$$ {}_tD_*^{\beta}u(x,t) = {}_xD_{\theta}^{\alpha}u(x,t), \quad u(x,0) = \delta(x), \quad x \in \mathbb{R},\ t \geq 0, \tag{3.1}$$

where $\{\alpha, \theta, \beta\}$ are real parameters restricted to the ranges

$$0 < \alpha \leq 2, \quad |\theta| \leq \min\{\alpha, 2-\alpha\},\ 0 < \beta \leq 1. \tag{3.2}$$

Here ${}_xD_{\theta}^{\alpha}$ denotes the *Riesz–Feller fractional derivative* of order α and skewness θ, acting on the space variable x, and ${}_tD_*^{\beta}$ denotes the *Caputo fractional derivative* of order β, acting on the time variable t. We recall the definitions of these fractional derivatives based on their representation in the Fourier and Laplace transform domain, respectively. So doing, we avoid the subtleties lying in the inversion of the corresponding fractional integrals; see, for example, the 2001 survey by Mainardi et al. [31]. For general information on fractional integrals and derivatives, we recommend the books [27, 49, 51].

3.1 The Riesz–Feller space-fractional derivative

We define the *Riesz–Feller* derivative as the pseudo-differential operator whose symbol is the logarithm of the characteristic function of a general *Lévy strictly stable* probability density with *index of stability* α and asymmetry parameter θ (improperly called *skewness*). As a consequence of equation (2.31), for a sufficiently well-behaved function $f(x)$, we define the *Riesz–Feller* space-fractional derivative of order α and skewness θ via the Fourier transform

$$\begin{cases} \mathcal{F}\{{}_xD_{\theta}^{\alpha}f(x);\kappa\} = -\psi_{\alpha}^{\theta}(\kappa)\widehat{f}(\kappa), \quad \psi_{\alpha}^{\theta}(\kappa) = |\kappa|^{\alpha} i^{i\theta\,\mathrm{sign}\,(\kappa)}, \\ 0 < \alpha \leq 2, \quad |\theta| \leq \min\{\alpha, 2-\alpha\}. \end{cases} \tag{3.3}$$

Notice that $i^{\theta\,\mathrm{sign}\,\kappa} = \exp[i(\mathrm{sign}\,\kappa)\theta\pi/2]$. For $\theta = 0$, we have a symmetric operator with respect to x, which can be interpreted as

$$ {}_xD_0^{\alpha} = -\left(-\frac{d^2}{dx^2}\right)^{\alpha/2}, \tag{3.4}$$

as can be formally deduced by writing $-|\kappa|^{\alpha} = -(\kappa^2)^{\alpha/2}$. We thus recognize that the operator D_0^{α} is related to a power of the positive definitive operator $-{}_xD^2 = -\frac{d^2}{dx^2}$ and must not be confused with a power of the first-order differential operator ${}_xD = \frac{d}{dx}$

for which the symbol is $-i\kappa$. An alternative illuminating notation for the symmetric fractional derivative is due to Zaslavsky [50], and reads

$$ {}_xD_0^\alpha = \frac{d^\alpha}{d|x|^\alpha}. \tag{3.5}$$

For $0 < \alpha < 2$ and $|\theta| \le \min\{\alpha, 2-\alpha\}$, the *Riesz–Feller* derivative reads

$$ {}_xD_\theta^\alpha f(x) = \frac{\Gamma(1+\alpha)}{\pi}\left\{\sin[(\alpha+\theta)\pi/2]\int\limits_0^\infty \frac{f(x+\xi)-f(x)}{\xi^{1+\alpha}}d\xi \right. \\ \left. + \sin[(\alpha-\theta)\pi/2]\int\limits_0^\infty \frac{f(x-\xi)-f(x)}{\xi^{1+\alpha}}d\xi\right\}. \tag{3.6}$$

3.2 The Caputo fractional derivative

For a sufficiently well-behaved function $f(t)$, we define the *Caputo* time-fractional derivative of order β with $0 < \beta \le 1$ through its Laplace transform

$$\mathcal{L}\{{}_tD_*^\beta f(t); s\} = s^\beta \widetilde{f}(s) - s^{\beta-1} f(0^+), \quad 0 < \beta \le 1. \tag{3.7}$$

This leads us to define

$$ {}_tD_*^\beta f(t) := \begin{cases} \frac{1}{\Gamma(1-\beta)} \int_0^t \frac{f^{(1)}(\tau)\,d\tau}{(t-\tau)^\beta}, & 0 < \beta < 1, \\ \frac{d}{dt} f(t), & \beta = 1. \end{cases} \tag{3.8}$$

For the essential properties of the Caputo derivative, see [3, 13, 49].

3.3 The fundamental solution of the space-time fractional diffusion equation

Let us note that the solution $u(x,t)$ of the Cauchy problem (3.1)–(3.2), known as the *Green function* or fundamental solution of the space-time fractional diffusion equation, is a probability density in the spatial variable x, evolving in time t. In the case $\alpha = 2$ and $\beta = 1$, we recover the standard diffusion equation for which the fundamental solution is the Gaussian density with variance $\sigma^2 = 2t$. Sometimes, to point out the parameters, we may denote the fundamental solution as

$$u(x,t) = G_{\alpha,\beta}^\theta(x,t). \tag{3.9}$$

For our purposes, let us here confine ourselves to recall the representation in the Laplace–Fourier domain of the (fundamental) solution as it results from the application of the transforms of Laplace and Fourier to equation (3.1). Using $\widehat{\delta}(\kappa) \equiv 1$, we have

$$s^\beta \widehat{\widetilde{u}}(\kappa,s) - s^{\beta-1} = -|\kappa|^\alpha i^{\theta\, \mathrm{sign}\, \kappa} \widehat{\widetilde{u}}(\kappa,s),$$

hence

$$\widehat{\widetilde{u}}(\kappa,s) = \widehat{\widetilde{G^\theta_{\alpha,\beta}}}(\kappa,s) = \frac{s^{\beta-1}}{s^\beta + |\kappa|^\alpha i^{\theta\, \mathrm{sign}\, \kappa}}. \tag{3.10}$$

For explicit expressions and plots of the fundamental solution of (3.1) in the space-time domain, we refer the reader to Mainardi, Luchko, and Pagnini [31]. There, starting from the fact that the Fourier transform of the fundamental solution can be written as a Mittag-Leffler function with complex argument,

$$\widehat{u}(\kappa,t) = \widehat{G^\theta_{\alpha,\beta}}(\kappa,t) = E_\beta(-|\kappa|^\alpha i^{\theta\, \mathrm{sign}\, \kappa} t^\beta), \tag{3.11}$$

these authors have derived a Mellin–Barnes integral representation of $u(x,t) = G^\theta_{\alpha,\beta}(x,t)$ with which they have proved the nonnegativity of the solution for values of the parameters $\{\alpha,\theta,\beta\}$ in the range (3.2) and analyzed the evolution in time of its moments. The representation of $u(x,t)$ in terms of Fox H-functions can be found in Mainardi, Pagnini, and Saxena [32]; see also Chapter 6 in the recent book by Mathai, Saxena, and Haubold [35]. We note, however, that the solution of the STFD equation (3.1) and its variants has been investigated by several authors; let us only mention some of them [1, 2, 7, 9, 23, 22, 24, 37, 38, 36, 44, 40, 43, 41, 42, 48, 54], where the connection with the *CTRW* was also pointed out.

In particular, the fundamental solution for the *space fractional diffusion* $\{0 < \alpha < 2, \beta = 1\}$ is expressed in terms of a stable density of order α and skewness θ,

$$G^\theta_{\alpha,1}(x,t) = t^{-1/\alpha} L^\theta_\alpha(x/t^{1/\alpha}), \quad -\infty < x < +\infty,\ t \ge 0, \tag{3.12}$$

whereas for the *time fractional diffusion* $\{\alpha = 2, 0 < \beta < 1\}$ in terms of a (symmetric) M-Wright function of order $\beta/2$,

$$G^0_{2,\beta}(x,t) = \frac{1}{2} t^{-\beta/2} M_{\beta/2}(|x|/t^{\beta/2}), \quad -\infty < x < +\infty,\ t \ge 0. \tag{3.13}$$

For the *standard diffusion* $\{\alpha = 2, \beta = 1\}$, we recover the Gaussian density

$$G^0_{2,1}(x,t) = \frac{1}{2\sqrt{\pi t}} \mathrm{e}^{-x^2/(4t)} = t^{-1/2} L^0_2(x/t^{1/2}) = \frac{1}{2} t^{-1/2} M_{1/2}(|x|/t^{1/2}).$$

Let us finally recall that the M-Wright function does appear also in the fundamental solution of the *rightward time fractional drift equation*,

$${}_tD^\beta_* u(x,t) = -\frac{\partial}{\partial x} u(x,t), \quad -\infty < x < +\infty,\ t \ge 0. \tag{3.14}$$

Denoting by $G^*_\beta(x,t)$ this fundamental solution, we have

$$G^*_\beta(x,t) = \begin{cases} t^{-\beta} M_\beta(\frac{x}{t^\beta}), & x > 0, \\ 0, & x < 0, \end{cases} \tag{3.15}$$

that for $\beta = 1$ reduces to the right running pulse $\delta(x - t)$ for $x > 0$. For details, see [15, 33].

3.4 Alternative forms of the space-time fractional diffusion equation

We note that in the literature there exist other forms alternative and equivalent to equation (3.1) with initial condition $u(x,0) = u_0(x)$ including the case $u_0(x) = \delta(x)$. For this purpose, we must briefly recall the definitions of fractional integral and fractional derivative according to Riemann–Liouville.

The Riemann–Liouville fractional integral for a sufficiently well-behaved function $f(t)$ $(t \geq 0)$ is defined for any order $\mu > 0$ as

$${}_tJ^\mu f(t) := \frac{1}{\Gamma(\mu)} \int_0^t (t-\tau)^{\mu-1} f(\tau)\, d\tau. \tag{3.16}$$

We note the convention ${}_tJ^0 = I$ (Identity) and the semigroup property

$${}_tJ^\mu\, {}_tJ^\nu = {}_tJ^\nu\, {}_tJ^\mu = {}_tJ^{\mu+\nu}, \quad \mu \geq 0,\ \nu \geq 0. \tag{3.17}$$

The fractional derivative of order $\mu > 0$ in the *Riemann–Liouville* sense is defined as the operator ${}_tD^\mu$ which is the left inverse of the Riemann–Liouville integral of order μ (in analogy with the ordinary derivative),

$${}_tD^\mu\, {}_tJ^\mu = I, \quad \mu > 0. \tag{3.18}$$

If m denote the positive integer such that such that $m - 1 < \mu \leq m$, we recognize from equations (3.16)–(3.18):

$${}_tD^\mu f(t) := {}_tD^m\, {}_tJ^{m-\mu} f(t). \tag{3.19}$$

Then, restricting our attention to a order β with $0 < \beta \leq 1$ (namely $m = 1$) the corresponding Riemann–Liouville fractional derivative turns out

$${}_tD^\beta f(t) = \begin{cases} \frac{d}{dt}\left[\frac{1}{\Gamma(1-\beta)} \int_0^t \frac{f(\tau)\, d\tau}{(t-\tau)^\beta}\right], & 0 < \beta < 1, \\ \frac{d}{dt} f(t). & \beta = 1. \end{cases} \tag{3.20}$$

Then we get the relationship among the Caputo fractional derivative with the classical Riemann–Liouville fractional integral and derivative:

$$ {}_tD_*^{\beta}f(t) := {}_tJ^{1-\beta}\,{}_tD^{1}f(t) = {}_tD^{\beta}[f(t)-f(0)] = {}_tD^{\beta}f(t) - \frac{f(0)}{\Gamma(1-\beta)t^{\beta}}, \tag{3.21} $$

and, as a consequence, the equivalence of (3.1) with the following problems:

$$ u(x,t) - u(x,0) = {}_tJ^{\beta}\,{}_xD_{\theta}^{\alpha}u(x,t), \quad u(x,0) = \delta(x), \tag{3.22} $$

$$ \frac{\partial}{\partial t}u(x,t) = {}_tD^{1-\beta}\,{}_xD_{\theta}^{\alpha}u(x,t), \quad u(x,0) = \delta(x). \tag{3.23} $$

4 Analytic and stochastic pathways to subordination in space-time fractional diffusion

Our starting key-point to introduce the analytical and stochastic approaches to subordination in space-time fractional diffusion processes is the fundamental solution of the space-time fractional diffusion equation in the Laplace–Fourier domain given by (3.10).

4.1 The analytical interpretation via operational time

Separating variables in (3.10) and using the trick to write $1/(z+a)$ for $\mathbb{R}(z+a) > 0$ as a Laplace integral

$$ \frac{1}{z+a} = \int_0^{\infty} \mathrm{e}^{-z\rho}\mathrm{e}^{-a\rho}\,d\rho $$

we have, identifying $\rho := t_*$ as *operational time*, the following instructive expression for (3.10):

$$ \widehat{\widetilde{u}}(\kappa,s) = \int_0^{\infty} [\exp(-t_*|\kappa|^{\alpha} i^{\theta\,\mathrm{sign}\,\kappa})][s^{\beta-1}\exp(-t_* s^{\beta})]\,dt_*. \tag{4.1} $$

We note that the first factor in (4.1),

$$ \widehat{f}_{\alpha,\theta}(\kappa,t_*) := \exp(-t_*|\kappa|^{\alpha} i^{\theta\,\mathrm{sign}\,\kappa}), \tag{4.2} $$

is the Fourier transform of a skewed stable density in x, evolving in operational time t_*, of a process $x = y(t_*)$ along the real axis x happening in operational time t_*, that we write as

$$ f_{\alpha,\theta}(x,t_*) = t_*^{-1/\alpha} L_{\alpha}^{\theta}(x/t_*^{1/\alpha}). \tag{4.3} $$

We can interpret the second factor

$$\widetilde{q}_\beta(t_*, s) := s^{\beta-1}\exp(-t_* s^\beta) \tag{4.4}$$

as Laplace representation of the probability density in t_* evolving in t of a process $t_* = t_*(t)$, generating the operational time t_* from the physical time t, that is expressed via a fractional integral of a skewed Lévy density as

$$q_\beta(t_*, t) = t_*^{-1/\beta}\,{}_tJ^{1-\beta}L_\beta^{-\beta}(t/t_*^{1/\beta}) = t^{-\beta}M_\beta(t_*/t^\beta); \tag{4.5}$$

see equation (2.26). To prove that $q_\beta(t_*, t)$ (surely positive for $t_* > 0$) is indeed a probability density, we must further prove that is normalized, $\int_{t_*=0}^{\infty} q_\beta(t_*, t)\,dt_* = 1$. For this purpose, it is sufficient to prove that its Laplace transform with respect to t_* is equal to 1 for $s_* = 0$. To get this Laplace transform $\widetilde{q}_\beta(s_*, t)$, we proceed as follows. Starting from the known Laplace transform with respect to t,

$$\widetilde{q}_\beta(t_*, s) = s^{\beta-1}\exp(-t_* s^\beta), \tag{4.6}$$

we apply a second Laplace transformation with respect to t_* with parameter s_* to get

$$\widetilde{\widetilde{q}}_\beta(s_*, s) = \frac{s^{\beta-1}}{s_* + s^\beta}, \tag{4.7}$$

so, by inversion with respect to t

$$\widetilde{q}_\beta(s_*, t) = \int_{t_*=0}^{\infty} \mathrm{e}^{-s_* t} q_\beta(t_*, t)\,dt_* = E_\beta(-s_* t^\beta), \tag{4.8}$$

and setting $s_* = 0$

$$\int_{t_*=0}^{\infty} q_\beta(t_*, t)\,dt_* = E_\beta(0) = 1. \tag{4.9}$$

Weighting the density of $x = y(t_*)$ with the density of $t_* = t_*(t)$ over $0 \le t < \infty$ yields the density $u(x, t)$ in x evolving with time t.

In physical variables $\{x, t\}$, using equations (4.1)–(4.5), we have the *subordination integral formula*

$$u(x, t) = \int_{t_*=0}^{\infty} f_{\alpha,\theta}(x, t_*) q_\beta(t_*, t)\,dt_*, \tag{4.10}$$

where $f_{\alpha,\theta}(x, t_*)$ (density in x evolving in t_*) refers to the process $x = y(t_*)$ ($t_* \to x$) generating in “operational time” t_* the spatial position x, and $q_\beta(t_*, t)$ (density in t_*

evolving in t) refers to the process $t_* = t_*(t)$ $(t \to t_*)$ generating from physical time t the "operational time" t_*.

Our aim is to construct a process $x = x(t)$ whose probability density is $u(x,t)$, density in x, evolving in t. We will soon find justification for denoting the variable of integration by t_*. We will exhibit it as the "operational time" for our fractional diffusion process, and for distinction we will call the variable t its "physical time." In fact, $f_{\alpha,\theta}(x,t_*)$ is a probability density in $x \in \mathbb{R}$, evolving in operational time $t_* > 0$ and $q_\beta(t_*,t)$ is a probability density in $t_* \geq 0$, evolving in physical time $t > 0$.

4.2 Stochastic interpretation

Clearly, $f_{\alpha,\theta}(x,t_*)$ characterizes a stochastic process describing a trajectory $x = y(t_*)$ in the (t_*,x) plane that can be visualized as a particle traveling along space x, as operational time t_* is proceeding. Is there also a process $t_* = t_*(t)$, a particle moving along the positive t_* axis, happening in physical time t? Naturally, we want $t_*(t)$ increasing, at least in the weak sense,

$$t_2 > t_1 \Longrightarrow t_*(t_2) \geq t_*(t_1).$$

We answer this question in the affirmative by showing that, by inverting the stable process $t = t(t_*)$ whose probability density (in t, evolving in operational time t_*) is the extremely positively skewed stable density

$$r_\beta(t,t_*) = t_*^{-1/\beta} L_\beta^{-\beta}(t/t_*^{1/\beta}). \tag{4.11}$$

In fact, recalling

$$\widetilde{r}_\beta(s,t_*) = \exp(-t_* s^\beta), \tag{4.12}$$

there exists the stable process $t = t(t_*)$, weakly increasing, with density in t evolving in t_* given by (4.11). We call this process *the leading process*.

Happily, we can invert this process. Inversion of a weakly increasing trajectory means that horizontal segments are converted to vertical segments and vice versa jumps (as vertical segments) to horizontal segments (in graphical visualization).

Consider a fixed sample trajectory $t = t(t_*)$ and its also fixed inversion $t_* = t_*(t)$. Fix an instant T of physical time and an instant T_* of operational time. Then, because $t = t(t_*)$ is increasing, we have the equivalence

$$t_*(T) \leq T_* \Longleftrightarrow T \leq t(T_*),$$

which, with notation slightly changed by

$$t_*(T) \to t_*', \quad T_* \to t_*, \quad T \to t, \quad t(T_*) \to t',$$

implies

$$\int_0^{t_*} q(t'_*, t)\, dt'_* = \int_t^{\infty} r_\beta(t', t_*)\, dt', \tag{4.13}$$

for the probability density $q(t_*, t)$ in t_* evolving in t. It follows

$$q(t_*, t) = \frac{\partial}{\partial t_*} \int_t^{\infty} r_\beta(t', t_*)\, dt' = \int_t^{\infty} \frac{\partial}{\partial t_*} r_\beta(t', t_*)\, dt'.$$

We continue in the s_*-Laplace domain assuming $t > 0$,

$$\bar{q}(s_*, t) = \int_t^{\infty} (s_* \bar{r}_\beta(t', s_*) - \delta(t'))\, dt'.$$

It suffices to consider $t > 0$, so that we have $\delta(t') = 0$ in this integral. Observing from (4.12),

$$\bar{\bar{r}}_\beta(s, s_*) = \frac{1}{s_* + s^\beta}, \tag{4.14}$$

we find

$$\bar{r}_\beta(t, s_*) = \beta t^{\beta-1} E'_\beta(-s_* t^\beta), \tag{4.15}$$

so that

$$\bar{q}(s_*, t) = \int_t^{\infty} s_* \beta t'^{\beta-1} E'_\beta(-s_* t'^\beta)\, dt' = E_\beta(-s_* t^\beta), \tag{4.16}$$

finally

$$q(t_*, t) = t^{-\beta} M_\beta(t_*/t^\beta). \tag{4.17}$$

From (4.16), we also see that

$$\bar{\bar{q}}(s_*, s) = \frac{s^{\beta-1}}{s_* + s^\beta} = \bar{\bar{q}}_\beta(s_*, s), \tag{4.18}$$

implying (4.6) and (see (4.7)),

$$q(t_*, t) \equiv q_\beta(t_*, t), \tag{4.19}$$

so that indeed the process $t_* = t_*(t)$ is the inverse to the stable process $t = t(t_*)$ and has density $q_\beta(t_*, t)$.

Remark. The process at hand, $t_* = t_*(t)$, which is referred to as the inverse stable subordinator, is honored with the name "Mittag-Leffler process" by Meerschaert at al. [37, 39]. Honoring this process by the name of Mittag-Leffler can be justified by the fact that by (4.16) the Laplace transform of its density is a Mittag-Leffler-type function or by the fact that it is a properly scaled diffusion limit of the counting function $N(t)$ of the fractional generalization of the Poisson process whose residual waiting time probability is the Mittag-Leffler-type function $E_\beta(-t^\beta)$; see our recent papers [10, 15]. In view of its probability density, it may also be called the M-Wright process.

Stipulating that there exists a weakly increasing process $t_* = t_*(t)$ with density $q_\beta(t_*, t)$, we can analogously find the density of its inverse $t = t(t_*)$ which comes just as $r_\beta(t, t_*)$. However, in the context of ours here presented considerations not being allowed to know that such process $t_* = t_*(t)$ exists, we have taken as a gift from God the process $t = t(t_*)$ and shown by its inversion that there exists a process $t_* = t_*(t)$ with the desired properties.

From the density $r_\beta(t, t_*)$ of *the leading process* $t = t(t_*)$, we have found the density of *the directing process* $t_* = t_*(t)$ as given by the Laplace transform pair (4.6), that is,

$$q_\beta(t_*, t) \div \bar{q}_\beta(t_*, s) = s^{\beta-1} \exp(-t_* s^\beta).$$

In physical coordinates, we have (4.5) and (4.17), so also an expression through an M-Wright function,

$$q_\beta(t_*, t) = {}_tJ^{1-\beta} r_\beta(t, t_*) = t^{-\beta} M_\beta(t_*/t^\beta); \tag{4.20}$$

see equation (2.26).

4.3 Evolution equations for the densities $r_\beta(t, t_*)$ of $t = t(t_*)$ and $q_\beta(t_*, t)$ of $t_* = t_*(t)$

The Laplace–Laplace representation of the density $r_\beta(t, t_*)$ of the process $t = t(t_*)$ is, according to (4.14),

$$\bar{\bar{r}}_\beta(s, s_*) = \frac{1}{s^\beta + s_*}.$$

This implies

$$s_* \bar{\bar{r}}_\beta(s, s_*) - 1 = -s^\beta \bar{\bar{r}}_\beta(s, s_*),$$

and by inverting the transforms and observing the initial condition $r_\beta(t, t_* = 0) = \delta(t)$ we arrive at the Cauchy problem

$$\frac{\partial}{\partial t_*} r_\beta(t, t_*) = -{}_tD_*^\beta r_\beta(t, t_*), \quad r_\beta(t, t_* = 0) = \delta(t). \tag{4.21}$$

Because it suffices to consider only $t > 0$ where $\delta(t) = 0$, we need not introduce a singular term on the right-hand side.

The Laplace–Laplace representation of the density $q_\beta(t_*, t)$ of the process $t_* = t_*(t)$ is, according to (4.18),

$$\bar{\bar{q}}_\beta(s_*, s) = \frac{s^{\beta-1}}{s_* + s^\beta}.$$

This implies

$$s^\beta \bar{\bar{q}}_\beta(s_*, s) - s^{\beta-1} = -s_* \bar{\bar{q}}_\beta(s_*, s),$$

and by inverting the transforms and observing the initial condition $q_\beta(t_*, t = 0) = \delta(t_*)$ we arrive at the Cauchy problem

$$_tD_*^\beta q_\beta(t_*, t) = -\frac{\partial}{\partial t_*} q_\beta(t_*, t) \quad q_\beta(t_*, t = 0) = \delta(t_*). \tag{4.22}$$

Because it suffices to consider only $t_* > 0$ where $\delta(t_*) = 0$, we can ignore the delta function on the right-hand side.

Remark. The fractional differential equations in the above Cauchy problems have the same form. By replacing t by t_* and r by q, one of them goes over into the other. However, in the first problem the delta initial condition refers to the fractional derivative (of order β), in the second problem to the ordinary (first-order) derivative. These equations are akin with the time-fractional drift equation treated in (3.14) and (3.15), with different coordinates and proper initial conditions, as explained above. The process $t = t(t_*)$ of the first problem is a positive-oriented (extreme) stable process, whereas the process $t_* = t_*(t)$ is a fractional drift process; see (3.14)–(3.15) with x replaced by t_*. The reason for the two evolution equations to have the same form is that the described two processes are inverse to each other; their graphical representations coincide just by interchanging the coordinate axes. The delta initial condition for each equation is given at value zero of the evolution variable for the variable in which the solution is a density.

4.4 The random walks

We can now construct the process $x = x(t)$ for the position x of the particle depending on physical time t as follows in two ways. With the variable t (physical time), t_* (operational time), x (position), we have the processes (i), (ii), and (iii), as follows:

(i) $t = t(t_*)$ with density $r_\beta(t, t_*)$ in t, evolving in t_*, *the leading process*,
(ii) $x = y(t_*)$ with density $f_{\alpha,\theta}(x, t_*)$ in x, evolving in t_*, *the parent process*,
(iii) $t_* = t_*(t)$ with density $q_\beta(t_*, t)$ in t_*, evolving in t, *the directing process*.

Observing that the processes (i) and (iii) are inverse to each other, and taking account of the subordination integral (4.10), we define *the space-time fractional diffusion process* as *the subordinated process*

$$x = x(t) = y(t_*(t)). \tag{4.23}$$

Simulation of a trajectory for the subordinated process means: generate in running physical time t the operational time t_*, then the operational process $y(t_*)$.

Now, the Mittag-Leffler (or M-Wright) process $t_* = t_*(t)$ is non-Markovian and not so easy to simulate. The alternative (we call it "parametric subordination") is to produce in dependence of the operational time t_* the processes (i) and (ii) and then eliminate t_* from the system

$$t = t(t_*), \quad x = y(t_*), \tag{4.24}$$

to get $x = x(t)$ from $x = y(t_*)$ by change of time from t_* to t.

We can produce a sequence of precise snapshots of $t = t(t_*)$ and $x = y(t_*)$ in the (t_*, t) plane and the (t_*, x) plane by setting, with a step-size $\tau_* > 0$,

$$t_{*,n} = n\tau_*, \quad \bar{t}_n = T_{*,1} + T_{*,2} \cdots + T_{*,n}, \quad \bar{x}_n = X_{*,1} + X_{*,2} + \cdots + X_{*,n}, \tag{4.25}$$

taking for $k = 1, 2, \ldots, n$ each $T_{*,k}$ as a random number with density $\tau_*^{-1/\beta} L_\beta^{-\beta}(t/\tau_*^{1/\beta})$ and each $X_{*,k}$ as a random number with density $\tau_*^{-1/\alpha} L_\alpha^\theta(x/\tau_*^{1/\alpha})$, corresponding by self-similarity to the step τ_*.

We can do this by taking random numbers T_k and X_k with density $L_\beta^{-\beta}(t)$ and $L_\alpha^\theta(x)$, respectively, and then with $\tau = \tau_*^{1/\beta}$ and $h = \tau_*^{1/\alpha}$, setting $T_{*,k} = \tau T_k$, $X_{*,k} = hX_k$. In other words, we produce (a renewal process at equidistant times with reward) a positively oriented random walk on the half-line $t \geq 0$ and a random walk on $-\infty < x < +\infty$ with jumps at equidistant operational time instants $t_* = n\tau_*$. We recognize the scaling relation $\tau^\beta/h^\alpha \equiv 1$, analogous to that used by us in earlier papers of ours on a well-scaled passage to the diffusion limit in *CTRW* under the power law regime; see [11, 15, 16]. Methods for producing stable random deviates can be found in the books [25, 26].

Finally, we transfer into the (t, x) plane the points with coordinates $\bar{t}_n, \bar{x}_n = \bar{y}_n$ and so obtain a sequence of precise snapshots of a true process $x = x(t)$. Finer details of the process $x = x(t)$ become visible by using smaller values of the operational step-size τ_*.

5 Graphical representations and conclusions

We recall that, denoting the physical time with t, the operational time with t_*, the physical space with x the density of the fractional diffusion process turns out to be given by the following subordination integral (see (4.10)):

$$u(x,t) = \int_{t_*=0}^{\infty} f_{\alpha,\theta}(x,t_*) q_\beta(t_*,t)\,dt_*, \tag{5.1}$$

where $f_{\alpha,\theta}(x,t_*)$, is the density (in x evolving in t_*) of the parent process $x = y(t_*) = x(t(t_*))$ and $q_\beta(t_*,t)$ is the density (in t_* evolving in t) of the directing process $t_* = t_*(t)$.

By using the Fourier–Laplace pathway, we recall the two densities related to the parameters α, θ, β from (4.3)–(4.5),

$$f_{\alpha,\theta}(x,t_*) = t_*^{-1/\alpha} L_\alpha^\theta(x/t^{1/\alpha}), \tag{5.2}$$

$$q_\beta(t_*,t) = t_*^{-1/\beta}\,{}_tJ^{1-\beta} L_\beta^{-\beta}(t/t_*^{1/\beta}) = t^{-\beta} M_\beta(t_*/t^\beta), \tag{5.3}$$

where L refers to the Lévy stable density and M to the Wright function, both introduced in Section 2. But for the *parametric subordination* the relevant density is $r_\beta(t,t_*)$ governing the *leading process*, a density in the physical time t evolving with the operational time t_*: it turns out to be the unilateral Lévy density of order β, namely (see (4.11)),

$$r_\beta(t,t_*) = t_*^{-1/\beta} L_\beta^{-\beta}(t/t_*^{1/\beta}). \tag{5.4}$$

We have shown in Section 4.4 that in our approach (referred to as *parametric subordination*) the process of space-time fractional diffusion (non-Markovian for $\beta < 1$) can be simulated by two Markovian processes governed by stable densities, provided by $f_{\alpha,\theta}(x,t_*)$ and $r_\beta(t,t_*)$, as pointed out in our 2007 paper with Vivoli [19], where we have dealt with the *CTRW* model. There, before passing to the diffusion limit, we have two Markov processes happening on a discrete set of equidistant instants (for simplicity the nonnegative integers) $n = 0,1,2,\ldots$, meaning $\tau_* = 1$, one of them moving randomly rightward along $t \geq 0$, the other moving randomly on the real line $-\infty < x < \infty$ with jumps T_n and X_n, respectively, for $n \geq 1$. By summing the "waiting times" T_k and the jumps X_k from 1 to n, we obtain sequences of jump instants $t = t_n$ and positions $x = x_n$ that we display in the (t,x) plane. In fact, CTRW is the virgin form of parametric subordination.

We note that our approach is akin to that based on two stochastic differential equations, known in physics as Langevin equations; see [6, 28, 63]. We have indicated these two stochastic differential equations in [19]. Here now, we are content with referring to the above cited papers.

In Section 4.4, we have split the fractional diffusion process into three processes (i), (ii), (iii), each of them containing two of the three coordinates: space x, physical time t, operational time t_*. We simulate *the leading process* by a random walk (rw_1), *the parent process* by a random walk (rw_2), and *the subordinated process* (which yields the desired trajectory) by a random walk (rw). The inversion of (rw_1) gives us a random walk (rw_3) for simulation of *the directing process* $t_* = t_*(t)$. Essentially, we need to carry out only (rw_1) and (rw_2) according to the equations (4.25). By transferring the points $(\bar{t}_n, \bar{x}_n)$ into the (t, x) plane, we get the random walk (rw) as visualization of a random trajectory $x = x(t) = y(t_*(t))$ according to the subordinated process, which is our space-time fractional diffusion process of interest.

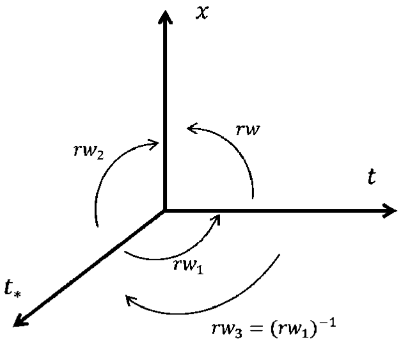

Figure 2: Diagram for the connections between the four random walks (rw_1), (rw_2), (rw_3), and (rw), related to the leading, parent, directing and subordinated processes, respectively.

To make the situation transparent, we display as a diagram in Figure 2 the connections between the four random walks. It is now instructive to show some numerical realizations of these random walks for two case studies of symmetric ($\theta = 0$) fractional diffusion processes: $\{\alpha = 2, \beta = 0.80\}$, $\{\alpha = 1.5, \beta = 0.90\}$. As explained in a previous subsection, for each case we need to construct the sample paths for three distinct processes, the leading process $t = t(t_*)$, the parent process $x = y(t_*)$ (both in the operational time), and finally, the subordinated process $x = x(t)$, corresponding to the required fractional diffusion process.

We shall depict the above sample paths in Figures 3, 4, 5, respectively, devoting the left and the right plates to the different case studies.

Plots in Figure 3 (devoted to the leading process, the limit of (rw_1)) thus represent sample paths in the (t_*, t) plane of unilateral Lévy motions of order β. By interchanging the coordinate axes, we can consider Figure 3 as representing sample paths of the directing process, the limit of (rw_3).

Plots in Figure 4 (devoted to the parent process, the limit of (rw_2)) represent sample paths in the (t_*, x) plane, produced in the way explained above, for Lévy motions of order α and skewness $\theta = 0$ (symmetric stable distributions).

By the indicated method (see (4.25)), we have with (for simplicity) $\tau_* = 1$, $\theta = 0$ (symmetry) produced 10000 numbers $\bar{t}_n$ and corresponding numbers $\bar{y}_n$. Plotting the points $(t_{*,n}, \bar{t}_n)$ into the (t_*, t) (operational time, physical time) plane, the points $(t_{*,n}, \bar{y}_n)$ into the (t_*, x) (operational time, position in space) plane we get Figure 3 and Figure 4 for visualization of (rw_1) and (rw_2), respectively. Figure 5 (as a visualization of (rw)) is obtained by plotting the points $(\bar{t}_n, \bar{y}_n)$ into the (t, x) (physical time and space) plane.

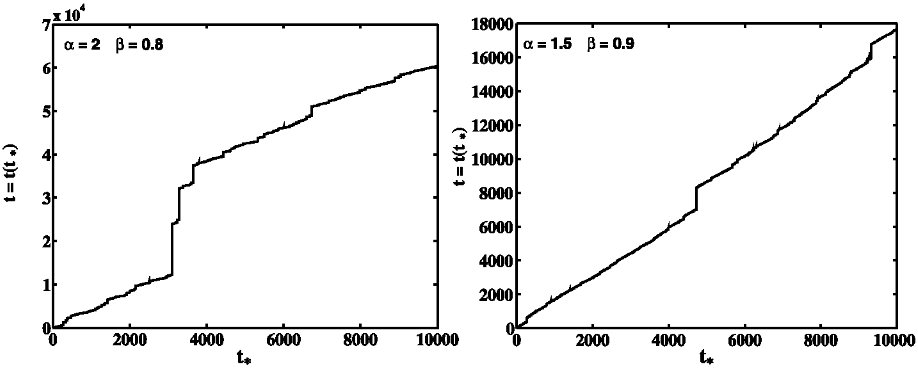

Figure 3: A sample path for (rw_1), the leading process $t = t(t_*)$. Left: $\{\alpha = 2, \beta = 0.80\}$; Right: $\{\alpha = 1.5, \beta = 0.90\}$.

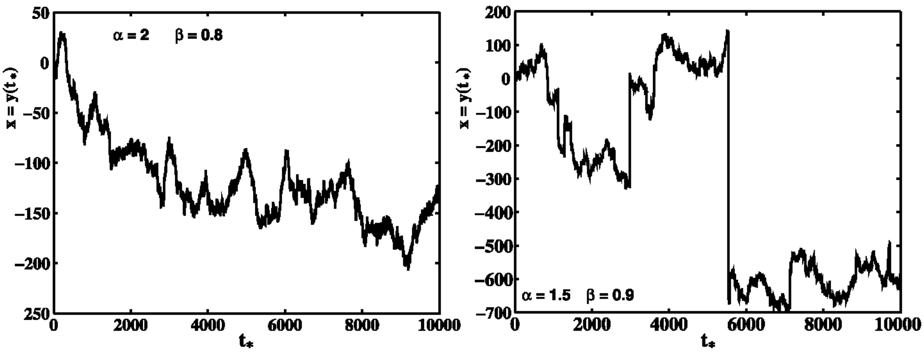

Figure 4: A sample path for (rw_2), the parent process $x = y(t_*)$. Left: $\{\alpha = 2, \beta = 0.80\}$; Right: $\{\alpha = 1.5, \beta = 0.90\}$.

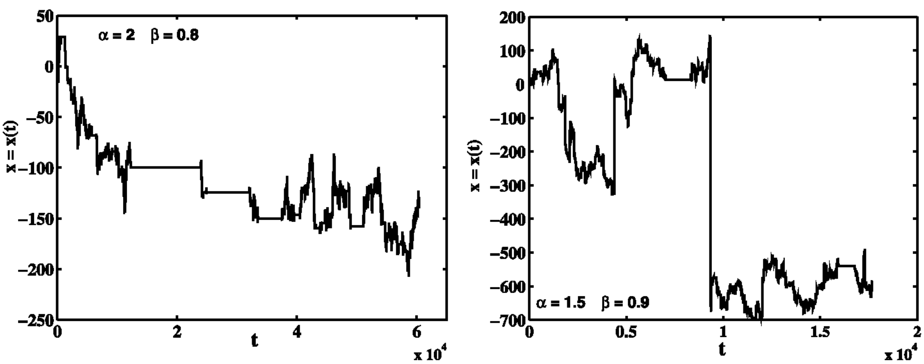

Figure 5: A sample path for (rw), the subordinated process $x = x(t)$. Left: $\{\alpha = 2, \beta = 0.80\}$; Right: $\{\alpha = 1.5, \beta = 0.90\}$.

Actually, we have invested a little bit more work in producing the figures. Namely, to make visible the jumps as vertical segments, we have in Figure 3 connected the points $(t_{*,n}, \bar{t}_n)$ and $(t_{*,n+1}, \bar{t}_n)$ by a horizontal segment, the points $(t_{*,n+1}, \bar{t}_n)$ and $(t_{*,n+1}, \bar{t}_{n+1})$ by a vertical segment. Analogously in Figure 4 with the indexed $\bar{t}$ replaced by indexed $\bar{y}$. In Figure 5, we have connected the points $(\bar{t}_n, \bar{y}_n)$ and $(\bar{t}_{n+1}, \bar{y}_n)$ by a horizontal segment, the points $(\bar{t}_{n+1}, \bar{y}_n)$ and $(\bar{t}_{n+1}, \bar{y}_{n+1})$ by a vertical segment.

Resuming, we can consider Figure 3 as a representation of (rw_1) for the leading process, or by interchange of axes as one of (rw_3) for the directing process, Figure 4 as one of (rw_2) for the parent process, and finally Figure 5 as a representation of (rw) for the subordinated process which is our space-time fractional diffusion process.

In our chapter in the book edited by Klafter, Lim, and Metzler in 2012 (see [18]), we have included additional figures, showing the effect of taking smaller step-sizes τ_*, equivalently larger values N of steps following our previous analysis for the *CTRW* [19]. These additional figures show the effect of making the operational step-length τ_* smaller or, equivalently, the number N of operational steps larger for the sample paths of the leading, parent, and subordinated processes, respectively. In these pictures $\tau_* = 1/N$, and we have taken $N = 10$, $N = 100$, and $N = 1000$. Finer details will become visible by choosing in the operational time t_* the step-length τ_* smaller and smaller. In those graphs, we can clearly see what happens for finer and finer discretization of the operational time t_*, by adopting 10^1, 10^2, 10^3 of number of steps. As a matter of fact, there is no visible difference in the transition for the successive decades 10^4, 10^5, 10^6, of the number of steps as the great majority of spatial jumps and waiting times even for very small steps τ_* of the operational time. This property also explains the visible persistence of large jumps and waiting times.

Bibliography

[1] E. Barkai, Fractional Fokker–Planck equation, solution, and application, *Phys. Rev. E*, **63** (2001), 046118/1-18.

[2] E. Barkai, CTRW pathways to the fractional diffusion equation, *Chem. Phys.*, **284** (2002), 13–27.

[3] K. Diethelm, *The Analysis of Fractional Differential Equations. An Application Oriented Exposition Using Differential Operators of Caputo Type*, Lecture Notes in Mathematics, vol. 2004, Springer, Berlin, 2010.

[4] A. Erdélyi, W. Magnus, F. Oberhettinger, and F. G. Tricomi, *Higher Transcendental Functions, vol. 3*, Ch. 18, McGraw-Hill, New-York, 1955.

[5] W. Feller, *An Introduction to Probability Theory and Its Applications, vol.ÎI*, Wiley, New York, 1971.

[6] H. C. Fogedby, Langevin equations for continuous time Lévy flights, *Phys. Rev. E*, **50** (1994), 1657–1660.

[7] D. Fulger, E. Scalas, and G. Germano, Monte Carlo simulation of uncoupled continuous-time random walks yielding a stochastic solution of the space-time fractional diffusion equation, *Phys. Rev. E*, **77** (2008), 021122/1-7.

[8] W. Gawronski, On the bell-shape of stable distributions, *Ann. Probab.*, **12** (1984), 230–242.

[9] G. Germano, M. Politi, E. Scalas, and R. L. Schilling, Stochastic calculus for uncoupled continuous-time random walks, *Phys. Rev. E*, **79** (2009), 066102/1-12.

[10] R. Gorenflo, Mittag-Leffler waiting time, power laws, rarefaction, continuous time random walk, diffusion limit, in S. S. Pai, N. Sebastian, S. S. Nair, D. P. Joseph, and D. Kumar (eds.) *Proceedings of the National Workshop on Fractional Calculus and Statistical Distributions, CMS Pala Campus, India*, pp. 1–22, 2010, http://arxiv.org/abs/1004.4413.

[11] R. Gorenflo and E. A. Abdel-Rehim, From power laws to fractional diffusion: the direct way, *Vietnam J. Math.*, **32**(SI) (2004), 65–75, http://arXiv.org/abs/0801.0142.

[12] R. Gorenflo, A. A. Kilbas, F. Mainardi, and S. V. Rogosin, *Mittag-Leffler Function, Related Topics and Applications*, Springer Verlag, Heidelberg, 2014.

[13] R. Gorenflo and F. Mainardi, Fractional calculus: integral and differential equations of fractional order, in A. Carpinteri and F. Mainardi (eds.) *Fractals and Fractional Calculus in Continuum Mechanics*, pp. 223–276, Springer Verlag, Wien, 1997, http://arxiv.org/abs/0805.3823.

[14] R. Gorenflo and F. Mainardi, Random walk models for space-fractional diffusion processes, *Fract. Calc. Appl. Anal.*, **1** (1998), 167–191.

[15] R. Gorenflo and F. Mainardi, Continuous time random walk, Mittag-Leffler waiting time and fractional diffusion: mathematical aspects, in R. Klages, G. Radons, and I. M. Sokolov (eds.) *Anomalous Transport, Foundations and Applications*, pp. 93–127, Wiley–VCH Verlag, Weinheim, Germany, 2008, http://arxiv.org/abs/0705.0797.

[16] R. Gorenflo and F. Mainardi, Some recent advances in theory and simulation of fractional diffusion processes, *J. Comput. Appl. Math.*, **229**(2) (2009), 400–415, http://arxiv.org/abs/0801.0146.

[17] R. Gorenflo and F. Mainardi, Subordination pathways to fractional diffusion, *Eur. Phys. J. Spec. Top.*, **193** (2011), 119–132, http://arxiv.org/abs/1104.4041.

[18] R. Gorenflo and F. Mainardi, Parametric subordination in fractional diffusion processes, in J. Klafter, S. C. Lim, and R. Metzler (eds.) *Fractional Dynamics, Recent Advances*, pp. 229–263, World Scientific, Singapore, 2012, Ch. 10, http://arxiv.org/abs/1210.841.

[19] R. Gorenflo, F. Mainardi, and A. Vivoli, Continuous time random walk and parametric subordination in fractional diffusion, *Chaos Solitons Fractals*, **34** (2007), 87–103, http://arxiv.org/abs/cond-mat/0701126.

[20] M. Hahn and S. Umarov, Fractional Kolmogorov–Planck type equations and their associated stochastic differential equations, *Fract. Calc. Appl. Anal.*, **14**(1) (2011), 56–79.

[21] M. Hahn, K. Kobayashi, and S. Umarov, SDEs driven by a time-changed Levy process and their associated time-fractional order pseudo-differential equations, *J. Theor. Probab.*, **25** (2012), 262–279.

[22] R. Hilfer, Exact solutions for a class of fractal time random walks, *Fractals*, **3** (1995), 211–216.

[23] R. Hilfer, Threefold introduction to fractional calculus, in R. Klages, G. Radons, and I. M. Sokolov (eds.) *Anomalous Transport, Foundations and Applications*, pp. 17–73, Wiley–VCH Verlag, Weinheim, Germany, 2008.

[24] R. Hilfer and L. Anton, Fractional master equations and fractal time random walks, *Phys. Rev. E*, **51** (1995), R848–R851.

[25] A. Janicki, *Numerical and Statistical Approximation of Stochastic Differential Equations with Non-Gaussian Measures*, Monograph No. 1, H. Steinhaus Center for Stochastic Methods in Science and Technology, Technical University, Wroclaw, Poland, 1996.

[26] A. Janicki and A. Weron, *Simulation and Chaotic Behavior of α-Stable Stochastic Processes*, Marcel Dekker, New York, 1994.

[27] A. A. Kilbas, H. M. Srivastava, and J. J. Trujillo, *Theory and Applications of Fractional Differential Equations*, Elsevier, Amsterdam, 2006.

[28] D. Kleinhans and R. Friedrich, Continuous-time random walks: Simulations of continuous trajectories, *Phys. Rev. E*, **76** (2007), 061102/1-6.

[29] F. Mainardi, *Fractional Calculus and Waves in Linear Viscoelasticity*, Imperial College Press, London, 2010.

[30] F. Mainardi and M. Tomirotti, Seismic pulse propagation with constant Q and stable probability distributions, *Ann. Geofis.*, **40** (1997), 1311–1328, http://arxiv.org/abs/1008.1341.

[31] F. Mainardi, Yu. Luchko, and G. Pagnini, The fundamental solution of the space-time fractional diffusion equation, *Fract. Calc. Appl. Anal.*, **4** (2001), 153–192, http://arxiv.org/abs/cond-mat/0702419.

[32] F. Mainardi, G. Pagnini, and R. K. Saxena, Fox H functions in fractional diffusion, *J. Comput. Appl. Math.*, **178** (2005), 321–331.

[33] F. Mainardi, A. Mura, and G. Pagnini, The M-Wright function in time-fractional diffusion processes: a tutorial survey, *Int. J. Differ. Equ.*, **2010** (2010), 104505, 29 pp., http://arxiv.org/abs/1004.2950.

[34] O. I. Marichev, *Handbook of Integral Transforms of Higher Transcendental Functions, Theory and Algorithmic Tables*, Ellis Horwood, Chichester, 1983.

[35] A. M. Mathai, R. K. Saxena, and H. J. Haubold, *The H-function, Theory and Applications*, Springer Verlag, New York, 2010.

[36] M. M. Meerschaert and H. P. Scheffler, Limit theorems for continuous-time random walks with infinite mean waiting times, *J. Appl. Probab.*, **41** (2004), 623–638.

[37] M. M. Meerschaert, D. A. Benson, H. P. Scheffler, and B. Baeumer, Stochastic solutions of space-fractional diffusion equation, *Phys. Rev. E*, **65** (2002), 041103/1-4.

[38] M. M. Meerschaert, D. A. Benson, H. P. Scheffler, and P. Becker-Kern, Governing equations and solutions of anomalous random walk limits, *Phys. Rev. E*, **66** (2002), 060102/1-4.

[39] M. M. Meerschaert, E. Nane, and P. Vellaisamy, The fractional Poisson process and the inverse stable subordinator, http://arxiv.org/abs/1007.505.

[40] R. Metzler and J. Klafter, From a generalized Chapman–Kolmogorov equation to the fractional Klein–Kramers equations, *J. Phys. Chem. B*, **104** (2000), 3851–3857.

[41] R. Metzler and J. Klafter, The random walk's guide to anomalous diffusion: a fractional dynamics approach, *Phys. Rep.*, **339** (2000), 1–77.

[42] R. Metzler and J. Klafter, The restaurant at the end of the random walk: Recent developments in the description of anomalous transport by fractional dynamics, *J. Phys. A, Math. Gen.*, **37** (2004), R161–R208.

[43] R. Metzler, J. Klafter, and I. M. Sokolov, Anomalous transport in external fields: Continuous time random walks and fractional diffusion equations extended, *Phys. Rev. E*, **58** (1998), 1621–1633.

[44] R. Metzler, E. Barkai, and J. Klafter, Deriving fractional Fokker–Planck equations from a generalised master equation, *Europhys. Lett.*, **46** (1999), 431–436.

[45] G. M. Mittag-Leffler, Sur la nouvelle fonction $E_\alpha(x)$, *C. R. Acad. Sci. Paris (Ser. II)*, **137** (1903), 554–558.

[46] G. M. Mittag-Leffler, Sopra la funzione $E_\alpha(x)$, *Rend. R. Accad. Lincei (Ser. V)*, **13** (1904), 3–5.

[47] G. M. Mittag-Leffler, Sur la représentation analytique d'une branche uniforme d'une fonction monogène, *Acta Math.*, **29** (1905), 101–181.

[48] A. Piryatinska, A. I. Saichev, and W. A. Woyczynski, Models of anomalous diffusion: the subdiffusive case, *Physica A*, **349** (2005), 375–420.

[49] I. Podlubny, *Fractional Differential Equations*, Academic Press, San Diego, 1999.

[50] A. Saichev and G. Zaslavsky, Fractional kinetic equations: solutions and applications, *Chaos*, **7** (1997), 753–764.

[51] S. G. Samko, A. A. Kilbas, and O. I. Marichev, *Fractional Integrals and Derivatives: Theory and Applications*, Gordon and Breach, New York, 1993.
[52] G. Samorodnitsky and M. S. Taqqu, *Stable non-Gaussian Random Processes*, Chapman & Hall, New York, 1994.
[53] K.-I. Sato, *Lévy Processes and Infinitely Divisible Distributions*, Cambridge University Press, Cambridge, 1999.
[54] E. Scalas, R. Gorenflo, and F. Mainardi, Uncoupled continuous-time random walks: Solution and limiting behavior of the master equation, *Phys. Rev. E*, **69** (2004), 011107/1-8.
[55] W. R. Schneider, Stable distributions: Fox function representation and generalization, in S. Albeverio, G. Casati, and D. Merlini (eds.) *Stochastic Processes in Classical and Quantum Systems*, Lecture Notes in Physics, vol. 262, pp. 497–511, Springer Verlag, Berlin, Heidelberg, 1986.
[56] H. Takayasu, *Fractals in the Physical Sciences*, Manchester University Press, Manchester and New York, 1990.
[57] V. V. Uchaikin and V. M. Zolotarev, *Chance and Stability. Stable Distributions and their Applications*, VSP, Utrecht, 1999.
[58] A. Wiman, Über den Fundamentalsatz der Theorie der Funktionen $E_\alpha(x)$, *Acta Math.*, **29** (1905), 191–201.
[59] E. M. Wright, On the coefficients of power series having exponential singularities, *J. Lond. Math. Soc.*, **8** (1933), 71–79.
[60] E. M. Wright, The asymptotic expansion of the generalized Bessel function, *Proc. Lond. Math. Soc. (Ser. II)*, **38** (1935), 257–270.
[61] E. M. Wright, The asymptotic expansion of the generalized hypergeometric function, *J. Lond. Math. Soc.*, **10** (1935), 287–293.
[62] E. M. Wright, The generalized Bessel function of order greater than one, *Quart. J. Math., Oxford Ser.*, **11** (1940), 36–48.
[63] Y. Zhang, M. M. Meerschaert, and B. Baeumer, Particle tracking for time-fractional diffusion, *Phys. Rev. E*, **78** (2008), 036705/1-7.
[64] V. M. Zolotarev, *One-Dimensional Stable Distributions*, Amer. Math. Soc., Providence, R. I., 1986.

James F. Kelly and Mark M. Meerschaert

The fractional advection-dispersion equation for contaminant transport

Abstract: Anomalous dispersion is observed throughout hydrology, yielding a contaminant plume with heavy leading tails. The fractional advection dispersion equation (FADE) captures this behavior by replacing the second-order spatial derivative with a Riemann–Liouville (RL) fractional derivative. The RL fractional derivative is a nonlocal operator and models large jumps of solute particles in heterogeneous media. This chapter reviews the FADE, including fundamental (point-source) solutions, which are expressed as stable probability density functions. The space FADE has been extended to space-dependent parameters (e. g., dispersivity) and multiple dimensions. Alternatively, the time FADE and fractional mobile immobile (FMIM) models, which utilize time-fractional derivatives to model long-waiting times (retention), are also used to model anomalous dispersion. Current applications of the FADE, including parameter estimation, source identification, space-time duality, and FADE models on bounded domains are discussed.

Keywords: Fractional dispersion, continuous time random walks, parameter fitting, source identification, space-time duality

MSC 2010: 26A33, 60G52

1 Introduction

Non-Fickian, or anomalous, dispersion is observed throughout hydrology in both surface [2, 26, 32, 53] and subsurface [10, 11, 19, 62] flows through heterogeneous porous media. Solute particles may experience long movements due to high-velocity preferential flow paths, yielding a particle plume with heavy leading tails. As a result, the solute spreads in a super-diffusive manner. The traditional advection dispersion equation (ADE) with constant coefficients cannot model this feature of anomalous dispersion. To address this problem, the fractional advection dispersion equation (FADE) was introduced in Benson et al. [8–10], replacing the second derivative in space with

Acknowledgement: JFK was partially supported by ARO MURI grant W911NF-15-1-0562 and NSF grant EAR-1344280. MMM was partially supported by ARO MURI grant W911NF-15-1-0562 and NSF grants DMS-1462156 and EAR-1344280. The authors thank Noah Schmadel and Adam S. Ward (Department of Environmental Engineering, Indiana University) for providing the Selke River data and Yong Zhang (Department of Geological Sciences, University of Alabama) for Figure 5.

James F. Kelly, Mark M. Meerschaert, Department of Statistics and Probability, Michigan State University, East Lansing, Michigan, USA, e-mails: kellyja8@stt.msu.edu, mcubed@stt.msu.edu

a fractional Riemann–Liouville (RL) derivative. Thus, the FADE introduces *spatial nonlocality* [20, 21, 23], using an integro-differential operator with a power-law kernel, to model a wide range of flow velocities.

The FADE has successfully modeled tracer tests in underground aquifers, including the MADE tracer tests in a highly heterogeneous aquifer located on a US Air Force base in Mississippi [10, 12, 17], tracer tests in the Cape Code sand and gravel aquifer [8], unsaturated soils [65], saturated porous media [73], streams and rivers [1, 25, 26], and overland solute transport due to rainfall [27]. More recently, the FADE has modeled anomalous mixing and reaction between multiple chemical species [13, 14]. Some of this success may be attributed to the simplicity of the FADE: a wide range of observed behavior in heterogeneous media is captured with a parsimonious model with just four parameters.

This chapter focuses on the spatial FADE in both 1D and multiple dimensions. In Section 2, we first discuss the one-dimensional FADE. We then discuss variants of the FADE with variable coefficients. Fundamental solutions to the FADE with constant coefficients are expressed in terms of a *stable* probability density function. In Section 3, we describe the multidimensional FADE [44]. Section 4 briefly surveys two time-fractional models: the time FADE [63] and the fractional mobile-immobile model (FMIM) [58]. Section 5 examines two inverse problems associated with the FADE: parameter estimation and source identification. Finally, current research and unsolved problems are discussed in Section 6.

2 The fractional advection-dispersion equation

The 1D space-fractional advection dispersion equation (FADE) for concentration $C(x,t)$ [M/L^3] with *constant coefficients* is given by

$$\frac{\partial C}{\partial t} + v\frac{\partial C}{\partial x} = D\frac{1+\beta}{2}\frac{\partial^\alpha C}{\partial x^\alpha} + D\frac{1-\beta}{2}\frac{\partial^\alpha C}{\partial(-x)^\alpha}, \tag{1}$$

where v [L/T] is the average plume velocity, D [L$^\alpha$/T] is a fractional dispersion coefficient that controls the rate of spreading, $1 \le \alpha \le 2$ (dimensionless) and $-1 \le \beta \le 1$ (dimensionless) is the skewness parameter. The first and second terms on the right hand of (1) are the positive (left) and negative (right) *Riemann–Liouville* (RL) fractional derivatives. If $\beta = 1$, then solutions to the FADE are positively-skewed, while if $\beta = -1$, solutions are negatively skewed. If $\beta = 0$, the sum of the two RL fractional derivatives is equivalent to the symmetric *Riesz* derivative, and the resulting solution is symmetric. The fractional order α codes for the heterogeneity of the velocity field, with a higher probability of large velocities as α decreases towards one, see Clarke et al. [17].

If $\alpha = 2$, the FADE reduces to the traditional advection-dispersion equation (ADE) for groundwater flow and transport (e. g., see Bear [6]). The FADE (1) was introduced by

Benson et al. [9] to model scale-dependent dispersivity in fitted groundwater plumes, i. e., the fact that the fitted parameter D grows with time when the ADE is applied to data. Such evidence of superdiffusion is an indicator that a space-fractional model may be preferable. Indeed, Benson et al. [8–10] show that the FADE (1) with $1 < \alpha < 2$ allows the same data to be fit with a constant coefficient model, where D does not vary over time.

The positive and negative RL derivatives in (1) may be computed using the (shifted) *Grünwald–Letnikov* finite difference formula introduced by Meerschaert and Tadjeran [42]:

$$\frac{\partial^\alpha C}{\partial x^\alpha} = \lim_{h\to 0} h^{-\alpha} \sum_{j=0}^{\infty} g_j^\alpha C(x-(j-1)h,t) \tag{2a}$$

$$\frac{\partial^\alpha C}{\partial (-x)^\alpha} = \lim_{h\to 0} h^{-\alpha} \sum_{j=0}^{\infty} g_j^\alpha C(x+(j-1)h,t), \tag{2b}$$

where the Grünwald weights g_j^α are given by

$$g_j^\alpha = (-1)^j \frac{\Gamma(\alpha+1)}{\Gamma(j+1)\Gamma(\alpha-j+1)} = \frac{-\alpha(1-\alpha)\cdots(j-1-\alpha)}{j!}.$$

From these definitions, we see that the RL fractional derivative is a nonlocal operator: the change in concentration at position x does not just depend on nearby locations, but distant locations as well. From a particle perspective, a combination of positive and negative RL derivatives allows a solute particle to *jump* to any point in the domain. Figure 1 illustrates this situation, and Schumer et al. [57] provide a derivation of (1) using this Eulerian particle picture. In brief, the FADE models contaminant transport through a heterogeneous porous medium, using a nonlocal fractional derivative that captures a highly variable velocity field.

The FADE (1) governs the long-time limit of a random walk with long-tailed particle jumps, and $C(x,t)$ is the probability density function (PDF) of the limiting stochas-

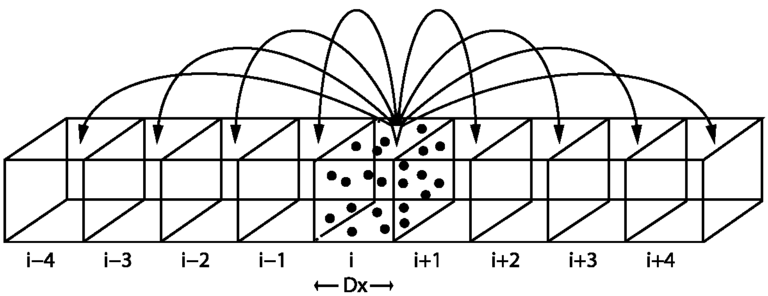

Figure 1: Fractional diffusion of particles between distant cells, illustrating the nonlocality of the RL fractional derivative, from [57].

tic process. Suppose that (X_n) are independent and identically distributed (IID) random variables that represent the particle jumps, and $S_n = X_1 + \cdots + X_n$ is a random walk that represents the position of a randomly selected particle after the nth jump. Suppose that $\mathbb{P}[X_n > x] = pCx^{-\alpha}$ and $\mathbb{P}[X_n < -x] = qCx^{-\alpha}$ for some $C > 0$ and $1 < \alpha < 2$, where p, q are nonnegative constants such that $p + q = 1$. Then the mean $v = \mathbb{E}[X_n]$ exists and we have

$$n^{-1/\alpha} \sum_{j=1}^{[nt]} (X_j - v) + n^{-1} \sum_{j=1}^{[nt]} v \Rightarrow Z_t + vt, \tag{3}$$

where Z_t is a stable Lévy motion with mean zero [40, Remark 4.17]. The PDF $C(x,t)$ of $Z_t + vt$ solves the FADE (1) with $D = C\Gamma(2-\alpha)/(\alpha-1)$ and $\beta = p - q$ [40, Proposition 4.16]. If X_n are IID with a finite variance $\sigma^2 = \mathbb{E}[(X_n - v)^2]$, then (3) holds with $\alpha = 2$, Z_t is a Brownian motion, and $C(x,t)$ solves the FADE (1) with $\alpha = 2$ and $D = \sigma^2/2$ [40, Section 1.1]. The latter connection between random walks, Brownian motion, and the diffusion equation was noted by Einstein [29] in his most cited research paper. The corresponding connection between heavy tailed random walks, stable Lévy motion, and the FADE extends this powerful idea, see Sokolov and Klafter [60] for further discussion.

2.1 Fractional-Flux ADE (FF-ADE)

In a heterogeneous porous medium, at a large enough scale where the geological character of the medium changes with location, the material parameters v and D can depend on space. There are at least three variants of the FADE with space-dependent coefficients: (1) the fractional-flux ADE (FF-ADE), (2) the fractional-divergence ADE (FD-ADE), and (3) the fully fractional divergence ADE (FFD-ADE).

The FF-ADE model is derived from the classical conservation of mass (continuity) equation

$$\frac{\partial C}{\partial t} + \frac{\partial q}{\partial x} = 0, \tag{4}$$

where $q(x,t)$ is the flux, complemented with a fractional flux constitutive equation [51, 57]

$$q(x,t) = v(x)C - D(x)\frac{1+\beta}{2}\frac{\partial^{\alpha-1}C}{\partial x^{\alpha-1}} + D(x)\frac{1-\beta}{2}\frac{\partial^{\alpha-1}C}{\partial(-x)^{\alpha-1}}. \tag{5}$$

The first term in (5) is the *advective flux*, which models the average drift of contaminant particles, while the second and third terms are the *dispersive flux* that model large particle jumps in the positive and negative directions, respectively. Combining (4) and (5) yields the FF-ADE from Zhang et al. [66] and Huang et al. [33]:

$$\frac{\partial C}{\partial t} = -\frac{\partial}{\partial x}\left[v(x)C - D(x)\frac{1+\beta}{2}\frac{\partial^{\alpha-1}C}{\partial x^{\alpha-1}} + D(x)\frac{1-\beta}{2}\frac{\partial^{\alpha-1}C}{\partial(-x)^{\alpha-1}}\right]. \tag{6}$$

Setting $\beta = 1$ yields the FF-ADE given by equation (4) in [67], while setting $v(x)$ and $D(x)$ constant yields (1).

2.2 Fractional-Divergence ADE (FD-ADE) and Fully Fractional Divergence ADE (FFD-ADE)

An alternative formulation replaces the divergence in the continuity equation (4) with a fractional divergence [47], yielding a fractional divergence-advection dispersion equation (FD-ADE)

$$\begin{aligned}\frac{\partial C}{\partial t} &= -\frac{\partial}{\partial x}[v(x)C] + \frac{1+\beta}{2}\frac{\partial^{\alpha-1}}{\partial x^{\alpha-1}}\left[D(x)\frac{\partial C}{\partial x}\right] \\ &\quad - \frac{1-\beta}{2}\frac{\partial^{\alpha-1}}{\partial(-x)^{\alpha-1}}\left[D(x)\frac{\partial C}{\partial x}\right]. \end{aligned} \tag{7}$$

Setting $\beta = 1$ yields the FD-ADE given by equation (11) in Zhang et al. [67]. By setting $v(x)$ and $D(x)$ constant in (7), we recover the *modified* FADE

$$\frac{\partial C}{\partial t} + v\frac{\partial C}{\partial x} = D\frac{1+\beta}{2}\frac{\partial^{\alpha-1}}{\partial x^{\alpha-1}}\left[\frac{\partial C}{\partial x}\right] - D\frac{1-\beta}{2}\frac{\partial^{\alpha-1}}{\partial(-x)^{\alpha-1}}\left[\frac{\partial C}{\partial x}\right], \tag{8}$$

proposed in Zhang et al. [68]. The modified FADE replaces the Riemann–Liouville fractional derivatives in the flux equation (5) with Caputo fractional derivatives. We will call the fractional derivatives on the right hand side of (8) *mixed Caputo* derivatives. These fractional derivatives, which lie in between the Riemann–Liouville and Caputo forms, have been used in various contexts, see for example Cushman and Ginn [21], Patie and Simon [52], and [47, Section 6]. On an infinite domain with sufficiently smooth concentration profiles that tend to zero at $\pm\infty$, both the FADE and the modified FADE are equivalent, because in that case the Riemann–Liouville and mixed Caputo derivatives are equal. On bounded domains, however, their behavior can be quite different. We will return to this issue in Subsection 6.2.

Finally, if we also fractionalize the advection term, we obtain the fully fractional divergence ADE (FFD-ADE):

$$\begin{aligned}\frac{\partial C}{\partial t} &= -\frac{\partial^{\alpha-1}}{\partial x^{\alpha-1}}[v(x)C] + \frac{1+\beta}{2}\frac{\partial^{\alpha-1}}{\partial x^{\alpha-1}}\left[D(x)\frac{\partial C}{\partial x}\right] \\ &\quad - \frac{1-\beta}{2}\frac{\partial^{\alpha-1}}{\partial(-x)^{\alpha-1}}\left[D(x)\frac{\partial C}{\partial x}\right]. \end{aligned} \tag{9}$$

All three versions of the FADE govern Markovian random walk processes, where the jump distribution depends on the current particle location [67]. The FF-ADE (6), FD-ADE (7), and FFD-ADE (9) can be discretized using an implicit Euler scheme, or alternatively a random walk particle tracking method [66]. The FF-ADE (6) and FD-ADE

(7) exhibit similar plume behavior if $D(x)$ varies linearly with position x; however, for nonlinear $D(x)$ and small α near one, there is a significant difference between these two models. Finally, solutions to the FFD-ADE (9) differ markedly from the FF-ADE and FD-ADE, with a much heavier leading tail. See Zhang et al. [67] for more details.

2.3 Fundamental solutions

The solution to the FADE (1) on the real line with point-source initial condition $C(x,0) = \delta(x)$ for any $1 < \alpha \le 2$ can be written in terms of a *stable* PDF $f(x;\alpha,\beta,\sigma,\delta)$ (e. g., see Samorodnitsky and Taqqu [55] or Meerschaert and Sikorskii [40, Proposition 5.8])

$$C(x,t) = f\big(x;\alpha,\beta,(Dt|\cos(\pi\alpha/2)|)^{1/\alpha}, vt\big). \tag{10}$$

For $\alpha = 2$, this solution reduces to a Gaussian. A brief derivation using Fourier transforms is included in Benson et al. [9] and [34]. Although the stable PDF with $1 < \alpha < 2$ cannot be written in closed form in terms of elementary functions, convenient computer codes are available to plot the stable PDF (e. g., see Nolan [50]) and these have been applied to the FADE [40, Chapter 5]. A MATLAB toolbox `FracFit`[1] to plot FADE solutions, and fit parameters to observed concentration data, is also available [35].

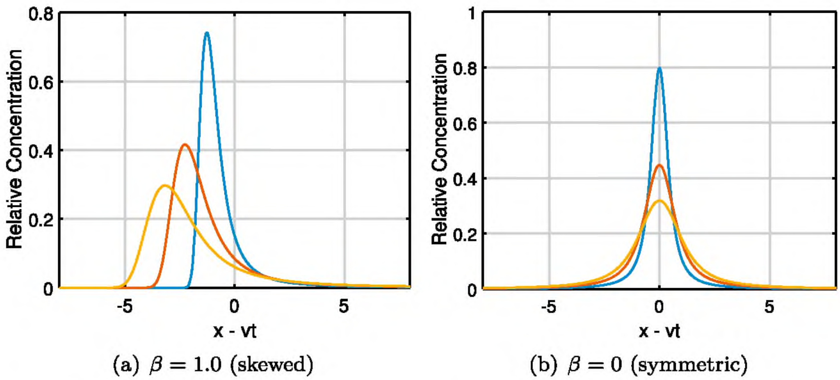

Figure 2: Evolution of the point-source solution (10) at times $t = 1$ (solid), 2 (dashed), and 3 (dotted) relative to the plume center of mass. A stable index of $\alpha = 1.2$ and fractional dispersion coefficient of $D = 1$ are used. Panel (a) shows a skewed plume with $\beta = 1$, while panel (b) shows a symmetric ($\beta = 0$) plume.

1 https://github.com/jfk-inspire/FracFit-v-0.9

Figure 2 displays the evolution of the point-source solution (10) at times $t = 1, 2,$ and 3 relative to the plume center of mass. A stable index of $\alpha = 1.2$ and fractional dispersion coefficient of $D = 1$ are used. Panel (a) shows a skewed plume with $\beta = 1$, while panel (b) shows a symmetric ($\beta = 0$) plume. In both panels, the solution has a nonlinear scaling rate proportional to $t^{1/\alpha}$, which grows faster than the classical Boltzmann rate $t^{1/2}$. That is, the point-source solution to the FADE exhibits super-diffusion. In addition, both figures exhibit heavy tails, which decay like inverse power laws with respect to x. For the skewed plume in panel (a), the plume has a heavy tail to the right (downstream) of the plume center of mass $x = vt$, while in the symmetric case shown in panel (b), the plume has heavy tails on both sides.

A second fundamental solution of interest to field and experimental hydrologists is a continuous injection solution. These solutions model continuous injection breakthrough curves (CBTCs) from laboratory experiments, such as transport of organic matter through porous media columns. These experiments display strong anomalous transport characteristics, for example, see Dietrich et al. [28] and McInnis et al. [38, 39].

At present, no closed-form analytical solution for the FADE or the FD-ADE using a continuous injection on the half-axis exists; however, an analytical approximation following what is done for the classical ADE ($\alpha = 2$) in Danckwerts [22] may be derived as follows. Consider the modified FADE (8) on $-\infty < x < \infty$ subject to initial condition $C_0(x, 0) = C_0$ for $x < 0$ and $C_0(x, 0) = 0$ for $x \geq 0$. Using the FADE pulse initial condition solution (10), the continuous injection solution is approximated by

$$C(x,t) = \int_{-\infty}^{\infty} C_0(x') f\left(x - x'; \alpha, \beta, \left(Dt|\cos(\pi\alpha/2)|\right)^{1/\alpha}, vt\right) dx'. \tag{11}$$

Evaluating the integral in (11) yields

$$C(x,t) = C_0\left[1 - F\left(x; \alpha, \beta, \left(Dt|\cos(\pi\alpha/2)|\right)^{1/\alpha}, vt\right)\right], \tag{12}$$

where $F(z; \alpha, \beta, \sigma, \delta)$ denotes the cumulative distribution function (CDF) for a stable random variable.

To verify this approximation, we compare it to a complete numerical solution from Zhang et al. [68]. A prescribed concentration boundary condition was imposed at the inlet $C(0, t) = C_0 H(t)$ and a free drainage boundary condition was imposed at $x = L = 200$. The parameters used in both simulations are $D = 2.5$, $v = 10.0$, $\alpha = 1.6$, which are identical to those used in Figure 3a of [68]. Agreement between (12) and the numerical solution is very good, indicating that (12) is a good approximation for continuous injection. For the case $\beta = 1$ shown in panel (a), we can see a heavier leading tail, while for the case $\beta = -1$ plotted in panel (b), we can observe a heavy trailing tail. See Figure 3.

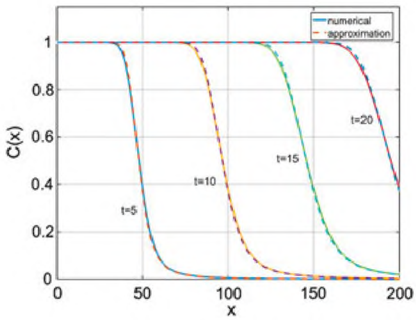

(a) $\beta = 1.0$

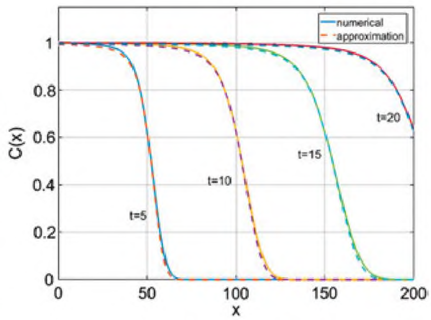

(b) $\beta = -1.0$

Figure 3: Comparison of the analytical approximation given by equation (12) and a semi-implicit discretization of the modified FADE (8). The unitless parameters for the two simulation are $C_0 = 1$, $\alpha = 1.6$, $v = 10$, $D = 2.5$. The left panel is positively-skewed ($\beta = 1.0$), while the right panel is negatively-skewed ($\beta = -1.0$).

3 Multidimensional fractional advection-dispersion equation

A multi-dimensional FADE was proposed in [44]

$$\frac{\partial C}{\partial t} + \mathbf{v} \cdot \nabla C(\mathbf{x}, t) = D\nabla_M^\alpha C(\mathbf{x}, t), \tag{13}$$

where $\mathbf{v}$ [L/T] is the d-dimensional average plume velocity and ∇_M^α is a vector fractional derivative [47] defined via an inverse spatial Fourier transform

$$\nabla_M^\alpha C(\mathbf{x}, t) = \mathcal{F}^{-1}\left[\int_{\|\boldsymbol{\theta}\|=1} (i\mathbf{k} \cdot \boldsymbol{\theta})^\alpha \hat{C}(\mathbf{k}, t) M(d\boldsymbol{\theta})\right], \tag{14}$$

where $\boldsymbol{\theta}$ is an d-dimensional unit vector, $\mathbf{k}$ is a wave-vector, $\hat{C}(\mathbf{k}, t) = \mathcal{F}[C(\mathbf{x}, t)] = \int e^{-i\mathbf{k}\cdot\mathbf{x}} C(\mathbf{x}, t)\, d\mathbf{x}$ is the spatial Fourier transform of concentration, and $M(d\boldsymbol{\theta})$ is a mixing measure defined over the unit sphere in d-dimensions. If $\alpha = 2$, (13) reduces to the traditional vector ADE

$$\frac{\partial C}{\partial t} + \mathbf{v} \cdot \nabla C(\mathbf{x}, t) = \nabla \cdot A \nabla C(\mathbf{x}, t)$$

where the 2-tensor

$$A = D \int \boldsymbol{\theta}\boldsymbol{\theta}^T M(d\boldsymbol{\theta})$$

is the dispersion tensor using the outer product [40, Section 6.5]. For a general mixing measure with $1 < \alpha < 2$, fundamental solutions to (13) cannot be expressed in closed form. We will consider two special cases, in which case we can write the fundamental solutions as products of stable PDFs. If jumps only occur along the standard coordinate vectors $\mathbf{e}_j : j = 1, 2, \ldots, d$ with probabilities $M\{\mathbf{e}_j\} = p/d$ and $M\{-\mathbf{e}_j\} = q/d$, then the fractional directional derivative (14) is evaluated as

$$\nabla_M^\alpha C(\mathbf{x}, t) = \frac{p}{d} \sum_{j=1}^{d} \frac{\partial^\alpha}{\partial x_j^\alpha} C(\mathbf{x}, t) + \frac{q}{d} \sum_{j=1}^{d} \frac{\partial^\alpha}{\partial(-x_j)^\alpha} C(\mathbf{x}, t). \tag{15}$$

Letting $D_0 = D/d$ and $\beta = p - q$ yields a vector fractional diffusion equation

$$\begin{aligned} &\frac{\partial}{\partial t} C(\mathbf{x}, t) + \mathbf{v} \cdot \nabla C(\mathbf{x}, t) \\ &\quad = D_0 \frac{1+\beta}{2} \sum_{j=1}^{d} \frac{\partial^\alpha}{\partial x_j^\alpha} C(\mathbf{x}, t) + D_0 \frac{1-\beta}{2} \sum_{j=1}^{d} \frac{\partial^\alpha}{\partial(-x_j)^\alpha} C(\mathbf{x}, t). \end{aligned} \tag{16}$$

Assuming a velocity $\mathbf{v} = \sum_{j=1}^{d} v_j \mathbf{e}_j$, the point source solution to (16) with $C(\mathbf{x}, 0) = \delta(\mathbf{x})$ may be computed via a Fourier transform, yielding

$$C(\mathbf{x}, t) = \prod_{j=1}^{d} f\left(x_j; \alpha, \beta, (D_0 t |\cos(\pi\alpha/2)|)^{1/\alpha}, v_j t\right). \tag{17}$$

Figure 4 shows level sets of (17) for $d = 2$ dimensions at time $t = 1$ relative to the plume center of mass. A stable index of $\alpha = 1.1$ and fractional dispersion coefficient of $D_0 = 1$ are used. Panel (a) shows contours of a skewed plume with $\beta = 1$, while panel (b) shows contours of a symmetric ($\beta = 0$) plume. Note that the contours are anisotropic in both cases, including panel (b) with symmetric jumps ($\beta = 0$). Except

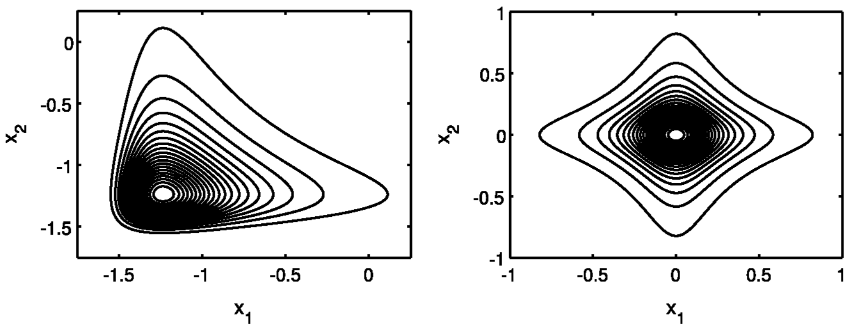

(a) $\beta = 1.0$ (skewed) (b) $\beta = 0$ (symmetric)

Figure 4: Level sets of the point-source solution to the multidimensional FADE ($d = 2$) at time $t = 1$ relative to the plume center of mass. A stable index of $\alpha = 1.1$ and fractional dispersion coefficient of $D_0 = 1$ are used. Panel (a) shows contours of a skewed plume with $\beta = 1$, while panel (b) shows contours of a symmetric ($\beta = 0$) plume.

for $\alpha = 2$, the plume spreads in an asymmetric fashion, thus providing a good model for anisotropic media.

Finally, consider the case where $M(d\boldsymbol{\theta})$ is uniform over the $(d-1)$-dimensional sphere. Using [40, Example 6.24], (14) is evaluated as the (symmetric) fractional Laplacian, yielding

$$\frac{\partial}{\partial t}C(\mathbf{x},t) + \mathbf{v}\cdot\nabla C(\mathbf{x},t) = c_\alpha D \Delta^{\alpha/2} C(\mathbf{x},t), \tag{18}$$

where $\Delta^{\alpha/2}C(\mathbf{x},t)$ has Fourier transform $-|\mathbf{k}|^\alpha \hat{C}(\mathbf{k},t)$ and c_α is a coefficient that only depends on the order α. The fundamental solution may be written as a subordinated normal PDF [40, Example 6.5], yielding a *symmetric* level set. Further extensions of the FADE in multiple dimensions are developed in Schumer et al. [59], see also [45, 67] and [40, Chapter 6]. This *operator scaling* FADE allows a different order of the space-fractional derivative in each coordinate.

4 Time-fractional models

Unlike the space FADE, which models long particle jumps, the time-fractional FADE models long waiting times between jumps, by replacing the first-order time-derivative in the ADE with a time-fractional derivative. In this section, we summarize two widely used time-fractional PDEs: the time-fractional FADE and the fractional mobile-immobile equation (FMIM). In Subsection 6.1, we will see how the space FADE and time FADE are related via duality.

4.1 Time-fractional FADE

The time-fractional advection dispersion equation from Zaslavsky [63] or Liu et al. [36] is given by

$$\left(\frac{\partial}{\partial t}\right)^\gamma C = -v\frac{\partial C}{\partial x} + D\frac{\partial^2 C}{\partial x^2}, \tag{19}$$

where the first term in (19) is a Caputo derivative with order $0 < \gamma < 1$ on the half-axis. In the case of $\gamma = 1$, (19) reduces to the classical ADE. In contrast to the spatial FADE (1), the units of the velocity parameter v are $\mathrm{L}/\mathrm{T}^\gamma$ and the units of the dispersion coefficient are $\mathrm{L}^2/\mathrm{T}^\gamma$.

This time-fractional equation governs the scaling limit of a continuous time random walk (CTRW). For simplicity, suppose that $v = 0$. Assume as in Section 2 that $S_n = X_1 + \cdots + X_n$ is a random walk of particle jumps. Now suppose that a random waiting time W_n occurs before the nth jump. The random walk $T_n = W_1 + \cdots + W_n$ gives the time of the nth jump, $N(t) = \max\{n \ge 0 : T_n \le t\}$ is the number of jumps by time $t \ge 0$, and the CTRW $S_{N(t)}$ is the location of a randomly selected particle at time $t \geq 0$. If the waiting times are heavy tailed with $\mathbb{P}[W_n > t] = At^{-\gamma}$ for some $A > 0$ and $0 < \gamma < 1$, then

$$n^{-1/\gamma} \sum_{j=1}^{[nt]} W_j = n^{-1/\gamma} T_{[nt]} \Rightarrow D_t, \tag{20}$$

another stable Lévy motion called a stable subordinator. The counting process $n^{-\gamma}N(nt) \Rightarrow E(t)$, where $E(t) = \inf\{u > 0 : D_u > t\}$ is called the inverse stable subordinator, and a continuous mapping argument yields the CTRW limit $Z_{E(t)}$ [40, Section 4.4]. The PDF $C(x,t)$ of the CTRW limit is the point source solution to the time-fractional dispersion equation (19) [46]. From a hydrological point of view, the waiting times model resting periods between particle movements.

Closed-form solutions to (19) are constructed via subordination. Starting with a solution $C_{\mathrm{ADE}}(x,t)$ to the ADE (19) with $\gamma = 1$, the time variable is randomized by the inverse stable subordinator (e. g., see Meerschaert and Straka [41]). For a pulse initial condition $C(x,0) = \delta(x)$ on the real axis, this subordination integral is written as [40, equation (4.39)]

$$C(x,t) = \int_0^\infty h_\gamma(u,t) \frac{1}{\sqrt{4\pi Du}} \exp\left(-\frac{(x - vu)^2}{4Du}\right) du, \tag{21}$$

where $h_\gamma(u,t)$ is the pdf of the inverse γ-stable subordinator $E(t)$. The density $h_\gamma(u,t)$ may be written in terms of a stable density [40, equation (4.47)], and evaluated using available codes (e. g., Nolan [50] or [35]).

4.2 Fractional mobile-immobile equation

The fractional mobile-immobile (FMIM) model from Schumer et al. [58] generalizes the classical mobile-immobile (MIM) model (e. g., see Coats and Smith.[18]), which partitions the concentration into mobile $C_m(x,t)$ and immobile $C_{im}(x,t)$ phases. All MIM models equate the divergence of the total (advective and dispersive) flux to a weighted sum of the time rate of change of each phase. The rate of change from the immobile to the mobile phase is expressed as a convolution with a memory function $f(t)$. In particular, the FMIM model [58] uses a power law memory function $f(t) = t^{-\gamma}/\Gamma(1-\gamma)$ with $0 < \gamma < 1$.

A CTRW model for the FMIM, that segregates mobile from immobile particles, was developed by Benson and Meerschaert [7]. It models the long waiting times experienced by solute particles in the immobile phase by a power law, exactly as for the time-FADE. The memory function is explicitly computed in terms of the CTRW model. Power law waiting times have been observed in river transport studies by Haggerty et al. [32] and Schmadel et al. [56].

The FMIM equation with Fickian flux for mobile concentration is given by Schumer et al. [58] as

$$\frac{\partial C_m}{\partial t} + \beta_c \frac{\partial^\gamma C_m}{\partial t^\gamma} = -v\frac{\partial C_m}{\partial x} + D\frac{\partial^2 C_m}{\partial x^2}, \tag{22}$$

where the second term in (22) is a Riemann–Liouville derivative on the half-axis, β_c [$T^{\gamma-1}$] is the capacity coefficient, defined as the ratio of the porosity in the immobile phase to that of the mobile phase (see Haggerty and Gorelick [30]), D [L^2/T] is the dispersion coefficient, and v [L/T] is the average velocity. This FMIM is similar to an earlier model proposed in Carrera et al. [15] and to a truncated power-law model proposed in Haggerty et al. [31].

Like the time-FADE, solutions to (22) may be expressed via a subordination integral [58, equation (21)]

$$C_m(x,t) = \int_0^t g_\gamma(t-u, \beta_c u)\frac{1}{\sqrt{4\pi D u}}\exp\left(-\frac{(x-vu)^2}{4Du}\right)du, \tag{23}$$

where $g_\gamma(t,u)$ is the density of the γ-stable subordinator D_u, with Laplace transform $\tilde{g}(s,u) = e^{-us^\gamma}$. A calculation [58] shows that $C_m(x,t)$ falls off like $t^{-\gamma-1}$ at late time.

5 Parameter estimation and source identification

Application of the FADE to observed field or laboratory data often requires solving an inverse problem. In this section, we briefly discuss two such inverse problems: source identification and parameter identification.

5.1 Source identification

In groundwater hydrology, source identification determines the source location, release history, and/or strength of a contaminant source given one or more measurements. One approach is to solve the forward equation multiple times to identify the source. While straightforward, this method is computationally expensive. Alternatively, one may derive a *backward equation* whose solution is a PDF for the source location/time. This backward equation only needs to be solved once, and is hence computationally more efficient.

A backward model for the classical ADE was derived in Neupauer and Wilson [49] using an adjoint-based approach. This method was extended to the FADE (specifically, the FD-ADE) in Zhang et al. [71] and later to bounded domains in Zhang et al. [72]. Since the primary application is groundwater flows, we consider a special case of the FD-ADE (7) with only positive jumps ($\beta = 1$) and source and sink terms given by [71, equation (1) with effective porosity $\theta = 1$]

$$\frac{\partial}{\partial t}C = -\frac{\partial}{\partial x}[v(x)C] + \frac{\partial}{\partial x}\left[D(x)\frac{\partial^{\alpha-1}C}{\partial x^{\alpha-1}}\right] + q_iC_i - q_0C, \tag{24}$$

where the mean velocity v and dispersion coefficient D may vary with x (heterogeneous), q_i is the source inflow rate, q_0 is the sink outflow rate, and C_i is the inflow concentration. Letting $A(x,t)$ be the adjoint state, the backward FADE is given by [71, equation (10) with $\theta = 1$]

$$\frac{\partial}{\partial t}A = \frac{\partial}{\partial x}[v(x)A] + \frac{\partial^{\alpha-1}}{\partial(-x)^{\alpha-1}}\left[D(x)\frac{\partial A}{\partial(-x)}\right] - q_iA + \delta(x - x_d)\delta(\tau), \tag{25}$$

where x_d is the detection location, T is the detection time, and $\tau = T - t$ is the "backward time". Given an observed contaminant at location x_d at backward time $\tau = 0$ assuming no other source or sink, the backward location PDF $f_x(x;\tau)$ satisfies (25) with $q_i = 0$. If both v and D are assumed constant, then (25) has an analytical solution specified by (10):

$$f_x(x;\tau) = f(x - x_d; \alpha, -1, (D\tau|\cos(\pi\alpha/2)|)^{1/\alpha}, v\tau). \tag{26}$$

Figure 5 evaluates the PDF (26) using MADE-2 concentration data [12] for day (a) 132, (b) 224, and (c) 328 using $\alpha = 1.1$, $v = 0.12$ m/day, and $D = 0.14$ m$^\alpha$/day. The vertical solid bar shows the actual release location, while the long and short dashed lines show the 75th and 25th percentiles of the displayed PDF. Although the predicted source location does not coincide with the median, the predicted source location does lie between the 25th and 75th percentiles. The variability in this estimation motivates further study, such as including a scale dependent dispersion coefficient and the effects of a finite boundary [72].

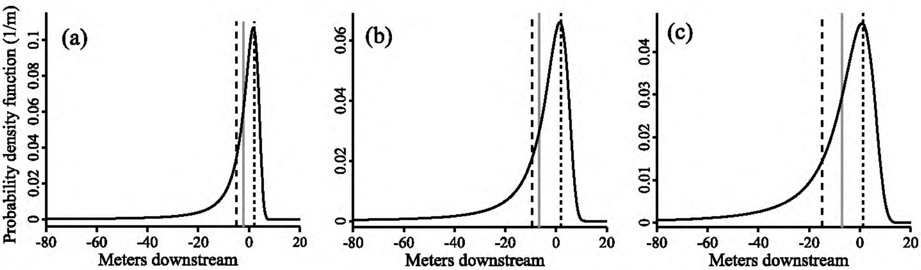

Figure 5: PDF of contaminant release location predicted by the backward FADE using MADE-2 concentration data for day (a) 132, (b) 224, and (c) 328 using $\alpha = 1.1$, $v = 0.12$ m/day, and $D = 0.14$ m$^\alpha$/day. The vertical solid bar shows the actual release location, while the long and short dashed lines show the 75th and 25th percentiles of the displayed PDF. Reprinted from [71].

5.2 Parameter estimation

A statistically optimal parameter estimation method based on the weighted nonlinear least squares (WNLS) approach is described in Chakraborty et al. [16]. This method is applicable to both snapshot data $x \mapsto C(x,t)$ with time t fixed and breakthrough curve (BTC) data $t \mapsto C(x,t)$ with position x fixed. Using a particle-tracking approach, [16] demonstrated that concentration variance is proportional to concentration (heteroscedasticity). As a result, weighted nonlinear regression is used where the weights are proportional to the reciprocal of measured concentration, thereby assigning a greater weight to lower concentration values. This WNLS approach is important for capturing anomalous transport characteristics (e. g., heavy leading or trailing tails). This estimation procedure was adapted to time-fractional, tempered time-fractional models (e. g., see [48]), and continuous injection data in [35].

To illustrate the WNLS approach, assume we have N measurements of a BTC $C_i = C(x,t_i)$ at times t_i, $1 \le i \le N$, and we wish to fit the parameters $\Theta = (\alpha,\beta,v,D)$ of the FADE to observed data by minimizing the weighted mean square error (WMSE) function

$$E(\Theta) = \frac{1}{N}\sum_{i=1}^{N} w_i\big(C_i - C(x,t_i)\big)^2, \tag{27}$$

where $C(x,t)$ is the modeled concentration (e. g., (10) for the space FADE) and the weights are given by $w_i = 1/C_i$. Either local optimization using a reasonable guess or global optimization (e. g., genetic algorithm) may be used to minimize (27) to find the optimal parameters Θ. We fit both the spatial FADE model (1) and the fractional mobile-immobile (FMIM) model, (22) and compare the results, using the `FracFit` package.

The first dataset is from a fluorescein dye tracer test conducted in the Red Cedar River (Michigan, USA) by Phanikumar et al. [53]. BTCs were measured at locations x = 1.4 km, 3.1 km, and 5.08 km downstream of the tracer source. The data was fit to the FADE (1) in previous work [16]. We replicated that fit at these three locations and also fit the FMIM model (22). The model fits and data are shown in panel (a) of Figure 6 for location $x = 3.1$ km. The FMIM parameters are $\gamma = 0.96$, $v = 0.145$ km/min, $\beta_c = 3.87\,\text{min}^{-0.04}$, and $D = 0.0012\,\text{km}^2/\text{min}$. The FADE parameters are $\alpha = 1.56$, $\beta = -1$, $v = 0.0259$ km/min, and $D = 0.0013\,\text{km}^{1.56}/\text{min}$. It is apparent that both models fit the data reasonably well.

The second dataset is a similar dye tracer test conducted in the Selke River (Germany) by Schmadel et al. [56]. Eight tracer injections were released and measured at seven downstream locations. We fit data from injection 7 at site 4, located 667 m downstream. The optimal fits and data are shown in panel (b) of Figure 6. The FMIM parameters are $\gamma = 0.906$, $v = 0.8549$ m/s, $\beta_c = 0.844\,\text{s}^{-0.094}$, and $D = 0.3204\,\text{m}^2/\text{s}$. The FADE parameters are $\alpha = 1.33$, $\beta = -1$, $v = 0.313$ m/s, and $D = 0.223\,\text{m}^{1.56}/\text{s}$. Again, both models match the data reasonably well. These parameter fits suggest that there could be a

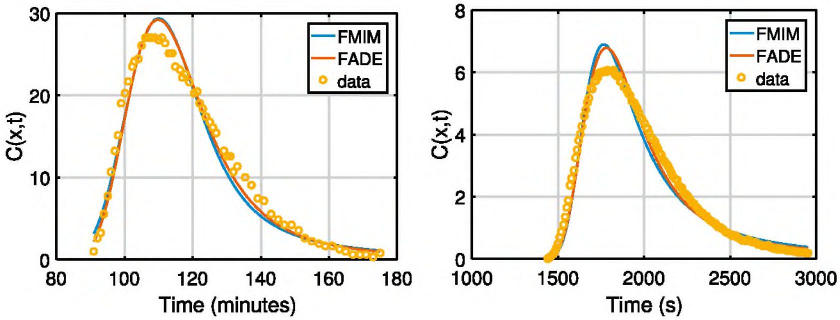

(a) Red Cedar river (b) Selke river

Figure 6: BTCs for the Red Cedar river at $x = 3.1$ km (panel a) and the Selke river at $x = 667$ m (panel b). The FADE (1) and time-fractional model (22) are fit using the `FracFit` toolbox. Parameters are given in the text.

relationship between time-fractional models and the space-FADE, which is discussed in the next section.

6 Current and future research

6.1 Space-time duality

As the parameter fits in Figure 6 illustrate, applications of the FADE to river flow hydrology employ a negatively skewed space-fractional derivative ($\beta = -1$), which models long upstream jumps in the random walk model outlined in Section 2. Deng et al. [25] suggest that this negatively skewed space-fractional derivative is capturing a “wide spectrum of dead zones” in the velocity field. The time-FADE models particle retention using a time-fractional derivative, which captures long resting periods between particle movements in the CTRW model discussed in Section 4. Zhang et al. [69] recommend the time-FADE (19) instead of the negatively skewed FADE (1) to model contaminant transport in rivers, because it does not seem physical for particles to make long upstream jumps. However, it is important to note that these jumps are moving upstream *relative to the center of mass*. In the space-FADE model, a particle moves downstream and then jumps back upstream. In the time-FADE model, the particle remains upstream while the bulk of the plume moves downstream. Either way, the particle ends up behind the plume center of mass.

This controversy between the space-FADE and the time-FADE for river flows was resolved in [34] by establishing a mathematical equivalence between the negatively skewed space-FADE and the time-FADE. This duality principle, which was applied to the space-fractional diffusion equation in Baeumer et al. [3], can be illustrated by considering the point source solution $C_0(x,t)$ to the negatively skewed FADE (1) with

$\beta = -1$, $v = 0$ and $D = 1$:

$$\frac{\partial C_0}{\partial t} = \frac{\partial^\alpha C_0}{\partial(-x)^\alpha}. \tag{28}$$

Apply a Fourier transform with respect to both x and t, yielding

$$[(i\omega) - (-ik)^\alpha]\hat{C}_0(k, \omega) = 0, \tag{29}$$

where k is the wavenumber and ω is the angular frequency. This *dispersion relationship* is equivalent to $(i\omega)^\gamma = (-ik)$ where $\gamma = 1/\alpha$. Substituting back into (29) and inverting the FT leads to the *dual equation*

$$\frac{\partial^\gamma C_0}{\partial t^\gamma} = -\frac{\partial C_0}{\partial x} \tag{30}$$

since $\partial/\partial(-x) = -\partial/\partial x$. Note that (30) is a special case of the time FADE (19) with $v = 1$ and $D = 0$ using a Caputo derivative. In the case $\alpha = 2$ ($\gamma = 1/2$), this space-time duality for the traditional diffusion equation was observed by Heaviside in 1871, perhaps the first real application of the fractional calculus. A rigorous derivation of space-time duality is laid out in [34], including the FADE (1) with any skewness. If the advection term in (1) is retained, it is shown in [34] that the dual time-fractional PDE involves the *fractional material derivative* from Sokolov and Metzler [61].

6.2 FADE in bounded domains

Most problems in hydrology and fluid dynamics occur on bounded domains, such as contaminant transport in column experiments [38, 39]. Application of the FADE on a bounded domain is a challenging problem, since the boundary condition may itself be nonlocal. Most available numerical schemes assume Dirichlet boundary conditions (BCs), including finite difference methods [42, 43, 54] and spectral methods [37, 64]; however, many problems involving the FADE in bounded domains require either mass conservation or a specification of flux. Considerable effort has been spent on developing mass-preserving, *reflecting* BCs for space fractional diffusion equations [4, 5, 24]. In particular, Baeumer et al. [4] proposed explicit Euler schemes for the one dimensional space-FADE using either a positive RL derivative or a mixed Caputo derivative. They show that the appropriate mass-preserving schemes involve a *fractional* boundary condition. The same fractional BCs were also applied to the (forward) FADE in Zhang et al. [70] and to the backward FADE in Zhang et al. [72].

As a simple example, consider the FADE model (1) on the unit interval $[0, 1]$ with $v(x) = 0$, $D(x) = 1$, and $\beta = 1$. Assume some initial mass $M_0 = \int_0^1 C(x, t)\,dx$ is conserved for all time t. Integrating the mass conservation equation (4) with respect to x and applying the fundamental theorem of calculus yields

$$\begin{aligned}\frac{\partial M_0}{\partial t} &= \int_0^1 \frac{\partial}{\partial t} C(x,t)\,dx \\ &= -\int_0^1 \frac{\partial}{\partial x} q(x,t)\,dx \\ &= q(0,t) - q(1,t).\end{aligned}$$

If the flux $q(0,t)$ and $q(1,t)$ at both endpoints is identically zero, then mass is conserved. From (5), the zero flux BC is

$$\left.\frac{\partial^{\alpha-1} C}{\partial x^{\alpha-1}}\right|_{x=0} = \left.\frac{\partial^{\alpha-1} C}{\partial x^{\alpha-1}}\right|_{x=1} = 0. \tag{31}$$

Figure 7 shows a numerical solutions using the explicit Euler method outlined in Baeumer et al. [4] of (a) the FADE (1) with Riemann–Liouville reflecting boundary conditions (31) and (b) the FADE with Caputo flux (8) with Caputo reflecting boundary conditions. As t increases, the solution in Figure 7(a) converges to the steady-state solution $C_\infty(x) = M_0(\alpha-1)x^{\alpha-2}$, which is singular at $x = 0$. Figure 7(b) shows numerical solutions of the modified FADE (8) with zero flux BCs. These BCs are the same as (31), except that the Riemann–Liouville fractional derivatives are replaced by Caputo derivatives. Since the Caputo fractional derivative of a constant is zero, the steady state solution is a constant $C_\infty(x) = M_0$. Consideration of the steady state solution is one useful method for selecting the appropriate FADE model on a bounded domain.

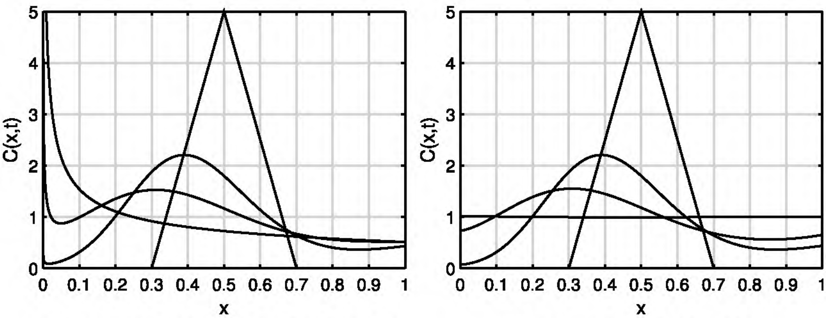

(a) Riemann-Liouville reflecting BC (b) Caputo reflecting BC

Figure 7: Numerical solution of (a) the FADE (1) with Riemann–Liouville reflecting boundary conditions (31) and (b) the FADE with Caputo flux (8) with Caputo reflecting boundary conditions. Both panels use parameters $\alpha = 1.5$, $v = 0$, $\beta = 1$, and $D = 1$ on $0 \le x \le 1$ at time $t = 0$ (solid line), $t = 0.05$ (dashed), $t = 0.1$ (dash dot), $t = 0.5$ (dotted).

7 Summary

The space FADE (1) models a wide range of observed anomalous dispersion using a fractional RL derivative in space. This RL derivative is a nonlocal operator and models large jumps of solute particles in heterogeneous media. The fundamental solutions to the space FADE in 1D exhibit both heavy tails and skewness, which are observed in many tracer tests. The space FADE has been extended to media with space-dependent material parameters and multiple dimensions. The time FADE and fractional mobile immobile (FMIM) models, which utilize time-fractional derivatives to model long-waiting times (retention), are also used to model anomalous dispersion. A connection between long upstream particle jumps and long waiting times is established using space-time duality, which provides an equivalence between the negatively-skewed space FADE and the time FADE. Finally, the FADE in bounded domains with nonlocal, reflecting boundary conditions is discussed.

Bibliography

[1] E. J. Anderson and M. S. Phanikumar, Surface storage dynamics in large rivers: Comparing three-dimensional particle transport, one-dimensional fractional derivative, and multirate transient storage models, *Water Resour. Res.*, **47**(9) (2011), W09511.

[2] A. Aubeneau, B. Hanrahan, D. Bolster, and J. Tank, Substrate size and heterogeneity control anomalous transport in small streams, *Geophys. Res. Lett.*, **41** (2014), 8335–8341.

[3] B. Baeumer, M. M. Meerschaert, and E. Nane, Space–time duality for fractional diffusion, *J. Appl. Probab.*, **46** (2009), 1100–1115.

[4] B. Baeumer, M. Kovács, M. M. Meerschaert, and H. Sankaranarayanan, Boundary conditions for fractional diffusion, *J. Comput. Appl. Math.*, **336** (2018), 408–424.

[5] B. Baeumer, M. Kovács, and H. Sankaranarayanan, Fractional partial differential equations with boundary conditions, *J. Differ. Equ.*, **264** (2018), 1377–1410.

[6] J. Bear, *Dynamics of Fluids in Porous Media*, Elsevier, New York, 1972.

[7] D. A. Benson and M. M. Meerschaert, A simple and efficient random walk solution of multi-rate mobile/immobile mass transport equations, *Adv. Water Resour.*, **32** (2009), 532–539.

[8] D. A. Benson, S. W. Wheatcraft, and M. M. Meerschaert, Application of a fractional advection-dispersion equation, *Water Resour. Res.*, **36**(6) (2000), 1403–1412.

[9] D. A. Benson, S. W. Wheatcraft, and M. M. Meerschaert, The fractional-order governing equation of Lévy motion, *Water Resour. Res.*, **36**(6) (2000), 1413–1423.

[10] D. M. Benson, R. Schumer, M. M. Meerschaert, and S. W. Wheatcraft, Fractional dispersion, Lévy motion, and the MADE tracer tests, *Transp. Porous Media*, **42** (2001), 211–240.

[11] B. Berkowitz and H. Scher, Anomalous transport in random fracture networks, *Phys. Rev. Lett.*, **79** (1997), 4038.

[12] J. M. Boggs, S. C. Young, L. M. Beard, L. W. Gelhar, K. R. Rehfeldt, and E. E. Adams, Field study of dispersion in a heterogeneous aquifer: 1. overview and site description, *Water Resour. Res.*, **28**(12) (1992), 3281–3291.

[13] D. Bolster, D. A. Benson, T. Le Borgne, and M. Dentz, Anomalous mixing and reaction induced by superdiffusive nonlocal transport, *Phys. Rev. E*, **82**(2) (2010), 021119.

[14] D. Bolster, D. A. Benson, M. M. Meerschaert, and B. Baeumer, Mixing-driven equilibrium reactions in multidimensional fractional advection–dispersion systems, *Phys. A, Stat. Mech. Appl.*, **392**(10) (2013), 2513–2525.
[15] J. Carrera, X. Sánchez-Vila, I. Benet, A. Medina, G. Galarza, and J. Guimerà, On matrix diffusion: Formulations, solution methods and qualitative effects, *Hydrogeol. J.*, **6**(1) (1998), 178–190.
[16] P. Chakraborty, M. M. Meerschaert, and C. Y. Lim, Parameter estimation for fractional transport: A particle-tracking approach, *Water Resour. Res.*, **45**(10) (2009), W10415.
[17] D. D. Clarke, M. M. Meerschaert, and S. W. Wheatcraft, Fractal travel time estimates for dispersive contaminants, *Groundwater*, **43**(3) (2005), 401–407.
[18] K. Coats and B. Smith, Dead-end pore volume and dispersion in porous media, *Soc. Pet. Eng. J.*, **4**(1) (1964), 73–84.
[19] A. Cortis and B. Berkowitz, Anomalous transport in "classical" soil and sand columns, *Soil Sci. Soc. Am. J.*, **68**(5) (2004), 1539–1548.
[20] J. H. Cushman and T. Ginn, Nonlocal dispersion in media with continuously evolving scales of heterogeneity, *Transp. Porous Media*, **13**(1) (1993), 123–138.
[21] J. H. Cushman and T. R. Ginn, Fractional advection-dispersion equation: a classical mass balance with convolution-Fickian flux, *Water Resour. Res.*, **36**(12) (2000), 3763–3766.
[22] P. Danckwerts, Continuous flow systems: Distribution of residence times, *Chem. Eng. Sci.*, **2**(1) (1953), 1–13.
[23] O. Defterli, M. D'Elia, Q. Du, M. Gunzburger, R. Lehoucq, and M. M. Meerschaert, Fractional diffusion on bounded domains, *Fract. Calc. Appl. Anal.*, **18**(2) (2015), 342–360.
[24] D. del-Castillo-Negrete, Fractional diffusion models of nonlocal transport, *Phys. Plasmas*, **13** (2006), 082308.
[25] Z.-Q. Deng, V. P. Singh, and L. Bengtsson, Numerical solution of fractional advection-dispersion equation, *J. Hydraul. Eng.*, **130**(5) (2004), 422–431.
[26] Z. Deng, L. Bengtsson, and V. P. Singh, Parameter estimation for fractional dispersion model for rivers, *Environ. Fluid Mech.*, **6**(5) (2006), 451–475.
[27] Z.-Q. Deng, J. L. De Lima, M. I. P. de Lima, and V. P. Singh, A fractional dispersion model for overland solute transport, *Water Resour. Res.*, **42**(3) (2006), W03416.
[28] L. Dietrich, D. McInnis, D. Bolster, and P. Maurice, Effect of polydispersity on natural organic matter transport, *Water Res.*, **47** (2013), 2231–2240.
[29] A. Einstein, On the movement of small particles suspended in a stationary liquid demanded by the molecular kinetic theory of heat, *Ann. Phys.*, **17** (1905), 549–560.
[30] R. Haggerty and S. M. Gorelick, Multiple-rate mass transfer for modeling diffusion and surface reactions in media with pore-scale heterogeneity, *Water Resour. Res.*, **31**(10) (1995), 2383–2400.
[31] R. Haggerty, S. A. McKenna, and L. C. Meigs, On the late-time behavior of tracer test breakthrough curves, *Water Resour. Res.*, **36**(12) (2000), 3467–3479.
[32] R. Haggerty, S. M. Wondzell, and M. A. Johnson, Power-law residence time distribution in the hyporheic zone of a 2nd-order mountain stream, *Geophys. Res. Lett.*, **29**(13) (2002), 18-1.
[33] G. Huang, Q. Huang, and H. Zhan, Evidence of one-dimensional scale-dependent fractional advection–dispersion, *J. Contam. Hydrol.*, **85**(1) (2006), 53–71.
[34] J. F. Kelly and M. M. Meerschaert, Space-time duality for the fractional advection dispersion equation, *Water Resour. Res.*, **53**(4) (2017), 3464–3475.
[35] J. F. Kelly, D. Bolster, M. M. Meerschaert, J. A. Drummond, and A. I. Packman, FracFit: A robust parameter estimation tool for fractional calculus models, *Water Resour. Res.*, **53**(3) (2017), 2559–2567.
[36] F. Liu, V. V. Anh, I. Turner, and P. Zhuang, Time fractional advection-dispersion equation, *J. Appl. Math. Comput.*, **13**(1) (2003), 233–245.

[37] Z. Mao, S. Chen, and J. Shen, Efficient and accurate spectral method using generalized Jacobi functions for solving Riesz fractional differential equations, *Appl. Numer. Math.*, **106** (2016), 165–181.
[38] D. P. McInnis, D. Bolster, and P. A. Maurice, Natural organic matter transport modeling with a continuous time random walk approach, *Environ. Eng. Sci.*, **31**(2) (2014), 98–106.
[39] D. P. McInnis, D. Bolster, and P. A. Maurice, Mobility of dissolved organic matter from the Suwannee River (Georgia, USA) in sand-packed columns, *Environ. Eng. Sci.*, **32**(1) (2015), 4–13.
[40] M. M. Meerschaert and A. Sikorskii, *Stochastic Models for Fractional Calculus, vol. 43*, Walter de Gruyter, Berlin, 2012.
[41] M. M. Meerschaert and P. Straka, Inverse stable subordinators, *Math. Model. Nat. Phenom.*, **8**(2) (2013), 1–16.
[42] M. M. Meerschaert and C. Tadjeran, Finite difference approximations for fractional advection–dispersion flow equations, *J. Comput. Appl. Math.*, **172**(1) (2004), 65–77.
[43] M. M. Meerschaert and C. Tadjeran, Finite difference approximations for two-sided space-fractional partial differential equations, *Appl. Numer. Math.*, **56**(1) (2006), 80–90.
[44] M. M. Meerschaert, D. A. Benson, and B. Baeumer, Multidimensional advection and fractional dispersion, *Phys. Rev. E*, **59**(5) (1999), 5026.
[45] M. M. Meerschaert, D. A. Benson, and B. Baeumer, Operator Lévy motion and multiscaling anomalous diffusion, *Phys. Rev. E*, **63** (2001), 021112–021117.
[46] M. M. Meerschaert, D. A. Benson, H.-P. Scheffler, and B. Baeumer, Stochastic solution of space-time fractional diffusion equations, *Phys. Rev. E*, **65**(4) (2002), 041103.
[47] M. M. Meerschaert, J. Mortensen, and S. W. Wheatcraft, Fractional vector calculus for fractional advection–dispersion, *Phys. A, Stat. Mech. Appl.*, **367** (2006), 181–190.
[48] M. M. Meerschaert, Y. Zhang, and B. Baeumer, Tempered anomalous diffusion in heterogeneous systems, *Geophys. Res. Lett.*, **35**(17) (2008), L17403.
[49] R. M. Neupauer and J. L. Wilson, Adjoint method for obtaining backward-in-time location and travel time probabilities of a conservative groundwater contaminant, *Water Resour. Res.*, **35**(11) (1999), 3389–3398.
[50] J. P. Nolan, Numerical calculation of stable densities and distribution functions, *Commun. Stat., Stoch. Models*, **13**(4) (1997), 759–774.
[51] P. Paradisi, R. Cesari, F. Mainardi, and F. Tampieri, The fractional Fick's law for non-local transport processes, *Phys. A, Stat. Mech. Appl.*, **293**(1) (2001), 130–142.
[52] P. Patie and T. Simon, Intertwining certain fractional derivatives, *Potential Anal.*, **36**(4) (2012), 569–587.
[53] M. S. Phanikumar, I. Aslam, C. Shen, D. T. Long, and T. C. Voice, Separating surface storage from hyporheic retention in natural streams using wavelet decomposition of acoustic Doppler current profiles, *Water Resour. Res.*, **43**(5) (2007), W05406.
[54] I. Podlubny, A. Chechkin, T. Skovranek, Y. Chen, and B. M. V. Jara, Matrix approach to discrete fractional calculus ii: Partial fractional differential equations, *J. Comput. Phys.*, **228**(8) (2009), 3137–3153.
[55] G. Samoradnitsky and M. S. Taqqu, *Stable non-Gaussian Random Processes: Stochastic Models with Infinite Variance, vol. 1*, CRC Press, 1994.
[56] N. M. Schmadel, A. S. Ward, M. J. Kurz, J. H. Fleckenstein, J. P. Zarnetske, D. M. Hannah, T. Blume, M. Vieweg, P. J. Blaen, and C. Schmidt et al., Stream solute tracer timescales changing with discharge and reach length confound process interpretation, *Water Resour. Res.*, **52**(4) (2016), 3227–3245.
[57] R. Schumer, D. A. Benson, M. M. Meerschaert, and S. W. Wheatcraft, Eulerian derivation of the fractional advection–dispersion equation, *J. Contam. Hydrol.*, **48**(1) (2001), 69–88.

[58] R. Schumer, D. A. Benson, M. M. Meerschaert, and B. Baeumer, Fractal mobile/immobile solute transport, *Water Resour. Res.*, **39**(10) (2003), 1296.
[59] R. Schumer, D. A. Benson, M. M. Meerschaert, and B. Baeumer, Multiscaling fractional advection-dispersion equations and their solutions, *Water Resour. Res.*, **39**(1) (2003), 1022–1032.
[60] I. M. Sokolov and J. Klafter, From diffusion to anomalous diffusion: A century after Einstein's Brownian motion, *Chaos*, **15** (2005), 026103.
[61] I. M. Sokolov and R. Metzler, Towards deterministic equations for Lévy walks: The fractional material derivative, *Phys. Rev. E*, **67**(1) (2003), 010101.
[62] L. Wang and M. Cardenas, Non-Fickian transport through two-dimensional rough fractures: Assessment and prediction, *Water Resour. Res.*, **50** (2014), 871–884.
[63] G. Zaslavsky, Fractional kinetic equation for Hamiltonian chaos, *Phys. D, Nonlinear Phenom.*, **76**(1–3) (1994), 110–122.
[64] M. Zayernouri and G. E. Karniadakis, Fractional Sturm–Liouville eigen-problems: theory and numerical approximation, *J. Comput. Phys.*, **252** (2013), 495–517.
[65] X. Zhang, J. W. Crawford, L. K. Deeks, M. I. Stutter, A. G. Bengough, and I. M. Young, A mass balance based numerical method for the fractional advection-dispersion equation: Theory and application, *Water Resour. Res.*, **41**(7) (2005), W07029.
[66] Y. Zhang, D. A. Benson, M. M. Meerschaert, and H.-P. Scheffler, On using random walks to solve the space-fractional advection-dispersion equations, *J. Stat. Phys.*, **123**(1) (2006), 89–110.
[67] Y. Zhang, D. A. Benson, M. M. Meerschaert, and E. M. LaBolle, Space-fractional advection-dispersion equations with variable parameters: Diverse formulas, numerical solutions, and application to the macrodispersion experiment site data, *Water Resour. Res.*, **43**(5) (2007), W05439.
[68] X. Zhang, M. Lv, J. W. Crawford, and I. M. Young, The impact of boundary on the fractional advection–dispersion equation for solute transport in soil: Defining the fractional dispersive flux with the Caputo derivatives, *Adv. Water Resour.*, **30**(5) (2007), 1205–1217.
[69] Y. Zhang, D. A. Benson, and D. M. Reeves, Time and space nonlocalities underlying fractional-derivative models: Distinction and literature review of field applications, *Adv. Water Resour.*, **32**(4) (2009), 561–581.
[70] Y. Zhang, C. T. Green, E. M. LaBolle, R. M. Neupauer, and H. Sun, Bounded fractional diffusion in geological media: Definition and Lagrangian approximation, *Water Resour. Res.*, **52** (2016), 8561–8577.
[71] Y. Zhang, M. M. Meerschaert, and R. M. Neupauer, Backward fractional advection dispersion model for contaminant source prediction, *Water Resour. Res.*, **52**(4) (2016), 2462–2473.
[72] Y. Zhang, H.-G. Sun, R. M. Neupauer, and P. Straka, Identification of pollutant source using backward probability density functions for bounded super-diffusion, *Water Resour. Res.* (2018), 10.1029/2018WR023011.
[73] L. Zhou and H. Selim, Application of the fractional advection-dispersion equation in porous media, *Soil Sci. Soc. Am. J.*, **67**(4) (2003), 1079–1084.

Vladimir V. Uchaikin and Renat T. Sibatov

Anomalous diffusion in interstellar medium

Abstract: Interstellar medium (ISM) consists of few components being in chaotic motion of turbulent kind. They interact with each other, exchange with energy, and some of them emit and absorb electromagnetic radiation and elementary particles. Neutral gas under the influence of gravity is crammed into molecular clouds with magnetic fields, charged particles born in supernova explosions and accelerated on their remnants fly in the magnetic fields and magnetized clouds and scattered on them, continuing their motion around wriggling magnetic lines. How far away this picture is from the slender motion of the planets in our solar system along the Keplerian orbits! On these giant scales, the Newton calm motion laws are replaced by the Kolmogorov stormy turbulence laws, molecular diffusion is replaced by turbulent diffusion, and integer-order differential equations are replaced by the fractional one. Some details of this change of paradigms are discussed in this chapter. In its conclusion, the authors dare to state a hypothesis that the deep reason for the appearance of fractional orders operators instead of the integer ones, is a transition from a closed mechanical system to an open system.

Keywords: Turbulence, cosmic rays, galaxy, molecular cloud, magnetic field

PACS: 02.50.-r, 05.40.-a, 98.70.Sa

1 Introduction

Looking at the cloudless night sky, we distinguish planets, stars, and a person with acute vision can even see clusters of stars—galaxies. We distinguish these objects, seeing them as bright points. This is because the light emitted by them propagates through ISM almost without deviations (without scattering). But it is not the only information source about cosmic objects. Nowadays, most of the information is delivered by other carriers: radio-waves, X-ray, gamma-radiation, and high-energy charged particles (cosmic rays). Like quanta of light (photons), charged particles come from far-localized sources, but if we had ability to see them, a different picture would appear before our eyes: we would see something resembling an uneven fragmented veil of

Acknowledgement: Authors thank the Russian Foundation for Basic Research (projects 16-01-00556, 18-51-53018) and the Ministry of Education and Science of the Russian Federation for financial support.

Vladimir V. Uchaikin, Ulyanovsk State University, Department of Theoretical Physics, Ulyanovsk, Russia, e-mail: vuchaikin@gmail.com
Renat T. Sibatov, Ulyanovsk State University, Laboratory of Diffusion Processes, Ulyanovsk, Russia, e-mail: ren_sib@bk.ru

clouds covering the sky in a rainy day. It is namely such a picture "seen" by devices measuring the fluxes of charged particles of cosmic origin. The reason for the difference between this picture and what the eye sees in the night sky is that the chaotic magnetic fields filling the space between sources and observers do not change the rectilinear character of the light propagation, but strongly distort the trajectories of the charged particles, giving to their motion character of a turbulent process. This motion is of a significantly different kind than the normal (Brownian) diffusion and for this reason is called the *anomalous diffusion*. The form of a diffusion packet and the law of its spreading in anomalous processes are quite different from normal ones. This review is devoted to discussion of *fractional models* of anomalous processes.

Weakly inhomogeneous magnetic fields are often represented by imaginary magnetic lines, around which the trajectories of charged particles are wound. For particles with energy higher than 10^{13} eV, the Larmor radii exceed 10^{15} cm. If the size of a domain significantly more that the rotating particle radius, say, several parsecs, then this domain can be considered as almost homogeneous, leading center in which moves almost uniformly and rectilinearly, like a free particle, and the particle itself expends time $t = r/(c\cos\alpha)$ (α is a pitch-angle) for passing distance r. Otherwise, the leading center changes its motion direction: the particle undergoes scattering on the inhomogeneity of the magnetic field.

In its entirity, the intragalactic magnetic field can be considered as a set of "clouds" randomly distributed in the space. The interstellar medium consists of a few components interacting with each other: (1) the neutral and partially or totally ionized gas (plasmas), (2) dust grains (small solid particles with sizes from the micron down to fraction of nanometers), (3) magnetic fields, permeating the ISM and characterized by average strength in the galactic plane of the order of 1 G, while the amplitude of the fluctuations is of the order of 5 G, (4) cosmic rays, being a high-energy wing of interstellar plasma including along with charged component (electrons, protons, other nuclei) also neutral particles of high energies (photons, neutrons, neutrinos, etc.), (5) the radiation field covering the full electromagnetic spectrum, both irradiated by local sources (supernova explosions, pulsars, quasars, gamma-ray bursts) and remained since the Big Bang time (relict or CMB radiation).

A common property of all ISM components is their high irregularities (fractality) in space, chaotic (turbulent) evolution in time, and close interaction with each other. Undoubtedly, the ISM is an instructive example of a complex system, and it should not be surprising that its mathematical analysis forces to involve such tools as derivatives of fractional orders which are less often applied to less complex systems.

Although other components of ISM reveal also various peculiarities in their diffusion in space, we focus here on the cosmic-ray charged component. As evidenced by one of leading experts in the cosmic ray physics, Pasquale Blasi, this direction needs a substantial update of the mathematical tools [5]: "Observations of diffuse backgrounds of radio and gamma ray emissions require a significant diffusion of CRs perpendicular to the Galactic disc, which reflects in the need to have substantial random walk of magnetic field lines. In all existing models of CR propagation in the Galaxy this very important effect is not taken into account, although some recent calculations have renewed the interest in this line of research." This statement, and the general trend in development of CR-theory have inspired this chapter.

2 Original CR-diffusion models

2.1 Ginzburg–Syrovatsky model

In 1953, Soviet physicist, V. L. Ginzburg wrote: "The motion of charged particles in the interstellar space resembles Brownian motion or motion of molecules in a gas. Indeed, due to the presence of the interstellar magnetic field, in the region where this field is quasihomogeneous, the trajectory of a particle winds around a magnetic field line and, upon averaging over the rotation period, is close to a straight line. However, on passing to a region with a different field direction, the trajectory changes and becomes a broken line as a whole. If the size of regions where the field direction noticeably changes is small compared to that of regions with a quasihomogeneous field, the particle motion can be treated as the motion of a molecule in a gas: the motion is free in the homogeneous field, and a change in the velocity direction at a boundary is similar to a collision with another molecule and can be usually assumed instantaneous. Hence, the size of the region with a quasi-homogeneous field plays the role of the mean free path l.

The mean free time is $\tau = l/v_0$, where v_0 is the translational velocity along the trajectory, which is by an order of magnitude equal to the usual velocity of the particle itself (and we therefore assume below that $\tau \sim l/v$, where v is the particle velocity). If magnetic fields do not change in time, this collision process leads only to the diffusion of particles and the "mixing" of their velocities over directions but not to a change in the energy of the particles. It is known from the diffusion theory that the mean square distance L passed by a particle during time t is $\sqrt{6Dt} \sim \sqrt{lvt}$ where $D \sim lv/3$ stands for the diffusion coefficient. According to astronomical data, in ISM $l > 10^{19}$ cm, so for v close to the light speed c and t close to proton life time $T \sim 10^{16}$ s, we obtain $L \sim 3{\cdot}10^{22}$ cm." ([15], pp. 368–369)[1]. This explained the *first feature* of CR-charged component: prevalence of single-nucleon nuclei (protons). The Fermi assumption on the exponentially distributed age of registered CR-particles in combination with the exponential growth of energy due to collisions with chaotically moving magnetic clouds led to understanding of the *second* important CR-attribute: the *inverse power energy spectrum*. Finally, this model successfully solved the *third mystery* of CR's: their *isotropy*. "The high degree of isotropy of cosmic rays was one of the first indications that cosmic

1 Translated by V. U.

rays fall on Earth not directly from sources but after complicated motion and scattering in interstellar magnetic fields. This motion can be considered as 'diffusion' of cosmic rays in the interstellar space during which particles 'forget' about their initial direction of motion" [16].

Recall, that the elementary 3D-diffusion equation is based on combination of two equations: the balance equation expressing the diffusant conservation law, and the Fick diffusion law. Combining these equalities yields the known *normal diffusion equation*

$$\frac{\partial N(\mathbf{x},t)}{\partial t} = \nabla\big(K\nabla N(\mathbf{x},t)\big),$$

or, if diffusion coefficient K doesn't depend on coordinates,

$$\frac{\partial N(\mathbf{x},t)}{\partial t} = K\Delta N(\mathbf{x},t).$$

Its Green function (called also *propagator*) reads

$$G(\mathbf{x},t) = \frac{1}{(4\pi Kt)^{3/2}} e^{-r^2/(4Kt)}, \quad r = |\mathbf{x}|.$$

In contrast to the strict first law, the second one has initially been introduced as an empirical fact. Later, it was derived together with related explicit expressions for the diffusion coefficient from some theoretical schemes as an approximate consequence. One of such schemes is the ideal gas model, in which particle-particle interactions are considered as instantaneous collisions. Each molecule flies independently of others until the next collision. A special property of this model is that the remainder of the path has the same exponential probability distribution as a whole path. This is interpreted as absence of memory: the molecule does not remember when it had experienced the previous collision (Markovian property). A more detailed description of such process is achieved by using the linear Bolzmann kinetic (LBK) equation for space-angle time-dependent distribution $n(\mathbf{x}, v\boldsymbol{\Omega}, t)$ ($\boldsymbol{\Omega} = \mathbf{v}/v$ is a unite directional vector). This equation begins with the material differential operator $d/dt = \partial/\partial t + \mathbf{v}\cdot\nabla$ and contains a collision integral, describing instantaneous changes of $\boldsymbol{\Omega}$. In the framework of the so-called P_1-approximation [7], its solution is of the form

$$n(\mathbf{x}, v\boldsymbol{\Omega}, t) = \frac{1}{4\pi} vN(\mathbf{x},t) + \frac{3}{4\pi}\boldsymbol{\Omega}\cdot\mathbf{j}(\mathbf{x},t),$$

where $N(\mathbf{x},t) = \int n(\mathbf{x}, v\boldsymbol{\Omega}, t)d\boldsymbol{\Omega}$ is the concentration of particles at point $\mathbf{x}$ at time t, and $\mathbf{j}(\mathbf{x},t) = \mathbf{v}N(\mathbf{x},t)$ is the current density vector. Inserting it into the LBK-equation, we arrive at normal diffusion with $K = \langle R\rangle v/3$, where $\langle R\rangle$ stands for the mean free path. One should stress that this approximation assumes very weak asymmetry of flux and, therefore, cannot be applicable near sharp boundaries and singular sources.

2.2 Brownian versus Boltzmann

Written in the form shown above, the classical diffusion equation conceals some peculiarities of the process, becoming clear in its pure mathematical model known as the *Wiener process*. Let us indicate the main ones.

- There is no ballistic regime between collisions. The particles do not possess an instantaneous velocity (the limit $\Delta\mathbf{x}/\Delta t$ does not exist) and for this reason their displacements are uncorrelated in consecutive time intervals.
- Trajectories of particles are continuous but nowhere differentiable curves. All directions of the further motion of a particle located at a given point are equally possible.
- The Bm trajectories are self-similar with the Hurst exponent $H = 1/2$.
- The length of Bm trajectory between any two points (even being close to each other) is infinite.
- Right away after switching on a point source, the probability to find out the particle becomes nonzero at all distances which contradicts to the relativistic principle of the limited velocity.

From a probabilistic point of view, the above properties occur through postulating independence of increments and self-similarity [36]. Physically, they result from the assumption about the background of the process: it is considered as something like an ideal gas consisting of uniformly and independently distributed over space molecules. However, the real situation is quite different, at least by two reasons: turbulence and magnetic field. Let us show what changes in equations is produced by involving these facts into consideration.

2.3 Compound model

Another, in some sense alternative model of CR-diffusion was set up by other Soviet astrophysicist, Getmantsev [13]. Estimating the influence of interstellar magnetic field on the motion of relativistic particles with $E \ll 10^{17}$ eV, he concluded that their gyroradii are very much less than the characteristic length of nonhomogeneities of the magnetic field, $l_1 \simeq 10^{20} \div 3\cdot 10^{20}$ cm. As a result of this, the motion of most of the cosmic particles is an almost entirely governed by the geometry of the magnetic force lines. One can say, Getmantsev made particles walk in magnetic tubes, instead of chaotic rushing between magnetic clouds from side to side. Getmantsev proposed to consider such a movement as compounded from two diffusion processes (one-dimensional diffusion along the tubes and three-dimensional diffusion on account of the randomly distributed breaks in the tubes). Such a model was used by its author to derive an expression for the probability that a particle passes by a certain distance from a given point in time t, as well as an expression for the mean-square displacement, $\langle R^2\rangle = l_1\sqrt{Dt/\pi}$, where $D = vl_1/2$ is the diffusion coefficient and v stands for velocity of the CR-particles along the force line of the interstellar field. He also assumed that the motion along a given tube of magnetic force lines is not free, but itself is a one-dimensional walk with a mean free path $l_2 \le 3 \cdot 10^{21}$ cm. With $l_1 \simeq 3 \cdot 10^{20}$ cm, $l_2 \simeq 3 \cdot 10^{21}$ cm and $t \simeq 10^{17}$ s, Getmantsev estimated $\sqrt{\langle R^2 \rangle} \simeq 10^{22}$ cm and concluded that in a period of time comparable with the age of the galaxy the particles move away from the galactic plane by an amount which is several times smaller than the radius of the halo, so that the exchange of cosmic rays between the flat subsystem and the halo cannot occur easily.

Let us make an important remark. In the framework of the Brownian motion model, transport of particles takes place in a structureless medium, consisting of independently distributed localized entities (atoms, molecules), but the compound model assumes long-range correlations realized by magnetic force lines. Such a picture resembles behavior of motes in a turbulent flow consisting of interwoven streamlines similar to an interstellar magnetic field, and essentially differs from the motion of the Brownian particle among neutral molecules of the ideal gas. This is the main reason for the mistrust of the normal diffusion model in the problem of the motion of cosmic rays. At a minimum, the constant deterministic diffusion coefficient should be replaced by an appropriate random field, but the need for subsequent averaging over statistical ensemble of the field transforms the diffusion equation into a system of nonlinear equations. Fractional calculus plays the role of some intermediate variant in this case. A deep interpretation of fractional calculus applied to turbulent kinetics can be found by the reader in books [47, 1, 34].

3 Fractional models of turbulent diffusion

3.1 Weizsäcker–Tchen's approach

We begin with consideration of the neutral particle diffusion model applicable, for example, to interstellar gas and turbulent processes in molecular clouds. The interstellar gas cannot remain stable at the average local density of 1 cm^{-3}, its density becomes in the range of 10 to 100 cm^{-3} for the cool phase, and much less, such as 0.1 cm^{-3}, in the warm neutral phase, given the total interstellar pressure. Any random motion inevitably partitions the gas into clouds and an intercloud medium; nowadays the the fractal point of view begins to predominate as recognition that the turbulent decomposition can produce fractal structures with well determined and universal properties.

The molecular clouds dynamics underlies understanding evolution of planets, stars and galaxies. One of the first fundamental works devoted to this problem was written by von Weizsäcker (1951). He considered that the motion of the cosmic gas obeys the equations of hydrodynamics and that in most cases it is turbulent and compressible. In accordance to Kolmogorov's hierarchical principle of turbulence, the ISM forms a hierarchical sequence—superclouds, complexes, molecular clouds (fragments), and cores (protostellar clouds), which may be identified by the variation along the hierarchy of the exponents of power-law scale relations between velocity spread and size, magnetic field and densities, and, in particular, between density ρ_n of a cloud of nth level and its size L_n,

$$\frac{\rho_{n+1}}{\rho_n} = \left(\frac{L_{n+1}}{L_n}\right)^{3c_n}, \tag{1}$$

where the exponent c_n called the degree of compression at the level n must be smaller than unity. Referring to observation data, Tchen estimated a limit value $c_\infty = c$ as lying between 0.09 and 0.23. Numerical simulations of compressible turbulence performed later have confirmed the scaling with $c = 0.15$ close to value 1/6, for which the density power spectrum becomes flat. The interrelations like (1) make the fractal concept to be related to turbulence with the spectral function

$$F(q) \propto q^{-5/3-2c} \tag{2}$$

in the inertial range (q_1, q_2). Later, Tchen [35] split the total tracer concentration into component N, averaged over the turbulent statistical ensemble, and pulsing component N', and excluded the latter from hydrodynamic equation system. Using the Heisenberg–Kolmogorov phenomenology with spectral function (2), he arrived at the equation for the Fourier transform $\tilde{N}(\mathbf{k})$ of the averaged concentration

$$\frac{\partial \tilde{N}(\mathbf{k}, t)}{\partial t} = -R(k)\tilde{N}(\mathbf{k}, t)$$

with inverse relaxation time

$$R(k) \propto k^2 \int_k^\infty \sqrt{F(q)/q^3}\,dq \propto k^{2/3-c}.$$

Returning to natural arguments yields equation

$$\frac{\partial N(\mathbf{x}, t)}{\partial t} = -K_\alpha(-\Delta)^{\alpha/2} N(\mathbf{x}, t)$$

containing fractional Laplacian $-(-\Delta)^{\alpha/2}$ determined by its Fourier image $-|\mathbf{k}|^\alpha$. Under initial condition $N(\mathbf{x}, 0) = \delta(\mathbf{x})$, its solution is expressed via 3D Lévy–Feldheim stable density with the characteristic exponent $\alpha = 2/3 - c$. When $\alpha = 2$, the equation takes the form of a normal diffusion equation.

Let us indicate main noteworthy features of the clouds. They are not, as has sometimes been assumed, isolated "billiard balls" moving about independently in space, but instead are just dense condensations in more a widely distributed, mostly atomic gas. Although molecular clouds may often appear to have sharp boundaries, these boundaries do not represent the edge of the matter distribution but just rapid transitions from the molecular gas to the surrounding atomic gas.

The molecular clouds are transient structures; their short lifetimes are directly indicated by the fact that the range in age of the young stars associated with them is only about 10 to 20 Myr, comparable to the internal dynamical timescales of large molecular clouds [23]. Finally, one should add that the clouds are highly irregular structures and may have very complex shapes.

3.2 Schönfeld's hydrodynamic approach

An alternative derivation of the turbulent diffusion equation was given by Schönfeld [31]. He considered an eddy characterized by a length measure ϱ, engaged at the point (x, y). The eddy produces a velocity w in a direction at an angle χ with the x-axis so the concentration at (x, y) incidentally deviates from the mean value $N(x, y)$. This deviating value was estimated by

$$N(x, y) \mapsto N(x - \varrho\cos\chi, y - \varrho\sin\chi),$$

so the contribution of this eddy into x-component of the diffusion flux was written as

$$\delta j_x = N(x - \varrho\cos\chi, y - \varrho\sin\chi)w\cos\chi.$$

The resulting flux is obtained via averaging the contribution of all possible position of the eddy and let $Wd\varrho/\varrho$ be the probability that the distance falls into the interval $(\varrho, \varrho + d\varrho)$. Assuming that all directions χ are equiprobable and that

$$\omega \equiv Ww$$

depends on ρ only, one obtains:

$$j_x = \frac{1}{2\pi}\int_0^\infty \frac{d\varrho}{\varrho}\omega(\varrho)N(x - \varrho\cos\chi, y - \varrho\sin\chi)\cos\chi.$$

Fourier transforming with respect to both spatial coordinates yields

$$\widetilde{j}_x = ik_x\widetilde{K}(k)\widetilde{N}(k_x, k_y),$$

and analogously

$$\widetilde{j}_y = ik_y\widetilde{K}(k)\widetilde{N}(k_x, k_y),$$

where k_x and k_y are projections of the wave vector $\mathbf{k}$,

$$\widetilde{K}(k) = \frac{1}{k}\int_0^\infty \frac{d\varrho}{\varrho}\omega(\varrho)J_1(\varrho k)$$

and $k = |\mathbf{k}| = \sqrt{k_x^2 + k_y^2}$. Substitution of these functions into the Fourier image of the continuity equation,

$$\frac{\partial \widetilde{N}}{\partial t} = ik_x\bar{j}_x + ik_y\bar{j}_y,$$

yields

$$\frac{\partial \widetilde{N}}{\partial t} + k^2\widetilde{K}(k)\widetilde{N}(\mathbf{k}, t) = 0. \tag{3}$$

This is the Fourier image of the turbulent diffusion equation.

Thus, in the case of molecular diffusion in a dilute gas, a tracer interacts with almost independent molecules per collisions and this fact makes the diffusion equation local, but in the case of turbulent diffusion the motion of neighboring fluid elements is correlated, and the tracers motion continuously affected by the elements is described by the nonlocal equation

$$\frac{\partial N(\mathbf{x}, t)}{\partial t} = \Delta \int d\mathbf{x}' K(\mathbf{x} - \mathbf{x}')N(\mathbf{x}', t). \tag{4}$$

3.3 Monin's hypothesis approach

The specificity of the turbulent diffusion of a particle arises because of the action on it of vortices of different sizes existing in a turbulent medium. The distance between two trial particles can significantly change during short time only under the action of a vortex whose size is comparable with this distance. This is the case in a turbulent medium that is filled with vortices of various sizes. The further apart these particles, the greater the size of the vortices that carry them from one another, and the more rapidly the relative distance l grows. In the framework of the classical diffusion theory, such an effect can be achieved by introducing the l-dependence of the diffusion coefficient: $D = D(l)$. This approach was used by Richardson, who wrote for the distribution density $p(l, t)$ of a random distances between a pair of impurity particles in the form

$$\frac{\partial p}{\partial t} = \frac{\partial}{\partial l}\left[D(l)\frac{\partial p}{\partial l}\right]$$

with the diffusivity $D(l) \propto l^{4/3}$, corresponding to observed law of the diffusion packet width growth $\Delta(t) \propto t^{3/2}$ instead of normal law $\Delta(t) \propto t^{1/2}$. The Richardson *4/3 law* was theoretically justified by Kolmogorov and Obukhov on the basis of the hypothesis on self-similarity of a local isotropic turbulence determined by only dimensional parameter ε (the rate of turbulent energy dissipation per unit of mass). Qualitatively, these results were consistent with experimental data, but the fact that the diffusion coefficient should depend on the spatial variable, created certain problems not only in the process of solving the equation, but also in the physical interpretation of the results obtained. The way to combine the accelerated character of the thermodynamic diffusion with the constancy of the coefficient characterizing the medium was found by A. S. Monin [25], who initiated the use of non-Gaussian stable distributions and equations with derivatives of fractional order in the turbulent diffusion theory (though did not use this terminology).

Considering the diffusion of a cloud of impurity particles in a coordinate system connected to the center of the cloud, Monin expressed the concentration distribution $f(\mathbf{x}, t)$ at time t through the initial distribution $f(\mathbf{x}, 0)$ by means of a time-dependent linear operator $\mathsf{A}(t)$,

$$f(\mathbf{x}, t) = \mathsf{A}(t) f(\mathbf{x}, 0), \quad t > 0.$$

In case of a stationary homogeneous and locally isotropic medium, the operator A^t is invariant with respect to shifts and rotations and depends on the only material parameter ε. After Fourier transformation, operator $\mathsf{A}(t)$ becomes the function $a(k, t, \varepsilon)$ of absolute value $k \equiv |\mathbf{k}|$ of wave-vector $\mathbf{k}$. Coordinating with the dimensionality principle, Monin represents it as a function of argument $\varepsilon^{1/3} k^{2/3} t$, so that

$$\tilde{f}(\mathbf{k}, t) = a(\varepsilon^{1/3} k^{2/3} t) \tilde{f}(\mathbf{k}, 0).$$

The Monin hypothesis, as Monin and Yaglom write in the second volume of their Statistical Hydromechanics [26], assumes that operators $\mathsf{A}(t)$ form a semigroup,

$$\mathsf{A}(t_1)\mathsf{A}(t_2) = \mathsf{A}(t_1 + t_2),$$

and consequently

$$a(\varepsilon^{1/3} k^{2/3} t_1) a(\varepsilon^{1/3} k^{2/3} t_2) = a(\varepsilon^{1/3} k^{2/3} (t_1 + t_2)).$$

In probabilistic terms, this is the Markovian property of the process. The solution to this equation is

$$a(\varepsilon^{1/3} k^{2/3} t) = \exp\{-c \varepsilon^{1/3} k^{2/3} t\},$$

and Fourier image of the sought-for concentration

$$\tilde{f}(\mathbf{k}, t) = \exp\{-c \varepsilon^{1/3} k^{2/3} t\} \tilde{f}(\mathbf{k}, 0)$$

obeys the differential equation

$$\frac{d\tilde{f}(\mathbf{k}, t)}{dt} = -c \varepsilon^{1/3} k^{2/3} \tilde{f}(\mathbf{k}, t)$$

with corresponding initial condition $\tilde{f}(\mathbf{k}, +0) = 1$. Factor $k^{2/3}$ in right-hand side of this equation just represents the Laplace operator in power 1/3; so, finally we have

$$\frac{\partial f(\mathbf{x}, t)}{\partial t} = -K(-\Delta)^{1/3} f(\mathbf{x}, t), \quad K = c\varepsilon^{1/3}.$$

4 Interstellar magnetic fields

4.1 Magnetic fields in numerical calculations

The GS model of charged particles possesses a significant imperfection. It ignores spatial structure of the interstellar magnetic field (ISMF). This is a provocative fact, because ISMF is closely connected to highly turbulent other components of ISM, and has in contrast to a classical hydro and aerodynamical media a complicated inner structure (lines, clouds, voids, traps, etc.) Thus, building an appropriate model for the magnetic field in the domain under consideration becomes essential and not a simple prelude to the CR's propagation calculations. As an example of such approach, the work [32] can be referred to. Modern simulations of the ISM have numerical resolution of order 1 pc, so the Larmor radius of CR's particles that dominate in energy density, is at least 10^6 times smaller than the resolved scales. For this reason, large-scale simulations, in the opinion of Snodin et al., rely on oversimplified forms of the diffusion tensor. They obtained explicit expressions for the CR's diffusion tensor for $R_L/l_c \ll 1$, where l_c is the magnetic correlation length. The diffusion coefficients, the authors note in the article, are closely connected with existing transport theories that include the random walk of magnetic lines and may be used in a subgrid model of cosmic ray diffusion. Authors of the work referred to the above-tested two models in their calculations. One of them is based on the simulation of a spatially homogeneous and an isotropic random component via its harmonic representation

$$\mathbf{b}(\mathbf{x}) = \sum_{n=1}^{N} [\mathbf{C}_n \cos(\mathbf{k}_n \cdot \mathbf{x}) + \mathbf{D}_n \sin(\mathbf{k}_n \cdot \mathbf{x})],$$

where $\mathbf{k}_n$ are randomly oriented wave vectors, and $\mathbf{C}_n$ and $\mathbf{D}_n$ are random vectors satisfying the condition $\nabla \cdot \mathbf{b} = 0$. The first model represents the magnetic field as a sum of a finite number of plane-wave modes with random polarizations, wave vectors, and phases. It can be shown (e. g., [4]) that the resulting field is spatially homogeneous and isotropic in the limit of an infinite number of modes. Giacalone and Jokipii [14] implemented this idea which has subsequently been used in many studies involving test particle simulations. Snodin et al. have used a special algorithm in order that the simulated magnetic field obeys the isotropic power spectrum $F(q) \propto q^{-s}$ with a given index s.

For simulated magnetic field, the authors solved the system of the charged particle motion equations

$$\frac{d\mathbf{x}}{dt} = \mathbf{v}, \quad \frac{d\mathbf{v}}{dt} = \frac{q}{mc\sqrt{1-(v/c)^2}}[\mathbf{v}, \mathbf{B}]$$

and found the parallel diffusivity as a function of time in the form:

$$K_\parallel = \frac{1}{2}\frac{d}{dt}\langle(\Delta x)^2\rangle = \langle v_x(t)\Delta x\rangle.$$

Here, Δx is the tracer displacement in the x-direction over some time t and $v_x(t)$ is the x-component of the tracer velocity at the end of the displacement.

One can note that due to scaling property, time-dependent diffusivity can be transformed into space-dependent one, leading how it will be shown in the next section, to fractional Laplacian.

The problem of the cosmic rays propagation in not reduced, however, to an increase in the accuracy of calculations. In fact, the uncertainties of the magnetic field changing in space-time and other components of the interstellar medium are oriented toward constructing qualitative models of the process with the exception of some particular cases when specific objects are being studied. This, in particular, explains wide development of approximate models that are derived not from the first principles of electrodynamics or magnetohydrodynamics, as we see in the analysis of processes observed in the plasmas laboratory, but from a general picture seen by astrophysicists owning information about various aspects of the process. This picture is formed initially as a complex process of interaction of cosmic rays with a turbulent magnetic. As an instructive example of such approach, one of the first articles published can be E. Fermi in connection with discussion of the cosmic rays origin problem.

4.2 Fermi's magnetic clouds

E. Fermi wrote that according to observations the interstellar space of the galaxy is not uniformly occupied by matter but there are domains where the density may be as much as ten or a hundred times as large than average and such domains (clouds) extend to dimensions of the order of 10 parsec. (1 parsec = 3.1×10^{18} cm = 3.3 light years). Referring to the measurements on the Doppler effect of interstellar absorption lines, he estimated the radial velocity with respect to the Sun of a sample of such clouds located at not too great distance from us, and found about 15 km/s, assuming that the root-mean-square velocity is obtained by multiplying this figure by the square root of 3, and is therefore about 26 km/s. Fermi arrives at a conclusion that such relatively dense clouds occupy approximately 5 % of the interstellar space. This estimation was in agreement with that given by Strömgren [33]. Here is a quotation from this article.

"We conclude that a relatively reliable upper limit to the density of the interstellar gas between the clouds can be derived, 0.1. The possibility cannot be entirely ruled out, however, that the hydrogen density between the clouds is considerably higher, while the sodium density here is extremely low (sodium being much more strongly concentrated in clouds than hydrogen is). With a view to this possibility, it would appear desirable to attempt a determination of the hydrogen density between the clouds with the help of observations of the interstellar hydrogen emission lines... We may thus conclude that sodium is quite strongly concentrated in the clouds—in fact, so strongly that the total mass of sodium present in the clouds (a = 0.05) is probably considerably larger than the total mass of sodium between the clouds." Observe, that referring to the Strömgren work devoted to gas clouds when dealing with magnetic clouds, Fermi implicitly assumed strong correlation between them. Below, we will also do it.

Improvement of observing technology with increasing sensitivity and resolving power allowed to get more information on the molecular, magnetic, and gas-dust clouds structure and properties. Clouds with mass $M \simeq 10^4 M_\odot$ and size R of tens of parsecs as well as complexes of them, with mass $M \simeq 10^5 \div 10^6 M_\odot$ and $R - 30 \div 300$ pc are observed in lines of the CO molecule and its isotopes.

Dudorov [11] introduced a key concept to understanding interstellar magnetic clouds statistics, their hierarchy. He showed that in cloud structures there exist hierarchical levels that differ not only with respect to mass, shape, size, and density, but also with respect to the dynamical influence of the magnetic field, rotation, and the type of turbulence and the mechanisms of its maintenance. Referring to astronomical measurements, Dudorov concludes also that at large scales of superclouds and cloud complexes, electromagnetic forces and turbulent and external pressure are dominant, the magnetic energy of superclouds and complexes of molecular clouds is estimated to be comparable to the gravitational energy. "Such a magnetic field, Dudorov writes, can support clouds both perpendicular to magnetic lines and along them, owing to the generation of MHD turbulence." It is assumed that

$$\sigma^2 = v_A^2 = B^2/4\pi\rho,$$

where v_A is the Alfvén velocity, B is the magnetic field, and ρ is the density. The scale correlations,

$$\sigma \propto R^{1/2} \propto M^{1/4}, \quad n \propto R^{-1},$$

where n is the number density, are a noteworthy property of the hierarchical structures."

Conclusion about the nature of the turbulence of magnetic clouds is drawn from the value of the exponent q_σ in the scale relation $\sigma \propto R^{q_\sigma}$, $0.3 \le q_\sigma \le 0.7$ ($q_\sigma = 1/3$ relates to Kolmogorov turbulence, $q_\sigma = 0.25$ characterizes MHD wave turbulence).

Bruce G. Elmegreen [12], refers to observations of a cloud structure, which supported the conclusion that it is fractal in nature, with a fractal dimension characteristic of turbulence, as found in the laboratory. Such structure has an open texture, with a volume filling factor of nearly 90 % for gas that is at low density. Turbulence makes such cavities by clearing away material during convective motions. The author proposes that most of the low-density intercloud medium is the result of turbulence and not overlapping supernova remnants. Elmegreen writes in the Abstract to the article cited, "Fractal clouds have a gradually decreasing average density with increasing distance... and are also highly clustered, making the mean free path for ionizing photons at least twice as large as in the 'standard cloud' model."

Referring to observation and simulation data, he collected in this work very useful information about interstellar clouds and expressed it in terms of fractal dimension

D: a distribution function for structures of size, a mass size relation ($M \propto S^D$), a mass distribution function for clouds ($n(M)d\log M \propto M^{-1}d\log M$), a density mass relation ($\rho \propto M/S^3 \propto M^{1-3/D}$), a distribution function for density ($n(\rho)d\rho \propto \rho^{(3-2D)/(D-3)}d\rho$), and so on.

In the paper [2], the two-dimensional numerical simulation of clouds in a square region of 1 kpc on a side in the Galactic plane (at roughly the solar circle) is described. The simulation gives the time evolution over 1.3×10^8 yr for all relevant physical quantities including the density, velocity, temperature, and magnetic field. Figures shown in Figure 2 represent clouds as a connected set of points whose densities are larger than an arbitrary threshold ρ_{T}.

The magnetic field inside clouds correlates with the mass density, and this correlation is usually expressed in the form of interrelation $|\mathbf{B}| \propto \rho^{\kappa}$ [9]. Since the ambipolar diffusion timescale is much shorter in a core than in an envelope, the core will become supercritical and collapse while the envelope remains subcritical and supported by the field. Hence, $|\mathbf{B}|$ in cloud envelopes remains virtually unchanged, so at lower densities no strong correlation between $|\mathbf{B}|$ and density ρ is predicted, and $\kappa \sim 0$.

The intercloud medium is presumably the low density part of the interstellar fractal. Another way of seeing why there must be a low density part to the ISM in a turbulent model is by considering the density of thermally stable gas in the local radiation field. This density is in the range of 10 to 100 cm^{-3} for the cool phase, and much less, such as 0.1 cm^{-3}, in the warm neutral phase, given the total interstellar pressure.

All of this is only a small part of the information about the interstellar magnetic fields, accumulated in processes of astronomical observations and mathematical simulations, and these results are used in Section 5.2.

4.3 Magnetic traps

Another kind of local nonhomogeneity is termed *magnetic traps*, regions confining charged particles for a long time [10]. The trap in the Earth's environment formed by the near-dipolar magnetic field exhibits a high degree of stability and considerable lifetime of particles in the trap. The traps in vicinities of chromospheric flares or in solar corpuscular streams of magnetized plasma are much more transparent for particles. The mode of particle ejection from such traps resembles the diffusion in irregular magnetic fields.

Traps of various kinds are also formed in the vicinities of normal stars, in particular, in the solar system and supernova shells. On the other hand, the Galaxy (the galactic disc and halo) also forms a peculiar trap of dimensions of many thousand of parsecs which can safely (with $\sim 10^7$ years life time) retain the particles of moderate and high energies and is very transparent for the super-high energy particles. It is quite possible that the clusters of galaxies form even more enormous traps of the super-high energy particles.

What formation in the space should be considered as a magnetic trap? Perhaps they are the formation with regular magnetic fields of peculiar configuration where the charged particle lifetime is very great and the accumulation effect is significant, or should the term be much extended? It seems to be expedient from the viewpoint of the study of the general regularities of the temporal variations of CR intensity to consider the CR traps as any magnetic formations in which the motion and time of residence of charged particles is substantially different from those in the free space of the same volume (it should be emphasized that the properties of the traps are essentially dependent on particle energy and that the same magnetic formation may be an excellent trap for particles with energies lower than some critical energy and, at the same time, may be practically transparent for particles of higher energies). The CR intensity inside a trap is determined by the powers of both internal and external source of particles, the absorption, nuclear conversions, loss owed interactions with magnetic fields (the latter is of importance to electrons) inside a trap, and the extent of the exchange with the outer space particles. The temporal variations of the above said factors will in their turn result in the temporal variations of the trapped radiation. Such an approach will permit the diverse types of CR to be uniquely considered and understood. The cosmic traps are characterized, first of all, by the structure of the magnetic fields that determine the charged particle's motion, the exchange with the outer space (ejection from a trap and the possibility of being trapped) and, to a great extent, by the particle absorption inside a trap. An extremely important characteristic of the traps is their dynamism; the traps can be static, moving, expanding, compressed, and besides that, can exhibit their internal dynamics." ([10], pp. 57–58).

5 Cosmic rays between clouds

5.1 Magnetic field lines

In a regular magnetic field topology between clouds, the transport of charged particles across the field is due to the collisions of the particles and their finite Larmor radii. However, a perturbation of the magnetic field results in a wandering of the field lines and a potentially much faster transport of the particles. This transport is widely attributed to the effect of the large-scale random field component, which would produce, following the quasilinear theory, a diffusion of the field lines across the direction of the average field [20, 21].

By considering the motion of cosmic-ray particles in regions of limited sizes where fluctuations of the direction and strength of the interstellar magnetic field are rela-

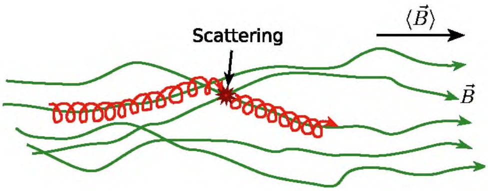

Figure 1: Transition between magnetic field lines due to scattering.

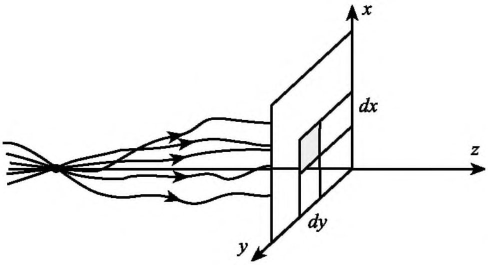

Figure 2: Ensemble of magnetic field line realizations.

tively small, it is convenient to imagine magnetic field lines on which the trajectories of charged particles are wound. The leading centers of particles move along these lines, slowing down their motion in front of "plugs," reflect from them, and return. In this case, the field lines do not remain motionless: they are displaced and bent, carrying the nearby charged particles with them, and the distances between line condensations and switchings change, complicating the motion of particles along field lines randomly walking in space and time (Figure 1) [18]. Following a set of such lines passing through the vicinity of point O in Figure 2, we see how they begin to diverge from each other, demonstrating a statistical ensemble, which has been described in many papers.

First, the model of this kind is called the *compound* or *splitting* model and was proposed in [13], with the ensemble of magnetic field lines represented as a family of independent three-dimensional trajectories consisting of successive independent segments with random lengths and random directions along which particles perform one-dimensional diffusive random walks. Such a combination caused the slowing down of CR diffusion in transverse directions to the law $\langle R^2(t)\rangle \propto \sqrt{t}$. A more strict and detailed justification of the compound model was performed in [8] in terms of fractional integrodifferential equation (see discussion in [38]). Recently, fractional Brownian motion was used for simulation of walking magnetic lines, because such trajectories seem to be more proper because they are smoother than simple Brownian ones.

The high energy charge particles are "magnetized" in the sense that their Larmor radius is much smaller than the mean free path between "collisions" implied by the diffusion coefficient. This means that particles diffuse primarily along the magnetic field, and only very slowly across it [20, 19].

In 1993, Chuvilgin and Ptuskin [8] have split of the quasihomogeneous magnetic field **B** into two components: a homogeneous mean field $\mathbf{B}_0$ and relatively small nonhomogeneous random term $\mathbf{b}$. The results were formulated in terms of the cosmic ray diffusion tensor

$$K_{ij} = K_\perp \delta_{ij} + (K_\parallel - K_\perp)\mathrm{B}_i\mathrm{B}_j,$$

where $\mathbf{B} = \mathbf{B}_0/B_0$, and $K_\parallel$ and $K_\perp$ are the CR-diffusivities along and across the mean magnetic field correspondingly. Such a splitting opens the way to be convenient for obtaining an analytical description of CR-transport in the framework of the linear (first) approximation of the perturbation theory and applicable to quasismooth domains of ISM or to interpretation of phenomena observed in laboratory plasma. Chuvilgin and Ptuskin obtained a closed equation for the averaged perpendicular component, and later this equation was rearranged by Webb et al. [45] to the form

$$D_t^{1/2} N_\perp = K_\perp \Delta_\perp N_\perp(\mathbf{x}_\perp, t) + N_\perp(\mathbf{x}_\perp, 0)\delta_{1/2}(t),$$

being in agreement with the Getmantsev estimation $\langle \mathbf{x}_\perp^2(t)\rangle \propto \sqrt{t}$ for the width.

However, it is worth to keep in mind that the accuracy of the first PT approximation is not high and the corresponding additions, as practice shows, are unworthy of confidence if their value exceeds 10 %.

5.2 Fractional Brownian lines

Consideration of three types of stochastic processes linked with Brownian motion: standard Bm $B^{(0)}(t) = D_t^0 B(t)$, integrated Bm $B^{(-1)}(t) = D_t^{-1}B(t)$, and differentiated Bm $B^{(1)}(t) = D_t^1 B(t)$, provoke us to introduce a generalized kind of *fractional Brownian motion (fBm)* $B^{(\nu)}(t) = D_t^\nu B(t)$ as a tool for simulation of magnetic force lines with a governed degree of smoothness. Similar to Bm, the fBm is a self-similar Gaussian process, characterized with the Hurst exponent

$$H = 1/2 - \nu,$$

using in its designation

$$B_H(t) \equiv \frac{1}{\Gamma(H + 1/2)} \int_0^t (t - t')^{H-1/2} dB(t'), \quad t > 0. \tag{5}$$

Though the process is self-similar, its increments are stationary only when $H = 1/2$ when it becomes the ordinary Bm:

$$B_{1/2}(t) = \int_0^t dB(t') = B(t).$$

Mandelbrot and van Ness [24] developed the widely accepted nowadays version of fBm using a modified fractional integral of Weyl type,

$$B_H(t) = \frac{1}{\Gamma(H+1/2)} \int_{-\infty}^{\infty} [(t-t')_+^{H-1/2} - (-t')_+^{H-1/2}]dB(t'), \quad -\infty < t < \infty.$$

By definition, the Hurst exponent H is a self-similarity index which should be positive. From the other side, if $H < 1$, the fBm is the only self-similar Gaussian process with stationary increments [30]. For these reasons, the Hurst exponent values are bounded by the region $0 < H \le 1$ and the fBm can be defined as a H-self-similar Gaussian process $\{X(t)\}$ with $\langle X(t)\rangle = 0$, $0 < H \le 1$ and stationary increments. When $H = 1/2$, fBm becomes the ordinary Bm: $\{B_{1/2}(t)\} = \{B(t)\}$. The case $1/2 < H < 1$ relates to *persistent* or *fractional superdiffusion* (enhanced diffusion), the process with $H < 1/2$ describes *antipersistent* or *fractional subdiffusion*. Note that all these processes are characterized by Gaussian one-dimensional distribution,

$$p(x,t) = \frac{1}{2\sqrt{\pi}\sigma t^H} \exp\left\{-\frac{x^2}{4\sigma^2 t^{2H}}\right\}, \quad t > 0.$$

obeying normal diffusion equation with time-dependent diffusivity $\sigma^2 t^{2H}$, whereas the fBm trajectories themselves satisfy the fractional differential equation.

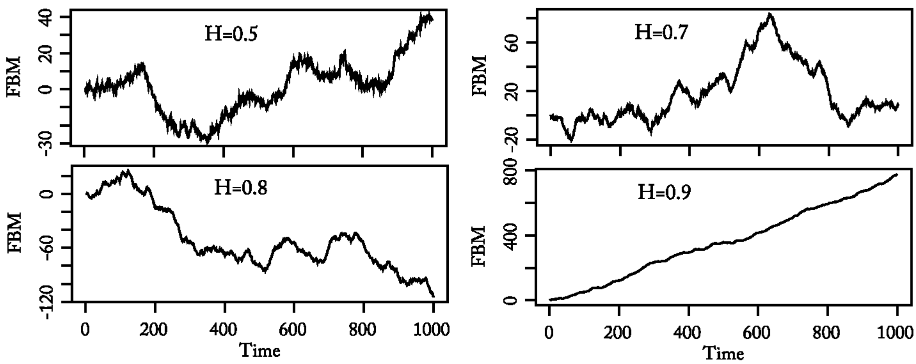

Figure 3: Trajectories of fBm for several values of H.

Figure 3 demonstrate peculiarities of the random lines as samples of fBm with different exponents. Observe, that the compound model as well as its fractional generalization can be interpreted as a *walk on walks*. Considering the Brownian walks as a way of randomization of the diffusion equation, one can term the compound model, by analogy with the quantum mechanics, the *secondary randomization*.

5.3 Electron propagation

In article [27], the bifractional equation was used for calculation of CR electrons propagation. The electrons moving with acceleration in magnetic fields, emit the synchrotron radiation which can be registered in X-ray astronomical observation at large distances. The magnetic domains, capturing CR-electrons and making them to perform a motion in a bounded region, are called magnetic traps. We discussed them in Section 4.3. Assumption that random trapping time is distributed according inverse power law with exponent $\beta \in (0, 1)$ involves into the equation the term with fractional time-derivative of order β, transforming the equation for propagator $G(\mathbf{x}, t)$ with a fractional Laplacian into a bifractional equation, whose Fourier–Laplace image,

$$G(\mathbf{x}, t) \mapsto \tilde{G}(\mathbf{k}, \lambda) = \int_0^\infty dt\, e^{-\lambda t} \int d\mathbf{x}\, e^{i\mathbf{kx}} G(\mathbf{x}, t),$$

obeys the algebraic equation

$$[b\lambda^\beta + a|\mathbf{k}|^\alpha]\tilde{G}(\mathbf{k}, \lambda) = b\lambda^{\beta-1}. \tag{6}$$

For more adequate understanding, we interpret it as asymptotical (as $\lambda \to 0$, and $|\mathbf{k}| \to 0$) form:

$$[1 - (1 - b\lambda^\beta)(1 - a|\mathbf{k}|^\alpha)]\tilde{G}(\mathbf{k}, \lambda) = \frac{1 - (1 - b\lambda^\beta)}{\lambda}. \tag{7}$$

The terms $1 - b\lambda^\beta$ and $1 - a|\mathbf{k}|^\alpha$ can be considered as main asymptotical terms in integral transforms of some time and space probability densities $q(t)$ and $p(\mathbf{x})$

$$\tilde{q}(\lambda) = \int_0^\infty e^{-\lambda t} q(t) dt \sim 1 - b\lambda^\beta, \quad \lambda \to 0 \tag{8}$$

and

$$\tilde{p}(\mathbf{k}) = \int_{\mathrm{R}^d} e^{-i\mathbf{kx}} p(\mathbf{x}) d\mathbf{x} \sim 1 - a|\mathbf{k}|^\alpha, \quad |\mathbf{k}| \to 0. \tag{9}$$

Thus, equation (7) can be considered as the asymptotical representation of some “exact” equation

$$[1 - \tilde{q}(\lambda)\tilde{p}(\mathbf{k})]\tilde{G}(\mathbf{k}, \lambda) = \frac{1 - \tilde{q}(\lambda)}{\lambda}, \tag{10}$$

looking in time-space variables as

$$G(\mathbf{x}, t) = \int_0^t \int d\mathbf{x}' q(t') p(\mathbf{x}') p(\mathbf{x} - \mathbf{x}', t - t') + \delta(\mathbf{x}) \bar{Q}(t), \tag{11}$$

where

$$\bar{Q}(t) = \mathsf{P}(T > t) = \int_t^\infty q(t')dt'$$

(the bar-sign distinguishes the complement distribution function from the ordinary cumulative distribution function $Q(t) = \mathsf{P}(T < t)$).

Equation (11) being a prelimit image of the bifractional differential equation

$$\frac{\partial G(\mathbf{x}, t)}{\partial t} = -K_{\alpha,\beta}\, {}_0D_t^{1-\beta}(-\Delta)^{\alpha/2} G(\mathbf{x}, t) \tag{12}$$

describes the following jump process. A particle placed at origin $\mathbf{x} = 0$ at time $t = 0$, stays there during a random time T distributed with probability density $q(t)$. At the moment T, it performs a jump on a random vector $\mathbf{x}$ distributed with 3-dimensional density $p(\mathbf{x})$ and stays in this new position at random time T' with the same distribution as T. Then the particle repeats such jumps again and again until the observation time t and solution of equation (11) gives pdf for random position of the walking particle at observation time t.

Processes with random instantaneous jumps between which the particle is immobile during random waiting time are known as CTRW (*Continuous Time Random Walk*) processes. For the sake of convenience, we will use for subfamily of this family satisfying conditions (8)–(9) abbreviation CTLF (*Continuous Time Lévy Flights*). Similar to the use of difference approximations for numerical solving of integer-order differential equations, the CTLF-approximation is a power tool for solving fractional-order differential equations. In addition, the CTRF-model has the clear probabilistic sense and for this reason it often occurs more close to the real process under numerical investigation, for which the fractional equation itself serves as asymptotical long-time and long-scale approximation. Nevertheless, the fractional calculus is a very effective tool for analytical investigation of non-Markovian processes running in nonhomogeneous (i. e., porous, turbulent, fractal) media.

Note also, that exponent β cannot be more 1, see the discussion of this question in [38], though the authors range the admitted domain as $0 < \beta \leq 2$. Incorrectness becomes obvious if one looks at formula (15) of this article. In our notation, it has the form

$$q(t) = \frac{1}{\tau_D} \frac{\beta}{\Gamma(1-\beta)} \left(\frac{t}{\tau_D}\right)^{-1-\beta}, \quad t \to \infty,$$

and cannot be a probability density due to the divergence of the integral for $\beta > 1$.

5.4 Proton propagation

Protons and heavier particles (nuclei) experience lesser accelerations and weaker effects of magnetic traps. Their motion in ISM filled in a fractal manner with scatterers

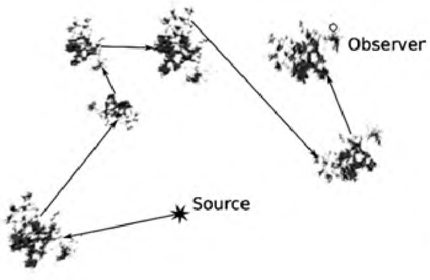

Figure 4: Walking particle trajectory scattering on magnetic clouds whose random positions are chosen by means of the Lévy–Mandelbrot algorithm.

(molecular clouds with their magnetic fields) is described by an equation of the evolutionary type (with the first time derivative):

$$\frac{\partial G}{\partial t} = -D_\alpha(-\Delta)^{\alpha/2}G(\mathbf{x}, t). \tag{13}$$

Recall that equation (13) was derived as a long-time asymptotic equation for CTRJ-process [44, 48].[2] In 1999, V. Uchaikin and A. Lagutin involved the equation into cosmic-ray propagation problem. A. Lagutin drew attention to the fact that the power asymptotics of this "anomalous" propagator can, at least qualitatively, reproduce the knee in the energy spectrum if to assume the power law dependence of the anomalous diffusion coefficient on energy. In the first joint work [22], V. Uchaikin gave a less formal derivation of this equation performed in natural (space-time) variables. It was obtained from integrodifferential equation

$$\frac{\partial f_\epsilon}{\partial t} = \sigma \int [f_\epsilon(\mathbf{x}', t) - f_\epsilon(\mathbf{x}, t)] W\left(\frac{\mathbf{x} - \mathbf{x}'}{\epsilon}\right)\frac{d\mathbf{x}'}{\epsilon^3} + S_\epsilon(\mathbf{x}, t),$$

where ϵ is an auxiliary parameter, and S stands for the source term. The equation describes the process of independent instantaneous jumps (see Figure 4) separated by random time intervals and distributed in accordance with the exponential law with the mean $1/\sigma$. The kernel W of the integral operator plays the role of the distribution density of the displacement vector in such a jump, and should therefore be integrable. For the equation represented in the second form, requirements imposed on the kernel W are relaxed, because the factor given by the difference of the solution values at nearby points serves as a regulator, and the integral can converge even if the kernel diverges. Assuming that the asymptotic form of the kernel for large ranges ("Lévy flights") is described by a power-law function, as is typical for fractal structures,

$$W(\mathbf{x}) \sim Ar^{-3-\alpha}, \quad r \to \infty,$$

2 A one-dimensional version of this equation was derived and involved. It was solved two years earlier in [29].

and introducing the notation $A' = A\sigma$, $t = \epsilon^\alpha s$, and $G(\mathbf{x}, t) = \lim_{\epsilon\to 0} f_\epsilon(\mathbf{x}, t\epsilon^{-\alpha})$, we obtain the equation for the three-dimensional isotropic Lévy motion:

$$\frac{\partial G(\mathbf{x}, t)}{\partial t} = A' \int \frac{G(\mathbf{x}', t) - G(\mathbf{x}, t)}{|\mathbf{x}' - \mathbf{x}|^{3+\alpha}} d\mathbf{x}', \quad 0 < \alpha < 1.$$

The range of α indicated here is determined by the convergence condition for the integral at $\mathbf{x}' \sim \mathbf{x}$. We assume that $G(\mathbf{x}, t)$ is a differentiable function of the coordinates and therefore, as $|\mathbf{x} - \mathbf{x}'| \to 0$, we have

$$|G(\mathbf{x}', t) - G(\mathbf{x}, t)| \propto |\mathbf{x}' - \mathbf{x}|$$

and the integral converges for $\alpha < 1$. This integral operator can be continued to the domain of larger α by several methods [38]. The regularization by calculating the finite (Hadamard's) part of the integral brings it to the form

$$J = \int \frac{[G(\mathbf{x}', t) - G(\mathbf{x}, t)]_2}{|\mathbf{x}' - \mathbf{x}|^{3+\alpha}} d\mathbf{x}', \quad 1 < \alpha < 2,$$

where $[\cdots]_2$ denotes a second-order difference.

In all of these cases, the equation for the Fourier transform with respect to spatial variables,

$$\frac{\partial \widetilde{G}(\mathbf{k}, t)}{\partial t} = -A_\alpha |\mathbf{k}|^\alpha \widetilde{G}(\mathbf{k}, t)$$

contains a term proportional to the fractional power α of the wave vector $|\mathbf{k}|$. Because $-|\mathbf{k}|^2$ is the Laplace operator transform, this term can be represented as

$$|\mathbf{k}|^\alpha \widetilde{G}(\mathbf{k}, t) \equiv \left(|\mathbf{k}|^2\right)^{\alpha/2} \widetilde{G}(\mathbf{k}, t) \Leftrightarrow (-\Delta)^{\alpha/2} G(\mathbf{x}, t),$$

and the equation is then written in the form (13).

From the physical standpoint, the fractional Laplacian can be regarded as the result of some averaging of the diffusion operator with a random diffusion coefficient $\tilde{D}$:

$$\left\langle \nabla(\tilde{D} \nabla G(\mathbf{x}, t)) \right\rangle \mapsto -K_\alpha (-\Delta)^{\alpha/2} \left\langle G(\mathbf{x}, t) \right\rangle.$$

It seems that the general derivation of this relation from the fractal structure of a medium where diffusion occurs does not exist, but there is a good example of a particular process of the propagation of excitations in plasma by resonance radiation. When averaging the transfer equation with an exponential range distribution (asymptotically equivalent to the standard diffusion equation) over the Lorentzian frequency distribution, the integral transfer operator is indeed transformed into the fractional Laplacian [38], and the equation exactly coincides with the one written above.

5.5 The model with a finite free-motion velocity

Both described above bifractional (12) and space-fractional (13) models possess a common imperfection: particles perform displacements with the infinite velocity, as instantaneous jumps. We cannot trace the particle: it spends some time at a fixed point in space, then disappears and immediately turns out to be at another, maybe a distant point of space. We cannot talk about the flux (the number of particles crossing the site) and we encounter other inconveniences. Spatial and time intervals between successive collisions are uncorrelated.

This situation has been improved in [37]. To explain the governing idea, we represent equation (6) in the form

$$L(\lambda,\mathbf{k})\tilde{G}(\mathbf{k},\lambda) = b\lambda^{\beta-1}, \tag{14}$$

where

$$L(\lambda,\mathbf{k}) = b\lambda^{\beta} + a|\mathbf{k}|^{\alpha}. \tag{15}$$

Involving a finite velocity between collisions changes equation (6) to the form

$$L_v(\lambda,\mathbf{k})\widetilde{G}(\mathbf{k},\lambda) \equiv [1 - p(\mathbf{k},\lambda/v)q(\lambda)]p(\mathbf{k},\lambda) = S_v(\lambda,\mathbf{k}), \tag{16}$$

where

$$S_v(\lambda,\mathbf{k}) = Q(\lambda) + (1/v)P(\mathbf{k},\lambda/v)q(\lambda).$$

Assuming

$$\mathsf{P}(R > r) \sim \frac{Ar^{-\alpha}}{\Gamma(1-\alpha)}, \quad r \to \infty, \quad \mathsf{P}(T > t) \sim \frac{Bt^{-\beta}}{\Gamma(1-\beta)}, \quad t \to \infty,$$

and applying Tauberian theorems, one can find the asymptotics

$$L_v(\lambda,\mathbf{k}) \sim B\lambda^{\beta} + \langle R\rangle\langle \lambda/v - i\mathbf{k}\mathbf{\Omega}\rangle + A\big\langle(\lambda/v - i\mathbf{k}\mathbf{\Omega})^{\alpha}\big\rangle, \quad \alpha > 1$$
$$L_v(\lambda,\mathbf{k}) \sim B\lambda^{\beta} + A\big\langle(\lambda/v - i\mathbf{k}\mathbf{\Omega})^{\alpha}\big\rangle, \quad \alpha < 1,$$

under $\mathbf{k} \to 0, \lambda \to 0$. Here, $\mathbf{\Omega}$ is a random direction of motion after collision assuming below to be isotropically distributed:

$$S_v(\lambda,\mathbf{k}) = B\lambda^{\beta-1} + \frac{A}{v}(1 - B\lambda^{\beta})\left\langle\left(\frac{\lambda}{v} + i\mathbf{k}\mathbf{\Omega}\right)^{\alpha-1}\right\rangle$$
$$\sim B\lambda^{\beta-1} + \frac{A}{v^{\alpha}}\big\langle(\lambda + iv\mathbf{k}\mathbf{\Omega})^{\alpha-1}\big\rangle.$$

For the sake of convenience, we will call this approximation of the process NoRD (Nonlocal Relativistic Diffusion) model.[3] Analyzing behavior of various terms as $\lambda \to 0$ leads to following conclusions.

In the case $v = \infty$, both expressions have the same asymptotic form

$$L_v(\lambda, \mathbf{k}) \sim B[\lambda^\beta + C_\infty |\mathbf{k}|^\alpha], \quad C_\infty = A|\cos(\alpha\pi/2)|/[(\alpha+1)B].$$

If $\alpha < \beta \le 1$, the asymptotic equation takes an unusual diffusion process form with the pseudodifferential operator: the averaged over all directions $\mathbf{\Omega}$ material derivative of fractional order $(\frac{\partial}{\partial t} + v\mathbf{\Omega}\nabla)^\alpha$:

$$(A/v^\alpha)\left\langle \left(\frac{\partial}{\partial t} + v\mathbf{\Omega}\nabla\right)^\alpha \right\rangle G(\mathbf{x}, t) = S_v(\mathbf{x}, t). \tag{17}$$

Here,

$$S_v(\mathbf{x}, t) \sim (A/v^\alpha)\left\langle \left(\frac{\partial}{\partial t} + v\mathbf{\Omega}\nabla\right)^{\alpha-1} \right\rangle \delta(\mathbf{x})\delta(t) = \frac{A}{v^\alpha}\frac{t^{-\alpha}}{\Gamma(1-\alpha)}\langle \delta(\mathbf{x} - v\mathbf{\Omega}t)\rangle.$$

Speed-dependence now remains at all times, but β-dependence disappears. The corresponding solution $G(\mathbf{x}, t)$ has a specific U- or W-shaped form in a bounded region (ball) of radius vt, beyond which it is zero.

Fourier–Laplace transform (16) allows us to compute the mean square root of the propagator,

$$\langle [R(t)]^2 \rangle = \int_{-\infty}^{\infty} r^2 G(\mathbf{x}, t) d\mathbf{x},$$

and for obtaining it the Laplace transform is enough:

$$\int_0^\infty e^{-\lambda t} \langle [R(t)]^2 \rangle dt = -[\partial^2 \widetilde{N}(\mathbf{k}, \lambda)/\partial k^2]_{\mathbf{k}=0} \equiv -\widetilde{N}''(0, \lambda).$$

Performing this differentiation with using asymptotical distributions $p(\mathbf{x})$ and $q(t)$ and Tauberian theorems yield results which can be formulated as follows. Let the mean free path $\langle \xi \rangle$ be finite,

$$p(\lambda) \sim 1 - \langle \xi \rangle \lambda + C\lambda^\delta, \quad 1 < \delta \le 2, \ \lambda \to 0,$$

and

$$q(\lambda) \sim 1 - B\Gamma(1-\beta)\lambda^\beta, \quad 0 < \beta < 1, \quad \lambda \to 0,$$

3 “Nonlocal” relates to fractional operators, ‘relativistic” indicates relativistic boundedness of particle speed.

then

$$\langle [R(t)]^2 \rangle \sim \frac{2C(\delta - 1)v^{2-\delta}}{B\Gamma(1-\beta)\Gamma(3-\delta+\beta)} t^{2-\delta+\beta}, \quad t \to \infty.$$

One can see that for $\beta = \delta - 1$ we have a normal law of the diffusion packet spreading, whereas in case $\beta < \delta - 1$, it spreads lower (the subdiffusion mode), and in the case of $\beta > \delta - 1$ we see faster spreading (superdiffusion model).

Now, let

$$p(\lambda) \sim 1 - A\Gamma(1-\alpha)\lambda^\alpha, \quad 0 < \alpha < 1,\ \lambda \to 0,$$

then

$$\langle [R(t)]^2 \rangle \sim (1-\alpha)v^2 t^2, \quad \alpha < \beta;$$

$$\langle [R(t)]^2 \rangle \sim \frac{A(1-\alpha)v^2}{A + Bv^\alpha} t^2, \quad \alpha = \beta;$$

$$\langle [R(t)]^2 \rangle \sim \frac{2A\Gamma(2-\alpha)v^{2-\alpha}}{B\Gamma(3-\alpha+\beta)\Gamma(1-\beta)} t^{2-\alpha+\beta}, \quad \alpha > \beta.$$

All of these cases relate to the superdiffusion mode.

When $v = \infty$, the mean square of the propagator diverges and cannot be used as a measure of its width. Thus, the free motion velocity finiteness drastically changes the asymptotic of the packet width as $t \to \infty$. Wherein, the subdiffusion mode arises only in case, if the mean free path is finite and trapping time is distributed according to inverse power law with β satisfying the condition $\beta < \delta - 1$. When $\beta > \delta - 1$, for any $\alpha < 1$, $\beta < 1$ (the mean free path and trapping times are infinite), the superdiffusion takes place. The linear dependence $\Delta \propto t$ under condition $\alpha \le \beta$ means that the leading contribution in longtime asymptotics is given by the ballistic mode, so in the case of $\alpha \to 0$ we observe a free motion in a pure form: $\Delta = vt$.

5.6 One-dimensional walks

In the framework of a one-dimensional version of a finite-speed model, the propagator can be expressed through elementary functions. Let us return to equation (17). In the one-dimensional case, vector $\mathbf{\Omega}$ takes two possible directions with equal (in case of isotropic walks) probabilities $p_\pm = 1/2$. Representing the Laplace c. f. of free paths as

$$\hat{p}(\lambda) \sim \begin{cases} 1 - c\lambda^\alpha, & 0 < \alpha < 1; \\ 1 - \langle R \rangle \lambda + c_1 \lambda^\alpha, & 1 < \alpha < 2, \end{cases}$$

we find Fourier–Laplace propagators of the first and second kind of expressions

$$\widetilde{G}_{\|}(k, \lambda) = \frac{2\langle R \rangle v^{\alpha-1} - c_1(\lambda + ivk)^{\alpha-1} - c_1(\lambda - ivk)^{\alpha-1}}{2\langle R \rangle v^{\alpha-1}\lambda - c_1(\lambda + ivk)^\alpha - c_1(\lambda - ivk)^\alpha}, \quad 1 < \alpha < 2, \tag{18}$$

and

$$\widetilde{G}_{\|}(k,\lambda) = \frac{(\lambda + ivk)^{\alpha-1} + (\lambda - ivk)^{\alpha-1}}{(\lambda + ivk)^{\alpha} + (\lambda - ivk)^{\alpha}} \quad 0 < \alpha < 1, \tag{19}$$

correspondingly.

For the first kind of process, the condition $|\lambda/vk| \to 0$ yields asymptotics

$$\begin{aligned}\widetilde{G}_{\|}(k,\lambda) &= \frac{2\langle R\rangle - c_1(\lambda/v - ik)^{\alpha-1} - c_1(\lambda/v + ik)^{\alpha-1}}{v[2\langle R\rangle(\lambda/v) - c_1(\lambda/v - ik)^{\alpha} - c_1(\lambda/v + ik)^{\alpha}]} \\ &\sim \frac{1}{[\lambda + \kappa|k|^{\alpha}]}, \quad \kappa = (c_1 v/\langle R\rangle)|\cos(\alpha\pi)/2|,\end{aligned}$$

inverting which (i. e., passing $\lambda \to t$) leads to the Fourier characteristic function

$$\widetilde{G}_{\|}(k,t) = \exp(-\kappa t|k|^{\alpha})$$

of a symmetric Levy stable density:

$$G_{\|}(x,t) = (\kappa t)^{-1/\alpha}\Psi_1^{(\alpha)}(x(\kappa t)^{-1/\alpha}), \quad 1 < \alpha \le 2. \tag{20}$$

For $\alpha = 2$, this coincides with the ordinary diffusion result.

The propagator of the second kind in a range of $\alpha \in (0,1)$ has the form

$$G_{\|}(x,t) = \frac{2\sin\pi\alpha}{\pi}\,\frac{(1 - x^2/v^2t^2)^{\alpha-1}}{(1 - x/vt)^{2\alpha} + (1 + x/vt)^{2\alpha} + 2(1 - x^2/v^2t^2)^{\alpha}\cos\pi\alpha}. \tag{21}$$

Plots of this propagator for some values of α are shown in Figure 5.

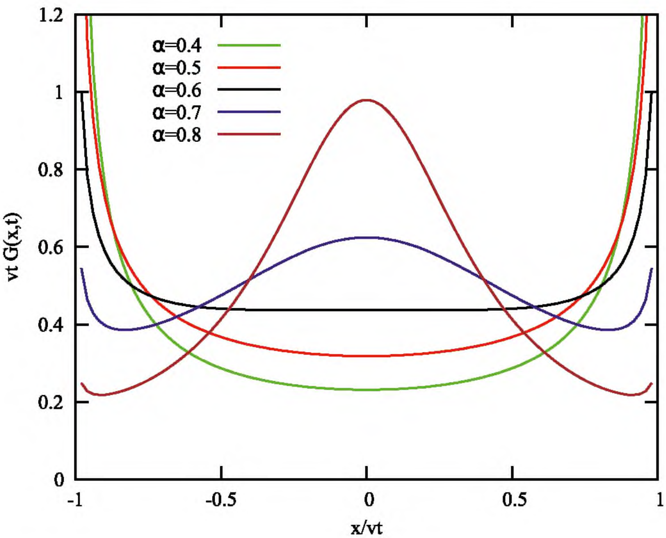

Figure 5: Propagators $G_{\|}(x,t)$ for different values of α.

Observe, that at small α transform (42) takes the form

$$\widetilde{G}_{\|}(k,\lambda) \sim \frac{1}{2}\left[\frac{1}{\lambda + ivk} + \frac{1}{\lambda - ivk}\right], \quad \alpha \to 0,$$

corresponding to the ballistic propagator

$$G_{\|}^{0}(x,t) \sim \frac{1}{2}[\delta(x - vt) + \delta(x + vt)],$$

describing symmetric free motion of two semipulses into two opposite directions. This example demonstrates the amazing ability of a fractional-differential apparatus not only to cover in the same equation such different modes as diffusion and ballistic motion, but also to ensure (that it is more interesting and important) a smooth transition from one regime to another via continuous change of control parameters α and β.

6 Radiowave propagation

Pulsars are rapidly rotating neutron stars with very strong magnetic fields. They are the pulse sources of radio waves and some of them emit high energy gamma radiation.

Known radio-pulsars appear to emit short pulses of radio radiation with pulse periods between 1.4 ms and 8.5 seconds. The word “pulsar” is a combination of “pulse” and “star,” however, actually pulsars are not pulsating stars. Radio-wave and gamma-quanta are emitted with a constant rate, but in a narrow beam rotating together with the source (a spinning neutron star) like a beacon beam scanning night space so a fixed observer sees only short repeated flashes. The variable intensity $I(t)$, measured by an observer at a great distance from such a source, would repeat (up to a shift) the temporal shape of the emitted signal $I_0(t)$, if not the scattering of waves (quanta) by the interstellar medium. Scattering is due to interaction of the radiation with electrons of the medium being in turbulent state. In fact, not only the time-shape of the observed pulses, but angular shape is also changed due to the scattering. These phenomena are called time- and angle-broadening correspondingly. Scattering is due to the interaction of radiation with the electrons of the medium in the turbulent state. The release of signals from these distortions is an important task of the theoretical astronomy.

Pulsars emit not only radio-wave but also optical, X-ray and gamma radiation. Propagation of radiation through a turbulent medium can often be described in terms of particles (photons) scattering theory and in terms of wave scattering theory. The differential scattering cross-section $w(\Theta)$ per unit length and unit solid angle is connected to the spectral density (Fourier transform) of the dielectric correlations function

$$\Phi_{\varepsilon}(\mathbf{q}) = \frac{1}{8\pi^3}\int_{\mathrm{R}^3} e^{-i\mathbf{q}\mathbf{x}}\langle[\varepsilon(\mathbf{x}_1) - \bar{\varepsilon}][\varepsilon(\mathbf{x}_1 + \mathbf{x}) - \bar{\varepsilon}]\rangle d\mathbf{x}.$$

In a statistically homogeneous and isotropic turbulent medium, the spectral density depends only on the absolute value of the vector argument, $q = |\mathbf{q}|$, and this link is expressed as

$$w(\Theta) = (1/2)\pi k_0^4 \Phi_\varepsilon(q),$$

where $q = 2k_0 \sin(\Theta/2)$, and k_0 is a wave number in the homogeneous medium with the dielectric constant $\bar{\varepsilon}$. According to Kolmogorov's two-thirds law,

$$\Phi_\varepsilon(q) = Cq^{-11/3}, \quad C = \text{const},$$

in the inertial interval of wave numbers (see equation (26.31) in the book [28]). This validates the small angle approximation with

$$w(\Theta) \approx A\Theta^{-\alpha-2}, \quad A = \text{const}, \quad \alpha = 5/3. \tag{22}$$

The more detailed description of the interstellar turbulence can be found in many works (see, e. g., [46]). For illustrative aims, we restrict ourselves by using the simplest representation (22).

As was repeatedly noted in the first chapter, an undoubted sign of the applicability of a fractional calculus to description of transport processes is appearance of distributions with power tails (such as the Lévy distribution). In the problem of pulsars, such a step was taken in the work [6]. But before discussing this point, we consider the multiple small-angle scattering from stationary source.

Let us assume that a one-directional point source is placed at origin and emits a photon along z-axis. In the small-angle approximation, z-coordinate of the photon is equated to its travel. For characterizing the deviation of the photon from the initial direction, the two-dimensional vector $\mathbf{u}$ is used. The kinetic equation for the angular distribution density $f(\mathbf{u}, z)$ reads

$$\frac{\partial f(\mathbf{u}, z)}{\partial z} = \int_{\mathrm{R}^2} [f(\mathbf{u} - \mathbf{u}', z) - f(\mathbf{u}, z)] w(|\mathbf{u}'|) d\mathbf{u}'. \tag{23}$$

Developing as series in $\mathbf{u}'$ and making integration (i. e., averaging over the scattering angle), one arrives at the diffusion equation for the main asymptotical part of the solution $f^{\mathrm{as}}(\mathbf{u}, z)$:

$$\frac{\partial f^{\mathrm{as}}(\mathbf{u}, z)}{\partial z} = \frac{\langle u^2 \rangle}{2} \Delta_{\mathbf{u}} f^{\mathrm{as}}(\mathbf{u}, z),$$

where $\Delta_{\mathbf{u}} = \partial^2/\partial u_x^2 + \partial^2/\partial u_y^2$ and

$$\langle u^2 \rangle = \int_{\mathbf{X}^2} w(|\mathbf{u}|) u^2 d\mathbf{u} \tag{24}$$

is the mean square scattering angle per unit length.

In case $\alpha \in (0,1)$, integral (23) diverges and instead of expanding into series, we insert ansatz (22) directly into integral term in the right-hand side of equation (23):

$$\frac{\partial f^{\mathrm{as}}(\mathbf{u},z)}{\partial z} = AJ(\mathbf{u}), \quad J(\mathbf{u}) = \int_{\mathrm{R}^2} [f^{\mathrm{as}}(\mathbf{u}-\mathbf{u}',z) - f^{\mathrm{as}}(\mathbf{u},z)]|\mathbf{u}'|^{-\alpha-2} d\mathbf{u}'.$$

When $\alpha \geq 1$, the collision integral $J(\mathbf{u})$ diverges again and we have to use the Hadamard regularization procedure, replacing the divergent integral $J(\mathbf{u})$ by its finite (in Hadamard's sense) part:

$$\begin{aligned} J(\mathbf{u}) \to \mathrm{p.f.}\, J(\mathbf{u}) &\equiv \int_{\mathrm{R}^2} [f^{\mathrm{as}}(\mathbf{u}-2\mathbf{u}',z) - 2f^{\mathrm{as}}(\mathbf{u}-\mathbf{u}',z) + f^{\mathrm{as}}(\mathbf{u},z)]|\mathbf{u}'|^{-\alpha-2} d\mathbf{u}' \\ &= -c(\alpha)(-\Delta_{\mathbf{u}})^{\alpha/2}, \end{aligned}$$

where

$$c(\alpha) = \frac{\pi^2(1-2^{1-\alpha})}{[\Gamma(1-\alpha/2)]^2 \sin(\alpha\pi/2)}.$$

Consequently, the asymptotical behavior of the angle distribution $f^{\mathrm{as}}(\mathbf{u},z)$ of photons traversed path z in a turbulent medium is described by the equation

$$\frac{\partial f(\mathbf{u},z)}{\partial z} = -c(\alpha)A(-\Delta_{\mathbf{u}})^{\alpha/2} f(\mathbf{u},z).$$

The solution to this equation is expressed through the two-dimensional isotropic Lévy–Feldheim stable density with the characteristic exponent $\alpha = 5/3$

$$g_2(r;\alpha) = \frac{1}{2\pi}\int_0^\infty e^{-k^\alpha} J_0(kr)k\,dk \tag{25}$$

by the relation

$$f(\mathbf{u},z) = [c(\alpha)Az]^{-2/\alpha} g_2([c(\alpha)Az]^{-1/\alpha}|\mathbf{u}|;\alpha). \tag{26}$$

Let us note three characteristic differences of scattering in a turbulent medium from analogous process in a medium with small-scale fluctuations of the refraction coefficient. The angle distribution width of the scattered photons grows with depth proportionally to $z^{3/5}$, but not to $z^{1/2}$, distribution tails have the power-law form but not the Gaussian one, and x- and y-projections of the vector $\mathbf{u}$ are not statistically independent anymore.

7 Conclusion

We would like to conclude this chapter with a few words on the general nature of the appearance of fractional operators in the astrophysical problems discussed here. Reconsidering various works performed with the use of fractional operators, we often meet as a reason for this a special property of a system under consideration: *fractality* (see reviews [38, 41, 42] and books [3, 43]). However, the linguistic consonance of words *fractal* and *fractional* cannot replace the logical conclusion, although, for the sake of justice, it should be noted that the operators of fractional differintegration possess the property of self-similarity which appears in the change of variables and in a certain sense corresponds to the self-similarity of fractals. On the other hand, there exists a deep distinction boundary between these two mathematical objects: fractional operators are completely continuous operators, whereas fractals are discontinuous geometric structures. Here is a convincing example: the diffusion equation describing the Brownian motion contains operators of integer orders, and but trajectories themselves are fractals.

Conversely, the evolution of the distribution of the particle performing the Lévy motion is described by an equation with a fractional Laplacian and has continuous (and even more, smooth) solutions, whereas the trajectories themselves, representing a real physical movement and not averaged over the ensemble, are fractal.

If this is the case, i. e. the way to reconcile fractality and fractionality runs through averaging, we must find some common cause for the appearance of fractional operators in different models, and first of all, a *cause of averaging*, the physical meaning of this operation. There may be useful in connection with this an idea expressed in the article [40]. On the base of consideration of the Liouville classical equation with the use of Mellin transformation in time, it was demonstrated there that *a subsystem of a closed Hamiltonian dynamical system, obeys the generalized Liouville equation, modified by adding a term with fractional time-derivative of distributed order.*

With respect to the problems under consideration, this assertion has been formulated in review [41]. Additional information, concerning fractional calculus and its application to physical problems can be found in books [34, 39, 17].

Bibliography

[1] O. G. Bakunin, *Turbulence and Diffusion: Scaling versus Equations*, Springer Science & Business Media, 2008.

[2] J. Ballesteros-Paredes and E. Vázquez-Semadeni, Cloud statistics in numerical simulations of the ISM, astro-ph/9601195.

[3] Y. Baryshev and P. Teerikorpi, *Discovery of Cosmic Fractals*, World Scientific, 2002.

[4] G. K. Batchelor, *The Theory of Homogeneous Turbulence*, Cambridge University Press, 1953.

[5] P. Blasi, Recent developments in cosmic ray physics, *Nucl. Phys. B, Proc. Suppl.*, **256** (2014), 36–47.
[6] S. Boldyrev and C. R. Gwinn, Lévy model for interstellar scintillations, *Phys. Rev. Lett.*, **91**(13) (2003), 131101.
[7] K. M. Case and P. F. Zweifel, *Linear Transport Theory*, Addison-Wesley, 1967.
[8] L. Chuvilgin and V. Ptuskin, Anomalous diffusion of cosmic rays across the magnetic field, *Astron. Astrophys.*, **279** (1993), 278–297.
[9] R. M. Crutcher, Observations of magnetic fields in molecular clouds, in *The Magnetized Interstellar Medium*, pp. 123–132, 2004.
[10] L. Dorman, *Cosmic Ray Interactions, Propagation, and Acceleration in Space Plasmas*, vol. 339, Springer Science & Business Media, 2006.
[11] A. Dudorov, Properties of the hierarchy of interstellar magnetic clouds, *Sov. Astron.*, **35** (1991), 342.
[12] B. G. Elmegreen, Diffuse Hα in a fractal interstellar medium, *Publ. Astron. Soc. Aust.*, **15**(1) (1998), 74–78.
[13] G. Getmantsev, On the isotropy of primary cosmic rays, *Sov. Astron.*, **6** (1963), 477.
[14] J. Giacalone and J. Jokipii, Charged-particle motion in multidimensional magnetic-field turbulence, *Astrophys. J.*, **430** (1994), L137–L140.
[15] V. Ginzburg, Origin of cosmic rays and radioastronomy, *Usp. Fiz. Nauk*, **51**(11) (1953), 343–392 (in Russian).
[16] V. Ginzburg and S. Syrovatskii, *The Origin of Cosmic Rays*, Pergamon Press, 1964.
[17] R. Herrmann, *Fractional Calculus: An Introduction for Physicists*, World Scientific, 2014.
[18] J. Jokipii, Cosmic-ray propagation. II. Diffusion in the interplanetary magnetic field, *Astrophys. J.*, **149** (1967), 405.
[19] J. Jokipii, Turbulence and scintillations in the interplanetary plasma, *Annu. Rev. Astron. Astrophys.*, **11**(1) (1973), 1–28.
[20] J. Jokipii and E. Parker, Stochastic aspects of magnetic lines of force with application to cosmic-ray propagation, *Astrophys. J.*, **155** (1969), 777.
[21] B. Kadomtsev and O. Pogutse, Electron heat conductivity of the plasma across a 'braided' magnetic field, in *Plasma Physics and Controlled Nuclear Fusion Research 1978, vol. 1*, pp. 649–662, 1979.
[22] A. Lagutin, Y. A. Nikulin, and V. Uchaikin, The "knee" in the primary cosmic ray spectrum as consequence of the anomalous diffusion of the particles in the fractal interstellar medium, *Nucl. Phys. B, Proc. Suppl.*, **97** (1–3) (2001), 267–270.
[23] R. B. Larson, Turbulence and star formation in molecular clouds, *Mon. Not. R. Astron. Soc.*, **194**(4) (1981), 809–826.
[24] B. B. Mandelbrot and J. W. Van Ness, Fractional Brownian motions, fractional noises and applications, *SIAM Rev.*, **10**(4) (1968), 422–437.
[25] A. Monin, The equation of turbulent diffusion, *Dokl. Akad. Nauk SSSR (in Russian)*, **105** (1955), 256–259.
[26] A. S. Monin and A. M. Yaglom, *Statistical Fluid Mechanics, Volume II: Mechanics of Turbulence*, Cambridge, 1971.
[27] B. Ragot and J. Kirk, Anomalous transport of cosmic ray electrons, astro-ph/9708041.
[28] S. Rytov, Y. A. Kravtsov, and V. Tatarskii, *Introduction to Statistical Radiophysics: vol. 2. Random Fields* (in Russian), Moscow, Nauka, 1978.
[29] A. I. Saichev and G. M. Zaslavsky, Fractional kinetic equations: solutions and applications, *Chaos, Interdiscip. J. Nonlinear Sci.*, **7**(4) (1997), 753–764.
[30] G. Samorodnitsky and M. S. Taqqu, *Stable Non-Gaussian Processes*, Chapman & Hall, New York, 1994.

[31] J. Schönfeld, Integral diffusivity, *J. Geophys. Res.*, **67**(8) (1962), 3187–3199.
[32] A. Snodin, A. Shukurov, G. Sarson, P. Bushby, and L. Rodrigues, Global diffusion of cosmic rays in random magnetic fields, *Mon. Not. R. Astron. Soc.*, **457**(4) (2016), 3975–3987.
[33] B. Strömgren, On the density distribution and chemical composition of the interstellar gas, *Astrophys. J.*, **108** (1948), 242.
[34] V. E. Tarasov, *Fractional Dynamics: Applications of Fractional Calculus to Dynamics of Particles, Fields and Media*, Springer Science & Business Media, 2011.
[35] C. Tchen, Diffusion of particles in turbulent flow, in *Advances in Geophysics*, vol. 6, pp. 165–174, Elsevier, 1959.
[36] V. V. Uchaikin, Self-similar anomalous diffusion and Lévy-stable laws, *Physics Uspekhi*, **46**(8) (2003), 821.
[37] V. V. Uchaikin, On the fractional derivative model of the transport of cosmic rays in the galaxy, *JETP Lett.*, **91**(3) (2010), 105–109.
[38] V. V. Uchaikin, Fractional phenomenology of cosmic ray anomalous diffusion, *Phys. Usp.*, **56**(11) (2013), 1074–1119.
[39] V. V. Uchaikin, *Fractional Derivatives for Physicists and Engineers, vols. I–II*, Springer – High Education Press, 2013.
[40] V. Uchaikin, On fractional differential Liouville equation describing open systems dynamics, *Belgorod State Univ. Sci. Bull., Math. Phys.*, **37**(25) (2014), 58–67.
[41] V. V. Uchaikin, Nonlocal models of cosmic ray transport in the Galaxy, *J. Appl. Math. Phys.*, **3**(2) (2015), 181–194.
[42] V. Uchaikin and R. Sibatov, Fractional derivatives on cosmic scales, *Chaos Solitons Fractals*, **102** (2017), 197–209.
[43] V. Uchaikin and R. Sibatov, *Fractional Kinetics in Space: Anomalous Transport Models*, World Scientific, 2018.
[44] V. V. Uchaikin and V. M. Zolotarev, *Chance and Stability: Stable Distributions and their Applications*, Walter de Gruyter, 1999.
[45] G. Webb, G. Zank, E. K. Kaghashvili, and J. Le Roux, Compound and perpendicular diffusion of cosmic rays and random walk of the field lines. I. Parallel particle transport models, *Astrophys. J.*, **651**(1) (2006), 211.
[46] S. Xu and B. Zhang, Scatter broadening of pulsars and implications on the interstellar medium turbulence, *Astrophys. J.*, **835**(1) (2017), 2.
[47] G. M. Zaslavsky, *Hamiltonian Chaos and Fractional Dynamics*, Oxford University Press on Demand, 2005.
[48] V. Zolotarev, V. Uchaikin, and V. Saenko, Superdiffusion and stable laws, *J. Exp. Theor. Phys.*, **88**(4) (1999), 780–787.

Gianni Pagnini

Fractional kinetics in random/complex media

Abstract: In this chapter, we consider a randomly-scaled Gaussian process and discuss a number of applications to model fractional diffusion. Actually, this approach can be understood as a Gaussian diffusion in a medium characterized by a population of scales. This interpretation supports the idea that fractional diffusion emerges from standard diffusion occurring in a complex medium.

Keywords: Fractional diffusion, fractional calculus, stochastic processes, randomly-scaled Gaussian processes, generalized grey Brownian motion

MSC 2010: 60G20, 60J60, 60G15, 26A33, 34A08, 35R11, 60J65

1 Introduction

The mathematical description of diffusion has a long history with many different formulations including phenomenological models based on: conservation of mass and constitutive laws, probabilistic models based on random walks and central limit theorems, stochastic models based on Wiener process or on the Langevin equation, as well as models based on master equations or on the Fokker–Planck equation. On the other hand many processes in life sciences, soft condensed matter, geology, and ecology show a diffusive behavior that cannot be modeled by classical methods. These phenomena are generally labeled with the term anomalous diffusion in order to distinguish them from the normal diffusion, where the adjective normal highlights that a Gaussian-based process is considered, and the mean square displacement of diffusing particles scales linearly with time. Numerous experimental measurements in which the mean square displacement of diffusing particles scales with a nonlinear power law in time are successfully modeled through fractional calculus, such that the corresponding process is referred to be a fractional diffusion phenomenon. Fractional diffusion can be interpreted as the consequence of the complexity, or randomness, of the medium in which a classical diffusion takes place. More explicitly, fractional diffusion emerges from a population of scales that characterizes the medium.

Acknowledgement: This research is supported by the Basque Government through the BERC 2014–2017 and BERC 2018–2021 programs, by the Spanish Ministry of Economy and Competitiveness MINECO through BCAM Severo Ochoa excellence accreditations SEV-2013-0323 and SEV-2017-0718 and through project MTM2016-76016-R "MIP."

Gianni Pagnini, BCAM and Ikerbasque, Bilbao, Basque Country, Spain, e-mail: gpagnini@bcamath.org

We consider here the motion of particles in such a random/complex medium. The randomness of the medium is described by a characteristic quantity, for example, the lengthscale, that depends on a parameter β. The role of β consists in tuning the degree of randomness of the medium by modulating the distribution of the lengthscale ℓ_β.

The considered approach is that of a randomly-scaled Gaussian process, that is, a Gaussian process multiplied times a non-negative independent random variable. This approach was inspired by the constitutive approach proposed by Mura [27] to built up processes meeting the characteristics of the so-called grey Brownian motion (gBm) [37, 38] and generalized grey Brownian motion (ggBm) [29, 28]. Actually, this approach is based on the product of the fractional Brownian motion (fBm) and an independent positive and constant random variable.

We can show that, in this scenario, a suitable choice of the length scale distribution ℓ_β allows to obtain a continuous transition from an ergodic to a nonergodic process through the parameter β. In particular, this is verified by the same condition that triggers the emergence of fractional kinetics, which is then straightforwardly associated with the occurrence of the ergodicity breaking.

The rest of the chapter is organized as follows: In Section 2, the modeling approach is described together with some properties. In Section 3, the formulation of stochastic processes with stationary increments is presented for the cases of Erdélyi–Kober fractional diffusion and space-time fractional diffusion. In Section 4, the formulation of stochastic processes with nonstationary increments is presented and the role of the dependence on time discussed. In Section 5, conclusions and final remarks are reported.

2 Modeling approach

2.1 Definition of the stochastic process

The proposed stochastic process $X(t)$ is expressed as

$$X(t) = \ell_\beta X_G(t) , \tag{2.1}$$

where $X_G(t)$ is a Gaussian stochastic process and ℓ_β a non-negative random variable. The process (2.1) is a randomly-scaled Gaussian process. In the following, the process $X_G(t)$ is chosen to be the fBm $X_H(t)$ where $0 < H < 1$ is the Hurst exponent and the ggBm is recovered, for example, [29].

With and **abuse** of terminology, we call ggBm a processes defined by the product of a Gaussian process and an independent and constant non-negative random variable.

Notice that ℓ_β is a random length scale labeling the single trajectory. Each trajectory can be interpreted as a different sample path performed by a particle in different experiments with the same particle initial conditions, but in different environmental conditions, which are parameterized by the random length scale ℓ_β.

2.2 Probability density function

It is well known that the probability density function (PDF) of the product of two independent random variables is given by an integral formula [34, 3, 21, 23].

Let Z_1 and Z_2 be two real independent random variables whose PDFs are $p_1(z_1)$ and $p_2(z_2)$, respectively, with $z_1 \in \mathbb{R}$ and $z_2 \in \mathbb{R}^+$. Let Z be the random variable obtained by the product of Z_1 and Z_2^γ, that is,

$$Z = Z_1 Z_2^\gamma \,. \tag{2.2}$$

Then, denoting with $p(z)$ the PDF of Z, it results

$$p(z) = \int_0^\infty p_1\left(\frac{z}{\lambda^\gamma}\right) p_2(\lambda) \frac{d\lambda}{\lambda^\gamma} \,. \tag{2.3}$$

From the PDF of the product of two variables (2.3), by applying the change of variables $z = xt^{-H}$ the PDF of the process $X(t)$ results to be

$$\frac{1}{t^H} p\left(\frac{x}{t^H}\right) = \int_0^\infty \frac{1}{\lambda^\gamma t^H} p_1\left(\frac{x}{\lambda^\gamma t^H}\right) p_2(\lambda) d\lambda \,, \tag{2.4}$$

where p_1 is the Gaussian density of X_G with variance $\langle x^2 \rangle \sim t^{2H}$ and p_2 is the density of ℓ_β^2.

2.3 Ergodicity breaking

The ergodicity of the process is evaluated through the limit for large T of the following quantity [1, 12, 8]

$$\mathrm{EB}(T, \Delta) = \frac{\langle [\overline{\delta^2}(T, \Delta)]^2 \rangle}{\langle \overline{\delta^2}(T, \Delta) \rangle^2} - 1, \tag{2.5}$$

where $\langle \cdot \rangle$ denotes the ensemble average and $\overline{\delta^2}(T, \Delta)$ the Time-Averaged Mean-Square Displacement (TA-MSD)

$$\overline{\delta^2}(T, \Delta) = \frac{\int_0^{T-\Delta} [X(\xi + \Delta) - X(\xi)]^2 \, d\xi}{T - \Delta} \,, \tag{2.6}$$

being Δ the time lag and $T \gg \Delta$ the measurement time. For an ergodic process, it has been shown that $\mathrm{EB}(T, \Delta)$ approaches 0 for large T. It is easy to see that, being computed as a time average on the single trajectory, the long-time ($T \to \infty$) TA-MSD of the process $X(t)$, equation (2.1), is given by

$$\overline{\delta^2}(T,\Delta) \xrightarrow{T\to\infty} 2\ell_\beta^2\Delta^{2H}\,, \tag{2.7}$$

so that the ensemble average of the long-time TA-MSD is simply given by [26]:

$$\langle\overline{\delta^2}(T,\Delta)\rangle \xrightarrow{T\to\infty} 2\langle\ell_\beta^2\rangle\Delta^{2H}\,. \tag{2.8}$$

From the ratio of (2.7) and (2.8), we have

$$\xi = \frac{\overline{\delta^2}}{\langle\overline{\delta^2}\rangle} \xrightarrow{T\to\infty} \frac{\ell_\beta^2}{\langle\ell_\beta^2\rangle}\,, \tag{2.9}$$

from which an indication about the distribution of ℓ_β can be obtained [26].

Indeed, setting a fixed and non-random length scale $\ell_\beta = 1$ in the stochastic process $X(t)$ defined in (2.1), it results

$$\mathrm{EB}_{\ell_\beta=1}(T,\Delta) = \mathrm{EB}_{\mathrm{fBm}}(T,\Delta) \xrightarrow{T\to\infty} 0\,. \tag{2.10}$$

In contrast, if ℓ_β is chosen as a random variable, it holds

$$\mathrm{EB}_{\ell_\beta}(T,\Delta) = \frac{\langle\ell_\beta^4\rangle}{\langle\ell_\beta^2\rangle^2}[\mathrm{EB}_{\mathrm{fBm}}(T,\Delta)+1] - 1 \xrightarrow{T\to\infty} \frac{\langle\ell_\beta^4\rangle}{\langle\ell_\beta^2\rangle^2} - 1\,, \tag{2.11}$$

then the nonergodicity of the process is shown by the parameter EB if the random length scale ℓ_β verifies the inequality $\langle\ell_\beta^4\rangle \neq \langle\ell_\beta^2\rangle^2$. Since ℓ_β is an independent random variable, equation (2.11) remarks that, in our approach, the EB is solely due to the randomness of the medium, and it is not affected by the particular choice of the stochastic process $X_G(t)$ at the basis of the trajectories. It is worth noting that, being $X(t)$ a monoscaling stochastic process, the dependence of EB on Δ disappears in the long-time limit $T \to \infty$.

2.4 p-variation test

Beside the EB analysis, another feature characterizing the stochastic trajectories and applicable as a criterion for the selection of stochastic processes consists in the p-variation test, defined as [16, 26]

$$V^{(p)}(t) = \lim_{n\to\infty} V_n^{(p)}(t)\,, \tag{2.12}$$

where, for $t \in [0,T]$,

$$V_n^{(p)}(t) = \sum_{j=0}^{2^n-1} \left| X\left(\frac{(j+1)T}{2^n} \wedge t\right) - X\left(\frac{jT}{2^n} \wedge t\right)\right|^p\,, \tag{2.13}$$

with $a \wedge b = \min\{a,b\}$.

It is easy to show that the stochastic process (2.1) maintains the same p-variation behavior as the fBm, in spite of the fact that EB occurs. Inserting (2.1) into (2.13) gives $V^{(p)}(t) = \ell_\beta^p \, V^{(p)}_{\mathrm{fBm}}(t)$.

2.5 Fractional diffusion as a consequence of ergodicity breaking

Let $p_\beta(\ell)$ be the density of the random scale ℓ_β. For a proper choice of $p_\beta(\ell)$, the PDF of $X(t)$ solves a fractional diffusion equation.

From the properties reported above, we observe that if it holds

$$\lim_{\beta\to\beta_0} p_\beta(\ell) \to \delta(\ell - \ell_0)\,, \tag{2.14}$$

then the PDF of the process $X(t)$ reduces to the Gaussian density of the process $X_G(t)$ and the ergodicity breaking parameter EB goes to 0, which means that the process is indeed ergodic.

This observation allows for relating the emergence of fractional diffusion to the emergence of ergodicity breaking providing a physical interpretation to fractional diffusion. Actually, parameter β describes the fluctuations of ℓ_β due to the complex/random medium where the diffusion occurs. The existence of these fluctuations causes the ergodicity breaking and a non-Gaussian diffusion. Since ℓ_β represents a scale of the process, we conclude that in a random/complex medium where a population of scales is expected, also ergodicity breaking is expected and for specific densities of the scales fractional diffusion emerges.

3 Stochastic processes with stationary increments

3.1 Erdélyi–Kober fractional diffusion

3.1.1 The fundamental solution to the Erdélyi–Kober fractional diffusion

Normal diffusion, or Gaussian diffusion, is a Markovian stochastic process driven by the classical parabolic equation

$$\frac{\partial P}{\partial t} = \frac{\partial^2 P}{\partial x^2}\,, \quad x \in \mathcal{R}\,,\; t \in \mathcal{R}_0^+\,, \tag{3.1}$$

with initial condition $P(x,0) = P_0(x)$. The fundamental solution of (3.1), which is named also the Green function, and corresponding to the case with initial condition $P(x,0) = P_0(x) = \delta(x)$, is the Gaussian density,

$$f(x,t) = \frac{1}{\sqrt{4\pi t}} \exp\left\{-\frac{x^2}{4t}\right\}, \tag{3.2}$$

whose variance grows linearly in time, that is, $\langle x^2\rangle = \int_{-\infty}^{+\infty} x^2 f(x,t)\,dx = 2t$. The density function $P(x,t)$ with general initial condition $P(x,0) = P_0(x)$ is related to the fundamental solution $f(x,t)$ by the following convolution integral:

$$P(x,t) = \int_{-\infty}^{+\infty} f(\xi,t)P_0(x-\xi)\,d\xi\,. \tag{3.3}$$

In order to generalize the classical Markovian setting to non-Markovian cases, the following integral equation has been introduced by A. Mura, M. S. Taqqu, and F. Mainardi [30]:

$$P(x,t) = P_0(x) + \int_0^t \frac{\partial g(s)}{\partial s} K[g(t)-g(s)] \frac{\partial^2 P(x,s)}{\partial x^2}\,ds\,, \tag{3.4}$$

where $K(t)$ is a memory kernel and $g(t)$, with $g(0) = 0$, is a smooth and increasing function describing a time stretching. The Green function of (3.4) $\mathcal{G}(x,t)$, which is the marginal one-point one-time PDF of the non-Markovian diffusion process, turns out to be

$$\mathcal{G}(x,t) = \int_0^{\infty} f(x,\tau)h(\tau,g(t))\,d\tau\,, \tag{3.5}$$

where $f(x,t)$ is the Gaussian density (3.2) that is the fundamental solution of the Markovian diffusion process, that is, $K(t) = \delta(t)$, and $h(\tau,t)$ is the fundamental solution of the so-called *non-Markovian forward drift equation*

$$u(\tau,t) = u_0(\tau) - \int_0^t K(t-s)\frac{\partial u(\tau,s)}{\partial \tau}\,ds\,, \quad \tau,t \in \mathcal{R}_0^+\,, \tag{3.6}$$

where $u_0(\tau) = u(\tau,0)$.

When the kernel and the time-stretching functions are stated as

$$K(t) = \frac{t^{\beta-1}}{\Gamma(\beta)}\,, \quad g(t) = t^{\alpha/\beta}\,, \quad 0 < \alpha \le 2\,,\ 0 < \beta \le 1\,, \tag{3.7}$$

Equation (3.4) becomes

$$P(x,t) = P_0(x) + \frac{1}{\Gamma(\beta)}\frac{\alpha}{\beta}\int_0^t \tau^{\alpha/\beta-1}\left(t^{\alpha/\beta} - \tau^{\alpha/\beta}\right)^{\beta-1} \frac{\partial^2 P(x,\tau)}{\partial x^2}\,d\tau\,, \tag{3.8}$$

that was originally introduced by A. Mura in his PhD thesis [27], and later discussed by him and collaborators in a number of papers [24, 28, 29, 30].

It is well known that there exists a relationship between the solutions of a certain class of integral equations that are used to model anomalous diffusion and stochastic processes. In this respect, the density function $P(x,t)$ which solves (3.8) is the marginal particle PDF, that is, the one-point one-time density function of particle dispersion, of the *generalized grey Brownian motion* (ggBm) [27, 28, 29].

The ggBm is a special class of H-sssi processes of order $H = \alpha$, or Hurst exponent $H = \alpha/2$, where, according to a common terminology, H-sssi means H-self-similar-stationary-increments. The ggBm provides non-Markovian stochastic models for anomalous diffusion, of both slow type $0 < \alpha < 1$ and fast type $1 < \alpha < 2$. The ggBm includes some well-known processes, so that it defines an interesting general theoretical framework. In fact, the fractional Brownian motion appears for $\beta = 1$, the grey Brownian motion, in the sense of W. R. Schneider [37, 38], corresponds to the choice $0 < \alpha = \beta < 1$, and finally the standard Brownian motion is recovered by setting $\alpha = \beta = 1$. It is worth noting to remark that only in the particular case of the Brownian motion the stochastic process is Markovian. Moreover, the ggBm is not an ergodic process [29].

The integral in the non-Markovian kinetic equation (3.8) can be expressed in terms of an Erdélyi–Kober fractional integral. In fact, let μ, η, and γ be $\mu > 0$, $\eta > 0$, and $\gamma \in \mathcal{R}$. The Erdélyi–Kober fractional integral operator $I_\eta^{\gamma,\mu}$, for a sufficiently well-behaved function $\varphi(t)$, is defined as [9, formula (1.1.17)]

$$\begin{aligned} I_\eta^{\gamma,\mu}\,\varphi(t) &= \frac{t^{-\eta(\mu+\gamma)}}{\Gamma(\mu)}\int_0^t \tau^{\eta\gamma}\left(t^\eta-\tau^\eta\right)^{\mu-1}\varphi(\tau)\,d(\tau^\eta) \\ &= \frac{\eta}{\Gamma(\mu)}t^{-\eta(\mu+\gamma)}\int_0^t \tau^{\eta(\gamma+1)-1}\left(t^\eta-\tau^\eta\right)^{\mu-1}\varphi(\tau)\,d\tau\,, \end{aligned} \tag{3.9}$$

hence equation (3.8) can be rewritten as

$$P(x,t) = P_0(x) + t^\alpha\left[I_{\alpha/\beta}^{0,\beta}\,\frac{\partial^2 P}{\partial x^2}\right]. \tag{3.10}$$

The integral operator $I_\eta^{\gamma,\mu}$ was introduced by I. N. Sneddon (see, e. g., [40, 41, 42]) who studied its basic properties and emphasized its useful applications to the generalized axially symmetric potential theory (GASPT) and other physical problems (say in electrostatics, elasticity, etc). When $\eta = 1$, one obtains the operators of fractional integration as originally introduced by H. Kober [10] and A. Erdélyi [2] and, when $\eta = 2$, those introduced by I. N. Sneddon [40, 41, 42]. In the special case $\gamma = 0$ and $\eta = 1$, the Erdélyi–Kober fractional integral operator (3.9) and the Riemann–Liouville fractional integral of order μ, here noted by J^μ, are related by the formula

$$I_1^{0,\mu}\,\varphi(t) = \frac{t^{-\mu}}{\Gamma(\mu)}\int_0^t (t-\tau)^{\mu-1}\varphi(\tau)\,d\tau = t^{-\mu}J^\mu\,\varphi(t)\,. \tag{3.11}$$

The possibility to rewrite equation (3.8) as (3.10) was briefly noted by the author in [32] and largely discussed in [33]. This correspondence between the ggBm and the Erdélyi–Kober fractional integral operator is here stressed, because, since the ggBm serves as a stochastic model for the anomalous diffusion, this leads to define the family of diffusive processes governed by the ggBm as *Erdélyi–Kober fractional diffusion*.

In order to establish the diffusion-type equation corresponding to (3.8), the Erdélyi–Kober fractional differential operator is here introduced. Let $n-1<\mu\leq n$, $n\in\mathbb{N}$. The Erdélyi–Kober fractional derivative is defined as [9, formula (1.5.19)]

$$D_\eta^{\gamma,\mu}\,\varphi(t)=\prod_{j=1}^{n}\left(\gamma+j+\frac{1}{\eta}t\frac{d}{dt}\right)\left(I_\eta^{\gamma+\mu,n-\mu}\,\varphi(t)\right). \tag{3.12}$$

The Riemann–Liouville fractional derivative of order μ, $m-1<\mu\leq m$, $m\in\mathbb{N}$ is defined as $D_{RL}^{\mu}\,\varphi(t)=\frac{d^m}{dt^m}J^{m-\mu}\,\varphi(t)$, and it emerges that the Erdélyi–Kober and the Riemann–Liouville fractional derivatives are related through the formula

$$D_1^{-\mu,\mu}\,\varphi(t)=t^{\mu}D_{RL}^{\mu}\,\varphi(t). \tag{3.13}$$

A further important property of the Erdélyi–Kober fractional derivative is the reduction to the identity operator when $\mu=0$, that is,

$$D_\eta^{\gamma,0}\varphi(t)=\varphi(t). \tag{3.14}$$

Recently, the notions of Erdélyi–Kober fractional integrals and derivatives have been further extended by Yu. Luchko [13] and Yu. Luchko and J. Trujillo [14].

Equation (3.10) in diffusive form is obtained by deriving in time both sides and it results

$$\begin{aligned}\frac{\partial P}{\partial t}&=\alpha\,t^{\alpha-1}I_{\alpha/\beta}^{0,\beta}\frac{\partial^2 P}{\partial x^2}+t^{\alpha}\frac{\partial}{\partial t}\left(I_{\alpha/\beta}^{0,\beta}\frac{\partial^2 P}{\partial x^2}\right)\\&=t^{\alpha-1}\left[\alpha+t\frac{\partial}{\partial t}\right]\left(I_{\alpha/\beta}^{0,\beta}\frac{\partial^2 P}{\partial x^2}\right),\end{aligned} \tag{3.15}$$

that can be recast as

$$\frac{\partial P}{\partial t}=\frac{\alpha}{\beta}t^{\alpha-1}\left[(\beta-1)+1+\frac{\beta}{\alpha}t\frac{\partial}{\partial t}\right]\left(I_{\alpha/\beta}^{0,\beta}\frac{\partial^2 P}{\partial x^2}\right), \tag{3.16}$$

and finally, by using (3.12),

$$\frac{\partial P}{\partial t}=\frac{\alpha}{\beta}t^{\alpha-1}\,D_{\alpha/\beta}^{\beta-1,1-\beta}\,\frac{\partial^2 P}{\partial x^2}. \tag{3.17}$$

A diffusion-type equation for the ggBm was previously proposed [24] but adopting, with an abuse of notation, the Riemann–Liouville fractional differential operator with a stretched time variable. Then, since the Erdélyi–Kober fractional differential operator is taken into account, equation (3.17) follows to be the correct formulation.

The Green function which corresponds to (3.10, 3.17) is [27, 28, 29, 30]

$$\mathcal{G}(x,t) = \frac{1}{2}\frac{1}{t^{\alpha/2}} M_{\beta/2}\left(\frac{|x|}{t^{\alpha/2}}\right), \tag{3.18}$$

where $M_\nu(z)$ is the M-Wright function, often referred to as Mainardi function in the literature devoted to fractional diffusion [18, 36], and it is defined as [17]

$$\begin{aligned} M_\nu(z) &= \sum_{n=0}^{\infty} \frac{(-z)^n}{n!\,\Gamma[-\nu n + (1-\nu)]} \\ &= \frac{1}{\pi}\sum_{n=1}^{\infty} \frac{(-z)^{n-1}}{(n-1)!}\Gamma(\nu n)\sin(\pi\nu n), \quad 0 < \nu < 1; \end{aligned} \tag{3.19}$$

see [6, 7, 24] for a review. Here, it is reminded the noteworthy composition, or subordination-type, formula [21],

$$t^{-\nu} M_\nu\left(\frac{\xi}{t^\nu}\right) = t^{-\ell}\int_0^\infty M_\lambda\left(\frac{\xi}{\tau^\lambda}\right) M_\ell\left(\frac{\tau}{t^\ell}\right)\frac{d\tau}{\tau^\lambda}, \quad \text{with } \nu = \lambda\,\ell, \tag{3.20}$$

where $0 < \nu, \lambda, \ell < 1$ and $\xi, t, \tau \in \mathcal{R}_0^+$. By using (3.20) and the special case $M_{1/2}(z) = (1/\sqrt{\pi})\exp(-z^2/4)$, Green function (3.18) can be expressed as [24, 29, 30]

$$\mathcal{G}(x,t) = \frac{1}{2}\frac{1}{t^{\alpha/2}} M_{\beta/2}\left(\frac{|x|}{t^{\alpha/2}}\right) \tag{3.21}$$

$$= \frac{1}{\sqrt{4t^\alpha}}\int_0^\infty M_{1/2}\left(\frac{|x|t^{-\alpha/2}}{\tau^{1/2}}\right) M_\beta(\tau)\,d\tau \tag{3.22}$$

$$= \int_0^\infty \frac{1}{\sqrt{4\pi\tau t^\alpha}}\exp\left\{-\frac{x^2}{4\tau t^\alpha}\right\} M_\beta(\tau)\,d\tau, \tag{3.23}$$

so that, under the view point of statistical mechanics, the ggBm or the *Erdélyi–Kober fractional diffusion*, emerges to be the superposition of processes with stretched Gaussian density $\frac{1}{\sqrt{4\pi\tau t^\alpha}}\exp\{-\frac{x^2}{4\tau t^\alpha}\}$, that is, fractional Brownian motions, whose variance is $\langle x^2\rangle = 2\tau t^\alpha$ where τ is a random coefficient distributed according to $M_\beta(\tau)$.

However, equation (3.23) can be further remanaged to exhibit a subordination type representation. In fact, after the change of variable $t_* = \tau t^\alpha$, it follows that

$$\mathcal{G}(x,t) = \int_0^\infty \frac{1}{\sqrt{4\pi t_*}}\exp\left\{-\frac{x^2}{4t_*}\right\}\frac{1}{t^\alpha} M_\beta\left(\frac{t_*}{t^\alpha}\right) dt_*, \tag{3.24}$$

which means that the random trajectory $x = x(t)$ can be obtained as a subordination process by $x = x(t) = y[t_*(t)]$, where $t_* = t_*(t)$ is a positive random variable that evolves in the natural time t and is referred to as operational time [4, 5]. The process $t_* = t_*(t)$ is the directing process that realizes in the (t, t_*)-plane whose PDF is $t^{-\alpha} M_\beta(t_* t^{-\alpha})$. Please note that the PDF of the directing process belongs to the same family of the Green function $\mathcal{G}(x,t)$ and they differ for the parameter pair. The process $y = y(t_*)$ is the parent process that is a random trajectory in the (t_*, y)-plane with Gaussian PDF evolving in the operational time t_*. Geometrically, identifying the spatial coordinates y and x, the subordination structure $x = x(t) = y[t_*(t)]$ is obtained by concatenation.

The marginal PDF of the non-Markovian diffusion process ggBm emerges to be related to the Mainardi function M_ν and it describes both slow and fast anomalous diffusion. In fact, the variance of the Green function (3.18) is $\langle x^2 \rangle = \int_{-\infty}^{+\infty} x^2 \mathcal{G}(x,t)\, dx = (2/\Gamma(\beta+1))\, t^\alpha$, then the resulting process turns out to be self-similar with Hurst exponent $H = \alpha/2$ and the variance law is consistent with slow diffusion for $0 < \alpha < 1$ and fast diffusion for $1 < \alpha \le 2$. However, it is worth noting to be remarked also that a linear variance growing is possible, but with non-Gaussian PDF, when $\beta \neq \alpha = 1$, and a Gaussian PDF with nonlinear variance growing when $\beta = 1$ and $\alpha \neq 1$.

3.1.2 The stochastic solution to the Erdélyi–Kober fractional diffusion

Let us consider the generalized grey Brownian motion (ggBm), which is obtained by setting $\ell_\beta = \sqrt{\Lambda_\beta}$,

$$X_{\beta,H}(t) = \sqrt{\Lambda_\beta}\, X_H(t)\,, \tag{3.25}$$

where the positive random variable Λ_β is distributed according to the one-side M-Wright/Mainardi function $M_\beta(\lambda)$, with $\lambda \ge 0$ and $0 < \beta < 1$. Hence with reference to (2.9), we have that the PDF of $\xi = \overline{\delta^2}/\langle \overline{\delta^2} \rangle$ is

$$p(\xi) = M_\beta(\xi) = \frac{1}{\beta \xi^{1/\beta+1}} L_\beta^{-\beta}\left(\frac{1}{\xi^{1/\beta}}\right), \tag{3.26}$$

where $L_\beta^{-\beta}(z)$ is an extremal Lévy density with stable parameter $0 < \beta < 1$.

The one-time PDF $\mathcal{P}(x;t)$ results to be

$$\begin{aligned}\mathcal{P}(x;t) &= \frac{1}{\sqrt{4\pi\lambda\, t^{2H}}} \int_0^\infty \exp\left\{-\frac{x^2}{4\lambda\, t^{2H}}\right\} M_\beta(\lambda)\, d\lambda \\ &= \frac{1}{2\, t^H} M_{\beta/2}\left(\frac{|x|}{t^H}\right),\end{aligned} \tag{3.27}$$

where it emerges that the shape of the displacement PDF is affected by the randomness of the complex medium, here represented by $M_\beta(\lambda)$. $\mathcal{P}(x;t)$ can also be expressed in terms of the H-function [22, 19]

$$\mathcal{P}(x;t) = \frac{1}{2t^H} H^{10}_{01}\left[\frac{|x|}{t^H}\left|\begin{array}{ccc} - & ; & (1-\beta/2,\beta/2) \\ (0,1) & ; & - \end{array}\right.\right], \tag{3.28}$$

and the asymptotic decay is $M_{\beta/2}(|x| \to \infty) \sim |x|^{\frac{c}{2}(\beta-1)} \mathrm{e}^{-b|x|^c}$, with $b = \frac{2^{1-c}}{c}\beta^{\beta c/2}$ and $c = \frac{2}{2-\beta}$ [20, 19].

The variance can be calculated as

$$\langle X^2_{\beta,H}\rangle = \frac{2}{\Gamma(1+\beta)} t^{2H}, \tag{3.29}$$

showing that the power law dependence of the particle displacement variance is not affected by the medium properties. It is noteworthy to observe that the ggBm can show both subdiffusion ($0 < H < 1/2$) and superdiffusion ($1/2 < H < 1$). Moreover, a remarkable case is obtained for $H = 1/2$, where the particle variance results to be linear in time (3.29) but, according to (3.27), the density function is not Gaussian. Gaussian density can be obtained from (3.27) as a special case when $\beta = 1$.

We remark that fractional kinetics, that is, $\beta \neq 1$, is directly associated to the occurrence of EB through the randomness of $\ell_\beta = \sqrt{\Lambda_\beta}$, being $M_{\beta\neq 1}(\lambda) \neq \delta(\lambda - 1)$. Moreover, the fractional order related to β can be experimentally computed by means of the long-time limit of EB(T). In fact, for large T, from (2.11) and $\ell_\beta = \sqrt{\Lambda_\beta}$ the limit of $\mathrm{EB}_{\mathrm{ggbm}}(t)$ results to be

$$\mathrm{EB}_{\mathrm{ggbm}}(T) \xrightarrow{T\to\infty} \frac{\langle\Lambda^2_\beta\rangle}{\langle\Lambda_\beta\rangle^2} - 1 = \beta\frac{\Gamma(\beta)\Gamma(\beta)}{\Gamma(2\beta)} - 1\,. \tag{3.30}$$

Interestingly, formula (3.30) provides the same expression obtained considering a Continuous Time Random Walk (CTRW) with infinite average sojourn time and power-law distribution of waiting times, that is, $\psi(\tau) \propto \tau^{-(1+\beta)}$, $0 < \beta < 1$ [8, 31].

3.1.3 Some special cases of EK fractional diffusion

(i) Fractional Brownian motion

In the case $\beta = 1$, we have $M_1(\lambda) = \delta(\lambda - 1)$ and the Λ_β turns to be a non-random length scale, that is, $\Lambda_\beta = 1$.

(ii) Brownian motion

The Brownian motion is recovered as a special case of the fBm, by setting $\beta = 2H = 1$.

(iii) Time-fractional diffusion equation

In the special case $0 < \beta = 2H < 1$, we obtain the grey Brownian motion whose PDF is the solution of the time-fractional diffusion equation, that is,

$$\mathcal{P}(x;t) = \frac{1}{2t^{\beta/2}} M_{\beta/2}\left(\frac{|x|}{t^{\beta/2}}\right), \quad \langle x^2\rangle \simeq t^\beta\,. \tag{3.31}$$

(iv) Brownian–non-Gaussian: M function

When $H = 1/2$, the linear dependence on time of the particle variance is obtained, but the PDF is not Gaussian, that is,

$$\mathcal{P}(x;t) = \frac{1}{2\,t^{1/2}} M_{\beta/2}\left(\frac{|x|}{t^{1/2}}\right), \quad \langle x^2 \rangle \simeq t\,. \tag{3.32}$$

(v) Brownian–non-Gaussian: exponential PDF

In particular, when $H = 1/2$ and $\beta = 0$, we get Brownian diffusion and the following exponential PDF:

$$\mathcal{P}(x;t) = \frac{1}{2\,t^{1/2}} \mathrm{e}^{-|x|/t^{1/2}}, \quad \langle x^2 \rangle \simeq t\,, \tag{3.33}$$

as follows from the special case $M_0(z) = \exp(-|z|)$.

3.2 Space-time fractional diffusion

3.2.1 The fundamental solution to the space-time fractional diffusion equation

The space-time fractional diffusion equation reads

$${}_tD_*^{\beta} u(x,t) = {}_xD_\theta^{\alpha} u(x,t)\,, \tag{3.34}$$

with

$$u(x,0) = \delta(x)\,, \quad u(\pm\infty,t) = 0\,, \quad -\infty < x < +\infty\,,\ t \geq 0\,, \tag{3.35}$$

Equation (3.34) is obtained from the ordinary diffusion equation by replacing the first-order time derivative and the second-order space derivative with the Caputo time-fractional derivative ${}_tD_*^{\beta}$, of real order β, and the Riesz–Feller space-fractional derivative ${}_xD_\theta^{\alpha}$, of real order α and asymmetry parameter θ, respectively. The real parameters α, θ, and β are restricted as follows:

$$0 < \alpha \leq 2, \quad |\theta| \leq \min\{\alpha, 2-\alpha\}, \quad 0 < \beta \leq 1 \text{ or } 1 < \beta \leq \alpha \leq 2. \tag{3.36}$$

The general solution of (3.34) can be represented as

$$u(x,t) = \int_{-\infty}^{+\infty} K_{\alpha,\beta}^{\theta}(x-\xi,t)\,u(\xi,0)\,d\xi\,, \tag{3.37}$$

where $K_{\alpha,\beta}^{\theta}$ is the fundamental solution, or Green function, which is obtained by setting in (3.35) the initial condition $u(x,0) = \delta(x)$. An important integral representation formula for the fundamental solution $K_{\alpha,\beta}^{\theta}(z)$ is [20, 21]:

$$K_{\alpha,\beta}^{\theta}(z) = \alpha \int_0^{\infty} \xi^{\alpha-1} M_\beta(\xi^\alpha) L_\alpha^\theta(z/\xi) \frac{d\xi}{\xi}\,, \quad 0 < \beta \leq 1\,, \tag{3.38}$$

where $L_\alpha^\theta(z)$ is the Lévy stable density and $M_\beta(\xi)$, $0 < \beta < 1$, is the M-Wright/Mainardi function. By replacing in (3.38) z with $x/t^{\beta/\alpha}$, and after the changes of variable $\xi = \tau^{1/\alpha}/t^{\beta/\alpha}$, it holds

$$t^{-\beta/\alpha} K_{\alpha,\beta}^\theta\left(\frac{x}{t^{\beta/\alpha}}\right) = K_{\alpha,\beta}^\theta(z) = \int_0^\infty \frac{1}{t^\beta} M_\beta\left(\frac{\tau}{t^\beta}\right) \frac{1}{\tau^{1/\alpha}} L_\alpha^\theta\left(\frac{x}{\tau^{1/\alpha}}\right) d\tau \,, \tag{3.39}$$

or

$$K_{\alpha,\beta}^\theta(x,t) = \int_0^\infty M_\beta(\tau,t) L_\alpha^\theta(x,\tau) d\tau \,, \quad 0 < \beta \le 1 \,. \tag{3.40}$$

By using formula (3.38), another integral representation formula for the space-time fractional diffusion can be derived [34]. Let $K_{\alpha,\beta}^\theta(x,t)$ be the fundamental solution of the space-time fractional diffusion equation (3.34) with initial and boundary conditions $u(x,0) = \delta(x)$ and $u(\pm\infty,t) = 0$ and parameters α, θ, β such that $0 < \alpha \le 2$, $|\theta| \le \min\{\alpha, 2-\alpha\}$, $0 < \beta \le 1$, then the following integral representation formula holds true for $0 < x < \infty$:

$$K_{\alpha,\beta}^\theta(x,t) = \int_0^\infty L_\eta^\gamma(x,\xi) K_{\nu,\beta}^{-\nu}(\xi,t) d\xi \,, \tag{3.41}$$

with

$$\alpha = \eta\nu \,, \quad \theta = \gamma\nu \,,$$

and

$$0 < \eta \le 2 \,, \quad |\gamma| \le \min\{\eta, 2-\eta\} \,, \quad 0 < \nu \le 1 \,.$$

In the particular case $\eta = 2$ and $\gamma = 0$, so that $\nu = \alpha/2$ and $\theta = 0$, the spatial variable x emerges to be distributed according to a Gaussian probability density and the integral representation formula (3.41) becomes

$$K_{\alpha,\beta}^0(x,t) = \int_0^\infty G(x,\xi) K_{\alpha/2,\beta}^{-\alpha/2}(\xi,t) d\xi \,, \quad 0 < \alpha \le 2 \,, \quad 0 < \beta \le 1 \,. \tag{3.42}$$

3.2.2 The stochastic solution to the space-time fractional diffusion

Then identifying functions and parameters as follows:

$$p(z) \equiv K_{\alpha,\beta}^0(z) \,, \quad p_1(z_1) \equiv G(z_1) \,, \quad p_2(z_2) \equiv K_{\alpha/2,\beta}^{-\alpha/2}(z_2) \,, \tag{3.43}$$

$$\gamma = \frac{1}{2} \,, \quad \omega = \frac{2\beta}{\alpha} \,, \quad \gamma\omega = \frac{\beta}{\alpha} \,, \tag{3.44}$$

formula (2.3) reduces to the new integral representation formula (3.42) for the symmetric space-time fractional diffusion equation.

In terms of random variables, it follows that [35, 34]

$$Z = Xt^{-\beta/\alpha} \quad \text{and} \quad Z = Z_1 Z_2^{1/2}, \tag{3.45}$$

hence it holds

$$X = Zt^{\beta/\alpha} = Z_1 t^{\beta/\alpha} Z_2^{1/2} = G_{2\beta/\alpha}(t)\sqrt{\Lambda_{\alpha/2,\beta}}\,. \tag{3.46}$$

Since $p_1(z_1) \equiv G(z_1)$, Z_1 is a Gaussian random variable. Consequently, the stochastic process $Z_1 t^{\beta/\alpha} = G_{2\beta/\alpha}(t)$ is a Gaussian process displaying anomalous diffusion. Further, the random variable $Z_2 = \Lambda_{\alpha/2,\beta}$ is distributed according to $p_2(z_2) \equiv K^{-\alpha/2}_{\alpha/2,\beta}, (z_2)$.

In summary, we define the following class of processes: Let $X_{\alpha,\beta}(t)$, $t \geq 0$, be a process defined by

$$X_{\alpha,\beta}(t) = \sqrt{\Lambda_{\alpha/2,\beta}}\, G_{2\beta/\alpha}(t)\,, \quad 0 < \beta \leq 1\,,\ 0 < \alpha \leq 2\,, \tag{3.47}$$

where the stochastic process $G_{2\beta/\alpha}(t)$ is a Gaussian process with power law variance $t^{2\beta/\alpha}$ and $\Lambda_{\alpha/2,\beta}$ is an independent constant non-negative random variable distributed according to the PDF $K^{-\alpha/2}_{\alpha/2,\beta}(\lambda)$, $\lambda \geq 0$, that is a special case of (3.40). The parametric class of Gaussian-based stochastic processes $X_{\alpha,\beta}(t)$ defined in (3.47), and depending on the parameters $0 < \beta \leq 1$ and $0 < \alpha \leq 2$, is a class of stochastic solutions to the space-time fractional diffusion equation (3.34) in the symmetric case. This means that the one-time one-point PDF of $X_{\alpha,\beta}(t)$ is the fundamental solution of equation (3.34) in the symmetric case, namely the PDF $K^0_{\alpha,\beta}(x,t)$ defined in (3.42). The stochastic process $X_{\alpha,\beta}(t)$ stated in (3.47) generalizes the Gaussian processes, which are recovered when $\alpha = 2$ and $\beta = 1$. Similar to the Gaussian process, even this process is uniquely determined by the mean and the autocovariance structure. This property directly follows from the fact that $G_{2\beta/\alpha}(t)$ is a Gaussian stochastic process and $\Lambda_{\alpha/2,\beta}$ is an independent constant non-negative random variable. For example, if we chose the fractional Brownian motion as the Gaussian process, the process $X_{\alpha,\beta}$ has stationary increments [34], by constraints of parameters α and β in the intervals $0 < \beta \leq 1$ and $0 < \beta < \alpha \leq 2$.

The simulation of such a stochastic process with stationary increments whose PDF is the solution of the space-time fractional diffusion equation can be performed by implementing the following process:

$$X_{\alpha,\beta} = \sqrt{\mathcal{L}^{\text{ext}}_{\alpha/2}} \cdot \left[\mathcal{L}^{\text{ext}}_{\beta}\right]^{-\beta/\alpha} X_{\beta/\alpha}(t)\,, \tag{3.48}$$

where β, such that $0 < \beta < 1$, is the fractional order of derivation in time and α, such that $0 < \beta < \alpha \leq 2$, is the fractional order of derivation in space. The process $X_{\beta/\alpha}(t)$ is a fBm with Hurst exponent $H = \beta/\alpha$ and $\mathcal{L}^{\text{ext}}_{\mu}$ is a positive random variable distributed according to an extremal one-side Lévy density $L^{-\mu}_{\mu}(z)$ with stable parameter $0 < \mu < 1$.

3.2.3 The symmetric space-fractional case

We know that $X_{\alpha,\beta}(t)$ defined in (3.47), and depending on the parameters $0 < \beta \le 1$ and $0 < \alpha \le 2$, is a class of stochastic solutions to the space-time fractional diffusion equation (3.34) in the symmetric case but we are interested to consider also the particular case of symmetric space-fractional diffusion equation. This means that the process $X_{\alpha,\beta}(t)$ becomes

$$X_{\alpha,1}(t) = \sqrt{\Lambda_{\alpha/2,1}}\, G_{2/\alpha}(t)\,, \quad 0 < \alpha < 2\,. \tag{3.49}$$

From the equation (3.46), we know that the random variable $\Lambda_{\alpha/2,\beta}$ is distributed according to $K^{-\alpha/2}_{\alpha/2,\beta'}(x,t)$. Moreover, by relation (3.40), that is,

$$K^{\theta}_{\alpha,\beta}(x,t) = \int_0^{\infty} M_\beta(\tau,t) L^{\theta}_{\alpha}(x,\tau)d\tau\,, \tag{3.50}$$

in the space-fractional case $\beta = 1$, we have

$$\begin{aligned} K^{-\alpha/2}_{\alpha/2,1}(x,t) &= \int_0^{\infty} M_1(\tau,t) L^{-\alpha/2}_{\alpha/2}(x,\tau)d\tau \\ &= \int_0^{\infty} \delta(t-\tau) L^{-\alpha/2}_{\alpha/2}(x,\tau)d\tau \\ &= L^{-\alpha/2}_{\alpha/2}(x,t)\,. \end{aligned} \tag{3.51}$$

Then we have shown that $\Lambda_{\alpha/2,1}$ is distributed according $L^{-\alpha/2}_{\alpha/2}(x,t)$, but we are interested in the distribution of $\sqrt{\Lambda_{\alpha/2,1}}$. For this goal, we use the following theorem. Let X be a continuous random variable having PDF f_X. Suppose that $g(x)$ is a strictly monotonic (increasing or decreasing), differentiable (and thus continuous) function of x. Then the random variable Y defined by $Y = g(X)$ has a PDF given by

$$f_Y(y) = \begin{cases} f_X[g^{-1}(y)]|\frac{d}{dy}g^{-1}(y)| & \text{if } y = g(y) \text{ for some } x\,, \\ 0 & \text{if } y \neq g(y) \text{ for all } x\,, \end{cases} \tag{3.52}$$

where $g^{-1}(y)$ is defined to equal that value of x such that $g(x) = y$. Considering the functions in the theorem as

$$\sqrt{y} \equiv g(y)\,, \quad y^2 \equiv g^{-1}(y)\,, \quad f_X \equiv L^{-\alpha/2}_{\alpha/2}\,, \tag{3.53}$$

we have that the PDF of $\sqrt{\Lambda_{\alpha/2,1}}$ is

$$q(\ell) = 2\ell L^{-\alpha/2}_{\alpha/2}(\ell^2)\,. \tag{3.54}$$

3.2.4 The symmetric time-fractional case

The stochastic process whose PDF is the solution of the symmetric time-fractional diffusion equation is actually the gBm proposed by Schneider [37, 38].

3.2.5 Some special cases of the space-time fractional diffusion

(i) Brownian motion

In the case $\beta = 1$ and $\alpha = 2$, the classical Brownian motion is recovered, because $H = 1/2$ and each one of the two Lévy variables result to be distributed according to a delta function.

(ii) Time-fractional diffusion: $0 < \beta < 1$

In the special case $\alpha = 2$, we obtain the grey Brownian motion whose PDF is the solution of the time-fractional diffusion equation.

(iii) Space-fractional diffusion: $1 < \alpha < 2$

In the special case $\beta = 1$ and then $1 < \alpha < 2$, the PDF of the resulting process is the solution of a space-fractional diffusion equation,

$$\mathcal{P}(x;t) = \frac{1}{t^{1/\alpha}} L_\alpha\left(\frac{x}{t^{1/\alpha}}\right). \tag{3.55}$$

(iv) Neutral diffusion: $0 < \alpha = \beta < 1$

In the special case $0 < \alpha = \beta < 1$, the PDF of the resulting process is the solution of the neutral fractional diffusion equation, and this PDF is a generalization of the Cauchy/Lorentz distribution:

$$\mathcal{P}(x;t) = \frac{1}{\pi} \frac{(x/t)^{\alpha-1} \sin[\alpha\pi/2]}{1 + 2(x/t)^\alpha \cos[\alpha\pi/2] + (x/t)^{2\alpha}} . \tag{3.56}$$

4 Stochastic processes with nonstationary increments

4.1 Definitions

The stochastic process under consideration is [25]

$$X(t) = \sqrt{t^\alpha \Lambda_\beta}\, X_H(t) , \quad t \geq 0 , \, \alpha \geq -1 , \tag{4.1}$$

with $X(0) = 0$. Here, $X_H(t)$, $0 < H < 1$, is the fBm whose displacement variance, or ensemble-average MSD (EAMSD), and correlation function are [1]

$$\langle X_H^2(t) \rangle = 2 D_H t^{2H} , \tag{4.2}$$

$$\langle X_H(t) X_H(s) \rangle = D_H \big(t^{2H} + s^{2H} - |t - s|^{2H}\big) , \tag{4.3}$$

and Λ_β is an independent positive random variable distributed according to the one-side M-Wright/Mainardi function, with $0 < \beta < 1$, and its mean is $\langle \Lambda_\beta \rangle = 1/\Gamma(1+\beta)$. Note that when $\alpha = 0$, the stochastic process (4.1) reduces to the ggBm [29].

It is specially remarkable the fact that every parameter of the process, that is, H, β, and α, has a clear physical meaning. In particular, we show in the following that H controls the exponent of the power-law of the variance although it is affected by α. In the case of an underlying Gaussian diffusion, that is, $H = 1/2$, subdiffusion occurs when $\alpha < 0$ and superdiffusion when $\alpha > 0$. β is the only parameter which controls the ergodicity/nonergodicity transition. α determines the power-law of aging.

Then the EAMSD of the process $X(t)$ stated in (4.1) results to be

$$\langle X^2 \rangle = \frac{2D_H}{\Gamma(1+\beta)} t^{2H+\alpha}, \tag{4.4}$$

where the power-law of the growing in time is actually that of the fBm but affected by the parameter α with an increasing or decreasing effect according to its sign.

4.2 Probability density function

The PDF of the process results to be

$$\mathcal{P}(x;t) = \frac{1}{2t^{H+\alpha/2}} M_{\beta/2}\left(\frac{|x|}{t^{H+\alpha/2}}\right). \tag{4.5}$$

Special cases follow from special cases of the PDF and they are similar to the special cases of the ggBm. In particular, it is here we report the following:

(a) Brownian diffusion $\langle x^2 \rangle \sim t$ is obtained when $\alpha = -2H$ and that means, in the case of the fBm, that the process $X_{\alpha/2}(t)$ is not the Wiener process but it shows a certain correlation.

(b) Brownian diffusion $\langle x^2 \rangle \sim t$ with an exponential PDF is obtained in the case $\alpha = -2H$ and $\beta = 0$.

4.3 Ergodicity breaking

In order to investigate the ergodicity of the process, we study in the following the so-called Ergodicity Breaking (EB) parameter defined as

$$\mathrm{EB} = \lim_{T\to\infty} \frac{\langle (\overline{\delta_X^2(t_a,T,\Delta)})^2 \rangle}{\langle \overline{\delta_X^2(t_a,T,\Delta)} \rangle^2} - 1, \tag{4.6}$$

where

$$\overline{\delta_X^2(t_a,T,\Delta)} = \frac{\int_{t_a}^{t_a+T-\Delta} [X(\tau+\Delta) - X(\tau)]^2 d\tau}{T-\Delta} \tag{4.7}$$

is the temporal-average MSD (TAMSD) and T, Δ, and t_a stand for the measurement time, lag time, and aging time, respectively.

Using the definition of TAMSD, and formulae (4.2) and (4.3), we obtain the ensemble-average TAMSD (EATAMSD)

$$\langle\overline{\delta_X^2(t_a, T, \Delta)}\rangle = \frac{2D_H \int_{t_a}^{t_a+T-\Delta} f(\tau, \Delta) d\tau}{(T-\Delta)\Gamma(1+\beta)}, \tag{4.8}$$

where

$$f(\tau, \Delta) = (\tau+\Delta)^{2H+\alpha} + \tau^{2H+\alpha} - \tau^{\alpha/2}(\tau+\Delta)^{\alpha/2}\left[\tau^{2H} + (\tau+\Delta)^{2H} - \Delta^{2H}\right].$$

We introduce the Taylor expansion of $f(\tau, \Delta)$ with $\Delta/\tau \ll 1$,

$$f(\tau, \Delta) \underset{\Delta \ll \tau}{=} \tau^{\alpha}\Delta^{2H} + O\big((\Delta/\tau) \wedge (\Delta/\tau)^{2-2H}\big), \tag{4.9}$$

where $a \wedge b = \min\{a, b\}$.

If $-1 < \alpha$, then the integration in (4.8) reads

$$\int_{t_a}^{t_a+T-\Delta} f(\tau, \Delta) d\tau \simeq \Delta^{2H} \frac{(t_a + T - \Delta)^{\alpha+1} - t_a^{\alpha+1}}{\alpha+1},$$

and the EATAMSD can be approximated by [25]

$$\langle\overline{\delta_X^2(t_a, T, \Delta)}\rangle \underset{\Delta \ll t_a \ll T}{\simeq} \frac{2D_H \Delta^{2H} T^{\alpha}}{\Gamma(1+\beta)(1+\alpha)}. \tag{4.10}$$

This means that as long as the limit $T \to \infty$ holds, EATAMSD follows a power-law with exponent α, growing infinitely for positive α and tending to 0 for negative $\alpha \in (-1, 0)$. This provides aging effects in the trajectories generated by the proposed stochastic process and relates it with existing studies on diffusion in biological systems [39].

When $\alpha = 0$ and $\Lambda_\beta = 1$, the result obtained in [1] for the fBm is recovered

$$\langle\overline{\delta_{X_H}^2(t_a, T, \Delta)}\rangle = 2D_H \Delta^{2H}.$$

In the special case of $\alpha = -1$, the EATAMSD also tends to zero but with the following law [25]:

$$\langle\overline{\delta_X^2(t_a, T, \Delta)}\rangle \underset{\Delta \ll t_a \ll T}{\simeq} \frac{2D_H \Delta^{2H}}{\Gamma(1+\beta)} \frac{\ln T}{T}. \tag{4.11}$$

Since the limit in (4.6) does not depend on the value of t_a, to simplify notation, hereinafter we consider $\overline{\delta_X^2(T, \Delta)} \equiv \overline{\delta_X^2(0, T, \Delta)}$.

With reference to (4.6), we now consider

$$\langle (\overline{\delta_X^2(T,\Delta)})^2 \rangle = \frac{\int_0^{T-\Delta} d\tau_1 \int_0^{T-\Delta} d\tau_2\, G(\tau_1,\tau_2)}{(T-\Delta)^2},$$

where

$$G(\tau_1,\tau_2) = \left\langle [X(\tau_1+\Delta) - X(\tau_1)]^2 [X(\tau_2+\Delta) - X(\tau_2)]^2 \right\rangle . \tag{4.12}$$

Using the following formula for Gaussian process with zero mean [11]:

$$\begin{aligned}\langle x(t_1)\, x(t_2)\, x(t_3)\, x(t_4)\rangle &= \langle x(t_1)\, x(t_2)\rangle \langle x(t_3)\, x(t_4)\rangle \\ &\quad + \langle x(t_1)\, x(t_3)\rangle \langle x(t_2)\, x(t_4)\rangle \\ &\quad + \langle x(t_1)\, x(t_4)\rangle \langle x(t_2)\, x(t_3)\rangle ,\end{aligned}$$

it results that

$$G(\tau_1,\tau_2) \underset{\Delta \ll \tau_1,\tau_2}{\approx} G_0 ,$$

where

$$\begin{aligned} G_0 &= 4D_H^2 \Delta^{4H} \langle \Lambda_\beta^2 \rangle [\tau_1\tau_2(\tau_1+\Delta)(\tau_2+\Delta)]^{\alpha/2} \\ &\quad + 2D_H^2 \langle \Lambda_\beta^2 \rangle \{ |\tau_1 + \Delta - \tau_2|^{2H} \tau_2^{\alpha/2} (\tau_1+\Delta)^{\alpha/2} \\ &\quad - |\tau_1 - \tau_2|^{2H} [(\tau_1\tau_2)^{\alpha/2} + (\tau_1+\Delta)^{\alpha/2}(\tau_2+\Delta)^{\alpha/2}] \\ &\quad + |\tau_2 + \Delta - \tau_1|^{2H} \tau_1^{\alpha/2} (\tau_2+\Delta)^{\alpha/2} \}^2 . \end{aligned} \tag{4.13}$$

After the approximation,

$$(\tau_i + \Delta)^{\alpha/2} \approx \tau_i^{\alpha/2}\left(1 + \frac{\alpha}{2}\frac{\Delta}{\tau_i}\right), \quad i = \overline{1,2},$$

we have

$$\begin{aligned} G(\tau_1,\tau_2) = \langle \Lambda_\beta^2 \rangle \tau_1^\alpha \tau_2^\alpha [4D_H^2 \Delta^{4H} &+ 2D_H^2 \{ |\tau_1 + \Delta - \tau_2|^{2H} \\ &+ |\tau_2 + \Delta - \tau_1|^{2H} - 2|\tau_1 - \tau_2|^{2H} \}^2] , \end{aligned}$$

and finally

$$\langle (\overline{\delta_X^2(T,\Delta)})^2 \rangle = \frac{\langle \Lambda_\beta^2 \rangle 4 D_H^2}{(T-\Delta)^2} \times \left\{ \int_0^{T-\Delta}\int_0^{T-\Delta} d\tau_1\, d\tau_2\, \tau_1^\alpha \tau_2^\alpha \Delta^{4H} + \frac{I}{2} \right\} , \tag{4.14}$$

where

$$I = \int_0^{T-\Delta}\int_0^{T-\Delta} d\tau_1\, d\tau_2\, \tau_1^\alpha \tau_2^\alpha \{ |\tau_1 - \tau_2 + \Delta|^{2H} + |\tau_2 - \tau_1 + \Delta|^{2H} - 2|\tau_1 - \tau_2|^{2H} \}^2 .$$

According to the value of H, the integral I follows two different power-laws of Δ and T [25]:

$$I \sim \begin{cases} \Delta^{4H+1}\, T^{2\alpha+1}\,, & 0 < H < \frac{3}{4}\,, \\ \Delta^{4}\, T^{4H+2\alpha-2}\,, & \frac{3}{4} < H < 1\,. \end{cases} \tag{4.15}$$

The EB parameter can now be written as

$$\mathrm{EB} = \lim_{T\to\infty} \frac{\langle \Lambda_\beta^2 \rangle}{\langle \Lambda_\beta \rangle^2} \left[1 + \frac{(1+\alpha)^2 I}{2\Delta^{4H}\, T^{2\alpha+2}} \right] - 1\,. \tag{4.16}$$

Taking into account (4.15), it holds

$$\mathrm{EB} = \frac{\langle \Lambda_\beta^2 \rangle}{\langle \Lambda_\beta \rangle^2} - 1 = \frac{\beta \Gamma^2(\beta)}{\Gamma(2\beta)} - 1\,. \tag{4.17}$$

The second equality in (4.17) is obtained from the Mellin transform of M_β, that is, $\int_0^\infty \lambda^{s-1} M_\beta(\lambda) d\lambda = \Gamma[1+(s-1)]/\Gamma[1+\beta(s-1)]\,, s > 0$ [21]. We have that $\mathrm{EB} \neq 0\,, \forall \beta \in (0,1)$ and only in the limit $\beta \to 1$ the process becomes ergodic.

5 Conclusions and final remarks

In the present chapter, we have presented a modeling approach for fractional diffusion based on randomly-scaled Gaussian processes. When the Gaussian process is the fBm and the scales are distributed according to the M-Wright/Mainardi function, the ggBm is recovered.

The main features of this approach is that the distribution of the scales leads to non-Gaussian densities of particle displacement and then for proper choice of scale fluctuations fractional diffusion is modeled. Moreover, the fluctuations of the scale leads also to the ergodicity breaking. Hence, we observe that since the distribution of the scale fluctuations causes non-Gaussianity and ergodicity breaking we claim that fractional diffusion is a specific ergodicity breaking due to the population of scales that characterizes the random/complex medium where diffusion occurs.

With reference to definition (2.1), it is here reported that the formalism holds for any choice of $\ell_\beta = \ell_\beta(t)$, with $\langle \ell_\beta^2 \rangle \sim t^\alpha$, and of any Gaussian processes such that

$$\langle X^2 \rangle = \langle \ell_\beta^2 \rangle \langle X_G^2 \rangle \sim t^\alpha \langle X_G^2 \rangle \sim t^\gamma\,, \tag{5.1}$$

where α is equal to 0 or not if the process has stationary or nonstationary increments, respectively, and γ corresponds to the desired power law for the particle variance. In particular, when $\ell_\beta(t) = \sqrt{t^\alpha \Lambda_\beta}$ the process defined in (4.1) is recovered. The choice of the fBm as Gaussian process, that is, $X_G(t) = X_H(t)$, is only the most simple choice for meeting this constraint.

The present approach has been used to model anomalous diffusion in biological systems [26]. In particular, the proposed stochastic process interpolates between the fBm and the CTRW, generating nonergodicity and nontrivial p-variation, as it is observed in experimental data [15]. Recently, it has been compared against the so-called approach *diffusion diffusivity* in [43], and again in view of the application in biological systems.

Bibliography

[1] W. Deng and E. Barkai, Ergodic properties of fractional Brownian–Langevin motion, *Phys. Rev. E*, **79** (2009), 011112.

[2] A. Erdélyi, On fractional integration and its applications to the theory of Hankel transforms, *Q. J. Math. Oxford*, **11** (1940), 293–303.

[3] W. Feller, *An Introduction to Probability Theory and Its Applications, vol. 2*, 2nd ed., Wiley, New York, 1971.

[4] R. Gorenflo and F. Mainardi, Subordination pathways to fractional diffusion, *Eur. Phys. J. Spec. Top.*, **193** (2011), 119–132.

[5] R. Gorenflo and F. Mainardi, Parametric subordination in fractional diffusion processes, in J. Klafter, S. C. Lim, and R. Metzler (eds.), *Fractional Dynamics. Recent Advances*, pp. 227–261, World Scientific, Singapore, 2012.

[6] R. Gorenflo, Yu. Luchko, and F. Mainardi, Analytical properties and applications of the Wright function, *Fract. Calc. Appl. Anal.*, **2** (1999), 383–414.

[7] R. Gorenflo, Yu. Luchko, and F. Mainardi, Wright functions as scale-invariant solutions of the diffusion-wave equation, *J. Comput. Appl. Math.*, **118** (2000), 175–191.

[8] Y. He, S. Burov, R. Metzler, and E. Barkai, Random time-scale invariant diffusion and transport coefficients, *Phys. Rev. Lett.*, **101** (2008), 058101.

[9] V. Kiryakova, *Generalized Fractional Calculus and Applications*, Longman Scientific & Technical/John Wiley & Sons Inc., Harlow/New York, Pitman Research Notes in Mathematics, vol. 301 1994.

[10] H. Kober, On a fractional integral and derivative, *Q. J. Math. Oxford*, **11** (1940), 193–211.

[11] R. Kubo, M. Toda, and N. Hashitsume, *Statistical Physics II: Nonequilibrium Statistical Mechanics*, vol. 31, Springer Science & Business Media, 2012.

[12] A. Lubelski, I. M. Sokolov, and J. Klafter, Nonergodicity mimics inhomogeneity in single particle tracking, *Phys. Rev. Lett.*, **100** (2008), 250602.

[13] Yu. Luchko, Operational rules for a mixed operator of the Erdélyi–Kober type, *Fract. Calc. Appl. Anal.*, **7** (2004), 339–364.

[14] Yu. Luchko and J. Trujillo, Caputo-type modification of the Erdélyi–Kober fractional derivative, *Fract. Calc. Appl. Anal.*, **10** (2007), 249–267.

[15] M. Magdziarz and J. Klafter, Detecting origins of subdiffusion: p-variation test for confined systems, *Phys. Rev. E*, **82**(1) (2010), 011129.

[16] M. Magdziarz, A. Weron, K. Burnecki, and J. Klafter, Fractional Brownian motion versus the Continuous-Time Random Walk: A simple test for subdiffusive dynamics, *Phys. Rev. Lett.*, **103** (2009), 180602.

[17] F. Mainardi, Fractional relaxation-oscillation and fractional diffusion-wave phenomena, *Chaos Solitons Fractals*, **7** (1996), 1461–1477.
[18] F. Mainardi, *Fractional Calculus and Waves in Linear Viscoelasticity*, Imperial College Press, 2010.
[19] F. Mainardi and G. Pagnini, The role of the Fox–Wright functions in fractional sub-diffusion of distributed order, *J. Comput. Appl. Math.*, **207** (2007), 245–257.
[20] F. Mainardi, Yu. Luchko, and G. Pagnini, The fundamental solution of the space-time fractional diffusion equation, *Fract. Calc. Appl. Anal.*, **4**(2) (2001), 153–192.
[21] F. Mainardi, G. Pagnini, and R. Gorenflo, Mellin transform and subordination laws in fractional diffusion processes, *Fract. Calc. Appl. Anal.*, **6**(4) (2003), 441–459.
[22] F. Mainardi, G. Pagnini, and R. K. Saxena, Fox H functions in fractional diffusion, *J. Comput. Appl. Math.*, **178** (2005), 321–331.
[23] F. Mainardi, G. Pagnini, and R. Gorenflo, Mellin convolution for subordinated stable processes, *J. Math. Sci.*, **132**(5) (2006), 637–642.
[24] F. Mainardi, A. Mura, and G. Pagnini, The M-Wright function in time-fractional diffusion processes: A tutorial survey, *Int. J. Differ. Equ.*, **2010** (2010), 104505.
[25] D. Molina-García, T. M. Pham, and G. Pagnini, A stochastic process for the puzzling framework of anomalous diffusion in biological systems, in V. Mladenov (ed.), *Non-Linear Systems, Nanotechnology (Proceedings of the 14th International Conference on Non-Linear Analysis, Non-Linear Systems and Chaos (NOLASC'15), Rome, Italy, November 7–9, 2015)*, Recent Advances in Electrical Engineering Series, vol. 55, pp. 75–80, WSEAS Press, 2015, ISSN: 1790-5117, ISBN: 978-1-61804-345-0.
[26] D. Molina-García, T. Minh Pham, P. Paradisi, C. Manzo, and G. Pagnini, Fractional kinetics emerging from ergodicity breaking in random media, *Phys. Rev. E*, **94** (2016), 052147.
[27] A. Mura, *Non-Markovian Stochastic Processes and Their Applications: From Anomalous Diffusion to Time Series Analysis*, Lambert Academic Publishing, 2011; Ph.D. Thesis, Physics Department, University of Bologna, defended in 2008.
[28] A. Mura and F. Mainardi, A class of self-similar stochastic processes with stationary increments to model anomalous diffusion in physics, *Integral Transforms Spec. Funct.*, **20**(3–4) (2009), 185–198.
[29] A. Mura and G. Pagnini, Characterizations and simulations of a class of stochastic processes to model anomalous diffusion, *J. Phys. A, Math. Theor.*, **41** (2008), 285003.
[30] A. Mura, M. S. Taqqu, and F. Mainardi, Non-Markovian diffusion equations and processes: Analysis and simulations, *Physica A*, **387** (2008), 5033–5064.
[31] T. Neusius, I. M. Sokolov, and J. C. Smith, Subdiffusion in time-averaged, confined random walks, *Phys. Rev. E*, **80** (2009), 011109.
[32] G. Pagnini, The evolution equation for the radius of a premixed flame ball in fractional diffusive media, *Eur. Phys. J. Spec. Top.*, **193** (2011), 105–117.
[33] G. Pagnini, Erdélyi–Kober fractional diffusion, *Fract. Calc. Appl. Anal.*, **15**(1) (2012), 117–127.
[34] G. Pagnini and P. Paradisi, A stochastic solution with Gaussian stationary increments of the symmetric space-time fractional diffusion equation, *Fract. Calc. Appl. Anal.*, **19**(2) (2016), 408–440.
[35] G. Pagnini, A. Mura, and F. Mainardi, Two-particle anomalous diffusion: Probability density functions and self-similar stochastic processes, *Philos. Trans. R. Soc. A*, **371** (2013), 20120154.
[36] I. Podlubny, *Fractional Differential Equations*, Academic Press, San Diego, 1999.
[37] W. R. Schneider, Grey noise, in *Stochastic Processes, Physics and Geometry*, pp. 676–681, World Scientific, Teaneck, 1990.
[38] W. R. Schneider, Grey noise, in *Ideas and Methods in Mathematical Analysis, Stochastics, and Applications, vol. I*, pp. 261–282, Cambridge University Press, Cambridge, 1992.

[39] J. H. P. Schulz, E. Barkai, and R. Metzler, Aging effects and population splitting in single-particle trajectory averages, *Phys. Rev. Lett.*, **110** (2013), 020602.
[40] I. N. Sneddon, *Mixed Boundary Value Problems in Potential Theory*, North–Holland Publ., Amsterdam, 1966.
[41] I. N. Sneddon, The use in mathematical analysis of the Erdélyi–Kober operators and some of their applications, in *Lecture Notes in Mathematics*, vol. 457, pp. 37–79, Springer-Verlag, New York, 1975.
[42] I. N. Sneddon, *The Use of Operators of Fractional Integration in Applied Mathematics*, RWN – Polish Sci. Publ., Warszawa, Poznan, 1979.
[43] V. Sposini, A. V. Chechkin, F. Seno, G. Pagnini, and R. Metzler, Random diffusivity from stochastic equations: comparison of two models for Brownian yet non-Gaussian diffusion, *New J. Phys.*, **20** (2018), 043044.

Nick Laskin

Nonlocal quantum mechanics: fractional calculus approach

Abstract: We show that a quantum system with long-range interparticle interaction can be described by invoking fractional calculus tools. The system under consideration is nonlocal exciton-phonon quantum dynamics on a 1D lattice.

It has been shown that long-range power-law exciton-exciton interaction leads to a nonlocal integral term in the motion equation of an exciton subsystem if we go from discrete to continuous space. In some particular cases for power-law interaction with noninteger power, the nonlocal integral term can be expressed through a spatial derivative of fractional order.

Considering exciton-phonon dynamics with long-range exciton-exciton interaction, we have obtained the system of two coupled equations, where one is the quantum fractional differential equation for the exciton subsystem while the other is a standard differential equation for the phonon subsystem. It has been found that the system of two coupled equations can be further simplified to come up with the following fractional nonlinear equations of motion: nonlinear fractional Schrödinger equation, nonlinear Hilbert–Schrödinger equation, fractional generalization of Zakharov system, and fractional Ginzburg–Landau equation.

The appearance of fractional differential equations in the continuum limit of lattice dynamics allows us to apply powerful tools of fractional calculus to study nonlocal quantum phenomena.

Keywords: Quantum nonlocal lattice dynamics, long-range interaction, fractional nonlinear Schrödinger equation, fractional Ginzburg–Landau equation, quantum lattice propagator

PACS: 03.65.-w, 03.65.Db, 05.30.-d, 05.40.Fb

1 Introduction

Our intention is to show that a quantum system with nonlocal interparticle interaction can be described by invoking fractional calculus tools. The system under consideration is nonlocal exciton-phonon quantum dynamics on 1D lattice.

Lattice dynamics is a very popular model of classical and quantum physics, applicable to study a broad set of physical phenomena and systems. The first 1D lattice model was introduced a long time ago by Frenkel and Kontorova [13] to study the structure and dynamics of dislocations in metals (for more details, see review

Nick Laskin, TopQuark Inc., Toronto, ON, Canada, e-mail: nlaskin@rocketmail.com

[4] and references therein). The Frenkel and Kontorova discrete classical dynamics is described as a 1D chain of atoms with the nearest-neighbor interatomic interaction and a periodic on-site potential. In the original Frenkel and Kontorova paper [13], the nearest-neighbor interatomic interaction is taken to be harmonic and on-site potential to be sinusoidal with a period commensurate to the equilibrium distance between atoms on the lattice. Despite its simplicity, the model has many applications in solid-state and nonlinear physics, including propagation of charge-density waves, the dynamics of absorbed layers of atoms on crystal surfaces, commensurable-incommensurable phase transitions, and the static and dynamical properties of domain walls in magnetically ordered structures; see for details [4, 5]. Moreover, the model is very attractive because it provides exactly integrable cases including the well-known sine-Gordon nonlinear equation in continuous approximation [5]. For this reason, the Frenkel–Kontorova model is also known as the "discrete sine-Gordon"equation. Since the Fermi, Pasta, and Ulam work [10], analytical developments and numerical simulation on discrete nonlinear dynamical equations have discovered numerous types of nonlinear excitations with various physical properties: solitons, continuous and discrete breathers [4, 11, 12], self-trapping states [42], and others.

Nonlocal dynamics can be modeled as a lattice model with long-range interatomic interaction. Examples include ferromagnetic chains [32], exciton transfer [8, 40], commensurable-incommensurable phase transitions [35], and the theory of Josephson junctions [3]. To model the long-range interaction in 1D lattice, a few potentials have been applied: power-law interaction [35], Lennard-Jones long-range coupling [16], and exponential interaction of Kac–Beker form [17]. Long-range coupling can be presented as nonlocality with finite space scale a if the coupling energy is proportional to $\exp(-|x_n - x_m|/a)$ for atoms located at the points x_n and x_m, or with scale-free interaction if the coupling energy is proportional to $|x_n - x_m|^{-s}$ $(s > 0)$. In addition to the well-known interaction with integer values of s, some complex media can be described by fractional values of s (see references in [46]).

Here, we present analytical developments on nonlocal quantum mechanics considering 1D exciton-phonon dynamics with long-range power-law exciton-exciton interaction. The long-range interaction leads in general to a nonlocal term in the quantum equation of motion if we go from discrete to continuous space. It has been shown that for power-law interaction with noninteger power s the nonlocal term can be expressed through a fractional order derivative. In other words, nonlocality originating from the long-range power-law interaction is revealed in the dynamical equations in the form of space derivatives of fractional order. The appearance of fractional differential equations in the continuum limit of lattice dynamics allows us to apply powerful tools of fractional calculus [14, 15, 18, 19, 30, 31, 33, 34, 37–39, 41, 45] to study nonlocal quantum dynamics.

In the early 1970s, a novel mechanism for the localization and transport of vibrational energy in certain types of molecular chains was proposed by A. S. Davydov [6] using a 1D lattice exciton-phonon model with nearest-neighbor exciton-exciton interaction. He pioneered the concept of the solitary excitons or the Davydov's solitons [9]. Our focus is analytical developments on nonlocal quantum 1D exciton-phonon dynamics with power-law long-range exciton-exciton interaction $\mathcal{J}_{n,m} = \mathcal{J}/|n-m|^s$, ($s > 0$) with interaction constant $\mathcal{J}$ for excitons located at lattice sites n and m. Using the ideas first developed by Laskin and Zaslavsky [27], we elaborate the Davydov model for the exciton-phonon system with a long-range power-law exciton-exciton interaction. It has been shown that 1D lattice nonlocal exciton-phonon dynamics in the long-wavelength approximation can be effectively presented by the system of two coupled equations for exciton and phonon subsystems. The dynamical equation describing the exciton subsystem is the fractional differential equation, which is a manifestation of nonlocality of interaction originating from the long-range interaction term. The dynamical equation describing the phonon subsystem is the differential equation. From this system of two coupled equations, we obtain fundamental fractional nonlinear equations of nonlocal quantum mechanics. They are: nonlinear fractional Schrödinger equation, nonlinear Hilbert–Schrödinger equation, fractional generalization of Zakharov system, fractional Ginzburg–Landau equation [25].

The impact of exciton-exciton long-range interaction on quantum lattice propagators has been studied. It has been found that the exciton propagator exhibits transition from the well-known Gaussian-like behavior to a power-law decay at some critical value of the power-law exponent. This transition can be treated as a phase transition accompanied by an infinite growth of the exciton's correlation length. The fractional Schrödinger equation has been derived for exciton propagator in the case of continuum space.

The nonlocal 1D quantum lattice dynamics with long-range interaction initiates a random walk in the imaginary time domain. It has been found that the transition probability of this random walk follows a fractional diffusion equation. The fractional diffusion equation has been obtained for transition probability of the random walk. It has been found that the newly introduced random walk model exhibits a cross-over from the Brownian random walk ($s > 3$) with finite correlation length to the symmetric α-stable Lévy random process ($\alpha = s - 1$ and $2 < s < 3$) with an infinite correlation length.

The paper is organized as follows. In Section 2, we introduce nonlocal quantum dynamics by considering 1D exciton-phonon dynamics—Davydov's model with long-range exciton-exciton interaction. Discrete motion equations for exciton and phonon subsystems have been developed. Section 3 presents transforms to go from discrete to continuum space in a long wave limit. It has been shown in Section 4 that depending on the long-range interaction parameter s, which is responsible for nonlocality of the interaction, the resulting quantum dynamical equations can be expressed in fractional differential form. The following fractional nonlinear dynamical equations have been developed: fractional nonlinear Schrödinger equation, nonlinear Hilbert–Schrödinger equation, fractional generalization of Zakharov system, fractional Ginzburg–Landau equation. The dimensionless form of all those equations was obtained and discussed.

The quantum nonlocal lattice propagator is introduced in Section 5. It has been found that depending on the parameter s the exciton propagator exhibits a transition from the well-known local Gaussian-like behavior to nonlocal power-law decay due to long-range exciton-exciton interaction. We show a link between the quantum lattice dynamics and random walk in the imaginary time domain. It has been found that the newly introduced random walk model exhibits a cross-over from the Brownian random walk ($s > 3$) to the symmetric α-stable Lévy random process ($\alpha = s - 1$ and $2 < s < 3$).

In the Appendix, the polylogarithm function and its series expansion are discussed.

The conclusion outlines our new developments and results on application of fractional calculus to study dynamical equations of nonlocal quantum mechanics.

2 Nonlocal quantum dynamics

2.1 Exciton-phonon system

To model 1D quantum lattice dynamics, let us consider a linear, rigid arrangement of sites with one molecule at each lattice site. Then, Davydov's Hamiltonian $\widehat{H}$ [7, 8] reads

$$\widehat{H} = \widehat{H}_{\text{ex}} + \widehat{H}_{\text{ph}} + \widehat{H}_{\text{int}}, \tag{1}$$

where $\widehat{H}_{\text{ex}}$ is exciton Hamilton operator, which describes quantum dynamics of intramolecular excitations, or simply excitons, $\widehat{H}_{\text{ph}}$ is phonon Hamiltonian operator which describes displacements of molecules from their equilibrium states or, in other words, the lattice vibrations, and H_{int} is the exciton-phonon operator which describes interaction of molecular excitations (excitons) with their displacements (lattice vibrations).

The exciton Hamiltonian H_{ex} is

$$\widehat{H}_{\text{ex}} = \varepsilon \sum_{n=-\infty}^{\infty} b_n^+ b_n - \mathcal{J} \sum_{n=-\infty}^{\infty} (b_n^+ b_{n+1} + b_n^+ b_{n-1}). \tag{2}$$

Here, b_n^+ is creation and b_n is annihilation operators of an excitation on a molecule on site n, parameter ε is exciton energy and $\mathcal{J}$ is interaction constant.

Operators b_n^+ and b_n satisfy the commutation relations $[b_n, b_m^+] = \delta_{n,m}$, $[b_n, b_m] = 0$, $[b_n^+, b_m^+] = 0$.

Alternatively, the Hamiltonian H_{ex} can be written as

$$\widehat{H}_{\text{ex}} = \varepsilon \sum_{n=-\infty}^{\infty} b_n^+ b_n - \sum_{n,m=-\infty}^{\infty} \mathcal{J}_{n,m} b_n^+ b_m, \tag{3}$$

if we introduce exciton transfer matrix $\mathcal{J}_{n,m}$, which describes exciton-exciton interaction,

$$\mathcal{J}_{n,m} = \mathcal{J}(\delta_{(n+1),m} + \delta_{(n-1),m}), \tag{4}$$

where the Kronecker symbols $\delta_{(n+1),m}$ mean that only the nearest-neighbor sites have been considered. In other words, the interaction term $\mathcal{J}_{n,m}b_n^+b_m$ in equation (3) is responsible for transfer from site n to the nearest-neighbor sites $n \pm 1$.

The phonon Hamiltonian H_{ph} is

$$\widehat{H}_{\text{ph}} = \sum_{n=-\infty}^{\infty}\left(\frac{\widehat{p}_n^2}{2\text{m}} + \frac{w}{2}(\widehat{u}_{n+1} - \widehat{u}_n)^2\right), \tag{5}$$

where w is the elasticity constant of the 1D lattice, and $\widehat{u}_n$ is the operator of displacement of a molecule from its equilibrium position on the site n, $\widehat{p}_n$ is the momentum operator of a molecule on site n, and m is molecular mass.

The exciton-phonon Hamiltonian $\widehat{H}_{\text{int}}$, which describes the coupling between internal molecular excitations with their displacements, has the form

$$\widehat{H}_{\text{int}} = \frac{\chi}{2}\sum_{n=-\infty}^{\infty}(\widehat{u}_{n+1} - \widehat{u}_n)b_n^+b_n, \tag{6}$$

with the coupling constant χ.

To extend Davydov's model and go beyond the nearest-neighbor interaction we introduce, following Laskin [25], the power-law interaction between excitons on sites n and m. Thus, to study long-range exciton-exciton interaction we introduce exciton transfer matrix $\mathcal{J}_{n,m}$ given by

$$\mathcal{J}_{n-m} = \frac{\mathcal{J}}{|n-m|^s}, \quad n \neq m, \tag{7}$$

where $\mathcal{J}$ is the interaction constant and parameter s covers different physical models; the nearest-neighbor approximation ($s = \infty$), the dipole-dipole interaction ($s = 3$), the Coulomb potential ($s = 1$). Our main interest will be in fractional values of s that can appear for more sophisticated interaction potentials attributed to complex media.

Aiming to obtain a system of coupled dynamical equations for the exciton-photon system under consideration, we introduce Davydov's ansatz.

2.2 Davydov's ansatz

To study the quantum system described by equation (1) with exciton transfer matrix given by equation (7), we introduce quantum state vector $|\phi(t)\rangle$ following [7] (see, also [40]):

$$|\phi(t)\rangle = |\Psi(t)\rangle|\Phi(t)\rangle, \tag{8}$$

where quantum vectors $|\Psi(t)\rangle$ and $|\Phi(t)\rangle$ are defined by

$$|\Psi(t)\rangle = \sum_n \psi_n(t) b_n^+ |0\rangle_{\text{ex}} \tag{9}$$

and

$$|\Phi(t)\rangle = \exp\left\{-\frac{i}{\hbar}\sum_n (\xi_n(t)\widehat{p}_n - \eta_n(t)\widehat{u}_n)\right\}|0\rangle_{\text{ph}}, \tag{10}$$

here $\hbar$ is Planck's constant, $|0\rangle_{\text{ex}}$ and $|0\rangle_{\text{ph}}$ are vacuum states of the exciton and phonon subsystems and $\xi_n(t)$ is the diagonal matrix element of the displacement operator $\widehat{u}_n$ in the basis defined by equation (8), while $\eta_n(t)$ is diagonal matrix element of the momentum operator $\widehat{p}_n$ in the same basis, that is,

$$\xi_n(t) = \langle \phi(t)|\widehat{u}_n|\phi(t)\rangle, \quad \eta_n(t) = \langle \phi(t)|\widehat{p}_n|\phi(t)\rangle. \tag{11}$$

The displacement $\widehat{u}_n$ and momentum $\widehat{p}_n$ operators satisfy the commutation relations

$$[\widehat{u}_n, \widehat{p}_m] = i\hbar\delta_{n,m}, \tag{12}$$

where $\hbar$ is Planck's constant and $\delta_{n,m}$ is the Kronecker symbol,

$$\delta_{n,m} = \begin{cases} 1 & n = m, \\ 0 & n \neq m. \end{cases}$$

The state vector $|\phi(t)\rangle$ satisfies the normalization condition

$$\langle \phi(t)|\phi(t)\rangle = \sum_n |\psi_n(t)|^2 = N, \tag{13}$$

with $|\psi_n(t)|^2$ being the probability to find exciton on the n^{th} site and N is the total number of excitons.

Therefore, the quantum dynamics of the exciton-photon system with Hamiltonian given by equation (1) can be described in terms of the functions $\psi_n(t)$, $\xi_n(t)$ and $\eta_n(t)$. In other words, Davydov's ansatz defined by equation (8)–(11) allows us to go from the quantum Hamilton operator introduced by equation (1) to the classical Hamiltonian function developed below. In the basis of the vectors $|\phi(t)\rangle$, the Hamilton operators $\widehat{H}_{\text{ex}}$, $\widehat{H}_{\text{ph}}$, and $\widehat{H}_{\text{int}}$ become the functions $H_{\text{ex}}(\psi_n, \psi_n^*)$, $H_{\text{ph}}(\xi_n, \eta_n)$, and $H_{\text{int}}(\psi_n, \psi_n^*, \xi_n)$ of classical dynamical variables $\psi_n(t)$, $\psi_n^*(t)$, $\xi_n(t)$, and $\eta_n(t)$.

Thus, the function $H_{\text{ex}}(\psi_n, \psi_n^*)$ is introduced as

$$\begin{aligned} H_{\text{ex}}(\psi_n, \psi_n^*) &= \langle \phi(t)|\widehat{H}_{\text{ex}}|\phi(t)\rangle \\ &= \varepsilon \sum_{n=-\infty}^{\infty} \psi_n^*(t)\psi_n(t) - \sum_{n,m=-\infty}^{\infty} \mathcal{J}_{n-m}\psi_n^*(t)\psi_m(t), \end{aligned} \tag{14}$$

here J_{n-m} given by equation (7) describes the nonlocal exciton-exciton interaction.

The function $H_{\text{ph}}(\xi_n, \eta_n)$ introduced as

$$H_{\text{ph}}(\xi_n, \eta_n) = \langle \phi(t)|\widehat{H}_{\text{ph}}|\phi(t)\rangle = \sum_{n=-\infty}^{\infty}\left(\frac{\eta_n^2}{2\text{m}} + \frac{w}{2}(\xi_{n+1} - \xi_n)^2\right) \tag{15}$$

is Hamiltonian function of phonon subsystem.

The function $H_{\text{int}}(\psi_n, \psi_n^*, \xi_n)$ introduced as

$$H_{\text{int}}(\psi_n, \psi_n^*, \xi_n) = \langle \phi(t)|\widehat{H}_{\text{int}}|\phi(t)\rangle = \frac{\chi}{2}\sum_{n=-\infty}^{\infty}(\xi_{n+1} - \xi_n)\psi_n^*(t)\psi_n(t), \tag{16}$$

describes interaction of exciton and phonon subsystems.

Combining together equations (14)–(16), we obtain the Hamiltonian function $H(\psi_n, \psi_n^*, \xi_n, \eta_n)$ of the exciton-phonon system under consideration

$$\begin{aligned} H(\psi_n, \psi_n^*, \xi_n, \eta_n) &= \langle \phi(t)|\widehat{H}|\phi(t)\rangle \\ &= H_{\text{ex}}(\psi_n, \psi_n^*) + H_{\text{ph}}(\xi_n, \eta_n) + H_{\text{int}}(\psi_n, \psi_n^*, \xi_n) \\ &= \varepsilon \sum_{n=-\infty}^{\infty} \psi_n^*(t)\psi_n(t) - \sum_{n,m=-\infty}^{\infty} \mathcal{J}_{n-m}\psi_n^*(t)\psi_m(t) \\ &\quad + \sum_{n=-\infty}^{\infty}\left(\frac{\eta_n^2}{2\text{m}} + \frac{w}{2}(\xi_{n+1} - \xi_n)^2\right) \\ &\quad + \frac{\chi}{2}\sum_{n=-\infty}^{\infty}(\xi_{n+1} - \xi_n)\psi_n^*(t)\psi_n(t). \end{aligned} \tag{17}$$

Having the Hamiltonian function $H(\psi_n, \psi_n^*, \xi_n, \eta_n)$, we can develop the motion equations for dynamical variables $\psi_n(t)$, $\psi_n^*(t)$, $\xi_n(t)$ and $\eta_n(t)$.

2.3 Nonlocal discrete equations of motion

Following [7] and identifying conjugate coordinates and momenta from the set of dynamical variables $\psi_n(t)$, $\psi_n^*(t)$, $\xi_n(t)$, and $\eta_n(t)$, we come up with the system of motion equations in terms of variational derivatives $\delta/\delta\psi_n^*(t)$, $\delta/\delta\psi_n(t)$, $\delta/\delta\eta_n(t)$, and $\delta/\delta\xi_n(t)$. For the variable $\psi_n(t)$, the motion equation is

$$i\hbar\frac{\partial\psi_n(t)}{\partial t} = \frac{\delta}{\delta\psi_n^*(t)}H(\psi_n, \psi_n^*, \xi_n, \eta_n). \tag{18}$$

For the complex conjugate variable $\psi_n^*(t)$, we have

$$i\hbar\frac{\partial\psi_n^*(t)}{\partial t} = -\frac{\delta}{\delta\psi_n(t)}H(\psi_n, \psi_n^*, \xi_n, \eta_n). \tag{19}$$

For the coordinate $\xi_n(t)$, the motion equation reads

$$\frac{\partial \xi_n(t)}{\partial t} = \frac{\delta}{\delta \eta_n(t)} H(\psi_n, \psi_n^*, \xi_n, \eta_n), \tag{20}$$

and for conjugate momenta $\eta_n(t)$ the motion equation is

$$\frac{\partial \eta_n(t)}{\partial t} = -\frac{\delta}{\delta \xi_n(t)} H(\psi_n, \psi_n^*, \xi_n, \eta_n), \tag{21}$$

here $H(\psi_n, \psi_n^*, \xi_n, \eta_n)$ is given by equation (16).

For our purposes, we will need the system of dynamical equations for $\psi_n(t)$, $\xi_n(t)$ and $\eta_n(t)$. Calculating the variational derivatives yields the following system of three coupled equations:

$$i\hbar \frac{\partial \psi_n(t)}{\partial t} = \Lambda \psi_n(t) - \sum_{\substack{m \\ (n \neq m)}} \mathcal{J}_{n-m} \psi_m(t) + \frac{\chi}{2}(\xi_{n+1} - \xi_n)\psi_n(t), \tag{22}$$

$$\frac{\partial \xi_n(t)}{\partial t} = \frac{\eta_n}{\mathrm{m}}, \tag{23}$$

and

$$\frac{\partial \eta_n(t)}{\partial t} = w(\xi_{n+1}(t) - 2\xi_n(t) + \xi_{n-1}(t)) + \frac{\chi}{2}(|\psi_{n+1}(t)^2| - |\psi_n(t)^2|), \tag{24}$$

where the constant Λ is introduced by

$$\Lambda = \varepsilon + \frac{1}{2} \sum_{n=-\infty}^{\infty} \left\{ \mathrm{m} \left(\frac{\partial \xi_n(t)}{\partial t} \right)^2 + w(\xi_{n+1} - \xi_n)^2 \right\}.$$

Further, substituting $\eta_n(t)$ from equation (23) into equation (24) yields

$$\mathrm{m} \frac{\partial^2 \xi_n(t)}{\partial t^2} = w(\xi_{n+1} - 2\xi_n + \xi_{n-1}) + \frac{\chi}{2}(|\psi_{n+1}(t)|^2 - |\psi_n(t)|^2). \tag{25}$$

Our focus now is the system of two coupled discrete dynamical equations (22) and (25).

3 From lattice to continuum

To go from discrete equations (22) and (25) to their continuum versions, we introduce function $\varphi(k, t)$

$$\varphi(k, t) = \sum_{n=-\infty}^{\infty} a e^{-ikna} \psi_n(t), \tag{26}$$

and function $v(k,t)$

$$v(k,t) = \sum_{n=-\infty}^{\infty} ae^{-ikna}\xi_n(t), \tag{27}$$

where $\psi_n(t)$ is related to $\varphi(k,t)$ as follows:

$$\psi_n(t) = \frac{1}{2\pi}\int_{-\pi}^{\pi} dke^{ikna}\varphi(k,t), \tag{28}$$

and $\xi_n(t)$ is related to $v(k,t)$ as follows

$$\xi_n(t) = \frac{1}{2\pi}\int_{-\pi}^{\pi} dke^{ikna}v(k,t). \tag{29}$$

Here, a is the lattice parameter, $a > 0$.

To go from lattice to continuum media, we consider the long-wavelength approximation when wavelength $\lambda = 2\pi/k$ exceeds the scale na, $k \ll (na)^{-1}$. In this case, we can substitute

$$\psi_n(t) \underset{k\ll(na)^{-1}}{\longrightarrow} \psi(x,t), \tag{30}$$

and

$$\xi_n(t) \underset{k\ll(na)^{-1}}{\longrightarrow} \xi(x,t), \tag{31}$$

where x is continuous variable, $x = na$. Then we expand the integration in equations (28) and (29) over the whole k space,

$$\frac{1}{2\pi}\int_{-\pi}^{\pi} dke^{ikna}\cdots \underset{k\ll(na)^{-1}}{\longrightarrow} \frac{1}{2\pi}\int_{-\infty}^{\infty} dke^{ikx}\cdots. \tag{32}$$

Therefore, from equations (28) and (29) we obtain

$$\psi(x,t) = \frac{1}{2\pi}\int_{-\infty}^{\infty} dke^{ikx}\varphi(k,t) \tag{33}$$

and

$$\xi(x,t) = \frac{1}{2\pi}\int_{-\infty}^{\infty} dke^{ikx}v(k,t). \tag{34}$$

Now we see that we can substitute

$$\sum_{n=-\infty}^{\infty} ae^{-ikna}\cdots \underset{k\ll(na)^{-1}}{\longrightarrow} \int_{-\infty}^{\infty} dxe^{ikx}\cdots \tag{35}$$

in equations (26) and (27). It gives us the following two equations:

$$\varphi(k,t) = \int_{-\infty}^{\infty} dx e^{-ikx}\psi(x,t) \tag{36}$$

and

$$\nu(k,t) = \int_{-\infty}^{\infty} dx e^{-ikx}\xi(x,t) \tag{37}$$

for the functions $\varphi(k,t)$ and $\nu(k,t)$ involved into equations (33) and (34).

Thus, equations (30), (31), and (32), (35) present the mapping to go from lattice to continuum space.

3.1 Nonlocal motion equations in continuum space

In terms of the functions $\psi(x,t)$ and $\xi(x,t)$ introduced by equations (33) and (34) the discrete equations (22) and (25) become continuous equations of motion

$$\begin{aligned} i\hbar\frac{\partial\psi(x,t)}{\partial t} &= \lambda\psi(x,t) \\ &\quad - \int_{-\infty}^{\infty} dy \frac{\partial}{\partial x} K(x-y)\frac{\partial}{\partial y}\psi(y,t) + \chi\frac{\partial\xi(x,t)}{\partial x}\psi(x,t), \end{aligned} \tag{38}$$

and

$$\mathrm{m}\frac{\partial^2\xi(x,t)}{\partial t^2} = w\frac{\partial^2\xi(x,t)}{\partial x^2} + \chi\frac{\partial|\psi(x,t)|^2}{\partial x}. \tag{39}$$

Quantum equation (38) is nonlocal due to the presence of the integral term. The kernel $K(x)$ in the integral term of equation (38) has the form

$$K(x) = \frac{1}{\pi}\int_{-\infty}^{\infty} dk e^{ikx}\frac{\mathcal{V}(k)}{k^2},$$

where the function $\mathcal{V}(k)$ is introduced as

$$\mathcal{V}(k) = \mathcal{J}(0) - \mathcal{J}(k), \tag{40}$$

and $\mathcal{J}(k)$ is defined by

$$\mathcal{J}(k) = \sum_{\substack{n=-\infty \\ (n\neq 0)}}^{\infty} e^{-ikna}\mathcal{J}_n, \tag{41}$$

with $\mathcal{J}_n$ given by equation (7) and, $\lambda = \Lambda - J(0)$.

Thus, we come to a new system of coupled dynamical equations (38) and (39) to model 1D exciton phonon dynamics with long-range exciton-exciton interaction introduced by equation (7). The field $\psi(x,t)$ describes the exciton sub-system, while the field $\xi(x,t)$ describes the phonon sub-system. Equation (38) is the integro-differential equation while equation (39) is the differential one. The integral term in equation (38) originates from nonlocal long-range exciton-exciton interaction term—the second term in $H_{\text{ex}}(\psi_n, \psi_n^*)$ introduced by equation (14).

4 Fractional nonlinear quantum equations

To transform the system (38) and (39) into the system of coupled differential equations of motion we use the properties of function $\mathcal{V}(k)$ defined by equation (40) in the continuum limit $a \to 0$ (long wave limit $k \to 0$), which can be obtained from the asymptotics of the polylogarithm (see the Appendix)

$$\mathcal{V}(k) \sim D_s |ak|^{s-1}, \quad 2 \leq s < 3, \tag{42}$$

$$\mathcal{V}(k) \sim -\mathcal{J}(ak)^2 \ln ak, \quad s = 3, \tag{43}$$

$$\mathcal{V}(k) \sim \frac{\mathcal{J}\zeta(s-2)}{2}(ak)^2, \quad s > 3, \tag{44}$$

where $\Gamma(s)$ is the Gamma function, $\zeta(s)$ is the Riemann zeta function and coefficient D_s is defined by

$$D_s = \frac{\pi \mathcal{J}}{\Gamma(s)\sin(\pi(s-1)/2)}. \tag{45}$$

It is seen from equation (42) that the fractional power of k occurs for interactions with $2 \leq s \leq 3$ only. In the coordinate space, the fractional power of $|ak|^{s-1}$ gives us the fractional Riesz derivative of order $s-1$ [27, 39] and we come to a fractional differential equation [25]

$$\begin{aligned} i\hbar \frac{\partial \psi(x,t)}{\partial t} &= \lambda \psi(x,t) \\ &\quad - D_s a^{s-1} \partial_x^{s-1} \psi(x,t) + \chi \frac{\partial \xi(x,t)}{\partial x} \psi(x,t), \end{aligned} \tag{46}$$

here ∂_x^{s-1} is the Riesz fractional derivative

$$\partial_x^{s-1} \psi(x,t) = -\frac{1}{2\pi} \int_{-\infty}^{\infty} dk e^{ikx} |k|^{s-1} \varphi(k,t), \quad 2 \leq s < 3, \tag{47}$$

where $\psi(x,t)$ and $\varphi(k,t)$ are related to each other by the Fourier transforms defined by equations (33) and (36).

Thus, we obtained the system of coupled equations (39) and (46) to study one-dimensional exciton-phonon quantum dynamics with long-range interaction.

4.1 Fractional nonlinear Schrödinger equation

The system of coupled equations, equations (39) and (46) can be further elaborated to get nonlinear fractional quantum and classical equations. Indeed, by assuming the existence of a stationary solution $\partial\xi(x,t)/\partial t = 0$ to equation (39), we obtain from equation (46) the following quantum fractional differential equation for wave function $\psi(x,t)$:

$$i\hbar\frac{\partial\psi(x,t)}{\partial t} = \lambda\psi(x,t) - D_s a^{s-1}\partial_x^{s-1}\psi(x,t) - \frac{\chi^2}{w}|\psi(x,t)|^2\psi(x,t), \quad 2 \le s < 3, \tag{48}$$

which can be rewritten in the form of fractional nonlinear Schrödinger equation [25],

$$i\hbar\frac{\partial\phi(x,t)}{\partial t} = -D_s a^{s-1}\partial_x^{s-1}\phi(x,t) - \frac{\chi^2}{w}|\phi(x,t)|^2\phi(x,t), \tag{49}$$

where ∂_x^{s-1} is fractional Riesz derivative defined by equation (47), $2 \le s < 3$ and the wave function $\phi(x,t)$ is related to the wave function $\psi(x,t)$ by

$$\phi(x,t) = \exp\{i\lambda t/\hbar\}\psi(x,t). \tag{50}$$

Note, that equation (49) is nonlinear generalization of linear fractional Schrödinger equation introduced into the quantum mechanics by Laskin [20–23, 26].

It is easy to see that equation (49) supports normalization condition for wave function $\phi(x,t)$

$$\int_{-\infty}^{\infty} dx|\phi(x,t)|^2 = 1. \tag{51}$$

Thus, using the system of coupled equations, equations (39) and (46), we discovered the fractional generalization of nonlinear Schrödinger equation (49) with a cubic focusing nonlinearity. The equation (49) has to be supplied with initial condition $\phi(x,t)|_{t=0} = \phi(x,0)$.

To express equation (49) in dimensionless form, let us apply the scaling transforms

$$t' = \omega t, \quad x' = \frac{x}{l}, \quad \phi'(x',t') = \sqrt{l}\phi(x,t), \tag{52}$$

where we introduce dimensionless time t' and length x', while ω is characteristic frequency and l is characteristic space scale. The transform $\phi'(x',t') = \sqrt{l}\phi(x,t)$ supports the normalization condition equation (51).

Applying the scale transforms to equation (49) results in

$$i\hbar\omega\frac{\partial\phi'(x',t')}{\partial t'} = -D_s a^{s-1}\frac{1}{l^{s-1}}\partial_{x'}^{s-1}\phi(x',t') - \frac{\chi^2}{wl}|\phi'(x',t')|^2\phi'(x',t'), \tag{53}$$

$$2 \le s < 3.$$

By choosing

$$l = \left(\frac{D_s}{\hbar\omega}\right)^{1/(s-1)} a, \tag{54}$$

we obtain the equation

$$i\frac{\partial\phi'(x',t')}{\partial t'} = -\partial_{x'}^{s-1}\phi'(x',t') - \varkappa\left|\phi'(x',t')\right|^2\phi'(x',t'),$$

where dimensionless parameter $\varkappa$ is introduced by

$$\varkappa = \frac{\chi^2(\hbar\omega)^{(2-s)/(s-1)}}{waD_s^{1/(s-1)}}. \tag{55}$$

Finally, by renaming $x' \to x$, $t' \to t$ and $\phi' \to \phi$, we come to the dimensionless fractional nonlinear Schrödinger equation

$$i\frac{\partial\phi(x,t)}{\partial t} = -\partial_x^{s-1}\phi(x,t) - \varkappa|\phi(x,t)|^2\phi(x,t), \quad 2 \le s < 3, \tag{56}$$

with $\varkappa$ given by equation (55), and ∂_x^{s-1} being the fractional Riesz derivative defined by equation (47).

Due to equation (44) for $s > 3$, equation (49) turns into the nonlinear Schrödinger equation with a cubic focusing nonlinearity [25],

$$i\hbar\frac{\partial\phi(x,t)}{\partial t} = -\frac{\mathcal{J}\zeta(s-2)}{2}a^2\partial_x^2\phi(x,t) - \frac{\chi^2}{w}|\phi(x,t)|^2\phi(x,t), \tag{57}$$

where $s > 3$ and $\partial_x^2 = \partial^2/\partial x^2$.

4.2 Nonlinear Hilbert–Schrödinger equation

It follows from equations (42) and (45) that in the case $s = 2$ the function $\mathcal{V}(k)$ in the long wave limit $k \to 0$ takes the form

$$\mathcal{V}(k) \sim \pi\mathcal{J}|ak|, \quad s = 2. \tag{58}$$

In this case, assuming the existence of a stationary solution $\partial\xi(x,t)/\partial t = 0$ to equation (39) we find from equation (38) the following nonlinear quantum fractional differential equation for wave function $\psi(x,t)$,

$$\begin{aligned} i\hbar\frac{\partial\psi(x,t)}{\partial t} &= \lambda\psi(x,t) \\ &\quad - \pi\mathcal{J}a\mathcal{H}\{\partial_x\psi(x,t)\} - \frac{\chi^2}{w}|\psi(x,t)|^2\psi(x,t), \quad s = 2. \end{aligned} \tag{59}$$

Here, $\mathcal{H}\{\cdots\}$ is the Hilbert integral transform defined by

$$\mathcal{H}\{\psi(x,t)\} = \frac{1}{\pi}\mathrm{PV}\int_{-\infty}^{\infty} dy \frac{\psi(y,t)}{x-y}, \tag{60}$$

where PV stands for the Cauchy principal value of the integral.

Introducing wave function $\phi(x,t)$ related to the wave function $\psi(x,t)$ by means of equation (50) brings us the nonlinear Hilbert–Schrödinger equation [25, 27]

$$i\hbar\frac{\partial\varphi(x,t)}{\partial t} = -\pi\mathcal{J}a\mathcal{H}\{\partial_x\varphi(x,t)\} - \frac{\chi^2}{w}|\varphi(x,t)|^2\varphi(x,t), \tag{61}$$

with normalization condition given by equation (51).

4.3 Fractional generalization of Zakharov system

Introducing a new variable $\sigma(x,t) = \partial\xi(x,t)/\partial x$ turns equations (39) and (48) into the following system of two coupled quantum equations for the fields $\psi(x,t)$ and $\sigma(x,t)$:

$$i\hbar\frac{\partial\psi(x,t)}{\partial t} = \lambda\psi(x,t) - D_s a^{s-1}\partial_x^{s-1}\psi(x,t) + \chi\sigma(x,t)\psi(x,t), \tag{62}$$

and

$$\left(\frac{\partial^2}{\partial t^2} - v^2\frac{\partial^2}{\partial x^2}\right)\sigma(x,t) = \frac{\chi}{\mathrm{m}}\frac{\partial^2}{\partial x^2}|\psi(x,t)|^2, \tag{63}$$

where $v = \sqrt{w/\mathrm{m}}$ is physical parameter with units of velocity, the parameter D_s is defined by equation (45), ∂_x^{s-1} is the fractional Riesz derivative introduced by equation (47), and parameter s is in the range $2 \le s < 3$. Equation (62) is fractional differential equation, while equation (63) includes spatial and temporal derivatives of second order.

Considering wave function $\phi(x,t)$ related to the wave function $\psi(x,t)$ by means of equation (50), we rewrite equations (62) and (63) in the form [25]

$$i\hbar\frac{\partial\phi(x,t)}{\partial t} = -D_s a^{s-1}\partial_x^{s-1}\phi(x,t) + \chi\sigma(x,t)\phi(x,t), \quad 2 \le s < 3, \tag{64}$$

and

$$\left(\frac{\partial^2}{\partial t^2} - v^2\frac{\partial^2}{\partial x^2}\right)\sigma(x,t) = \frac{\chi}{\mathrm{m}}\frac{\partial^2}{\partial x^2}|\phi(x,t)|^2. \tag{65}$$

To express equations (64) and (65) in dimensionless form, let us apply the scaling transforms

$$t' = \omega t, \quad x' = \frac{x}{l}, \tag{66}$$

$$\phi'(x',t') = \sqrt{l}\phi(x,t), \quad \sigma'(x',t') = l\sigma(x,t),$$

where we introduce dimensionless time t' and length x', while ω is characteristic frequency and l is characteristic space scale. The transform $\phi'(x',t') = \sqrt{l}\phi(x,t)$ supports the normalization condition equation (51).

Plugging those transforms into equations (64) and (65) results in

$$i\hbar\omega\frac{\partial\phi'(x',t')}{\partial t'} = -D_s\left(\frac{a}{l}\right)^{s-1}\partial_{x'}^{s-1}\phi(x',t') + \chi\sigma'(x',t')\phi'(x',t'),$$

with $2 \le s < 3$, and

$$\left(\omega^2\frac{\partial^2}{\partial t'^2} - \frac{v^2}{l^2}\frac{\partial^2}{\partial x'^2}\right)\sigma'(x',t') = \frac{\chi}{\mathrm{m}l^2}\frac{\partial^2}{\partial x'^2}|\phi'(x',t')|^2.$$

Further, by choosing

$$l = \left(\frac{D_s}{\hbar\omega}\right)^{1/(s-1)}, \tag{67}$$

we have the system of coupled equations

$$i\frac{\partial\phi'(x',t')}{\partial t'} = -\partial_{x'}^{s-1}\phi'(x',t') + \gamma\sigma'(x',t')\phi'(x',t'), \tag{68}$$

and

$$\left(\frac{\partial^2}{\partial t'^2} - \varkappa^2\frac{\partial^2}{\partial x'^2}\right)\sigma'(x',t') = \beta\frac{\partial^2}{\partial x'^2}|\phi'(x',t')|^2, \tag{69}$$

with dimensionless parameters $\gamma, \varkappa$ and β introduced by

$$\gamma = \frac{\chi}{\hbar\omega}, \quad \varkappa = \frac{v}{\omega l}, \quad \beta = \frac{\chi}{l^2\omega^2\mathrm{m}}. \tag{70}$$

Finally, by renaming $x' \to x$, $t' \to t$, $\phi' \to \phi$ and $\sigma' \to \sigma$ we come to the following system of coupled equations for the fields $\phi(x,t)$ and $\sigma(x,t)$,

$$i\frac{\partial\phi(x,t)}{\partial t} = -\partial_x^{s-1}\phi(x,t) + \gamma\sigma(x,t)\phi(x,t), \quad 2 \le s < 3, \tag{71}$$

and

$$\left(\frac{\partial^2}{\partial t^2} - \varkappa^2\frac{\partial^2}{\partial x^2}\right)\sigma(x,t) = \beta\frac{\partial^2}{\partial x^2}|\phi(x,t)|^2, \tag{72}$$

with $\gamma, \varkappa$ and β given by equation (68).

The system of coupled equations (71) and (72) is a fractional generalization of the Zakharov system originally introduced in 1972 to study the Langmuir waves propagation in an ionized plasma [44].

In our approach, we came to the system of equations (71) and (72) by studying the nonlocal quantum 1D exciton-phonon system assuming that the exciton-exciton interaction has power-law long-range behavior.

4.4 Fractional Ginzburg–Landau equation

In the case of propagating waves, one can search for the solution to the system of equations (64) and (65) in the form of traveling waves

$$\psi(x,t) = \psi(x - \mathrm{v}t) \quad \text{and} \quad \xi(x,t) = \xi(x - \mathrm{v}t), \tag{73}$$

where v is wave velocity.

By introducing the notation $\zeta = (x - \mathrm{v}t)$, we can rewrite equations (64) and (65) as

$$i\hbar\mathrm{v}\frac{\partial\phi(\zeta)}{\partial\zeta} = -D_s a^{s-1}\partial_\zeta^{s-1}\phi(\zeta) + \chi\sigma(\zeta)\phi(\zeta), \quad 2 \leq s < 3, \tag{74}$$

and

$$(\mathrm{v}^2 - v^2)\frac{\partial^2}{\partial\zeta^2}\sigma(\zeta) = \frac{\chi}{\mathrm{m}}\frac{\partial^2}{\partial\zeta^2}|\phi(\zeta)|^2. \tag{75}$$

It is easy to see that the solution to equation (75) is

$$\sigma(\zeta) = \frac{\chi}{\mathrm{m}(\mathrm{v}^2 - v^2)}|\phi(\zeta)|^2. \tag{76}$$

Then equation (74) results in nonlinear fractional equation

$$i\hbar\mathrm{v}\frac{\partial\phi(\zeta)}{\partial\zeta} = -D_s a^{s-1}\partial_\zeta^{s-1}\phi(\zeta) + \gamma|\phi(\zeta)|^2\phi(\zeta), \tag{77}$$

where nonlinearity parameter γ has been introduced as

$$\gamma = \frac{\chi^2}{\mathrm{m}(\mathrm{v}^2 - v^2)}.$$

We call equation (77) the fractional Ginzburg–Landau equation, which was initially developed in [43]. This is the quantum nonlinear fractional differential equation in the framework of fractional quantum mechanics [20–23, 26].

To express equation (77) in dimensionless form, let us apply the scaling transforms

$$\zeta' = \frac{\zeta}{b}, \quad \phi'(\zeta') = \sqrt{b}\phi(\zeta), \quad \sigma'(\zeta') = b\sigma(\zeta), \tag{78}$$

where we introduce dimensionless length ζ' and characteristic scale b. The transform $\phi'(\zeta') = \sqrt{b}\phi(\zeta)$ supports the normalization condition equation (51).

By performing the scaling transforms and then omitting the prime symbol, we obtain fractional nonlinear differential equation

$$i\frac{\partial\phi(\zeta)}{\partial\zeta} = -\epsilon_s\partial_\zeta^{s-1}\phi(\zeta) + \delta|\phi(\zeta)|^2\phi(\zeta), \quad 2 \leq s < 3, \tag{79}$$

with dimensionless coefficients ϵ_s and δ introduced by

$$\epsilon_s = \frac{D_s a^{s-1}}{b^{s-2}\hbar \mathrm{v}}, \quad \delta = \frac{\gamma b}{\hbar \mathrm{v}} = \frac{\chi^2 b}{\hbar \mathrm{v} m(\mathrm{v}^2 - \nu^2)}. \tag{80}$$

Thus, we came to the fractional Ginzburg–Landau equation (79) in dimensionless form.

5 Quantum lattice propagator

To study impact of long-range interaction on 1D quantum dynamics, let us focus on the exciton sub-system only. Hence, following [25, 27] we consider discrete nonlocal linear problem associated with the exciton Hamiltonian $H_{\mathrm{ex}}(\psi_n, \psi_n^*)$ given by equation (14).

Suppose that we know the solution $\psi_{n'}(t')$ to equation (14) at some time instant t' at the lattice site n'. Then the solution $\psi_n(t)$ at later time t, $(t > t')$ at the lattice site n will be

$$\psi_n(t) = \sum_{n'} G_{n,n'}(t|t')\psi_{n'}(t'), \tag{81}$$

where $G_{n,n'}(t|t')$ is exciton 1D lattice quantum propagator, that is, the probability of exciton transition from site n' at the time moment t' to site n at the time moment t.

It follows from equations (14) and (81) that $G_{n,n'}(t|t')$ is governed by the motion equation

$$i\hbar \frac{\partial G_{n,n'}(t|t')}{\partial t} = \varepsilon G_{n,n'}(t|t') - \sum_{\substack{m \\ (m \neq n)}} \mathcal{J}_{n-m} G_{m,n'}(t|t'), \quad t \geq t', \tag{82}$$

with the initial condition

$$G_{n,n'}(t|t')\big|_{t=t'} = \delta_{n,n'}, \tag{83}$$

here $\delta_{n,n'}$ is the Kronecker symbol.

To avoid bulky notations let us choose $n' = 0$, $t' = 0$ and introduce $G_n(t)$ as

$$G_n(t) = G_{n,0}(t|0). \tag{84}$$

It yields

$$i\hbar \frac{\partial G_n(t)}{\partial t} = \varepsilon G_n(t) - \sum_{\substack{m \\ (m \neq n)}} \mathcal{J}_{n-m} G_n(t), \quad t \geq t', \tag{85}$$

with the initial condition

$$G_n(t)|_{t=0} = \delta_{n,0}. \tag{86}$$

At this point, we take into consideration the propagator $G(k,t)$ related to $G_n(t)$ as

$$G(k,t) = \sum_{n=-\infty}^{\infty} e^{-ikn} G_n(t), \tag{87}$$

here we put the lattice parameter, $a = 1$ for simplify.

Hence, in terms of $G(k,t)$ the quantum lattice propagator $G_n(t)$ is given by[1]

$$G_n(t) = \frac{1}{2\pi} \int_{-\pi}^{\pi} dk e^{ikn} G(k,t). \tag{88}$$

It follows from equations (85), (87), and (41) that

$$i\hbar \frac{\partial G(k,t)}{\partial t} = \big(\omega + \mathcal{V}(k)\big) G(k,t), \quad t \geq 0, \tag{89}$$

where $\mathcal{V}(k)$ is defined by equations (40) and (41), energy ω is given by

$$\omega = \varepsilon - \mathcal{J}(0) \tag{90}$$

and

$$\mathcal{J}(0) = \sum_{\substack{n=-\infty \\ (n\neq 0)}}^{\infty} \mathcal{J}_n, \tag{91}$$

with $\mathcal{J}_n$ given by equation (7). Then it is easy to see from equations (86) and (87) that the initial condition for $G(k,t)$ is

$$G(k, t = 0) = 1. \tag{92}$$

To solve equation (89) with the initial condition (92) let us introduce quantum propagator $g(k,t)$

$$g(k,t) = \exp(i\omega t/\hbar) G(k,t). \tag{93}$$

Thus, $G(k,t)$ can be expressed in terms of $g(k,t)$ as

$$G(k,t) = \exp(-i\omega t/\hbar) g(k,t). \tag{94}$$

1 the formula (1.17.17) [1]

$$\frac{1}{2\pi} \sum_{n=-\infty}^{\infty} e^{-ikn} \left(\int_{-\pi}^{\pi} dk' e^{ik'n} G(k',t) \right) = G(k,t)$$

has been used.

It follows from equation (89) that the propagator $g(k,t)$ is governed by the equation

$$i\hbar\frac{\partial g(k,t)}{\partial t} = \mathcal{V}(k)g(k,t), \quad t \geq 0, \tag{95}$$

with the initial condition

$$g(k,t=0) = 1. \tag{96}$$

The solution to the problem defined by equations (95) and (96) is

$$g(k,t) = \exp(-i\mathcal{V}(k)t/\hbar). \tag{97}$$

By substituting this solution into equations (88) and (94), we obtain

$$G_n(t) = \frac{1}{2\pi}\int_{-\pi}^{\pi} dk \exp(ikn - i(\omega + \mathcal{V}(k))t/\hbar). \tag{98}$$

Similar to (94), we write

$$G_n(t) = \exp(-i\omega t/\hbar)g_n(t), \tag{99}$$

where the quantum lattice propagator $g_n(t)$ has been introduced by

$$g_n(t) = \frac{1}{2\pi}\int_{-\pi}^{\pi} dk \exp(ikn - i\mathcal{V}(k)t/\hbar). \tag{100}$$

The generalization to quantum lattice propagator $g_{n,n'}(t|t')$, which describes transition of an exciton from site n' at the time moment t' to site n at the time moment t $(t > t')$, is obvious that

$$g_{n,n'}(t|t') = \frac{1}{2\pi}\int_{-\pi}^{\pi} dk \exp(ik(n-n') - i\mathcal{V}(k)(t-t')/\hbar). \tag{101}$$

Therefore, the quantum lattice propagator $g_{n,n'}(t|t')$ can be considered as quantum transition amplitude. The propagator $g_{n,n'}(t|t')$ describes 1D exciton transport discrete in space and continuous in time. It is obvious that the propagator $G_{n,n'}(t|t')$ defined by equations (82) and (83) can be expressed in terms of the propagator $g_{n,n'}(t|t')$ as

$$G_{n,n'}(t|t') = \exp(-i\omega t/\hbar)g_{n,n'}(t|t'). \tag{102}$$

Let us note that $g_{n,n'}(t|t')$ satisfies the following fundamental criteria:

1. Normalization condition

$$\sum_{n=-\infty}^{\infty} g_{n,n'}(t|t') = 1. \tag{103}$$

2. Rule for two events successive in time

$$g_{n,n'}(t_1|t_2) = \sum_{m=-\infty}^{\infty} g_{n,m}(t_1|t')g_{m,n'}(t'|t_2). \tag{104}$$

The last condition means that for exciton propagations occurring in succession in time the quantum transition amplitudes are multiplied.

Our intent now is to study behavior of $g_n(t)$ at large $|n|$, when the main contribution to the integral equation (100) comes from small k. Therefore, we can expand integral over k from $-\infty$ up to ∞,

$$g_n(t) = \frac{1}{2\pi}\int_{-\infty}^{\infty} dk \exp(ikn - i\gamma_s|k|^{\upsilon(s)}t/\hbar), \tag{105}$$

where

$$\upsilon(s) = \begin{cases} 2, & \text{for } s > 3, \\ s-1, & \text{for } 2 < s < 3, \end{cases} \tag{106}$$

and

$$\gamma_s = \begin{cases} \frac{\mathcal{J}\zeta(s-2)}{2}, & \text{for } s > 3, \\ D_s, & \text{for } 2 < s < 3, \end{cases} \tag{107}$$

here D_s is given by equation (45).

Asymptotic behavior of the lattice quantum 1D propagator $g_n(t)$ at large $|n|$ depends on the value of the parameter s. Indeed, when $s > 3$, equation (105) goes to

$$g_n(t) = (\hbar/2\pi i\mathcal{J}\zeta(s-2)t)^{1/2} \exp\left\{-\frac{\hbar}{2i\mathcal{J}\zeta(s-2)t}|n|^2\right\}, \quad s > 3, \tag{108}$$

if we take into account equations (106) and (107).

When $2 < s < 3$ the integral in equation (105) is expressed in terms of Fox's H-function [24] and [29],

$$g_n(t) = \frac{1}{|n|(s-1)} H^{1,1}_{2,2}\left[\left(\frac{\hbar}{iD_s t}\right)^{1/(s-1)} |n| \,\middle|\, \begin{matrix} (1, 1/(s-1)), (1, 1/2) \\ (1, 1), (1, 1/2) \end{matrix}\right]. \tag{109}$$

Therefore, the propagator $G_n(t)$ defined by equation (99) can be presented as

$$G_n(t) = \frac{\exp(-i\omega t/\hbar)}{|n|(s-1)} H^{1,1}_{2,2}\left[\left(\frac{\hbar}{iD_s t}\right)^{1/(s-1)} |n| \,\middle|\, \begin{matrix} (1, 1/(s-1)), (1, 1/2) \\ (1, 1), (1, 1/2) \end{matrix}\right]. \tag{110}$$

On the other hand, in the long-wavelength approximation for $2 < s < 3$ the integral in equation (105) can be estimated as

$$g_n(t) \simeq \frac{1}{\pi}\Gamma(s)\sin\left(\frac{\pi(s-1)}{2}\right)\left(\frac{iD_s t}{\hbar}\right)^{s/(s-1)}\frac{1}{|n|^s}. \tag{111}$$

Thus, the asymptotics of the lattice quantum exciton propagator $g_n(t)$ exhibits the power-law behavior at large $|n|$ for $2 < s < 3$. Transition from Gaussian-like behavior equation (108) to power-law decay equation (111) is due to long-range interaction (the second term on the right-hand side of equation (14)). This transition can be interpreted as phase transition. In fact, when $s > 3$, the propagator $g_n(t)$ defined by equation (108) has correlation length[2] Δn

$$\Delta n \simeq \left(\frac{2\mathcal{J}\zeta(s-2)t}{\hbar}\right)^{1/2}, \quad s > 3. \tag{112}$$

When $2 < s < 3$, the propagator $g_n(t)$ defined by equation (111) exhibits power-law behavior with infinite correlation length, that is in the case $2 < s < 3$ the correlation length does not exist for a 1D lattice system with long-range exciton-exciton interaction given by equation (7).

5.1 Exciton propagator in continuum space

Considering exciton lattice propagator in continuum space gives us insight on how the fractional Schrödinger equation for a free particle quantum propagator emerges in fractional quantum mechanics. In the case of continuum space, equation (105) with substitution $k = p/\hbar$ brings

$$g(x,t) = \frac{1}{2\pi\hbar}\int_{-\infty}^{\infty} dp\,\exp(ipx/\hbar - i\gamma_s|p|^{\nu(s)}t/\hbar^{\nu(s)+1}), \tag{113}$$

where $\nu(s)$ and γ_s are defined by equations (106) and (12), respectively.

At this point, we define the quantum Riesz fractional derivative $(\hbar\nabla)^{\nu(s)}$ by means of equation

$$(\hbar\nabla)^{\nu(s)}g(x,t) = -\frac{1}{2\pi\hbar}\int_{-\infty}^{\infty} dp|p|^{\nu(s)}\exp(px/\hbar)g(p,t), \tag{114}$$

where operator ∇ is $\nabla = \partial/\partial x$ and functions $g(x,t)$ and $g(p,t)$ are related to each other by the Fourier transforms

$$g(x,t) = \frac{1}{2\pi\hbar}\int_{-\infty}^{\infty} dp\,\exp(ipx/\hbar)g(p,t) \tag{115}$$

2 Let us note that the lattice scale a is equal to 1, $a = 1$.

and

$$g(p,t) = \int_{-\infty}^{\infty} dx \exp(-ipx/\hbar) g(x,t). \tag{116}$$

It is easy to see from equations (113) and (114) that the following quantum fractional differential equation holds:

$$i\hbar \frac{\partial}{\partial t} g(x,t) = \mathcal{D}_{\nu(s)} (\hbar \nabla)^{\nu(s)} g(x,t), \tag{117}$$

where $\mathcal{D}_{\nu(s)}$ is scale coefficient

$$\mathcal{D}_{\nu(s)} = \frac{\gamma_s}{\hbar^{\nu(s)}} \tag{118}$$

with units of $[\mathcal{D}_{\nu(s)}] = \mathrm{erg}^{1-\nu(s)} \cdot \mathrm{cm}^{\nu(s)} \cdot \mathrm{sec}^{-\nu(s)}$. The initial condition to equation (117) is

$$g(x,0) = \delta(x), \tag{119}$$

as seen from equations (96) and (115).

To solve equation (117) with initial condition (119), we use the method developed in [24] to obtain $g(x,t)$ terms of Fox's H-function [29],

$$g(x,t) = \frac{1}{|x|\nu(s)} H^{1,1}_{2,2} \left[\frac{1}{\hbar} \left(\frac{\hbar}{i\mathcal{D}_{\nu(s)} t} \right)^{1/\nu(s)} |x| \,\middle|\, \begin{matrix} (1, 1/\nu(s)), (1, 1/2) \\ (1,1), (1, 1/2) \end{matrix} \right], \tag{120}$$

where the scale coefficient $\mathcal{D}_{\nu(s)}$ has been introduced by equation (117) and $\nu(s)$ is given by equation (106).

It is easy to see that the solution (120) is in agreement with its discrete version given by equation (109).

5.2 Crossover in random walk on 1D lattice

Exciton-exciton 1D lattice quantum dynamics initiates a 1D random walk model. Indeed, if we put $it \to \tau$, introduce $w(k)$

$$w(k) = \mathcal{V}(k)/\hbar \tag{121}$$

and rename

$$g_{n,n'}(t|t')|_{it\to\tau, it'\to\tau'} \to P_{n,n'}(\tau|\tau'),$$

then equation (101) becomes

$$P_{n,n'}(\tau|\tau') = \frac{1}{2\pi} \int_{-\pi}^{\pi} dk \exp\{ik(n-n') - w(k)(\tau-\tau')\}, \tag{122}$$

which is the definition of random walk transition probability $P_{n,n'}(\tau|\tau')$.

The transition probability answers the question: What is the probability that a walker will be on site n at the time moment τ if at some previous time moment τ' ($\tau' < \tau$) he was on site n'. It is easy to see that $P_{n,n'}(\tau|\tau')$ is normalized

$$\sum_{n=-\infty}^{\infty} P_{n,n'}(\tau|\tau') = 1, \tag{123}$$

and satisfies the Chapman–Kolmogorov equation

$$P_{n,n'}(\tau_1|\tau_2) = \sum_{m=-\infty}^{\infty} P_{n,m}(\tau_1|\tau')P_{m,n'}(\tau'|\tau_2), \tag{124}$$

with the initial condition

$$P_{n,n'}(\tau|\tau')\big|_{\tau=\tau'} = \delta(n - n'). \tag{125}$$

We came to a continuous in time τ and discrete in space (1D lattice) random walk model [27]. From equation (124), we conclude that the random walk model under consideration is a Markov random process. As we will see, the obtained random walk model exhibits a cross-over from the Brownian random walk ($s > 3$) with finite correlation length to the symmetric α-stable Lévy random process (with $\alpha = s - 1$ and $2 < s < 3$) with an infinite correlation length.

Let us choose $n' = 0$, $\tau' = 0$ and introduce $P_n(\tau)$ as

$$P_n(\tau) = P_{n,n'}(\tau|\tau')\big|_{n'=0,\tau'=0} = \frac{1}{2\pi}\int_{-\pi}^{\pi} dk \exp\{ikn - w(k)\tau\}. \tag{126}$$

The probability $P_n(\tau)$ can be expressed as

$$P_n(\tau) = \frac{1}{2\pi}\int_{-\pi}^{\pi} dk \exp(ikn)P(k,\tau), \tag{127}$$

where $P(k,\tau)$ is given by

$$P(k,\tau) = \sum_{n=-\infty}^{\infty} e^{-ikn}P_n(\tau) = \exp\{-w(k)\tau\}, \tag{128}$$

and $w(k)$ is defined by equation (121).

It follows straightforwardly from equation (128) that the probability $P(k,\tau)$ satisfies motion equation,

$$\frac{\partial}{\partial \tau}P(k,\tau) = -w(k)P(k,\tau), \tag{129}$$

with the initial condition

$$P(k, t = 0) = 1.$$

In the case of continuum space, the integral over k equation (127) can be expanded from $-\infty$ up to ∞ and we obtain probability distribution function $P(x,\tau)$,

$$P(x,\tau)=\frac{1}{2\pi}\int_{-\infty}^{\infty}dk\exp(ikx)P(k,\tau), \tag{130}$$

where $P(k,\tau)$ is the inverse Fourier transform

$$P(k,\tau)=\int_{-\infty}^{\infty}dx\exp(-ikx)P(x,\tau). \tag{131}$$

Thus, we have

$$P(x,\tau)=\frac{1}{2\pi}\int_{-\infty}^{\infty}dk\exp\{ikx-w(k)\tau\}.$$

Further, using equations (42) and (44), we write the probability distribution function $P(x,\tau)$ in the form

$$P(x,\tau)=\frac{1}{2\pi}\int_{-\infty}^{\infty}dk\exp(ikx-\gamma_s|k|^{\upsilon(s)}\tau), \tag{132}$$

which satisfies the initial condition

$$P(x,\tau=0)=\delta(x), \tag{133}$$

where $\upsilon(s)$ and γ_s are defined by equation (106) and equation (107), respectively. This probability distribution function bears dependency on index s and exhibits cross-over from Gaussian behavior at $s>3$ to α-stable ($\alpha=s-1$) Lévy law at $2<s<3$.

It follows from equation (132) that $P(x,\tau)$ satisfies fractional diffusion equation

$$\begin{aligned}\frac{\partial}{\partial\tau}P(x,\tau)&=-\frac{\gamma_s}{2\pi}\int_{-\infty}^{\infty}dk|k|^{\upsilon(s)}\exp(ikx-\gamma_s|k|^{\upsilon(s)}\tau)\\&=\gamma_s(\nabla)^{\upsilon(s)}P(x,\tau),\end{aligned} \tag{134}$$

where $(\nabla)^{\upsilon(s)}$ stands for the Riesz fractional derivative introduced by

$$(\nabla)^{\upsilon(s)}P(x,\tau)=-\frac{1}{2\pi}\int_{-\infty}^{\infty}dk|k|^{\upsilon(s)}\exp(ikx)P(k,\tau). \tag{135}$$

Here, $P(x,\tau)$ and $P(k,\tau)$ are related to each other by the Fourier transforms defined by equations (130) and (131). The initial condition to the fractional differential equation (134) is given by equation (133).

The solution to equation (134) with initial condition (133) is

$$P(x,\tau) = \frac{1}{|x|\nu(s)} H^{1,1}_{2,2} \left[\left(\frac{1}{\gamma_s \tau} \right)^{1/\nu(s)} |x| \,\middle|\, \begin{matrix} (1, 1/\nu(s)), (1, 1/2) \\ (1,1), (1,1/2) \end{matrix} \right]. \tag{136}$$

6 Conclusion

To illustrate how fractional dynamical equations emerge in nonlocal quantum mechanics, we introduced and elaborated a 1D exciton-phonon system with long-range power-law exciton-exciton interaction. It has been shown that the long-range power-law interaction leads, in general, to a nonlocal integral term in the motion equation of an exciton subsystem if we go from discrete to continuous space. In some particular cases for power-law interaction with noninteger power, the nonlocal integral term can be expressed through a spatial derivative of fractional order. In other words, the nonlocality originating from the long-range interparticle interaction is revealed in the dynamical equations in the form of space derivatives of fractional order.

Considering exciton-phonon system with long-range power-law exciton-exciton interaction, we have obtained the system of two coupled equations, where one is quantum fractional differential equation for exciton subsystem while the other is a standard differential equation for phonon subsystem. It has been found that the system of two coupled equations can be further simplified to come to the following fractional nonlinear equations of motion: fractional nonlinear Schrödinger equation, nonlinear Hilbert–Schrödinger equation, fractional generalization of Zakharov system and fractional Ginzburg–Landau equation.

The quantum lattice propagator for exciton subsystem has been introduced. The propagator describes exciton transport, which is discrete in space and continuous in time. Asymptotic behavior at large interatomic scales of the quantum lattice propagator has been studied. It has been found that depending on the value of the parameter s involved into long-range power-law interaction, the quantum lattice propagator exhibits the transition from Gaussian-like behavior to power-law decay due to nonlocal interaction.

Nonlocal exciton-exciton lattice quantum dynamics initiates a new 1D random walk model if we go to imaginary time domain. It has been shown that the evolution equation for transition probability density of the random walk is fractional diffusion equation. The transition probability density shows a cross-over from normal to fractional mode, that is from Gaussian behavior to α-stable Lévy law.

On a final note, let us emphasize that the appearance of fractional differential equations in the continuum limit of lattice dynamics allows us to apply powerful tools of fractional calculus to study nonlocal quantum dynamics.

Appendix A

A.1 Polylogarithm as a power series

The polylogarithm $\mathrm{Li}_s(z)$ is defined by [2, 28]

$$\mathrm{Li}_s(z) = \sum_{n=1}^{\infty} \frac{z^n}{n^s} = \frac{z}{\Gamma(s)} \int_0^{\infty} dt \frac{t^{s-1}}{e^t - z}. \tag{137}$$

Here, s is a real parameter and z is the complex argument. The name *polylogarithm* comes from the fact that the function $\mathrm{Li}_s(z)$ may be introduced as the repeated integral of itself,

$$\mathrm{Li}_{s+1}(z) = \int_0^{z} dt \frac{\mathrm{Li}_s(t)}{t}. \tag{138}$$

It is easy to see that for $z = 1$ the polylogarithm $\mathrm{Li}_s(1)$ reduces to the well-known Riemann zeta function $\zeta(s)$,

$$\mathrm{Li}_s(1) = \zeta(s) = \sum_{n=1}^{\infty} \frac{1}{n^s}, \quad \mathrm{Re}(s) > 1. \tag{139}$$

Quantum statistical mechanics is the best known field where the polylogarithm arises in a natural way. Indeed, if we note that the Bose–Einstein distribution function $\mathrm{BE}(t)$ is given by

$$\mathrm{BE}(t) = \frac{t^{s-1}}{e^{t-\mu} - 1}, \tag{140}$$

and the Fermi–Dirac distribution function $\mathrm{FD}(t)$ is given by

$$\mathrm{FD}(t) = \frac{t^{s-1}}{e^{t-\mu} + 1}, \tag{141}$$

then the integrals of the Bose–Einstein distribution function and the Fermi–Dirac distribution function are respectively

$$\int_0^{\infty} dt\, \mathrm{BE}(t) = \int_0^{\infty} dt \frac{t^{s-1}}{e^{t-\mu} - 1} = \Gamma(s)\mathrm{Li}_s(e^{\mu}), \tag{142}$$

and

$$\int_0^{\infty} dt\, \mathrm{FD}(t) = \int_0^{\infty} dt \frac{t^{s-1}}{e^{t-\mu} + 1} = -\Gamma(s)\mathrm{Li}_s(-e^{\mu}), \tag{143}$$

where $\Gamma(s)$ is the Gamma function.

For our purposes, we are looking for power series representation (about $\mu = 0$) of the polylogarithm $\mathrm{Li}_s(e^{-\mu})$,

$$\mathrm{Li}_s(e^{-\mu}) = \frac{1}{\Gamma(s)} \int_0^\infty dt \frac{t^{s-1}}{e^{t+\mu} - 1}. \tag{144}$$

The power series representation of the polylogarithm $\mathrm{Li}_s(e^{-\mu})$ can be found by using the Mellin transform (see [36])

$$M_s(r) = \int_0^\infty du u^{r-1} \mathrm{Li}_s(e^{-u}) = \int_0^\infty du u^{r-1} \sum_{n=1}^\infty \frac{e^{-nu}}{n^s} = \Gamma(r)\zeta(s+r), \tag{145}$$

where $\zeta(s+r)$ is the Riemann zeta function defined by equation (139).

The inverse Mellin transform then gives

$$\begin{aligned} \mathrm{Li}_s(e^{-u}) &= \frac{1}{2\pi i} \int_{c-i\infty}^{c+i\infty} dr u^{-r} M_s(r) \\ &= \frac{1}{2\pi i} \int_{c-i\infty}^{c+i\infty} dr u^{-r} \Gamma(r)\zeta(s+r), \quad r > 0, \end{aligned} \tag{146}$$

where c is a constant to the right of the poles of the integrand. The path of integration may be converted into a closed contour, and the simple poles of the integrand are those of the Riemann zeta function $\zeta(s+r)$ at $r = 1 - s$ with residue +1 and the Gamma function $\Gamma(r)$ at $r = -l$ with residues $(-1)^l/l!$. Here, $l = 0, -1, -2, \ldots$.

Summing the residues yields, for $|\mu| < 2\pi$ and $s \neq 1, 2, 3, \ldots$

$$\mathrm{Li}_s(e^{-\mu}) = \Gamma(1-s)\mu^{s-1} + \sum_{l=0}^\infty \frac{\zeta(s-l)}{l!}(-\mu)^l. \tag{147}$$

This equation gives us the power series representation of the polylogarithm $\mathrm{Li}_s(e^{-\mu})$ (about $\mu = 0$).

If the parameter s is a positive integer n, both the Gamma function $\Gamma(1-s)$ and the $l = n - 1$ term become infinite, although their sum remains finite [36].

For integer $l > 0$, we have

$$\begin{aligned} &\lim_{s \to l+1} \left[\Gamma(1-s)(\mu)^{s-1} + \frac{\zeta(s-l)}{l!}(-\mu)^l \right] \\ &= \frac{(-\mu)^l}{l!} \left(\sum_{m=1}^{l} \frac{1}{m} - \ln(\mu) \right), \end{aligned} \tag{148}$$

and for $l = 0$

$$\lim_{s \to 1} [\Gamma(1-s)(\mu)^{s-1} + \zeta(s)] = -\ln(\mu). \tag{149}$$

A.2 Properties of function $\mathcal{V}(k)$

It is easy to see that $\mathcal{J}(k)$ given by equation (41) with $\mathcal{J}_n$ defined by equation (7) can be expressed in terms of the polylogarithm

$$\mathcal{J}(k) = 2\mathcal{J} \sum_{n=1}^{\infty} \frac{\cos(kna)}{n^s} = 2\mathcal{J}\,\mathrm{Re}\{\mathrm{Li}_s(e^{-ika})\}. \tag{150}$$

Then the function $\mathcal{V}(k)$ defined by equation (40) is written as

$$\mathcal{V}(k) = 2\mathcal{J}\zeta(s)\,\mathrm{Re}\left\{1 - \frac{\mathrm{Li}_s(e^{-ika})}{\zeta(s)}\right\}, \tag{151}$$

where $\zeta(s)$ is the Riemann zeta function given by equation (139).

Taking into account power series representation given by equation (147), we find from equation (151) that in the limit $a \to 0$ function $\mathcal{V}(k)$ has the following behavior, depending on value of the parameter s, [27]:

$$\mathcal{V}(k) \sim D_s|ka|^{s-1}, \quad 2 \le s < 3, \tag{152}$$

$$\mathcal{V}(k) \sim -J(ka)^2 \ln ka, \quad s = 3, \tag{153}$$

$$\mathcal{V}(k) \sim \frac{J\zeta(s-2)}{2}(ka)^2, \quad s > 3, \tag{154}$$

where $\zeta(s)$ is the Riemann zeta function and the coefficient D_s is defined by

$$D_s = \frac{\pi\mathcal{J}}{\Gamma(s)\sin(\pi(s-1)/2)}, \tag{155}$$

with $\Gamma(s)$ being the Gamma function.

Bibliography

[1] http://dlmf.nist.gov/1.17.

[2] http://dlmf.nist.gov/25.12.

[3] A. Barone and G. Paterno, *Physics and Applications of the Josephson Effect*, Wiley, New York, 1982.

[4] O. M. Braun and Y. S. Kivshar, Nonlinear dynamics of the Frenkel–Kontorova model, *Phys. Rep.*, **306** (1998), 1–108.

[5] O. M. Braun and Yu. S. Kivshar, *The Frenkel–Kontorova Model: Concepts, Methods and Applications*, Springer-Verlag, Berlin, 1998.

[6] A. S. Davydov, Bio-soliton condensation in human body, *J. Theor. Biol.*, **38** (1973), 559–569.

[7] A. S. Davydov, Solitons in quasi-one-dimensional molecular structures, *Sov. Phys. Usp.*, **25** (1982), 898–918.

[8] A. S. Davydov, *Solitons in Molecular Systems*, 2nd ed., Reidel, Dordrecht, 1991.

[9] A. S. Davydov and N. I. Kislukha, Solitary excitons in one-dimensional molecular chains, *Phys. Status Solidi B*, **59** (1973), 465–470.

[10] E. Fermi, J. Pasta, and S. Ulam, *Studies in Nonlinear Problems, I. Los Alamos report LA-1940, 1955*, reproduced in A. C. Newell (ed.) *Nonlinear Wave Motion*, Amer. Math. Soc., Providence, 1974.
[11] S. Flach, Breathers on lattices with long range interaction, *Phys. Rev. E*, **58** (1998), R4116.
[12] S. Flach and C. R. Willis, Discrete breathers, *Phys. Rep.*, **295** (1998), 181–264.
[13] Ya. Frenkel and T. Kontorova, On theory of plastic deformation and twinning, *Phys. Z. Sowjetunion*, **13** (1938), 1–12.
[14] R. Herrmann, *Fractional Calculus: An Introduction for Physicists*, World Scientific, 2011.
[15] R. Hilfer (ed.), *Applications of Fractional Calculus in Physics*, World Scientific, 2000.
[16] Y. Ishimori, Solitons in a one-dimensional Lennard-Jones lattice, *Prog. Theor. Phys.*, **68** (1982), 402–410.
[17] M. Kac and E. Helfand, Study of several lattice systems with long-range forces, *J. Math. Phys.*, **4** (1973), 1078–1088.
[18] A. A. Kilbas, H. M. Srivastava, and J. J. Trujillo, *Theory and Applications of Fractional Differential Equations*, Elsevier Science, 2006.
[19] J. Klafter, S. C. Lim, and R. Metzler, *Fractional Dynamics*, World Scientific, 2011.
[20] N. Laskin, Fractional quantum mechanics and Lévy path integrals, *Phys. Lett. A*, **268** (2000), 298–305.
[21] N. Laskin, Fractional quantum mechanics, *Phys. Rev. E*, **62** (2000), 3135–3145.
[22] N. Laskin, Fractals and quantum mechanics, *Chaos*, **10** (2000), 780–790.
[23] N. Laskin, Fractional Schrödinger equation, *Phys. Rev. E*, **66** (2002), 056108.
[24] N. Laskin, Lévy flights over quantum paths, *Commun. Nonlinear Sci. Numer. Simul.*, **12** (2007), 2–18, https://arxiv.org/pdf/quant-ph/0504106v1.pdf.
[25] N. Laskin, Exciton-phonon dynamics with long-range interaction, in A. C. J. Luo, J. A. T. Machado, and D. Baleanu (eds.) *Dynamical Systems and Methods*, pp. 311–322, Springer, 2012, https://arxiv.org/ftp/arxiv/papers/1104/1104.1310.pdf.
[26] N. Laskin, *Fractional Quantum Mechanics*, World Scientific, 2018.
[27] N. Laskin and G. M. Zaslavsky, Nonlinear fractional dynamics on a lattice with long-range interactions, *Physica A*, **368** (2006), 38–54.
[28] L. Lewin, *Polylogarithms and Associated Function*, Elsevier, Amsterdam, 1981.
[29] A. M. Mathai and R. K. Saxena, *The H-function with Applications in Statistics and Other Disciplines*, Wiley Eastern, New Delhi, 1978.
[30] R. Metzler and J. Klafter, The random walk's guide to anomalous diffusion: a fractional dynamics approach, *Phys. Rep.*, **339** (2000), 1–77.
[31] K. S. Miller and B. Ross, *An Introduction to the Fractional Calculus and Fractional Differential Equations*, Wiley, New York, 1993.
[32] H. Nakano and M. Takahashi, Magnetic properties of quantum Heisenberg ferromagnets with long-range interactions, *Phys. Rev. B*, **52** (1995), 6606–6610.
[33] K. B. Oldham and J. Spanier, *The Fractional Calculus*, Academic Press, 1974.
[34] I. Podlubny, *Fractional Differential Equations*, Mathematics in Science and Engineering, vol. 198, Academic Press, 1999.
[35] V. L. Pokrovsky and A. Virosztek, Long-range interactions in commensurate-incommensurate phase transition, *J. Phys. C*, **16** (1983), 4513–4525.
[36] J. E. Robinson, Note on the Bose–Einstein integral functions, *Phys. Rev.*, **83** (1951), 678–679.
[37] J. Sabatier, O. P. Agrawal, and J. A. Tenreiro Machado (eds.), *Advances in Fractional Calculus: Theoretical Developments and Applications in Physics and Engineering*, Springer Science & Business Media, 2007.
[38] A. I. Saichev and G. M. Zaslavsky, Fractional kinetic equations: solutions and applications, *Chaos*, **7** (1997), 753–764.

[39] S. G. Samko, A. A. Kilbas, and O. I. Marichev, *Fractional Integrals and Derivatives, Theory and Applications*, Gordon and Breach, Amsterdam, 1993.
[40] A. Scott, Davydov's soliton, *Phys. Rep.*, **217** (1992), 1–67.
[41] V. I. Tarasov, *Fractional Dynamics: Application of Fractional Calculus to Dynamics of Particles, Fields and Media*, Springer, 2011.
[42] J. A. Tuszyński, M. L. A. Nip, P. L. Christiansen, M. Rose, and Ole Bang, Exciton self-trapping in the Ginzburg–Landau framework, *Phys. Scr.*, **51** (1995), 423–430.
[43] H. Weitzner and G. M. Zaslavsky, Some applications of fractional equations, *Commun. Nonlinear Sci. Numer. Simul.*, **8** (2003), 273–281.
[44] V. E. Zakharov, Collapse of Langmuir waves, *Sov. Phys. JETP*, **35** (1972), 1745–1759.
[45] G. M. Zaslavsky, Chaos, fractional kinetics, and anomalous transport, *Phys. Rep.*, **371** (2002), 461–580.
[46] G. M. Zaslavsky, A. A. Stanislavsky, and M. Edelman, Chaotic and pseudochaotic attractors of perturbed fractional oscillator, nlin.CD/0508018, https://arxiv.org/pdf/nlin/0508018.pdf, 2005.

S. C. Lim and Chai Hok Eab

Fractional quantum fields

Abstract: Fractional Klein–Gordon field at zero and positive temperature can be obtained as an infinite collection of corresponding fractional oscillators. Free energy associated with the fractional field and topological symmetry breaking of quartic self-interacting fractional Klein–Gordon scalar massive and massless field theories on toroidal spacetime are discussed. Generalization of fractional field to variable order is briefly considered.

Keywords: Fractional Langevin equation, fractional Klein–Gordon field, Casimir energy, fractional boundary condition, topological symmetry breaking, multifractional Klein–Gordon field

PACS: 26A33, 60G22, 60H10, 81T08, 81T55, 82C31

1 Introduction

Fractional derivatives and integrals [30, 35, 76, 89] are nonlocal operators which can describe processes with nonlocality in time (memory) and space (large jumps). As a result, fractional differential equations seem to be well suited for describing the evolution of transport processes in complex and fluctuating media and environments, such as anomalous diffusion, fractional advection-dispersion, non-Debye relaxation processes, etc. Applications of fractional differential equations to describe various phenomena in complex heterogeneous and disordered materials in condensed matter physics have become more widespread during the past few decades, and they have now extended to other areas such as engineering, internet traffic, biology, economics, and many other complex natural processes and man-made events. However, the applications of fractional calculus in quantum theory is still quite recent, especially the use of fractional calculus in quantum fields is rather limited.

An important impetus to the increasing use of fractional calculus in quantum theory is the recent results from quantum gravity. Various approaches to quantum gravity, which include the asymptotically safe quantum Einstein gravity [47, 68, 78, 79], causal dynamical triangulations [4, 5, 91], loop quantum gravity and spin foams [60, 74, 83], Hořava–Lifshitz gravity [32, 90], nonlocal quantum gravity [10, 13, 61], etc., all lead to a common feature that the dimension of spacetime changes with the scale despite great differences in these inequivalent models of quantum gravity. All known theories

S. C. Lim, Faculty of Engineering, Multimedia University Malaysia, 63100 Putrajaya, Selangor Darul Ehsan, Malaysia, e-mail: sclim47@gmail.com
Chai Hok Eab, 386/23 Phetchbury 14, Bangkok 10400, Thailand, e-mail: chaihok.e@gmail.com

of quantum gravity are multiscale in nature since they have an anomalous scaling of the spacetime dimension. The multifractal character of quantum spacetime is manifested in the change of its topological dimension from two in the ultraviolet (i. e., short length scale or large energy) limit to four at the infrared (i. e., large length scale or low energy) limit.

A precursor to the incorporation of fractional calculus into quantum theory is the use of fractal processes in quantum physics since these processes can be described by fractional integro-differential operators. Brownian motion can be regarded as the first fractal process used in quantum theory. The trajectories of Brownian motion have been extensively used in the Feynman path integral approach to (Euclidean) quantum mechanics [23]. Brownian motion also played an important role in Nelson's stochastic mechanics [64, 67], which attempts to provide an alternative formulation to quantum mechanics. Early applications of fractal geometry in quantum field theory have focused mainly on the studies of quantum field models in fractal sets and fractal spacetime, and quantum field theory of spin systems such as the Ising spin model [20, 21, 93] (see also [43] for a review of early work on fractal geometry in quantum theory). The applications were subsequently extended to fractal Wilson loops in lattice gauge theory [82], and fractal geometry of random surfaces in quantum gravity [16].

The use of fractional calculus in quantum theory is a relatively recent development. It is interesting to note that the concept of fractional quantum field preceded that of fractional quantum mechanics by almost a decade. Fractional scalar massless and massive fields have been considered by various authors [6, 7, 11, 15], with fractional Dirac equation followed somewhat later [77, 98]. The fractional Klein–Gordon operator has been treated from a purely mathematical point of view in [69], and the Euclidean fractional scalar field was studied within the framework of constructive quantum field theory as a convoluted white noise [2, 3, 27]. In the study of the QED radiative corrections, the fractional propagator has been introduced [28, 29]. Stochastic quantization of fractional field have been considered [48, 50]. The Casimir effect associated with the massive and massless fractional fields at zero and finite temperature have been investigated [17, 54, 57]. There exist studies on transition from the lattice and continuum fractional quantum field [94], and quantum field in multifractional spacetime from the quantum gravity point of view [12, 14].

In the case of fractional generalization of quantum mechanics, one can draw an analogy from the diffusion equation, which is extended to fractional diffusion equation to describe anomalous diffusion. By noting that Euclidean Schrödinger equation is the same as diffusion equation up to some constants, its fractional generalization can be carried out just like fractional diffusion equation. Mathematical treatment of the fractional Schrödinger operator has been considered in [70, 89]. The fractional Schrödinger equation and path integral approach to fractional quantum mechanics has been studied [44–46, 63].

This article aims to provide a brief review on the fractional Klein–Gordon field at zero and at a positive temperature. The fractional scalar field can be obtained from the fractional oscillator via the box quantization method. By treating the fractional field as convoluted white noise, it is possible to generalize the fractional field from a single index to two indices. Free energy with fractional boundary conditions and topological symmetry breaking of quartic self-interacting fractional Klein–Gordon field on toroidal spacetime are considered. Finally, a brief discussion on the possible generalization to the multifractional field or fractional field with variable order is given.

2 Fractional Klein–Gordon field

In this article, the fractional quantum field would be considered in Euclidean spacetime such that it can be regarded as fractional random field and mathematical tools from probability theory and stochastic differential equations apply.

The fractional scalar massive field can be obtained by usual box quantization. In the case of the fractional field, the Markov oscillator process for the usual quantum field is to be replaced by the non-Markovian fractional oscillator process. Consider the fractional oscillator process obtained from the following fractional generalization of Langevin equation with two fractional indices:

$$[{}_aD_t^\gamma + \omega]^\alpha Q(t) = \eta(t), \tag{1}$$

where $0 < \gamma \leq 1$, $\alpha > 0$, and $\omega \geq 0$. $\eta(t)$ is the usual white noise defined by its mean and covariance

$$\langle \eta(t) \rangle = 0, \quad \langle \eta(t)\eta(s) \rangle = \delta(t-s). \tag{2}$$

Note that the condition $\alpha\gamma \geq 1/2$ is required to ensure the process $Q(t)$ is an ordinary stochastic process; otherwise, it needs to be considered as a generalized process defined on the Schwarz space of test functions $S(\mathbb{R})$ [25]. The fractional derivative ${}_aD_t^\gamma$ is defined by [30, 35, 76, 89]

$${}_aD_t^\gamma f(t) = \frac{1}{\Gamma(n-\gamma)} \left(\frac{d}{dt}\right)^n \int_a^t \frac{f(u)}{(t-u)^{\gamma-n+1}} du, \quad n-1 < \gamma < n. \tag{3}$$

For $a = 0$, ${}_0D_t^\gamma$ is known as the Riemann–Liouville fractional derivative; when $a = -\infty$, ${}_{-\infty}D_t^\gamma$ is called the Liouville–Weyl fractional derivative. Note the Liouville–Weyl fractional derivative is also known as Weyl derivative in physics literature; the latter term will be preferred in this paper.

Note that one can formally defined the “shifted” fractional derivative $({}_aD_t^\gamma + \omega)^\alpha$ in terms of the unshifted derivative D_t^γ. By using binomial expansion, it is possible to express the shifted fractional derivative in terms of unshifted ones:

$$[{}_aD_t^\gamma + \omega]^\alpha = \sum_{j=0}^{\infty} \binom{\alpha}{j} \omega^j D_t^{\gamma(\alpha-j)}. \tag{4}$$

It can also be treated in a more rigorous way by using hypersingular integrals [87].

For the Riemann–Liouville derivative, (1) subjected to the boundary condition ${}_0D_t^{\gamma-1}Q_{\alpha,\gamma}^{\mathrm{RL}}(t) = 0$ has the solution

$$Q_{\alpha,\gamma}^{\mathrm{RL}}(t) = \int_0^t H_{\alpha,\gamma}(t-u)\eta(u)du \tag{5a}$$

with

$$H_{\alpha,\gamma}(t) = L^{-1}\left((s^\gamma + \omega)^{-\alpha}\right) = \frac{1}{\Gamma(\alpha)}\sum_{j=0}^{\infty}\frac{(-1)^j\omega^j}{j!}\frac{\Gamma(\alpha+j)}{\Gamma(\gamma(\alpha+j))}t^{\gamma(\alpha+j)-1}. \tag{5b}$$

Note that the condition $\alpha\gamma > 1/2$ is imposed to ensure the existence of the integral (5). $Q_{\alpha,\gamma}^{\mathrm{RL}}(t)$ is a nonstationary Gaussian process. It has zero mean and for $s < t$ its covariance is

$$\begin{aligned} C_{\alpha,\gamma}^{\mathrm{RL}}(t,s) &= \langle Q_{\alpha,\gamma}^{\mathrm{RL}}(t)Q_{\alpha,\gamma}^{\mathrm{RL}}(s)\rangle \\ &= \frac{1}{(\Gamma(\alpha))^2}\sum_{j=0}^{\infty}\sum_{l=0}^{\infty}\frac{\Gamma(j+\alpha)\Gamma(l+\alpha)}{\Gamma(\gamma(\alpha+j)+1)\Gamma(\gamma(\alpha+l))}s^{\gamma(\alpha+j)}t^{\gamma(\alpha+l)-1} \\ &\qquad \times {}_2F_1(1-\gamma(\alpha+l),1,1+\gamma(\alpha+j),s/t), \end{aligned} \tag{6}$$

where ${}_2F_1$ is the Gauss hypergeometric function. Note that (6) has a less complicated form for $\gamma = 1$, $\alpha > 0$ and $\gamma > 0$, $\alpha = 1$, but these covariances do not indicate any connection with fractional quantum theory. Therefore, the Riemann–Liouville fractional oscillator is not a suitable candidate for constructing fractional quantum field. Detailed discussion on the properties of $Q_{\alpha,\gamma}^{\mathrm{RL}}(t)$ can be found in [49, 55, 58, 59].

The solution of (1) with the Weyl derivative is given by

$$Q_{\alpha,\gamma}^{W}(t) = \frac{1}{\sqrt{2\pi}}\int_{\mathbb{R}}\frac{e^{ikt}\hat{\eta}(k)dk}{((ik)^\gamma+\alpha)^\alpha}, \tag{7}$$

where $\hat{\eta}(k)$ is the Fourier transform of $\eta(t)$, and again the condition $\alpha\gamma > 1/2$ is to ensure the finiteness of the integral (7). The covariance of $Q_{\alpha,\gamma}^{W}(t)$ is

$$C_{\alpha,\gamma}^{W}(t,s) = \langle Q_{\alpha,\gamma}^{W}(t)Q_{\alpha,\gamma}^{W}(s)\rangle = \frac{1}{2\pi}\int_{\mathbb{R}}\frac{e^{ik(t-s)}dk}{(|k|^{2\gamma}+2\omega|k|^\gamma\cos(\gamma\pi/2)+\omega^2)^\alpha}. \tag{8}$$

It has a closed form for $\alpha > 1/2$, $\gamma = 1$,

$$C_{\alpha,1}(t,s) = \frac{2^{1/2-\alpha}}{\sqrt{\pi}\Gamma(\alpha)}\left(\frac{|t-s|}{\omega}\right)^{\alpha-1/2}K_{\alpha-1/2}(\omega|t-s|), \tag{9}$$

where $K_\nu(t)$ is the McDonald function or the modified Bessel function of the second kind [26]. Fourier transform of (9) is $(2\pi)^{-1}(|k|^2+\omega^2)^{-\alpha}$, which can be regarded as the propagator of one-dimensional Euclidean fractional field of mass ω.

The usual box quantization method can be applied to the fractional Klein–Gordon field $\phi_\alpha(\mathbf{x}, t)$ in d-dimensional Euclidean spacetime $\mathbb{R}^d$. One can impose spatial cutoffs on and work in a finite volume say, a cube of volume L^{d-1} with periodic boundary conditions. The system can then be treated as a collection of harmonic oscillators with the following Fourier decomposition:

$$\phi_\alpha(\mathbf{x}, t) = L^{(d-1)/2} \sum_{\mathbf{k}} Q_{\mathbf{k}}(t) e^{i\mathbf{k}\cdot\mathbf{x}} \tag{10}$$

with $k_i = 2\pi n_i/L$, n_i integer. Here, the fractional oscillator $Q_{\mathbf{k}}(t)$ is the solution of the fractional Langevin equation

$$({}_{-\infty}D_t + \omega_{\mathbf{k}})^\alpha Q_{\mathbf{k}}(t) = \eta_{\mathbf{k}}(t), \tag{11}$$

where $\omega_{\mathbf{k}} = \sqrt{\mathbf{k}^2 + m^2}$, $\mathbf{k} = \sum_{i-1}^{d-1} k_i^2$ and $\langle \eta_{\mathbf{k}}(t)\eta_{\mathbf{k}}(s)\rangle = \delta(t-s)\delta_{\mathbf{k},\mathbf{k}'}$. Using Fourier transform to solve (11) with the boundary condition $Q_{\mathbf{k}}(0) = 0$ gives the solution $Q_{\mathbf{k}}(t)$, a Gaussian process with zero mean and covariance

$$\langle Q_{\mathbf{k}}(t) Q_{\mathbf{k}'}(s)\rangle = \frac{2^{\frac{1}{2}-\alpha}}{\sqrt{\pi}\Gamma(\alpha)} \left(\frac{|t-s|}{\omega_{\mathbf{k}}}\right)^{\alpha-1/2} K_{\alpha-\frac{1}{2}}(\omega_{\mathbf{k}}|t-s|)\delta_{\mathbf{k},\mathbf{k}'}. \tag{12}$$

By combining (10) and (12), substituting $\omega_{\mathbf{k}} = \sqrt{\mathbf{k}^2 + m^2}$ and removing the cutoffs lead to

$$\langle \phi_\alpha(\mathbf{x}, t)\phi_\alpha(\mathbf{y}, s)\rangle = \frac{1}{(2\pi)^d} \int_{\mathbb{R}^d} \frac{e^{i\mathbf{k}\cdot(\mathbf{x}-\mathbf{y}) + ik_d(t-s)}}{(\mathbf{k}^2 + k_d^2 + m^2)^\alpha} d^d k, \tag{13}$$

and the propagator of the fractional Klein–Gordon field $(|k|^2 + m^2)^{-\alpha}$, with $|k|^2 = \mathbf{k}^2 + k_d^2$, $\mathbf{k} \in \mathbb{R}^{d-1}$, $k_d \in \mathbb{R}$.

The solutions of (1) with the Weyl derivative for the two special cases $0 < \alpha \le 1$, $\gamma = 0$ and $\alpha = 0$, $\gamma > 0$, and the general case $0 < \gamma \le 1$, $\alpha > 0$, and their properties have been studied [49, 55, 58, 59]. Note that (6) does not lead to propagator in the form $1/(|k|^{2\gamma} + \omega^2)^\alpha$ which can be associated to Euclidean fractional scalar massive field with two indices. In order to achieve this objective, it is necessary to introduce a modified fractional oscillator which is the solution of the following stochastic pseudodifferential equation:

$$(\mathbf{D}_t^\gamma + \omega^2)^{\alpha/2} Q_{\alpha,\gamma}(t) = \eta(t), \tag{14}$$

where the Riesz derivative (in one-dimension) $\mathbf{D}_t^\gamma = (-d^2/dt^2)^{\gamma/2}$ is defined by the inverse Fourier transform [80, 89]:

$$\mathbf{D}_t^\gamma f = (-d^2/dt^2 f)^{\gamma/2} = \mathcal{F}^{-1}(|k_d|^\gamma \hat{f}(k_d)), \quad \gamma > 0, \tag{15}$$

where $\hat{f}(k_d)$ is the Fourier transform of $f(t)$. From

$$(\mathbf{D}_t^{2\gamma} + \omega^2)^{\alpha/2} f(t) = \mathcal{F}^{-1}\big((|k_a|^{2\gamma} + \omega^2)^{\alpha/2}\hat{f}(k_d)\big), \tag{16}$$

one gets the solution of (14) as

$$Q_{\alpha,\gamma}(t) = \frac{1}{(2\pi)^{1/2}} \int_{\mathbb{R}} \frac{e^{ik_d t}\hat{\eta}(k_d)}{(|k_d|^{2\gamma} + \omega^2)^{\alpha/2}} dk_d, \tag{17}$$

which is the modified fractional oscillator process indexed by two parameters.

Unlike the case with $\gamma = 1$, the usual box quantization method does not lead to a fractional field with the desired propagator $(|k|^{2\gamma} + m^2)^{-\alpha}$. One can employ Parisi–Wu stochastic quantization method to the Euclidean fractional field $\phi_{\alpha,\gamma}(x)$ [50, 55]. Alternatively, it can be considered as the solution of the stochastic pseudodifferential equation

$$\big((-\Delta)^\gamma + m^2\big)^{\alpha/2} \phi_{\alpha,\gamma}(x) = \eta(x), \tag{18}$$

where $(-\Delta)^\gamma$, the fractional power of the negative Laplacian operator on $\mathbb{R}^d$, is also known as Riesz fractional derivative [80, 89]. It is defined just like the one-dimensional case $\mathbf{D}_t^\gamma$ as given by (15), with

$$(-\Delta)^\gamma f(x) = \mathcal{F}^{-1}\big(|k|^{2\gamma}\hat{f}\big)(x), \quad \gamma > 0. \tag{19}$$

Let $G_{\alpha,\gamma}$ be the Green function of the pseudo-differential operator $((-\Delta)^\gamma + m^2)^{\alpha/2}$ with $\gamma > 0$ and $\alpha > 0$. Then

$$(\mathcal{F}G_{\alpha,\gamma})(k) = \frac{1}{(2\pi)^{d/2}(|k|^{2\gamma} + m^2)^{\alpha/2}}, \tag{20}$$

or

$$G_{\alpha,\gamma}(x) = \frac{1}{(2\pi)^d} \int_{\mathbb{R}^d} \frac{e^{ik.x} d^d k}{(|k|^{2\gamma} + m^2)^{\alpha/2}}. \tag{21}$$

The solution is given by the stochastic integral $\phi_{\alpha,\gamma} = ((-\Delta)^\gamma + m^2)^{-\alpha/2} * \eta$, which is the convoluted white noise with the Green function. Since the function $(|k|^\gamma + m^2)^{-\alpha/2}$ is in $L_2(\mathbb{R}^d)$ if and only if $\alpha\gamma > d/2$, so $\phi_{\alpha,\gamma}(x)$ is an ordinary random field if this condition is satisfied. When $\alpha\gamma \leq d/2$, the fractional field needs to be regarded as a generalized random field over the Schwarz space of test functions $S(\mathbb{R}^d)$ [25]. Fourier transform of the Euclidean two-point function or Schwinger function $\langle\phi_{\alpha,\gamma}(x)\phi_{\alpha,\gamma}(y)\rangle = G_{\alpha,\gamma}(x - y)$ gives the Euclidean field propagator $(2\pi)^{-d}(|k|^{2\gamma} + m^2)^{-\alpha}$.

When $\gamma = 1$ and $\alpha > 1$, $\phi_{\alpha,\gamma}(x)$ reduces to the fractional Klein–Gordon field $\phi_\alpha(x)$ which is the solution of the stochastic pseudodifferential equation $(-\Delta + m^2)^{\alpha/2}\phi_\alpha(x) =$

$\eta(x)$. The convoluted white noise $\phi_\alpha = G_\alpha * \eta$ which gives the fractional field with two-point Schwinger function $(2\pi)^{-d/2}2^{1-\alpha}\Gamma^{-1}(\alpha/2)(m/|x|)^{(d-2\alpha)/2}K_{(d-2\alpha)/2}(m|x|)$. Note that the fractional operator $(-\Delta + m^2)^{\alpha/2}$ is closely related to the Bessel potential with the covariance equals to the Bessel kernel up to a multiplication constant [89]. The Euclidean fractional field ϕ_α is also known as Bessel field in mathematical literature. Note that for the massless case $m = 0$, $(-\Delta)^{-\alpha\gamma/2}\eta$ is a fractional random field only for $0 < \alpha\gamma < d/2$.

It would be interesting to examine briefly the long and short "distance" behavior of the Schwinger two-point function of $\phi_{\alpha,\gamma}(x)$. Note that the two-point function can be represented by [56]

$$\frac{-|x|^{\frac{2-d}{2}}}{2^{\frac{d-2}{2}}\pi^{\frac{2+d}{2}}}\operatorname{Im}\int_0^\infty \frac{K_{\frac{d-2}{2}}(u|x|)}{(e^{i\gamma\pi}u^{2\gamma}+m^2)^\alpha}u^{d/2}du. \tag{22}$$

For all $\gamma \in (0,1)$ and $\alpha > 0$, the above integral is convergent if $x \neq 0$. (22) can be used to study the large $|x|$ behavior of the Schwinger function of $\phi_{\alpha,\gamma}(x)$. It can be shown that when $|x| \to \infty$,

$$\begin{aligned} C_{\alpha,\gamma}(x) \sim{}& \frac{1}{\pi^{1+d/2}}\sum_{j=1}^\infty \frac{(-1)^{j-1}2^{2\gamma j}\Gamma(\alpha+j)}{j!\Gamma(a)}\Gamma(\gamma j+1)\Gamma(\gamma j+d/2) \\ &\times m^{-2\alpha-j}\sin(\gamma j\pi)|x|^{2\gamma j-d} \end{aligned} \tag{23}$$

with the leading term given by $2^{2\gamma}\pi^{-1-d/2}\alpha m^{-2\alpha-1}\Gamma(\gamma+1)\Gamma(\gamma+d/2)\sin(\gamma\pi)|x|^{-2\gamma-d}$. Therefore, at long distance the two-point function decays as $|x|^{-2\gamma-d}$ and does not depend on α. When $\gamma = 1$, (22) cannot be employed to obtain the long distance behavior. Instead, by using the asymptotic property of $K_\nu(z)$ one gets

$$\begin{aligned} C_{\alpha,1}(x) ={}& \frac{2^{(1-2\alpha-d)/2}e^{-m|x|}}{\pi^{(d-1)/2}\Gamma(\alpha)}\sum_{j=0}^\infty\Bigg[\frac{\Gamma(\alpha+j-(d-1)/2)}{2^j j!\Gamma(\alpha-j-(d-1)/2)} \\ &\times m^{-\alpha-j+(d-1)/2}|x|^{\alpha-j+(d+1)/2}\Bigg] \end{aligned} \tag{24}$$

with the leading term $2^{(1-2\alpha-d)/2}\pi^{(1-d)/2}\Gamma^{-1}(\alpha)e^{-m|x|}m^{-\alpha+(d-1)/2}|x|^{\alpha-(d+1)/2}$, which shows exponential decay of the two-point function in the large $|x|$ limit.

As $|x| \to 0$, one can derive the following behavior for the two-point function [56]

$$C_{\alpha,\gamma}(x) - C_{\alpha,\gamma}(0) = \begin{cases} c_1|x|^{2\alpha\gamma-d} + O(|x|^{2\alpha\gamma-d}) & \text{if } \alpha\gamma \in (d/2, 1+d/2), \\ c_2|x|^2\log(\frac{1}{|x|}) + O(|x|^2) & \text{if } \alpha\gamma = 1+d/2, \\ c_3|x|^2 + O(|x|^2) & \text{if } \alpha\gamma > 1+d/2, \end{cases} \tag{25}$$

where c_1, c_2, c_3 some constants. In the case $\alpha\gamma \in (d/2, 1+d/2)$, the two-point function varies as $|x|^{2\alpha\gamma-d}$ in the short distance regime. Since the dependency of α and γ

is through the product $\alpha\gamma$, one can let $\alpha = \alpha'/\gamma$ such that $\alpha\gamma = \alpha'$. Thus, in the limit $|x| \to 0$, the two-point function behaves as $|x|^{2\alpha'-d}$ and is independent of γ. Note that the constant c_1 is independent of mass m, hence this result also holds for the massless case.

It is interesting to note in the short- and long-distance regimes, the two-point function of the fractional Gaussian field $\phi_{\alpha,\gamma}(x)$ is characterized separately by the parameter α and γ. Since all n-point functions of the free field theory can be expressed as sums of products of two-point functions, these asymptotic properties hold for all Schwinger functions of $\phi_{\alpha,\gamma}(x)$.

Analytic continuation of the Schwinger functions of the fractional Klein–Gordon field $\phi_\alpha(x)$ to the corresponding Wightman functions in the Minkowskian spacetime based on the Osterwalder–Schrader reconstruction framework [71, 72] has been carried out [2, 3]. One of the basic property that allows the analytic continuation of Schwinger functions to Wightman functions is the reflection positivity condition. Denote by C the two-point function of the Euclidean field, and θ be the time reflection with respect to the hyperplane $t = 0$, $\theta x = (-t, \mathbf{x})$, $x = (t, \mathbf{x}) \in \mathbb{R} \times \mathbb{R}^{d-1}$, and P_+ be the orthogonal projection in L^2 onto $t \geq 0$. The reflection positivity property states that $P_+\theta P_+ \geq 0$. This condition is satisfied by the free field with $0 < \alpha \leq 1$, and it has an analytic continuation to a relativistic fractional quantum field in Hilbert space with positive metric. However, for $\alpha > 1$ the Euclidean two-point function fails to satisfy the reflection positivity condition, hence it results in relativistic fractional quantum field with indefinite metric Hilbert space. In general, it is necessary to consider relativistic fractional field within the framework of Hilbert space with indefinite metric [3]. It has been shown that a local and invariant quantization is not possible in a Hilbert space with positive-definite metric. However, it can be formulated on a Krein space with modified Wightman axioms [62, 92].

One interesting property of the free Euclidean Klein–Gordon field ($\alpha = 1/2$, $\gamma = 1$) is that it satisfies the global Markov property [65, 66]. One would like to know whether this property or a modified version still holds for free fractional Klein–Gordon field. By considering its reproducing kernel Hilbert space defined by the covariance of Bessel field, which is isomorphic to the fractional order Sobolev space $L^{\alpha,2}(\mathbb{R}^d)$, Pitt and Robeva [75, 81] have studied the sharp Markov property of the Bessel field on $\mathbb{R}^d$, $d < 3$. They have shown that under certain technical conditions the Bessel field satisfies the sharp Markov property for some integer $\ell \geq 1$ and $\ell < \alpha < \ell + 1$. A similar result for Levy fractional Brownian field indexed by α in $\mathbb{R}^d$ has also been obtained. It would be interesting to see whether this result can be generalized to fractional field indexed by two parameters $\phi_{\alpha,\gamma}(x)$.

Finally, one remarks briefly on the fractal dimension of the random field $\phi_{\alpha,\gamma}(x)$. It can be shown [55, 59] that for $d/2 < \alpha\gamma < (d+2)/2$, then with probability one the fractal dimension of the graph of the sample path of $\phi_{\alpha,\gamma}(x)$ is $\frac{3d}{2}+1-\alpha\gamma$, which agrees with the result based on a general theorem [22]. Note that fractal dimension is a local property, and it depends on the parameters α and γ in the combination $\alpha\gamma$. By replacing α by

α/γ, one finds the fractal dimension depends on single parameter independent of γ. This is consistent with the local behavior of the Schwinger functions discussed earlier.

3 Fractional field at positive temperature

Discussion given in previous section applies to fractional field with positive temperature if the fractional oscillators are replaced by fractional thermal oscillators [48]. For an oscillator at positive temperature $T = 1/\beta > 0$, denoted by $Q^{\beta}(t)$, one imposes the periodic time condition $Q^{\beta}(t+\beta) = Q^{\beta}(t)$. The usual definitions of fractional derivatives are not suited to deal with periodic functions since they do not preserve periodicity. Following Samko et al. [89], the definitions of fractional integrodifferential operators can be modified such that they transform a periodic function into another periodic one. Note that fractional derivative and integral of periodic functions expressed in terms of Fourier series was first considered by Weyl. For a periodic function $f(t)$ on $\mathbb{R}$ with period β, its Fourier series is given by

$$f(t) = \sum_{n=-\infty}^{\infty} c_n e^{i\omega_n t}, \quad c_n = \frac{1}{\beta}\int_0^{\beta} f(t)e^{-i\omega_n t}, \tag{26}$$

where $\omega_n = 2n\pi/\beta$. In order not to include constants, it is assumed that the mean of the function considered vanishes or $c_0 = 0$. Fractional integral and derivative are then defined as

$$D_t^{\alpha} f(t) = \sum_{n=-\infty}^{\infty} (i\omega_n)^{\alpha} c_n e^{i\omega_n t}, \quad I_t^{\alpha} f(t) = \sum_{n=-\infty}^{\infty} (i\omega_n)^{-\alpha} c_n e^{i\omega_n t}. \tag{27}$$

By using the above definitions, fractional thermal oscillator is given by the solution of the following fractional Langevin equation:

$$(D_t + \omega)^{\alpha} Q_{\alpha}^{\beta}(t) = \eta_{\beta}(t) \tag{28}$$

with the periodic boundary condition $Q_{\alpha}^{\beta}(t+\beta) = Q_{\alpha}^{\beta}(t)$, and $\eta_{\beta}(t)$ is the periodic white noise $\eta_{\beta}(t+\beta) = \eta_{\beta}(t)$. The solution is given by

$$Q_{\alpha}^{\beta}(t) = \int_0^{\beta} G_{\beta}(t-u)\eta_{\beta}(u)du, \tag{29}$$

where $G_{\beta}(t)$ is the Green function

$$G_{\beta}(t) = \frac{1}{\beta}\sum_{n=-\infty}^{\infty} \frac{e^{i\omega_n t}}{(i\omega_n + \omega)^{\alpha}}. \tag{30}$$

The covariance of $Q_\alpha^\beta(t)$ is

$$\langle Q_\alpha^\beta(t) Q_\alpha^\beta(s)\rangle = \frac{1}{\beta}\sum_{n=-\infty}^{\infty}\frac{e^{i\omega_n(t-s)}}{(\omega_n^2+\omega^2)^\alpha}. \tag{31}$$

Again, one can employ box quantization method to obtain the fractional Klein–Gordon field $\phi_\alpha^\beta(x)$ at positive temperature β^{-1}. The resulting Euclidean thermal two-point function of the fractional field is

$$\langle \phi_\alpha^\beta(x)\phi_\alpha^\beta(y)\rangle = \frac{1}{(2\pi)^{d-1}\beta}\sum_{-\infty}^{\infty}\frac{e^{ik_n\cdot(x-y)}}{(k_n^2+m^2)^\alpha}, \tag{32}$$

where $k_n = (\omega_n, \mathbf{k})$, $k_n^2 = \omega_n^2 + \mathbf{k}^2$. When $\alpha = 1$, it reduces to the usual positive temperature Klein–Gordon field, which satisfies the two-sided Markov property on the circle [38]. $\phi_\alpha^\beta(x)$ fails to observe this property when $\alpha \neq 1$. The Euclidean propagator for $\alpha = 1$ is also known as Matsubara propagator.

In the conventional finite temperature field theories, it is important to determine the asymptotic high temperature behavior of many field-theoretic thermodynamic quantities such as partition function, free energy, etc. The techniques used in these calculations also apply to fractional fields. For example, the method of Riemann zeta function regularization and heat kernel can be used in the derivation of the high temperature expansion of free energy associated to fractional thermal Klein–Gordon field at positive temperature. Using the thermal zeta function [19, 37] associated with the fractional Klein–Gordon operator $(-\Delta + m^2)^\alpha$,

$$\zeta_K(s) = \frac{V}{(2\pi)^3}\sum_{n=-\infty}^{\infty}\int_{\mathbb{R}^{d-1}}\frac{e^{ik_n(x-y)}d^{d-1}k}{(4\pi^2\beta^2n^2+\mathbf{k}^2+m^2)^{\alpha s}}, \tag{33}$$

one can calculate the high temperature expansion of the free energy density as

$$F = -\alpha\left(\frac{\pi^2}{90}T^4 + \frac{1}{24}m^2T^2 - \frac{1}{12}m^3T + \cdots\right), \tag{34}$$

which equals to the free energy for the ordinary Klein–Gordon field multiply by the fractional parameter α [48].

The free energy calculation for the more general case of fractional field parametrised by two indices is complicated, so far only the one-dimensional case has been obtained [55]. In this case, the renormalized free energy is

$$\begin{aligned} F = \frac{\alpha}{\beta}\Bigg(&\gamma\log m + \gamma\log\beta - \sum_{l\in\mathbb{N}, l\neq\frac{1}{2\gamma}}\frac{(-1)^l m^{2l}}{l}\left(\frac{\beta}{2\pi}\right)^{2\gamma l}\zeta(2\gamma l)\Bigg) \\ &+ \epsilon_\gamma(-1)^{\frac{1}{2\gamma}}\left(\frac{\beta m}{\pi}\right)\left[\gamma\left(\log\left(\frac{2\pi}{\beta m}\right)+\psi(1)\right) - \frac{1}{2}\left(\psi\left(\frac{1}{2\gamma}\right)+\psi(1)\right)\right], \end{aligned} \tag{35}$$

where $\zeta(s) = \sum_{n=1}^{\infty} n^{-s}$ is the Riemann zeta function, $\psi(z) = \Gamma'(z)/\Gamma(z)$ is the logarithmic derivative of the Gamma function, and $\epsilon_\gamma = 1$ if and only if $1/(2\gamma)$ is an integer, otherwise $\epsilon_\gamma = 0$.

An interesting topic in fractional calculus is regarding the use of the fractional derivative boundary conditions or fractional Neumann conditions [35, 89]. The following example [17, 54] illustrates how such boundary conditions can provide an interpolation to various usual boundary conditions. For simplicity, consider a free fractional scalar massless field $\phi_\alpha(x)$, $x = (\mathbf{x}, t) \in \mathbb{R}^{d-1} \times \mathbb{R}$ inside a rectangular box $\Omega = [0, L_1] \times \cdots \times [0, L_{d-2}] \times [0, D]$ such that $D \ll L_i$, $i = 1, \ldots, d-2$. L_i is finally allowed to approach infinity to result space between the two hyperplanes $x_{d-1} = 0$ and $x_{d-1} = \ell$ in $\mathbb{R}^{d-1}$. The fractional Neumann boundary conditions for the parallel plates are

$$\frac{\partial^\mu}{\partial x_{d-1}^\mu}\phi(\mathbf{x}, x_{d-1}, t)\Big|_{x_{d-1}=0}, \quad \frac{\partial^\nu}{\partial x_{d-1}^\nu}\phi(\mathbf{x}, x_{d-1}, t)\Big|_{x_{d-1}=\ell}, \tag{36}$$

where $\mathbf{x} \in \mathbb{R}^{d-2}$, $x_{d-1} \in \mathbb{R}$ and $\mu, \nu \in [0, 1]$. Here, it is convenient to define the fractional derivative in terms of Fourier transform:

$$\frac{\partial^\mu}{\partial x^\mu} f(x) = \frac{1}{2\pi} \int_{-\infty}^{\infty} (ik)^\mu e^{ikx} \hat{f}(-k) dk \tag{37a}$$

with

$$(\pm ik)^\mu = |k|^\mu e^{\pm i\mu\pi/2} \operatorname{sgn}(k). \tag{37b}$$

For $\mu = \nu = 0$, the boundary conditions for both plates are of Dirichlet type; for $\mu = \nu = 1$, one gets the Neumann boundary condition for both plates. When $\mu = 0$, $\nu = 1$, or $\mu = 1$, $\nu = 0$, the boundary condition is of Boyer type. One has the fractional boundary condition for both plates if the values of (μ, ν) differ from the above values.

Zeta function technique can be used in the computation of free energy (and Casimir energy). Basically, it involves three main steps. In the case for scalar massless fractional Klein–Gordon field, they are as follows: (i) determination the eigenvalues λ of the fractional d'Alembertian operator $(-\Delta)^\alpha$ with suitable boundary conditions, hence the spectral zeta function $\zeta_{(-\Delta)^\alpha}(s) = \sum_\lambda \lambda^{-s}$; (ii) analytic continuation of the zeta function to a meromorphic function of the entire complex plane; (iii) evaluation of $\det(-\Delta)^\alpha$ in term of the $\zeta_{(-\Delta)^\alpha}(s)$ using $\det(-\Delta)^\alpha = \exp(\zeta'_{(-\Delta)^\alpha}(0))$.

The results obtained for the free energy density at positive temperature β^{-1} with various boundary conditions can be summarized in the following compact form [17]:

$$F_{\alpha;\mu,\nu} = \frac{\sigma_{\mu,\nu} \alpha \pi^{d/2} \Gamma(d/2)}{\ell^{d-1}} \left(\left(\frac{\ell}{\pi\beta}\right)^d \zeta_R(d) + \frac{1}{(2\pi)^d} \sum_{n=1}^{\infty} \frac{\cos(n(\mu-\nu)\pi)}{n^d} \right.$$
$$\left. + 2\left(\frac{\ell}{\pi\beta}\right)^d \sum_{l=1}^{\infty} \sum_{n=1}^{\infty} \frac{\cos(n(\mu-\nu)\pi)}{(l^2 + (2n\ell/\beta)^2)^{d/2}} \right.$$

$$+\frac{\epsilon_{\mu,\nu}(\ell/\beta)^{d-1}\Gamma((d-1)/2)}{2\pi^{d-1/2}\Gamma(d/2)}\zeta_R(d-1)\Bigg), \tag{38a}$$

where

$$\sigma_{\mu,\nu}=\begin{cases}1 & \text{if } (\mu,\nu)=\{(0,0),(1,0),(0,1),(1,1)\},\\ 2 & \text{otherwise,}\end{cases} \tag{38b}$$

$$\epsilon_{\mu,\nu}=\begin{cases}1 & \text{if } (\mu,\nu)=(1,1),\\ -1 & \text{if } (\mu,\nu)=(0,0),\\ 0 & \text{otherwise.}\end{cases} \tag{38c}$$

The high temperature behavior of the free energy for various boundary conditions can be then derived and is given by [17]

$$\begin{aligned} F_{\alpha;\mu,\nu} \sim & -\frac{\sigma_{\mu,\nu}\alpha}{\ell^{d-1}}\Bigg[\left(\frac{\ell}{\sqrt{\pi}\beta}\right)^d\Gamma(d/2)\zeta_R(d)+\frac{\Gamma((d-1)/2)}{2^{d-1}\pi^{d/2}\beta}\sum_{n=1}^{\infty}\frac{\cos(n(\mu-\nu)\pi)}{n^{d-1}} \\ & + 2^{1-d/2}\left(\frac{\ell}{\beta}\right)^d\cos((\mu-\nu)\pi) \\ & \times\left(1+\sum_{l=1}^{\infty}\left(\frac{\beta}{8\pi\ell}\right)^l\frac{e^{-4\pi D/\beta}}{2^{2l}l!}\prod_{j=1}^{l}((d-1)^2-(2j-1)^2)\right)\Bigg] \\ & + O(e^{-8\pi\ell/\beta}). \end{aligned} \tag{39}$$

The leading term $-\sigma_{\mu,\nu}\alpha\ell\Gamma(d/2)\zeta_R(d)/(\sqrt{\pi}\beta)^d$ varies with T^d and does not depend on $\mu-\nu$. It gives $F_{\alpha;\mu,\nu}=-\sigma_{\mu,\nu}\alpha\pi^2\ell T^4/90$ for $d=4$. One can verify the consistency of the results with ordinary massless field ($\alpha=1$) for the appropriate values of μ and ν corresponding to the usual ordinary Dirichlet, Neumann, and Boyer boundary conditions [17].

4 Spontaneously symmetry breaking

This section considers briefly the possibilities of topological mass generation and symmetry breaking mechanism for a fractional scalar field with interaction in a toroidal spacetime. A massless field can develop a mass as a consequence of both self-interaction and nontrivial spacetime topology, a phenomenon known as topological mass generation [24, 95]. For ordinary quantum fields, topological mass generation in toroidal spacetime has been studied by several authors using the zeta function regularization technique [1, 18, 36].

The possibilities of topological mass generation and symmetry breaking mechanism for a quartic self-interacting fractional Klein–Gordon scalar field ϕ_α^4 in a

d-dimensional toroidal spacetime has been studied [52]. The Lagrangian is

$$L = -\frac{1}{2}\phi_\alpha(x,t)[(-\Delta + m^2)^\alpha]\phi_\alpha(x,t) - \frac{\lambda}{4!}\phi_\alpha^4(x,t). \tag{40}$$

By using the Epstein zeta function regularization method with some appropriate modifications, the one loop effective potential for both the massive and massless ϕ_α^4 theory in the toroidal spacetime $\mathbf{T}^p \times \mathbb{R}^q$, $d = p + q$ can be derived in terms of power series of $\lambda\breve{\phi}_\alpha^2$, where $\breve{\phi}_\alpha$ is the constant classical background field. The renormalized mass m_{ren} is obtained explicitly. For the massive case, it is related to the bare mass m by

$$m_{\text{ren}}^{2\alpha} = m^{2\alpha} + \frac{\lambda\pi^\alpha m^{\frac{d}{2}-\alpha}}{(2\pi)^{\frac{d}{2}+\alpha}\Gamma(\alpha)} \sum_{\mathbf{n}\in\mathbb{Z}^p\setminus\{0\}} \left(\sum_{i=1}^p |L_i n_i|^2\right)^{\frac{d-2\alpha}{4}} K_{\frac{d-2\alpha}{2}}\left(m\sqrt{\sum_{i=1}^p |L_i n_i|^2}\right), \tag{41}$$

with L_i, $i = 1,\ldots,p$, the compactification lengths of the torus $\mathbf{T}^p$. The renormalized topologically generated mass reduces to bare mass $m_{\text{ren}}^{2\alpha} = m^{2\alpha}$ when $p = 0$. It agrees with the result in [52] for $\alpha = 1$, $d = 4$. We note that in the massive case, $m_{\text{ren}}^{2\alpha}$ is always positive, hence there is no symmetry breaking due to quantum fluctuations.

For the massless case, the renormalized topologically generated mass is given by

$$\begin{aligned} m_{\text{ren}}^{2\alpha} &= \frac{\lambda\Gamma(\alpha - \frac{q}{2})}{2^{q+1}\pi^{q/2}\Gamma(\alpha)}\left(\prod_{i=1}^p L_i\right)^{-1} Z_p\left(\alpha - \frac{q}{2}; \frac{2\pi}{L_1},\ldots,\frac{2\pi}{L_p}\right) \\ &= \frac{\lambda\Gamma(\frac{d}{2} - \alpha)}{2^{\alpha+1}\pi^{d/2}\Gamma(\alpha)} Z_p\left(\frac{d}{2} - \alpha; L_1,\ldots,L_p\right) \qquad \text{if } \alpha \neq \frac{q}{2}, \end{aligned} \tag{42a}$$

$$\begin{aligned} m_{\text{ren}}^{2\alpha} &= \frac{\lambda}{2^{q+1}\pi^{q/2}\Gamma(\alpha+1)}\left(\prod_{i=1}^p L_i\right)^{-1} \\ &\quad \times \left\{1 + \alpha[\psi(\alpha) - \psi(1)] + \alpha Z_p'\left(0; \frac{2\pi}{L_1},\ldots,\frac{2\pi}{L_p}\right)\right\} \qquad \text{if } \alpha = \frac{q}{2}, \end{aligned} \tag{42b}$$

where the zeta function $Z_p(s; a_1,\ldots,a_p) = \sum_{\mathbf{n}\in\mathbb{Z}^p}(\sum_{i=1}^p (a_i n_i)^2)^{-s}$. When $d = 4$ and $\alpha = 1$, (42) agrees with the corresponding results in [18]. For a fixed compactified dimension $p \le 9$, symmetry breaking occurs if $0 < d - 2\alpha \le p$. However, when $p \ge 10$, symmetry breaking is possible only for values of $d - 2\alpha$ that lie in the proper subset of $(0, p]$.

It is interesting to note that essentially the same results can be derived if the fractional scalar field of order α in a d-dimensional toroidal spacetime $\mathbf{T}^p \times \mathbb{R}^{d-p}$ considered above is replaced by an ordinary scalar field ($\alpha = 1$) in a toroidal spacetime $\mathbf{T}^p \times \mathbb{R}^{d-p+2-\alpha}$ with fractional dimension $d + 2 - \alpha$. More detailed discussion can be found in [18].

One possible extension of the above discussion is to include local structure like spacetime curvature in addition to nontrivial global topology. Another useful generalization is to study the topological mass generation for fractional quantum field with variable order (or multifractional quantum field, see next section) in view of the possible multifractional character of spacetime at sub-Planckian scale.

5 Multifractional quantum field

In complex disordered physical systems, there are certain physical processes with the fractal dimensions dependent on some physical parameters such as time, position, energy, etc. [41, 42, 97]. Such processes can have variable memory and their modeling requires the use of integrodifferential operators with variable fractional order [85, 86, 88]. In other words, it is necessary introduce multifractional random processes with variable local Hölder exponents in the study of these systems.

Random processes generated by pseudodifferential operators with variable fractional order such as multifractional stable-like processes associated with $-(-\Delta)^{\alpha(x)}$, $0 < \alpha(x) < 1$, were studied by various authors [8, 34, 96]. The subsequent results [31, 33] show the existence a Feller semigroup generated by the pseudodifferential operator with symbol given by $-(1 + |\lambda|^2)^{\alpha(x)}$, $0 < \inf\alpha \leq \sup\alpha \leq 2$. Gaussian random processes such as multifractional Brownian motion with covariance functions defined by an elliptic pseudodifferential operator of variable fractional order have also been considered [9, 73].

It would be interesting to see whether oscillator process with single fractional variable index can be regarded as one-dimensional Euclidean multifractional quantum field. One can define multifractional oscillator process of Weyl type in a similar way as multifractional Brownian motion [51, 73],

$$Q^W_{\alpha(t)}(t) = \frac{1}{\Gamma(\alpha(t))} \int_{-\infty}^{t} (t-u)^{\alpha(t)-1} e^{\omega(t-u)} \eta(u)du. \tag{43}$$

In contrast to the Weyl fractional oscillator $Q^W_{\alpha,1}$ which is obtained as solution of (1), it is unlikely that $Q^W_{\alpha(t)}(t)$ can be obtained as a solution of an variable order fractional Langevin-like equation. The covariance of the multifractional oscillator can be computed [51] and it is given by

$$\langle Q^W_{\alpha(t)}(t) Q^W_{\alpha(s)}(s)\rangle = \frac{e^{-\omega(t-s)}(t-s)^{\alpha(s)+\alpha(t)-1}}{\Gamma(\alpha(t))} \Psi(\alpha(s), \alpha(s)+\alpha(t), 2\omega(t-s)), \tag{44}$$

where $\Psi(a, b, c)$ is the confluent hypergeometric function [26]. Note that $Q^W_{\alpha(t)}(t)$ is in general a nonstationary process in contrast to the Weyl fractional oscillator with covariance given by (9). It can be shown that multifractional Brownian motion is the "massless limit" $\omega \to 0$ of the "reduced" multifractional Weyl oscillator process $Q^W_{\alpha(t)}(t) - Q^W_{\alpha(t)}(0)$. The multifractional oscillator of the Riemann–Liouville type can be defined in a similar way; its covariance can be expressed as a summation of the Gauss hypergeometric functions; for details, see [51]. The above discussion indicates that the multifractional oscillator defined by (44) is not a suitable candidate for Euclidean fractional field of variable order in one dimension.

It is possible to define multifractional field on $\mathbb{R}^d$s a convoluted white noise $\phi_{\alpha(x)}(x) = G_{\alpha(x)} * \eta(x)$ with the Green's function

$$G_{\alpha(x)}(x) = (2\pi)^{-d} \int_{\mathbb{R}^d} \frac{e^{ik\cdot x} d^d k}{(|k|^2 + m^2)^{\alpha(x)/2}}. \tag{45}$$

$\phi_{\alpha(x)}(x)$ can be formally regarded as the solution to the stochastic pseudodifferential equation with variable order

$$\left((-\Delta) + m^2\right)^{\alpha(x)/2} \phi_{\alpha(x)}(x) = \eta(x). \tag{46}$$

The two-point Schwinger function of the field $\phi_{\alpha(x)}(x)$ is

$$\begin{aligned} C_{\alpha(x)\alpha(y)}(x, y) = {} & \frac{2^{d-[\alpha(x)+\alpha(y)]/2}}{(2\pi)^d \Gamma([\alpha(x) + \alpha(y)]/2)} \left(\frac{m}{|x - y|} \right)^{(d-\alpha(x)-\alpha(y))/2} \\ & \times K_{(d-\alpha(x)-\alpha(y))/2}(m|x - y|). \end{aligned} \tag{47}$$

The Schwinger function behaves as $|x - y|^{(\alpha(x)+\alpha(y)-d-1)/2} e^{-m|x-y|}$ in the long-distance limit, it decays exponentially just like in the fractional field with constant fractional order. The local behavior of the two-point Schwinger function of $\phi_{\alpha(x)}(x)$ is similar to $\phi_\alpha(x)$, it follows the power law-type behavior $|x - y|^{\alpha(x)+\alpha(y)-1}$.

One multifractional random field that is of interest to Euclidean quantum field is the Riesz–Bessel field of variable fractional order $\phi^{\mathrm{RB}}_{\alpha(x),\gamma(x)}(x)$ on $\mathbb{R}^d$. It allows the interpolation between multifractional massive and massless scalar fields [53, 84]. The multifractional Riesz–Bessel field can formally be considered as the solution of the following stochastic pseudodifferential equation:

$$(-\Delta)^{\gamma(x)/2} \left(-\Delta + m^2\right)^{\alpha(x)/2} \phi^{\mathrm{RB}}_{\alpha(x),\gamma(x)}(x) = \eta(x). \tag{48}$$

Conditions for (48) to define an ordinary random field are $0 \le \gamma(x) < d/2$ and $\alpha(x) + \gamma(x) > d/2$ for all x. Otherwise, $\phi^{\mathrm{RB}}_{\alpha(x),\gamma(x)}(x)$ is a generalized field on $S(\mathbb{R}^d)$. Its covariance is given by

$$\begin{aligned} C_{\alpha(\cdot),\gamma(\cdot)}(x, y) &= \langle \phi^{\mathrm{RB}}_{\alpha(x),\gamma(x)}(x) \phi^{\mathrm{RB}}_{\alpha(x),\gamma(x)}(x) \rangle \\ &= \frac{1}{(2\pi)^d} \int_{\mathbb{R}^d} \frac{e^{ik\cdot(x-y)} d^d k}{|k|^{\gamma(x)+\gamma(y)} (|k|^2 + m^2)^{(\alpha(x)+\alpha(y))/2}}. \end{aligned} \tag{49}$$

Equation (49) can be evaluated to give a rather complicated expression involved the Gauss hypergeometric functions [53]. When $\gamma(x) = 0$, $\phi^{\mathrm{RB}}_{\alpha(x),0}(x)$ reduces to the fractional scalar massive field $\phi_{\alpha(x)}(x)$ of variable order with covariance (47). On the other hand, if $\alpha(x) = 0$, $\phi^{\mathrm{RB}}_{0,\gamma(x)}(x)$ becomes multifractional scalar massless field $\phi_{\gamma(x)}(x)$.

It can be shown [53] that the Hausdorff dimension of the graph of the fractional Riesz–Bessel field of variable order $\phi^{\mathrm{RB}}_{\alpha(x),\gamma(x)}(x)$ over a hypercube $I = \prod_{i=1}^d [a_i, b_i]$ is $1 + \frac{3d}{2} - m_I[\alpha(x) + \gamma(x)]$ with $m_I[\alpha(x) + \gamma(x)] = \min\{\alpha(x) + \gamma(x); x \in I\}$. It reduces to the result for the massive multifractional field $\phi_{\alpha(x)}(x)$ when $\gamma(x) = 0$.

6 Concluding remarks

This paper provides a brief discussion on some basic properties of fractional quantum field in Euclidean spacetime. Various types of fractional oscillators have been considered to identify the appropriate one suitable to realise the box quantization. Fractional thermal oscillators are used to construct fractional quantum field at positive temperature. Free energy and its high temperature limit are considered. The use of fractional Neumann boundary conditions in the computation of the Casimir-free energy allows the interpolation between the usual Dirichlet, Neumann, and Boyer boundary conditions. Topological mass generation and symmetry breaking is briefly discussed. Many of the mathematical methods such as zeta function regularization technique used in the calculation of Casimir-free energy and topological mass generation for ordinary quantum fields also apply to fractional field with some appropriate modifications.

Fractional quantum field in Minkowskian spacetime can be recovered by the analytic continuation of Schwinger functions of the fractional field to the corresponding Wightman functions using Osterwalder–Schrader reconstruction scheme. Note that in general, the Schwinger functions of fractional field do not satisfy the reflection positivity, hence the resulting Wightman functions do not stay in Hilbert space with positive metric. Modified Wightman axioms in indefinite metric Hilbert space apply to fractional quantum field.

Generalization of the above results to free fractional electromagnetic field in various gauges can be carried out in both zero and positive temperature [48, 50]. Path integral representations of fractional oscillator with single and two indices have been studied [49, 87]. The use of path integrals in fractional fields has recently been considered [39, 40].

Work on multifractional quantum field theory is still lacking, substantial research needs to be carried out both in terms of the mathematical aspects as well as physical interpretations. In view of the strong indication of the multifractal character of quantum spacetime supported by various models of quantum gravity, one can expect quantum fields in multifractional spacetime would subsequently attract more interest. One looks forward to a feasible and workable multifractional quantum field theory in time to come.

Bibliography

[1] A. Actor, Topological generation of gauge field mass by toroidal spacetime, *Class. Quantum Gravity*, **7** (1980), 663–683.

[2] S. Albeverio, H. Gottschalk, and J. L. Wu, Convoluted generalized white noise, Schwinger functions and their analytic continuation to Wrightman functions, *Rev. Math. Phys.*, **8** (1996), 763–817.

[3] S. Albeverio, H. Gottschalk, and J. L. Wu, Models of local relativistic quantum fields with indefinite metric (in all dimensions), *Commun. Math. Phys.*, **184** (1997), 509–531.
[4] J. Ambjørn, J. Jurkiewicz, and R. Loll, Spectral dimension of the universe, *Phys. Rev. Lett.*, **95**, (2005), 171301, 4 pp.
[5] J. Ambjørn, A. Goerlich, J. Jurkiewicz, and R. Loll, Nonperturbative quantum gravity, *Phys. Rep.*, **519** (2012), 127–210.
[6] D. G. Barci, L. E. Oxman, and M. Rocca, Canonical quantization of non-local field equations, *Int. J. Mod. Phys. A*, **11** (1996), 2111–2126.
[7] D. G. Barci, C. G. Bollini, L. E. Oxman, and M. C. Rocca, Lorentz-invariant pseudo-differential wave equations, *Int. J. Theor. Phys.*, **37** (1998), 3015–3030.
[8] R. F. Bass, Uniqueness in law for pure jump type Markov processes, *Probab. Theory Relat. Fields*, **79** (1988), 271–287.
[9] A. Benassi, S. Jaffard, and D. Roux, Gaussian processes and pseudodifferential elliptic operators, *Rev. Mat. Iberoam.*, **13** (1997), 19–90.
[10] T. Biswas, E. Gerwick, T. Koivisto, and A. Mazumdar, Towards singularity- and ghost-free theories of gravity, *Phys. Rev. Lett.*, **108**, (2012), 03110, 4 pp.
[11] C. G. Bollini and J. J. Giambiagi, Arbitrary powers of d'Alembertian and the Huygens' principle, *J. Math. Phys.*, **34** (1993), 610–621.
[12] G. Calcagni, Geometry and field theory in multi-fractional spacetime, *J. High Energy Phys.*, **1201** (2012), 65, 82 pp.
[13] G. Calcagni and L. Modesto, Nonlocal quantum gravity and M-theory, *Phys. Rev. D*, **91**, (2015), 124059, 16 pp.
[14] G. Calcagni and G. Nardelli, Symmetries and propagator in multifractional scalar field theory, *Phys. Rev. D*, **87** (2013), 085008, 15 pp.
[15] R. L. P. G. do Amaral and Marino EC, Canonical quantization of theories containing fractional powers of the d'Alembertian operator, *J. Phys. A, Math. Gen.*, **25** (1992), 5183–5200.
[16] B. J. Durhuus and J. Ambjørn, *Quantum Geometry: A Statistical Field Theory Approach*, Cambridge University Press, Cambridge, UK, 1997.
[17] C. H. Eab, S. C. Lim, and L. P. Teo, Finite temperature Casimir effect for a massless fractional Klein–Gordon field with fractional Neumann conditions, *J. Math. Phys.*, **48** (2007), 082301, 24 pp.
[18] E. Elizalde and K. Kirsten, Topological symmetry breaking in self-interacting theories on toroidal space-time, *J. Math. Phys.*, **35** (1994), 1260–1273.
[19] E. Elizalde, S. D. Odintsov, A. Romeo, A. A. Bytsenko, and S. Zerbini, *Zeta Regularization Techniques with Applications*, World Scientific, Singapore, 1994.
[20] G. Eyink, Quantum field theory models on fractal space-time 1: introduction and overview, *Commun. Math. Phys.*, **125** (1989), 613–636.
[21] G. Eyink, Quantum field theory models on fractal space-time 2: hierarchical propagators, *Commun. Math. Phys.*, **126** (1989), 85–101.
[22] K. J. Falconer, *Fractal Geometry: Mathematical Foundations and Applications*, 3rd ed., John Wiley & Sons, New York, USA, 2014.
[23] R. P. Feynman and A. R. Hibbs, *Quantum Mechanics and Path Integrals*, McGraw-Hill, New York, USA, 1965.
[24] L. H. Ford and T. Yoshimura, Mass generation by self-interaction in non-Minkowskian spacetimes, *Phys. Lett. A*, **70** (1979), 89–91.
[25] I. M. Gelfand and G. E. Shilov, *Generalized Functions, vol. I*, Academic Press, New York, USA, 1964.
[26] I. S. Gradshteyn and I. M. Ryzhik, *Tables of Integrals, Series and Products*, Academic Press, New York, USA, 1980.

[27] M. Grothaus and L. Streit, Construction of relativistic quantum fields in the framework of white noise analysis, *J. Math. Phys.*, **40** (1999), 5387–5405.
[28] S. Gulzari, J. Swain, and A. Widom, Asymptotic infrared fractal structure of the propagator for a charged fermion, *Mod. Phys. Lett. A*, **21** (2006), 2861–2872.
[29] S. Gulzari, Y. Srivastava, J. Swain, and A. Widom, Fractal propagators in QED and QCD and implications for the problem of confinement, *Braz. J. Phys.*, **37** (2007), 286–289.
[30] R. Herrman, *Fractional Calculus: An Introduction for Physicists*, 2nd ed., World Scientific, Singapore, 2014.
[31] W. Hoh, Pseudo differential operators with negative definite symbols of variable order, *Rev. Mat. Iberoam.*, **16** (2000), 219–241.
[32] Petr Hořava, Spectral dimension of the universe in quantum gravity at a Lifshitz point, *Phys. Rev. Lett.*, **102** (2009), 161301-4.
[33] N. Jacob and H. G. Leopold, Pseudo-differential operators with variable order of differentiation generating Feller semigroups, *Integral Equ. Oper. Theory*, **17** (1993), 544–553.
[34] K. Kikuchi and A. Negoro, On Markov process generated by pseudodifferential operator of variable order, *Osaka J. Math.*, **34** (1997), 319–335.
[35] A. A. Kilbas, H. M. Srivastava, and J. J. Trujillo, *Theory and Applications of Fractional Differential Equations*, Elsevier, Armsterdam, Netherlands, 2006.
[36] K. Kirsten, Topological gauge field mass generation by toroidal spacetime, *J. Phys. A, Math. Gen.*, **26** (1993), 2421–2435.
[37] K. Kirsten, *Spectral Fuxnctions in Mathematics and Physics*, CRC Press, Boca Raton, Fl, USA, 2002.
[38] A. Klein and L. J. Landau, Periodic Gaussian Osterwalder–Schrader positive processes and the two-sided Markov property on the circle, *Pac. J. Math.*, **94** (1981), 341–367.
[39] H. Kleinert, Fractional quantum field theory, path integral, and stochastic differential equation for strongly interacting many-particle systems, *Europhys. Lett.*, **100** (2013), 10001-5.
[40] H. Kleinert, Quantum field theory of black-swan events, *Found. Phys.*, **44** (2014), 546–556.
[41] Y. Kobelev, L. Y. Kobelev, and Y. L. Klimontovich, Anomalous diffusion with time-and coordinate-dependent memory, *Dokl. Phys.*, **48** (2003), 264–268.
[42] Y. Kobelev, L. Y. Kobelev, and Y. L. Klimontovich, Statistical physics of dynamic systems with variable memory, *Dokl. Phys.*, **48** (2003), 285–289.
[43] H. Kröger, Fractal geometry in quantum mechanics, field theory and spin systems, *Phys. Rep.*, **323** (2000), 81–181.
[44] N. Laskin, Fractional quantum mechanics, *Phys. Rev. E*, **62** (2000), 3135–3145.
[45] N. Laskin, Fractional Schrödinger equation, *Phys. Rev. E*, **66** (2002), 056108, 7 pp.
[46] N. Laskin, *Fractional Quantum Mechanics*, World Scientific, Singapore, 2018.
[47] O. Lauscher and M. Reuter, Fractal spacetime structure in asymptotically safe gravity, *J. High Energy Phys.*, **0510** (2005), 050, 15 pp.
[48] S. C. Lim, Fractional derivative quantum fields at positive temperature, *Physica A*, **363** (2006), 269–281.
[49] S. C. Lim and C. H. Eab, Riemann–Liouville and Weyl fractional oscillator processes, *Phys. Lett. A*, **355** (2006), 87–93.
[50] S. C. Lim and S. V. Muniandy, Stochastic quantization of nonlocal fields, *Phys. Lett. A*, **324** (2004), 396–405.
[51] S. C. Lim and L. P. Teo, Weyl and Riemann–Liouville multifractional Ornstein–Uhlenbeck processes, *J. Phys. A, Math. Theor.*, **40** (2007), 6035–6060.
[52] S. C. Lim and L. P. Teo, Topological symmetry breaking of self-interacting fractional Klein–Gordon field theories on toroidal spacetime, *J. Phys. A, Math. Theor.*, **41** (2008), 145403, 29 pp.

[53] S. C. Lim and L. P. Teo, Sample path properties of fractional Riesz–Bessel field of variable order, *J. Math. Phys.*, **49** (2008), 013509, 31 pp.

[54] S. C. Lim and L. P. Teo, Repulsive Casimir force from fractional Neumann boundary conditions, *Phys. Lett. B*, **679** (2009), 130–137.

[55] S. C. Lim and L. P. Teo, The fractional oscillator process with two indices, *J. Phys. A, Math. Theor.*, **42** (2009), 065208, 34 pp.

[56] S. C. Lim and L. P. Teo, Generalized Whittle–Matérn random field as a model of correlated fluctuations, *J. Phys. A, Math. Theor.*, **42** (2009), 105202, 21 pp.

[57] S. C. Lim and L. P. Teo, Casimir effect associated with fractional Klein–Gordon field, in J. Klafter, S. C. Lim, R. Metzler (eds.) *Fractional Dynamics: Recent Advances*, pp. 483–506, World Scientific, Singapore, 2012.

[58] S. C. Lim, M. Li, and L. P. Teo, Locally self-similar fractional oscillator processes, *Fluct. Noise Lett.*, **7** (2007), L169–L179.

[59] S. C. Lim, M. Li, and L. P. Teo, Langevin equation with two fractional orders, *Phys. Lett. A*, **372** (2008), 6309–6320.

[60] L. Modesto, Fractal structure of loop quantum gravity, *Class. Quantum Gravity*, **26**, (2009), 242002, 9 pp.

[61] L. Modesto, Super-renormalizable quantum gravity, *Phys. Rev. D*, **86**, (2012), 044005, 20 pp.

[62] G. Morchio and F. Strocchi, Infrared singularities, vacuum structure and pure phase in local quantum field theory, *Ann. Inst. H. Poincaré*, **A33** (1980), 251–282.

[63] M. Naber, Time fractional Schrödinger equation, *J. Math. Phys.*, **45** (2004), 3339–3352.

[64] E. Nelson, Derivation of Shrödinger equation from Newtonian mechanics, *Phys. Rev.*, **150** (1966), 1079–1085.

[65] E. Nelson, Construction of quantum fields from Markoff fields, *J. Funct. Anal.*, **12** (1973), 97–112.

[66] E. Nelson, The free Markoff field, *J. Funct. Anal.*, **12** (1973), 211–227.

[67] E. Nelson, *Quantum Fluctuations*, Princeton University Press, Princeton, NJ, USA, 1985.

[68] M. Niedermaier and M. Reuter, The asymptotic safety scenario in quantum gravity, *Living Rev. Relativ.*, **9** (2006), 5–173.

[69] V. A. Nogin and E. V. Sukhinin, Fractional powers of the Klein–Gordon Fock operator in L_p-spaces, *Russ. Acad. Sci. Dokl. Math.*, **341** (1995), 166–168.

[70] V. A. Nogin and E. V. Sukhinin, Fractional powers of the Schrödinger operators is L_p-spaces, *Dokl. Akad. Nauk*, **360** (1998), 608–610.

[71] K. Osterwalder and R. Schrader, Axioms for Euclidean Green's functions I, *Commun. Math. Phys.*, **31** (1973), 83–112.

[72] K. Osterwalder and R. Schrader, Axioms for Euclidean Green's functions II, *Commun. Math. Phys.*, **42** (1975), 281–305.

[73] P. Peltier and J. Lévy-Vehel, *Multifractional Brownian Motion: Definition and Preliminary Results*, Research Report RR-2645, INRIA, 1995.

[74] A. Perez, The spin-foam approach to quantum gravity, *Living Rev. Relativ.*, **16** (2013), 3–128.

[75] L. D. Pitt and R. S. Robeva, On the sharp Markov property for Gaussian random fields and spectral synthesis in spaces of Bessel potentials, *Ann. Probab.*, **31** (2003), 1338–1376.

[76] I. Podlubny, *Fractional Differential Equations*, Academic Press, New York, USA, 1999.

[77] A. Raspini, Simple solution of fractional Dirac equation of order 2/3, *Phys. Scr.*, **64** (2001), 20–22.

[78] M. Reuter and F. Saueressig, Fractal space-times under the microscope: a renormalization group view on Monte Carlo data. *J. High Energy Phys.*, **2011** (2011), 12, 26 pp.

[79] M. Reuter and F. Saueressig, Asymptotic safety, fractals, and cosmology, in G. Calcagni, L. Papantonopoulos, G. Siopsis, N. Tsamis N (eds.) *Quantum Gravity and Quantum Cosmology*. Lecture Notes in Physics, vol. 863, pp. 185–226, Springer, Berlin, Heidelberg, 2013.

[80] M. Riesz, L'intégrale de Riemann–Liouville et le problème de Cauchy, *Acta Math.*, **81** (1949), 1–222.

[81] R. S. Robeva and L. D. Pitt On the equality of sharp and germ σ-fields for Gaussian processes and fields, *Pliska Stud. Math. Bulgar.*, **16** (2004), 183–205.

[82] H. J. Rothe, *Lattice Gauge Theories: An Introduction*, 3rd ed., World Scientific, Singapore, 2005.

[83] C. Rovelli, *Quantum Gravity*, Cambridge University Press, Cambridge, UK, 2007.

[84] M. D. Ruiz-Medina, V. V. Anh, and J. M. Angulo, Fractional generalized random fields of variable order, *Stoch. Anal. Appl.*, **22** (2004), 775–799.

[85] S. G. Samko, Fractional integration and differentiation of variable order, *Anal. Math.*, **21** (1995), 213–236.

[86] S. G. Samko, Fractional differentiation and integration of variable order, *Dokl. Math.*, **51** (1995), 401–403.

[87] S. G. Samko, *Hypersingular Integrals and Their Applications*, Taylor and Francis, London, UK, 2002.

[88] S. G. Samko and B. Ross, Integration and differentiation to a variable fractional order, *Integral Transforms Spec. Funct.*, **1** (1993), 277–300.

[89] S. Samko, A. A. Kilbas, and D. I. Maritchev, *Integrals and Derivatives of the Fractional Order and Some of Their Applications*, Gordon & Breach Publishers, New York, USA, 1993.

[90] T. P. Sotiriou, Hořava–Lifshitz gravity: a status report, *J. Phys. Conf. Ser.*, **283** (2011), 012034, 17 pp.

[91] T. P. Sotiriou, M. Visser, and S. Weinfurtner, Spectral dimension as a probe of the ultraviolet continuum regime of causal dynamical triangulations, *Phys. Rev. Lett.*, **107** (2011), 131303, 4 pp.

[92] F. Strocchi, *An Introduction to Non-Perturbative Foundations of Quantum Field Theory*, Oxford University Press, Oxford, UK, 2013.

[93] K. Svozil, Quantum field theory on fractal space-time, *J. Phys. A*, **20** (1987), 3861–3867.

[94] V. E. Tarasov, Fractional quantum field theory: from lattice to continuum, *Adv. High Energy Phys.*, **2014** (2014), 957863, 14 pp.

[95] D. J. Toms, Symmetry breaking and mass generation by space-time topology, *Phys. Rev. D*, **21** (1980), 2805–2817.

[96] M. Tsuchiya, Lévy measure with generalized polar decomposition and the associated SDE with jumps, *Stoch. Stoch. Rep.*, **38** (1992), 95–117.

[97] S. Umarov and S. Steinberg, Variable order differential equations and diffusion with changing modes, *Z. Anal. Anwend.*, **28** (2009), 431–450.

[98] P. Zavada, Relativistic wave equations with fractional derivatives and pseudo-differential operators, *J. Appl. Math.*, **2** (2002), 163–197.

Vasily E. Tarasov

Fractional quantum mechanics of open quantum systems

Abstract: Fractional dynamics of open quantum systems with power-law memory is described. We show that the quantum processes can demonstrate a universal dynamic behavior caused by the effects of power-law fading memory. We propose generalizations of time-ordered exponential and time-ordered product for processes with power-law memory. As examples, we consider equations of the N-level open quantum system with memory, quantum oscillator with friction and memory. The solutions of the corresponding fractional differential equations with derivatives of noninteger orders are obtained.

Keywords: Quantum mechanics, open quantum system, non-Hamiltonian system, dissipative system, memory, dynamic memory, fading memory, fractional calculus, fractional dynamics, fractional derivative, derivative of noninteger order, fractional differential equations

PACS: 45.10.Hj, 03.65.Ta, 03.65.Yz

1 Introduction

Fractional quantum dynamics is a branch of quantum physics, in which processes and systems are characterized by memory and/or nonlocality. The powerful mathematical tool, which allows us to describe power-law memory and non-locality is the fractional calculus [12, 20, 21, 28, 30].

It should be noted that the concept of memory is actively used in modern physics [2, 3, 11, 24, 27, 29, 44, 45]. The term “memory” means the property that characterizes a dependence of the process state at a given time from the change history of state in the past [64, 65]. The memory can be considered as nonlocality in time. One of the most important properties of memory is a fading (dissipation). The fading of memory means that it is less probable to expect strengthening of the memory with respect to the more distant events. We will consider memory with power-law fading. It allows us to use the fractional calculus and fractional differential equations to describe quantum processes with power-law fading memory.

Any quantum system is really embedded in some environment and, therefore, it can be considered as an open quantum system. In many cases, the corresponding environments are unknown or are unobservable. Therefore, the theory of open

Vasily E. Tarasov, Skobeltsyn Institute of Nuclear Physics, Lomonosov Moscow State University, Moscow 119991, Russia, e-mail: tarasov@theory.sinp.msu.ru

quantum systems is a fundamental generalization of standard quantum mechanics of closed and Hamiltonian systems [39]. A general form of the quantum Markov equations, which describes the dynamics of quantum observables and states, were proposed by Gorini, Kossakowski, Sudarshan, and Lindblad in [14, 15, 22, 23] (see also [17, 18, 31, 39]). These equations do not take into account the memory effects. Fractional calculus [12, 20, 21, 28, 30] is a powerful tool to describe processes with power-law memory in physical sciences. The power-law memory can be described by equations with fractional derivatives of noninteger orders with respect to time variable. It should be noted that the memory can be caused by interactions with environment [1, 46].

In this chapter, we show that the quantum systems with memory, such as N-level open quantum system and quantum oscillator with friction, can demonstrate the universal behavior. To describe time-dependent fractional dynamics of quantum processes, we propose a generalization of the time-ordered product (also called the Dyson product) and time-ordered exponential, which are actively used in quantum physics, by taking into account power-law memory. The memory-ordered exponential, which is a generalization of time-ordered exponential, is a mathematical operation that is defined in matrix algebras and noncommutative operator algebras. It can be considered as a matrix (operator) analog of the exponential of the integral in the commutative algebras of functions. The expressions of memory-ordered exponential (time-ordered exponential with memory) and corresponding memory-ordered product (time-ordered product with memory) are derived by using the matrix fractional differential equation, which describes open quantum systems with memory.

2 Quantum dynamics with power-law memory

The dynamics of open quantum systems can be described in terms of the infinitesimal change of the system. This change is defined by some form of infinitesimal generator. The most general explicit form of the infinitesimal superoperator was suggested by Gorini, Kossakowski, Sudarshan, and Lindblad in [14, 15, 22, 23] (see also [17, 18, 31, 39]). There exists a one-to-one correspondence between the completely positive norm continuous semigroups and the completely dissipative generating superoperators [4, 6, 9, 16, 39].

In order to take into account a power-law memory, we can use fractional differentiation with respect to time [47, 62, 63, 65]. It allows us to describe fading memory that corresponds to intrinsic dissipative processes [7, 8, 25, 26]. Let us consider fractional generalizations of quantum Markovian equation for quantum observables and states [32–44, 47–50, 63].

The equation for bounded quantum observable $X(t)$ of an open quantum system with power-law memory has the form

$$D^{\alpha}_{t_0,t}[\tau]X(\tau) = -\frac{1}{i\hbar}[\mathcal{H}, X(t)] + \frac{1}{2\hbar}\sum_{k=1}^{\infty}(V_k^*[X(t), V_k] + [V_k^*, X(t)]V_k), \tag{1}$$

where $D^{\alpha}_{t_0,t}[\tau]$ is the Caputo fractional derivative with respect to time t (dimensionless variable), V_k are elements of C^*-algebra. For noninteger values of $\alpha > 0$, equation (1) describes the quantum processes with power-law memory. If all operators V_k are equal to zero ($V_k = 0$), then we have a fractional generalization of the Heisenberg equation for Hamiltonian system with memory

$$D^{\alpha}_{t_0,t}[\tau]X(\tau) = \frac{i}{\hbar}[\mathcal{H}, X(t)]. \tag{2}$$

For $\alpha = 1$, equation (1) takes the form of the standard quantum Markovian equation [17, 18, 22, 23] since $D^{1}_{t_0,t}[\tau]X(\tau) = dX(t)/dt$. Equation (2) with $\alpha = 1$ is the standard Heisenberg equation.

The proposed generalization of the Lindblad equation for quantum observables can be represented in the superoperator form

$$D^{\alpha}_{t_0,t}[\tau]X(\tau) = -\mathcal{L}_V X(t), \tag{3}$$

where $\mathcal{L}_V$ is the superoperator (the operator that acts on operators), which is defined by

$$\mathcal{L}_V X(t) = \frac{1}{i\hbar}[\mathcal{H}, X(t)] - \frac{1}{2\hbar}\sum_{k=1}^{\infty}(V_k^*[X(t), V_k] + [V_k^*, X(t)]V_k). \tag{4}$$

If we consider the Cauchy-type problem for equation (3) in which the initial condition is given at the time $t = 0$ by $X(0)$, then its solution can be represented [47] in the form

$$X(t) = \Phi_t(\alpha)X(0), \quad (t \geq 0),$$

where

$$\Phi_t(\alpha) = E_{\alpha}[-t^{\alpha}\mathcal{L}_V]. \tag{5}$$

Here, $E_{\alpha}[-t^{\alpha}\mathcal{L}]$ with $t \geq 0$ is the Mittag-Leffler function with the superoperator argument

$$E_{\alpha}[-t^{\alpha}\mathcal{L}] = \sum_{k=0}^{\infty}\frac{(-t^{\alpha})^k}{\Gamma(\alpha k + 1)}\mathcal{L}^k.$$

Note that the relation

$$D^{\alpha}_{t_0,t}[\tau]E_{\alpha}[\lambda(\tau - t_0)^{\alpha}] = \lambda E_{\alpha}[\lambda(t - t_0)^{\alpha}]$$

holds for $\lambda \in \mathbb{C}$, $t > t_0 \in \mathbb{R}$, and $\alpha > 0$ (see Lemma 2.23 in [20]).

The superoperators $\Phi_t(\alpha)$, $t \geq 0$, describe dynamics of open quantum systems with power-law memory. The superoperator $\mathcal{L}_V$ can be considered as a generator of the one-parameter groupoid $\Phi_t(\alpha)$ on operator algebra of quantum observables:

$$D^{\alpha}_{t_0,t}[\tau]\Phi_\tau(\alpha) = -\mathcal{L}_V \Phi_t(\alpha).$$

The set $\{\Phi_t(\alpha) \mid t \geq 0\}$ will be called a quantum dynamical groupoid. Note that the following properties are realized:

$$\Phi_t(\alpha) I = I,$$

$$(\Phi_t(\alpha) X)^* = \Phi_t(\alpha) X$$

for self-adjoint operators X ($X^* = X$), and

$$\lim_{t \to 0+} \Phi_t(\alpha) = L_I,$$

where L_I is an identity superoperator ($L_I X = X$). As a result, the superoperators $\Phi_t(\alpha)$, $t \geq 0$, are real and unit preserving maps on operator algebra of quantum observables.

For $\alpha = 1$, we have

$$\Phi_t(1) = E_1[-t\mathcal{L}_V] = \exp\{-t\mathcal{L}_V\}.$$

The superoperators $\Phi_t = \Phi_t(1)$ form a semigroup such that

$$\Phi_t \Phi_s = \Phi_{t+s}, \quad (t, s > 0), \quad \Phi_0 = L_I.$$

This property holds since

$$\exp\{-t\mathcal{L}_V\} \exp\{-s\mathcal{L}_V\} = \exp\{-(t+s)\mathcal{L}_V\}.$$

For $\alpha \notin \mathbb{N}$, we have

$$E_\alpha[-t^\alpha \mathcal{L}_V] E_\alpha[-s^\alpha \mathcal{L}_V] \neq E_\alpha[-(t+s)^\alpha \mathcal{L}_V].$$

Therefore, the semigroup property is not satisfied for noninteger values of α:

$$\Phi_t(\alpha)\Phi_s(\alpha) \neq \Phi_{t+s}(\alpha), \quad (t, s > 0).$$

As a result, the superoperators $\Phi_t(\alpha)$ with $\alpha \notin \mathbb{N}$ cannot form a semigroup. This property means that we have a quantum processes with memory. The superoperators $\Phi_t(\alpha)$ describe quantum dynamics of open systems with memory. The violation of this semigroup property is a characteristic property of dynamics with memory.

3 Quantum oscillator with friction and memory

In general, the operators $\mathcal{H}$ and V_k should be considered as time dependent, that is, $\mathcal{H} = \mathcal{H}(t)$, $V_k = V_k(t)$. In this case, equation (1) describes time-dependent open quantum systems with power-law memory.

Let us describe quantum observables $Q(t)$ and $P(t)$ of oscillator with linear friction and power-like memory. For this description, the basic assumption is that the general form of a bounded completely dissipative generator holds for an unbounded generator [10]. We will assume that the operators $\mathcal{H}$ and V_k are functions of the operators Q and P such that the obtained model is exactly solvable [17, 18, 31, 39]. Therefore, we will consider $V_k = V_k(Q,P,t)$ as the first-degree polynomials in Q and P, and the Hamiltonian $\mathcal{H} = \mathcal{H}(Q,P,t)$ as a second degree polynomial in Q and P with time-dependent parameters. As a result, we have

$$\mathcal{H} = \mathcal{H}(Q,P,t) = \frac{1}{2m(t)}P^2 + \frac{m(t)\omega^2(t)}{2}Q^2 + \frac{\mu(t)}{2}(QP + PQ), \tag{6}$$

$$V_k = V_k(Q,P,t) = a_k(t)P + b_k(t)Q, \tag{7}$$

where $a_k(t)$ and $b_k(t)$, $(k = 1,2)$, are complex-valued functions.

Using the canonical commutation relations for operators Q and P, we obtain equation (1) for $Q(t)$ and $P(t)$ in the form

$$D^{\alpha}_{t_0,t}[\tau]Q(\tau) = \big(\mu(t) - \lambda(t)\big)Q(t) + \frac{1}{m(t)}P(t), \tag{8}$$

$$D^{\alpha}_{t_0,t}[\tau]P(\tau) = -m(t)\omega^2(t)Q(t) - \big(\mu(t) + \lambda t\big)P(t), \tag{9}$$

where $\lambda(t) = \mathrm{Im}(a_1(t)b_1^*(t) + a_2(t)b_2^*(t))$. Equations (8)–(9) can be rewritten in the matrix form

$$D^{\alpha}_{t_0,t}[\tau]X(\tau) = g^{\alpha}H(t)X(t), \tag{10}$$

where the matrices $H(t)$ and $X(t)$ are defined by the expressions

$$X(t) = \begin{pmatrix} Q(t) \\ P(t) \end{pmatrix}; \quad H(t) = \begin{pmatrix} \mu(t) - \lambda(t) & m^{-1}(t) \\ -m(t)\omega^2(t) & -\mu(t) - \lambda(t) \end{pmatrix}. \tag{11}$$

It should be noted that the matrix $H(t)$ can be represented in the form

$$H(t) = N^{-1}(t)F(t)N(t), \tag{12}$$

where

$$N(t) = \begin{pmatrix} m(t)\omega^2(t) & \mu(t) + \nu(t) \\ m(t)\omega^2(t) & \mu(t) - \nu(t) \end{pmatrix}, \tag{13}$$

$$F(t) = \begin{pmatrix} -\lambda(t) - \nu(t) & 0 \\ 0 & -\lambda(t) + \nu(t) \end{pmatrix}, \tag{14}$$

and $\nu(t)$ is a we use the complex-valued function such that $\nu^2(t) = \mu^2(t) - \omega^2(t)$.

For the constant operator $\mathcal{H}$ and matrix C_{kl}, which does not change with time, and $n-1 < \alpha < n$ the solution of equation (10) can be written [31] by the equation

$$X(t) = \sum_{k=0}^{n-1} (t-t_0)^k N^{-1} E_{\alpha,k+1}[g^\alpha (t-t_0)^\alpha F] N X^{(k)}(t_0), \tag{15}$$

where $E_{\alpha,\beta}[z]$ is the two-parametric Mittag-Leffler function of [13], p. 56. Equation (15) describes time-dependent quantum oscillator with power-law memory as an open quantum system, parameters of which depend on time.

4 *N*-level open quantum system with memory

For a N-level open quantum system with power-law memory, the equation for quantum observable $X(t)$ has the form

$$D^\alpha_{t_0,t}[\tau]X(\tau) = -\frac{1}{i\hbar}[\mathcal{H}, X(t)] + \frac{1}{2\hbar}\sum_{k,l=1}^{N^2-1} C_{kl}(V_k^*[X(t), V_l] + [V_k^*, X(t)]V_l), \tag{16}$$

where $D^\alpha_{t_0,t}[\tau]$ is the Caputo fractional derivative of the order $\alpha \geq 0$ [11, 29], $\mathcal{H}^* = \mathcal{H}$ is a self-adjoint operator with $\mathrm{Tr}(\mathcal{H}) = 0$, C_{kl} is a complete positive matrix, and $\{V_k, k = 1 \dots N^2\}$ is a complete orthogonal set on a Hilbert space such that

$$\mathrm{Tr}(V_k^* V_l) = \delta_{kl}; \quad \mathrm{Tr}(V_k) = 0 \quad (k = 1, \dots, N^2 - 1); \quad V_N^2 = \frac{1}{\sqrt{N}}E.$$

It should be noted that for $\alpha = 1$, equation (16) gives the equation of the standard quantum Markovian equation, which is suggested by Gorini, Kossakowski, Sudarshan [14, 15] (see also [39]).

In the general case, the operator $\mathcal{H}$, and matrix C_{kl} depend on time, that is, $\mathcal{H} = \mathcal{H}(t)$, $C_{kl} = C_{kl}(t)$. Then equation (16) describes the time-dependent N-level open quantum system with power-law fading memory.

Let us consider two-level open quantum system with power-law memory. We can represent an arbitrary quantum observable $X(\tau)$ of two-level quantum system in terms of the Pauli matrices

$$X(t) = \frac{1}{2}\sum_{\mu=0}^{3} \sigma_\mu X_\mu(t), \tag{17}$$

where $X_\mu(t) = \mathrm{Tr}(\sigma_\mu X(t))$ and σ_μ are the Pauli matrices. Suppose $\{V_\mu, \mu = 0, 1, 2, 3\}$ is a complete orthogonal set of the self-adjoint matrices $V_\mu = \frac{1}{\sqrt{2}}\sigma_\mu$, such that we have the condition $\mathrm{Tr}(V_k^* V_l) = \delta_{kl}$, where $(A, B) := \mathrm{Tr}(A^* B)$ is the scalar product. The basic assumption imposed on the operators $\mathcal{H}$ and $X(t)$ is that they can be represented through the Pauli matrices by the equations

$$X(t) = \frac{1}{2} X_0(t) + \frac{1}{2} \sum_{k=1}^{3} \sigma_k X_k(t), \tag{18}$$

$$\mathcal{H}(t) = \frac{1}{2} \mathcal{H}_0(t) + \frac{1}{2} \sum_{k=1}^{3} \sigma_k \mathcal{H}_k(t). \tag{19}$$

Using the properties of the Pauli matrices, we obtain the matrix equation

$$D^{\alpha}_{t_0,t}[\tau] X(\tau) = g^{\alpha} H(t) X(t), \tag{20}$$

where g is a small constant that has the dimensionality of time and that describes, for example, the smallest time scale in the considered process. The elements $H_{\mu\nu}(t)$ of the matrix $H(t)$ are defined by the expressions

$$H_{kl}(t) = \frac{1}{\hbar} \sum_{s=1}^{3} \varepsilon_{kls} H_s(t) + \frac{1}{\hbar} (C(t)\delta_{kl} - C_{(kl)}(t)), \tag{21}$$

$$H_{0l}(t) = \frac{1}{\hbar} \sum_{i,j=1}^{3} \varepsilon_{ijl} \mathrm{Im}(C_{ij}(t)), \tag{22}$$

$$H_{00}(t) = H_{k0}(t) = 0, \tag{23}$$

where $k, l = 1, 2, 3$, and

$$C(t) = \sum_{k=1}^{3} C_{kk}; \quad C_{(kl)} = \frac{1}{2} (C_{kl}(t) + C_{lk}(t)). \tag{24}$$

As a result, matrix equation (20) for quantum observables (17) and matrices (21)–(24) describe a two-level open quantum system with power-law memory.

5 Time-dependent fractional dynamics with memory

Let us consider fractional differential equations (20) and (10), which describe quantum processes with power-law memory. We can write these equations in the form

$$(D^{\alpha}_{t_0+} X)(t) = g^{\alpha} H(t) X(t), \tag{25}$$

where g is a small time constant that describes, for example, the smallest time scale in the considered process. We can use the time t as a dimensionless variable.

Let us consider an action of the left-sided Riemann–Liouville fractional integral $I^{\alpha}_{t_0,t}$ of order $\alpha > 0$ [20], pp. 69–70, on equation (25). The action of fractional integral gives

$$(I^{\alpha}_{t_0+}D^{\alpha}_{t_0+}X)(t) = g^{\alpha} I^{\alpha}_{t_0,t}[\tau] H(\tau) X(\tau). \tag{26}$$

It is known that the Caputo derivative is inversed to the Riemann–Liouville integral [20], p. 96. In other words, for any continuous function $X(t) \in C[t_0, t]$, the generalized Newton–Leibniz formula (see equation (2.4.42) of [20], p. 96) has the form

$$(I^{\alpha}_{t_0+}D^{\alpha}_{t_0+}X)(t) = X(t) - \sum_{k=0}^{n-1} \frac{X^{(k)}(t_0)}{k!}(t-t_0)^k, \tag{27}$$

where $n-1 < \alpha < n$, $n := [\alpha]+1$ and $X^{(0)}(t_0) = X(t_0)$. Using (27), equation (26) can be written in the form

$$X(t) = \sum_{k=0}^{n-1} X^{(k)}(t_0) \frac{(t-t_0)^k}{k!} + g^{\alpha} I^{\alpha}_{t_0,t}[\tau] H(\tau) X(\tau), \tag{28}$$

where $n-1 < \alpha < n$. As a result, equation (25) can be solved by iteration of integral equation (28), where we take into account the initial conditions.

To obtain a solution as an expansion in powers of the characteristic time scale g, we rewrite equation (31) with $t = \tau_m$ and $\tau = \tau_{m+1}$ with $m = 1, 2, \ldots, N$ in the form

$$X(\tau_m) = \sum_{k=0}^{n-1} X^{(k)}(t_0) \frac{(\tau_m - t_0)^k}{k!} + g^{\alpha} I^{\alpha}_{t_0,\tau_m}[\tau_{m+1}] H(\tau_{m+1}) X(\tau_{m+1}). \tag{29}$$

Consecutive substitutions of (29) with $m = 1, 2, \ldots, N$ into equation (27) give

$$\begin{aligned} X(t) = {} & \sum_{k=0}^{n-1} X^{(k)}(t_0) \frac{(t-t_0)^k}{k!} + g^{\alpha} \sum_{k=0}^{n-1} I^{\alpha}_{t_0,t}[\tau_1] H(\tau_1) X^{(k)}(t_0) \frac{(\tau_1 - t_0)^k}{k!} \\ & + \sum_{m=2}^{N} g^{\alpha m} \sum_{k=0}^{n-1} I^{\alpha}_{t_0,t}[\tau_1] \cdots I^{\alpha}_{t_0,\tau_{m-1}}[\tau_m] H(\tau_1) \cdots H(\tau_m) \frac{(\tau_m - t_0)^k}{k!} X^{(k)}(t_0) \\ & + g^{\alpha(N+1)} I^{\alpha}_{t_0,t}[\tau_1] \cdots I^{\alpha}_{t_0,\tau_N}[\tau_{N+1}] H(\tau_1) \cdots H(\tau_{N+1}) X(\tau_{N+1}), \end{aligned} \tag{30}$$

where $t_0 \le \tau_1 \le \tau_2 \le \cdots \le \tau_N \le \tau_{N+1} \le t$ and $N \ge 2$. For the limit $N \to \infty$, we get the representation

$$X(t) = \sum_{k=0}^{n-1} S_k(t,t_0) X^{(k)}(t_0), \tag{31}$$

where we use the matrix operators

$$S_k(t,t_0) = \sum_{m=0}^{\infty} g^{\alpha m} I^{\alpha}_{t_0,t}[\tau_1] \cdots I^{\alpha}_{t_0,\tau_{m-1}}[\tau_m] H(\tau_1) \cdots H(\tau_m) \frac{(\tau_m - t_0)^k}{k!}, \tag{32}$$

with $k = 0, 1, 2, \dots, n-1$, $n-1 < \alpha < n$ and $t_0 \leq \tau_1 \leq \dots \leq \tau_m \leq t$. Note that equation (32) is a shorter symbolic form of the expression

$$S_k(t,t_0) = \frac{(t-t_0)^k}{k!}E + g^{\alpha} I^{\alpha}_{t_0,t}[\tau_1]H(\tau_1)\frac{(\tau_1-t_0)^k}{k!} + \sum_{m=2}^{\infty} g^{\alpha m} I^{\alpha}_{t_0,t}[\tau_1]\cdots I^{\alpha}_{t_0,\tau_{m-1}}[tau_m]H(\tau_1)\cdots H(\tau_m)\frac{(\tau_m-t_0)^k}{k!}. \quad (33)$$

For $\alpha = 1$ ($n = 1$), equations (31) and (32) take the standard form

$$X(t) = S(t,t_0)X(t_0) \quad (34)$$

with the matrix

$$S(t,t_0) = \sum_{m=0}^{\infty} g^{\alpha m} \int_{t_0}^{t} d\tau_1 \cdots \int_{t_0}^{\tau_{m-1}} d\tau_m H(\tau_1)\cdots H(\tau_m), \quad (35)$$

where $t_0 \leq \tau_1 \leq \dots \leq \tau_m \leq t$.

Let us derive a generalization of the time-ordered product for processes with power-law memory. For simplicity, we first consider term of (32) with $m = 2$ and $k = 0$, that is,

$$I^{\alpha}_{t_0,t}[\tau_1]H(\tau_1)I^{\alpha}_{t_0,\tau_1}[\tau_2]H(\tau_2) = \frac{1}{\Gamma^2(\alpha)}\int_{t_0}^{t}\frac{H(\tau_1)d\tau_1}{(t-\tau_1)^{1-\alpha}}\int_{t_0}^{\tau_1}\frac{H(\tau_2)d\tau_2}{(\tau_1-\tau_2)^{1-\alpha}}. \quad (36)$$

Using the Heaviside step function,

$$\theta(\tau_1-\tau_2) = \begin{cases} 1, & \text{for } \tau_1 \geq \tau_2, \\ 0, & \text{for } \tau_2 > \tau_1, \end{cases} \quad (37)$$

expression (36) can be written in the form

$$I^{\alpha}_{t_0,t}[\tau_1]H(\tau_1)I^{\alpha}_{t_0,\tau_1}[\tau_2]H(\tau_2) = \frac{1}{2}\int_{t_0}^{t} d\tau_1 \int_{t_0}^{t} d\tau_2 \frac{1}{\Gamma^2(\alpha)}\left(\frac{\theta(\tau_1-\tau_2)H(\tau_1)H(\tau_2)}{(t-\tau_1)^{1-\alpha}(\tau_1-\tau_2)^{1-\alpha}} + \frac{\theta(\tau_2-\tau_1)H(\tau_2)H(\tau_1)}{(t-\tau_2)^{1-\alpha}(\tau_2-\tau_1)^{1-\alpha}}\right). \quad (38)$$

For $k > 0$, the term of (32) with $m = 2$ can be written as

$$I^{\alpha}_{t_0,t}[\tau_1]I^{\alpha}_{t_0,\tau_2}[\tau_2]\left\{H(\tau_1)H(\tau_2)\frac{(\tau_2-t_0)^k}{k!}\right\} = \frac{1}{2}\int_{t_0}^{t} d\tau_1 \int_{t_0}^{t} d\tau_2 \left\{\frac{\theta(\tau_1-\tau_2)H(\tau_1)H(\tau_2)}{(t-\tau_1)^{1-\alpha}(\tau_1-\tau_2)^{1-\alpha}}\frac{(\tau_2-t_0)^k}{k!\Gamma^2(\alpha)} + \frac{\theta(\tau_2-\tau_1)H(\tau_2)H(\tau_1)}{(t-\tau_2)^{1-\alpha}(\tau_2-\tau_1)^{1-\alpha}}\frac{(\tau_1-t_0)^k}{k!\Gamma^2(\alpha)}\right\}, \quad (39)$$

where $k = 0, 1, 2, \ldots, n-1$, $n-1 < \alpha < n$. It is easy to see that product (39) with $k = 0$ gives expression (38).

Let us define the memory-ordered product $T_{\alpha,k}$ (the time-ordered product with power-law memory) by the equation

$$\begin{aligned} T_{\alpha,k}\{H(\tau_1)H(\tau_2)\} &= \theta(\tau_1 - \tau_2)\frac{(t-\tau_2)^{1-\alpha}}{(\tau_1-\tau_2)^{1-\alpha}}\frac{(\tau_2-t_0)^k}{k!}H(\tau_1)H(\tau_2) \\ &+ \theta(\tau_2 - \tau_1)\frac{(t-\tau_1)^{1-\alpha}}{(\tau_2-\tau_1)^{1-\alpha}}\frac{(\tau_1-t_0)^k}{k!}H(\tau_2)H(\tau_1). \end{aligned} \tag{40}$$

The operation (40) is the time-ordered product with power-law memory, which memory fading is equal to $\alpha > 0$, such that $n-1 < \alpha < n$. The product is called the memory-ordered product [63]. For $\alpha = 1$, the time-ordered product (40) has the standard time-ordered product that is used in quantum physics [5], pp. 141–146, [19], pp. 177–179, in the form

$$T_{1,0}\{H(\tau_1)H(\tau_2)\} = T\{H(\tau_1)H(\tau_2)\} = \begin{cases} H(\tau_1)H(\tau_2), & \tau_1 > \tau_2; \\ H(\tau_2)H(\tau_1), & \tau_2 > \tau_1. \end{cases} \tag{41}$$

Then expression (38) can be represented by the fractional integration in the symmetric form

$$\begin{aligned} I^{\alpha}_{t_0,t}[\tau_1] I^{\alpha}_{t_0,\tau_1}[\tau_2]\left\{H(\tau_1)H(\tau_2)\frac{(\tau_2-t_0)^k}{k!}\right\} \\ = \frac{1}{2} I^{\alpha}_{t_0,t}[\tau_1] I^{\alpha}_{t_0,t}[\tau_2] T_{\alpha,k}\{H(\tau_1)H(\tau_2)\}, \end{aligned} \tag{42}$$

where $k = 0, 1, 2, \ldots, n-1$, $n-1 < \alpha < n$.

Similarly, we can consider $m = 3, 4, \ldots$. As a result, the changing of the variable notation in fractional integration of (32), we obtain the identity

$$\begin{aligned} I^{\alpha}_{t_0,t}[\tau_1] \cdots I^{\alpha}_{t_0,\tau_{m-1}}[\tau_m] H(\tau_1)\cdots H(\tau_m)\frac{(\tau_m-t_0)^k}{k!} \\ = \frac{1}{m!} I^{\alpha}_{t_0,t}[\tau_1]\cdots I^{\alpha}_{t_0,t}[\tau_m] T_{\alpha,k}\{H(\tau_1)\cdots H(\tau_m)\}. \end{aligned} \tag{43}$$

The time-ordered product $T_{\alpha,k}$ with power-law memory, which is used in equation (43), is defined by the equation

$$\begin{aligned} &T_{\alpha,k}\{H(\tau_1)\cdots H(\tau_m)\} \\ &= \sum_P \frac{\theta(\tau_{P1},\ldots,\tau_{Pm})\prod_{i=1}^m (t-\tau_i)^{1-\alpha}}{(t-\tau_{P1})^{1-\alpha}\prod_{j=1}^{m-1}(\tau_{Pj}-\tau_{P(j+1)})^{1-\alpha}}\frac{(\tau_{Pm}-t_0)^k}{k!} H(\tau_{P1})\cdots H(\tau_{Pm}), \end{aligned} \tag{44}$$

where the sum runs all permutations P, and the unit step function $\theta(\tau_{P1},\ldots,\tau_{Pm})$ enforces the condition $\tau_{P1} \geq \tau_{P2} \geq \cdots \geq \tau_{Pm}$, where $t \geq \tau_{P1}$ and $\tau_{Pm} \geq t_0$. Multiplication of matrices $H(t)$, which is defined by equation (44), can be called memory-orders product.

For $\alpha = 1$, the memory-ordered product (44) takes the form of the standard time-ordered product

$$\begin{aligned} T_{1,0}\{H(\tau_1)\cdots H(\tau_m)\} &= T\{H(\tau_1)\cdots H(\tau_m)\} \\ &= \sum_P \theta(\tau_{P1},\dots,\tau_{Pm})H(\tau_{P1})\cdots H(\tau_{Pm}). \end{aligned} \tag{45}$$

Using product (44), operator (32) can be written in the symmetric form

$$S_k(t,t_0) = \sum_{m=0}^{\infty} \frac{1}{m!} g^{\alpha m} I^{\alpha}_{t_0,t}[\tau_1]\cdots I^{\alpha}_{t_0,t}[\tau_m] T_{\alpha,k}\{H(\tau_1)\cdots H(\tau_m)\}. \tag{46}$$

As a result, we obtain the generalization of the time-ordered exponent (memory-ordered exponent) for processes with power-law memory

$$\begin{aligned} &T_k\{\exp(g^{\alpha} I^{\alpha}_{t_0,t}[\tau]H(\tau))\} \\ &:= \sum_{m=0}^{\infty} \frac{1}{m!} g^{\alpha m} I^{\alpha}_{t_0,t}[\tau_1]\cdots I^{\alpha}_{t_0,t}[\tau_m] T_{\alpha,k}\{H(\tau_1)\cdots H(\tau_m)\}, \end{aligned} \tag{47}$$

where $k = 0,1,2,\dots,n-1$, $n-1 < \alpha < n$. The left-hand side of equation (47) is a symbolic form of the right-hand side of (47), that is, in fact, it is a notation of the series. Therefore, the memory ordering must be applied before the fractional integration.

As a result, the solution of equation (25) can be represented in the form

$$X(t) = \sum_{k=0}^{n-1} S_k(t,t_0) X^{(k)}(t_0), \tag{48}$$

where $n-1 < \alpha < n$, and

$$S_k(t,t_0) = T_k\{\exp(g^{\alpha} I^{\alpha}_{t_0,t}[\tau]H(\tau))\} \tag{49}$$

are the evolution operators (S-matrices), where $k = 0,1,2,\dots,n-1$.

For $\alpha = 1$, expression (49) takes the standard form

$$S(t,t_0) = T\left\{\exp\left(g\int_{t_0}^{t} d\tau H(\tau)\right)\right\}, \tag{50}$$

where the time-ordered exponential is defined by the equation

$$\begin{aligned} &T\left\{\exp\left(g\int_{t_0}^{t} d\tau H(\tau)\right)\right\} \\ &= \sum_{m=0}^{\infty} \frac{1}{m!} g^m \int_{t_0}^{t} d\tau_1 \cdots \int_{t_0}^{t} d\tau_m T\{H(\tau_1)\cdots H(\tau_m)\}. \end{aligned} \tag{51}$$

Equations (48) and (49) describe the time-dependent fractional dynamics of the N-level open quantum system with power-law memory and the dynamics of quantum oscillator with friction and memory, when friction, mass, and frequency depend on time.

6 Fractional dynamics of two-level open quantum system with memory

Let us consider fractional differential equation (25) with the power-law matrix

$$H(t) = H_c(t - t_0)^{\beta}, \tag{52}$$

where $\beta > -1$. In this case, we can use equation (2.1.16) of book [20], p. 71, in the form

$$I^{\alpha}_{t_0,t}[\tau](\tau - t_0)^{\beta} = \frac{\Gamma(\beta + 1)}{\Gamma(\alpha + \beta + 1)}(t - t_0)^{\beta+\alpha}, \tag{53}$$

where $\beta > -1$. To write solutions of (25), we define [63] a new special function, which is a generalization of the Mittag-Leffler functions [13] by the equation

$$W^{\alpha}_{\beta,\gamma}[z] = \sum_{m=0}^{\infty} \left\{ \prod_{k=0}^{m} \frac{\Gamma(k\alpha + \beta)}{\Gamma(k\alpha + \gamma)} \right\} \frac{z^m}{\Gamma(m\alpha + \beta)}, \tag{54}$$

where α, β, γ are the parameters. Function (54) can be considered as a generalization of the Mittag-Leffler function. For $\beta = \gamma$, the W-function is the two-parametric Mittag-Leffler function of [13], p. 56, that is, $W^{\alpha}_{\beta,\beta}[z] = E_{\alpha,\beta}[z]$. For $\beta = 1$ and $\gamma = 1$, the W-function (54) is the Mittag-Leffler function [61, p. 17], that is, $W^{\alpha}_{1,1}[z] = E_{\alpha}[z]$. For $\alpha = 1$, $\beta = 1$, and $\gamma = 1$, the W-function (54) is the exponential function of [13], p. 20, that is, $W^{1}_{1,1}[z] = e^z$.

Let us consider the matrix operators, which are defined by equation (32). Using equation (53) and $\Gamma(k + 1)= k!$, the mth fractional integrations with H-matrix (52) give

$$\begin{aligned} &I^{\alpha}_{t_0,t}[\tau_1] \cdots I^{\alpha}_{t_0,\tau_{m-1}}[\tau_m] H(\tau_1) \cdots H(\tau_{m-1}) H(\tau_m) \frac{(\tau_m - t_0)^k}{k!} \\ &= \left\{ \prod_{j=0}^{m} \frac{\Gamma(j(\alpha + \beta) + \beta + k + 1)}{\Gamma(j(\alpha + \beta) + k + 1)} \right\} \frac{(t - t_0)^{m(\alpha+\beta)+k}}{\Gamma(m(\alpha + \beta) + \beta + k + 1)} H_c^m. \end{aligned} \tag{55}$$

As a result, matrix operators (32) can be written in the form

$$S_k(t,t_0) = (t - t_0)^k \sum_{m=0}^{\infty} \left\{ \prod_{j=0}^{m} \frac{\Gamma(j(\alpha + \beta) + \beta + k + 1)}{\Gamma(j(\alpha + \beta) + k + 1)} \right\} \frac{\left(g^{\alpha}(t - t_0)^{(\alpha+\beta)} H_c\right)^m}{\Gamma(m(\alpha + \beta) + \beta + k + 1)}, \tag{56}$$

where $k = 0, 1, 2, \ldots, n - 1$, $n - 1 < \alpha < n$.

This allows us to write S-matrices (49) in the form

$$S_k(t,t_0) = (t-t_0)^k W^{\alpha+\beta}_{\beta+k+1,k+1}[g^\alpha (t-t_0)^{(\alpha+\beta)} H_c], \tag{57}$$

where $k = 0,1,2,\dots,n-1$, $n-1 < \alpha < n$ and W-function is defined by (54). The solution of equation (25) with matrix (52) has the form

$$X(t) = \sum_{k=0}^{n-1} (t-t_0)^k W^{\alpha+\beta}_{\beta+k+1,k+1}[g^\alpha (t-t_0)^{(\alpha+\beta)} H_c] X^{(k)}(t_0), \tag{58}$$

where $n-1 < \alpha < n$. The solution of fractional differential equation (25) is represented through the new special function that is proposed in [63]. Equation (58) describes time-dependent dynamics of quantum processes with power-law memory.

7 Time-independent quantum dynamics with memory

Let us consider equation (25) with $0 < \alpha < 2$ and constant matrix $H(t) = H = \text{const}$ for all $t > 0$. In this case, the solution of equation (25) is represented by (58) with $\beta = 0$. This solution can be written as

$$X(t) = \sum_{k=0}^{n-1} (t-t_0)^k E_{\alpha,k+1}[g^\alpha (t-t_0)^\alpha H] X^{(k)}(t_0). \tag{59}$$

For the scalar case (1×1 matrices), solution (59) coincides with the Solution 4.1.64 that is given in book [20], p. 231.

The general solution of fractional differential equations (25) can be represented in the form

$$X(t) = \sum_{k=1}^{n} c_k X_k E_\alpha[\lambda_k t^\alpha], \tag{60}$$

where $n-1 < \alpha < n$, λ_k are the eigenvalues of the matrix H; the vectors $X_k = (X_{ki})$ are the eigenvectors of the matrix H; and the coefficients c_k are determined by the initial condition

$$\sum_{k=1}^{n} c_k X_k = X(0). \tag{61}$$

As a result, solution (60) is a linear combination of the functions $E_\alpha[\lambda_k t^\alpha]$ with $k = 1,\dots,n$. Therefore, in general, the fractional dynamics of the quantum process with memory cannot be described by $X(t) = X(0)E_\alpha[\lambda t^\alpha]$, that is, with the uniform parameter λ for all components of $X(t)$.

Let us consider the dominant behavior of processes with power-law memory at $t \to \infty$. Using equations (3.4.14) and (3.4.15) of [13], pp. 25–26, we have the asymptotic expression of the Mittag-Leffler functions $E_\alpha[\lambda_k t^\alpha]$ at $t \to \infty$ and $0 < \alpha < 2$ in the form

$$E_\alpha[\lambda t^\alpha] = \frac{1}{\alpha}\exp(\lambda^{1/\alpha} t) - \sum_{k=1}^{m} \frac{\lambda^{-k}}{\Gamma(1-\alpha k)} \frac{1}{t^{\alpha k}} + O\left(\frac{1}{t^{\alpha(m+1)}}\right) \tag{62}$$

for real values of λ and for complex roots with $|\arg(\lambda)| \le \theta$, where

$$\arg(\lambda) = \operatorname{arctg}\left(\frac{\operatorname{Im}(\lambda)}{\operatorname{Re}(\lambda)}\right), \ \frac{\pi\alpha}{2} < \theta < \min\{\pi, \pi\alpha\}. \tag{63}$$

For complex values of λ, for which $\theta \le |\arg(\lambda)| \le \pi$, we have

$$E_\alpha[\lambda t^\alpha] = -\sum_{k=1}^{m} \frac{\lambda^{-k}}{\Gamma(1-\alpha k)} \frac{1}{t^{\alpha k}} + O\left(\frac{1}{t^{\alpha(m+1)}}\right), \tag{64}$$

where $\Gamma(1-\alpha) < 0$ for $0 < \alpha < 1$ and $\Gamma(1-\alpha) > 0$ for $1 < \alpha < 2$.

As a result, for the real values of λ, we find that the growth rate of the fractional dynamics with memory does not coincide with the eigenvalues λ_k of the matrix H. The growth rate is equal to the values

$$\lambda_{k,\mathrm{eff}}(\alpha) := \lambda_k^{1/\alpha}, \tag{65}$$

which will be interpreted as the effective growth rates. For complex values of λ, for which $\theta \le |\arg(\lambda)| \le \pi$, the dynamics at $t \to \infty$ is determined by the inverse proportionality $t^{-\alpha}$ instead of the exponential functions. In the presence of terms with the exponential behavior at $t \to \infty$, the contribution of the terms with $t^{-\alpha}$ can be neglected at $t \to \infty$.

As a result, solution (60) is a combination of the Mittag-Leffler functions $E_\alpha[\lambda_k t^\alpha]$ with different parameter λ_k, which correspond to different effective growth rates $\lambda_{k,\mathrm{eff}}(\alpha)$. In solution (60) at $t \to \infty$, the term with the maximum real part of $\lambda_{k,\mathrm{eff}}(\alpha)$, for which $c_k \neq 0$ and $|\arg(\lambda_k)| \le \theta$, where θ satisfies inequality (63), will dominate. If the dominant term has the effective growth rate

$$\lambda_{\max,\mathrm{eff}}(\alpha) = \lambda_{\max}^{1/\alpha}, \tag{66}$$

then the growth rates of all components of $X(t)$ at $t \to \infty$ tend to the effective growth rate (66). In this case, the dynamics at $t \to \infty$ is determined by the proportion between the coordinates of the eigenvector $X_{\max}$, which corresponds to $\lambda_{\max}$. If the dominant is a term with $\lambda_{k,\mathrm{eff}}(\alpha) \neq \lambda_{\max,\mathrm{eff}}(\alpha)$, then the dynamics of $X(t)$ at $t \to \infty$ is defined by the corresponding eigenvector X_k, which coordinates can have different signs [63]. Note that the growth rates can increase and decrease in comparison with the processes without memory.

The dominant behavior allows us to formulate the principle of changing of growth rates: For low growth rates of the processes without memory ($\lambda_{\max} < 1$), the accounting the memory with fading parameter $0 < \alpha < 1$ leads to a decrease in the growth rate, and it leads to an increase in the growth rate for $1 < \alpha < 2$. For high rates of the growth rate of the processes without memory ($\lambda_{max} > 1$), the accounting the memory with the fading parameter $0 < \alpha < 1$ leads to an increase in growth, and it leads to a decrease in the growth rate for $1 < \alpha < 2$.

8 Fractional dynamics of quantum oscillator with friction and memory

Let us consider the fractional dynamics of the time-dependent quantum oscillator with friction and memory, which is defined by equation (1) with (6) and (7), where the mass, frequency, and friction depend on time. The variances and covariance of the observables $Q(t)$ and $P(t)$ are defined by the equations

$$\sigma_{PP}(t) = \mathrm{Tr}(\rho P^2(t)) - (\sigma_P(t))^2, \tag{67}$$

$$\sigma_{QQ}(t) = \mathrm{Tr}(\rho Q^2(t)) - (\sigma_Q(t))^2, \tag{68}$$

$$\sigma_{PQ}(t) = \mathrm{Tr}\left(\rho \frac{1}{2}(P(t)Q(t)+Q(t)P(t))\right) - \sigma_P(t)\sigma_P(t), \tag{69}$$

where $\sigma_A(t)$ is the mean value of the quantum observable $A(t)$ such that $\sigma_A(t) = \mathrm{Tr}(\rho A(t))$, and ρ is the density matrix that describes quantum state of this oscillator. Equations for the variances and covariance of quantum observables $Q(t)$ and $P(t)$ can be rewritten in the matrix form

$$D^{\alpha}_{t_0,t}[\tau]X(\tau) = g^{\alpha}H(t)X(t) + D(t). \tag{70}$$

The matrices $H(t)$, $D(t)$ and $X(t)$ are defined by the expressions

$$H(t) = \begin{pmatrix} 2(\mu(t) - \lambda(t)) & 0 & 2\omega(t) \\ 0 & 2(-\mu(t) - \lambda(t)) & -2\omega(t) \\ -\omega(t) & \omega(t) & -2\lambda(t) \end{pmatrix}, \tag{71}$$

$$X(t) = \begin{pmatrix} m(t)\omega(t)\sigma_{QQ}(t) \\ m^{-1}(t)\omega^{-1}(t)\sigma_{PP}(t) \\ \sigma_{PQ}(t) \end{pmatrix}, \tag{72}$$

$$D(t) = \begin{pmatrix} 2m(t)\omega(t)D_{QQ}(t) \\ 2m^{-1}(t)\omega^{-1}(t)D_{PP}(t) \\ 2D_{PQ}(t) \end{pmatrix}, \tag{73}$$

where

$$D_{QQ}(t) = \frac{\hbar}{2}(a_1^*(t)a_1(t) + a_2^*(t)a_2(t)), \tag{74}$$

$$D_{PP}(t) = \frac{\hbar}{2}\big(b_1^*(t)b_1(t) + b_2^*(t)b_2(t)\big), \tag{75}$$

$$D_{QP}(t) = -\frac{\hbar}{2}\operatorname{Re}\big(a_1^*(t)b_1(t) + a_2^*(t)b_2(t)\big). \tag{76}$$

Equation (70) is nonhomogeneous fractional differential equation. Matrix (71) can be represented in the form

$$H(t) = T(t)L(t)T(t), \tag{77}$$

where

$$T(t) = \frac{1}{2\nu(t)}\begin{pmatrix} \mu(t)+\nu(t) & \mu(t)-\nu(t) & 2\omega(t) \\ \mu(t)-\nu(t) & \mu(t)+\nu(t) & 2\omega(t) \\ -\omega(t) & -\omega(t) & -2\mu(t) \end{pmatrix}, \tag{78}$$

$$L(t) = \frac{1}{2\nu(t)}\begin{pmatrix} 2(\nu(t)-\lambda(t)) & 0 & 0 \\ 0 & 2(-\nu(t)-\lambda(t)) & 0 \\ 0 & 0 & -2\lambda(t) \end{pmatrix}, \tag{79}$$

and $\nu(t)$ is the complex-valued function such that $\nu^2(t) = \mu^2(t) - \omega^2(t)$.

The general solution of the nonhomogeneous fractional differential equation (70) can be written as a sum of solutions of the corresponding homogeneous equation and particular solution the nonhomogeneous equation.

Using the action of the left-sided Riemann–Liouville fractional integral $I^{\alpha}_{t_0,t}$ of order $\alpha > 0$ on equations (70) and the generalized Newton–Leibniz formula (27), we get [63] the expression

$$\begin{aligned} X(t) &= \sum_{k=0}^{n-1} F(t,t_0) + g^{\alpha}\sum_{k=0}^{n-1} I^{\alpha}_{t_0,t}[\tau_1]H(\tau_1)F(\tau_1,t_0) \\ &\quad + \sum_{m=2}^{N} g^{\alpha m}\sum_{k=0}^{n-1} I^{\alpha}_{t_0,t}[\tau_1]\cdots I^{\alpha}_{t_0,\tau_{m-1}}[\tau_m]H(\tau_1)\cdots H(\tau_m)F(\tau_m,t_0) \\ &\quad + g^{\alpha(N+1)}I^{\alpha}_{t_0,t}[\tau_1]\cdots I^{\alpha}_{t_0,\tau_N}[\tau_{N+1}]H(\tau_1)\cdots H(\tau_{N+1})X(\tau_{N+1}), \end{aligned} \tag{80}$$

where $t_0 \le \tau_1 \le \tau_2 \le \cdots \le \tau_N \le \tau_{N+1} \le t$, $N \ge 2$ and

$$F(t,t_0) := \sum_{k=0}^{n-1} X^{(k)}(t_0)\frac{(t-t_0)^k}{k!} + g^{\alpha}I^{\alpha}_{t_0,t}[\tau]D(\tau). \tag{81}$$

For $D(t) = 0$, expression (80) gives (30). Considering the limit $N \to \infty$, we obtain the solutions of equation (70) in the form

$$X(t) = \sum_{k=0}^{n-1} S_k(t,t_0)X^{(k)}(t_0) + K(t,t_0), \tag{82}$$

where the matrices $S_k(t,t_0)$ are defined by equations (32) or (46) and

$$K(t,t_0) := \sum_{m=0}^{\infty} g^{\alpha(m+1)} I^{\alpha}_{t_0,t}[\tau_1]\cdots I^{\alpha}_{t_0,\tau_{m-1}}[\tau_m]H(\tau_1)\cdots H(\tau_m)(I^{\alpha}_{t_0,\tau_m}[\tau]D(\tau)). \tag{83}$$

Let us consider the matrix $K(t,t_0)$ that is defined by equation (83) with the H-matrix (52) and the D-matrix in the form

$$D(t) = D_0(t-t_0)^{\gamma}, \tag{84}$$

where $\gamma > -1$.

As a result, we get [63] the K-matrices (83) in the form

$$K(t,t_0) = g^{\alpha}\Gamma(\gamma+1)(t-t_0)^{\gamma+\alpha} W^{\alpha+\beta}_{\alpha+\beta+\gamma+1,\alpha+\gamma+1}[g^{\alpha}(t-t_0)^{(\alpha+\beta)}H_c]D_0, \tag{85}$$

where $k = 0,1,2,\ldots,n-1$, $n-1 < \alpha < n$.

Equation (82) with (85) describes time-dependent fractional dynamics of the time-dependent open quantum oscillator (70) with power-law fading memory.

For the constant matrices H and D, which does not change with time, and $n-1 < \alpha < n$ the solution of equations (70) can be represented by equation (82) with (85) with $\beta = \gamma = 0$. In this case, the solution can be written as

$$\begin{aligned} X(t) = {} & \sum_{k=0}^{n-1} (t-t_0)^k E_{\alpha,k+1}[g^{\alpha}(t-t_0)^{\alpha}H_c]X^{(k)}(t_0) \\ & + g^{\alpha}(t-t_0)^{\alpha}E_{\alpha,\alpha+1}[g^{\alpha}(t-t_0)^{\alpha}H_c]D_0, \end{aligned} \tag{86}$$

where $E_{\alpha,\beta}[z]$ is the two-parametric Mittag-Leffler function [13], p. 56.

If the matrix H_c is nondegenerate and, therefore, there is an inverse matrix H_c^{-1}, then equation (86) can be simplified [63]. Equation (86) is represented in the form

$$\begin{aligned} X(t) = {} & \sum_{k=0}^{n-1} (t-t_0)^k E_{\alpha,k+1}[g^{\alpha}(t-t_0)^{\alpha}H_c]X^{(k)}(t_0) \\ & + (E_{\alpha,1}[g^{\alpha}(t-t_0)^{\alpha}H_c] - E)H_c^{-1}D_0. \end{aligned} \tag{87}$$

Equations (86) and (87) describe the quantum processes with power-law fading memory, where the parameters are time-dependent.

For processes without memory ($\alpha = 1$), equation (87) takes the form

$$X(t) = \exp(g(t-t_0)H_c)X(t_0) + (\exp(g(t-t_0)H_c) - E)H_c^{-1}D_0, \tag{88}$$

where we can go to the dimensional time variable ($gt \to t$).

The solution that describes quantum oscillator with friction and memory can be written in the form

$$X(t) = \sum_{k=0}^{n-1} (t - t_0)^k T E_{\alpha,k+1}[g^\alpha (t - t_0)^\alpha L] T X^{(k)}(t_0) + T(E_{\alpha,1}[g^\alpha (t - t_0)^\alpha L] - E) L^{-1} T D_0, \tag{89}$$

where the matrices T and L are defined by equations (78) and (79). Equation (89) describes fractional dynamics of the variances and covariance of quantum observables $Q(t)$ and $P(t)$ of the quantum oscillator with friction and power-law memory that are time independent. For quantum processes without memory, we can use $\alpha = 1$, and solution (89) takes the form

$$X(t) = T \exp(g(t - t_0)L) T X(t_0) + T(\exp(g(t - t_0)L) - E) L^{-1} T D_0, \tag{90}$$

where we can go to the dimensional time variable ($gt \to t$). Expression (90) coincides with the solution that is derived by Sandulescu and Scutaru (see equation (3.44) of paper [31]).

9 Conclusion

In this chapter, we consider some aspects of the fractional dynamics of open quantum systems that are described in [39, 47, 63] and [32–38, 40–43, 49]. Methods and solutions of time-independent and time-dependent dynamics of quantum processes with power-law memory are proposed [63]. The suggested matrix operators $S_k(t, t_0)$ are evolution operators that describe the fractional dynamics of the vector variables $X(t)$ at time point t. These operators are analogous to the S-matrix that are used in quantum field theory [5, 19]. Solutions of the equations of quantum processes with memory are written by using the memory-ordered product (the time-ordered product with memory) and the memory-ordered exponent (the time-ordered exponent with memory). The memory can be caused by interactions with environment [1, 46]. In quantum theory, the memory effects can lead to new properties of the quantum processes. Influence of memory can significantly change the dynamics of quantum processes. The growth rates can increase and decrease in comparison with the processes without memory.

We assume that the fractional quantum dynamics with memory and nonlocality can be realized in the discrete and lattice form by using the lattice fractional derivatives [52, 54, 56], exact fractional differences [55, 57, 61], [53, 58, 59]. The proposed approach can be generalized for quantum field theory, where the space-time power-law nonlocality is taken into account. It should be noted that the interaction picture (the Dirac picture) cannot be realized in the simple form for quantum processes with memory because the violation of the standard Leibniz rule for fractional derivatives of noninteger order [51, 60]. The suggested approach, methods and results can be applied not only to the description of quantum processes, but also to a wide class of processes with memory in natural and social sciences.

Bibliography

[1] L. Accardi, Y. G. Lu, and I. V. Volovich, *Quantum Theory and Its Stochastic Limit*, Springer Verlag, New York, 2002.

[2] H. D. Alber, *Materials with Memory. Initial Boundary Value Problems for Constitutive Equations with Internal Variables*, Springer-Verlag, Berlin, 1998, 171 pp.

[3] G. Amendola, M. Fabrizio, and J. M. Golden, *Thermodynamics of Materials with Memory: Theory and Applications*, Springer Science and Business Media, 2011 576 pp., 10.1007/978-1-4614-1692-0.

[4] S. Attal, A. Joye, and C. A. Pillet (eds.), *Open Quantum Systems: The Markovian Approach*, Springer, 2006.

[5] N. N. Bogoliubov and D. V. Shirkov, *Quantum Fields*, Benjamin/Cumming, New York, 1983, 388 pp.

[6] H. P. Breuer and F. Petruccione, *Theory of Open Quantum Systems*, Oxford University Press, 2002.

[7] M. Caputo and F. Mainardi, Linear models of dissipation in anelastic solids, *Riv. Nuovo Cimento II*, **1** (1971), 161–198.

[8] M. Caputo and F. Mainardi, A new dissipation model based on memory mechanism, *Pure Appl. Geophys.*, **91** (1971), 134–147.

[9] E. B. Davies, *Quantum Theory of Open Systems*, Academic Press, London, 1976.

[10] E. B. Davies, Quantum dynamical semi-groups and neutron diffusion equation, *Rep. Math. Phys.*, **11** (1977), 169–188.

[11] W. A. Day, *The Thermodynamics of Simple Materials with Fading Memory*, Springer-Verlag, Berlin, 1972, 134 pp.

[12] K. Diethelm, *The Analysis of Fractional Differential Equations: An Application-Oriented Exposition Using Differential Operators of Caputo Type*, Springer-Verlag, Berlin, 2010 247 pp, 10.1007/978-3-642-14574-2.

[13] R. Gorenflo, A. A. Kilbas, F. Mainardi, and S. V. Rogosin, *Mittag-Leffler Functions, Related Topics and Applications*, Springer-Verlag, Berlin, 2014 443 pp.

[14] V. Gorini, A. Kossakowski, and E. C. G. Sudarshan Completely positive dynamical semigroups of *N*-level systems, *J. Math. Phys.*, **17**(5) (1976), 821–825.

[15] V. Gorini, A. Frigerio, M. Verri, A. Kossakowski, and E. C. G. Sudarshan, Properties of quantum Markovian master equations, *Rep. Math. Phys.*, **13** (1978), 149–173.

[16] R. S. Ingarden, A. Kossakowski, and M. Ohya, *Information Dynamics and Open Systems: Classical and Quantum Approach*, Kluwer, New York, 1997.

[17] A. Isar, A. Sandulescu, H. Scutaru, E. Stefanescu, and W. Scheid, Open quantum systems, *Int. J. Mod. Phys. E*, **3**(2) (1994), 635–714, quant-ph/0411189.

[18] A. Isar, A. Sandulescu, and W. Scheid, Phase space representation for open quantum systems with the Lindblad theory, *Int. J. Mod. Phys. B*, **10**(22) (1996), 2767–2779, quant-ph/9605041.

[19] C. Itzykson and J. B. Zuber, *Quantum Field Theory*, McGraw-Hill, New York, 1980 705 pp.

[20] A. A. Kilbas, H. M. Srivastava, and J. J. Trujillo, *Theory and Application of Fractional Differential Equations*, Elsevier, Amsterdam, 2006.

[21] V. S. Kiryakova, *Generalized Fractional Calculus and Applications*, Longman and J. Wiley, New York, 1994, 360 pp.

[22] G. Lindblad, On the generators of quantum dynamical semigroups, *Commun. Math. Phys.*, **48**(2) (1976), 119–130.

[23] G. Lindblad, Brownian motion of a quantum harmonic oscillator, *Rep. Math. Phys.*, **10**(3) (1976), 393–406.

[24] A. A. Lokshin and Yu. V. Suvorova, *Mathematical Theory of Wave Propagation in Media with Memory*, Moscow State University, Moscow, 1982, 152 pp. (Russian).
[25] F. Mainardi, Fractional relaxation-oscillation and fractional diffusion-wave phenomena, *Chaos Solitons Fractals*, **7** (1996), 1461–1477.
[26] F. Mainardi, The fundamental solutions for the fractional diffusion-wave equation, *Appl. Math. Lett.*, **9**(6) (1996), 23–28.
[27] F. Mainardi, *Fractional Calculus and Waves Linear Viscoelasticity: An Introduction to Mathematical Models*, Imperial College Press, London, 2010, 368 pp.
[28] I. Podlubny, *Fractional Differential Equations*, Academic Press, San Diego, 1998, 340 pp.
[29] Yu. N. Rabotnov, *Elements of Hereditary Solid Mechanics*, Mir Publishers, Moscow, 1980, 387 pp.
[30] S. G. Samko, A. A. Kilbas, and O. I. Marichev, *Fractional Integrals and Derivatives Theory and Applications*, Gordon and Breach, New York, 1993.
[31] A. Sandulescu and H. Scutaru, Open quantum systems and the damping of collective models in deep inelastic collisions, *Ann. Phys.*, **173** (1987), 277–317.
[32] V. E. Tarasov, Quantum dissipative systems: IV. Analogues of Lie algebras and groups, *Theor. Math. Phys.*, **110**(2) (1997), 168–178.
[33] V. E. Tarasov, Quantization of non-Hamiltonian and dissipative systems, *Phys. Lett. A*, **288**(3/4) (2001), 173–182. quant-ph/0311159.
[34] V. E. Tarasov, Weyl quantization of dynamical systems with flat phase space, *Moscow Univ. Phys. Bull.*, **56**(6) (2001), 5–10.
[35] V. E. Tarasov, Pure stationary states of open quantum systems, *Phys. Rev. E*, **66**(5) (2002), 056116, quant-ph/0311177.
[36] V. E. Tarasov, Stationary states of dissipative quantum systems, *Phys. Lett. A*, **299**(2/3) (2002), 173–178, arXiv:1107.5907.
[37] V. E. Tarasov, Quantum computer with mixed states and four-valued logic, *J. Phys. A*, **35**(25) (2002), 5207–5235, quant-ph/0312131.
[38] V. E. Tarasov, Path integral for quantum operations, *J. Phys. A*, **37**(9) (2004), 3241–3257, arXiv:0706.2142.
[39] V. E. Tarasov, *Quantum Mechanics of Non-Hamiltonian and Dissipative Systems*, Elsevier, Amsterdam, London, 2008, 540 pp.
[40] V. E. Tarasov, Fractional Heisenberg equation, *Phys. Lett. A*, **372**(17) (2008), 2984–2988, arXiv:0804.0586.
[41] V. E. Tarasov, Weyl quantization of fractional derivatives, *J. Math. Phys.*, **49**(10) (2008), 102112.
[42] V. E. Tarasov, Fractional generalization of the quantum Markovian master equation, *Theor. Math. Phys.*, **158**(2) (2009), 179–195, arXiv:0909.0965.
[43] V. E. Tarasov, Quantum nanotechnology, *Int. J. Nanosci.*, **8**(4–5) (2009) 337–344.
[44] V. E. Tarasov, *Fractional Dynamics: Applications of Fractional Calculus to Dynamics of Particles, Fields and Media*, Springer, New York, 2010, 505 pp, 10.1007/978-3-642-14003-7.
[45] V. E. Tarasov, *Theoretical Physics Models with Integro-Differentiation of Fractional Order*, IKI, RCD, 2011, (Russian).
[46] V. E. Tarasov, The fractional oscillator as an open system, *Cent. Eur. J. Phys.*, **10**(2) (2012), 382–389, 10.2478/s11534-012-0008-0.
[47] V. E. Tarasov, Quantum dissipation from power-law memory, *Ann. Phys.*, **327**(6) (2012), 1719–1729.
[48] V. E. Tarasov, Fractional dynamics of open quantum systems, in *Fractional Dynamics in Physics: Recent Advances*, pp. 447–480, Chapter 19, World Scientific, Singapore, 2012, 10.1142/9789814340595_0019.

[49] V. E. Tarasov, Uncertainty relation for non-Hamiltonian quantum systems, *J. Math. Phys.*, **54**(1) (2013), 012112, 13 pp.

[50] V. E. Tarasov, Fractional diffusion equations for open quantum systems, *Nonlinear Dyn.*, **71**(4) (2013), 663–670.

[51] V. E. Tarasov, No violation of the Leibniz rule. No fractional derivative, *Commun. Nonlinear Sci. Numer. Simul.*, **18**(11) (2013), 2945–2948.

[52] V. E. Tarasov, Toward lattice fractional vector calculus, *J. Phys. A*, **47**(35) (2014), 355204. 51 pp, 10.1088/1751-8113/47/35/355204.

[53] V. E. Tarasov, Fractional quantum field theory: From lattice to continuum, *Adv. High Energy Phys.*, **2014** (2014), 957863, 14 pp., 10.1155/2014/957863.

[54] V. E. Tarasov, Lattice fractional calculus, *Appl. Math. Comput.*, **257** (2015), 12–33, 10.1016/j.amc.2014.11.033.

[55] V. E. Tarasov, Exact discrete analogs of derivatives of integer orders: Differences as infinite series, *J. Math.*, **2015** (2015), 134842, 10.1155/2015/134842.

[56] V. E. Tarasov, United lattice fractional integro-differentiation, *Fract. Calc. Appl. Anal.*, **19**(3) (2016), 625–664, 10.1515/fca-2016-0034.

[57] V. E. Tarasov, Exact discretization by Fourier transforms, *Commun. Nonlinear Sci. Numer. Simul.*, **37** (2016), 31–61, 10.1016/j.cnsns.2016.01.006.

[58] V. E. Tarasov, Exact discretization of Schrodinger equation, *Phys. Lett. A*, **380**(1–2) (2016), 68–75, 10.1016/j.physleta.2015.10.039.

[59] V. E. Tarasov, Exact discrete analogs of canonical commutation and uncertainty relations, *Mathematics*, **4**(3) (2016), 44, 10.3390/math4030044.

[60] V. E. Tarasov, Leibniz rule and fractional derivatives of power functions, *J. Comput. Nonlinear Dyn.*, **11**(3) (2016), 031014.

[61] V. E. Tarasov, Exact discretization of fractional Laplacian, *Comput. Math. Appl.*, **73**(5) (2017), 855–863, 10.1016/j.camwa.2017.01.012.

[62] V. E. Tarasov, No nonlocality. No fractional derivative, *Commun. Nonlinear Sci. Numer. Simul.*, **62** (2018), 157–163, 10.1016/j.cnsns.2018.02.019, arXiv:1803.00750.

[63] V. E. Tarasov and V. v. Tarasova, Time-dependent fractional dynamics with memory in quantum and economic physics, *Ann. Phys.*, **383** (2017), 579–599, 10.1016/j.aop.2017.05.017.

[64] V. E. Tarasov and V. V. Tarasova, Criterion of existence of power-law memory for economic processes, *Entropy*, **20**(6) (2018), 414, 24 pp., 10.3390/e20060414.

[65] V. V. Tarasova and V. E. Tarasov, Concept of dynamic memory in economics, *Commun. Nonlinear Sci. Numer. Simul.*, **55** (2018), 127–145, 10.1016/j.cnsns.2017.06.032.

Alexander Iomin

Fractional quantum mechanics with topological constraint

Abstract: An application of fractional integrodifferentiation in quantum processes is presented. We considered two examples of Lévy flights in finite configuration space, which are the examples of the application of the fractional space derivatives in quantum dynamics with topological constraint. These are Lévy flights in an infinite well potential and a quantum damping dynamics of a fractional kicked rotor. It is shown that the Riesz fractional derivative corresponds to the Hamiltonian dynamics. We present a detailed analysis of this quantization in the framework of the path integral approach construction for the system with topological constraint. We also show that the Weyl fractional derivative can quantize an open system. To this end, a fractional kicked rotor is studied in the framework of the fractional Schrödinger equation. The system is described by the non-Hermitian Hamiltonian by virtue of the Weyl fractional derivative. Violation of space symmetry leads to acceleration of the orbital momentum. Quantum localization saturates this acceleration, such that the average value of the orbital momentum can be a direct current and the system behaves like a ratchet. The classical counterpart is a nonlinear kicked rotor with absorbing boundary conditions.

Keywords: Fractional integral, Lévy flight, topological constraints, oath integral

PACS: 05.45.Mt, 05.40.-a

1 Introduction

The introduction of a fractional concept in quantum mechanics with motivating new implementations of nonlocal physics leads to many technical questions and often needs special care. A typical example is the "quantum Lévy flights" in systems with a so-called topological constraint, like a rotor and a kicked rotor [15], or a particle in an infinite well potential [22]. The latter "simple" example has evoked an active discussion in the literature on how a nonlocal operator, defined on the infinite scale, acts in a finite-size range, such as a quantum box. This discussion is reviewed and resolved in [16]. Here, we discuss two examples of the Lévy flights in quantum mechanics with topological constraint. Among many possible applications of the problem, of special

Acknowledgement: This research was supported by the Israel Science Foundation (ISF).

Alexander Iomin, Department of Physics, Technion, Haifa, 32000, Israel, e-mail: iomin@physics.technion.ac.il

interest is the first-passage analysis [11], which is important for the investigation of the transport properties, for example, of Lévy glasses [2].

In quantum mechanics, the fractional concept has been introduced by means of the Feynman propagator for nonrelativistic quantum mechanics as for Brownian path integrals [22, 28]. Equivalence between the Wiener and the Feynman path integrals [12], established by Kac [21], is natural, since both are Markov processes and indicates equivalence between the Laplace operators for classical diffusion equation and the Schrödinger equation. The same, the appearance of the space fractional derivatives in the Schrödinger equation is natural, since both the standard Schrödinger equation and the space fractional one obey the Markov process. As shown in the seminal papers [22, 28], the appearance of the space fractional derivatives in the Schrödinger equation is natural and relates to the path integrals approach. The path integral approach for Lévy stable processes, considered for the fractional diffusion equation, in particular, for the fractional Fokker–Planck equation (FFPE), has been extended to a quantum Feynman–Lévy measure that leads to the space fractional Schrödinger equation (FSE) [22, 28].

The introduction of the Lévy measure in quantum mechanics is based on the generalization of the self-consistency condition, known as the Bachelor–Smoluchowski–Kolmogorov chain equation (or the Einstein–Smoluchowski–Kolmogorov–Chapman equation; see, e. g., [24]), established for the Wiener process for the conditional probability $W(x,t|x_0,t_0)$[1]

$$W(x,t|x_0,t_0) = \int_{-\infty}^{\infty} W(x,t|x',t')W(x',t'|x_0,t_0)\,dx'. \tag{1}$$

In the case of the translational invariance, it reads $W(x,t|x_0,t_0) = W(x-x_0,t|t_0)$. Straightforward generalization of this expression by the Lévy process is expressed through the Fourier transform

$$W(x,t|x_0,t_0) = \int_{-\infty}^{\infty} e^{ip(x-x_0)}e^{-K_\alpha(t-t_0)|p|^\alpha}\,dp, \tag{2}$$

where $0 < \alpha \le 2$ and K_α is a generalized diffusion coefficient [23]. Using equations (1) and (2), one defines the integration of function $f[x(\tau)]$ over the generalized measure

$$\int f[x(\tau)]d_Lx(\tau) \equiv \lim_{N\to\infty}\frac{1}{(2\pi\hbar)^n}\int_{-\infty}^{\infty}dx_1\cdots\int_{-\infty}^{\infty}dx_N\int_{-\infty}^{\infty}dp_1\cdots\int_{-\infty}^{\infty}dp_N \\ \times f(x_1,\dots,x_N)e^{-i[(x_1-x_0)p_1+\dots+(x_{N+1}-x_N)p_N]}e^{-K_\alpha[|p_1|^\alpha\Delta t+\dots+|p_N|^\alpha\Delta t]}. \tag{3}$$

1 In the case of the translational invariance, equation (1) has the solution in the Fourier space $\mathcal{F}[W(x,t|x_0,t_0)](p,t-t_0) = e^{-K_\alpha(t-t_0)|p|^\alpha} = e^{-K_\alpha(t-t')|p|^\alpha}e^{-K_\alpha(t'-t_0)|p|^\alpha}$, which is in accordance with equation (2).

Here, $\Delta t = (t - t_0)/N$. The Lévy distribution is defined by the Fox function [22] and in the r. h. s. of equation (3) it is presented by means of the Fourier integral with a stretched exponential kernel. When

$$f[x(\tau)] = \exp\left\{-\int_{t_0}^{t} V[x(\tau)]d\tau\right\},$$

with $V(x)$ being a potential, expression (3) is a generalized Feynman–Kac formula [22, 27].

One should recognize that the general form of the path integral in equation (3) does not correctly describe systems when integrations over coordinates $x_1, x_2, \ldots, x_N$ have finite limits, which is a topological constraint [7]. As the first example of such systems, we consider fractional quantum mechanics in an infinite well potential. We show that the condition of the restriction of the integration in both the formulation of the problem in equation (3) and correspondingly, in the fractional Riesz derivative must be taken into account. Otherwise, the FSE for the infinite well potential cannot be obtained.

2 Lévy quantum mechanics in potential well

In complete analogy with fractional diffusion, fractional quantum mechanics can be constructed from the Feynman–Kac formula and $V(x)$ is the potential. Following Laskin's theory [22], we determine a wave function at the moment $t + \Delta t$ by means of equation (3)

$$\psi(x, t + \Delta t) = \int_{-\infty}^{\infty} \frac{dp}{2\pi\hbar} e^{-iK_\alpha \Delta t |p|^\alpha} \int_{-\infty}^{\infty} dy\, e^{-\frac{i}{\hbar}p(x-y)} e^{-\frac{i}{\hbar}V(y)\Delta t} \psi(y, t). \tag{4}$$

In the limit $\Delta t \to 0$, one obtains

$$i\hbar\partial_t \psi(x, t) = \frac{K_\alpha}{2\pi\hbar} \int_{-\infty}^{\infty} dy \int_{-\infty}^{\infty} |p|^\alpha e^{-\frac{i}{\hbar}p(x-y)} \psi(y, t) dp + V(x)\psi(x, t). \tag{5}$$

If one introduces the fractional Laplacian $(-\Delta)^{\alpha/2}$ by means of the Riesz fractional derivative [25],

$$(-i\hbar\partial_x)^\alpha \psi \equiv \hbar^\alpha (-\Delta)^{\alpha/2} \psi = \frac{1}{2\pi\hbar} \int_{-\infty}^{\infty} e^{-ipx} |p|^\alpha \phi(p) dp, \tag{6}$$

where $\phi(p) = \int_{-\infty}^{\infty} e^{ipy} \psi(y) dy$ is the Fourier image, the FSE is obtained from equation (5)

$$i\hbar\partial_t \psi = K_\alpha (-i\hbar)^\alpha \partial_x^\alpha \psi + V(x)\psi. \tag{7}$$

One sees that for $\alpha = 2$, the FSE (7) reduces to a conventional Hamiltonian mechanics with $K_2 = 1/2m$ being a half inverse mass of a particle.

It should be noted that this equation is valid only for the smooth potentials $V(x)$, which ensures infinite limits of integration in the Laplace operator (6). However, if the limits are finite, for example, for the infinite potential well

$$V(x) = \begin{cases} 0 & \text{if } |x| \le L \\ \infty & \text{if } |x| > L, \end{cases} \tag{8}$$

one cannot obtain the Schrödinger equation (7) from equations (4) and (5). A simple explanation of this problem relates to the absence of the expansion over $V\Delta t$ in equation (4), since

$$\exp\left[-\frac{i}{\hbar}\Delta t V(x)\right]$$

is an infinitely fast oscillating function for any arbitrary small but finite Δt. Note that one first performs this expansion and then takes the limit $\Delta t \to 0$. To overcome this obstacle, the cutoff of the limits of integration over y is performed. Moreover, this is a correct formulation of the problem with the topological constraints, as in the case of the infinite potential well. This notion is also relevant for conventional local quantum mechanics; see, for example, [7]. Therefore, FSEs (5) and (7) reduce to a well-defined problem of a free particle in a finite-size range with the FSE,

$$i\hbar\partial_t\psi = \frac{K_\alpha}{2\pi\hbar}\int_{-L}^{L} dy \int_{-\infty}^{\infty} |p|^\alpha e^{-\frac{i}{\hbar}p(x-y)}\psi(y,t)dp, \tag{9}$$

which is furnished with the boundary conditions $\psi(x = \pm L) = 0$. Obviously, the Riesz fractional derivative (6) can no longer be used for the potential well, and in addition the Fourier image $\phi(p)$ is not appropriately defined.

Next, we follow the theory of [16], which in its tern is a standard approach as well [7]. Let us perform the Fourier inversion in equation (9) over $k = p/\hbar$. This yields

$$\frac{\hbar^\alpha}{2\pi}\int_{-\infty}^{\infty} |k|^\alpha e^{-ik(x-y)}dk = \frac{\hbar^\alpha}{2\pi}(i\partial_x)^2\int_{-\infty}^{\infty} |k|^{\alpha-2}e^{-ik(x-y)}dk. \tag{10}$$

One obtains this expression with the double differentiation for $1 < \alpha < 2$, while for $0 < \alpha < 1$ one differentiates only once. Therefore, we have the integration

$$\int_{-\infty}^{\infty} |k|^{-\nu}e^{-ikz}dk = 2\int_{0}^{\infty} |k|^{-\nu}\cos kz = \frac{2\pi|z|^{\nu-1}}{2\Gamma(\nu)\cos(\nu\pi/2)}, \tag{11}$$

where $\nu = 2 - \alpha$ for $1 < \alpha \le 2$ and $\nu = 1 - \alpha$ for $0 < \alpha \le 1$, and $\Gamma(\nu) = (\nu - 1)!$ is a gamma function. Following [16], we consider $1 < \alpha \le 2$. The integration in equations (10) and (11) yields the fractional Laplace operator $(-\Delta)^{\frac{\alpha}{2}}$ for the FSE (9) in the form of the Riemann–Liouville fractional derivative, also known as the Riesz fractional derivative [25]

$$\mathcal{R}^{\alpha}\psi(x) = \frac{\hbar^{\alpha}K_{\alpha}}{2\Gamma(2-\alpha)\cos\frac{\alpha\pi}{2}}\partial_x^2 \int_{-L}^{L} |x-y|^{1-\alpha}\psi(y)\,dy. \tag{12}$$

Note that

$$I^{\nu}_{[a,b]}\phi(z) = \frac{1}{2\Gamma(\nu)\cos\frac{\nu\pi}{2}} \int_a^b \frac{\phi(z)dz}{|x-z|^{1-\nu}}$$

is the Riesz fractional integral on the finite interval $[a,b]$ [25] with $a \le x \le b$ and $0 < \nu < 1$. It can be presented as the sum of the left and right Riemann–Liouville fractional integrals

$$\int_a^x \frac{\phi(z)dz}{(x-z)^{1-\nu}} + \int_x^b \frac{\phi(z)dz}{(z-x)^{1-\nu}} \equiv I^{\nu}_{a+}\phi(x) + I^{\nu}_{b-}\phi(x).$$

2.1 Eigenvalue problem for the fractional Laplace operator

Let us consider the eigenvalue problem

$$\mathcal{R}^{\alpha}\Psi_E = E\Psi_E \tag{13}$$

with boundary conditions $\Psi_E(x = \pm L) = 0$ that yields the solution of FSE (9)

$$\psi(x,t) = \sum_E a_E e^{-iEt}\Psi_E,$$

where coefficients a_E are defined by the initial conditions $\psi_0(x) = \psi(x, t = 0)$. We rewrite the fractional Laplace operator in the form of the FSE (9), which is convenient in the following analysis:

$$\mathcal{R}^{\alpha}f(y) = K_{\alpha}\hbar^{\alpha}(i\partial_x)\int_{-L}^{L}\left[\frac{1}{2\pi}\int_{-\infty}^{\infty}|k|^{\alpha-2}ke^{-ik(x-y)}dk\right]f(y)dy. \tag{14}$$

Here, we use again that on the real axis $|k|^2 = k^2$. One easily finds that the antisymmetric (odd) eigenfunction Ψ_E^{odd} can be found in the form

$$\Psi_E^{\mathrm{odd}}(x) = \Psi_m^{\mathrm{odd}}(x) = \frac{1}{\sqrt{L}}\sin\frac{m\pi x}{L}, \quad m = 1, 2, \ldots, \tag{15}$$

which satisfies the boundary condition $\Psi_m^{\mathrm{odd}}(x = \pm L) = 0$. Substituting solution (15) with $f(y) = \Psi_E(y)$ in equation (14) and performing integration straightforwardly, one obtains

$$\mathcal{R}^\alpha \sin\frac{m\pi x}{L} = K_\alpha\left(\frac{\hbar m\pi}{L}\right)^\alpha \sin\frac{m\pi x}{L}.$$

Therefore, $\Psi_m^{\mathrm{odd}}(x)$ is the eigenfunction with corresponding eigenvalue

$$E^{\mathrm{odd}} \equiv E_m^{\mathrm{odd}} = K_\alpha\left(\frac{\hbar m\pi}{L}\right)^\alpha = K_\alpha(\hbar k_m)^\alpha, \tag{16}$$

where $k_m \equiv \frac{\pi m}{L}$. The analytical solution of the eigenvalue problem has been suggested in [16] and the numerical verification for the odd eigenfunctions was also performed in [17] The same procedure can be performed to find symmetric (even) eigenfunctions as well [16].

3 Fractional path integral

One should bear in mind that the Feynman–Kac formula in equation (4) and FSE (5) are introduced in unbounded Euclidean (configuration) space. In contrast, the configuration space of a particle in the infinite potential well is contracted to the finite size of the potential well. This leads to the quantum mechanics in a space with topological constraints. Even for the conventional local quantum mechanics, the path integral presentation is not an easy task, as stated in [7]. Fortunately, since eigenvalue solutions (13)–(16) are known, the path integral for the Lévy process in the finite area can be constructed. Therefore, one can obtain equation (7) with infinite limits of integration for the Riesz operator. Let us define for convenience $|x\rangle \equiv \Psi_m^{\mathrm{odd}}(x)$. Then equation (4) can be rewritten as

$$\psi(x,\Delta t) \equiv \langle x|\psi(\Delta t)\rangle = \langle x|e^{-i\mathcal{R}^\alpha\Delta t/\hbar}|\psi_0\rangle = \int_{-L}^{L} dx_1\langle x|e^{-i\mathcal{R}^\alpha\Delta t/\hbar}|x_1\rangle\langle x_1|\psi_0\rangle. \tag{17}$$

We focus on the evolution of the Green's function $G(x, t+\Delta t|x_1, t) \equiv G(x,\Delta t; x_1)$, which reads

$$G(x,\Delta t;x_1) = \langle x|e^{-i\mathcal{R}^\alpha\Delta t/\hbar}|x_1\rangle = \int_{-\infty}^{\infty}\frac{dk}{2\pi}e^{-i|k|^\alpha K_\alpha\Delta t}\int_{-L}^{L} dy e^{-ik(x_1-y)}\langle x|y\rangle. \tag{18}$$

Taking into account the scalar product $\langle x|y\rangle = \frac{1}{L}\sum_{n=0}^\infty \sin(k_n x)\sin(k_n y)$ and the Poisson summation formula $\sum_{l=-\infty}^\infty e^{2\pi i x l} = \sum_{m=-\infty}^\infty \delta(x-m)$, one obtains (see also [7])

$$G(x,\Delta t;x_1) = \frac{1}{2}\sum_{l=-\infty}^{\infty}\int_{-\infty}^{\infty}\frac{dk}{2\pi}e^{-i\hbar^{\alpha-1}|k|^\alpha K_\alpha\Delta t}\left[e^{ik(x-x_1+2Ll)} - e^{ik(x+x_1+2Ll)}\right]$$

$$= \frac{1}{2}\sum_{z=\pm x}\sum_{l=-\infty}^{\infty}\int_{-\infty}^{\infty}\frac{dk}{2\pi}e^{-i\hbar^{\alpha-1}|k|^{\alpha}K_{\alpha}\Delta t}$$
$$\times \exp\{ik(z - x_1 + 2Ll) + i\pi[H(-z) - H(x_1)]\}, \quad (19)$$

where the Heaviside $H(z)$ functions in the exponential provide the correct signs for $z = \pm x$. Now, we take into account

$$\frac{1}{2}\sum_{z=\pm x}\sum_{l=-\infty}^{\infty}\int_{-L}^{L} dx_1 \longleftrightarrow \int_{-\infty}^{\infty} dx_1, \quad (20)$$

which returns one to the fractional integration with infinite limits, as in equation (4). The essential difference here is the appearance of the topological phase due the Heaviside functions in Green's function (19). Continuing this procedure by repeating it N times ($t = N\Delta t$), one arrives at the correct analogy of equation (3) for the infinite well potential

$$G(x,t|x_0,0) \equiv G(x,t;x_0) = \sum_{l=-\infty}^{\infty}\sum_{z=\pm x+2lL}\prod_{j=1}^{N}\int_{-\infty}^{\infty}dx_j\prod_{j=1}^{N+1}\int_{-\infty}^{\infty}\frac{dk_j}{2\pi}$$
$$\times \exp\left\{i\sum_{j=1}^{N+1}[k_j(x_j - x_{j-1}) + \pi H(-x_j) - \pi H(-x_{j-1}) - \hbar^{\alpha-1}|k_j|^{\alpha}K_{\alpha}\Delta t]\right\}, \quad (21)$$

where $x_{N+1} \equiv z$. The topological term is purely a boundary expression[2] and, therefore, integration over all x_j in equation (21) yields a product of δ functions $\prod_{j=1}^{N}\delta(k_j - k_{j+1})$, which finally yields the Fourier inversion of the Green function in the form of Fox's $H_{2,2}^{1,1}(x)$ function [22, 29] in its Fourier form

$$G(x,t;x_0) = \sum_{l=-\infty}^{\infty}\frac{1}{4\pi}\int_{-\infty}^{\infty}dk e^{-i\hbar^{\alpha-1}|k|^{\alpha}K_{\alpha}t}[e^{ik(x-x_0+2lL)} - e^{-ik(x+x_0+2lL)}]. \quad (22)$$

Because of the properties of $H_{2,2}^{1,1}(x)$ Fox's function, at $\alpha = 2$, the Green function (22) reduces to the Green function of a free particle with a unit mass in the box [7]

$$\langle x,t|x_0,0\rangle_{\text{box}} = \sum_{l=-\infty}^{\infty}\frac{1}{\sqrt{8i\pi\hbar t}}[e^{\frac{i}{2\hbar}\frac{(x-x_0+2lL)^2}{t}} - e^{\frac{-i}{2\hbar}\frac{(x+x_0+2lL)^2}{t}}]. \quad (23)$$

2 For $\alpha = 2$, this expression coincides with the results in [7]. For the self-contained presentation, we shall adjust some formulae thereof. Namely, taking the continuous time limit, one arrives at the path integral $G(x,t;x_0) = \frac{1}{2}\sum_{l=-\infty}^{\infty}\sum_{z=\pm x+2lL}\int Dx(\tau)\int\frac{Dp(\tau)}{2\pi\hbar}\exp\{\frac{i}{\hbar}S\}$, where the action $S[z] = \int_0^t d\tau[p\dot{x} - \mathcal{H}(|p|) - \hbar\pi\dot{x}\delta(x)]$ contains the new topological term $S_{\text{top}}[z] = -\hbar\pi\int_0^t d\tau[\dot{x}\delta(x)] = \hbar\pi[H(-z) - H(-x_0)]$, which is purely a boundary expression.

4 Example I: Moving walls in adiabatic approximation

Handling the path integral expression in such a simple form as equation (22), one can consider a system of a Lévy particle inside moving walls. For $\alpha = 2$, this problem corresponds to the so-called Fermi acceleration [9], where chaotic dynamics can be realized because of the interaction of nonlinear resonances. However, for $1 < \alpha < 2$, the physical implementation of the classical limit of the problem is vague, since a particle is really not free; it is a Lévy particle. Therefore, the interaction of nonlinear resonances is not considered. Here, the problem is treated in the adiabatic approximation. In this case, equation (22) can be used for further quantum mechanical analysis. Let the infinite walls at $x = \pm L$ move periodically, such that the boundary conditions for the wave function are $\psi(x = \pm L(t)) = 0$, where $L(t) = L + \varepsilon \sin(\nu t)$ with $\varepsilon/L \ll 1$. To calculate the density of states, we are interested in the trace of the Green function

$$g(t) = \int_{-L}^{L} dx_0 G(x_0, t; x_0) \tag{24}$$

where $G(x = x_0, t; x_0)$ can be obtained from equation (22) in the form

$$G(x_0, t; x_0) = \sum_{l=-\infty}^{\infty} \frac{1}{4\pi} \int_{-\infty}^{\infty} dk e^{-i\hbar^{\alpha-1}|k|^{\alpha} K_\alpha t} \left[e^{ik(2lL)} - e^{-ik(2x_0+2lL)} \right]. \tag{25}$$

Performing summation over l by the Poisson summation formula

$$\sum_{l=-\infty}^{\infty} e^{\pm 2iklL} = 1 + 2 \sum_{l=1}^{\infty} e^{2iklL} = \frac{\pi}{L} \sum_{m=-\infty}^{\infty} \delta\left(k - \frac{\pi m}{L}\right),$$

one performs integration over k, that leads to summation over the spectrum $k = k_m = \pi m/L$. Then, performing integration over x_0, one obtains for the trace

$$g_0(t) = \sum_{m=1}^{\infty} \exp\left[-i|\hbar\pi m/L|^{\alpha} K_\alpha t/\hbar\right]. \tag{26}$$

One also obtains this result from the expression for the Green function

$$G(x_0, t; x_0) = \sum_n \exp(-iE_n^{\text{odd}} t/\hbar) \Psi_n^{\text{odd}}(x_0) \Psi_n^{*\text{odd}}(x_0).$$

The Fourier transform $\mathcal{G}_0(E) = \mathcal{F}[g_0(t)]$ yields the density of states $\rho_0(E) = -\frac{1}{\pi}\Im \mathcal{G}_0(E)$

$$\rho_0(E) = \hbar \sum_m \delta(E - K_\alpha |\hbar k_m|^{\alpha}), \tag{27}$$

where $E \equiv E^{\text{odd}}$, which satisfies the eigenvalue problem, discussed in Section 2.1.

In the case of the moving walls, at the replacement $L \to L(t)$, the adiabatic approximation makes it possible to obtain the trace of the Green's function in the form

$$g_\varepsilon(t) = e^{(\varepsilon \sin \nu t)\frac{d}{dL}} g_0(t) = \sum_m e^{-i(\hbar\pi m/L(t))^\alpha K_\alpha t/\hbar}. \tag{28}$$

Let us present the shift operator in equation (28) as follows:

$$e^{(\varepsilon \sin \nu t)\frac{d}{dL}} = \sum_{n=-\infty}^{\infty} \frac{1}{2\pi} \int_{-\pi}^{\pi} d\xi e^{\varepsilon \sin \xi \frac{d}{dL}} e^{in(\xi - \nu t)}. \tag{29}$$

Then the Fourier transform over time can be easily performed, which yields the following expression for the density of states:

$$\rho_\varepsilon(E) = \sum_{n=-\infty}^{\infty} \frac{\hbar}{2\pi} \int_{-\pi}^{\pi} d\xi e^{(\varepsilon \sin \xi)\frac{d}{dL}} e^{in\xi} 2L \sum_m \delta\left(E - \hbar n\nu - K_\alpha \left|\frac{\hbar\pi m}{L}\right|^\alpha\right). \tag{30}$$

Parameter ξ determines the quasi-energy spectrum, namely, its band structure. Therefore, for the moving walls the discrete spectrum (16) changes essentially even in the adiabatic consideration. The spectrum reads

$$E_m \to E_{m,n}(\xi) = \hbar n\nu + K_\alpha \left|\frac{\hbar\pi m}{L + \varepsilon \sin \xi}\right|^\alpha \approx E_m + \hbar n\nu - \varepsilon\alpha K_\alpha \frac{|\hbar\pi m|^\alpha}{L^{\alpha+1}} \sin \xi. \tag{31}$$

This solution corresponds to the reconstruction of the energy spectrum of the stationary problem (13): it becomes the quasienergy spectrum with a narrow band structure.

5 Example II: Fractional kicked rotor

The situation changes dramatically, when the adiabatic approximation for the moving walls cannot be used. In the classical counterpart ($\hbar = 0$), it corresponds to the chaotic dynamics, which is known as the Fermi acceleration, and its simplified scheme can be described by a kicked rotor model [8]. An interaction with the environment, can be modeled by means of the fractional space derivatives, as well. This task relates to the quantum-to-classical crossover [19] where the role of dissipation in quantum systems is a subject of extensive studies [14, 4, 26]. A quantum kicked rotor with dissipation is an example where a quantization of a strange attractor has been considered in the framework of both the master equation [13, 10] and the Hamiltonian approach [19], as well.. Fractional space derivatives make it possible to introduce quantum dissipation in such a way that quantum dynamics can be still described by means of a wave function in the framework of the Schrödinger equation. This approach will be demonstrated for the quantum kicked rotor. The topological constraint here is due to the operator algebra of the angular momentum, which describes a motion of a particle on a circle.

5.1 Fractional particle on a circle

The dynamics of a point particle on a unit circle is described by an angular phase $\phi \in [0, 2\pi]$. If a wave function is the same at $\phi = 0$ and $\phi = 2\pi$, the time evolution of a particle of a unit mass $m = 1$ between two points ϕ_0 and $\phi = \phi(t)$ in time interval $(0, t)$ is determined by the transition amplitude (see, e. g., [7])

$$G(\phi, t|\phi_0, 0) \equiv G(\phi, t; \phi_0) = \sum_{l=-\infty}^{\infty} \int_{-\infty}^{\infty} \frac{dp}{2\pi\hbar} \exp\left\{\frac{i}{\hbar}\left[p(\phi - \phi_0 + 2\pi l) - \frac{p^2}{2m}t\right]\right\}. \tag{32}$$

Here, p corresponds to the orbital momentum operator $\hat{p} = -i\hbar\frac{\partial}{\partial\phi}$. As it is shown in Section 3, a generalization of this expression on the fractional dynamics is straightforward, by substitute $p^2/2 \to K_\alpha|p|^\alpha$ in the exponential with $1 < \alpha < 2$.

$$G(\phi, t; \phi_0) = \sum_{l=-\infty}^{\infty} \int_{-\infty}^{\infty} \frac{dp}{2\pi\hbar} \exp\left\{\frac{i}{\hbar}[p(\phi - \phi_0 + 2\pi l) - K_\alpha|p|^\alpha t]\right\}. \tag{33}$$

Here, modulus $|p|$ ensures the unitary transformation. We also pay attention that in equation (32), the action in the exponential is dimensionless, therefore, to keep this property in the fractional Green's function (33), we introduce the coefficient K_α, in complete analogy with the precedent sections. For $\alpha = 2$, it is a half of the moment of inertia of a particle with unit mass on a circle of the unit radius. One can easily check that $G(\phi, t; \phi_0)$ is the Green function with corresponding properties as the initial condition

$$\lim_{t\to 0} G(\phi, t; \phi_0) = \sum_l \delta(\phi - \phi_0 + 2\pi l)$$

and the chain rule

$$G(\phi, t; \phi_0) = \int_0^{2\pi} G(\phi, t|\phi', t')G(\phi', t'; \phi_0)d\phi'.$$

The Hamiltonian, which produces the Green function, can be obtained by differentiation of equation (33) with respect to time $t > 0$ [28]. This yields

$$i\hbar\partial_t G(\phi, t; \phi_0) = \sum_{l=-\infty}^{\infty} \int_{-\infty}^{\infty} \frac{K_\alpha|p|^\alpha dp}{2\pi\hbar} \exp\left\{\frac{i}{\hbar}[p(\phi - \phi_0 + 2\pi l) - K_\alpha|p|^\alpha t]\right\}. \tag{34}$$

However, the r. h. s. of equation (34) can be obtained by means of the left and right fractional derivatives $D^\alpha_{-\infty+}$ and $D^\alpha_{\infty-}$, correspondingly, which is also know as Weyl's derivatives [29]. The Fourier transform of the derivatives yields

$$\mathcal{F}[D^\alpha_{-\infty+}f(x)] = (ik)^\alpha f(k), \quad \mathcal{F}[D^\alpha_{\infty-}f(x)] = (-ik)^\alpha f(k) \tag{35}$$

Therefore, the term $|p|^\alpha e^{\frac{i}{\hbar}pz}$ can be expressed by means of the Weyl fractional integrals (35). This yields the Schrödinger equation for the Green's function for $t > 0$

$$i\hbar\partial_t G = \frac{K_\alpha}{2}[(-i\hbar)^\alpha D^\alpha_{-\infty+} + (i\hbar)^\alpha D^\alpha_{\infty-}]G \equiv \hat{\mathcal{H}}G. \tag{36}$$

This equation describes the fractional dynamics of a quantum particle on a unit circle with the Hamiltonian $\hat{\mathcal{H}}$. In what follows, we consider an example of a perturbed motion on the circle, and we also violate the unitary property of the evolution operator.

5.2 Fractional kicked rotor

The quantum chaotic dynamics of a fractional kicked rotor (FKR) is described by the Hamiltonian

$$\hat{\mathcal{H}} = \hat{\mathcal{T}} + \epsilon \cos x \sum_{n=-\infty}^{\infty} \delta(t-n), \tag{37}$$

where ϵ is an amplitude of the periodic perturbation which is a train of δ kicks and $\phi \equiv x \in (-\infty, \infty)$. The kinetic part of the Hamiltonian is due to equation (36)

$$\hat{\mathcal{T}} = (-i\tilde{h})^\alpha K_\alpha D^\alpha_{-\infty}, \tag{38}$$

where $\tilde{h} = \hbar(K_\alpha/2)^{\frac{1}{\alpha}}$ is the dimensionless Planck constant. When $\alpha = 2$, equation (37) is the quantum kicked rotor [6]. The kinetic term in the Hamiltonian (37) is defined on the basis $|k\rangle = e^{ikx}/\sqrt{2\pi}$ as follows:

$$\hat{\mathcal{T}}|k\rangle = \mathcal{T}(k)|k\rangle = (\tilde{h}k)^{2-\beta}|k\rangle \tag{39}$$

where $\alpha = 2 - \beta$ with $0 < \beta < 1$. This non-Hermitian operator has complex eigenvalues for $k < 0$, which are defined on the complex plane with a cut from 0 to $-\infty$, such that $1^{-\beta} = 1$ and $(-1)^{-\beta} = \cos\beta\pi - i\sin\beta\pi$ and, therefore, $k^{-\beta} = |k|^{-\beta}e^{-i\pi\beta(k)}$, where $\beta(k) = \beta[1 - \mathrm{sgn}(k)]/2$. Note that when $\alpha > 2$, one chooses $(-1) = e^{-i\pi}$, such that $(-1)^\beta = e^{-i\pi\beta}$.

A quantum map for the wave function $\psi(\phi, t)$ is

$$\psi(x, t+1) = \hat{U}\psi(x,t), \tag{40}$$

where the evolution operator on the period

$$\hat{U} = \exp\left[\frac{-i\epsilon\cos x}{\tilde{h}}\right]\exp\left[\frac{-i\hat{\mathcal{T}}}{\tilde{h}}\right] \tag{41}$$

describes a free dissipative motion and then a kick. Dynamics of the FKR is studied numerically, where equation (39) enables one to use the fast Fourier transform as an efficient way to iterate the quantum map (40). A specific property of this Hamiltonian dynamics is quantum dissipation resulting in probability leakage and described by the survival probability

$$P(t) = \langle \psi(t)|\psi(t)\rangle = \sum_{n=-\infty}^{\infty} |f_n|^2, \tag{42}$$

where $|f_n|^2$ is the level occupation distribution at time t. The initial occupation is $f_n(t = 0) = \delta_{n,0}$. Another specific characteristic is the nonzero mean value of the orbital momentum

$$\langle p(t)\rangle = \tilde{h}\frac{\sum_n n|f_n(t)|^2}{\sum_n |f_n(t)|^2}, \tag{43}$$

due to the asymmetry of the quantum kinetic term $\hat{T}$.

Results of the numerical study of the quantum map (40) are shown in Figures 1–4. The quantum dissipation leads to the asymmetrical distribution of the level occupation $|f_n(t)|$, shown in Figure 1 that results in the nonzero first moment of the orbital momentum $\langle p\rangle \sim t^{\gamma_1}$ in Figure 2, where $\gamma_1 > 0$. This accelerator dynamics is accompanied by the power law decay of the survival probability $P(t) \sim t^{-\gamma_2}$ with the exponent $0 < \gamma_2 < 1$ (in Figure 3 $\gamma_2 \approx 0.71$), and then the decay rate increases with the time due to quantum effects. Quantum localization affects strongly both γ_1 and γ_2. By increasing the quantum parameter, when $\tilde{h} = 0.76$, the exponent γ_1 approaches zero (in Figure 4 the slope is 10^{-5}), and the survival probability decays at the rate $\gamma_2 \approx 0.99$. This means that quantum localization saturates the acceleration with time and leads to the exponential restriction of the initial profile spreading in the orbital momentum space from above. This property results in saturation of acceleration of $\langle p(t)\rangle$; namely, at $t \to \infty$ it follows that $\langle p(t)\rangle \to \text{const}$. Such a behavior is found for a special selection of the parameters $\tilde{h} = 0.76$, $\beta = 0.05$, and $\epsilon = 3$. In Figure 4, one sees a direct current of $\langle p(t)\rangle$

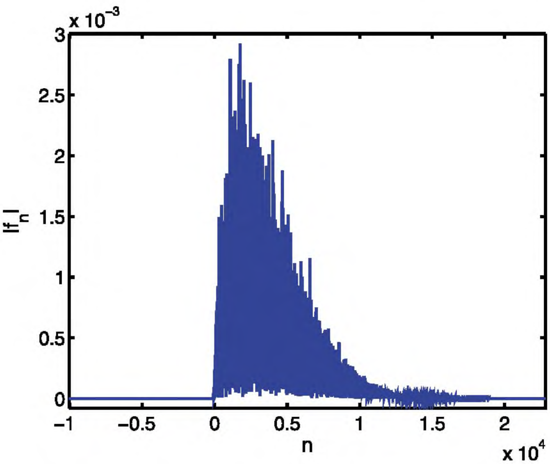

Figure 1: Level occupation distribution (after 2000 iterations) for $\epsilon = 3$, $\beta = 0.01$, $\tilde{h} = 0.02$. Reprinted figure with permission from A. Iomin, Phys. Rev. E, 75, 037201 (2007). Copyright 2007 by the American Physical Society.

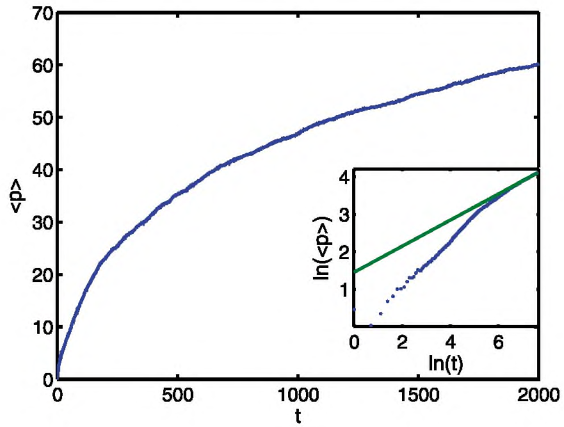

Figure 2: Acceleration of the average orbital momentum for the same parameters as in Figure 1. The insert is the log-log plot, and the solid line corresponds to $\gamma_1 = 0.35$ obtained by the least squared calculation. Reprinted figure with permission from A. Iomin, Phys. Rev. E, 75, 037201 (2007). Copyright 2007 by the American Physical Society.

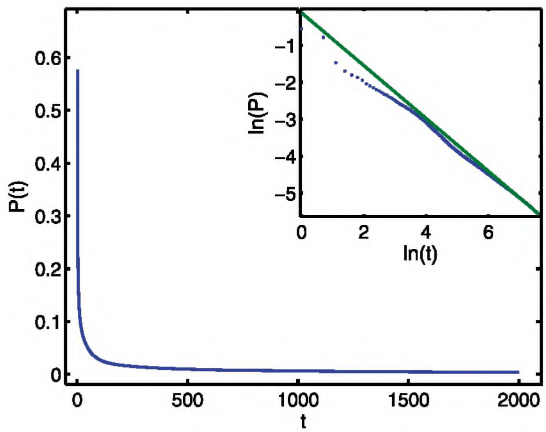

Figure 3: Decay of the survival probability $P(t)$. The insert is the log-log plot, and the solid line corresponds to $\gamma_2 = 0.71$ obtained by the least squared calculation. Reprinted figure with permission from A. Iomin, Phys. Rev. E, 75, 037201 (2007). Copyright 2007 by the American Physical Society.

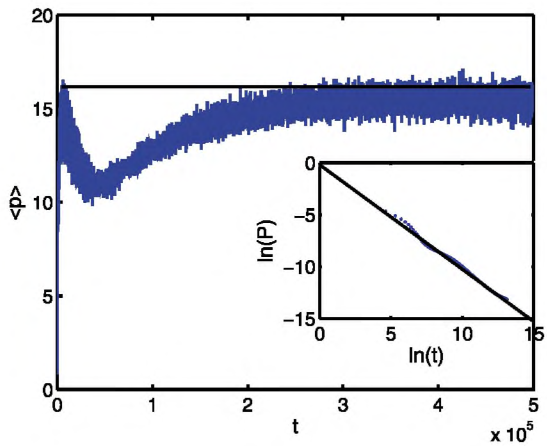

Figure 4: Quantum saturation of $\langle p(t) \rangle$ due to localization when $\tilde{h} = 0.76$, $\beta = 0.05$, and the same ϵ, as in Figures 1–3. The slope of the solid line is 10^{-5}. The insert shows the power low decay of $P(t) \sim t^{-\gamma_2}$ with $\gamma_2 \approx 0.99$ due to the linear interpolation. Reprinted figure with permission from A. Iomin, Phys. Rev. E, 75, 037201 (2007). Copyright 2007 by the American Physical Society.

for $5 \cdot 10^5$ iterations. This double quantum impact of asymmetric dissipation and localization leads, asymptotically, to a quantum like ratchet which differs from quantum one obtained for a classical chaotic attractor [5].

5.3 Wigner representation

To understand the physical relevance of the fractional Schrödinger equation with dissipation, the classical limit $\tilde{h} \to 0$ is performed in the Wigner representation. Thus, the system is described by the Wigner function $\rho_W(x,p,t)$ which is a c-number projection of the density matrix in the Weyl rule of association between c-numbers and operators. The Weyl transformation of an arbitrary operator function $f(\hat{x},\hat{p})$ is [30, 1]

$$F(x,p) = \mathrm{Tr}\left[f(\hat{x},\hat{p})\Delta(x-\hat{x},p-\hat{p})\right], \tag{44}$$

where $F(x,p)$ is a c-number function and $\Delta(x-\hat{x},p-\hat{p})$ is a projection operator which acts as the two dimensional Fourier transform. For the cylindrical phase space, the projection operator is [3]

$$\Delta(x-\hat{x},p-\hat{p}) = \sum_{m=-\infty}^{\infty} \frac{1}{2\pi} \int_{-\pi}^{\pi} d\xi e^{im(x-\hat{x})+i\xi(p-\hat{p})}. \tag{45}$$

This operator determines an inverse transform as well:

$$f(\hat{x},\hat{p}) = \sum_{k=-\infty}^{\infty} \frac{1}{2\pi} \int_{-\pi}^{\pi} F(x,\tilde{h}k)\Delta(x-\hat{x},\tilde{h}k-\hat{p}), \tag{46}$$

where $p = \tilde{h}k$. The quantum map for the density matrix $\hat{\rho}(t)$ is

$$\hat{\rho}(t+1) = \hat{U}^{\dagger}\hat{\rho}(t)\hat{U}. \tag{47}$$

Therefore, evolution of the Wigner function

$$\rho_W(t,x,p) = \mathrm{Tr}\left[\hat{\rho}(t)\Delta(x-\hat{x},p-\hat{p})\right],$$

for the period determined by the map (47), is

$$\begin{aligned}\rho_W(t+1,x,p) &= \mathrm{Tr}\left[\hat{U}^{\dagger}\hat{\rho}(t)\hat{U}\Delta(x-\hat{x},p-\hat{p})\right] \\ &= \sum_{k'=-\infty}^{\infty} \int_{0}^{2\pi} G_{\tilde{h}}(x,p|x',p')\rho_W(t,x',p')dx',\end{aligned} \tag{48}$$

where $G_{\tilde{h}}(x,p|x',p')$ is Green's function for the period

$$G_{\tilde{h}}(x,p|x',p') = \sum_{m} \frac{1}{2\pi} \int_{-\pi}^{\pi} e^{im(x-x'+\xi')} e^{i\xi'(p'-p)}$$

$$\times \exp\left[\frac{i}{\tilde{h}}\mathcal{T}^*(p+\tilde{h}m/2) - \frac{i}{\tilde{h}}\mathcal{T}(p-\tilde{h}m/2)\right]$$
$$\times \exp\left[\frac{i\epsilon}{\tilde{h}}\cos(x'+\tilde{h}\xi'/2) - \frac{i\epsilon}{\tilde{h}}\cos(x'-\tilde{h}\xi'/2)\right]. \quad (49)$$

The trace here is $\mathrm{Tr}[\cdots] = \sum_k \langle k|\cdots|k\rangle$.

In the classical limit $\tilde{h} \to 0$, we obtain in equation (49) that the difference of the perturbations in the exponential is $-i\epsilon$, $\cos x$, while the difference of the kinetic terms is

$$\mathcal{T}^*(p+\tilde{h}m/2) - \mathcal{T}(p-\tilde{h}m/2) = \begin{cases} im\omega(p) \equiv imp^{1-\beta} & \text{for } p>0 \\ -2\sin(\beta\pi)\mathcal{T}(|p|)/\tilde{h} & \text{for } p<0. \end{cases}$$

The last term diverges at $\tilde{h} = 0$ and yields identical zero for Green's function $G_0 \equiv G_{\tilde{h}=0}(p<0) \equiv 0$. Thus, the classical Green function

$$G_0(x,p|x'p') = H(p)\delta(x-x'-\omega(p))\delta(p-p'-\epsilon\sin x') \quad (50)$$

corresponds to the classical map $\mathcal{M}$

$$p_{n+1} = p_n + \epsilon\sin x_n, \quad x_{n+1} = x_n + \omega(p_{n+1}) \quad (51)$$

of the nonlinear kicked rotor with the nonlinear frequency $\omega(p)$, and absorbing boundary conditions for $p<0$, that the Heaviside function $H(p)$ reflects. Therefore, the fractional Hamiltonian (37) corresponds to the open system, described by equations (50), (51).

5.3.1 Chaotic dynamics of fractional map

Chaotic dynamics of this open system takes place in the upper half of the cylindrical phase space. The stability property is determined by the trace of the linearized map $\partial\mathcal{M}$

$$\mathrm{Tr}[\partial\mathcal{M}] = 2 + \epsilon(1-\beta)p^{-\beta}\cos x. \quad (52)$$

For any ϵ, there are stable regions $\{\Delta x, \Delta p\}$ determined by the locus of elliptic points $\{x_e, p_e\}$, (see Figure 5),

$$x_e = \arccos\left(-\frac{2p_e^{\beta}}{\epsilon(1-\beta)}\right). \quad (53)$$

The presence of this infinite regular elliptic island structure, which leads to the stickiness of chaotic trajectories [31], also results in the power law decay of the survival probability for the quantum counterpart in Figure 3. It should be stressed that

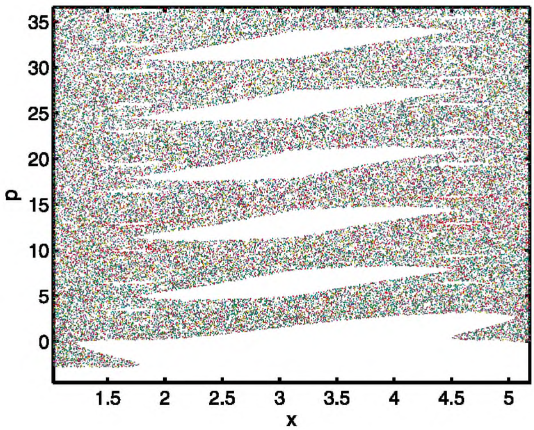

Figure 5: Phase portrait of the classical map without absorption, after 20 000 iterations of 15 initial conditions for $\epsilon = 3$ and $\beta = 0.01$. Reprinted figure with permission from A. Iomin, Phys. Rev. E, 75, 037201 (2007). Copyright 2007 by the American Physical Society.

the nature of the power law decay of the quantum long time dynamics differs from the classical one. On the Ehrenfest time scale, when quantum dynamics is described approximately by the classical trajectories, the rate of the quantum probability leakage is determined by the classical exponent due to the classical stickiness phenomenon [18]. The situation changes essentially for the long time quantum dynamics. Namely, the power law decay of the survival probability, which is shown in Figure 3, is now due to the quantum tunneling between integrable interior of the stability islands and the chaotic sea. This power law phenomenon due to quantum tunneling has been an issue of extensive studies in quantum chaos; see the discussion in [20] and references therein.

It is worth mentioning that on the class of periodic functions, eigenvalues of the unperturbed Hamiltonian $\mathcal{T}$ coincide with $\hat{\mathcal{H}}_0(\hat{p}) = (-i\tilde{h}\frac{\partial}{\partial x})^\alpha$, and have the same classical limit of equation (50). This local derivative has the classical counterpart with the Hamiltonian $\mathcal{H}_0(p) = p^\alpha$ which does not coincide with equation (50). Namely, the Hamiltonian $\mathcal{H}_0(p)$ is the classical system with dissipation for $p < 0$, while the map $\mathcal{M}$ in equations (50) and (51) is the open system where a particle is set apart from the dynamics for $p < 0$.

6 Conclusion

The introduction of the quantum Lévy process depends essentially on the structure of the phase space that leads to accounting for the topological constraints in the construction of the quantum dynamics. We concerned with two examples of quantum mechanical systems, where the topological constraints relate both to the boundary condition as for Lévy flights in a box, and to the operator algebra, as for the fractional rotor. Both problems are treated in the framework of the path integral formalism with the Lévy measure. A correct path integral consideration is possible when the eigenvalue problem (13) is appropriately defined on a class of periodic functions, which is done for the infinite well potential (8) and for a particle on a unite circle (33). An analytical expression for the evolution operator is obtained in the path integral presentation, which corresponds to the dynamics with the nonlocal operator D^α. For $\alpha = 2$, the path integral has the correct limit, which is well known in the local quantum mechanics with the topological constraints [7].

An important point of any "fractional quantum mechanics" is the classical limit $\hbar \to 0$, where a serious question emerges about the physical meaning of its classical counterpart. As an example, the Lévy process in a box is considered for oscillating walls. For $\alpha = 2$, this problem corresponds to a so-called Fermi acceleration [9] leading to classical and quantum chaos due to the interaction of nonlinear resonances. For $1 < \alpha < 2$, we suggested two considerations of the problem. In the first one, it is treated in the adiabatic, perturbative approach, where an analytical expression for the quasienergy spectrum is obtained. In the second approach, which is an example of nonlocal quantum chaos, a simplified scheme of the Fermi acceleration of the Lévy walk is described in the framework of the fractional kicked rotor.

It is interesting to admit that by means of the fractional operator D^α, a decay mechanism can be easily introduced for Hamiltonian treatment of the quantum dynamics, which itself is not an easy task [26]. Another important conclusion from the second example relates to the classical limit. The fractional Schrödinger equation

$$i\tilde{h}\partial_t \psi = (-i\tilde{h})^\alpha D^\alpha_{-\infty}\psi \tag{54}$$

describes the quantum *dissipative Hamiltonian* dynamics. The classical counterpart is a nonlinear motion with a nonlinear frequency $\omega(p)$ realized on the upper half-plane of the phase space with absorption in the lower half-plane. It has well-defined physical meaning. Therefore, the fractional Schrödinger equation (54) can be a generalized approach for any functions for which the Fourier transform is valid. In this case, the opposite classical-to-quantum transition can be performed by determining the Heaviside function in equation (49)

$$e^{i\omega(p)z}H(p) = \lim_{\tilde{h}\to 0} \exp\left[\frac{i}{\tilde{h}}\mathcal{T}^*\left(p + \frac{\tilde{h}z}{2}\right) - \frac{i}{\tilde{h}}\mathcal{T}\left(p - \frac{\tilde{h}z}{2}\right)\right],$$

where $\mathcal{T}(p)$ is uniquely defined by the condition $\omega(p) = \mathcal{T}'(p)$. Thus, fractional derivatives quantize classical open systems in the framework of the non-Hermitian Hamiltonian.

Bibliography

[1] G. S. Agarwal and E. Wolf, Calculus for functions of noncommuting operators and general phase-space methods in quantum mechanics I, *Phys. Rev. D*, **2** (1970), 2161–2186.

[2] P. Barthelemy, J. Bertolotti, and D. Wiersma, A Lévy flight for light, *Nature*, **453** (2008), 495–498.

[3] G. P. Berman, A. R. Kolovsky, F. M. Izrailev, and A. M. Iomin, Quantum chaos in the Wigner representation, *Chaos*, **1** (1991), 220–223.

[4] D. Braun, *Dissipative Quantum Chaos Decoherence*, Springer, Berlin, Heidelberg, 2001.

[5] G. G. Carlo, G. Benenti, G. Casati, and D.Ł. Shepelyansky, Quantum ratchets in dissipative chaotic systems, *Phys. Rev. Lett.*, **94** (2005), 164101.

[6] G. Casati, B. V. Chirikov, F. M. Izrailev, and J. Ford, Stochastic behavior of a quantum pendulum under a periodic perturbation, in G. Casati and J. Ford (eds.) *Stochastic Behavior in Classical and Quantum Hamiltonian Systems*, Springer, New York, 1979.

[7] M. Chaichian and A. Demichev, *Path Integrals in Physics*, vol. 1, Institute of Physics Publishing, Bristol, 2001.

[8] B. V. Chirikov, A universal instability of many-dimensional oscillator systems, *Phys. Rep.*, **52** (1979), 263–379.

[9] B. V. Chirikov and G. M. Zaslavsky, On the mechanism of one-dimensional Fermi acceleration, *Dokl. Akad. Nauk SSSR*, **159** (1964), 306–309.

[10] T. Dittrich and R. Graham, Quantum effects in the long-time behavior of the dissipative standard map, *Phys. Scr.*, **40** (1989), 409–415.

[11] B. Dybiec, E. Gudowska-Nowak, and P. Hänggi, Lévy–Brownian motion on finite intervals: Mean first passage time analysis, *Phys. Rev. E*, **73** (2006), 046104.

[12] R. P. Feynman and A. R. Hibbs, *Quantum Mechanics and Path Integrals*, McGraw–Hill, New York, 1965.

[13] R. Graham, Dissipative quantum maps, *Phys. Scr.*, **35** (1987), 111–118.

[14] F. Haake, *Quantum Signature of Chaos*, Springer, Berlin, Heidelberg, 2000.

[15] A. Iomin, Accelerator dynamics of a fractional kicked rotor, *Phys. Rev. E*, **75** (2007), 037201.

[16] A. Iomin, Lévy flights in a box, *Chaos Solitons Fractals*, **71** (2015), 73–77.

[17] A. Iomin and T. Sandev, Lévy transport in slab geometry of inhomogeneous media, *Math. Model. Nat. Phenom.*, **11** (2016), 51–62.

[18] A. Iomin and G. M. Zaslavsky, Quantum breaking time scaling in superdiffusive dynamics, *Phys. Rev. E*, **63** (2001), 047203.

[19] A. Iomin and G. M. Zaslavsky, Breaking time for the quantum chaotic attractor, *Phys. Rev. E*, **67** (2003), 027203.

[20] A. Iomin, S. Fishman, and G. M. Zaslavsky, Quantum localization for a kicked rotor with accelerator mode islands, *Phys. Rev. E*, **65** (2002), 036215.

[21] M. Kac, *Probability and Related Topics in Physical Sciences*, Interscience, New York, 1959.

[22] N. Laskin, Fractals and quantum mechanics, *Chaos*, **10** (2000), 780–790.

[23] R. Metzler and J. Klafter, The random walk guide to anomalous diffusion: A fractional dynamics approach, *Phys. Rep.*, **339** (2000), 1–77.

[24] E. W. Montroll and M. F. Shlesinger, The wonderful world of random walks, in J. Lebowitz and E. W. Montroll (eds.) *Studies in Statistical Mechanics*, vol. 11, Noth-Holland, Amsterdam, 1984.

[25] S. G. Samko, A. A. Kilbas, and O. I. Marichev, *OI. Fractional Integrals and Derivatives: Theory and Applications*, Gordon and Breach, New York, 1993.

[26] V. E. Tarasov, *Quantum Mechanics of Non-Hamiltonian and Dissipative Systems*, Elsevier, Amsterdam, 2008.

[27] V. E. Tarasov and G. M. Zaslavsky, Fractional generalization of Kac integral, *Commun. Nonlinear Sci. Numer. Simul.*, **13** (2008), 248–258.

[28] B. J. West, Quantum Lévy propagators, *J. Phys. Chem. B*, **104** (2000), 3830–3832.

[29] B. J. West, P. Grigolini, R. Metzler, and T. F. Nonnenmacher, Fractional diffusion and Lévy stable processes, *Phys. Rev. E*, **55** (1997), 99–106.
[30] E. P. Wigner, On the quantum correction for thermodynamic equilibrium, *Phys. Rev.*, **40** (1932), 749–759.
[31] G. M. Zaslavsky, M. Edelman, and B. A. Niyazov, Self-similarity, renormalization, and phase space nonuniformity of Hamiltonian chaotic dynamics, *Chaos*, **7** (1997), 159–181.

Alexander Iomin

Fractional time quantum mechanics

Abstract: An overview of quantum mechanics with fractional time derivatives is presented. Examples of physically relevant time fractional Schrödinger equations (FSE) are considered. A correct form of the FSE is discussed and its justification based on the correct form of analytic continuation of time is suggested.

Keywords: Caputo fractional derivative, Riemann–Liouville fractional derivative, fractional Schrödinger equation, fractional Fokker–Planck equation, analytic continuation of time, quantum comb model, parabolic equation approximation

PACS: 05.45.Mt, 05.40.-a

1 Introduction

Application of the fractional calculus to quantum processes is a new and fast developing part of quantum physics, which studies nonlocal quantum phenomena [23, 47, 48]. It aims to explore nonlocal effects found for either long-range interactions or time-dependent processes with many scales [5, 31, 48]. As it is shown in the seminal papers [23, 47], the fractional concept can be introduced in quantum physics by means of the Feynman propagator for nonrelativistic quantum mechanics in complete analogy with the Brownian path integrals [10]. The path integral approach for Lévy stable processes, leading to the fractional diffusion equation, can be extended to a quantum Feynman–Lévy measure, which leads to the natural appearance of the space fractional Schrödinger equation [23, 47].

A way of introduction of a fractional time derivative in quantum mechanics is not so "easy." It is tempting to introduce it in quantum mechanics by analogy with the fractional Fokker–Planck equation (FFPE) by means of the Wick rotation of time $t \to -it/\hbar$ [32]. However, this way is completely vague from its physical interpretation. An important discrepancy between the Fokker–Planck and the Schrödinger equations is that the latter is the fundamental quantum-mechanical postulate, while the former is just an asymptotic limit of a kinetic equation for the Markovian random process. It is worth noting that, contrary to the space fractional derivative, the time fractional Schrödinger equation (FSE) describes non-Markovian evolution with a memory effect [43]. For the Markovian processes, the link between the Schrödinger equation and the Fokker–Planck equation is established by the path integral presentation [8, 19, 38].

Acknowledgement: This work was supported by the Israel Science Foundation (ISF).

Alexander Iomin, Department of Physics, Technion, Haifa, 32000, Israel, e-mail: iomin@physics.technion.ac.il

Contrary to this for the non-Markovian processes this path integral relation is broken, since the path integral does not exist for either FSE or FFPE (due to violation of the Stone theorem). The FSE violates the Stone's theorem on the one-parameter unitary group[1] [32]. Therefore the relation between FSE and FFPE is not obvious, at least it can be differed from the Wick rotation.

However, these arguments do not discard a mathematical attractivity of the FSE. As shown in [12, 13, 16, 50], the FSE is an effective way to describe the dynamics of a quantum system interacting with the environment, in particular time fractional quantum dynamics can be interpreted as an interaction of quantum systems with an environment with power-law spectral density [43, 44]. In this case, fractional time derivative is an effect of the interaction of the quantum system with the environment, where part of the quantum information is lost [13, 50].

Time evolution of realistic quantum systems, like open systems is not Markovian due to interaction with the environment. Such systems are well described by the density matrix in the framework of the von Neumann equation. Summing out the environmental variables one eventually arrives at the a Lindblad scheme [28]. The situation differs completely, when one describes the quantum "friction" or decay processes by wave function in the framework of the generalized Schrödinger equation, which reads [37, 43]

$$i\tilde{h}\int_0^t \lambda(t-\tau)\partial_\tau\psi(x,\tau)d\tau = \hat{\mathcal{H}}(x)\psi(x,t), \tag{1}$$

where $x \equiv \mathbf{x} \in \mathbb{R}_d$ are coordinates in d dimensional configuration space, $\lambda(t)$ is a memory kernel, such that its Laplace transform exists $\Lambda(s) = \mathcal{L}[\lambda(t)](s)$, and when $\lambda(t) = \delta(t)$, the Hermitian operator $\hat{\mathcal{H}}(x)$ is the Hamiltonian, then equation (1) reduces to the standard time Schrödinger equation. The effective Planck constant $\tilde{h}$ is a dimensionless parameter, such that all variables and parameters in equation (1) are dimensionless as well.[2]

Contrary to open systems, here the process of relaxation is intrinsic property of fractional quantum evolution, as quantum "friction." This also involves a strong machinery of fractional calculus as new mathematical tool for fractional quantum mechanics, whose mathematical and physical properties are in the field of extensive

1 Stone's theorem [40] on one-parameter unitary groups is a basic theorem of functional analysis that establishes a one-to-one correspondence between self-adjoint operators in the Hilbert space and one-parameter families of unitary operators, which are evolution operators in quantum mechanics. In other words, for the evolution (unitary) operator $\hat{U}(t)$, there is a group property $\hat{U}(t)\hat{U}(s) = \hat{U}(t+s)$.

2 See footnote 4, where the dimensionless Planck constant is explained. In many theories, like quantum field theory, it is used as $\hbar = 1$. For some theories like quantum chaos, a kind of dimensionless $\hbar \to \tilde{h}$ is introduced, since it is a convenient parameter for the semiclassical consideration. In the present work, it appears naturally, for example, in Section 3 on 'parabolic equation approximation."

studies [4, 9, 11–13, 16, 24, 32, 33, 37, 42–44, 46, 50]. Therefore, we do not consider these violations of the Markovian property as shortcomings but properties of time fractional quantum mechanics. However, a starting point of this time fractional quantum mechanics should be physical systems, where appearance of the nonlocal memory kernels are well justified. There are few examples where these properties have physically justified realizations [13, 16, 33, 43, 44, 50]. These are quantum comb model [13], effective description of dynamics of spontaneous emission in photonic crystals [50], fractional Lindblad equation [43], and fractional oscillator as an open system with friction and memory [44], and fractional Lèvy processes in slab geometry in the parabolic equation approximation [16]. Another approach, based on Euler–Lagrange fractional variational principal, has been suggested in [33].

Discussing the violation of the quantum Markov property due to the nonlocal dynamics, we consider this generalization by means of the memory kernel in the power law form

$$\lambda(t-\tau) = (i\hbar)^{\bar{\alpha}} \frac{(t-\tau)^{-\alpha}}{\Gamma(1-\alpha)}, \qquad 0 < \alpha \leq 1, \tag{2}$$

where $\Gamma(\nu+1) = \nu\Gamma(\nu)$ is the gamma function. We will concern with two cases both $\bar{\alpha} = \alpha - 1$ and $\bar{\alpha} = 0$. The l. h. s. of equation (1) is the Caputo fractional derivative ${}^{\mathrm{C}}D_t^{\alpha}$ [7]

$$ {}^{\mathrm{C}}D_0^{\alpha}\psi(t) \equiv {}^{\mathrm{C}}D^{\alpha}\psi(x,t) = \int_0^t \frac{(t-\tau)^{-\alpha}\partial_\tau\psi(x,\tau)}{\Gamma(1-\alpha)} d\tau. \tag{3}$$

This formulation of the Caputo fractional derivative also relates to the fractional integration of the order $\nu > 0$, which reads[3]

$$I_0^{\nu} f(t) \equiv I^{\nu} f(t) = \frac{1}{\Gamma(\nu)} \int_0^t f(t')(t-t')^{\nu-1} dt'. \tag{4}$$

As the inverse procedure, one obtains the fractional derivative

$$D^{\nu} f(t) = I^{-\nu} f(t) \equiv \frac{1}{\Gamma(-\nu)} \int_0^t f(t')(t-t')^{-\nu-1} dt'. \tag{5}$$

For arbitrary $\nu > 0$, this integral diverges, and as a result of this a regularization procedure is introduced with two alternative definitions. The first one is the Riemann–Liouville fractional derivative of the form

$$ {}^{\mathrm{RL}}D^{\nu} f(t) = \frac{d^n}{dt^n} I^{n-\nu} f(t), \tag{6}$$

3 See, for example, [34, 35].

where $n-1 < \nu \leq n$. The second one is fractional derivative in the Caputo form

$$ {}^{\mathrm{C}}D^{\nu} f(t) = I^{n-\nu} f^{(n)}(t), \tag{7} $$

where $f^{(n)}(t) \equiv \frac{d^n}{dt^n} f(t)$. For $n = 1$, definition (7) coincides with equation (3) with $\nu = \alpha$ The Laplace transform of the Caputo fractional derivative yields

$$ \mathcal{L}[{}^{\mathrm{C}}D^{\nu} f(t)] = s^{\nu} F(s) - \sum_{k=0}^{n-1} f^{(k)}(0^+) s^{\nu-1-k}, \tag{8} $$

where $\mathcal{L}[f(t)] = F(s)$, which is convenient for the present analysis, where the initial conditions are imposed in terms of integer derivatives. We also use here a convolution rule for $0 < \alpha < 1$,

$$ \mathcal{L}[I^{\alpha} f(t)] = s^{-\alpha} F(s). \tag{9} $$

For both $\bar{\alpha} = \alpha - 1$ and $\bar{\alpha} = 0$, equation (1) reads in the form of the time FSE

$$ (i\tilde{h})^{\beta}\, {}^{\mathrm{C}}D^{\alpha} \psi(x,t) = \hat{\mathcal{H}}(x) \psi(x,t). \tag{10} $$

In the former case of $\beta = \alpha$, equation (10) has been introduced in quantum mechanics by analogy with the FFPE [32]. The latter case of $\beta = 1$ corresponds to the FSE, obtained independently in [33] in the framework the path integral quantization of a fractional Newton equation and in [16] as an effective parabolic wave approximation of Helmholtz equation. This "small" change in β leads to essential differences in solutions of (10) and their physical interpretations. In what follows, we will discuss both cases in some details.

2 Quantum evolution

Considering initial value, or Cauchy problem with the initial condition $\psi(x, t = 0) = \psi_0(x)$, one obtains that the dynamics of the wave function, as a solution of equation (10), is determined by the evolution operator $\hat{U}(t)$ in the form of the power series, which is the Mittag-Leffler function $E_{\alpha}(z)$

$$ \psi(x,t) = \hat{U}(t)\psi_0(x) = E_{\alpha}\left(\frac{t^{\alpha}\hat{\mathcal{H}}}{(i\tilde{h})^{\beta}}\right)\psi_0(x) = \sum_{n=0}^{\infty} \frac{[(t^{\alpha}/(i\tilde{h})^{\beta})\hat{\mathcal{H}}]^n}{\Gamma(n\alpha+1)} \psi_0(x). \tag{11} $$

As it has been admitted by many authors (see, e. g., review [24]), this evolution operator for $\alpha \neq 1$ violates fundamental properties of quantum mechanics as unitary evolution, conservation probability, which also affects existence of stationary states. These properties are related with non-Markovian quantum mechanics, also established in open quantum systems (see, e. g., [42]). However, contrary to open systems, here it is intrinsic property of fractional quantum evolution, as quantum "friction," or long-term memory, which are much more sophisticated than relaxation. This also involves a strong machinery of fractional calculus as a new mathematical tool for fractional quantum mechanics.

2.1 Mittag-Leffler function: oscillation and relaxation

Let us consider the case with $\beta = \alpha$. We present the Mittag-Leffler function in the form of the inverse Laplace transform [3], which reads

$$E_\alpha(zt) = \frac{1}{2\pi i} \oint_C \frac{e^{st} s^{\alpha-1} ds}{s^\alpha - z}, \tag{12}$$

where C is a suitable contour of integration; it can be reduced to the Hankel contour for the gamma function [3, 32, 35]. This expression makes it possible to split the evolution operator to the oscillating and decay parts. The former is due to the pole at $s = z^{1/\alpha}$, while the latter is due to the Hankel contour with the branch point at $s = 0$, obtained with branch cut along the negative part of the real axis. Performing this procedure [32], one obtains from equation (12)

$$E_\alpha(zt^\alpha) = \text{Residue} - \frac{1}{2\pi} \int_{\text{Ha}} [\cdots] = \frac{e^{tz^{\frac{1}{\alpha}}}}{\alpha} - \frac{z\sin(\alpha\pi)}{\pi} \int_0^\infty \frac{e^{-rt} r^{\alpha-1} dr}{r^{2\alpha} - 2z\cos(\alpha\pi) + z^2}. \tag{13}$$

Therefore, evolution operator $\hat{U}(t)$ in equation (11) reads

$$\begin{aligned} \hat{U}(t) &= \hat{U}_{\text{Res}}(t) + \hat{U}_{\text{dec}}(t) \\ &= \frac{\exp(\frac{-i\hat{\mathcal{H}}^{\frac{1}{\alpha}} t}{\tilde{h}})}{\alpha} - \frac{(i\tilde{h})^\alpha \hat{\mathcal{H}} \sin(\alpha\pi)}{\pi} \int_0^\infty \frac{e^{-rt} r^{\alpha-1} dr}{(i\tilde{h}r)^{2\alpha} - 2(i\tilde{h})^\alpha \hat{\mathcal{H}} \cos(\alpha\pi) + \hat{\mathcal{H}}^2}. \end{aligned} \tag{14}$$

The second, decay term can be simplified in the semiclassical limit $\tilde{h} \to 0$. In this case, the denominator in the integrand is $1/\hat{\mathcal{H}}^2$, and integration yields the gamma function. Eventually, the decay term reads

$$\hat{U}_{\text{dec}}(t) \sim (i\tilde{h})^\alpha \sin(\alpha\pi)\Gamma(\alpha)/\pi\hat{\mathcal{H}}t^\alpha. \tag{15}$$

Therefore, for the large time asymptotic the oscillatory term is dominant and increases the probability by factor $1/\alpha^2$. This means that the quantum "friction" increases the probability inside the system for $\alpha < 1$. Moreover, in this case, the dynamics is essentially nonlinear due to the operator $\mathcal{H}^{\frac{1}{\alpha}}$.

This increase of the probability by factor $1/\alpha^2 > 1$ is problematic and not physical, until $\psi(x)$ does not contain a complete information about the system, such that pdf $\rho(x,t) = |\psi(x,t)|^2$ is a marginal pdf of some more general system, for example, in $d+1$ space. We shall discuss this problem latter in Section 2.2.

This violation of the probability conservation needs more detailed insight into the dynamics in the framework of continuity equation for the probability density $\rho(x,t) = |\psi(x,t)|^2$. To shed light on all these deficiencies of the fractional evolution, we consider physical examples, where the FSE appears naturally as a result of effective description of quantum mechanics of a particle in the $x \in \mathbb{R}^d$ space, which interacts with the environmental space, where a part of the information about the environment and the interaction can be reasonably neglected and other part of the information is accounted by the time fractional derivative.

2.2 Quantum comb

A special quantum behavior of a particle on the comb can be defined as the quantum motion in the $\mathbb{R}_{d+1}$ configuration space $(\mathbf{x}, y)$, such that the dynamics in the d dimensional configuration space $\mathbf{x} \equiv x$ is possible only at $y = 0$, and motions in the x and y directions commute. Therefore, the quantum dynamics is described by the following Schrödinger equation

$$i\tilde{h}\frac{\partial\psi}{\partial t} = \delta(y)\hat{\mathcal{H}}(x)\psi - \frac{\tilde{h}^2}{2}\frac{\partial^2\Psi}{\partial y^2}, \tag{16}$$

where the Hamiltonian $\hat{\mathcal{H}}(x) = -\frac{\tilde{h}^2}{2}\nabla_x^2 + V(x)$ governs the dynamics with a potential $V(x)$ in the $x \in \mathbb{R}_d$ space, while the y coordinate corresponds to the 1d free motion. All the parameters and variables are dimensionless.[4]

By analogy with the diffusion (classical) comb model [1], we concern with the dynamics in the one-dimensional x space. In contrast to the diffusion model, integration of the wave function over the y coordinate is not valid, since it destroys the probabilistic nature of the pdf $|\psi(x,y,t)|^2$ and correspondingly the marginal pdf $P(x,t) = \int_{-\infty}^{\infty} |\psi(x,y,t)|^2 dy \neq |\int \psi(x,y,t)dy|^2$. Therefore, one carries out the Fourier transform in the y space $\mathcal{F}_y[\psi(x,y,t)](l) = \Psi(x,l,t) \equiv \Psi_l(x,t)$, and as a result of this, equation

4 Analogously to the FSE (1), following [32], one introduces the Planck length $L_P = \sqrt{\hbar G/c^3}$, time $T_P = \sqrt{\hbar G/c^5}$, mass $M_P = \sqrt{\hbar c/G}$, and energy $E_P = M_P c^2$, where $\hbar$, G, and c are the Planck constant, the gravitational constant and the speed of light, respectively. Therefore, quantum mechanics of a particle with mass m is described by the dimensionless units $x/L_P \to x$, $y/L_P \to y$, $t/T_P \to t$, while the dimensionless Planck constant is defined as the inverse dimensionless mass $\tilde{h} = M_P/m$. Note that the dimensionless potential is now $V(x) \to V(x)/M_P c^2$.

(16) reads

$$i\tilde{h}\frac{\partial\Psi_l}{\partial t} = \hat{\mathcal{H}}(x)\psi(x,0,t) + \frac{\tilde{h}l^2}{2}\Psi_l. \tag{17}$$

To obtain this equation in a closed form, one needs to express the wave function at $y = 0$, $\psi(x,0,t)$, by means of the Fourier image Ψ_l. To this end, the Laplace transform of equation (16) is performed $\mathcal{L}[\psi(x,y,t)](s) = \Psi(x,y,s)$. The solution in the Laplace domain reads

$$\Psi(x,y,s) = \Psi(x,0,s)\exp\big[i(1+i)\sqrt{s/\tilde{h}}|y|\big], \tag{18}$$

where we used $\sqrt{2i} = (1+i)$. Performing the Fourier transform $\Psi_l(x,s) = \mathcal{F}_y[\Psi(x,y,s)]$ one obtains from equation (18)

$$\Psi_l(x,s) = \Psi(x,0,s)\mathcal{F}_y e^{i(1+i)\sqrt{s/\tilde{h}}|y|} = \frac{2i(1+i)\sqrt{s/\tilde{h}}}{l^2 - 2is/\tilde{h}}\Psi(x,0,s). \tag{19}$$

Finally, the Laplace inversion for $\Psi(x,0,s)$ determines the wave function at $y = 0$,

$$\psi(x,0,t) = \mathcal{L}^{-1}\left[\Psi_l(x,s)\frac{l^2 - 2is/h}{2i(1+i)\sqrt{s/\tilde{h}}}\right]. \tag{20}$$

Let us, first, consider a simple case with zero mode $l = 0$. We have from equation (20)

$$\psi(x,0,s) = -\sqrt{\frac{s}{2\tilde{h}i}}\Psi_0(x,s).$$

Then we redefine $\Psi_0(x,t) = \psi(x,t)$, and, carrying out the Laplace transform in equation (17), we arrive at the definition of the Caputo fractional derivative (8) in the Laplace domain

$$\mathcal{L}[{}^{\mathrm{C}}D^{\frac{1}{2}}\psi(t)] = s^{1/2}\Psi(s) - s^{-1/2}\psi(0).$$

Finally, carrying out the inverse Laplace transform and redefining $\frac{i\hat{\mathcal{H}}}{\sqrt{2\tilde{h}}} \to \hat{\mathcal{H}}$, one obtains the time FSE which coincides exactly with equation (10) for $\alpha = 1/2$.[5] This term does not contain any information about the dynamics of all other modes with $l \neq 0$. Consequently, the violation of the probability conservation (namely increasing it as

5 This fractional parameter $\alpha = 1/2$ appears naturally from the comb geometry. The initial Schrödinger equation (16) is the standard local quantum mechanics with topological comb constraint. However, here this topology leads to the fractional time derivative, where the index is defined by topology and cannot be changed. Therefore, it is a real physical system, where the time fractional derivative of the order of 1/2 appears naturally.

twice) of $\Psi(x, l = 0, t)$ due to the oscillating term in equation (14) results from the interaction with other modes.

Repeating the same procedure for arbitrary l, one performs the Laplace transform of the term proportional to $l^2/\sqrt{s}$ in equation (20). Performing simple operations of fractional calculus and taking into account equations (7), (8), (9), one obtains

$$(i\tilde{h})^{\frac{1}{2}}\,{}^{\mathrm{C}}D^{\frac{1}{2}}\Psi_l(x,t) = -\frac{l^2}{2\sqrt{2}} I^1 \hat{\mathcal{H}}\Psi_l(x,t) + \frac{i}{\sqrt{2\tilde{h}}}\hat{\mathcal{H}}\Psi_l(x,t) + \frac{\tilde{h}^2 l^2}{2}\Psi_l(x,t). \tag{21}$$

This comb FSE describes the quantum dynamics in the x configuration space. The index l corresponds to an effective interaction of a quantum system with an additional degree of freedom, while the fractional time derivatives, with $\alpha = 1/2$, reflect this interaction in the form of non-Markov memory effects.

3 Parabolic equation approximation

Considering FSE with $\beta = 1$ in equation (10), we show haw it appears from a general form of the wave diffusive process, which relates, for example, to the Lévy process in the 2D slab geometry in the parabolic equation approximation.[6] where the paraxial small angle approximation is naturally applied. Therefore, our main concern now is the Helmholtz fractional equation,

$${}^{\mathrm{C}}D_z^{\nu} W(z,x) + D_{|x|}^{\nu} W(z,x) + \omega^2 W(z,x) = 0, \tag{22}$$

where $W(z,x)$ is the stationary wave amplitude at the point (z,x) with frequency ω and it is described by dimensionless (x,z) slab variables, where $z \in (0,\infty)$ and $x \in [-L, L]$ are longitudinal and transversal coordinates, correspondingly. The equation involves both the Caputo and the Riemann–Liouville fractional derivatives of the order $0 < \nu < 2$. In a variety of physical realizations from underwater acoustics [17] to optical lattices [27] it is used that the wave frequency is determined by the wave number k and refractive index n: $\omega^2 \approx 2k^2\Delta n$, where Δn is fluctuation of the refractive index for inhomogeneous media. The Caputo fractional derivative relates to the dimensionless longitudinal direction $z(0,\infty)$. In this case, the Laplace transform is determined explicitly by the boundary condition at $z = 0$, $W(z = 0, x) = W_0(x)$, which is used as the "initial" condition in further analysis. For the transversal direction $x \in [-L, L]$, the following notation for the Riemann–Liouville fractional derivative is used

$$D_{|x|}^{\nu} f(z) \equiv {}^{\mathrm{RL}}D_{-L}^{\nu} x f(x) + {}^{\mathrm{RL}}D_L^{\nu} f(x). \tag{23}$$

6 The method of parabolic equation approximation was first applied by Leontovich in study of radiowaves spreading [25] and later developed in detail by Khokhlov [21] (see also [41]). In modern experimental and theoretical research, it naturally appears in investigations of a wave propagation in random optical lattices [26, 27] and quantum chaos in underwater acoustics [17].

It should be stressed that this approach has not only academic interest, but also describes both waves and relaxation processes in a variety of applications like diffusion-wave phenomena in inhomogeneous media. In particular, we specify here optical ray dynamics in Lévy glasses [2], where Lévy walks can be described by equation (23).[7] Another interesting phenomenon, which is described by equation (22), is a superdiffusion of ultracold atoms in an optical lattice [36].[8]

When the height L is less than the Lévy flight lengths in the longitudinal direction, the transport is of a small grazing angle with respect to the longitudinal direction. In this case, we are looking for the solution $W(z,x)$ in the form

$$W(z,x) = e^{ikz}\psi(z,x), \tag{24}$$

which after substitution in equation (22) yields the following integration:

$${}^{C}D^{\nu}W(z,x) = \frac{1}{\Gamma(2-\nu)}\int_0^z (z-z')^{2-\nu-1}\frac{d^2}{dz'^2}[e^{ikz'}\psi(z',x)]dz'. \tag{25}$$

Note that the "initial" conditions at $z = 0$ for both ψ and W are the same: $\psi(z = 0) = W(z = 0)$.

Now the parabolic equation in the paraxial approximation can be obtained. Taking into account that $\psi(z,x)$ is a slowly-varying function of z, such that

$$\left|\frac{\partial^2\psi}{\partial z^2}\right| \ll \left|2k\frac{\partial\psi}{\partial z}\right|, \tag{26}$$

one obtains

$$\frac{d^2}{dz^2}[e^{ikz}\psi(z,x)] \approx 2ike^{ikz}\frac{d}{dz}\psi(z,x). \tag{27}$$

Substituting this approximation in equation (25), one obtains from equations (22), (24), and (25)

$$2ikI_z^{2-\nu}[e^{ikz}\partial_z\psi(z,x)] + D_{|x|}^{\nu}\psi(z,x)e^{ikz} + \omega^2\psi(z,x)e^{ikz} = 0. \tag{28}$$

---

7 Lévy glasses are specially prepared optical material in which the Lévy flights are controlled by the power law distribution of the step-length of a free ray dynamics, which can be specially chosen in the power law form $\sim 1/l^{\nu+1}$.

8 There are Lévy walks, and the theoretical explanation of this fact, presented within the standard semiclassical treatment of Sisyphus cooling [20, 30], is based on a study of the microscopic characteristics of the atomic motion in optical lattices and recoil distributions resulting in macroscopic Lévy walks in space, such that the Lévy distribution of the flights depends on the lattice potential depth [30]. The flight times and velocities of atoms are coupled, and these relations, established in asymptotically logarithmic potential, have been studied for different regimes of the atomic dynamics, [20], so the cold atom problem is a variant of the Lévy walks. An alternating approach based on a comb model has been suggested as well [14].

To get rid of the exponential e^{ikz} in equation (28), we insert it inside the derivative $e^{ikz}\partial_z\psi(z,x) = \partial_z[e^{ikz}\psi(z,x)] + O(k)$. The term $O(k) = ike^{ikz}\psi(z,x)$ can be neglected in equation (28) since it is of the order of $O(k^2)$, which is neglected in the paraxial approximation with $k \ll 1$. Note also that $I_z^{2-\nu}\frac{d}{dz}f(z) = \partial_z^\alpha f(z)$, where $\alpha = \nu - 1$ and $0 < \alpha < 1$ is the same as for the FSE (10). The Laplace transform can be performed: $\mathcal{L}[e^{ikz}\psi(z)] = \Psi(s - ik)$. Therefore, one obtains from equation (28)

$$2ik[s^\alpha\Psi(s-ik) - s^{\alpha-1}\psi(z=0)] + D_{|x|}^\nu\Psi(s-ik) + \omega^2\Psi(s-ik). \qquad (29)$$

Performing the shift $s - ik \to s$ and neglecting again the terms of the order of $o(k)$ in equation (29), and then performing the Laplace inversion, one obtains the Helmholtz equation in the form of the effective FSE. Accounting that $z \equiv t$ coordinates play a role of an effective time and $\tilde{h} = 1/k$ is an effective dimensionless Planck constant, we have eventually arrived at equation (10) with $\beta = 1$. Multiplying equation (29) by $\tilde{h}^\nu$, we obtain

$$i\tilde{h}^\alpha\, {}^{\mathrm{C}}D_t^\alpha\psi + \frac{\tilde{h}^\nu}{2}D_{|x|}^\nu\psi + V(x)\psi = 0, \qquad (30)$$

where $V(x) = \tilde{h}^{\nu-2}\Delta n(x)$ is a slab profile potential. The "initial" condition at $t = z = 0$ corresponds to the boundary condition for the initial problem in equation (22). One supposes that there is a source of the signal at $z = 0$, therefore, we have the initial condition $\psi(t = 0, x) = \psi_0(x)$. The boundary conditions at $x = \pm L$ are $\psi(t, x = \pm L) = 0$. Since our main concern is the time fractional derivative, we generalizing this expression with an arbitrary "Hamiltonian" form $\hat{\mathcal{H}}$ that yields

$$i\tilde{h}^\alpha\, {}^{\mathrm{C}}D_t^\alpha\psi = \hat{\mathcal{H}}\psi, \qquad (31)$$

where the "Hamiltonian" is

$$\hat{\mathcal{H}} = -\frac{\tilde{h}^\nu}{2}D_{|x|}^\nu + V(x). \qquad (32)$$

3.1 Properties of the FSE (31)

(i) We admit some specific properties of the quantum operator $\hat{\mathcal{H}}$ in equation (32), which is the Hermitian operator and it is the Hamiltonian only for $\alpha = 1$. Even for homogeneous media, when $V(x) = 0$ it is not a free particle for all values of $0 < \nu \le 2$, since it is fractional particle (Lévy walk) in an infinite well potential [15], defined by the boundary conditions.

(ii) Another important property is a continuity equation, which is valid only for a free particle with the "Hamiltonian" $\hat{\mathcal{H}} = -\tilde{h}^2\partial_x^2$. To show this, we use the property of fractional differentiation

$${}^{\mathrm{RL}}D^{1-\alpha}\, {}^{\mathrm{C}}D_t^\alpha f(t) = D_t I^\alpha I^{1-\alpha} D_t f(t) = D_t[f(t) - f(0)] = \partial_t f(t), \qquad (33)$$

where $0 < \alpha < 1$. Therefore, we have from equation (33) for the pdf $\rho(x,t) = |\psi(x,t)|^2$

$$\begin{aligned}\partial_t \rho(x,t) &= {}^{\mathrm{RL}}D^{1-\alpha}\,{}^{\mathrm{C}}D_t^{\alpha}|\psi(x,t)|^2 \\ &= i\tilde{h}^{2-\alpha}\big[\big({}^{\mathrm{RL}}D^{1-\alpha}\partial_x^2\psi(x,t)\big)\psi^*(x,t) - \big({}^{\mathrm{RL}}D^{1-\alpha}\partial_x^2\psi^*(x,t)\big)\psi(x,t)\big].\end{aligned} \tag{34}$$

Introducing a new function $\tilde{\psi}(x.t) = {}^{\mathrm{RL}}D^{1-\alpha}\psi(x,t)$ and the fractional quantum probability current [33]

$$J(x,t) = -i\tilde{h}(\tilde{\psi}^*\partial_x\psi - \psi\partial_x\tilde{\psi}^*), \tag{35}$$

equation (34) reads as the continuity equation

$$\partial_t\rho(x,t) + \partial_x J(x,t) = 0. \tag{36}$$

For all other cases, the continuity equation in the form of equation (36) is an open question, since there is a problem of definition of the fractional quantum probability current J.

(iii) Let us consider a generalization of the FSE (31) for an arbitrary Hermitian operator $\hat{\mathcal{H}}$. The solution of the generalized FSE (31) for an arbitrary Hermitian operator $\hat{\mathcal{H}}$ is the Mittag-Leffler function. Now the evolution operator in equation (11) reads

$$\hat{U}(t) = E_\alpha\left(-i\frac{t^\alpha\hat{\mathcal{H}}}{\tilde{h}^\alpha}\right) = \sum_{n=0}^{\infty}\frac{[-i(t^\alpha/\tilde{h}^\alpha)\hat{\mathcal{H}}]^n}{\Gamma(n\alpha+1)}. \tag{37}$$

Let us present the last term as a superposition of two sums over odd and even numbers

$$\begin{aligned}\hat{U}(t) &= \sum_{n=0}^{\infty}\left\{\frac{[-i(t^\alpha/\tilde{h}^\alpha)\hat{\mathcal{H}}]^{2n}}{\Gamma(2n\alpha+1)} + \frac{[-i(t^\alpha/\tilde{h}^\alpha)\hat{\mathcal{H}}]^{2n+1}}{\Gamma(2n\alpha+1+\alpha)}\right\} \\ &= E_{2\alpha}\left(-\frac{t^{2\alpha}\hat{\mathcal{H}}^2}{\tilde{h}^{2\alpha}}\right) - i\frac{t^\alpha\hat{\mathcal{H}}}{\tilde{h}^\alpha}E_{2\alpha,\alpha+1}\left(-\frac{t^{2\alpha}\hat{\mathcal{H}}^2}{\tilde{h}^{2\alpha}}\right).\end{aligned} \tag{38}$$

Therefore, the large time asymptotic behavior corresponds to the power law decay. This result also follows from the residue part of the evolution operator (14), which now changes dramatically. Indeed, this residue part of the evolution operator reads

$$\hat{U}_{\mathrm{Res}}(t) = \frac{1}{\alpha}\exp\left[\frac{(-i\hat{\mathcal{H}})^{\frac{1}{\alpha}}t}{\tilde{h}}\right], \tag{39}$$

where $(-i)^{\frac{1}{\alpha}} = \cos\frac{\pi}{2\alpha} - i\sin\frac{\pi}{2\alpha}$. Since $0 < \alpha < 1$, $\cos\frac{\pi}{2\alpha} < 0$, which yields the exponential decay of the amplitude of the evolution operator. Therefore, the large time asymptotic dynamics is due to the decay term, which coincides with equations (15), [33].

(iv) As a simple example, we consider a fractional dynamics, which is a decay process, in a harmonic oscillator. The latter is described by the Hermitian operator

$$\hat{\mathcal{H}} = \tilde{h}\omega(\hat{a}^\dagger\hat{a} + 1/2), \tag{40}$$

where $\hat{a}^\dagger$ and $\hat{a}$ are creation and annihilation operators with the commutator $[\hat{a}, \hat{a}^\dagger] = 1$ and ω is a frequency of harmonic oscillations. Projecting the evolution operator on the basis of eigenfunctions $|n\rangle$, with $\hat{a}^\dagger \hat{a}|n\rangle = n|n\rangle$, one obtains the matrix elements of the evolution operator from equations (38) and (40) as follows:

$$\begin{aligned}\langle m|\hat{U}(t)|n\rangle &= E_{2\alpha}(-\tilde{h}^{2(1-\alpha)} t^{2\alpha} \omega^2 (n+1/2)^2)\delta_{m,n} \\ &\quad - it^\alpha \tilde{h}^{1-\alpha} \omega(n+1/2) E_{2\alpha,\alpha+1}(-t^{2\alpha}\tilde{h}^{2(1-\alpha)}\omega^2(n+1/2)^2)\delta_{m,n}. \end{aligned} \tag{41}$$

The Mittag-Leffler function is a decay function, such that for the small argument of the Mittag-Leffler function, which corresponds to the initial time dynamics, the evolution operator is determined by the first term in equation (41). Thus for the short time dynamics the matrix elements of the evolution operator read [3, 31]

$$\langle m|\hat{U}(t \ll 1)|n\rangle \approx \exp[-\tilde{h}^{2(1-\alpha)} t^{2\alpha} \omega^2 (n+1/2)^2 / \Gamma(2\alpha+1)]\delta_{m,n}. \tag{42}$$

In the opposite case of the large time dynamics, the second term in equation (41) is dominant. Thus we have [3, 31]

$$\langle m|\hat{U}(t \gg 1)|n\rangle \approx \frac{-i\tilde{h}^{(\alpha-1)}}{t^\alpha \omega(n+1/2)\Gamma(\alpha-1)}\delta_{m,n}. \tag{43}$$

For simplicity, let us take the initial wave function $\psi_0(x)$ in terms of the Hermite polynomial $\psi_0(x) = \langle x|n\rangle$. Accounting its evolution for the short and large time scales according equations (42) and (43), we obtain the evolution of the pdf as the survival probability, where the initial stretched exponential decay $\rho(x,t) \sim e^{-t^{2\alpha}}$ is replaced by the power law decay $\rho(x,t) \sim 1/t^{2\alpha}$. For $\alpha = 1$, it is a well-known phenomenon in quantum chaos for systems with phase space structures, which attracts researches for more than twenty years (see, e. g., [18, 22, 29]).

3.2 On relation between FFPE and FSE: analytic continuation of time

Albeit the above example sheds lights on our intuitive understanding of the FSE in equation (31), an important question about insofar this form is generic and correct from the physical point of view should be clarified with more details. To that end, let us first consider a FFPE for a pdf $P(x,t)$ of finding a random walker at a position x at time t,

$${}^{C}D^\alpha P(x,t) = K_\alpha \partial_x^2 P(x,t), \tag{44}$$

where K_α is a generalized diffusion coefficient [31] and $0 < \alpha < 1$. A relation between the FFPE (44) and the FSE (10) with $\beta = 1$ can be established by the analytic continuation of time in complex plane[9] $t \to t(-i/\tilde{h})^{\frac{1}{\alpha}}$. Replacing the Fokker–Planck operator by the "Hamiltonian" $K_\alpha \partial_x^2 \to \hat{\mathcal{H}}(x)$, and $P(x,t) \to \psi(x,t)$, one obtains the FSE

$$i\tilde{h}\,{}^{\mathrm{C}}D^{\alpha}\psi(x,t) = \hat{\mathcal{H}}(x)\psi(x,t). \tag{45}$$

Therefore, our question in task is to understand this analytic continuation of time, which differs from the standard Wick rotation suggested in [32]. It is well known that analytic continuation is natural for solutions (Green's functions) expressed in the path integral form. However, equation (44) does not produce any path integral forms, since the Stone's theorem is violated, which means that a chain rule for the Green's function does not exist. Therefore, we reconsider fractional diffusion in such a form, which can be described by path integrals with the same space-time scaling as in equation (44). This problem has been solved in [39] with further development in [6, 49].

It has been shown [6, 39, 49] that overdamped dynamics of a particle affected by a Gaussian correlated noise,

$$\dot{x} = {}^{\mathrm{RL}}D^{\frac{1-\alpha}{2}}\xi(t),$$

corresponds to fractional diffusion, which is described by the Fokker–Planck equation

$$\partial_t P(x,t) = K_\alpha t^{\alpha-1}\partial_x^2 P(x,t). \tag{46}$$

Here, $\xi(t)$ is the Gaussian white noise. The path integral solution for the Green's function reads

$$G(x(t),t|x_0,0) = \frac{1}{\sqrt{4\pi K_\alpha t^\alpha}}\exp\left[\frac{-\alpha(x(t)-x_0)^2}{4K_\alpha t^\alpha}\right], \tag{47}$$

and its Fourier image has the form

$$\mathcal{G}(k,t|0) = \mathcal{F}[G(x(t),t|x_0,0)] = \exp\left[\frac{-k^2K_\alpha t^\alpha}{\alpha}\right]. \tag{48}$$

Therefore, rescaling $t \to t/(i\tilde{h})^{\frac{1}{\alpha}}$ and denoting $K_\alpha = \tilde{h}^2/2m$, we arrive at quantum mechanics of a particle with mass m. The latter is described by the time dependent Hamiltonian

$$\hat{\mathcal{H}} = -\frac{\tilde{h}^2 t^{\alpha-1}}{2m}\partial_x^2.$$

It is worth stressing that this system is Hamiltonian.

9 To establish this relation for equation (31), one introduce the analytic continuation of time as follows: $t \to t(-i)^{\frac{1}{\alpha}}/\tilde{h}$.

Let us show that this rescaling, which is just the analytic continuation of time, is also correct for the FFPE (44). Performing Fourier transform, we obtain the solution in the form of the Mittag-Leffler function

$$\mathcal{F}[P(x,t)](k,t) = E_\alpha(-K_\alpha k^2 t^\alpha). \tag{49}$$

Now we take into account that for the small argument, the Mittag-Leffler function is the exponential and coincides with the Fourier form (48). Then we immediately obtain that the analytic continuation

$$t \to (-i/\tilde{h})^{\frac{1}{\alpha}} t \tag{50}$$

is the desired result, which ensures the correct form of the FSE (10) with $\beta = 1$. We also admit that another form, $t \to (-i)^{\frac{1}{\alpha}}/\tilde{h}t$, is also correct, which leads to the FSE (31) with corresponding dimensionality of $\tilde{h}$.

4 Conclusion

Concluding this review on the fractional time Schrödinger equation (FSE), we are first admitting that the theory of time fractional quantum mechanics is still in its infancy, despite the numerous publications. Many authors are attracted by mathematical beauty of the fractional calculus and its novelty, and as well as by the physical implementation of the time fractional derivative in the Schrödinger picture of quantum mechanics with long-term memory. However, many questions are still opened, like fractional time quantization in the Heisenberg representation [45]. Moreover, the physical justification of the FSE is an open question as well. In this sense, the work by Naber [32] is rather opening these serious questions on the physical meaning and implementation of the time fractional derivative in quantum mechanics. This intuitive introduction of the FSE by analogy with the time fractional Fokker–Planck equation (FFPE) by means of the Wick rotation of time $t \to -it/\tilde{h}$ is vague from its physical interpretation. The Markov chain property, which establishes the relation between the FFPE and quantum mechanics is broken, or at least, not obvious for the non-Markovian processes. We discussed the main deficiencies related with this approach in Section 2, where we have admitted that increasing the pdf $\rho(x,t)$ by factor $1/\alpha^2 > 1$ does not have any physical nature for closed systems. This problem can be resolved when $\psi(x)$ does not contain a complete information about the system, such that pdf $\rho(x,t) = |\psi(x,t)|^2$ is a subsystem pdf of some more general system, for example, in $d+1$ space. The physical relevance of this statement is explained in the framework of the quantum comb (16) consideration.

Physical examples [13, 16], considered here, indicate that the situation is more sophisticated, and the picture of fractional quantum dynamics is richer. However, these stimulating results do not shed light on the general approach to the FSE and do not explain the correct form of the FSE. In [33], the authors have obtained another form of the FSE in the framework of the of path integral quantisation of a fractional particle. However, any path integral solution of the FSE does not exist due to violation of the Stone's theorem. Here, we have justified this result, considering a fractional diffusion processes, where path integral can be rigorously constructed [6, 39, 49]. This method is based on a simple fact that fractional (turbulent) diffusion can be described by a Fokker–Planck equation (46) with a time dependent diffusion coefficient. In this case, the path integral consideration is valid. Also, in this case, analytic continuation of time $t \to (-i/\tilde{h})^{\frac{1}{\alpha}} t$ leads to quantum mechanics with time dependent Hamiltonian. Moreover, for the infinitesimally small time $T < \varepsilon \to 0$, the fractional evolution operator in the form of the Mittag-Leffler function coincides with the exponential unitary evolution (due to the time dependent Hamiltonian). In this case, a relation between fractional quantum mechanics and fractional diffusion can be established, which also results in the correct relation between the FSE and the FFPE (50). Another important consequence is that the FSE (31) describes correctly the relaxation process, which leads to the power law decay of the pdf $p(x,t) \xrightarrow{t\to\infty} 0$.

Bibliography

[1] V. E. Arkhincheev and E. M. Baskin, Anomalous diffusion and drift in the comb model of percolation clusters, *Sov. Phys. JETP*, **73** (1991), 161–165.

[2] P. Barthelemy, J. Bertolotti, and D. S. Wiersma, A Lévy flight for light, *Nature*, **453** (2008), 495–498.

[3] H. Bateman and A. Erdélyi, *Higher Transcendental Functions, vols. I–III*, McGraw-Hill, New York, 1953.

[4] S. Bayin, Time fractional Schrödinger equation: Fox's H-functions and the effective potential, *J. Math. Phys.*, **54** (2013), 012103.

[5] J.-P. Bouchaud and A. Georges, Anomalous diffusion in disordered media: Statistical mechanisms, models and physical applications, *Phys. Rep.*, **195** (1990), 127–293.

[6] I. Calvo and R. Sánchez, The path integral formulation of fractional Brownian motion for the general Hurst exponent, *J. Phys. A, Math. Theor.*, **41** (2008), 282002.

[7] M. Caputo, Linear models of dissipation whose *Q* almost frequency independent – II, *Geophys. J. R. Astron. Soc.*, **13** (1967), 529–539.

[8] M. Chaichian and A. Demichev, *Path Integrals in Physics: Stochastic Process and Quantum Mechanics*, vol. 1, IOP Publishing, Bristol, 2001.

[9] J. Dong and M. Xu, Space-time fractional Schrödinger equation with time-independent potentials, *J. Math. Anal. Appl.*, **344** (2008), 1005–1017.

[10] R. P. Feynman and A. R. Hibbs, *Quantum Mechanics and Path Integrals*, McGraw–Hill, New York, 1965.

[11] P. Górka, H. Prado, and J. Trujillo, The time fractional Schrödinger equation on Hilbert space, *Integral Equ. Oper. Theory*, **87** (2017), 1–14.

[12] A. Iomin, Fractional-time quantum dynamics, *Phys. Rev. E*, **80** (2009), 022103.

[13] A. Iomin, Fractional-time Schrödinger equation: Fractional dynamics on a comb, *Chaos Solitons Fractals*, **44** (2011), 348–352.
[14] A. Iomin, Superdiffusive comb: Application to experimental observation of anomalous diffusion in one dimension, *Phys. Rev. E*, **86** (2012), 032101.
[15] A. Iomin, Lévy flights in a box, *Chaos Solitons Fractals*, **71** (2015), 73–77.
[16] A. Iomin and T. Sandev, Lévy transport in slab geometry of inhomogeneous media, *Math. Model. Nat. Phenom.*, **11** (2016), 51–62.
[17] G. M. Iomin and A. Zaslavsky, Sensitivity of ray paths to initial conditions, *Commun. Nonlinear Sci. Numer. Simul.*, **8** (203), 401–413.
[18] A. Iomin, S. Fishman, and G. M. Zaslavsky, Quantum localization for a kicked rotor with accelerator mode islands, *Phys. Rev. E*, **65** (2002), 036215.
[19] M. Kac, *Probability and Related Topics in Physical Sciences*, Interscience, NY, 1959.
[20] D. A. Kessler and E. Barkai, Theory of fractional Lévy kinetics for cold atoms diffusing in optical lattices, *Phys. Rev. Lett.*, **108** (2012), 230602.
[21] R. V. Khokhlov, Wave propagation in nonlinear dispersive lines, *Radioteh. Elektron.*, **6** (1961), 1116–1120.
[22] Y.-C. Lai, R. Bliimel, E. Ott, and C. Grebogi, Quantum manifestations of chaotic scattering, *Phys. Rev. Lett.*, **68** (1992), 3491–3494.
[23] N. Laskin, Fractals and quantum mechanics, *Chaos*, **10** (2000), 780–790.
[24] N. Laskin, Time fractional quantum mechanics, *Chaos Solitons Fractals*, **102** (2017), 16–28.
[25] M. A. Leontovich, On a method of solving the problem of propagation of electromagnetic waves along the earth's surface, *Proc. Acad. Sci. USSR, Phys.*, **8** (1944), 16–22 (Russian).
[26] L. Levi, M. Rechtsman, B. Freedman, T. Schwartz, O. Manela, and M. Segev, Disorder-enhanced transport in photonic quasicrystals, *Science*, **332** (2011), 1541–1544.
[27] L. Levi, Y. Krivolapov, S. Fishman, and M. Segev, Hyper-transport of light and stochastic acceleration by evolving disorder, *Nat. Phys.*, **8** (2012), 912–916.
[28] G. Lindblad, On the generators of quantum dynamical semigroups, *Commun. Math. Phys.*, **48** (1976), 119–130.
[29] S. Löck, A. Bäcker, R. Ketzmerick, and P. Schlagheck, Regular-to-chaotic tunneling rates: From the quantum to the semiclassical regime, *Phys. Rev. Lett.*, **104** (2010), 114101.
[30] S. Marksteiner, K. Ellinger, and P. Zoller, Anomalous diffusion and Lévy walks in optical lattices, *Phys. Rev. A*, **53** (1996), 3409–3429.
[31] R. Metzler and J. Klafter, The random walk guide to anomalous diffusion: A fractional dynamics approach, *Phys. Rep.*, **339** (2000), 1–77.
[32] M. Naber, Time fractional Schrodinger equation, *J. Math. Phys.*, **45** (2004), 3339–3352.
[33] B. N. Narahari Achar, B. T. Yale, and J. W. Hanneken, Time fractional Schrödinger equation revisited, *Adv. Math. Phys.*, **2013** (2013), 290216.
[34] K. B. Oldham and J. Spanier, *The Fractional Calculus*, Academic Press, Orlando, 1974.
[35] I. Podlubny, *Fractional Differential Equations*, Academic Press, San Diego, 1999.
[36] Y. Sagi, M. Brook, I. Almog, and N. Davidson, Observation of anomalous diffusion and fractional self-similarity in one dimension, *Phys. Rev. Lett.*, **108** (2012), 093002.
[37] T. Sandev, I. Petreska, and E. K. Lenzi, Time-dependent Schrödinger-like equation with nonlocal term, *J. Math. Phys.*, **55** (2014), 092105.
[38] L. Schulman, *Techniques and Applications of Path Integration*, Wiley, New York, 1981.
[39] K. L. Sebastian, Path integral representation for fractional Brownian motion, *J. Phys. A, Math. Gen.*, **28** (1995), 4305–4311.
[40] M. H. Stone, On one-parameter unitary groups in Hilbert space, *Ann. Math.*, **33** (1932), 643–648.

[41] E. D. Tappert, The parabolic approximation method, in J. B. Keller and J. S. Papadakis (eds.) *Wave Propagation and Underwater Acoustics*, Lectures Notes in Physics, vol. 70, pp. 224–287, Springer, New York, 1977.

[42] V. E. Tarasov, *Quantum Mechanics of Non-Hamiltonian and Dissipative Systems*, Elsevier, Amsterdam, 2008.

[43] V. E. Tarasov, Quantum dissipation from power-law memory, *Ann. Phys.*, **327** (2012), 1719–1729.

[44] V. E. Tarasov, The fractional oscillator as an open system, *Cent. Eur. J. Phys.*, **10** (2012), 382–389.

[45] V. E. Tarasov and V. V. Tarasova, Time-dependent fractional dynamics with memory in quantum and economic physics, *Ann. Phys.*, **383** (2017), 579–599.

[46] S. Wang and M. Xu, Generalized fractional Schrödinger equation with space-time fractional derivatives, *J. Math. Phys.*, **48** (2007), 043502.

[47] B. J. West, Quantum Lévy propagators, *J. Phys. Chem. B*, **104** (2000), 3830–3832.

[48] B. J. West, M. Bologna, and P. Grigolini, *Physics of Fractal Operators*, Springer, New York, 2002.

[49] H. Wio, *Path Integrals For Stochastic Processes*, World Scientific, New Jersey, 2013.

[50] J.-N. Wu, C.-H. Huang, S.-C. Cheng, and W.-F. Hsieh, Spontaneous emission from a two-level atom in anisotropic one-band photonic crystals: A fractional calculus approach, *Phys. Rev. A*, **81** (2010), 023827.

Index